A Thesis Entitled

MULTIELEMENT GEOCHEMICAL RECONNAISSANCE FOR URANIUM IN THE PALMYRIDES REGION OF CENTRAL SYRIA

by

YOUSSEF Maarouf JUBELI

Submitted for the Degree of

Doctor of Philosophy

in

The Faculty of Science

The University of London

Applied Geochemistry Research Group

Department of Geology

Royal School of Mines

Imperial College

London SW7 2BP

A

THESIS

entitled

MULTIELEMENT GEOCHEMICAL RECONNAISSANCE FOR URANIUM IN THE PALMYRIDES REGION, CENTRAL SYRIA

Submitted for the

Degree of

DOCTOR OF PHILOSOPHY

in the

FACULTY OF SCIENCE OF THE UNIVERSITY OF LONDON

by

YOUSSEF MAAROUF JUBELI

Applied Geochemistry Research Group
Department of Geology
Imperial College
London S W 7

July 1986

ABSTRACT

This research work is concerned with the application of orientation and reconnaissance multielement geochemistry coupled with ground scintillation gamma ray measurements to investigate the dispersion patterns of uranium and other major and trace elements in the arid Palmyrides region of central Syria. Rocks, wadi and playa sediments, overburden and groundwaters have been studied.

The region occupies an interplatform depression in the northern part of the Arabia Plate, upon which sediments up to 10km thick have accumulated. Outcrops of strongly fractured Mesozoic and Cenozoic rocks form two major mountain belts, the northern and southern Palmyrides, between which is located the closed Ad-Daww basin, with a thick Neogene and Quaternary clastic cover. Among the various lithologies, phosphorites, enriched in U, are well represented. In and around these phosphorites numerous traces of secondary U mineralization occur.

Lexan-fission track registration was performed on selected samples to investigate the distribution of uranium. Results of this technique show that U is closely related to phosphate particles, collophane mud and organic matter in the carbonate rocks. Secondary U enrichment along fractures and micro-fissures was also found. Integrated mineralogical and geochemical procedures utilizing optical and scanning electron microscopy, electron microprobe and various x-ray diffractometric methods indicated the presence of carnotite, tyuyamunite, meta-tyuyamunite and un-named urano-vanadate mineral similar to ferghanite.

Univariate and multivariate statistical methods are used to interpret the geochemical data. These methods involve generating histograms, boxplots, scattergams, QQ plots, interelement correlations, multiple linear regression using ridge constants, hierarchical cluster analysis and principal component analysis. The aerial distribution of U, its associated elements and multivariate geochemical functions and factor scores are mapped using computer graphics.

Low order anomalies of U, accompanied by various combinations of anomalous concentrations of Mo, Se, Sr, As, Ba, Cd, P and V are recognized in all the sampling media used in this work. Lithogeochemistry provides geochemical dispersion patterns with good contrast, and the hydrogeochemical anomalies are of particular interest: multielement signatures similar to those related to known sedimentary uranium deposits elsewhere in the world occur in an aquifer of coarse clastic Neogene sediments.

It is concluded that U and associated elements have been incorporated into the Upper-Cretaceous and Lower Palaeogene sediments, especially the phosphate rocks, from three possible sources, namely, sea water, Lower Cretaceous volcanism and metalliferous fluids leaking along taphrogenic lineaments. Results of the factor analysis indicated that the dispersion patterns of U and associated elements are controlled by a combination of structural, lithological and environmental factors. Uranium and associated elements have subsequently been leached out of the

phosphorite and other U enriched clayey limestone and carbonate rocks into the hydrogeologic regime. Redistribution of these elements is taking place along fracture zones and major faults. A degree of U accumulation in the Neogene-Quaternary aquifer of the Ad-Daww basin is evident. There is also some evidence of U concentration in recently formed thin duricrusts of calcrete and gypcrete. Indications of bifacies of oxidized and reduced lacustrine formations of the lower Neogene suggest a further means of U precipitation; this phenomenon merits further investigation. Recommendations for further uranium exploration in Syria are reported.

ACKNOWLEDGEMENTS

The author would like to thank the Atomic Energy Commission of Syria for kindly granting him leave of study to undertake the research described in this thesis. The support and encouragement of Prof. I. Haddad, Director General of the AEC is sincerely acknowledged.

I am most grateful to Dr. Martin Hale of the Department of Geology, Imperial College for his supervision, constructive advice in the field particularly during sampling W. Om Jorn and for reading and correcting of the manuscript and suggesting many improvements.

I wish to express my deep and sincere thanks to the Arab-British Chamber Charitable Foundation and the Committee of Vice-Chancellors and Principals of the Universities of the United Kingdom for the awards recieved during the present research work.

The author gratefully thanks Dr. P. Simpson of the British Geological Survey for his guidance and help in the field of fission track registration and U mineralogy. His help in other aspects (library and literature) is also warmly acknowledged.

Analysis at Imperial College Reactor Centre was made through the assistance of Dr. Susan Parry, Mr. Ian Sinclair and Mr. Tom Jones to whom I am grateful.

I would also like to thank Drs. R. J. Howarth, M. Wheatley and Mr. M. Turner for their assistance with computing techniques and statistical applications.

Technical and other help recieved from Messrs. A. Ahmad, B. Coles, D. Campain, A. Doyle and Mrs. E. Banerjee and other members of staff within the Applied Geochemistry Research Group and the Geology Department, Imperial College is also acknowledged.

A note of appreciation is directed to Messrs. P. Watkins for his help in REE analysis, R. Giddens for his assistance in SEM imagery and probe analysis, A. Cash and N. Morton for their help in many aspects of photography.

Special thanks are extended to Mrs. E.G. Ng. Chieng Hin and Mrs. G. Bello; the former for her invaluable help in typing long tables and reading the whole manuscript, and the latter for kindly providing various typing help.

The following members of the Geology Department at the AEC, Syria are warmly acknowledged.

Drs. M. Mouty and A.K. El Maleh for their support; Messrs. B. Ghaleb, M. Sanawbara, A. Safarjalani, K. Shaker, Y. Radwan, A. Kassim and M. El Bahri for their help during sampling and shipping of the samples to London.

Special thanks are also extended to Drs. S. Kheir and W.R. Agha of Damascus University for their encouragement and support.

I would like to register my sincere appreciation and thanks to Mrs. Judy Heeley and Mr. Gordon Heeley for their patient typing and interpreting my handwritten manuscript to the present neat form.

The friendship provided by my colleagues in the research room and within the Group is highly appreciated.

Finally, I wish to thank sincerely with love my wife Mukarram and my four sons Bazegh, Majd, Aouj and Rand; the former for her wholehearted support and the latter for their patience and the hardship caused by my absence during the period of this research work.

CONTENTS

	Page No.
Abstract	i
Acknowledgements	iii
Contents	v
List of Figures	xiv
List of Tables	xxx
List of Plates	xxxiv

CHAPTER I

1. Introduction	1
1.1. Background to the Research.	1
1.1.1. Aims of the Research.	3
1.1.2. Approach used in the Study.	3
1.1.2.1. Objectives of the Orientation Survey.	6
1.1.2.2. Handling and Processing of the Data.	6
1.1.3. Description of the Thesis.	9
1.2. Chemical Properties and Geochemical Cycle of U.	10
1.2.1. Chemical Properties.	10
1.2.2. Geochemical Cycle of U.	12
1.3. Uranium Deposits.	20
1.3.1. Uranium Provinces.	20
1.3.2. Classification of U Deposits.	23
1.4. Uranium Exploration.	25
1.4.1. Historical Background.	25
1.4.2. Methods of Exploration.	27

CHAPTER II

2. Geology 30

2.1. History of geological investigations 30

2.2. Geology of the Palmyrides in the light of plate tectonics 33

2.2.1. The Palmyrides aulacogen 33

2.2.2. Plate tectonic movements 35

2.2.3. Faulting 49

2.3. Stratigraphy 52

2.4. Phosphorite deposits 58

2.4.1. Distributions 58

2.4.2. Types of phosphorite 61

2.4.3. The major Palmyrides phosphorite deposits 62

2.5. Occurrence of uranium 63

2.5.1. Review of previous work 63

2.5.2. Observations during current research 67

CHAPTER III

3. Physiography 70

3.1 General 70

3.2 Topography 70

3.3 Climate 78

3.3.1 General 78

3.3.2 Temperature 78

3.3.3 Winds 81

3.3.4 Precipitation 81

3.3.5 Vegetation 86

3.3.6 Animals 86

3.3.7 Population 68

3.4 The geochemical environment of the Palmyrides 87

3.4.1 General 87

3.4.2 Physical weathering 87

3.4.3 Chemical weathering 87

3.4.4 Combined effects of physical and chemical weathering in the Palmyrides 89

3.5 Erosion and transport 89

3.5.1 General 89

3.5.2 The effect of wind 90

3.5.3 The effect of rain water 90

3.5.4 Landslides 92

3.5.5 Drainage 93

3.5.6 Soil 93

3.6 Characteristics of the surficial geochemical environment of the Palmyrides 94

3.6.1 Principal features 94

3.6.2 Formation of the duricrusts 95

3.6.3 Brief review of the factors of calcrete formations 95

3.6.4 Classification of calcretes and U favourability 98

3.6.5 Duricrusts of the Palmyrides 98

CHAPTER IV

4.Sampling, analysis and data processing 102

4.1 General 102

4.2 Sampling 102

4.2.1 The orientation survey 102

4.2.2 The reconnaissance survey 105

4.3 Physical preparation of samples for analysis 108

4.3.1 The orientation samples 108

4.3.2 The reconnaissance samples 109

4.4 Instrumental analysis 109

4.4.1 Total chemical extraction and ICP analysis 111

4.4.2 Hydride generation and ICP analysis 111

4.4.3 Uranium and rare-earth elements analysis 112

4.4.3.3 Principles of INAA 113

4.4.3.2 Application of INAA in this study 113

4.4.4 Fission track radiography 115

4.5 Suitability of the data produced 116

CHAPTER V

5. Region selection and orientation survey 123

5.1 Investigation to optimize the size fraction to be analysed 123

5.2 Analysis of Uranium minerals 125

5.2.1 General 125

5.2.2 Sample preparation and analytical techniques 126

5.2.3 Scanning electron microscopy 126

5.2.4 X-ray photography and fluorescence 130

5.3 Fission track registrations 134

5.3.1 General 134

5.3.2 Results and discussion 134

5.3.3 Reasons for variations in Uranium content 144

5.3.4 Conclusions of fission track studies 151

5.4 Geochemical results and region selection 152

5.4.1 General 152

5.4.2 Quality of the data 152

5.4.3 Data interpretation 154

5.4.3.1 Symbolic geochemical maps 154

5.4.3.2 Boxplots 162

5.4.3.3 Histograms and frequency distributions 167

5.4.3.4 Interelement correlations 171

5.4.3.5 Variation diagrams 171

5.4.3.6 Elemental ratios 174

5.4.4 Wadi sediment data 177

5.4.5 Overburden data 179

5.4.6 Bedrock data 185

5.5 General conclusions of the orientation survey 186

5.6 Recommendations for the reconnaissance stage 187

CHAPTER VI.

6. Drainage survey 189

6.1 Detailed wadi sediment survey 189

6.2 Location and geology 189

6.3 Wadi sediment geochemistry 191

6.3.1 Sampling and analysis 191

6.3.2 Results and discussion 191

6.3.2.1 Basic statistics and histograms 191

6.3.2.2 Correlation and cluster analysis 193

6.3.2.3 Uranium anomalies 204

6.3.2.4 Regression analysis 213

6.4 Conclusions 217

CHAPTER VII

7. Hydrogeochemistry of the Palmyrides 219

7.1 General 219

7.2 Sample location and local geology 221

7.2.1 Sample location 221

7.1.2 Geology 221

7.3 Hydrogeology 225

7.3.1 Units (the aquifers) 225

7.3.2 System 226

7.3.3 Water flow 226

7.4 Methods of analysis 229

7.5 Results and discussion 230

7.5.1 General characteristics 230

7.5.2 Frequency distribution 235

7.5.3 Interelemental correlations 237

7.5.4 Cluster analysis 240

7.5.5 Ridge regression 245

7.5.6 Box plots 215

7.6 Spatial distribution 255

7.6.1 Symbolic distribution 255

7.6.2 Uranium anomalies 258

7.7 Model of Uranium enrichments 262

7.8 Conclusions 265

Chapter VIII

8. Geochemistry of Sabkhet El Mouh 267

8.1 Introduction 267

8.2 Objectives of the playa geochemistry 269

8.3 Description of the area 270

8.4 Sampling and geology 272

8.4.1 Sampling 272

8.4.2 Geology 273

8.5 Analysis and data control 275

8.6 Results and interpretation 277

8.6.1 Element abundance 277

8.6.2 Univariate element distribution 279

8.6.3 Spatial distribution of selected elements 282

8.7 Multivariate statistical analysis of the data 295

8.7.1 Interelement relationships 295

8.7.2 Cluster analysis 297

8.7.3 Principal component and factor analysis 300

8.7.3.1 General 300

8.7.3.2 Application of the method 302

8.7.3.3 Results and interpretation 304

8.7.4 Regression analysis 304

8.8 Conclusions 327

CHAPTER IX

9. Lithogeochemistry of the Palmyrides. 329

9.1 Introduction 329

9.2 Aims of lithogeochemistry in this study 331

9.3. Surface geology and the phosphorite rocks 332

9.3.1 Surface geology 332

9.3.2 The Palmyrides mountain belts 335

9.3.3 The basins 335

9.3.4 Phosphorite deposits of the Palmyrides 336

9.4 Uranium content of the Palmyrides phosphorite 337

9.5 Sample locations and analysis 339

9.5.1 Sample location 339

9.5.2 Analysis and data control 343

9.5.3 Petrography and mineralogy 343

9.6 Statistical and areal distribution of the lithogeochemical data 347
9.6.1 Statistical parameters 347
9.6.2 Single element areal distribution 356
9.6.2.1 Uranium 356
9.6.2.2 Radioactivity (CPS) 365
9.6.2.3 Thorium 369
9.6.2.4 Arsenic 371
9.6.2.5 Selenium 373
9.6.2.6 Phosphorus 377
9.6.2.7 Strontium 380
9.6.2.8 Vanadium 382
9.6.2.9 Molybdenum 385
9.6.2.10 Potassium 387
9.7 Lithological studies 389
9.7.1 General 389
9.7.2 Geochemistry of the two main rock groups 390
9.7.3 Distribution of U and its associated elements in the phosphate group 393
9.7.4 Distribution of U and associated elements in the nonphosphate group 396
9.7.5 Uranium and Phosphorus in the phosphorite deposits 402
9.7.6 Uranium in fault-controlled zones 403
9.7.7 Geochemistry of various lithostratigraphical units 405
9.7.7.1 General characteristics 405
9.7.7.2 Boxplots 409

9.7.7.3 Lithogeochemistry of typical regional traverses 413
9.8 Interelement correlation analysis 423
9.9 Cluster analysis 429
9.10 Factor analysis 435
9.10.1 General 435
9.10.2 The six factor model 435
9.10.3 Factors controlling U in the phosphate rocks 448
9.11 Regression analysis 463
9.11.1 Regression models 463
9.11.2 Interpretation of the residuals 468
9.11.3 Regression of U in the phosphate rocks 470
9.12 Conclusions 474

Chapter X

10. Summary, conclusions and recommendations for further work 477
10.1 Summary 477
10.2 General conclusions 478
10.2.1 Approach 478
10.2.2 Radioactivity measurements 478
10.2.3 Geology 479
10.2.4 Uranium minerals 484
10.2.5 Fission track registrations 485
10.2.6 Drainage geochemistry 486
10.2.7 Hydrogeochemistry 487
10.2.8 Playa geochemistry 490
10.2.9 Lithogeochemistry 491
10.3 Further work and recommendations 498

LIST OF FIGURES

		Page No.
Fig.1.1	Location map of the orientation survey areas.	5
Fig.1.2	Reconnaissance sampling of the Palmyrides region.	8
Fig.1.3	Decay series of ^{238}U and ^{235}U.	11
Fig.1.4	Uranyl complexes versus pH and the main U hydroxide species.	13
Fig.1.5	Geochemical cycle of U.	15
Fig.1.6	Exogenous part of the geochemical cycle of U.	16
Fig.1.7	Time bound of major U deposits.	18
Fig.1.8	Uranium provinces.	21
Fig.2.1	Symblified geological map of the Palmyrides region.	32
Fig.2.2	Location and schematic sections showing the main structural units of the basement.	34
Fig.2.3	Correlation of development stage and cycles of some aulacogens (from Milanovsky, 1981).	36
Fig.2.4	General regional tectonic setting.	38
Fig.2.5	Structural pattern of Levant, Red Sea, Gulf of Aden and East Africa area.	40
Fig.2.6	Compression and thrust deformation in the Palmyrides following the collision of the Arabia and Anatolia plates.	42
Fig.2.7	Asymmetrical thrust shape of the southern Palmyrides Mountains.	44

Fig.2.8	The Levant shear system.	46
Fig.2.9	Development of volcanic activities outside the Palmyrides compression zone.	48
Fig.2.10	Interpretration of fault lineaments from the Landsat image (from Khouri and Droubi, 1980).	50
Fig 2.11	Fault contact between Maestrichtian marls and Lower Cretaceous or Jurassic rocks.	51
Fig.2.12	Sharifeh borehole (from Technoexport,1966).	56
Fig.2.13	The major phosphorite deposits (modified after Atfeh, 1967).	59
Fig.2.14	Distribution of the phosphorites in the stratigraphic column of the Palmyrides.	60
Fig.2.15	The relationship of U, P_2O_5 and the radioactivity (from Hunting, 1975).	66
Fig.2.16	Uranium occurrences in the Palmyrides.	68
Fig.3.1	The major topographic features of the region.	71
Fig.3.2	Various mountains of the Palmyrides.	72
Fig.3.3	Rose diagrams of the winds.	82
Fig.3.4	Isohytee of the Palmyrides and Syria.	85
Fig.3.5	Pleistocene and recent drainage basins.	91
Fig.3.6	Piedmont and stony desert formation.	96
Fig.3 7	Schematic calcrete profil.	96
Fig.3.8	Genetic classification of calcretes , their U favorability and world wide distribution.	100
Fig.4.1	Accuracy of U determination by NAA.	118
Fig.4.2	Accuracy of measuring the major and trace elements in HRM1.	119
Fig.4.3	Accuracy of measuring the major and trace elements in HRM2.	119

Fig.4.4	Precision of duplicate results for P and Ca.	121
Fig.4.5	Precision of duplicate results for K and V.	121
Fig.4.6	Accuracy of duplicate results for U.	122
Fig.5.1	Relative concentrations of U and associated elements in different size fractions.	124
Fig.5.2	Scanning electron microprobe photomicrograph of U minerals.	129
Fig.5.3	X-ray fluorescence of an unnamed U mineral.	150
Fig.5.4	Microprobe analysis of U minerals.	150
Fig.5.5	Spatial distribution of U in the orientation areas solid surface (a), symbolic map (b), contour map (c).	155
Fig.5.6	Spatial distribution of P in the orientation areas; solid surface (a), symbolic map (b).	156
Fig.5.7	Spatial distribution of Sr in the orientation areas; solid surface (a), symbolic map (b).	157
Fig.5.8	Spatial distribution of V in the orientation areas; solid surface (a), symbolic map (b).	158
Fig.5.9	Spatial distribution of Th in the orientation areas; solid surface (a), symbolic map (b).	159
Fig.5.10	Spatial distribution of Hf in the orientation areas; solid surface (a), symbolic map (b).	160
Fig.5.11	Spatial distribution of the CPS in the orientation areas; solid surface (a), symbolic map (b).	161
Fig.5.12	Boxplot of U, Hf, As, CPS, Th and P of the orientation survey by sample type.	163
Fig.5.13	Boxplot of Ca, Sr, Ba, Al and Ti of the orientation survey by sample type.	164

Fig.5.14 Boxplot of V, Cr, Mo, Mn, Fe and Co in the orientation survey by sample type. 165

Fig.5.15 Boxplot of Zn, Cu, Mg, Na, K and Li in the orientation survey by sample type. 166

Fig.5.16 Histograms of U, P and V in the orientation samples. 168

Fig.5.17 Histograms of Sr and Ca in the orientation samples. 169

Fig.5.18 Normal Cumulative probability plot for U and P. 170

Fig.5.19 Scatterplots of U, Th and K Vs CPS. 173

Fig.5.20 Relationship of U and P_2O_5 content. 175

Fig.5.21 Histograms of U, V, As, P, Sr and CPS in the wadi sediments. 180

Fig.5.22 Histograms of U in the overburden and rocks. 180

Fig.6.1 Surface geology and location of wadi Om Jorm. 190

Fig.6.2 Histograms of U, As, Se, P, Sr, Ba, V, Mo and Ni. 195

Fig.6.3 Histograms of Cu, Zn, Cd, Li, Na, K, Mg, Ca and Ti. 196

Fig.6.4 Normal cumulative probability plots of U, Se, Mo and P. 197

Fig.6.5 Geochemical dispersion patterns of U, Se, Ba and Sr in wadi Om Jorn. 198

Fig.6.6 Geochemical dispersion patterns of As, Zn, P and Mo in wadi Om Jorn. 199

Fig.6.7 Geochemical dispertion patterns of V, Cu, Ni and Cd in wadi Om Jorn. 200

Fig.6.8 Cluster analysis of 20 variables of the drainage geochemistry. 203

Fig.6.9 Cluster analysis of 10 variables of the drainage geochemistry. 205

Fig.6.10 The Trees clustering pattern of the whole data set. 206

Fig.6.11 Cluster analysis of the upper section of wadi Om Jorn. 211

Fig.6.12 Cluster analysis of the lower section of wadi Om Jorn. 212

Fig.6.13 Ridge trace for a regression model of U Vs 15 other geochemical variables in the wadi geochemistry. 216

Fig.7.1 Mobility of various elements in the surface environment (from Rose et al.,1979 and Plant et al., 1985). 220

Fig.7.2 Sample location in relation to the surface geology. 222

Fig.7.3 The Palmyrides aquifers in relation to the lithostratigraphic column. 223

Fig.7.4 Direction of the groundwater movement in the region. 228

Fig.7.5 The relationship of U contents measured by various techniques. 231

Fig.7.6 Accuracy (a) and precision (b) of U determination by the ^{239}U (NAA). 233

Fig.7.7 Ternary diagram of the major alkaline elements in the Palmyrides hydrogeochemistry. 234

Fig.7.8 Histogram and QQ plot of U in the groundwaters. 236

Fig.7.9 Cluster analysis of 22 hydrogeochemical variables. 241

Fig.7.10 Cluster analysis of 13 hydrogeochemical variables. 242

Fig.7.11 Cluster analysis of 15 hydrogeochemical variables. 243

Fig.7.12 Zonation of Roll-Front type of U deposit (from Chester, 1984). 246

Fig.7.13 Ridge trace for regression of U vs 18 variables in the hydrogeochemistry. 248

Fig.7.14 Ridge trace for regression of U Vs 11 variables in the hydrogeochemistry. 248

Fig.7.15 Optimum ridge regression of U in the hydrogeochemical data. 250

Fig.7.16 Residual probability plot of U in the groundwaters. 252

Fig.7.17 Boxplot of U, TDS, Mo and S of the hydrogeochemistry. 253

Fig.7.18 Boxplot of Sr, V and Ca of the hydrogochemistry. 254

Fig.7.19 Spatial distribution of U, Se and V in the Palmyrides hydrogeochemistry. 256

Fig.7.20 Spatial distribution of As, Sr and Mo in the Palmyrides hydrogeochemistry. 257

Fig.7.21 Solid surface distribution of U and Se in the Palmyrides hydrogeochemistry. 259

Fig.7.22 Areal distribution of U anomalies. 260

Fig.7.23 An explanatory model of U enrichment in the Neogene-Quaternary aquifer of the region. 263

Fig.8.1 Schematic diagram and profile of Sabkhet El Mouh. 271

Fig.8.2 Surface geology of Sabkhet El Mouh. 274

Fig.8.3 Relative concentrations of U, Sr, V, Na, K and P in different size fractions of the sabkha sediments. 276

Fig.8.4 Histograms of V, Mo, As and Mg in the sabkha geochemistry. 280

Fig.8.5 Histograms of U and CPS of the sabkha geochemistry. 280

Fig.8.6 Normal probability plots showing bimodal distributions. 281

Fig.8.7 Normal probability plots of Sr, Li, Na and K showing anomalous levels. 281

Fig.8.8 Symbolic areal distribution of U and Sr in the sabkha sediments. 283

Fig.8.9 Symbolic areal distribution of P and As in the sabkha sediments. 284

Fig.8.10 Symbolic areal distribution of V and Mo in the sabkha sediments. 285

Fig.8.11 Symbolic areal distribution of Mg and Ti in the sabkha sediments. 286

Fig.8.12 Symbolic areal distribution of K and Fe in the sabkha sediments. 287

Fig.8.13 Solid surface distribution of U in the sabkha. 289

Fig.8.14 Solid surface distribution of As in the sabkha. 290

Fig.8.15 Solid surface distribution of Sr in the sabkha. 291

Fig.8.16 Solid surface distribution of Mo in the sabkha. 292

Fig.8.17 Solid surface distribution of V in the sabkha. 293

Fig.8.18 Contour map of U and As in the sabkha sediments illustrating anomalous trends. 294

Fig.8.19 Scatterplots showing very good linear relationship between Al and Fe and less obvious one between U and As. 296

Fig.8.20 Dendrogram showing R-mode cluster analysis of 21 geochemical variable of the sabkha. 299

Fig.8.21 Solid surface distribution of the scores of factor 1 association of the sabkha sediments. 309

Fig.8.22 Solid surface distribution of the scores of factor 1 association of the sabkha sediments (a), compared to C distribution (b). 311

Fig.8.23 Solid surface distribution of the scores of factor 6 (a) compared to P distribution (b) in the sabkha sediments. 313

Fig.8.24 Solid surface distribution of the scores of factor 2 association in the sabkha sediments. 314

Fig.8.25 Solid surface distribution of the scores of factor 4 association in the sabkha sediments. 316

Fig.8.26 Solid surface distribution of the scores of factor 5 association in the sabkha sediments. 318

Fig.8.27 Ridge trace of U regression vs 19 geochemical variables in the sabkha sediments. 324

Fig.8.28 Ridge trace of U regression Vs 11 geochemical variables in the sabkha sediments. 324

Fig.8.29 Normal probability plot of U residuals in the sabkha sediments. 326

Fig.9.1 Location map and surface geology of the Palmyrides region. 333

Fig.9.2 Simplified lithostratigraphic column. 334

Fig.9.3 Sample location in relation to surface geology. 340

Fig.9.4 Sample location in each of the nine traverses. 341

Fig.9.5 Flow diagram of the sampling scheme. 342

Fig.9.6 A typical geological cross-section of the region coinciding with traverse 600. 344

Fig.9.7 Precision of duplicate measurements of U and Th of the lithogeochemistry. 346

Fig.9.8 Histograms of U and CPS in the Palmyrides lithogeochemistry. 348

Fig.9.9 Stem-and-Leaf display of U, CPS, Th and As. 349

Fig.9.10 Stem-and-Leaf display of Se, Sr, Ba and P. 350

Fig.9.11 Stem-and-Leaf display of V, K, Mo and Cd. 351

Fig.9.12 Stem-and-Leaf display of Na, Li, Mn and Fe. 352

Fig.9.13 Stem-and-Leaf display of Ca, Mg, Ti and Cr. 353

Fig.9.14 Stem-and-Leaf display of Cu, Zn, Al and La. 354

Fig.9.15 Stem-and-Leaf display of Co, Pb and Ni. 355

Fig.9.16 Symbolic areal distribution of U in the region. 357

Fig.9.17 X-ray diffractogram of sample 710. 358

Fig.9.18 Solid surface distribution of U in the region. 366

Fig.9.19 Symbolic areal distribution of CPS in the region. 367

Fig.9.20 Solid surface distribution of CPS in the region. 367

Fig.9.21 Symbolic areal distribution of Th in the region. 370

Fig.9.22 Solid surface distribution of Th in the region. 370

Fig.9.23 Symbolic areal distribution of As in the region. 372

Fig.9.24 Solid surface distribution of As in the region. 372

Fig.9.25 Symbolic areal distribution of Se in the region. 374

Fig.9.26 Solid surface distribution of Se in the region. 374

Fig.9.27 Solid surface distribution of Se in the hydrogeochemistry. 376

Fig.9.28 Symbolic areal distribution of P in the region. 378

Fig.9.29 Solid surface distribution of P in the region. 378

Fig.9.30 Symbolic areal distribution of Sr in the region. 381

Fig.9.31 Solid surface distribution of Sr in the region. 381

Fig.9.32 Symbolic areal distribution of V in the region. 383

Fig.9.33 Solid surface distribution of V in the region. 383

Fig.9.48 Scatterplot showing the relationship of U and P_2O_5 in the phosphate group. 404

Fig.9.49 Boxplot of U, CPS and Th by rock type. 410

Fig.9.50 Boxplot of As, Se and Sr by rock type. 411

Fig.9.51 Boxplot of V, Mo and K by rock type. 412

Fig.9.52 Distribution of CPS, U and P along traverse 600. 414

Fig.9.53 Distribution of CPS, U and P along traverse 100. 415

Fig.9.54 Distribution of Th, As and Se along traverse 600. 416

Fig.9.55 Distribution of Th, As and Se along traverse 100. 417

Fig.9.56 Distribution of V, Mo and K along traverse 600. 418

Fig.9.57 Distribution of V, Mo and K along traverse 100. 419

Fig.9.58 Distribution of Sr, Li and Ca along traverse 600. 420

Fig.9.59 Distribution of Sr, Li and Ca along traverse 100. 421

Fig.9.60 Scatterplots of U, Th and K contents of the rocks vs CPS. 425

Fig.9.61 Scatterplot of P content in the rocks vs CPS. 426

Fig.9.62 Summary of the important correlations of U, CPS and P with selected elements in the two groups of rocks (phosphate and nonphosphate). 428

Fig.9.63 Summary of U correlations with selected elements of the lithostratigraphic units. 428

Fig.9.64 Dendrogram of R-mode cluster analysis of 20 variables of the litogeochemistry. 431

Fig.9.65 Dendrogram of R-mode cluster analysis of 14 variables of the lithogeochemistry. 432

Fig.9.66 Dendrogram of R-mode cluster analysis of 20 variables in the phosphate group. 434

Fig.9.67 Dendrogram of R-mode cluster analysis of 20 variables in the nonphosphate group. 434

Fig.9.68 Solid surface distribution of the scores of factor 1 in the whole data set. 439

Fig.9.69 Solid surface distribution of the scores of factor 2 of the whole data set. 441

Fig.9.70 Solid surface distribution of the scores of factor 3 in the whole data set. 443

Fig.9.71 Solid surface distribution of the scores of factor 4 in the whole data set. 445

Fig.9.72 Solid surface distribution of the scores of factor 5 in the whole data set. 447

Fig.9.73 Solid surface distribution of the scores of factor 6 in the whole data set. 449

Fig.9.74 Solid surface distribution of the scores of factor 1 in the phosphate rocks. 453

Fig.9.75 Solid surface distribution of the scores of factor 2 in the phosphate rocks. 453

Fig.9.76 Solid surface distribution of the scores of factor 3 in the phosphate rocks. 458

Fig.9.77 Microchemical analysis of Pt grain. 456

Fig.9.78 X-ray diffraction of sample 119 showing high temperature minerals. 456

Fig.9.79 Solid surface distribution of the scores of factor 4 in the phosphate rocks. 458

Fig.9.80 Solid surface distribution of the scores of factor 5 in the phosphate rocks. 460

Fig.9.81 Zonation shown by the regional distribution of the scores of the five factors. 460

Fig.9.82 Ridge trace of U regression against 20 variables of the lithogeochemical data. 465

Fig.9.83 Ridge trace of U regression against 14 variables of the lithogeochemical data. 465

Fig.9.84 Ridge trace of the optimum U regression model with 16 variables of the lithogeochemical data. 467

Fig.9.85 Solid surface distribution of U residuals after ridge regression of the lithogeochemical data. 467

Fig.9.86 Ridge trace of regression for U vs 13 variables of the phosphate rocks. 472

Fig.9.87 Solid surface distribution of U residuals in the phosphate rocks. 472

Fig.10.1 A suggested model for phosphogenesis and U incorporation in the Palmyrides phosphorites. 480

Fig.10.2 Variation of U contents with geological history since Upper Cretaceous to Recent. 493

Fig.10.3 Structurally controlled U enriched areas in the Palmyrides region (areas for follow-up work). 493

Fig.10.4 Contour map of U in the Palmyrides region. 495

Fig.10.5 Contour map of P in the Palmyrides region. 496

LIST OF TABLES

		Page No.
Table 1.1	Classification of U deposits (from Young, 1984).	24
Table 1.2	Uranium exploration methods.	28,29
Table 2.1	Stratigraphic interpretation of the Dbayyat borehole and the Triassic, Jurassic and Cretaceous systems (from, Technoexport, 1966).	55
Table 2.2	The Palaeogene system.	57
Table 3.1	Annual average temperature, 1970-1981.	80
Table 3.2	Average maximum and minimum temperature for the year 1981.	80
Table 3.3	Atmospheric pressure, hours of sunshine and average daily evaporation for the year 1981.	83
Table 3.4	Precipitation and weather phenomena for the year 1981.	83
Table 3.5	Annual precipitation (mm), 1970-1981.	84
Table 3.6	Genetic classification of calcretes (from Carlesli, 1977).	99
Table 4.1	List of the elements determined during this study, the methods of analysis and the detection limits.	110
Table 5.1	Uranium contents in miniralized specimens measured by (NAA).	127

Table 5.2	Microprobe analysis of U minerals; identification = carnotite group, formula $K_2(UO_2)_2V_2O_8.3H_2O$.	127
Table 5.3	Microprobe analysis of an unnamed urano-vanadate mica.	128
Table 5.4	Microprobe analysis of carnotite mineral.	133
Table 5.5	Microprobe analysis of U mineral possibly schroekingerite; formula $NaCa_3(UO_2)(CO_3)_3SO_4F.10H_2O$.	133
Table 5.6	Summary statistics of the orientation samples.	153
Table 5.7	Correlation coefficient matrix of the orientation data.	172
Table 5.8	Elemental ratios (P_2O_5 and Ca are in per cent, others in ppm).	176
Table 5.9	Summary statistics of the wadi sediments.	178
Table 5.10	Correlation coeffitients for U with other elements wadi, overburden and rock samples of the orientation survey.	181
Table 5.11	Summary statistics of the overburden data.	182
Table 5.12	Normal content of U in rocks.	184
Table 5.13	Typical concentrations of U in the natural environment.	184
Table 6.1	Summary statistics of wadi Om Jorn sediments.	194
Table 6.2	Correlation matrix of the drainage geochemistry.	202
Table 6.3	Regression coefficient of wadi Om Jorn sediments.	215

Table 7.1	Uranium concentration in the groundwaters.	232
Table 7.2	Summary statistics of the hydrogeochemical data.	238
Table 7.3	Correlation matrix of the hydrogeochemical data.	239
Table 7.4	Standardized estimators and regression coefficients.	247
Table 7.5	Statistics of the ridge regression (R^2 and F-ratio).	247
Table 8.1	Summary statistics of the sabkha geochemistry.	278
Table 8.2	Correlation matrix of the Box-Cox transformed data of the sabkha.	298
Table 8.3	Summary of factor loadings for 4, 5, 6 and 10 factor models.	303
Table 8.4	Loadings of six components for a principal component analysis of the sabkha geochemistry.	305
Table 8.5	Loadings of six factor model for factor analysis of the sabkha geochemistry.	306
Table 8.6	Loadings of five factor model for factor analysis of the sabkha geochemistry.	319
Table 8.7	Standardized estimators and the regression coefficients for U Vs 19 variables of the sabkha geochemistry.	323
Table 8.8	Standardized estimators and the regression coefficients for U Vs 11 variables of the sabkha geochemistry.	323

Table 8.9	Analysis of variance and the regression statistics (R^2 and F-ratio).	323
Table 9.1	Geochemical data on U and P_2O_5 in the Palmyrides phosphorites (from Hunting, 1975).	338
Table 9.2	The major lithosratigraphic units in the region.	345
Table 9.3	Summary statistics of the systematic lithogeochemical data in the Palmyrides region.	391
Table 9.4	Summary statistics of all the rock groups compared to the whole data set.	391
Table 9.5	Comparision of U and P_2O_5contents of this study with that of Hunting (1975) for the phosphorite samples.	404
Table 9.6	Summary statistics of various lithostratigraphic units.	406
Table 9.7	Robust correlation matrix of the lithogeochemical data.	424
Table 9.8	Summary of the correlations of U with other variables in the six lithostratigraphic units.	424
Table 9.9	Loadings of the six factor model for the Palmyrides lithogeochemistry.	437
Table 9.10	Loadings of the five factor model for the phosphate and phosphorite rocks.	450
Table 9.11	Standardized estimators of U in the 16 variable model of ridge regression and the regression coefficient.	464

Table 9.12 Standardized estimators of U in the optimum ridge regression and the regression coefficients. 464

Table 9.13 Statistics of the regression and analysis of the variance (R^2 and F-ratio). 464

Table 9.14 Standardized estimators of U in the phosphate and phosphorite rocks and the regression coefficients. 471

LIST OF PLATES

Plate A	Different mode of occurrences of secondary U minerals.	2
Plate 1	A typical box fold of the Southern Palmyrides mountains (J.Al Abtar).	74
Plate 2	General view of Sabkhet El Mouh (playa).	76
Plate 3	General view of Ad Daww basin.	77
Plate 4	The dry surface of Sabkhet El Mouh.	79
Plate 5	Sampling tools (steel corer, hammer and auger with three channel spectro-scintillometer for insitu radiometric measurements.	104
Plate 6	The uppermost profile of the playa surface.	107
Plate 7	Scanning electron microphotograph illustrating the crystal morphology of U minerals (a) and their association with the mineral celestite (b, c).	131

Plate 8 Photomicrographs of polished thin sections (I and III) and corresponding lexan fission track registrations (II and IV); showing U distribution in phosphate particles. 136

Plate 9 Photomicrographs of Polished thin sections (I and III) and corresponding fission track registration (II and IV); showing uneven distribution of U. 137

Plate 10 Photomicrographs of thin section and a superimposed lexan print with a slight offset (I). In (II) tracks are related to fractures and fissures filled with collophane mud. 138

Plate 11 Photomicrograph showing dense tracks (I) and lexan print in (II). 139

Plate 12 Matched photomicrographs of thin section of phosphatized glauconitic limestone (I, cross nicols) and lexan print (II). 140

Plate 13 Matched thin section (I) and fission track image on lexan film (II). 142

Plate 14 Matched thin section (I) and fission track registration (II) showing a complex history of diagenesis. 143

Plate 15 Photomicrograph of thin section superimposed by lexan print with a slight offset (I). In II the tracks are entirely related to the secondary phase and not to the rock constituents. 145

Plate 16 Matching thin section (I) and fission track registration (II), the tracks are generated by secondary U minerals. 146

Plate 17 Photomicrographs of thin section (I) and fission track registration (II), secondary U minerals seem to be resposible for dense tracks. 147

Plate 18 Photomicrographs of thin sections (I and III), bright U minerals are formed within bone microfractures (I) and in the matrix (III). In II and IV the X-ray electron images show the distribution of U in the corresponding grains. 148

Plate 19 Photomicrographs of thin sections with U mineralization. 149

Plate 20 Uppermost part of wadi Om Jorn showing secondary U occurrence and the main features of the wadi sediments. 192

Plate 21 Backscattered photomicrograph showing U, Zn, Fe, Cu, Ba and Mo mineralization in a quartz vein of sample 710. 360

Plate 22 Backscattered photomicrograph showing U, Pt, Zn, Cu and Fe mineralizations and high temperature zinc-phosphate and barium minerals in sample 119 and 121. 361

Plate 23 Backscattered photomicrograph showing U, Pt, Zn, Cu and Fe mineralizations and high temperature zinc-phosphate and barium minerals in sample 119 and 121. 362

Chapter I.

1. INTRODUCTION.

1.1 Background to the Research.

There are events in the geological history of the Palmyrides region, Central Syria which have first incorporated many elements including U into a source rock, and thereafter remobilized these elements under different environmental conditions. Evidence of U remobilization is represented by numerous manifestations of secondary uranium mineral occurrences throughout the Palmyrides and beyond. Many are closely associated with the widespread phosphorite deposits. Nevertheless, several other U occurrences and radiometric anomalies, not directly related to phosphorite, have been found. Those manifestations appear to be associated with secondary uranium mineralizations such as uranyl oxides and uranyl vanadates along faults and ancient taphrogenic lineaments (deep rooted into lower crust or upper mantle), as well as disseminated in recently developed duricrusts or young surficial formations. These oxidized uranium minerals occur in calcareous and gypsiferous rocks as thin films, spots, pods, powdery coatings on fissures and crack surfaces and infilling of porous rocks. Occasionally they are formed within a host rock parallel to the bedding planes or disseminated in small areas; their colours are bright yellow, greenish yellow and canary yellow sometimes with a waxy appearance (Plate A). According to investigation reports during the geological mapping of the country by Technoexport (1966 and 1967), these oxidized types of minerals are tyuyamunite, autunite, carnotite and torbernite.

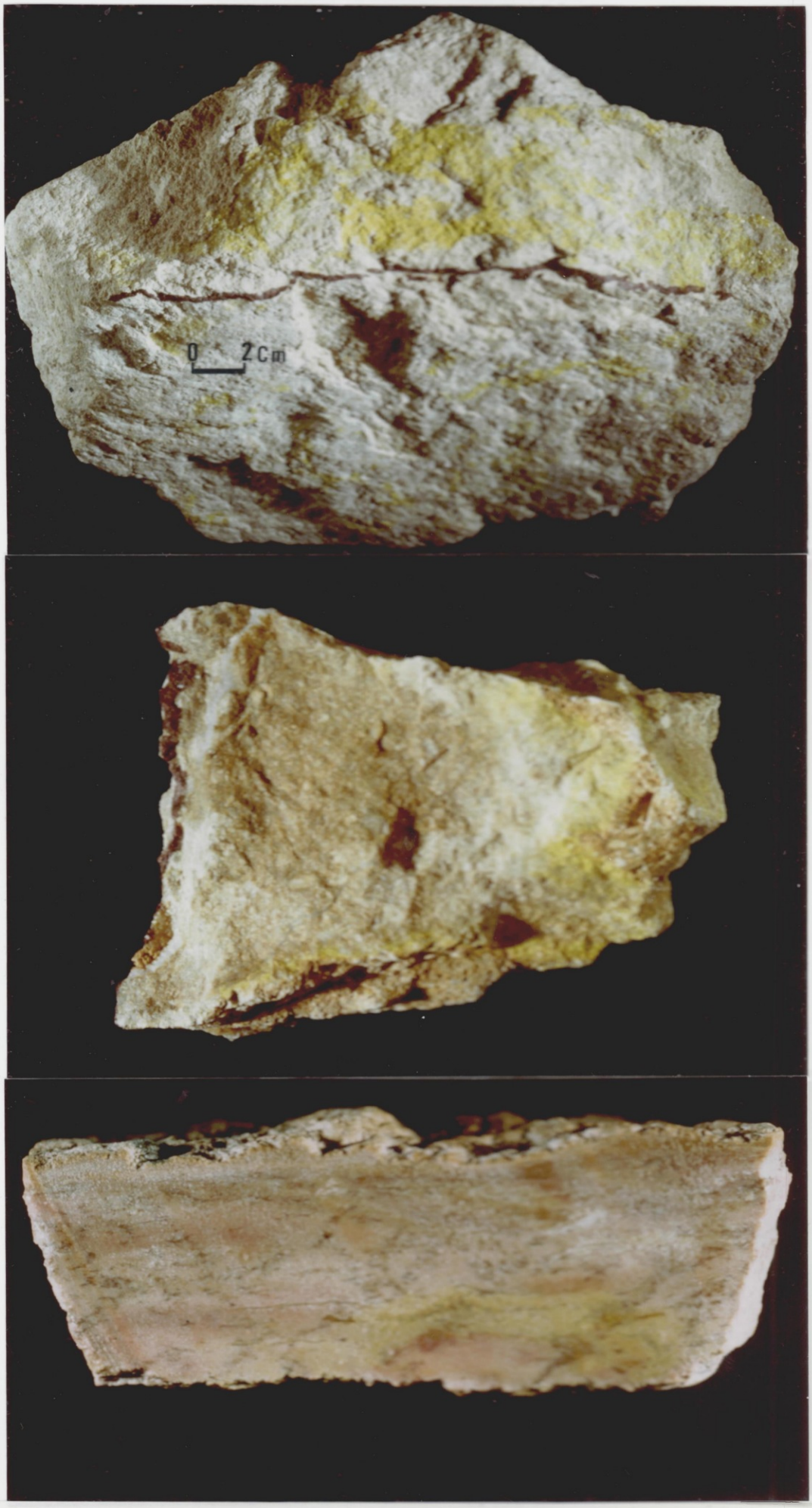


Plate A Different modes of occurrence of secondary U minerals; a = coatings, b = haloes within the rock, c = fillings of micro fissures of a fault-deformed rock.

The present work describes the application of a geochemical approach to study the secondary and the primary dispersion patterns of U and associated elements in the semi-arid region of the Palmyrides.

1.1.1. Aims of the Research.

The primary objectives of the present research programme are as follows:

1) To achieve a basic knowledge of the distribution of uranium and other elements in the Palmyrides region (Central Syria).
2) To discern areas, rock types or other media which are enriched in uranium and associated elements.
3) To define regional geochemical features which may be related to the presence or absence of uranium resources.
4) To use the foregoing geochemical data to consider whether or not phosphorite is the source rock for uranium mineralization in the area.
5) To acquire an understanding of how the visible uranium occurrences are reworked by the geological processes in the region.

1.1.2. Approach used in this study.

Among the techniques currently used in uranium exploration and reviewed by Bowie and Cameron (1976); De Voto (1984) and Chester (1984), a combination of ground radiometric measurements and geochemical reconnaissance survey could be an appropriate approach to achieve the foregoing objectives.

In Syria, the oxidizing environment facilitates the mobility of uranium. Geochemical investigation, using various sampling media, is therefore a feasible approach in order to detect uranium dispersion patterns. Basically, this research consists of an orientation survey followed by geochemical reconnaissance sampling with radiometric measurements. In the geochemical orientation sampling programme, 72 samples of rocks, detrital overburden (soil) and wadi sediment samples were collected in both background and mineralized areas, and in situ radiometric measurements were recorded. Location of the areas involved in this survey can be found in Fig. 1.1. These samples were analysed for uranium, thorium and the rare earth elements by Instrumental Neutron Activation Analysis (INAA), and for 30 major and trace elements by Inductively Coupled Plasma Atomic Emission Spectrometry (ICPAES), Pb and As by Atomic Absorption Spectrophotometry (AAS) and F by Specific Ion Electrode (SIE).

Mineralized specimens were studied by applying integrated geochemical, petrographical and mineralogical techniques including scanning electron imagery, microchemical probe analysis, X-ray diffraction photography, X-ray fluorescence, microscopic examination and Lexan-fission track registration. Interpretation of the results of these studies was likely to provide a better understanding of the secondary uranium minerals and their incorporation in various samples.

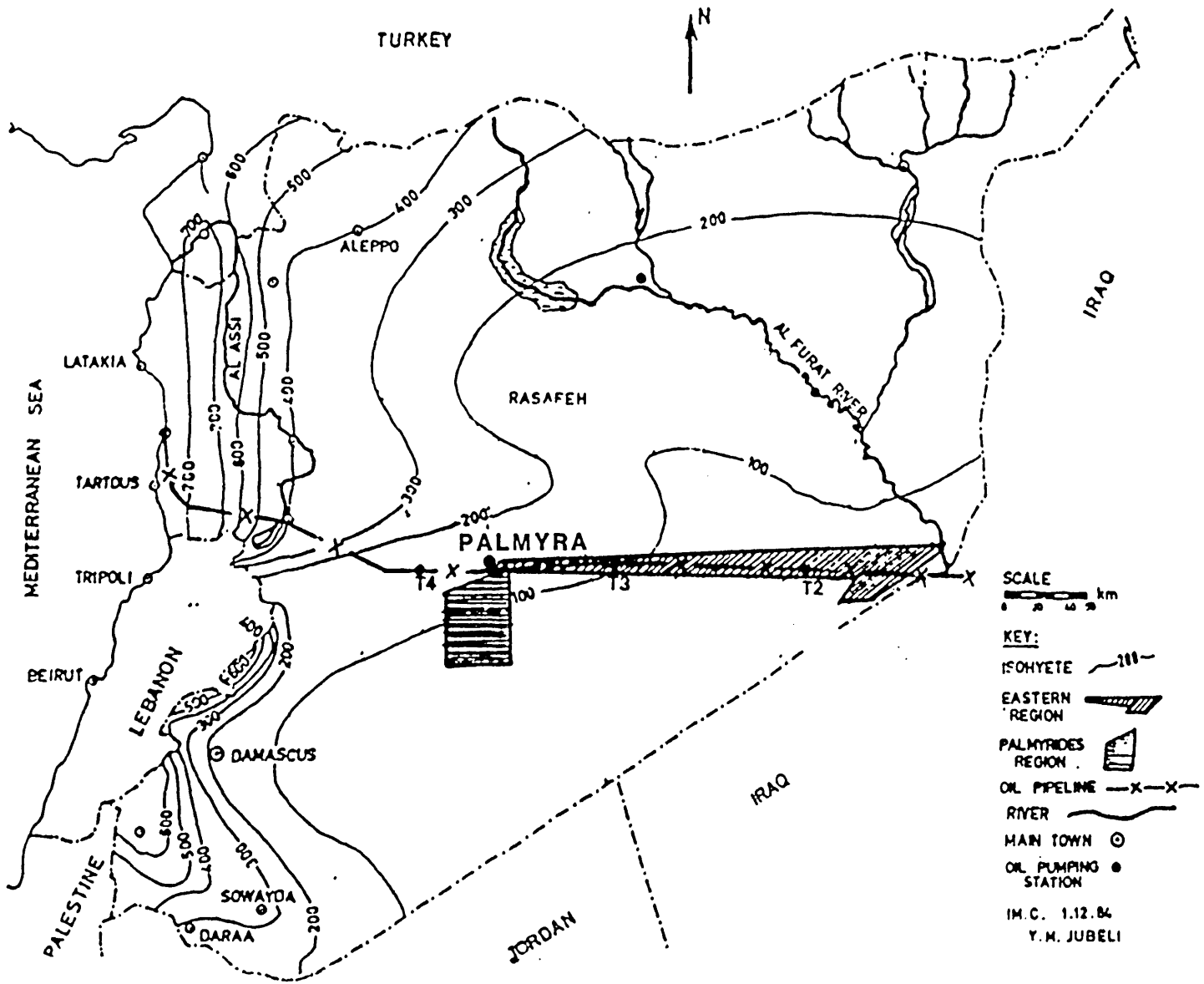


Fig.1.1 Location map of the orientation survey areas .

1.1.2.1. Objectives of the orientation survey.

1) To obtain the necessary geochemical and mineralogical information about the secondary uranium minerals found in the mineralized specimens.
2) To test the usefulness and response of the different sample types and establish site-selection criteria for the reconnaissance stage.
3) To select where relevant the optimum size fraction to be analysed with particular reference to uranium.
4) To recognize, if possible, relationships between uranium and other elements.
5) To provide preliminary information about the background levels of uranium and associated elements and the magnitude of variations in their concentrations.
6) To select from first-hand experience the most appropriate geochemical analytical methodology for measuring uranium and the associated elements in various sample types in the main survey.

1.1.2.2. Handling and processing of the data.

All geochemical data were transferred onto magnetic tapes at Imperial College mainframe (CDC 6500/Cyber 855 and 174) computers from output of various analytical instruments. Handling and processing of these geochemical data was carried out with the aid of available statistical packages and methods. Univariate statistics were used to establish histograms (frequency and Stem and Leaf distributions), normal cumulative probability plots, means, medians and standard deviations using the MINITAB

statistical package (Ryan et al., 1981). Graphical presentation of the elemental distribution patterns was achieved using KPLOT (Wheatley, AGRG, Pers. Comm.) and Conicon solid surface (Imperial College, 1985). Multivariate analysis including correlation analysis (Pearson; Box-Cox transformed and robust data) hierarchical R-mode cluster analysis (Kleiner and Hartigan, 1981) was performed using the modified BTREE version (Turner, AGRG, Pers. Comm.), ridge regression analysis (Howarth, 1984) and R-mode principal component and factor analysis (PCA2, Imperial College, 1985).

Interpretation of the geochemical data was based on separation of the elemental concentrations into background and anomalous populations using the foregoing statistical techniques and common sense in establishing threshold values and then generating the areal distribution patterns. Attempts to identify areas favourable for uranium mineralization and enrichment were based on visual inspection of the distribution patterns, field observations, previous and present geological information, as well as geochemical principals and derivatives of the univariate and multivariate statistics (elemental ratios, scattergrams, residuals and scores).

Following preliminary, but satisfactory assessment of the orientation results, the second stage, comprising the reconnaissance survey, was undertaken, during which a total of 610 samples of groundwaters, rocks, wadi and playa sediments were collected from the most promising areas in the Palmyrides region (Fig. 1.2). The same analytical techniques were adopted as were used for the orientation samples. This was undertaken in order to

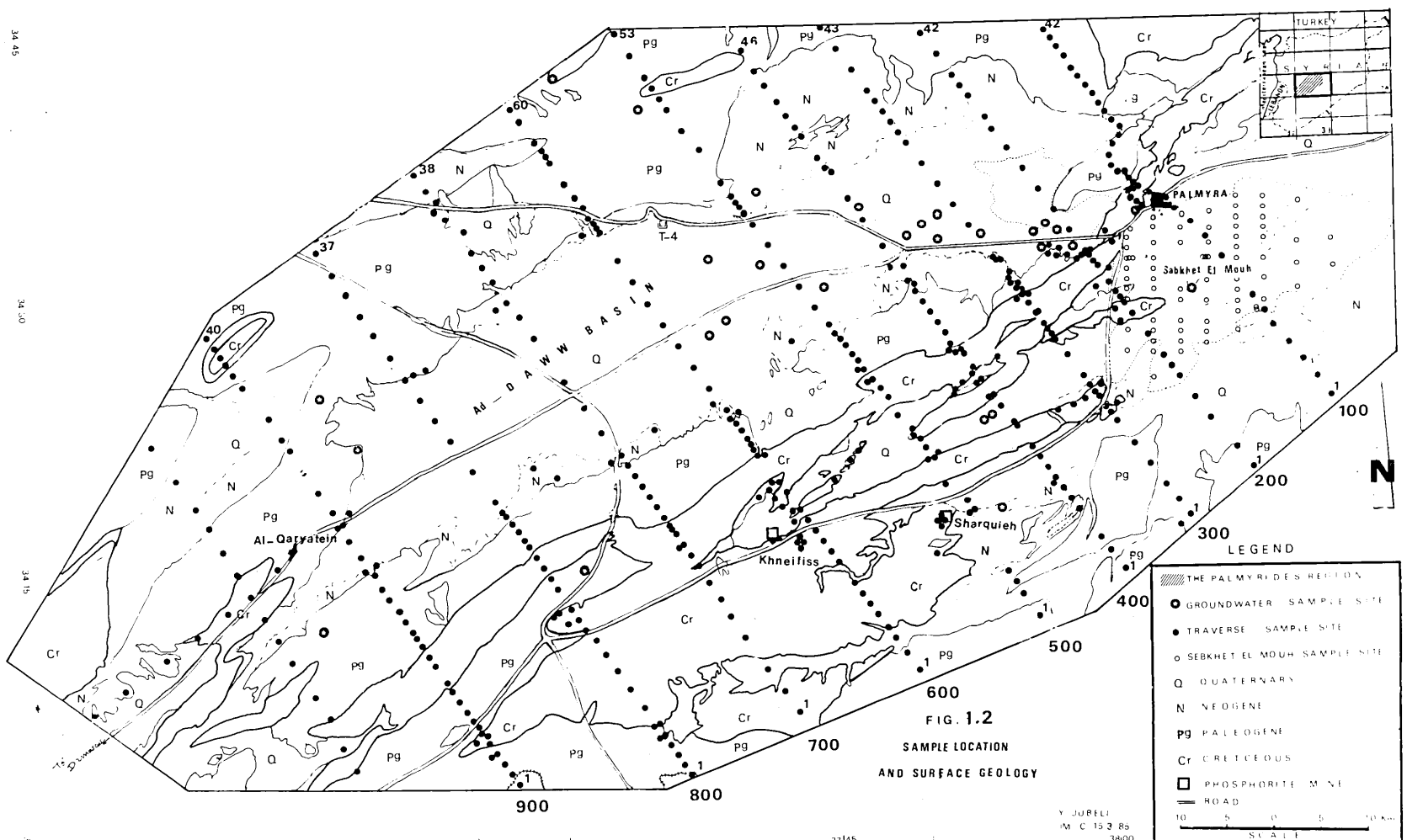


FIG. 1.2
SAMPLE LOCATION
AND SURFACE GEOLOGY

Fig. 1.2 Scheme of reconnaissance sampling of the Palmyrides region.

achieve the aims and objectives that were outlined above.

1.1.3. Description of thesis

The thesis begins with a chapter introducing the main objectives and broadly outlines the approach used in this research work. It proceeds, very briefly, to summarize the main features of uranium provinces, its exploration methods and classification (Chapter I). In Chapter II, the geology of the region interpreted in the light of plate tectonics, the phosphorite formations and their uranium content are described. The theme of Chapter III is physiography and the geochemical characteristics of the Palmyrides environment. Chapter IV covers sampling programmes, analysis and the analytical techniques applied to data organization, data quality control and processing of the geochemical data. The geochemistry of the orientation survey is discussed in detail through Chapter V along with the fission track, uranium minerals and investigation of the optimum size fraction. The subsequent chapters deal with the reconnaissance stage which was carried out based on the conclusions of the orientation survey.

In Chapter VI, the drainage geochemistry of detailed wadi sediment sampling is presented. It shows the elemental association in wadi sediments near to a known mineralized occurrence.

Investigation of the hydrogeochemistry is described in Chapter VII, and a model for U concentration in one of the aquifers is presented. In Chapter VIII, the general picture of the geochemistry of U in Sabkhet El Mouh (playa) is outlined. Chapter

IX is devoted to the lithogeochemistry of the region and delimits areas and rock units of particular interest. Finally, Chapter X presents a review of the main results and conclusions as well as recommendations for further work, and a proposed model of phosphogenesis in the Palmyrides is outlined.

1.2 Chemical properties and geochemical cycle of uranium.

1.2.1. Chemical Properties.

Uranium is a lithophile and oxiphile element, with an atomic number of 92 and three naturally occuring radioactive isotopes, ^{238}U, ^{235}U, and ^{234}U; their relative abundances are 99.274, 0.720 and 0.006 respectively. The first two isotopes, ^{238}U and ^{235}U, are parents for two decay series (Fig. 1.3), which yield ^{206}Pb and ^{207}Pb respectively.

Uranium has valence states ranging between 2+ and 6+; the first three (U^{2+}, U^{3+}, U^{4+}) are analogous to the lanthanides, the last three (U^{4+}, U^{5+}, U^{6+}) to Ti, Zr, Hf, V, Mo, Ta, Nb, Cr and W, but in its natural occurrences, U forms complexes in which it is either quadrivalent, U^{4+} (uranous), or hexavalent, U^{6+} (uranic), and to a lesser degree pentavlent (U^{5+}). Quadrivalent U is about 1Å in ionic size similar to Th^{4+}, Ce^{3+}, Y^{3+}, Ca^{2+} and Na^{+}; uranous complexes tend to be insoluble at low temperatures and at pH 4.5 to 7. At temperatures above 150°C, their mobility increases and may become important depending on ligand concentrations such as fluoride, phosphate, sulphate and especially hydroxide; uranous

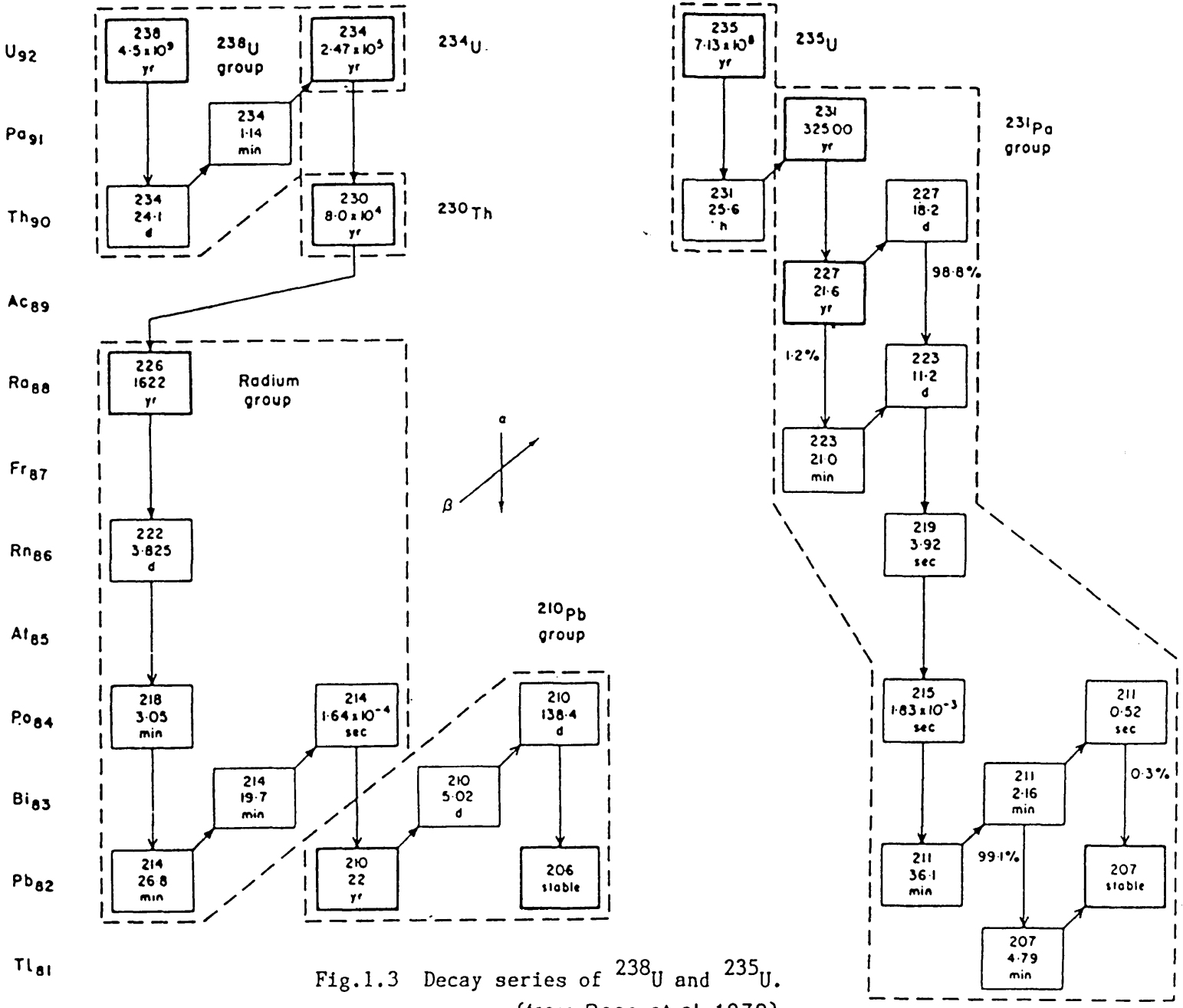
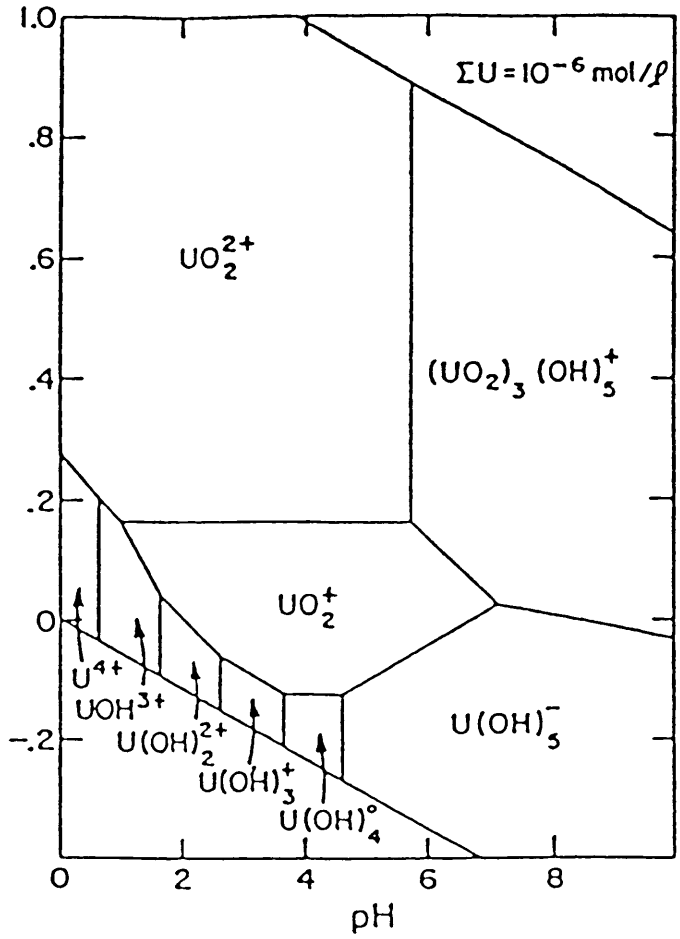


Fig.1.3 Decay series of ^{238}U and ^{235}U.
(from Rose et al., 1979)

carbonate complexes are however unstable. Hexavalent U is soluble over a wide range of conditions. At 25°C, uranyl fluoride (UF_6) complexes are dominant at pH<4, uranyl phosphates at pH 4-7.5 and uranyl di- and tricarbonate complexes at pH>7.5. Uranyl silicates are insignificant, and at temperatures near 100°C uranyl hydroxides predominate, whereas uranyl carbonate complexes dissociate. The uranyl sulphate complexes, bisulphate $UO_2(SO_4)_2^{2-}$ and trisulphate, $UO_2(SO_4)_3^{4-}$, are stable at pH 4, while humic and fulvic complexes arise at low to neutral pH values (Fig. 1.4). Precipitation from solution occurs as a result of reduction of the uranyl ion to a uranous ion with modifications of pH, pressure, temperature and other ligands. Soluble U complexes may be fixed by clays, Fe-Mn hydroxides, phosphate and organic matter.

1.2.2 Geochemical cycle.

The zonal formation of the terrestrial globe at 4.6-3.6 Ga, and upward migration of the radioactive materials was the first step in a typical geochemical cycle of U (Simov, 1985). This was followed by the fractionation of the mantle and transfer of U to the upper levels since 3.5 Ga under high heat-flow conditions (Ferguson, 1985). The second step was the migration of U from the mantle to the upper crust through establishment of convecting cycles at 2.5 Ga (Locardi, 1985). This vertical distribution process seems to have been more regular than the subsequent lateral one which has been taking place in the earth's crust in the last 2 Ga, leading to the formation of U provinces (Simpson et al., 1979; 1982).



. Eh-pH diagram showing the relative importance of +4, +5 (as UO_2^+) and +6 valent uranium species at 25°C, for $\Sigma U = 10^{-6}$ M.

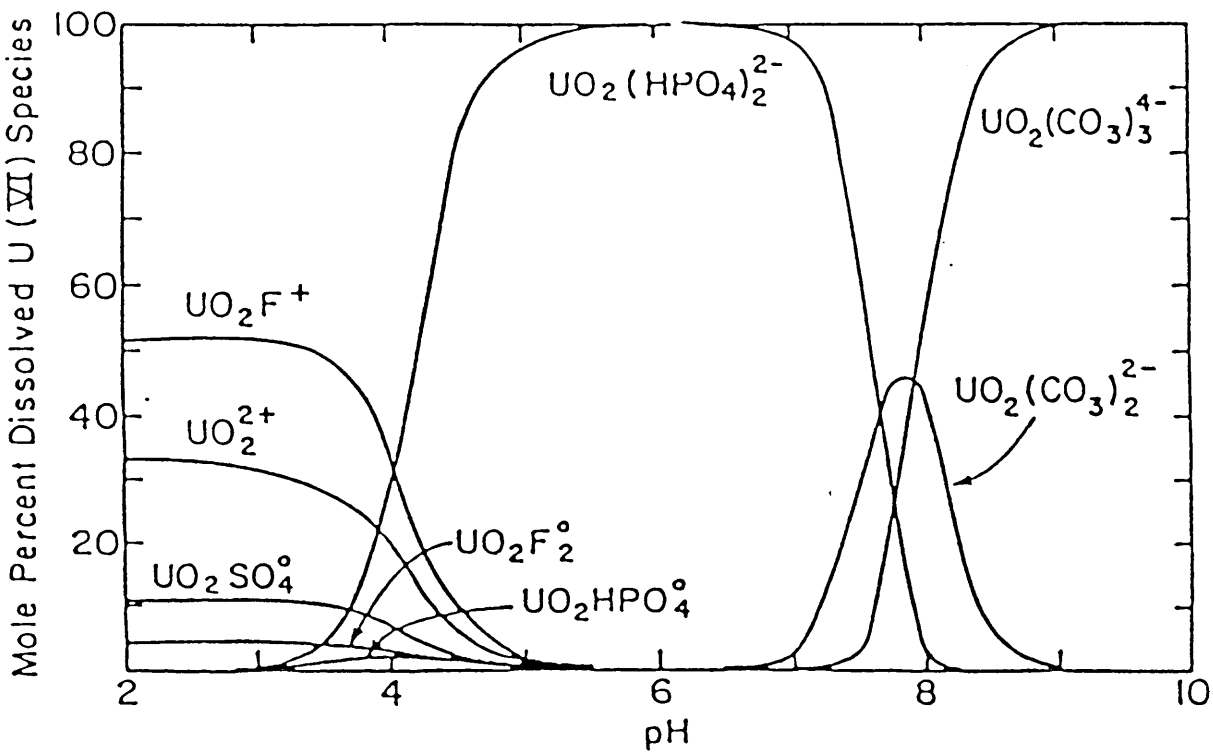
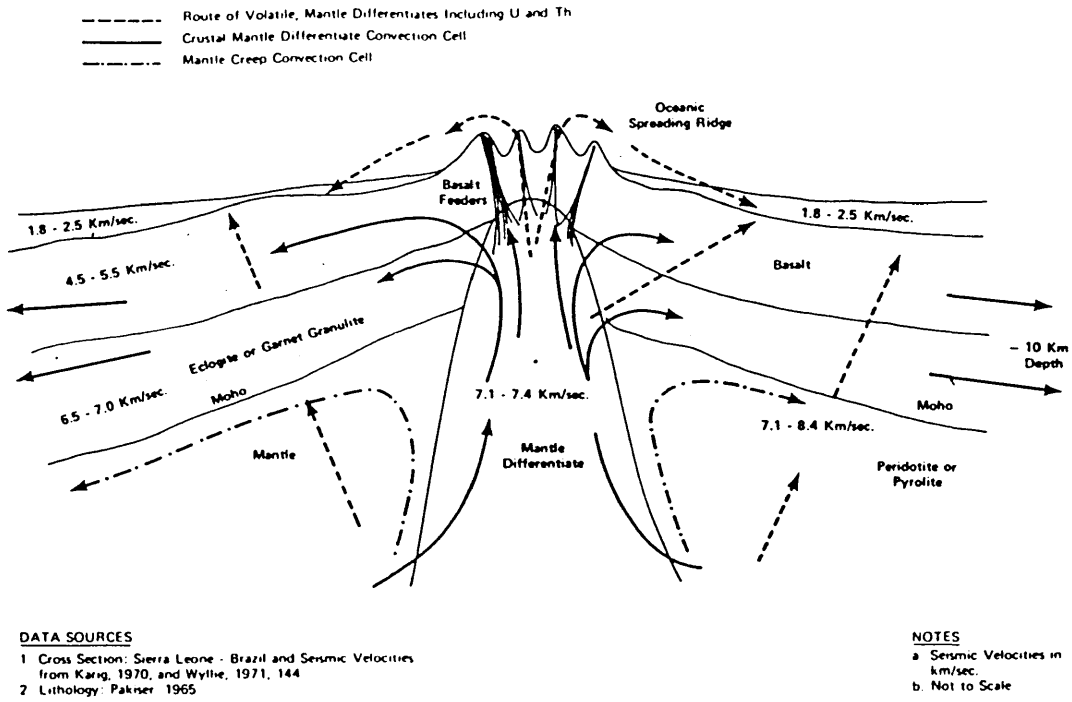


Fig. 1.4 Distribution of uranyl complexes versus pH for some typical ligand concentrations in ground waters of the Wind River Formation at 25°C. $P_{CO_2} = 10^{-2.5}$ atm, ΣF = 0.3 ppm, ΣCl = 10 ppm, ΣSO_4 = 100 ppm, ΣPO_4 = 0.1 ppm, ΣSiO_2 = 30 ppm. (from Langmuir, 1978)

The mode of U transfer into the ocean and upper crust is a more complicated process. The common rock forming minerals do not easily accommodate U, and consequently, it is either concentrated in late magmatic fluids or expelled from magma chambers (Armstrong, 1974; Hambleton-Jones, 1978). Therefore, U tends to form its own minerals such as uraninite under low oxygen fugacity conditions or tends to be transported as uranyl carbonate as suggested by the investigations of fluid inclusions in granites (Poty et al. 1974). Gabelman (1977) suggested that mantle convection is essentially a mechanism for the solid state transfer of U beneath the mid-ocean ridges (Fig. 1.5). However, as a result of convection and partial melting, the upper mantle and the earths crust became relatively enriched in U compared to the lower mantle (0.013 ppm U; Sun, 1982; 1980), and this process continued the separation of mafic from the felsic crust. Such fractionation during the early crustal thickening appears to have been produced first by moderately U-enriched Na-magma, followed by an extensive development of the K-magma which was accompanied by U-rich granitoids.

The crystalline and igneous rocks are the starting point of the exogenous part of the geochemical cylcle of U (Fig. 1.6). It includes recycling of crustal material by subduction, differentiation, magmatism, migmatization, anatexis and hydrothermal processes. These last-named take place under open system conditions and constitutes the major part of the geochemical cycle (Gaetano Dongarra, 1984), including mobilization of U from a source rock, fixation and U-ore forming processes. One process for U mobilization and preferential enrichment is that demonstrated by Simpson and Plant (1984), through their model of magma emplacement



hypothetical cross section showing convection and volatile paths; ocean-ridge spreading axis.

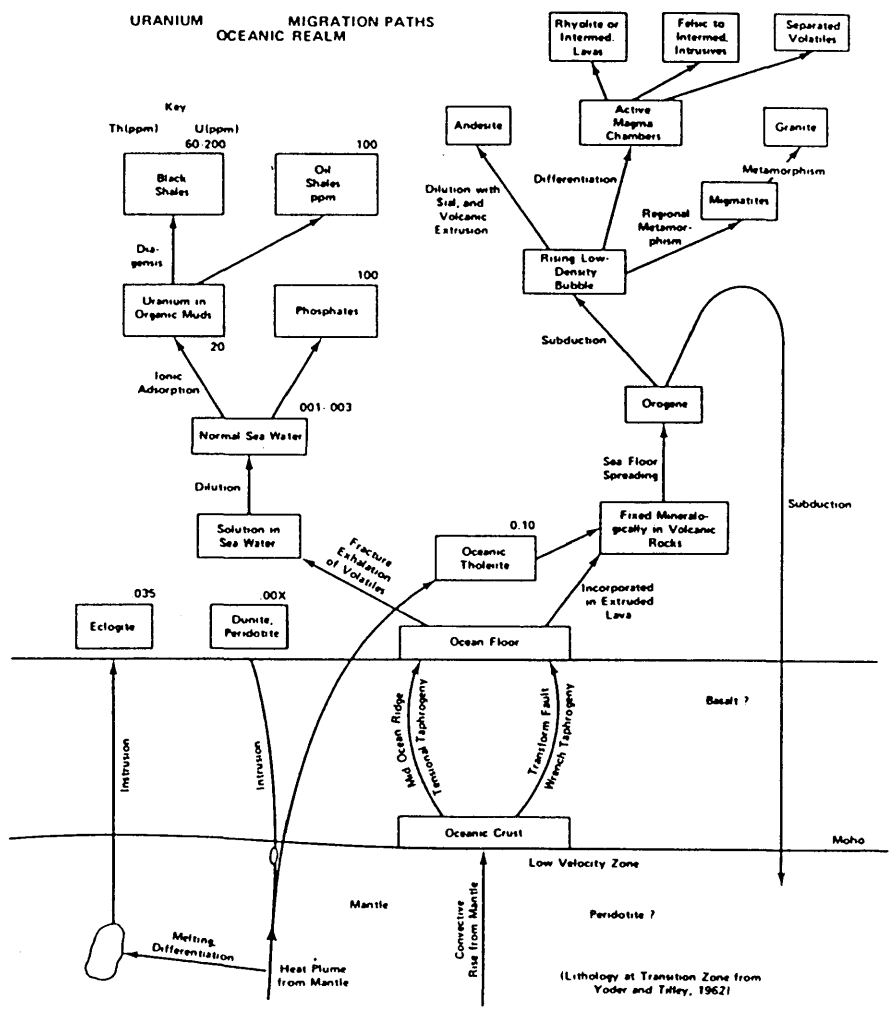
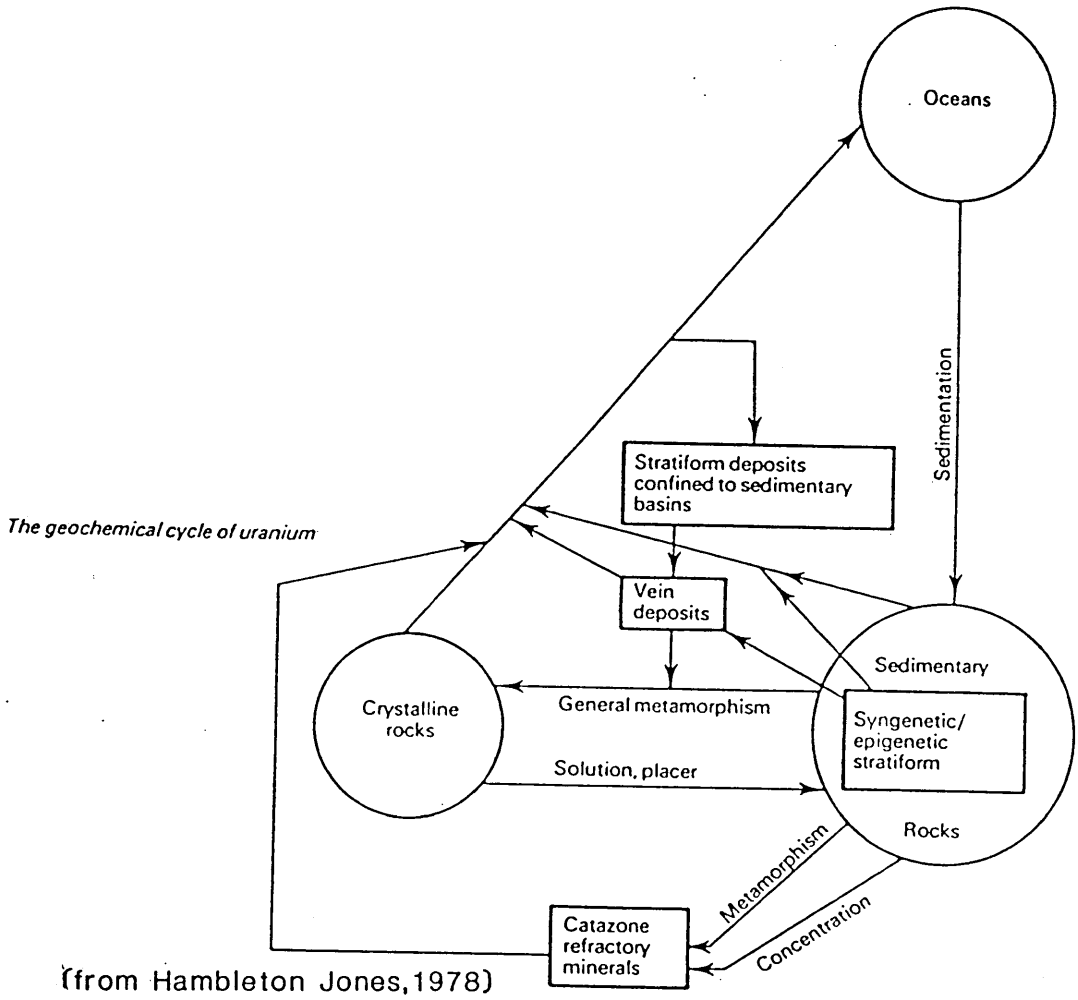
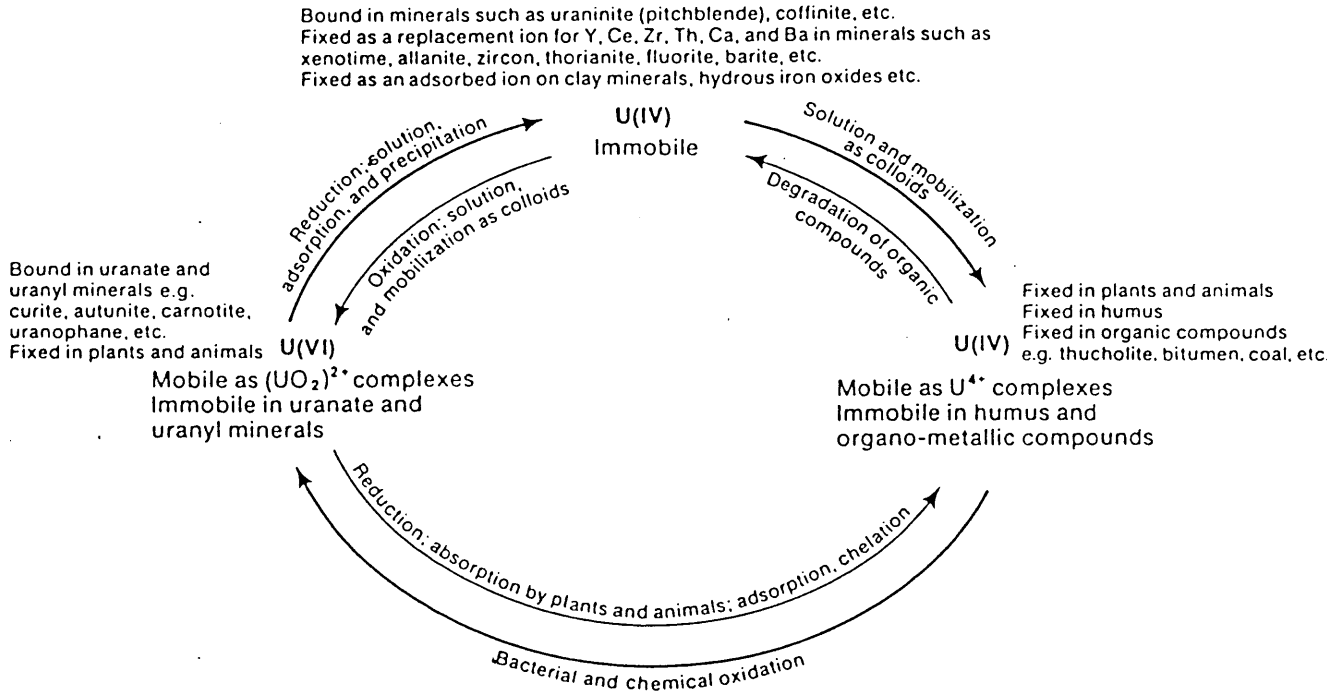


Fig.1.5 Geochemical cycle of U.(from Gableman,1977)



The geochemical cycle of uranium

(from Hambleton Jones, 1978)



U (V) state is possible and may occur where low oxidation potentials prevail in nature

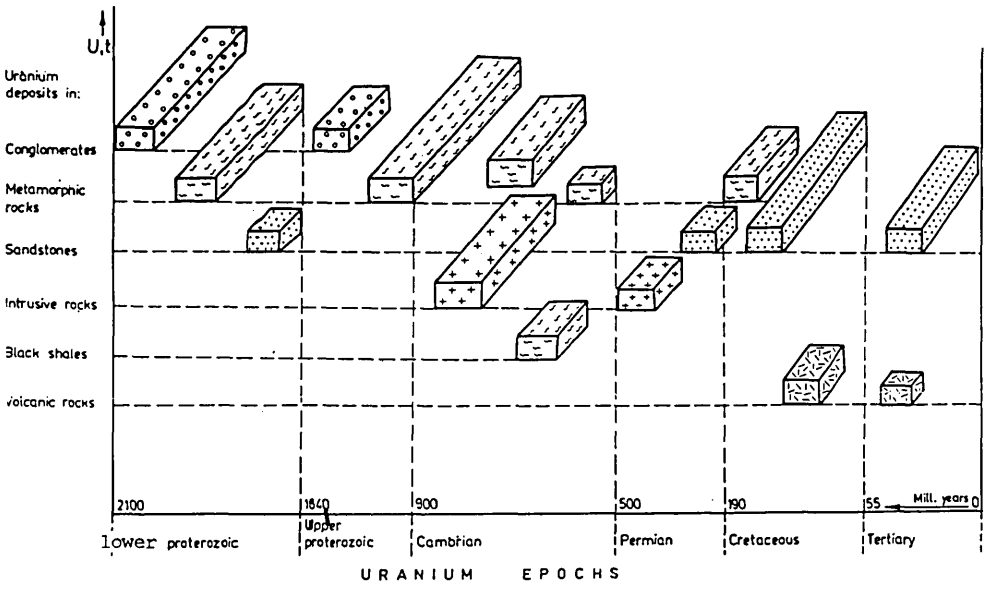
Cycle of U(IV) and U(VI) interconversions in nature. (From Boyle, 1982)

Fig.1.6 Exogenous part of the geochemical cycle of U.

in an adequately hydrous environment. This involves the interaction between anhydrous mantle-derived granitic magma enriched in U, volatiles and metals, and country rock-derived meteoric and metamorphic waters, generating a hydrothermal convective system at a relatively high level in the crust. Mobilization and transportation of U and associated elements into the host or mineralization sites can be associated with such a hydrothermal convective system. The roles of low temperature fluids (<200°C) with a broad range of salinities from zero to 24 wt% NaCl in mobilizing U can also be inferred from recent fluid inclusion studies (Rankin and Alderton, 1985).

Crustals reformation by magmatism, erosion, weathering and sedimentation leads to recycling of U in the surficial part of the geochemical cycle of U. The means of U transport and accumulation in the sediments may be dominantly biochemical (Fyfe, 1979); however the ultimate sink for recycling U is in ocean water, altered sea-floor basalts, marine sediments (black shale, pelagic sediments, phosphorites) and other clastic sedimentary U deposits especially those of post-Archaean age. The distribution of U during recycling appears to be time-controlled (Fig. 1.7), reflecting major developments in the environment (Toens, 1981). Quartz conglomeratic-type U deposits (Witwatersrand and Elliot Lake) lie within Proterozoic rocks restricted to 2.8 to 2.2 Ga, when the atmosphere was poorly oxygenated (reduced?). Unconformity related vein-type U deposits in both Canada and Australia occur in the sedimentary environment in the post-2.2 Ga period, when meteoric waters became oxidizing (Needlham et al., 1985). However, the majority of these deposits are restricted to the time-bound 1.7 to

(a)



(b)

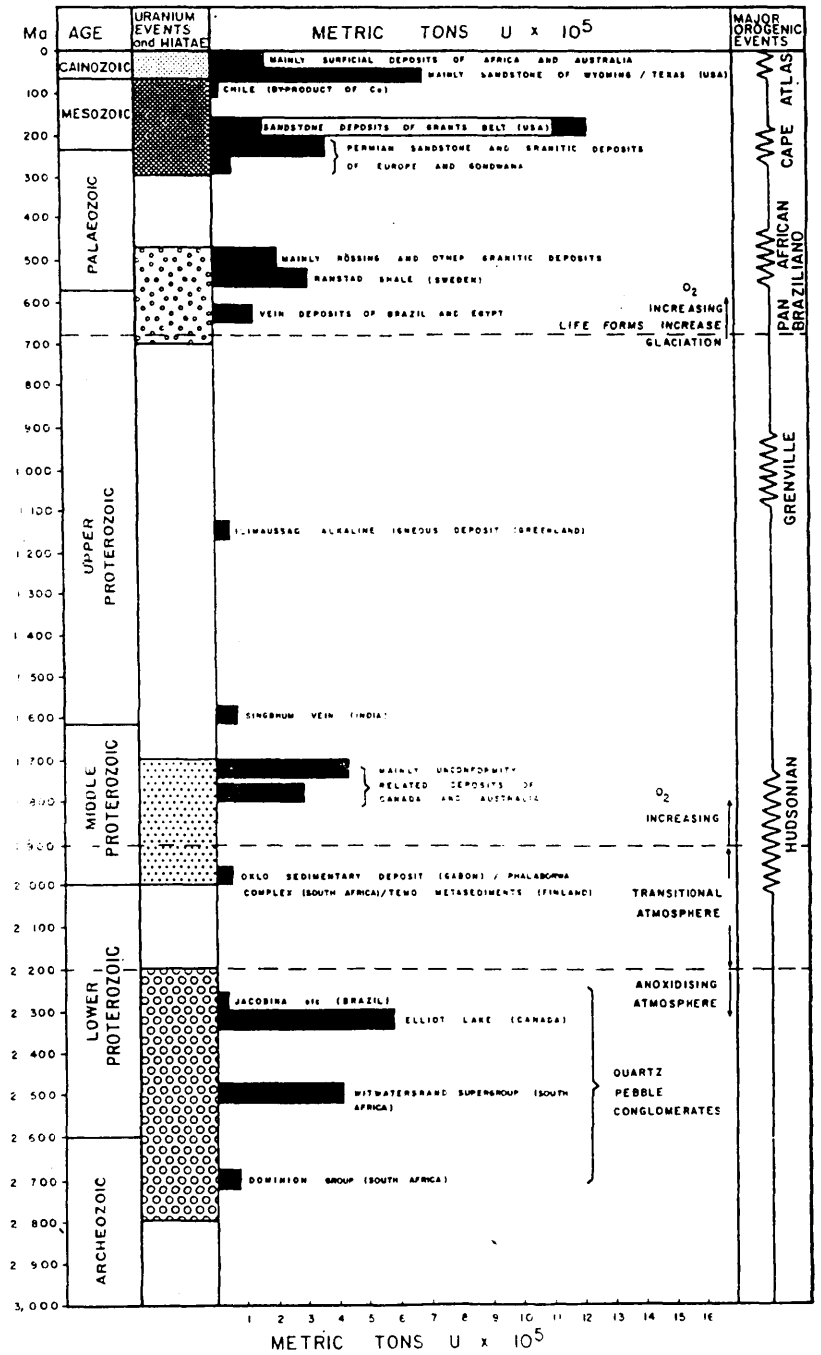


Fig.1.7 Time bound of the major U deposits(from Simov, 1985(a);Toens, 1981(b).

1.4 Ga. Other Proterozoic unconformity strata-bound and stratiform metasedimentary U deposits of Middle to Late Proterozoic age can be found (Athabasca basin, Olympic Dam, Aillik Group, Pine Creek and Katanga system). In most situations, the unconformity separates the Lower Proterozoic from the Middle Proterozoic (Ferguson, 1985, Meneghel, 1984; Roberts and Hudson, 1984; Nutt, 1984; Gandhi, 1984, Ward, 1984). In the post-1.4 Ga period, the atmosphere appears to have been similar to that existing today, therefore, all the U in the hydrosphere would have been mobile and transported in the hexavalent state, but fixed and sometimes concentrated under strongly reducing conditions in clastic sediments and carbonaceous shale and sandstones. Most of the sandstone-type U deposits are, for exploration purposes, restricted to Phanerozoic rocks younger than 0.2 Ga. The U in these deposits was removed by oxidizing rain and groundwater from igneous rocks (granite or lavas), and fixed in a reducing sedimentary environment created by organic matter, pyrite, H_2S or hydrocarbons within permeable sediments. Roll fronts, tabular and channel deposits may be formed in this way (Nash and Adams, 1981; Finch, 1985; Comte and Varlet, 1985; Sanford, 1985). Under arid conditions, U leached from igneous and metamorphic rocks tends to concentrate in drainage channels (as at Yeelirrie) and in other surficial sediments, forming the so-called "surficial U deposits" (IAEA, 1984). These deposits are very young and some are being formed at the present time (Butt, 1985).

1.3. Uranium deposits.

1.3.1. Uranium provinces.

At a technical meeting on the recognition of U provinces held in Vienna, 1975, the IAEA experts in U geology defined the U province as a region in which U is enriched in rocks of successive ages (IAEA, 1977). Those discrete segments of the earths crust which show enriched levels of U regardless of geological processes, environment or age of mineralization were listed by Hunter and Michie (1985) during a recent technical meeting of the IAEA on the same topic. They rightly emphasized the individual characteristics displayed by many U provinces, notwithstanding the significance of U enrichment in some regions as a guide for exploration.

From Fig. 1.8 it can be seen that the authors included clusters of spatially or genetically related U occurrences irrespective of area or size (above an arbitrary cut-off value chosen by them to be about 70–100 ppm U). The source of U in these provinces as well as in other models proposed for their recognition (Sibbald, 1985; Cuny, 1978; Sanford, 1982; Briot, 1984; Simov, 1985; Parslow, 1985, 1982; Locardi, 1985; Galloway, 1985; and Turner, 1985) is said to be either debatable or cryptic and ill-defined (Hunter and Michie, 1985).

According to Hunter and Michie, U provinces can be described and recognized under the following characteristics;

a) Geological setting, related to major structural lineaments.

b) Deep fertile precursor zones in the lower crust/upper mantle.

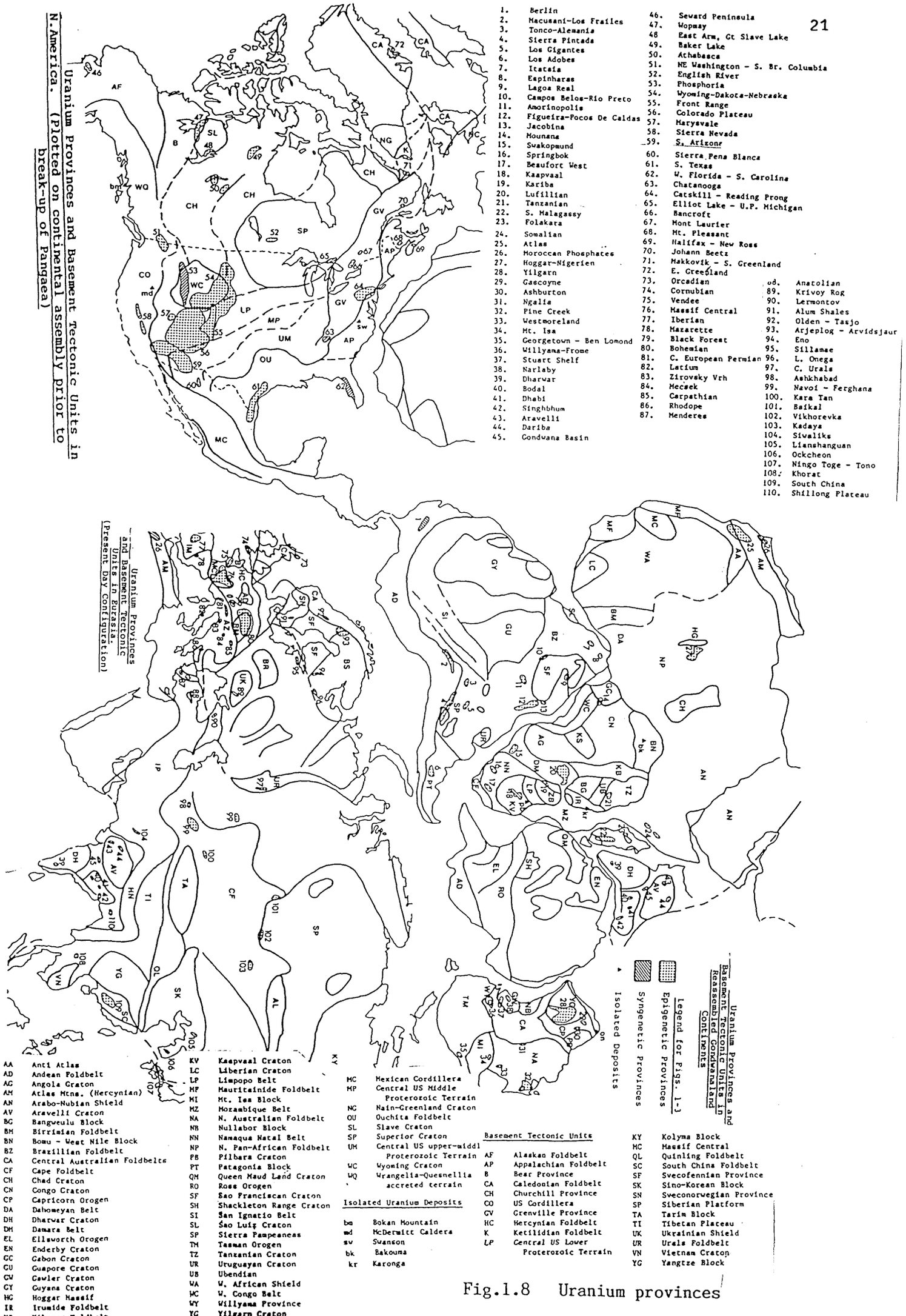


Fig.1.8 Uranium provinces (combined from Hunter and Michie, 1985).

c) Uraniferous source areas in the crust.

d) Regional geophysical and geochemical signatures.

e) Recycling of U concentrations.

f) Depositional processes.

It should be noted, however, that the first of these characteristics is the only unifying criterion, whereby all known U provinces seem to occur in continental type crust, whether a stable part of a craton, orogenic belt, or segment formed by stabilization. Moreover the lineaments were found to be usable in recognition of U provinces (Gabelman, 1977; Darnley, 1981). Kutina (1981) was able to predict the position of the Swanson deposit (Appalachian, USA) by studying U occurences along basement lineament before its actual discovery in 1982. Simpson et al. (1979, 1982), Watson and Plant (1979), Ostle (1982) and Watson et al. (1982), suggested that U provinces can be formed by mass transfer of radioelements entrained in high heat producing acid magma, from subcontinental lithosphere to the upper crust during cratonization following orogenesis. Rapid uplift and displacement along deep faults, hot spring activities and circulating groundwaters may then redistribute U into various types of U deposits (Simpson and Plant, 1984). Similarly Simpson et al. (1979) and Plant et al. (1980, 1983) demonstrated the importance of factors such as mineralogical composition, level of emplacement of the granitic magma, metamorphism, plate tectonics and regional geochemistry in defining U provinces.

1.3.2. Classification of U deposits.

Many attempts by various workers have been made to classify U deposits, but any simple classification has proved extremely difficult. Among the well known classifications are those of Little (1970), which was modified from Lang et al. (1962); Barnes and Ruzicka (1970); Ziegler (1974); Sorensen (1970); and Cornelius (1976). Most of these proposals were based on genetic criteria, but, in a few cases, their characteristic suite of elements was considered in a more or less geochemical sense. Gabelman (1977) pointed out that a geochemical guide in classification is a great aid to exploration. During 1978 more schemes were produced by Dahlkamp (1978); Roger et al. (1978); McMillan (1978) and Hambleton-Jones (1978), who suggested four criteria which could be used to classify U deposits;

(i) genetic; (ii) metallotectonic; (iii) morphological relations to host rocks; and (iv) elemental associations. Robertson (1978) added to those criteria the concept of age. More recently Young (1984) put forward a modified version after Dahlkamp, and this classification is presented in Table 1.1.

The IAEA panel on U provinces (held in London, 1985) uses the following guidelines in classifying U deposits.

1) Quartz-Pebble conglomerate not younger than 2.2 Ga and not oxidized.
2) Unconformity-related deposits aged between 1.8 and 2.5 Ga.
3) Vein and vein-like deposits.

Table 1.1 Classification of U deposits (from Young, 1984).

Mode of origin	Host rock/type deposit	Example
Sedimentary	Quartz-pebble conglomerate	Blind River–Elliot Lake (Canada)
	Black shales	Chattanooga Shale (U.S.A.)
	Muds	Walvis Bay (Namibia)
	Phosphorites	Western U.S.A.
	Bauxites	Arkansas (U.S.A.)
	Placers	Southeastern U.S.A.
	Brines	Sea water
Effusive	Silicic volcanics	Peña Blanca (Mexico)
	Mafic volcanics	Olympic Dam (Australia)
Intrusive	Peralkaline nepheline syenites	Ilímaussaq (Greenland)
	Carbonatites	Araxá (Brazil)
	Anatectics	Rössing (Namibia)
	Pegmatitic alkalitic granites	Bokan Mountain (U.S.A.)
	Granites	Spokane Mountain (U.S.A.)
	Pegmatites	Bancroft (Canada)
	Hydrothermal veins	Schwartzwalder (U.S.A.)
		Shinkolobwe (Zaire)
Metasomatic	Contact	Mary Kathleen (Australia)
	Sodic	Ukranian Shield (U.S.S.R.)
Metamorphic	Phyllites	Forstau (Austria)
	Schists	Portugal
Uncertain (vein-like)	Unconformity-related	Rabbit Lake (Canada)
		Jabiluka II (Australia)
	Vein-like in metamorphics	Beaverlodge (Canada)
		Echo Bay–Eldorado (Canada)
	Vein-like in sediments	Orphan mine (U.S.A.)
Epigenetic	Sandstones	
	Peneconcordant	Grants (U.S.A.)
	Roll-type	Gas Hills (U.S.A.)
	Stack	Franceville Basin (Gabon)
	Calcretes	Yeelirrie (Australia)
	Lignites, coals and carboniferous shales	Williston Basin (U.S.A.)
	Limestones	Todilto LS (U.S.A.)
	Epigenetic phosphates	Baukoma (Zaire)

4) Sandstone type U deposits.

-stable platform and intercratonic basins.

-intermontane basins.

-graben and regional extentional basins.

-continental basins.

-closed volcanogenic and small fluvial basins.

5) Dessiminations in magmatic and metamorphic rocks.

6) Others such as:

-surficial deposits and duricrusts.

-phosphorites, black shales, bauxites, lignite and coal.

1.4. Uranium exploration.

1.4.1. Historical background.

Several uranium prospecting booms have contributed significantly to the development of U exploration methods. Four periods can be distinguished on the basis of its consumption and industrial usage;

i) radium demand (beginning of this century, 1900's)

ii) vanadium demand (1920's to 1940's)

iii) atomic weapon military demand (starting from 1940's and culminating in the 1960's)

iv) nuclear-power demand (mid 1960's and still developing).

During each of these periods, there has been renewed interest in improving prospecting techniques or developing new ones. However, during the seventies the crisis of oil prices and the fear of fuel shortages led to an increase in the importance of U as a nuclear fuel

for electricity generation and other requirements. Therfore, another major upsurge in the scale of U exploration activities took place worldwide, until it stabilized again in the early 1980's.

An extensive review of the literature on geochemical exploration methods of U is beyond the scope of this thesis. Until recently, geochemical exploration techniques were not widely used in U exploration (Bowie, 1972; Bailey and Childers, 1977). Geophysical methods, particularly gamma-ray spectrometry and magnetometric surveys were the main methods of prospecting. But in the last two decades or so, the application of geochemistry has been greatly facilitated by major advances in more sensitive and automated analytical instrumentation, computerized data handling and the application of geostatistics to data interpretation (Kane, 1977; Howarth, 1984; Zhao, 1984).

A particularly important development in the use of geochemistry after the pioneer work by Fix (1956) and Denson (1956) was the initiation of the Natural Uranium Resource Evaluation (NURE) programme in the USA, the results of which are reported in open files (Arendt et al., 1979; Bell, 1982). Similarly, the National Geochemical Reconnaissance (NGR) programme in Canada resulted in large numbers of published papers (Cameron and Hornbrook, 1976). Almost all known geochemical techniques were applied during a programme of Research and Development (R&D) work in U exploration which was carried out by a joint group of the OCED Nuclear Energy Agency (NEA) and the International Atomic Energy Agency (IAEA), the results of which were published in proceedings of "Symposium on U exploration methods", Paris (OCED, 1982). Comparative studies of

exploration methods applied by experts of the NEA/IAEA in Athabasca basin, Canada **also resulted** in a special publication edited by Cameron (1983). In many other recent projects, a geochemical approach seems to play the leading role (Rose et al., 1983; Boyle, 1984).

A comprehensive list of authors, methods and references can be found in the publications of the (IAEA), Vienna, since 1968 as well as in Boyle (1982).

1.4.2. Methods of U exploration.

Aerial, water, surface and subsurface methods have been extensively developed to support U exploration. They include various techniques and applications as summarized in Table 1.2.

TABLE 1.2 Summary of U exploration methods

METHODS	APPLICATION	AUTHORS
1. Geological concepts, mapping, modelling and related data compilation and interpretation	Establishing character features for recognition of U provinces; Narrowing down prospecting areas and indicating favourable geologic settings and targets; Interpretation within applicable geological framework	Simpson et al. (1985, 82, 79); Hunter and Michie (1985); Everhart (1985); Ruzicka (1985); Finch (1985) a, b, c; Sanford (1985); Barthel and Hahn (1985); Locardi (1985); Mahadevan (1985); Andreoli et al. (1985); Roberts (1985); Sibbald (1985); Barretto (1985); Simpson and Hurdley (1985); Needham et al. (1985); Bull (1985); Ward (1984); De Veto 1984, 80); Scott (1983); Gregory (1983); Bowie (1979, 76, 72, 70); Ostel (1982); Harshman and Adams (1981); Tilsley (1980); Dahlkamp (1979, 77); Regland and Roger (1980); Davidson and Bowie 1956
2. Geophysical methods	Measuring the radioactivity of the rocks, depending on requirements, the instrumentation can be:	Darnley (1985,75,72,70); Dodd (1984, 80, 76); Richardson (1983); George (1982); Killeen (1982); Lovborg (1982; Bristow and Killeen (1982); Tommer (1982); Smit (1982); Grasty et al. (1979); Duray (1982)
I Radiometric techniques i total gamma-ray counts (Geiger counters and scintillometers) ii gamma-ray spectrometry	- airborne - carborne - underwater - ground (portable) - borehole logging	
II Non-radiometric techniques (indirect geophysical methods for U exploration) gravity; magnetic and gradiometry: electromagnetic; induced polarization; resistivity; seismic; and temperature measurements	Measurements of other physical properties of the media: - airborne; - carborne; - waterborne; - borehole logging	Sobczak (1983); Kornik (1983, 82); Sinha (1983); Stolz (1983) a, b; Hajnal et al. (1983); Osterlund (1982); Pigott et al. (1982); Bosschart and Pemberton (1969); George and Scott (1982); Lubecki et al. (1982)
III Exploration drilling - rotary drilling - non-core drilling - non-diamond in general	Most U exploration drilling programmes run in depth from surface to approximately 300 deep, in some cases up to 750 m and very rare to more than 1000 m. It may be applied as subsurface geological mapping in which both geophysical techniques, radiometric and non-radiometric can be used	Deveto (1984); Bailey and Childerns (1977); Scott and Daniels (1976); Smith et al. (1976); Dodd and Eschliman (1972)
IV Thermoluminescence detection techniques	Measuring comulative radiation damage	Ypma and Hoshman (1985); Charlet et al. (1982)
3. Remote sensing	Selection of regional targets	Cole (1985; Raines (1982); Hambleton-Jones (1984);
i Landsat imagery	Delineation of palaeodrainage	Krische and Queil (1984); Offield et al. (1982);
ii ERTS imagery	Outlining valley-fill U deposits especially	Monget (1982); Offield (1976); Fisher (1976)
iii Other satellite data	calcrete type Surficial U deposits in deserts	
iv Aerial photogeology	Establishing important linear features	

Cont. Table 1.2 Uranium exploration methods.

4. Geochemical methods:	Applying geochemical principles and analytical techniques to determine U, its decay daughters and isotopes	Simpson et al.(1985,84,82, 81,79,77,76);Plant et al. (1985,83,80);Watson et al. (1982); Watson and Plant (1979); Reimer (1985); Wenrich (1985, 89); Boyle (1984; Gallaway (1984); Koval (1984); Sopuck et al. (1983), Rose et al. (1983); Dyck (1983, 82, 80); Boyle and Ballantyne (1980); Cameron (1980); Leachetal (1980); Hofman (1983); Wallers (1983); Kunsendorf et al. (1983); Cardigan and Felmlee (1977); Arendt et al. (1977); Butz (1977); Gallagher (1972) Giblin (1985); Anderson (1984); Wanty et al. (1985, 81); Coker and Dunn (1983); Giblin and Snelling (1983); Langmuir and Chatham (1980); Runnelells et al. (1980); Dyck (1979, 77, 75, 74); Dall'Aglio (1974, 72, 70)
(a) Lithogeochemistry		
i Reconnaissance		
ii - detailed	Detecting the primary and secondary dispersion haloes either directly or indirectly using various sampling media (rocks, soil, till, stream, playa and lake sediments overburden and all kinds analysis of waters	
(b) Drainage geochemistry		
Lake sediments		
Stream sediments		
Playa sediments		
Marine sediments		
Boulders		
(c) Hydrogeochemistry		
i Groundwaters		
ii Surface waters		
Stream waters		
Snow		
(d) Pedogeochemistry		Simpson and Sopuck (1983); Bradshaw and Lett (1980); Pogorski et al. (1977)
Soil		
Till and drift		
Overburden		
(e) Vapour and gas geochemistry	Determination of radiogenic and non-radiogenic gases: Rn, Hg, CO_2 , O_2 H_2S and He	Hilton et al. (1986); Gregory and Durrance (1985); Ishak et al. (1985); Dyck and Jonasson (1983); Pacer (1982); Pochet (1982); Bell and Card (1981, 80, 79); Hambleton-Jones and Smit (1981)
The techniques used are:		
i emanometry		
ii alphametry		
iii track-etch		
iv radon on activated charcoal		
(f) Biogeochemistry and geobotany	Using the whole plant and/or vegetation or part of it such as twigs, roots, leaves and branches	Morrison et al. (1969); Brook et al. (1985); Dunn (1983, 82, 80); KK (1982); Levinson and Coelzee (1978)
(g) Isotope-geochemistry	Natural fractionation of isotopes and their ratios such as: $^{234}U/^{238}U$	Stuckless (1985); Chatterjee (1985, 82); Card and Bell (1985); Ludwig (1980)
Radioisotopes		
Stable isotopes	U-TH-Pb systematics, $^{222}Rn/^{220}Rn$, $^{207}Pb/^{204}Pb$; $^{18}O/^{16}O$; $^{3}He/^{4}He$	
(h) Mineral-chemistry	Identification of minerals with high U content and their relationship	Basham et al. (1982, 81, 80, 77, 74); Simpson et al. (1981, 79, 77); Bowie et al. (1973)
i autoradiography		
ii fission-track registration		
iii solution-mineral equilibria	Considering mineral solubilities using both thermo-dynamic principles and experimental results	Wanty et al. (1985); Goldhaber et al. (1985); Lepka (1985); Miller et al. (1984); Robb and Meyer (1985); Hambleton-Jones (1984); Silver (1982);
iv scanning electron microscopy and microprobe techniques	Using integrated optical and microchemical analysis	Pagel (1984, 82); Langmuir (1980, 78); Poty et al. (1974); Garrels (1965); Hasteler and Garrels (1962)
(i) Airborne geochemistry	Utilising natural aerosols which are collected first on nylon tape or passed directly into the analytical instrument	Weiss (1971); Barringer (1985);
(j) Other geochemical techniques include:		
i colour change due to alteration in a redox front	Identifying chemical reduction in sandstone roll-front type U deposits	Adams and Cramer (1985); Meunier et al. (1985); Adams and Smith (1981); Goldhaber and Reynolds (1979); Harshman (1974, 72, 66, 62); Adler (1973, 70); Fisher (1970); Rose (1977); Winager (1975); King (1966); Shawe (1959, 56)
ii non-radiogenic path-finders	Using the element association V, Mo, As, Se, Cu, Pb and conductivity	
5. Integrated methods include combinations of variety of techniques and possibly organizations	A systematic gathering of aerial, surface and subsurface geological, geophysical and geochemical data	Cameron (1983); Bell (1982)

CHAPTER II

2. GEOLOGY

2.1. History of geological investigations in the region

Systematic geological studies were begun in the region in the early 1920s by European geologists as a result of rising interest in the petroleum reservoirs of the Middle East. The first geological information from the Palmyrides was outlined by Dubertret et al. (1932); and more detailed information was given in his later papers (1938, 1941). A collection of all the papers devoted to the geology of the region and the country as a whole has been available since 1933 under the title of "Notes et Memoires" (Dubertret, 1933) and "Notes et Memoires sur Le Moyen Orient" (Arambourg et al., 1959). In these publications,Arambourg et al. concluded that thickness of the sedimentary cover increases in the north and northeastwrds of Palmyra (Tudmor), suggesting general subsidence of the basement in this direction. Chenevart (1950) reported in more detail the rock succession and thickness distribution of the Upper Cretaceous sequence in the Palmyra area. Among the many investigations conducted by oil companies in the region, drilling of deep exploratory boreholes such as the Sharifeh well in the western part and Dbayyat just outside the area surveyed has yielded useful geological information.

The period 1958 to 1962 was associated with the work of the Soviet specialists, who conducted more detailed geological, geophysical, hydrogeological and structural investigations. Their

surveys made use of extensive palaeontological studies, and was accompanied by stratigraphic mapping of nearly all the geological systems outcropping in the region, dividing them into series, stages and zones. The Soviet team of experts compiled good quality geological maps of 1:200,000 scale for Palmyra (sheet XV), and Al Qaryatem (sheet XIV) which cover the whole study area of the present reconnaissance survey and provide the geological base for the simplified geological map of the Palmyrides region presented in Fig. 2.1. There are also tectonic and geomorphological maps, a map of mineral occurrences, and a map of groundwater horizons. Primary investigations of the phosphorite formations were also carried out along with the search for other sedimentary mineral resources. Uranium, however, was not included.

Syrian geologists began their investigations of the region in the early 1960s (Atfeh, 1964, 1965, 1966, 1967, 1970 and 1975 ; and Katmeh, 1968, 1969). More comprehensive investigations were undertaken by Mouty (1973, 1978, 1984). The present author was a member of a team of geologists headed by Professor Mouty, which carried out the most recent geological studies of the Palmyrides (Mouty et al., 1983). Geological mapping of the central part of the Palmyrides in 1:50,000 scale began in 1975 by geologists of the General Establishment of Geology and Mineral Resources (GEGMR), and is still continuing.

As early as 1935, Khabaz started limited hydrogeological work in the Ad Daww basin. More systematic studies were carried out by Safadi (1954); Burdon (1961); Khouri (1966, 1970, 1971, 1972 and 1973); Agha (1976); Khouri and Hadj (1983) and Agha and Droubi

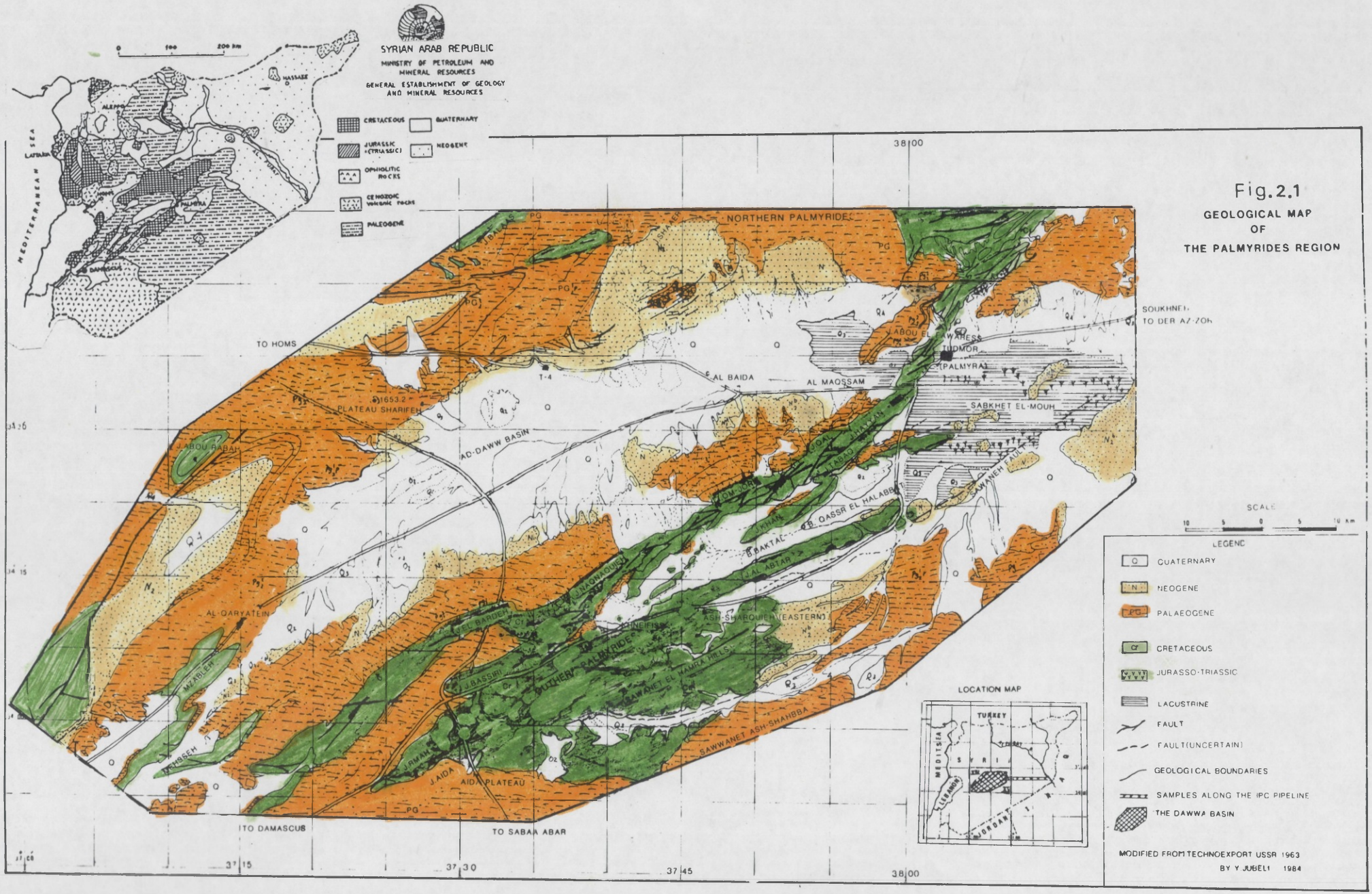


Fig. 2.1

GEOLOGICAL MAP OF THE PALMYRIDES REGION

(1983).

2.2 Geology of the Palmyrides in the light of the plate tectonics

An attempt is made here to consider the available geological information about the region within a framework of the kinematic model of the plate tectonics of the Middle East.

2.2.1 The Palmyrides aulacogen

Without referring to plate tectonics, the Technoexport specialists (Ponikarov et al., 1966) reported that the Palmyrides folded region occupied an ancient, northeasterly trending, elongated depression within the mobile northern slope of the Afro-Arabian platform. The depression is bounded in the southeast and north by two distinct basement highs. The first, the Rutbah uplift, is situated southward towards the border with Iraq, actually doming in the vicinity the town of Rutbah, Iraq, with outcrops of nearly horizontal or slightly dipping (1° to 2°) Triassic and Jurassic beds. The second, The Halab (Aleppo) Uplift, borders the folded Palmyrides at its northern and northwestern margins, close to the border with Turkey. The relationship of these three structural features is illustrated in Fig. 2.2. It can be seen that deep faults within the basement were inferred to be ancient lineaments and faults probably prior to Palaeozoic times, implying that the Palmyrides trough was possibly structurally controlled since late Pre-Cambrian. It should be noted, however, that no field geological evidence was found to indicate an obvious fault control prior to Mesozoic times.

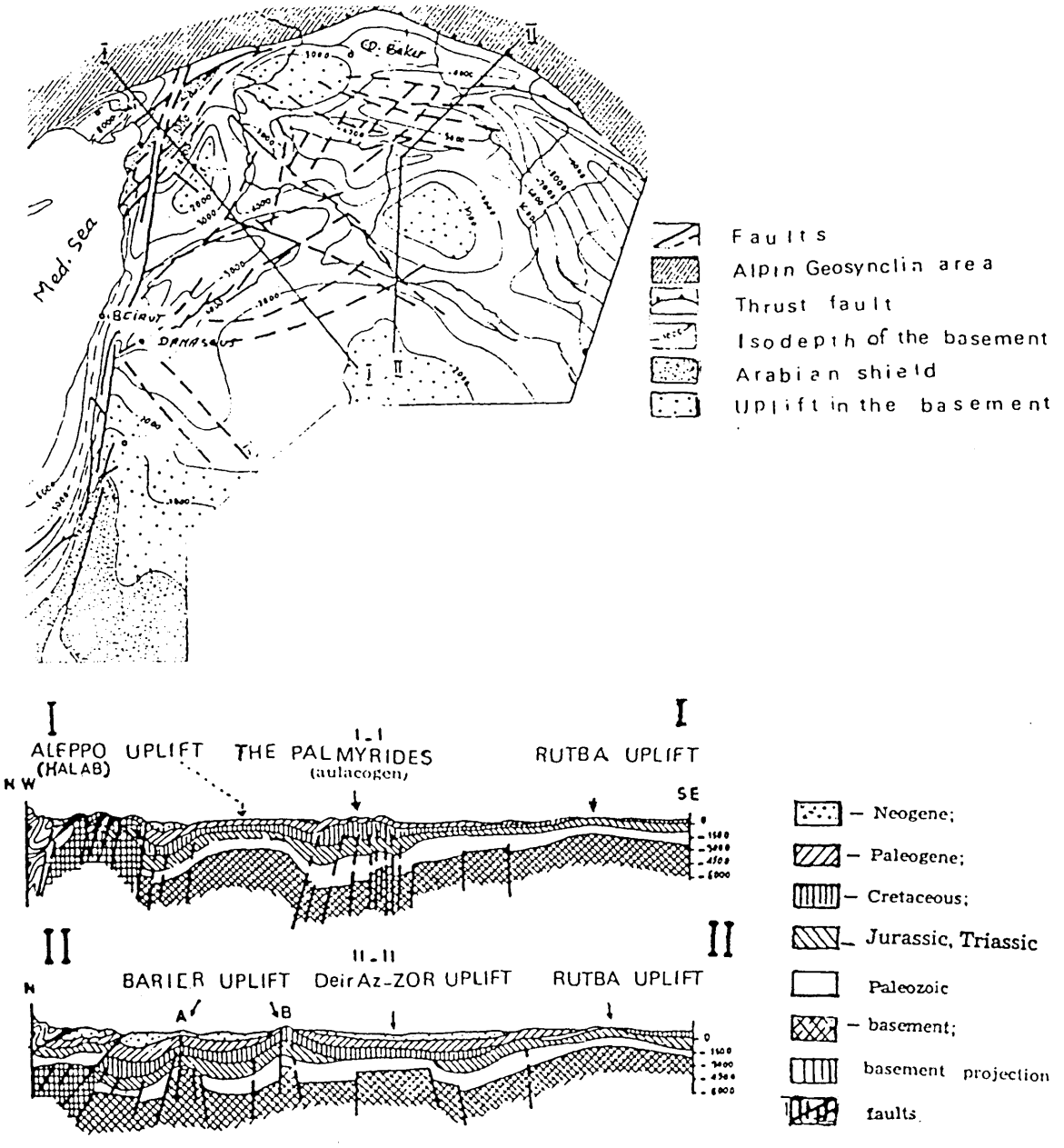


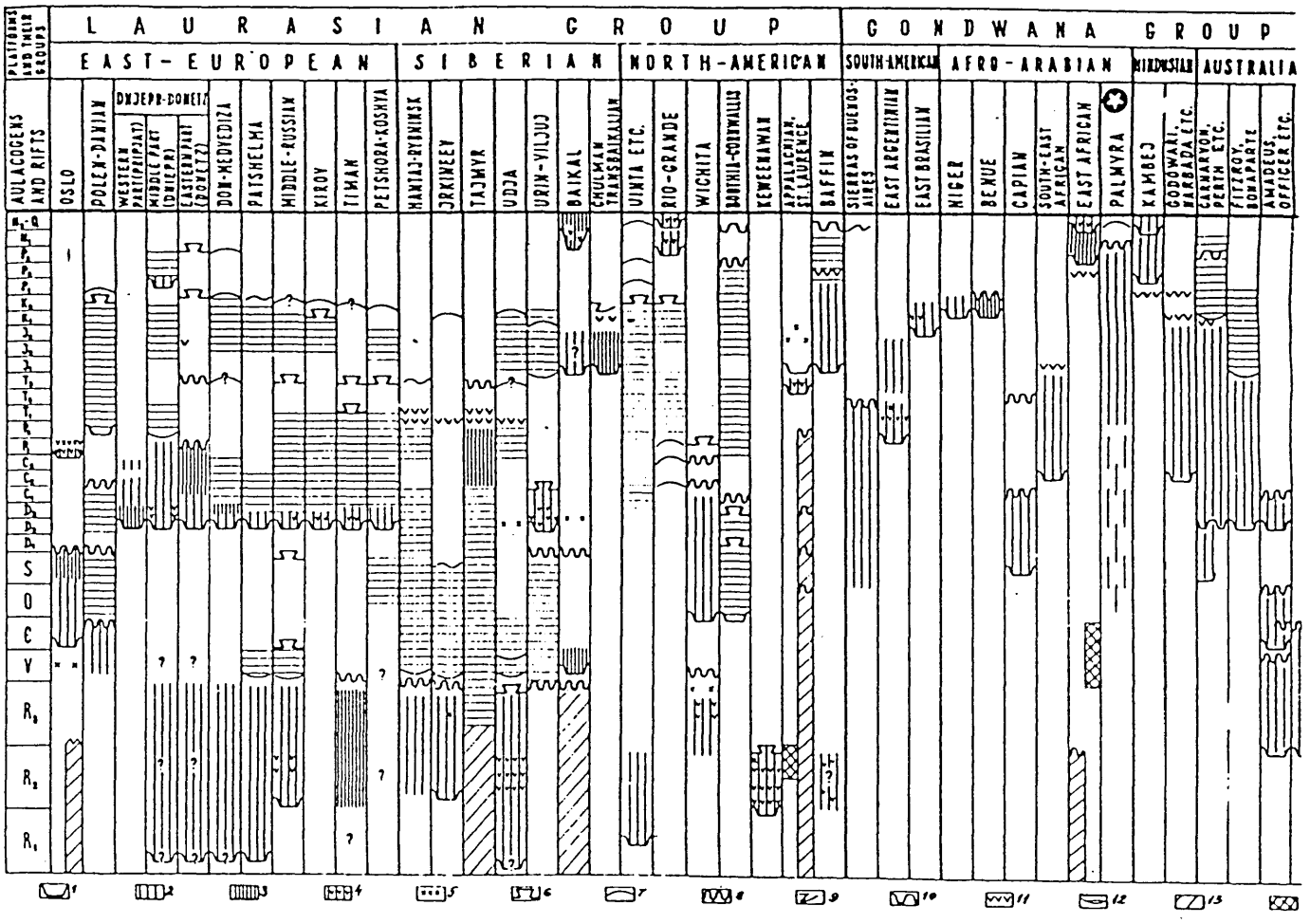
Fig.2.2 Location and schematic sections showing the main structural units of the basement.

In their explanatory notes of the geological maps of the region, Soulidi-Kondratiyev et al. (1966), considered the folded Palmyrides as a suture trough striking northeastwards,with an active tectonic lineament along its southern margin. They accepted the idea of Shatsky and Bogdonov (1961) that this sharp boundary lies deep within the basement rocks of the Arabian platform, and described the Palmyrides as an aulacogen. This term was first used by Shatsky and Bogdonov (1961) without any combrehensive definition, implying a mainly vertical fault movement. Milanovsky (1981), defines the term aulacogen as "Riphean and Palaeozoic linear graben-like platform depressions jointly with linear swell uplifts in a platform cover, interplatform folded zones and Meso-Cenozoic epi-platform rift". He accepted that the early stages of an aulacogen evolution occur under horizontal extensional conditions, whereas the inversion stage take place under a compressional regime. According to him, the Palmyrides belong to a Gondwana group of aulacogens on the Afro-Arabian platform (Fig.2.3).

2.2.2 Plate tectonic movements

The structural development of the region can be interpreted in terms of plate boundary movements and their resulting features of rifting and compression. The two stages of tension and compression occur in the region,and they correspond respectively to:

(i) The break-up of the coherent Afro-Arabian plate along the Gulf of Aden and the opening of the Red Sea spreading centre further



1 = Stage of incipience (or regeneration) of aulacogen or rift; *2* = Stage of subsidence and infilling of aulacogen (rift) by sediments; *3* = the same, more intensive; *4* = the same, accompanied by basic and basic-alkaline volcanism; *5* = basic and alkaline intrusions; *6* = stage of inversion represented by block uplift of basement (partly-along upthrusts); *7* = the same represented by swell-like uplift of platform cover; *8* = folding and fold-overthrust deformations; *9* = marginal upthrusts and overthrusts on the borders of grabens and graben-like depressions; *10* = differential block movements; *11* = trap volcanism; *12* = formation of wider and flater platform depression (syneclise) above aulacogen and its moderate or slight subsidence; *13* = pre-platform (geosynclinal-orogenic) stages of development; *14* = epochs of tectono-magmatic activisation.

✪ Palmyra

Fig.2.3 Correlation of development stages and cycles of some aulacogens (from Milanovsky, 1981).

south, which created the horizontal movement and its extensional component; and

(ii) The continental collision which followed between the Arabian and Anatolian plates in the north and northeast, along the Amanous-Taurus and Zagros mountains. This stage generated the compressional component within The Palmyrides region (Fig.2.4). The first stage, however, was preceded by epi-orogenic movement that manifested itself prior to the break-up of the plates by alternation of subsidence and uplift periods which produced transgression and regression cycles within the Palaeo Tethys basins. The conspicuous diferences in the sedimentary sections between the Palmyrides depression and the Rutbah Uplift are related to this down warping and uplift. While the Rutbah area was receiving very thick Lower Palaeozoic clastic sediments, which lie undisturbed over the Pre-Cambrian basement, and then a much reduced Upper Palaeozoic through to Cenozoic series, the Palmyrides showed a very reduced Lower Palaeozoic lagoonal to continental terrigenous sediments, and, afterwards, began to subside in the late Upper Palaeozoic, causing accumulation of very thick shelf-type carbonate and evaporite sequences. In the Palmyrides, the downwarping continued during the Triassic and Lower Jurassic times and ended when a major Middle Jurassic uplift took place. This uplift is well marked throughout the region by distinct hard grounds and ferruginous crusts, as well as the lack of all Upper Jurassic series. (The work of Mouty (1973, 1978, 1984) disputed the reported presence of Upper Jurassic rocks by the Soviet workers and provided evidence for their absence).

The first rift activity within the study area perhaps

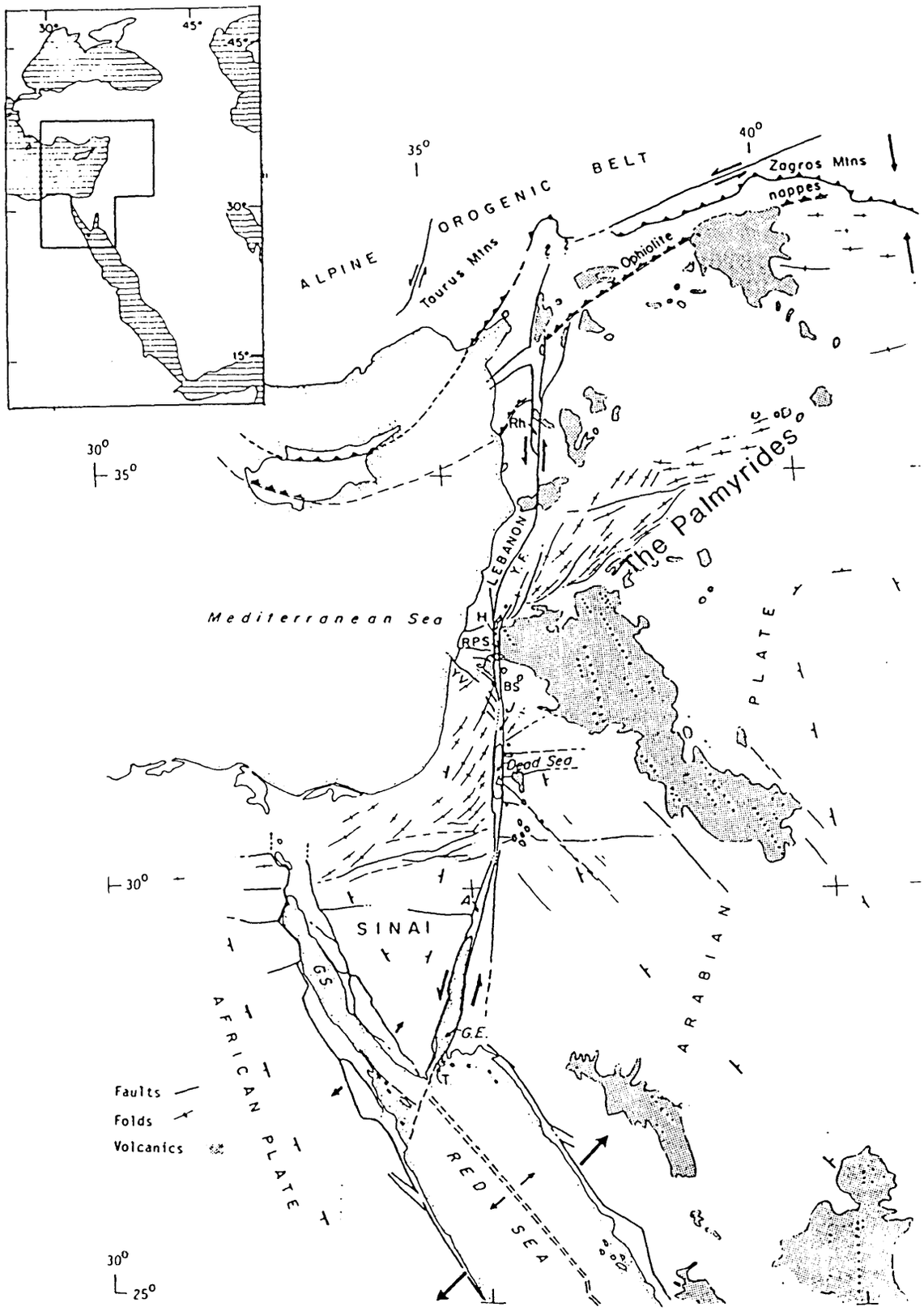


Fig. 2.4 General setting of the Dead Sea transform. *Rh* = Rhab depression; *YF* = Yammuneh faults; *H* = Hula depression; *RPS* = Rosh Pinna saddle; *YV* = Yizreel Valley; *BS* = Bet Shean; *J* = Jordan Valley; *A* = Arava; *G.E.* = Gulf of Aqaba ; *T* = Island of Tiran; *G.S.* = Gulf of Suez. (from Garfunkel, 1981)

occurred in the early Cretaceous and marked the Aptian transgression. It was accompanied by volcanic activities, possibly related to deep taphrogenic events spatially associated with the southern boundary of the Palmyrides region. It corresponds to tectonic activities that began (according to Karpoff, 1957; Carella and Scarpa, 1963; and Azzaroli, 1968) in Jurassic or Cretaceous times, leading to the separation of Somalia from Arabia and the failure that originated the opening of the Red Sea between Africa (Nubia plate) and Arabia as shown in Fig.2.5.

Although this rifting phase is obviously fault-controlled within the Palmyrides, its surface expression is very weak and shows no strike-slip indications. Therefore, it is evident that up to late Cretaceous, the region did not experience inversion or compression and its development towards a mature aulacogen took place under extensional conditions, which manifested themselves in renewed subsidence that appears to have been fualt controlled.This control was reflected through lithological variations of the Upper Cretaceous series and even within the rock sequences of its individual stages (Coniasian, Santonian, Campanian Maestrichtian and Danian). This is particularly evident in the rapid alternation of limestone, chert, marly limestone, thick phosphorites and coquina which are followed by thick pelagic sediments. Such great variation in rock-type and thickness can be related to the above mentioned fault control. Hence, it can be inferred that the deposition of the Palmyrides phosphorites was closely associated with rifting and faulting which, in turn, was a result of the horizontal movements of the plate boundary. The much stronger effect during Campanian and Maestrichtian times was contemporaneous

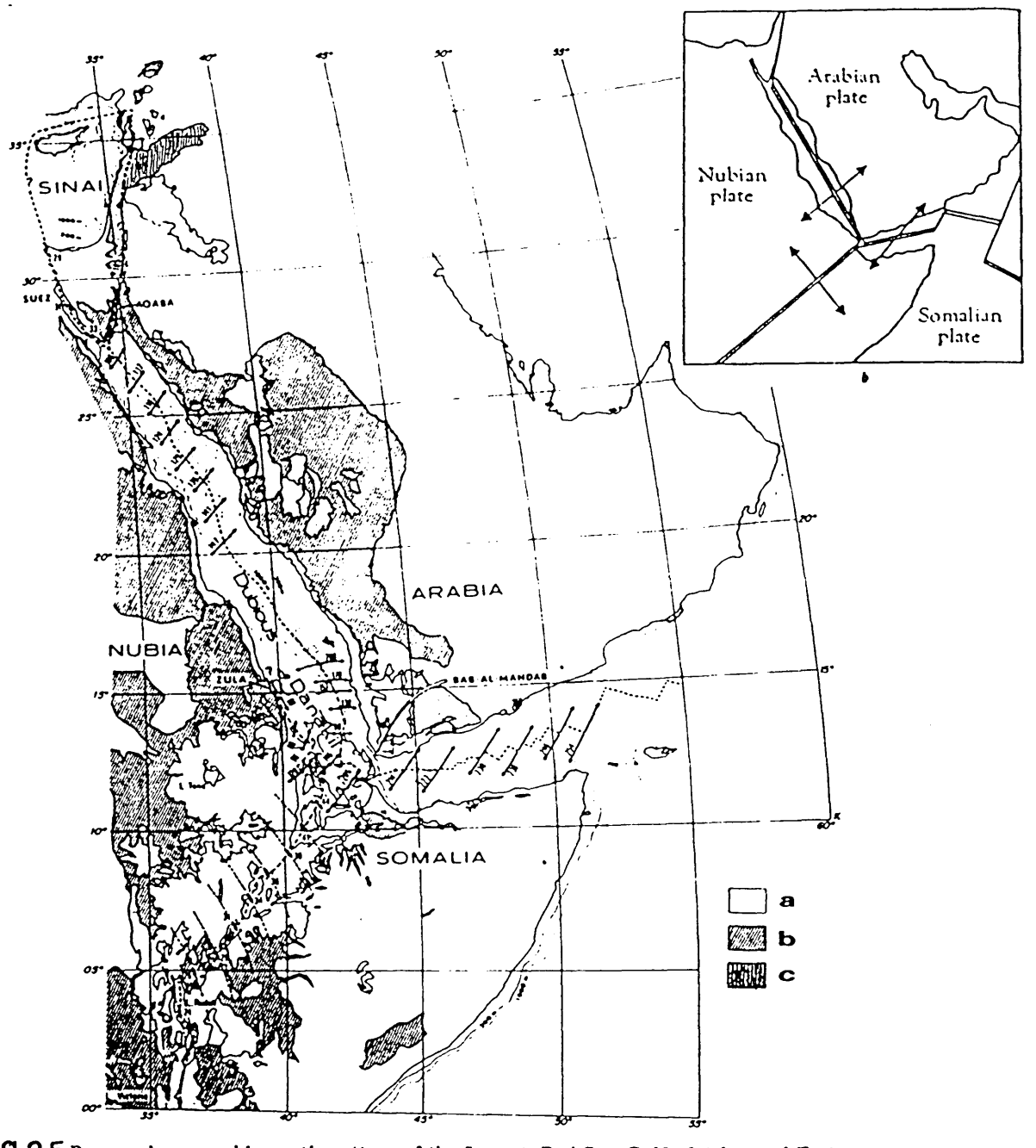


Fig.25 Proposed average kinematic pattern of the Levant, Red Sea, Gulf of Aden and East Africa area since the Early Miocene on a base of the International Tectonic Map of Africa (ASGA, UNESCO, 1968). The boundaries between plates are shown dashed. The vectors of total motion, according to the rotations listed in Table IV are shown at the scale of the map with magnitude in kilometers. Legend: *a* = Recent volcanics, *b* = Precambrian basement, *c* = folded belt (Palmyra chain). G. Postel, azimuthal projection.

(from Le Pichon and Francheteau, 1978)

with the revolution of the Neo-Tethys tectonism that led to the closure of the Palaeo-Tethys basins in the northwest of Syria, Turkey and the neighbouring regions (Sengor and Yilmaz, 1981). According to their studies, the renewed tectonism was connected to the convergence of Afro-Arabia against Eurasia along a north-dipping subduction zone beneath southern Turkey prior to their final collision in Miocene times. Geological evidence for a consumption of the floor of an inner Mediterranean sea basin during these stages can be provided by the presence of the ophiolitic arc in NW syria and Southern Turkey. The onset of these ophiolites was reported to be of Campano-Maestrichtian age (Al-Maleh, 1976). However, differentiation into regions or transition zones near the consumption boundaries of this sea led to complex geology within the collision zone as well as some distance away (Fig.2.6).

It has been recognised that in the whole Middle East region the seismic creep or slip rates were considerably lower than other known plate motions, regardless of fault type and setting (Davies and Brune, 1971; North, 1974). Garfunkel et al. (1981) estimated the recent rate along the Dead Sea fault system to be half that of Pliocene-Pleistocene movement indicating that, due to collision in Turkey between the Arabia and Anatolia plates the movement became more difficult along the Levant Shear system.

Vertical displacement occurred along the Southern Palmyrides zone of faults as well as other regional lineaments in the area, suggesting the rejuvenation of the continental rifting and revival of the ancient Taphrogenic elements in response to major plate boundary movements and accompanying deformation. It is recognized

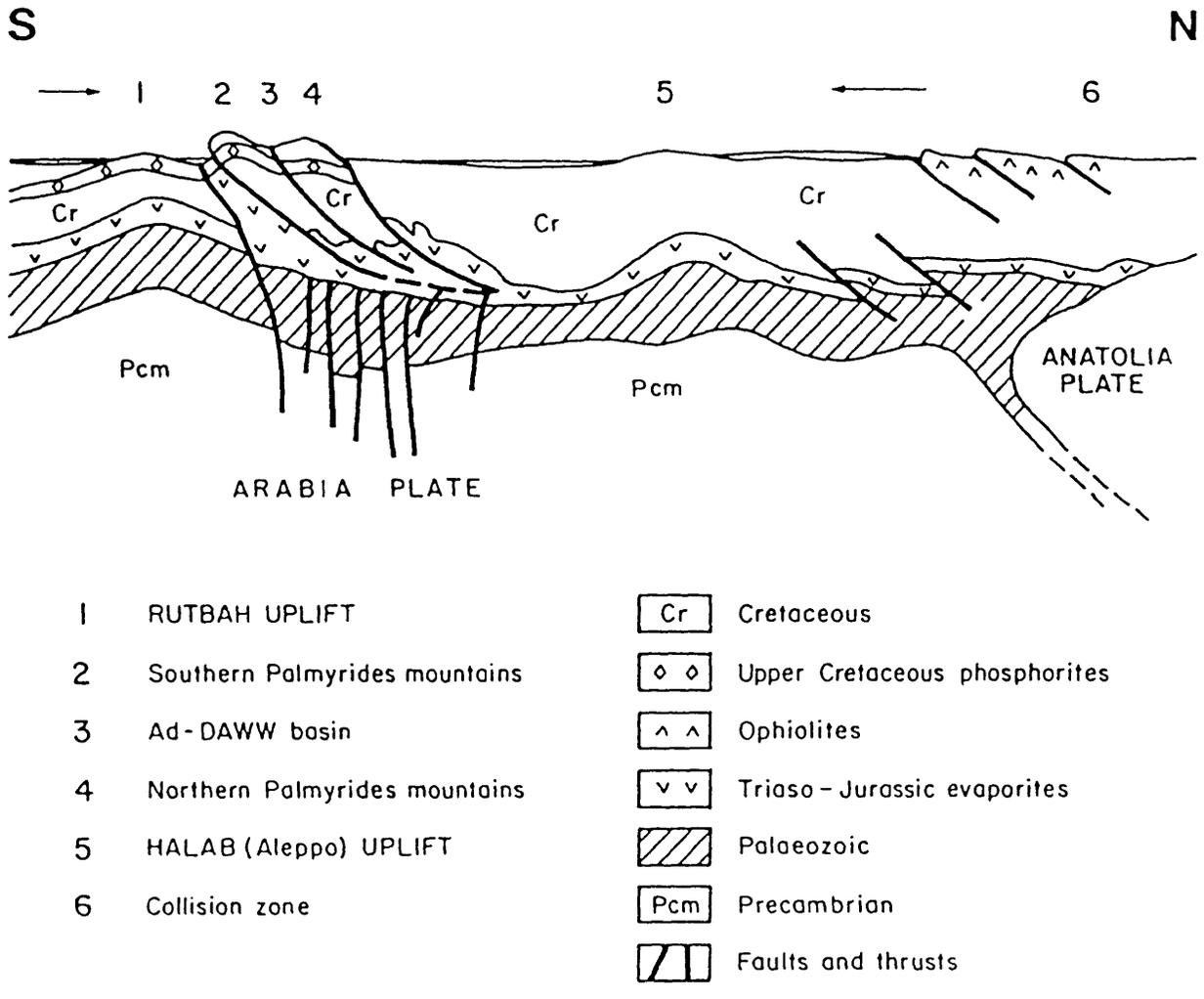
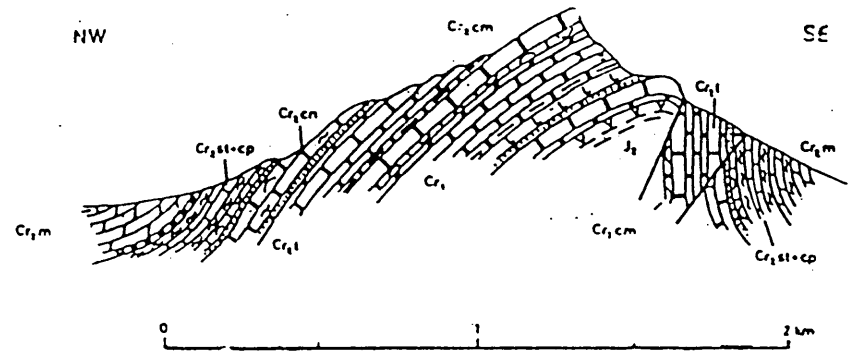


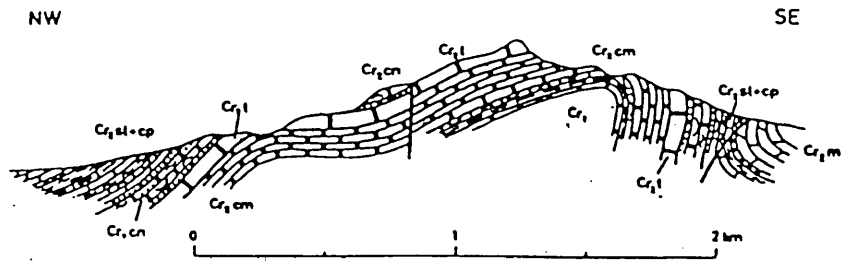
Fig. 2.6 Schematic representation of the structural setting of the Palmyrides illustrating the thrust deformation due to collision in the north between Arabia plate and Anatolia plate
(Notice the role of the Jurasso-Triassic evaporites)

also however, that the Triasso-Jurassic evaporites played a great role in deforming these faults into shallower north-dipping thrust faults. This deformation is particularly evident along the southern limbs of many Southern Palmyrides mountains. The folds reflect by their asymmetrical shape (coffer and box folds), the shallow detachment on the top of the thick evaporite which acted as lubricant for underthrusting deformation (see Fig.2.6). The sharp southern limbs of these mountains represent the thrust contact (Fig.2.7), where the deformation events have a clear thrust motion component along the northeasterly trending Southern Palmyrides faults owing to the compression caused by the faster motion of the Arabia plate.

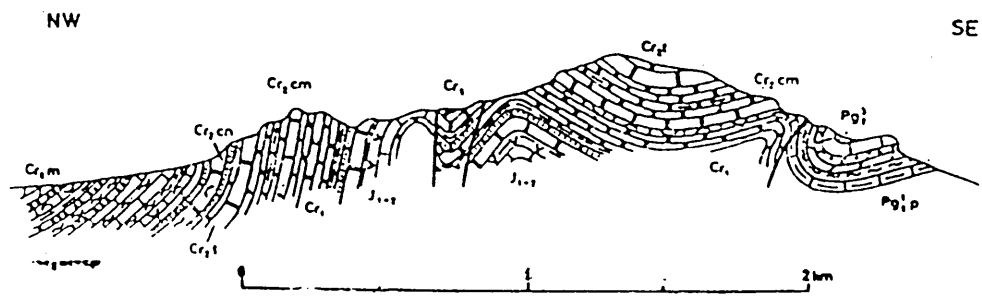
Further northeastward, outside the folded Palmyrides lateral motion with a tensional component occurred along the northwestward trending Al-Furat fault system, which controls the course of the Euphrates river. In the late Neogene-early Pleistocene, the southernmost part of this fault (within Syrian territory) formed a distinct graben reflecting the extentional feature. This was accompanied by volcanic activities. Similar extentional components can be also inferred in areas with extensive Neogene and Quaternary volcanisms, in the southwest and west of the region. These volcanic activities started in mid-Miocene, and seem to be associated with the opening of the Red Sea and the movement of the two boundaries along the irregular Levant shear system of faults extending along the Gulf of Suez triple junction, Gulf of Aqaba, Dead Sea fault system, Yemmuneh fault (Lebanon) and to the Syrian rift valley west of the Palmyrides (see Fig.2.4). The lack of similar volcanic activity within the folded Palmyrides gives additional support to



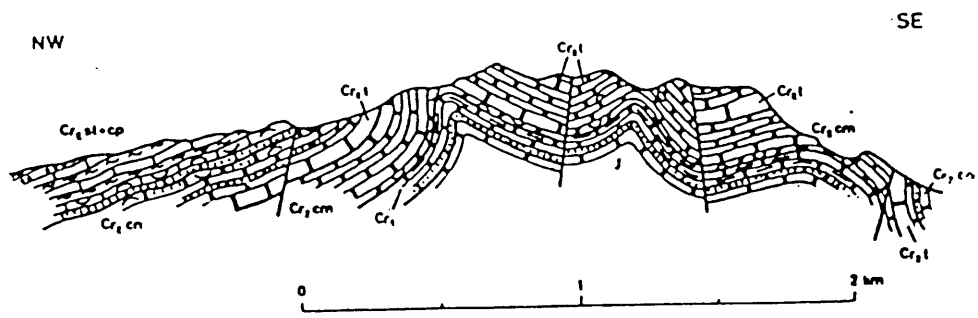
Rmah anticline



Bassiri anticline



Naqnaqiyeh anticline



Tboug anticline

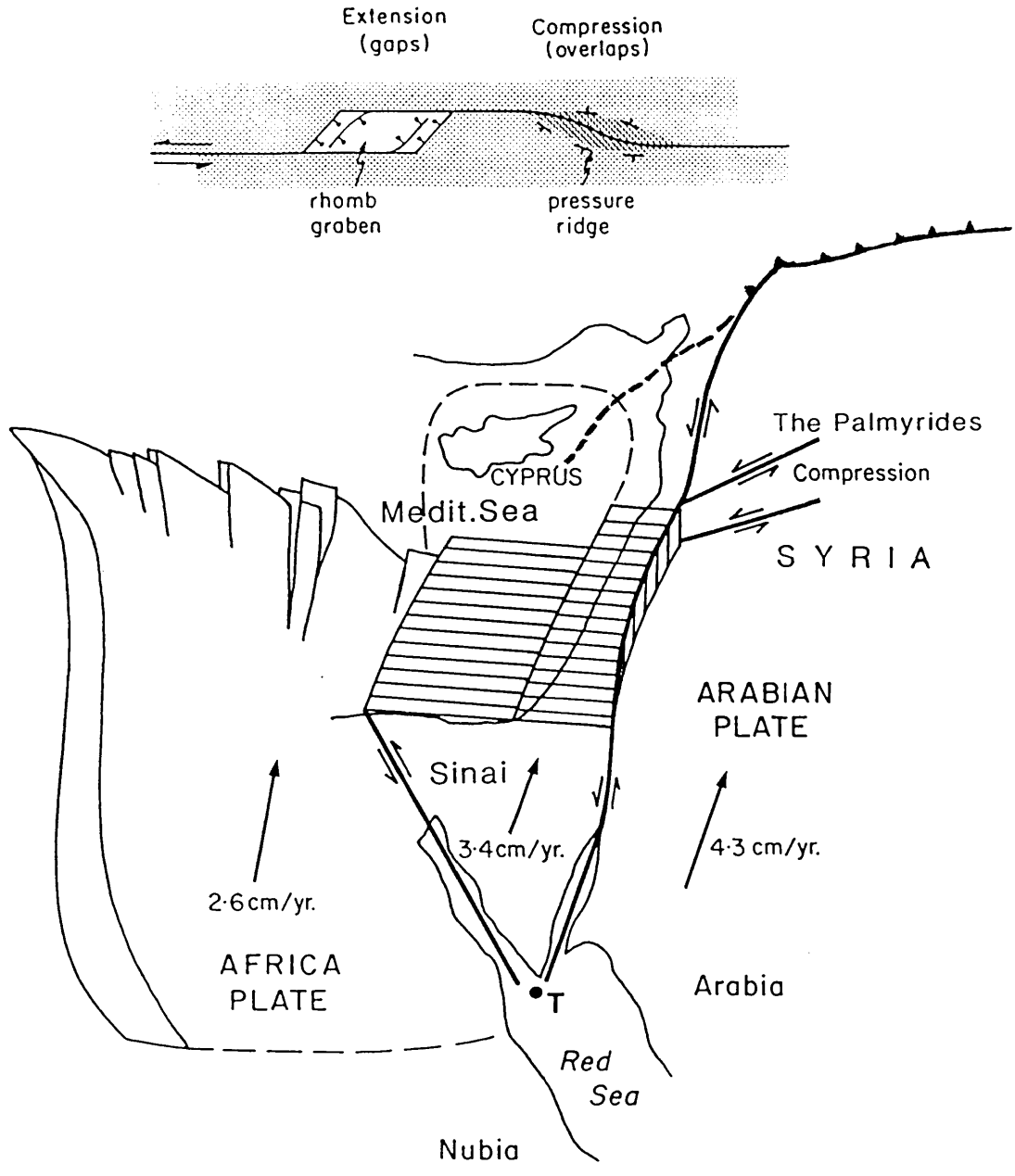
Fig.2.7 Asymmetrical thrust shape of the southern Palmyrides Mountains. (from Technoexport,1966)

its compressional nature, which appears to prevent lava outflow to the surface. The presence of magmatic activity below the present surface is still an open quistion.

It is widely accepted now that movement of 107 km on the eastern block of the Levant Shear system took place in two stages, starting immediately after the break-up of the Gulf of Suez triple junction. In each the horizontal movement component was much greater than the vertical (Quennell, 1958). The first phase of movement, totalling 62 km started in the Lower Miocene, continued well into the Pliocene and ceased for a period of horizontal standstill with up and down thrusts which were reflected on the surface. The irregularity of the fault system (Fig. 2.8) assisted in producing strong compression in some sections, and the separation of margins of blocks along others, and the Lower Miocene volcanism was contemporaneous with this phase of motion. The standstill was terminated by the second stage of horizontal movement (45 km), in the late Pleistocene and is still continuing. It has negligible vertical displacements and minor volcanic activities, but frequent earthquakes. In the Palmyrides most of the E-W and NW-SE trending faults appear to be associated more with the second phase of the horizontal movements.

The major events of the inversion and compression stages of the Palmyrides aulacogen development can be summarized as follows:

(a) A faster movement of the Arabia plate away from Africa in a north-northeasterly direction due to the failure of the Gulf of Suez triple junction in southern Sinai. The instrumental force



T = Gulf of Suez Triple Junction

Fig.2.8 The Levant shear system

(combined and redrawn after Nur and Ben Avraham, 1978; and Ben Avraham, 1978)

in this motion is related to the earlier opening of the Red Sea. This phase culminated in the continental collision of the Arabia and Anatolia plates along southern and southeastern Turkey (Amanus-Taurus and Bitlis suture) in early to mid-Miocene times.

(b) In response, a strong deformation occurred, particularly in the area adjacent to the collision and some 600 km or more away. This manifested itself in compression within the Palmyrides, due to the fact that this area occupies a depression in the basement between two highs (Rutbah and Haleb). Therefore, it is more amenable to compression than the other locations. Basement highs, on the contrary, seem to be deformed under a tensional component (eg. Al Furat fault and graben) over the Der-Az-Zor basement high. The extensive folding within the Palymrides was associated with the compression that followed the collision (Upper Miocen to early Pliocene).

(c) Thrust development, particularly underthrusting of the southern Palymrides along the major fault zone at its Southern border, in which the thick Triasso-Jurassic evaporites played a major role, resulted in extensive deformation and asymmetrical folds.

(d) Volcanic activities during Neogene and Quaternary times are lacking within the folded Palymrides and extensive outside its limits, especially along the Syrian rift zones in the far west and southwest of the country, as well as close to the Al-Furat tensional fault (Fig. 2.9).

(e) The deposition of the phosphorite seems to be closely associated with the late Cretaceous Neo Tethys plate tectonic activities.

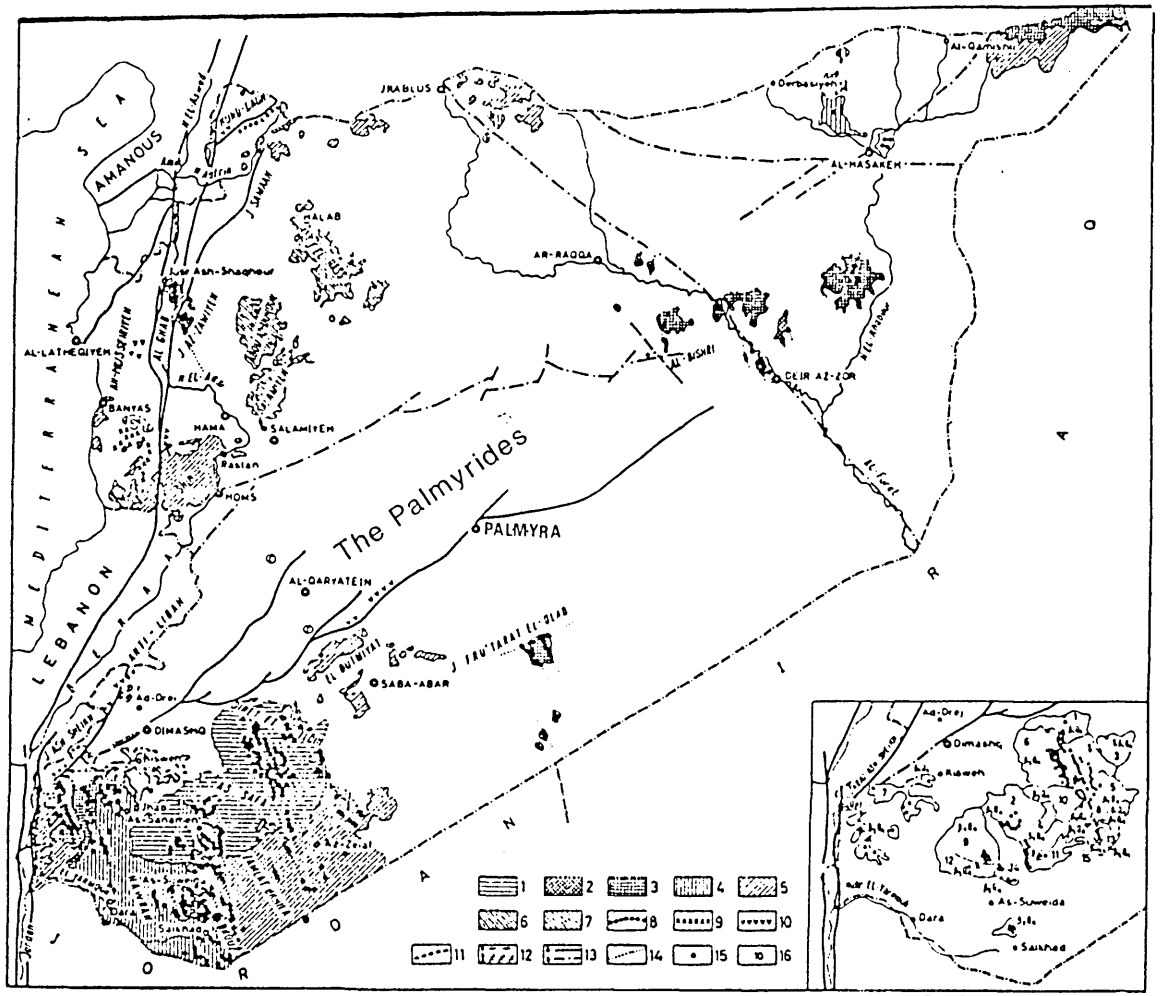


Fig.2.9 Development of volcanic activities outside the Palmyrides

1 – Recent basalt; *2* – Upper Quaternary basalt; *3* – Middle Quaternary basalt; *4* – Lower Quaternary basalt; *5* – Pliocene basalt; *6* – Upper Miocene basalt; *7* – Middle Miocene basalt; *8* – Lower Eocene basalt; *9* – Upper Cretaceous basalt; *10* – Lower Cretaceous basalt; *11* – Middle Jurassic basalt, *12* – hypabyssal basaltic rocks: *a* – Quaternary, *b* – Pliocene, *c* – Miocene, *13* – faults: *a* – proved, *b* – inferred; *14* – faults-feeding channels of lava flows; *15* – cones of extinct volcanoes; *16* – numbers of recent basalt sheets

On the right – a scheme of basalt sheets of different ages. Names of recent basalt sheets: 1 – Dmer; 2 – Arid el Hamra; 3 – Tell Salman; 4 – Deir Ad-Drouz; 5 – Rhayyet As-Sumra; 6 – Diret; 7 – Hadar; 8 – Tell Om El-Janbris; 9 – Al-Laja; 10 – As-Safa; 11 – Al-Kra'; 12 – Tell Shihan; 13 – As Safa; 14 – Tlool Rgheleh; 15 – Tell As-Safa

2.2.3. Faulting

Interpretation of the Landsat image (Fig. 2.10) shows four principal trends of faults. These are north-south, north-east, north-west and east-west systems. The north-south faults are distinguished only outside the study area.

Among the most important north-easterly trending faults are the South Palymrides zone of faults which constitute the boundary between two distinct tectonic zones within the Syrian part of the Arabian platform. These are the stable part of the platform in the south and the relatively mobile part of the platform slope in the north. These faults are generally steep with magnitudes of displacement often exceeding 1000 m, bringing into contact the Maestrichtian or Palaeogene series with the Jurassic or the Lower Cretaceous ones (Fig. 2.11). On the northern side of the Palymrides, there is also an extensive north-easterly running zone of faults hidden by Neogene sediments.

Important north-westerly trending faults (which seem to be younger than north-easterly trending faults), are found parallel to the Al-Furat (Euphrate) fault. Outside the Palymrides region, these faults have provided conduits for lava flows. Inside the region, however, they have a smaller extent, and are rather poorly marked in the surface structures.

East-west faults are the least important, extending for a few

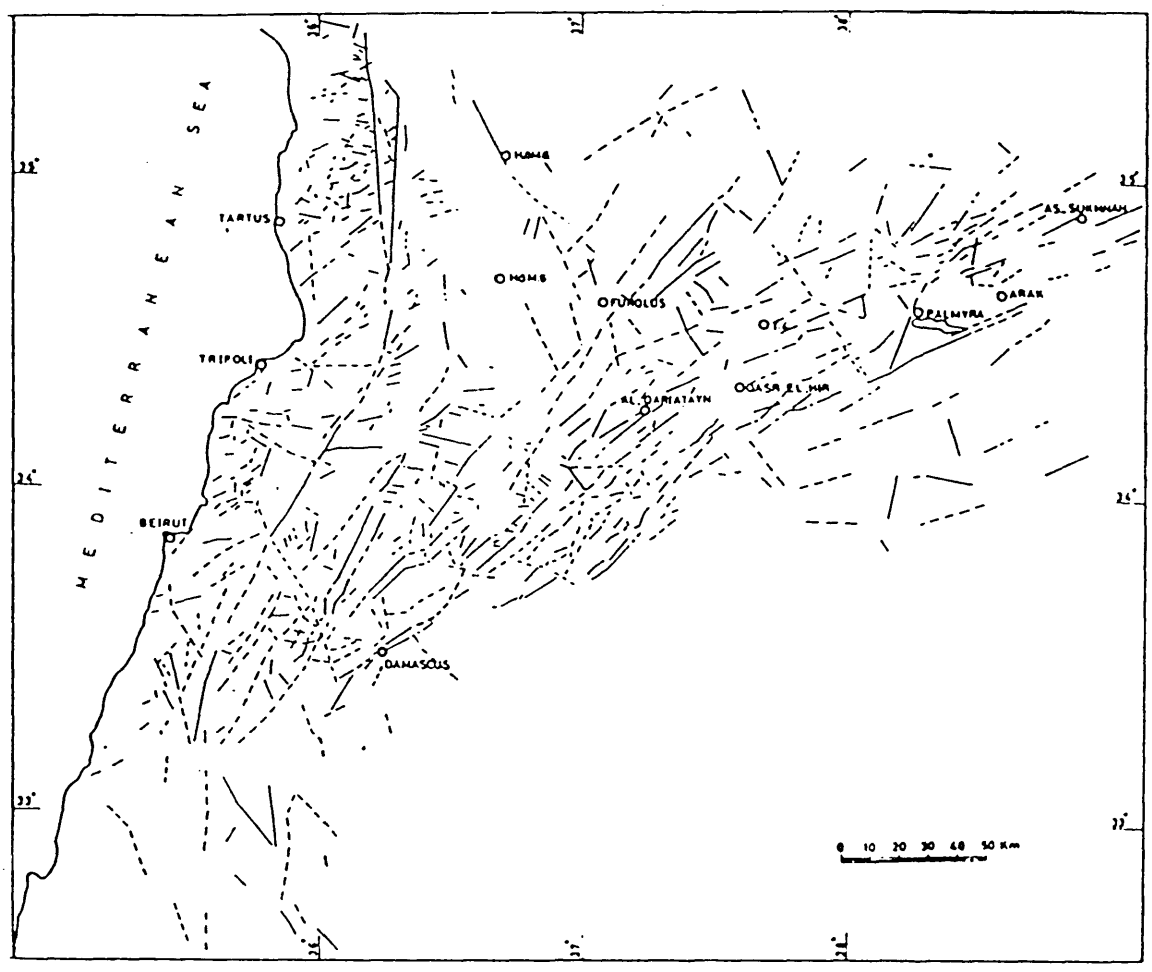


Fig.2.10 Interpretration of fault lineaments from the Landsat image (from Khouri and Droubi, 1981).

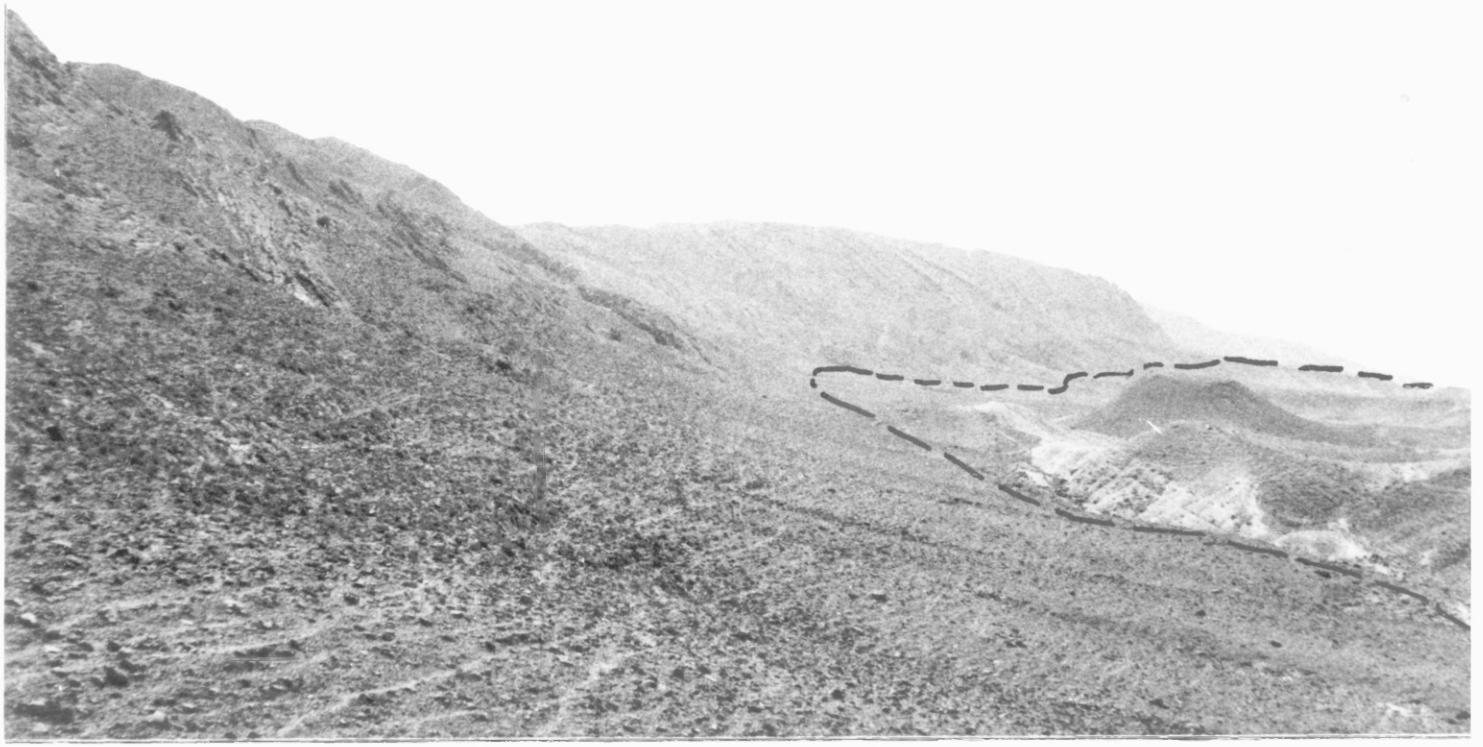


Fig. 2.11 Fault contact between Maestrichtion Marls (right) and Jurassic Lower Cretaceous rock (left).

kilometers and mapped only for a very short distance. They are probably the youngest sytem of faults, and the most noticeable is that which cuts the Khneifiss phosphorite deposit into two northern and southern parts.

Thermal and mineral springs are generally confined to recently active faults, they are represented by J. Abou Rabah's vapour vent and Palmyra and As-Sukhneh hot springs.

The latest reported earthquakes in the Palymrides region, which occurred during 1970 (NE of Palymra, October 5th, 1970, focal depth 32 km, intensity less than 4.7) and 1974 (SW Palymra, July 12th, 1974, focal depth 36 km, intensity less than 4.3), are geological evidence that the Palymrides region is stil structually active.

2.3 Stratigraphy

Except for restricted Triassic evaporite outcrops in the core of J. Hayyan (BRGM, 1977), the oldest Mesozoic rocks outcropping and accessible to study in the Palymrides region are of Jurassic age. Details of the stratigraphy relevant to this study are written separately. However a brief summary follows.

Lagoonal conditions which prevailed during the Triassic and Jurassic times are represented by approximately 100 m of arenaceous and gypsiferous clays, green shales, dolomitic limestone, gypsum, anhydrite and dolomite. Only two series of the Jurassic system,

namely, the Lias and Dogger, are represented in the region. The uppermost part of the Dogger is characterized by ferruginous crusts and hardgrounds expressing a major uplift, which may explain the absence of the Mahn sequence of Upper Jurassic.

The Lower Cretaceous marine transgression deposited on unconformable varigated ferruginous basal sandstone and irregular nodules of restricted thickness of iron ores during the Aptian times. These formations were gradually replaced by dolomitic limestone, dolomite and clayey-marly limestone during the Albian period and mainly dolomite during the Cenomanian stage. In some parts of the region the Turonian seems to be deposited with discontinuity at the base which is represented by conglomeratic breccias of dolomite and sandstone; however, everywhere the Turonian ends with a marked erosional surface. Arenaceous facies occur at the base of the Coniacian stage of Upper Cretaceous and are gradually replaced by dolomite and marly limestone with a distinct limestone bed rich in fosils and organic matter. These facies seem to reflect changes in the sea level owing to a response of the sea floor to the earlier discussed plate tectonics. Such a response culminates during Santonian, Campanian and Lower Maestrichtian times, resulting in major lithological variations and changes of the palaeogeographical environment. The distinctive feature of this period is the deposition and rapid alternation of phosphorite, marly limestone, chert and coquina rocks. This was followed by thick pelagic sediments of monotonous marls and clayey-chalky limestone of the Upper Maestrichtian and Danian stages, indicating conspicuous changes to deeper sea environment and much calmer tectonic activities in the very late Cretaceous

(for thickness and lithologies refer to Table 2.1 and fig. 2.12).

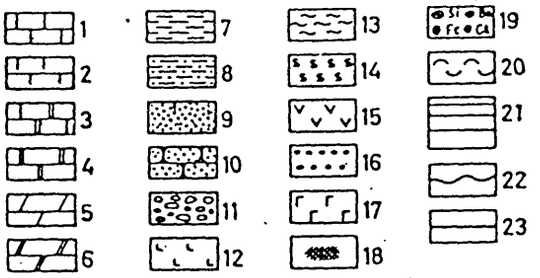
The stable conditions continued during the Palaeogene times. However, the Palaeogene system can be divided into two major sedimentary cycles comprising five series with seven subseries and eleven zones (Table 2.2). The first is characterized by pelagic sediments of marls, clayey glauconitic carbonate, phosphatized limestone, well developed phosphorite beds and chalk-like limestone with concretional flints lasting up to Middle Eocene. The second cycle comprises the Upper Eocene and Oligocene; the former is represented by nummulitic limestones which are laterally and gradually replaced by a marble-like limestone, whereas the latter shows distinct terrigenous sediments and sandstones replacing reef limestone. This marks the permanent late Oligocene marine regression which has since left the Palmyrides region above sea level. Continental conditions prevailed during the Neogene and Quaternary period. The Neogene sediments rest with angular unconformity ($>10^{o}$) on the Palaeogene rocks, and are represented by lacustrine, fluvial and terrigeneous materials with subordinate autochthonous carbonate sediments.

The Quaternary formations comprising locally-derived proluvium, alluvium and aeolian sediments, are widely distributed in the Palmyrides especially in the Ad-Daww basin and Sabkhet El Mouh playa. The lithologies are mainly sandstone, loam, clays and carbonate and gypsum duricrusts.

Table 2.1 Stratigraphic interpretation of the Dbayyat borehole and the Triassic, Jurassic and Cretaceous systems (from, Technoexport, 1966).

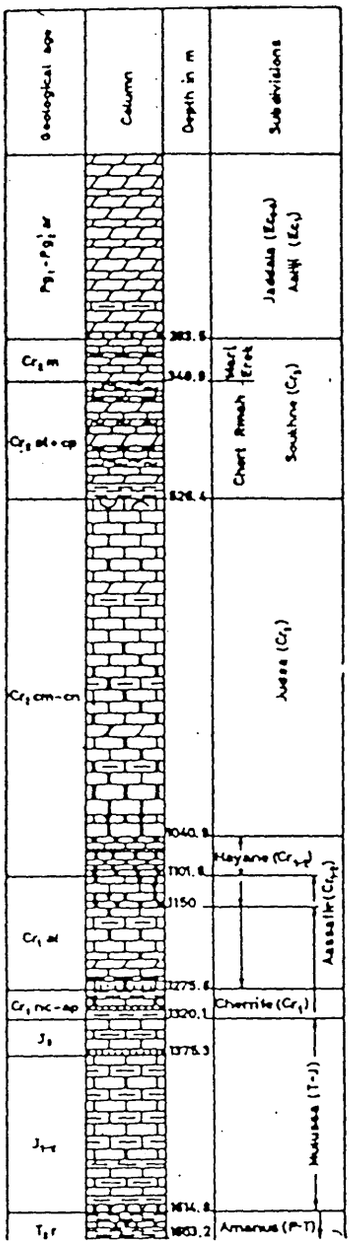
Data of Syrian Oil Company for the Dbayyat well					An interpretation of Dbayyat well on the basis of the geological survey on the 1:200,000 scale under Contract 944 (1961)		
Formation	System	Lithological and faunistic characteristic	Thickness, m	Depth from surface, m	System	Series	Stage
Aalili	Paleogene	Grey marl, white limestone. - Hantkenina	186	186.0	Paleogene	Middle Eocene	
		Grey marl, black flint	112.7	298.7		Upper part of Lower Eocene	
		Grey-green marl; grey bituminous marl; blue, brown glauconitic marl. Fauna: *Guterelina irregularis, Haplophragnoides sphaeriloculus, Anomalina navarroensis*	310.9	609.6		Paleocene-Lower Eocene	
Shiranish	Cretaceous	Grey, lighyt-ellow marl; at the base grey-brown marl, glauconitic marl, phosphorites. In the middle part fauna: *Globotruncana arca, Gumbelina* aff. *plummerae, Bolivina incrassata, Bulliminella* aff. *carseyi, Gumbelina globulosa*	229.8	839.4	Cretaceous	Upper	Danian
							Maestrichtian
Soukhne		Phosphatic shale, green marl, grey limestone with oysters, laminated shale. Black and white flint, marl, dolomite in the lower part	56.7	896.1			Campanian
Judea		Grey, grey-yellow dolomite	185.9	1082.0			Santonian
							Coniacian
		Grey dolomite, white marly dolomite, gypseous bands of green arenaceous shale and green marl	131.1	1213.1			Turonian
							Cenomanian
		Grey marl, dark-grey dolomite, grey-pink arenaceous dolomite	13.7	1226.8		Lower	
Aassalir	Jurassic	White and dark-grey gypsum and anhydrite alternating with black marl	209.4	1436.2	Jurassic	Middle	
Mulussa		Grey dolomite with anhydrite inclusions alternating with black marl and black and white anhydrite. In the lower part grey, light-grey and yellow-grey dolomite alternating with grey-green marl. Possible unconformity	316.4	1752.6		Lower	

Data of Syrian Oil Company for the Dbayyat well					An interpretation of Dbayyat well on the basis of the geological survey on the 1:200,000 scale under Contract 944 (1961)		
Formation	System	Lithological and faunistic characteristic	Thickness, m	Depth from surface, m	System	Series	Stage
Amanus group	Triassic	Green and white ferruginous sandstone alternating with green and red shale. Red shale, arenaceous clay, blue shale, grey and red sandstone, grey dolomite in the lower part. Unconformity	519.7	2272.3	Triassic		
	Permian	Brown and blue shale, arenaceous clay; bands of red and purple, shale, grey dolomite, sandstone and limestone. Fauna: *Ostracode pormien, Hollinella* aff. *nevensis*	150.9	2423.2	Permian		
	Carboniferous: Middle and Upper Pensilvanian	Grey sandstone, blue shale, limestone bands with brachiopods and crinoids. In the middle and lower parts blue micaceous shale, grey-brown and red-purple shale, thin limestone bands, green and white sandstone. Fauna: *Pentagonocyclopae* aff. *diapar*	123.4	2546.6	Carboniferous	Upper	
	Lower Pensilvanian	Blue and grey shale, limestone bands, white and grey-green sandstone. Several thin coal bands at the base. Fauna: *Fusulina, Productus, Bryozaires, Bairdia auricula Knight.*	135.6	2682.2		Middle	
	Mississippian	Black shale, sandstone, arenaceous clays	51.8	2734.0		Lower	



Lithological signs

1 — limestone; *2* — chalky limestone; *3* — dolomitized limestone; *4* — dolomite; *5* — marl; *6* — dolomitic marl; *7* — clay and clayey varieties of rocks; *8* — siltstone; *9* — sand and sandy varieties of rocks; *10* — sandstone; *11* — conglomerate; *12* — basalt, diabase; *13* — silicite; *14* — opoka; *15* — gypsum; *16* — phosphate; *17* — glauconite; *18* — limonite and ferruginous rocks; *19* — flint, barite, iron and calcareous concretions; *20* — microfossils; *21* — bedding: thin, medium, thick, coarse and massive; *22* — unconformities; *23* — stratigraphical units boundaries. Number of strata on the left, thickness in metres on the right



The Sharifeh well log
Geological age (in the opinion); subdivisions of previous investigators

Fig.2.12 Sharifeh borehole (from Technoexport,1966).

Table 2.2 The Palaeogene system.

System	Series	Subseries	Zone (subzone) and its index	The mapped units and their indexes adopted for sheet I-37-XV	Division of Paleogene sediments of the territory of the USSR which is close to the West European division
Paleogene	Oligocene		Almaena taurica Pg_3al	Oligocene Pg_3	Oligocene
	Eocene	Upper	Globigerina corpulenta Pg_2^3cp	Upper Eocene Pg_2^3	Upper Eocene
		Middle	Truncorotaloides rohri Pg_2^2r	Middle Eocene Pg_2^2	
			Hantkenina alabamensis Pg_2^2al		
			Acarinina rotundimarginata Pg_2^2rt		
			Acarinina bullbrooki Pg_2^2bl		
		Lower	Subzone Acarinina pentacamerata Pg_2^1p	Lower Eocene Pg_2^1p (subzone Acarinina pentacamerata)	Middle Eocene
			Subzone Globorotalia aragonensis Pg_2^1ar	Paleocene—Lower Eocene Pg_1—Pg_2^1ar	
			Globorotalia subbotinae Pg_2^1sb		Lower Eocene
	Paleocene	Upper	Globorotalia velascoensis Pg_1^2		Paleocene
		Lower	Globorotalia angulata Pg_1^1		

2.4 Phosphorite Deposits

Early information about the presence of phosphate formations in Syria was registered by Vautrin in Dubertret (1933) from observations near As Soukhneh, 25 km north-east of Palymra. Cayeux (1935, 1939) studied petrographically three of Vautrin's samples and gave the first brief description of the Syrian phosphorite. In 1960, Soviet geologists carried out detailed phosphate exploration work which has led to the discovery of several phosphorite deposits.

2.4.1 Distribution

The *most important phosphorite deposits of Syria* (Fig 2.13) are those of:

(1) - the Palymrides region, comprising Wadi Ghadir El Hamel area (45-60 km southwest of Palymra), As-Sukhneh (25 km northeast of Palymra), and Wadi Er-Kheime (60 km west-north-west of Palymra);

(2) - Ain Layloun (about 30 km east of the main coastal town Latheqiyeh); and

(3) - the Tarraq El Hbari-Abar Sijri deposits (in the Syrian desert 120 km southeast of Palmyra).

The stratigraphic column (Fig 2.14) shows several phosphorite horizons ranging in age from Upper Cretaceous to Middle Palaeogene. The principal commercial deposits are of Campanian-Maestrichtian age.

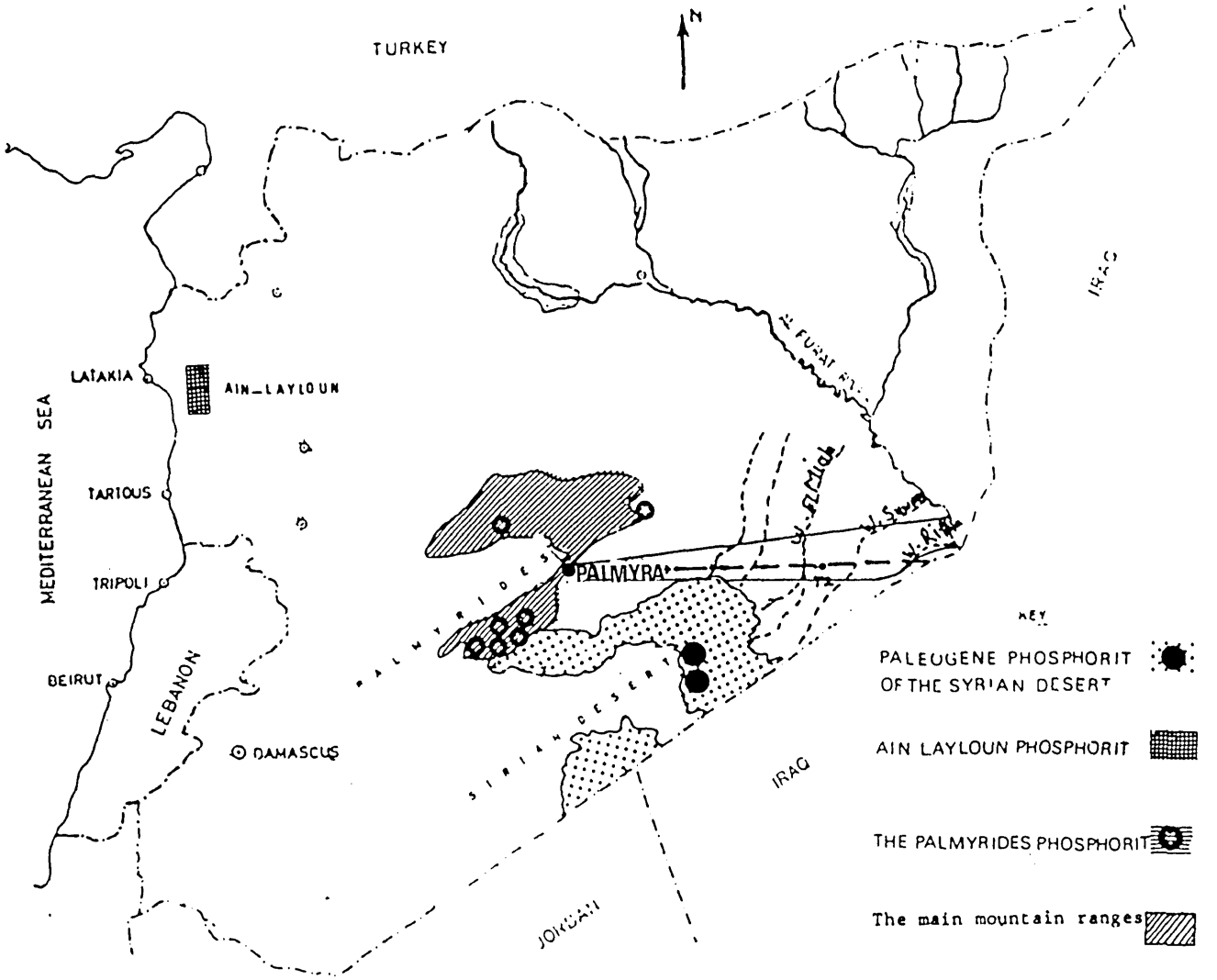


Fig.2.13 The major phosphorite deposits (modified after Atfeh, 1967).

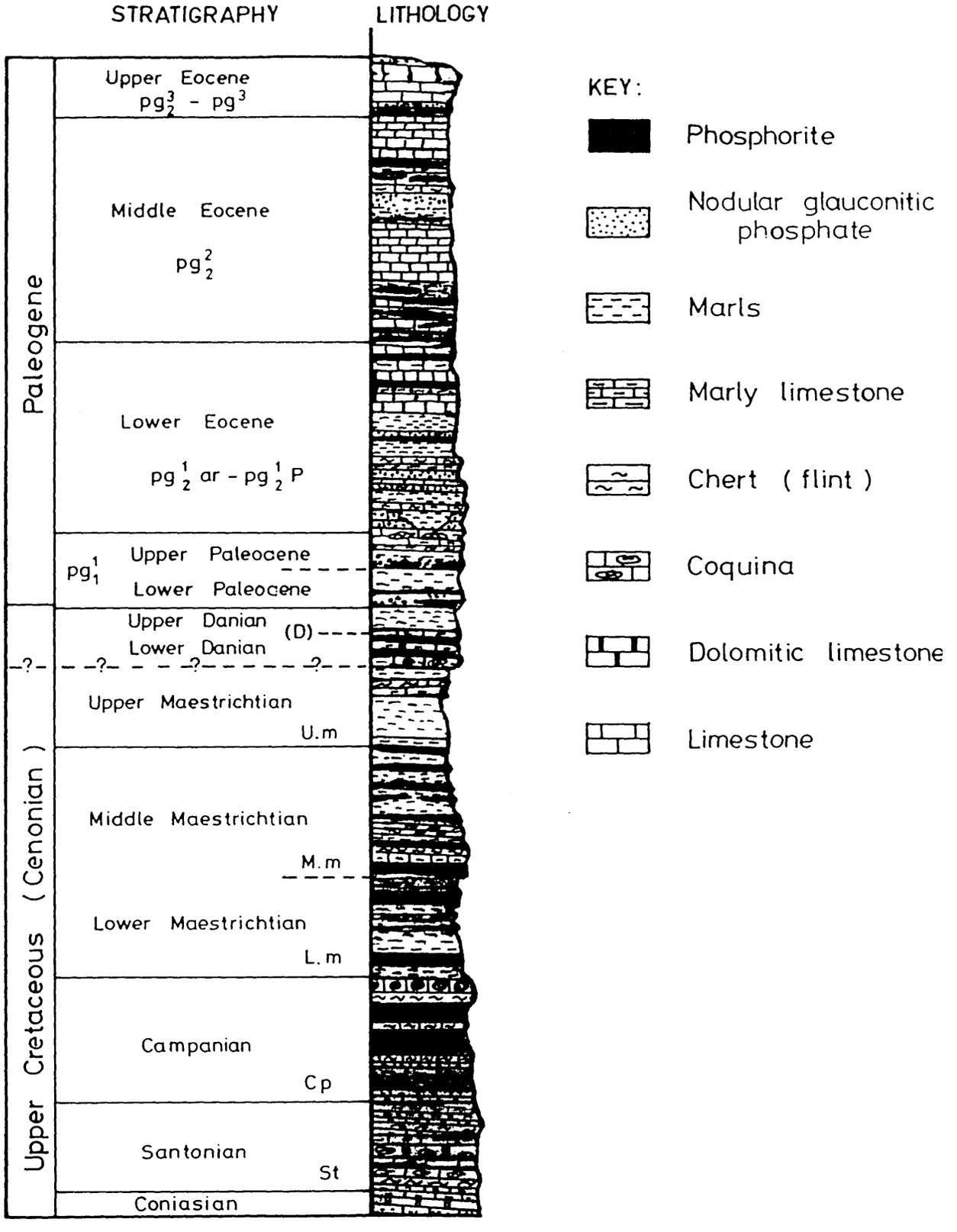


Fig.2.14 Distribution of the phosphorites in the stratigraphic column of the Palmyrides.

2.4.2 Types of Phosphorite

Syrian phosphorites are either compact solid, semi-compact or friable, and either the platform or geosynclinal type. Remarkable changes in lithology, reflecting nonuniform structure and increased tectonic activity associated with piedmont troughs and differential subsidence in the marginal basins of the northern slope of the Arabian platform, are especially pronounced in the Palmyrides phosphorites.

These phophorites consist of phosphatic grains (ovules), pellets, nodules, concretions (mainly of coprolitic origin) and elongated and angular particles of various organic fragments. Organic phosphate material is represented by bones, vertebrae, teeth, shells (Foraminifera and pelecypodes), sponge spicules and scales of fish. The size of concretions range from fractions of a millimetre to 15 mm; often they are cracked into fragments.

Four phosphorite varieties are distinguished in the Palmyrides according to their cement composition: calcareous, argillaceous, siliceous and mixed. The richest beds have a calcareous cement and are confined to the Upper Campanian-Lower Maestrichtian stages in the Palymrides. The phosphatic grains account for 65-80% of the rock and are 0.05 to 0.4 mm in size. They are made of slightly crystallized or amorphous, pure, brown to gold-brown phosphate minerals among which the most common are fluor-apatite, chlor-apatite, hydroxy-apatite, francolite (carbonate fluor-apatite) and dahllite (carbonate hydroxy-apatite). The term 'collophane' is also used to indicate the very finely

microcrystalline and crypto-crystalline apatite. The average P_2O_5 content of the Campanian - Maestrichtian phosphorite is about 24.5%, with the extreme values of 16 and 39.6%.

Within the study area, Palaeogene phosphorites occur as thin streaks (0.3m thick) and beds 0.7 to 4m thick of the nodular type or irregular lenses and non-persistent layers, with P_2O_5 content ranging from 6 to 15%. The cement is chalcedony, and glauconite in these deposits is an important rock-forming mineral. The quality and thickness of these phosphate beds improves in the Syrian Desert, forming a phosphorite bearing sequence.

2.4.3 The major Palmyrides phosphorite deposits

Only the Ghadir El-Hamel phosphorite field falls within the study area, and includes the deposits below:

(i) Khneifiss deposit, located at the southwestern end of Jabal El Abtar range.

(ii) Ash-Sharquieh (Eastern) deposits, located 45 km southwest of the town of Palmyra.

(iii) Al Abtar deposit which extends along the foot of the Al-Abtar mountain.

(iv) The Central deposit, located about 5 km south of the Khneifiss deposit.

(v) The Ghadir El-Hamel deposit, occupying the western flank of the

Ghadir El-Hamel valley.

2.5 Occurrence of Uranium

2.5.1 Review of previous work

Although no special systematic geochemical prospecting for uranium has yet been carried out, some preliminary geological and geophysical investigations were reported to explain the presence of secondary U minerals, and their special association with phosphorite.

In an early attempt to investigate the possibilities of uranium mineralisation in Syria, Drovenik (1957) pointed out that a suite of deep faults accompanying the Dead sea fault could have made passageways for the migration of uranium mineralising fluids. Such fluids might have been generated from the basement. Abdul-Moneim (1959) conducted air-borne radiometric surveys at an altitude of 15-30 m over the country. Thirteen anomalies were recorded, ten of them within the Palymrides region. This was followed by radiometric ground checking and follow up investigations by Syrian and Egyptian geologists, which revealed negative results at the time. However, the exact position of the airborne radiometric traverses was not adequately known, since the airborne survey lacked the use of a tracking camera.

Hussein (1961) and his Egyptian co-workers investigated these radiometric anomalies, and they came to the conclusion that the secondary uranium minerals responsible for radioactive anomalies

are closely connected with phosphorite beds.

Technoexport geologists from the USSR, using radiometric methods, recorded many uranium occurrences during the geological mapping of the territory of Syria. Atfeh (1964) summarised this Russian work.

Western Knapp Engineering (WKE, 1963) reported an average of 130 and 70 ppm U for Khneifiss and Sharquieh (Eastern) phosphorites deposits, respectively. These results were obtained by chemical analysis carried out at Battelle Memorial Institute (Ohio, USA) during the first stage of evaluation and beneficiation tests for those phosphorites.

Atfeh and Faradzhev (1965) examined the radioactive nature of the Syrian phosphorite. They defined, with the help of drill logs, the depth, thickness and structure of the phosphorite layers.

Evaluation of the U content of the Palymrides phosphorites and some other occurrences was by the Soviet experts. Liaschenko and Tatarnikov (1968), who carried out local ground radiometric checking, sampling and radiometric analysis. Their recommendations for subsequent work speak of the necessity for further investigations for uranium.

In a review of all previous data available at the time, Atfeh (1970) emphasised the very localised nature of the uranium occurrences. He reported the Russian analytical results for uranium in the phosphate to vary between 30 - 210 ppm. Although Atfeh took

the view that Syria is a "uranium bearing province", he concluded that possibilities for uranium enrichment other than in phosphate are not good.

Hunting Geology and Geophysics (1975) reviewed all the previous data and conducted fieldwork and measurements in operating mines. They found that the relationship of P_2O_5 and radioactivity is indeed indirect (Fig 2.15) and the relationship of P_2O_5 and U_3O_8 is not linear. They demonstrated that in the phosphate samples containing above 22% P_2O_5, uranium increased almost by an order of magnitude more than equivalent P_2O_5. The report also pointed out that the possibility of the occurrence of concentration processes similar to those forming the uranium deposit at Yeelirrie, Australia, encourages a systematic search in surficial materials and sedimentary basins. Hunting noted that[a] geochemical search for uranium would also provide the opportunity to seek other minerals or elements as well.

The study by Mouty et al.(1983)which included the auther,was accompanied by radiometric measurements along the geochemical cross-sections; the only significant anomaly found was in Jabal Om-Jorn area with readings within one very limited area exceeding 100-fold of the natural background,and was subsequently recorded by geologists of the GEGMR.

Early in 1982,the author also carried out ground radiometric checking in the region and along the oil pipeline extending towards the border with Iraq. Two types of scintillometers were used, one (SAPHYMO SRAT SPP2), producing total count, and the other a multi-channel spectrometer (Scintrex GIS4). Several radiometric

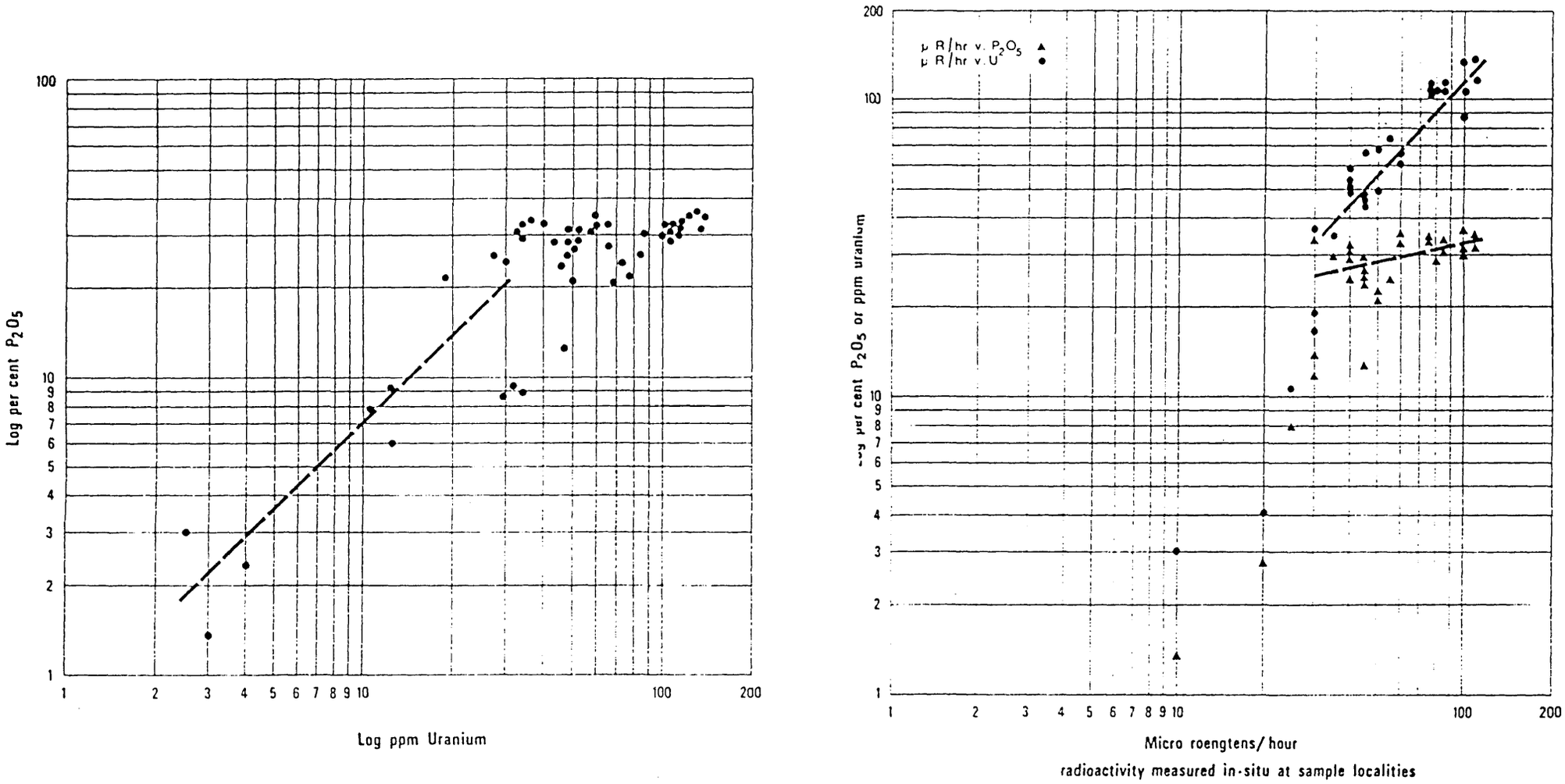


Fig.2.15 The relationship of U, P_2O_5 and the radioactivity (from Hunting, 1975).

anomalies were recorded in areas where there is no obvious phosphorite, especially within the Palaeogene (Jubeli, 1982). Furthermore, a study of gamma logs of 21 bore-holes in an adjacent Basin (Jubeli et al., 1982) revealed that 80% of the significant gamma anomalies (more than sixfold of the natural background) were confined to argillaceous limestone rocks of Palaeogene age and the other 20% to younger sediments mainly of Neogene age.

2.5.2 Observations during current research

In the course of the present fieldwork, numerous new occurrences of secondary uranium minerals were encountered along various traverses covering the study area (Fig. 2.16). The most important ones were found to extend a few tens of metres in Jabal Om Jorn within intensively faulted zones. The same features were found in areas of Jebel Tabaque, J. Al Abtar, J. Bassiri, J. Hayyan, J. Qal, J. El Bardeh and in several other localities, especially in the wadis draining the eastern part of Ad-Daww basin. Also, they were found in southeastern Al Qaryatein and in J. Abou El Fawaress, west and northwest of Palmyra. Secondary uranium minerals were found to be patchily distributed and disseminated, particularly in phosphorites, clayey calcareous glauconitic rocks, organic-rich limestone, and caliche-like or gypcrete crusts. Fractures and fissures were filled with bright-yellow to yellow and greenish yellow powdery coatings of uranium minerals, which also penetrate into the pores of the rocks (see Plate A).

It was obvious during the present work that the majority of U manifestations were confined to the Upper Cretaceous and Upper

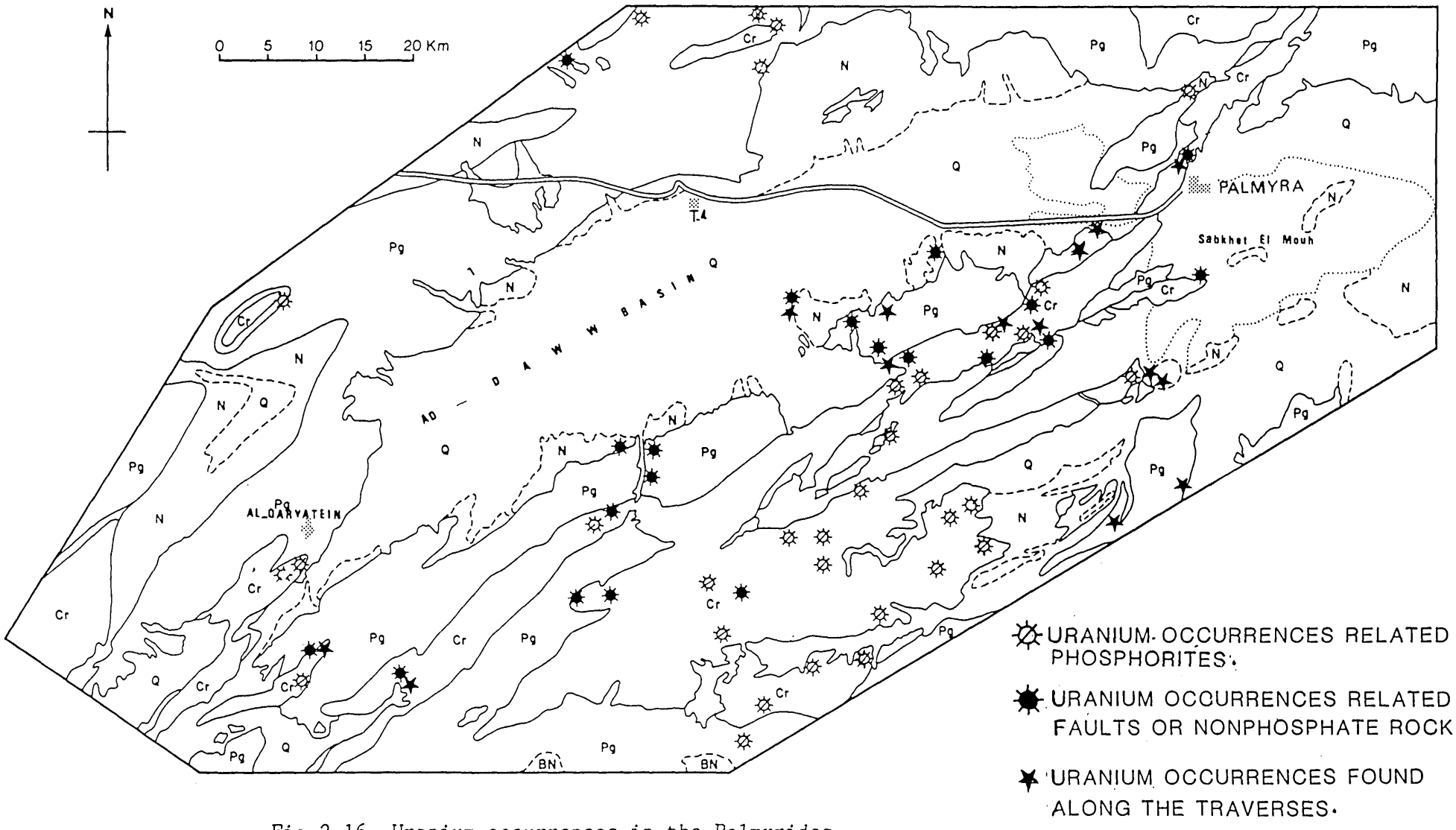


Fig.2.16 Uranium occurrences in the Palmyrides.

Palaeogene-Lower Neogene. An apparent relationship between secondary uranium mineralisation and certain lithotypes resulted in grouping the occurrences as follows:

(a) occurrences associated with phosphorite;
(b) occurrences possibly associated with phosphatic or clayey glauconitic limestones;
(c) occurrences associated with organic-rich carbonate rocks; and
(d) occurrences associated with gypcrete and calcrete-like duricrusts.

However, except for the nearby phosphorite deposits, no clear evidence of a primary uranium source was linked to the showings of uranium minerals.

CHAPTER III

3. PHYSIOGRAPHY

3.1 General

The region under investigation covers the territory of the Al-Qaryatein sheet (I-37 XIV), with exception of its extreme north western corner, and the western part of the Palmyra sheet (I-31 XV) of the geological map of Syria, scale 1:200,000. The total surveyed area is in excess of 9000 km^2. It is bounded by latitudes 34° 00 and 34° 45' North and longitudes 37° 00 and 38° 30' East. It occupies the major upland part of central Syria.

3.2 Topography

Three types of relief can be distinguished in the region and are illustrated in Fig. 3.1.

(a) The first is the Palmyrides ranges which have a fairly rugged topography and occupy 15% of the area. They are represented by Southern, Northern and Central belts.

(i) The Southern Palmyrides mountains are linearly elongated ranges with an elevation of 1000 to 1400m above sea level. These ranges consist of monoclinal horsts with asymmetric slopes and slightly flattened, narrow watersheds coinciding with the apex of the mountains (see Fig. 2.7). The Southern Palmyrides ranges extend in a northeasterly direction across the whole central part of the region. The main orographical features of this part are shown in Fig. 3.2.

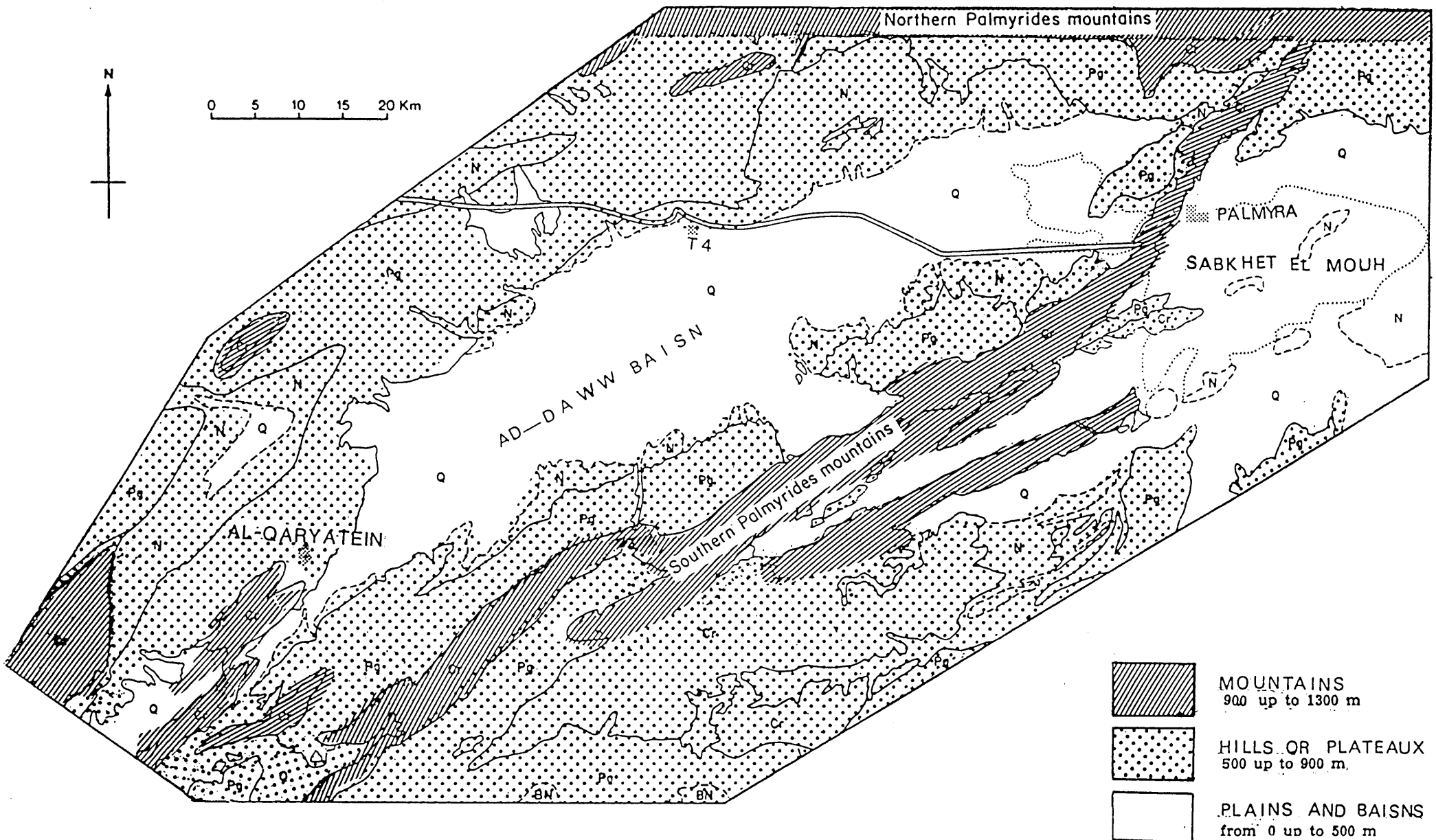


Fig.3.1 The major topographic features of the region.

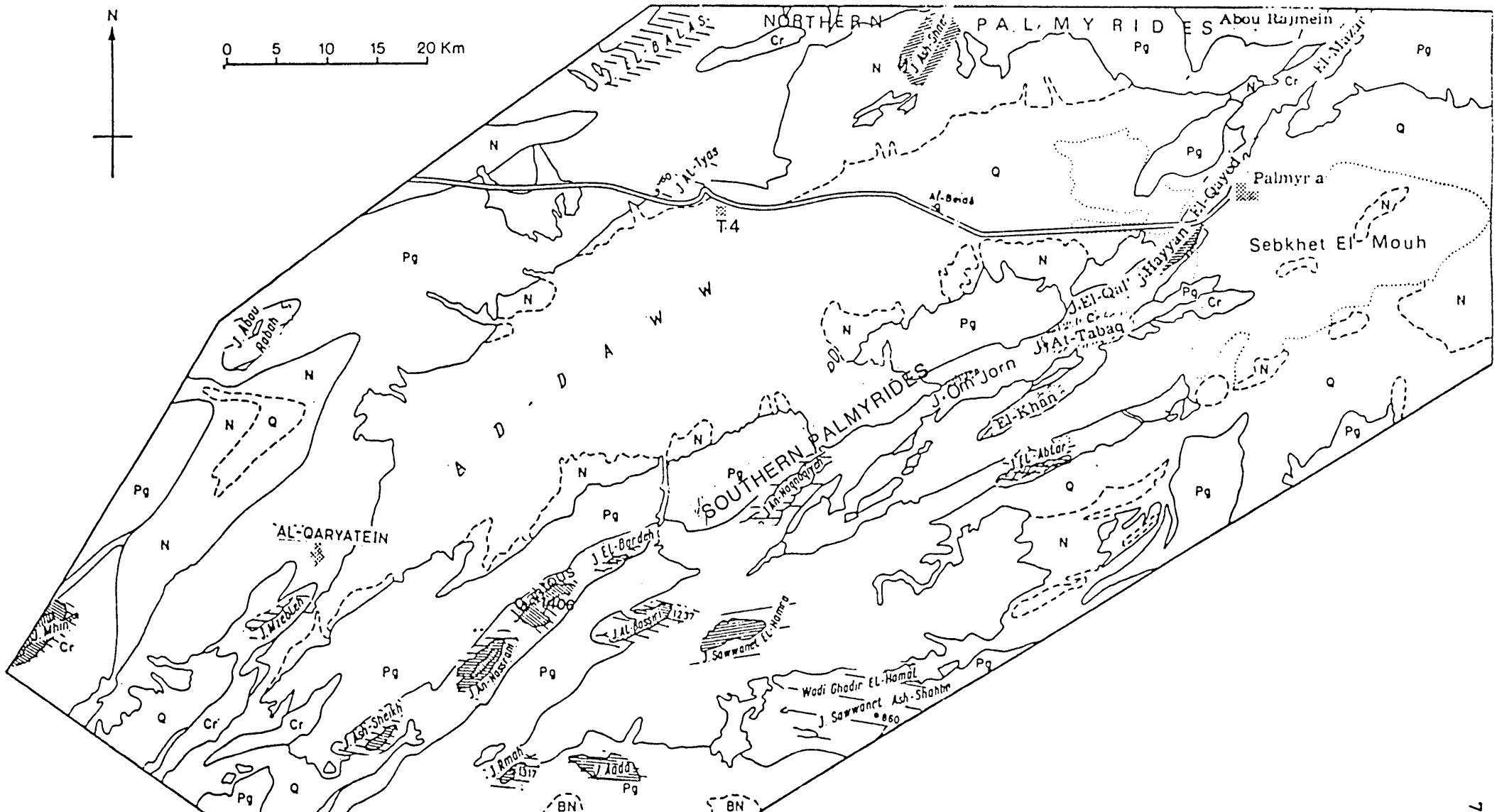


Fig.3.2 Various mountains of the Palmyrides.

Ghantous forms the highest mountain (1,406m) while, the most important ranges are; Jabal Hayyan, J.Qal, J.Tabaque, J.Om Jorn, J.Naqnaqueih, J.Abtar, J.Bassiri, J.Bardeh, J.Nassrani, J.Rmah, and Jabal Mehsseh.

(ii) The Northern Palmyrides belt is characterized by a developement of large, gently dipping brachyform uplifts and anticlinal folds. The folds run sub-latitudinally, with the exception of some minor folds that are genetically associated with faults and have northeasterly and northwesterly trends. The largest ranges are, from west to east: Jabal Balaas (1036m), J.Shoumariyeh (1060m), J.Shaer (1260m), J.Abou Rajmein (1350m) and J.El.Mazar (900m). They extend along their axes for 25 to 30km. The cross sections of the folds are box or coffer-like (Plate 1).

(iii) The Central Palmyrides consists of relatively low ranges, slightly asymmetrical, broad anticlines. The principal antiforms in this belt are: Jabal Abou Rabah, Tyas anticline and Jhar brachyanticline, all of which have northeasterly trending axes. The dips in the northwestern limb are between 5° and 20° while the southern limb is generally more steeply inclined with an average dip of 30°, and it is partly faulted.

(b) The second type of relief found in the southern part of the study area is formed by a few plateau-like escarpments, with an average elevation of 780 to 1000m and a steeply dipping slope to the south (Aida and Ash-Shahba plateaux). The Aida plateau, its name derived from the highest point of the plateau





Plate 1 Typical box and coffer like southern palmyrides fold (J. Al Abtar).

(1,287m), is a steeply sloping high cliff with an average rise of 250m above the general land surface. The Ash-Shahba plateau has a lower elevation with slopes gentler than that of Aida. Between these two plateaux and the mountainous range of the Southern Palmyrides, flat-topped hills of Sawwanet El Hammra are located. Similar hills are found in the western part of the region such as Sharifeh and Turaq Ghor hills. This type of topography occupies 40% of the total area.

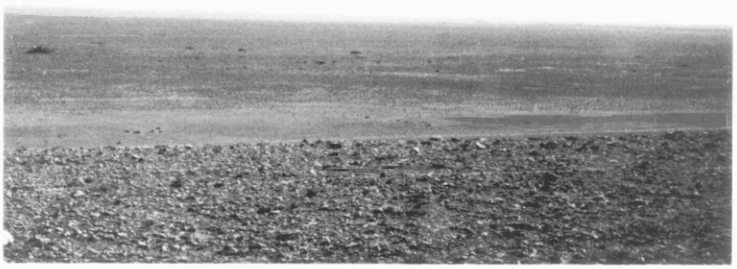
(c) The third type of relief is represented by two plains of flat topography with gentle undulations reflecting the position of Ad-Daww and Sabkhet El Mouh (Playa) basins (Plate 2), and it occupies the remaining 35% of the region. The Ad-Daww basin is an intermontane synform located between the Northern Palmyrides in the north and the Southern Palmyrides in both the east and the south. It has a flat relief extending in a north-easterly direction across a distance of 120km from the south of Al-Qaryatien town to the north-western suburbs of Palmyra town, where the two Palmyrides belts merge together. The minimum elevation in this basin is 450m above sea level. Its southern flank is very gentle with dips less than 8°, while the dip of the northern flank increases to about 20° and reaches a maximum of 40° in some localities. The axis of the basin is shifted towards the north-western limb. In general, it is a large closed basin with no permanent drainage. However, its sides especially the eastern and northern ones, are intensively dissected by erosional valleys and dry wadis (Plate 3).

The second flat plain relief is found in the area occupied by

A



B



C



Plate 2 General views showing the flat topography of Sebket El Mouh (Playa) close to its dry sides (A and B); in C, the southern palmyrides ranges can be seen in the western horizons of the Playa.

A



B



C



Plate 3 General views showing part of Ad Daww basin (A); the extreme northeastern part where the two palmyrides mountain belts intercept (B) and the eastern side where a few weathering rills are developing towards wadis(C).

Sabkhet El Mouh Playa. It has an elevation of 370m above sea level. The central part consists of a drying lacustrine basin, hills are scattered in the basin rising between 10 and 15m above the general present day plain surface (Plate 4). Sebkhet El Mouh is an asymmetrical basin with a sharply uplifted northern limb, where the beds dip 60° to 70°, while the southern limb has a very gentle dip of 2° to 3°. The surface of the central part is usually flooded in winter and wet to very wet in summer; high salinity limits the growth of vegetation (Plate 4.B).

3.3 Climate

3.3.1 General

The present climate of the survey area is semi-arid in the north-western part and arid to extremely arid in the southern and eastern parts. It is that of a continental desert with hot summers and cold winters. However, the presence of very long and wide wadis and historical evidence e.g. Roman dams, irrigation channels and gardens of Palmyra indicate wetter periods in the historic past.

3.3.2 Temperature

The annual average temperature is $18.4^{o}C$ to $19.3^{o}C$, but with a great seasonal variation (Table 3.1). The hottest months are July and August, when temperatures reach $44^{o}C$, and the coldest months are December and January, when the minimum temperature is about $-1^{o}C$ and $-6^{o}C$ to $-9^{o}C$ in exceptional cases. There is also a remarkable difference between daily maximum and daily minimum

A



B



Plate 4 The surface of a dry portion of Sebkhet El Mouh looking towards J. Hayyan (A); the northern part of the Playa towards the gardens of Palmyra (B); restricted vegetations can be found when getting close to the Playa.

Table 3.1 Annual average temperature, 1970–1981.

STATION	1970	1975	1979	1980	1981
Damascus	16.7	16.1	17.2	16.2	16.5
Palmyra	19.0	18.4	19.3	18.5	18.8
Lattakia	20.1	19.1	19.9	19.3	19.7
Aleppo	17.9	17.1	18.1	17.1	17.9
Al-Kamishli	19.1	18.5	19.3	18.5	19.0
Deir-ez-Zoor	20.1	19.4	20.5	19.5	19.8

Table 3.2 Average maximum and minimum temperature for the year 1981.

STATION	YEARLY TEMPERATURE IN °C											
	ABSOLUTE MIN.			ABSOLUTE MAX.			DEV. FROM MEAN	AVE-RAGE MIN.	DEV. FROM MEAN	AVE-RAGE MAX.	DEV. FROM MEAN	AVE-RAGE
	MONTH	DAY	°C	MONTH	DAY	°C						
Damascus	Dec.	10	-4.6	Aug.	4	42.0	-0.2	8.0	+0.1	25.2	-0.1	16.5
Palmyra	Jan.	14	-0.8	July	26	43.6	+0.8	12.6	-0.2	25.6	+0.1	18.8
				Aug.	1	43.6						
Lattakia	Jan.	1	5.4	Sep.	25	38.2	+0.3	16.2	-0.1	23.0	+0.1	19.7
Aleppo	Jan.	1	-1.0	July	27	43.0	+0.4	11.7	-0.2	23.9	+0.7	17.9
Al-Kamishli	Feb.	3	-0.5	July	15	44.5	+0.8	13.2	0.0	25.3	+0.1	19.0
				Aug.	1							
Deir-ez-Zoor	Jan.	1	0.1	July	27	44.6	+0.5	13.6	-0.6	26.4	0.0	19.8

temperatures (Table 3.2).

3.3.3 Winds

In Fig. (3.3) rose-diagrams of different winds are illustrated. The air circulation which controls the timing, amount and place of precipitation in Palmyra has a westerly and west-northwesterly direction. The usual speed of the wind is 17 to 21 knots but it can reach 40 to 50 knots on some days. Such winds may cause dust and sand storms. Other weather phenomena are listed in Table (3.3).

3.3.4 Precipitation

There is a scarcity of rainfall over the whole year (Table 3.4). However, the average annual rainfall varies from one year to another (Table 3.5). It can be estimated as 106 to 150mm in the lowland areas and it increases to 200mm on the mountain ridges (Fig. 3.4). Precipitation is brought by winds from the Mediterranean Sea. However, the wind is generally intercepted by the mountains of Lebanon on which much of their moisture content falls, and therefore the air currents arrive dry at the inland Palmyrides region. Nevertheless the wettest period of the year is that of mid-November to mid-January with December being the wettest month and January having the maximum humidity. In summer time, particularly in July and August, there is no rainfall whatsoever.

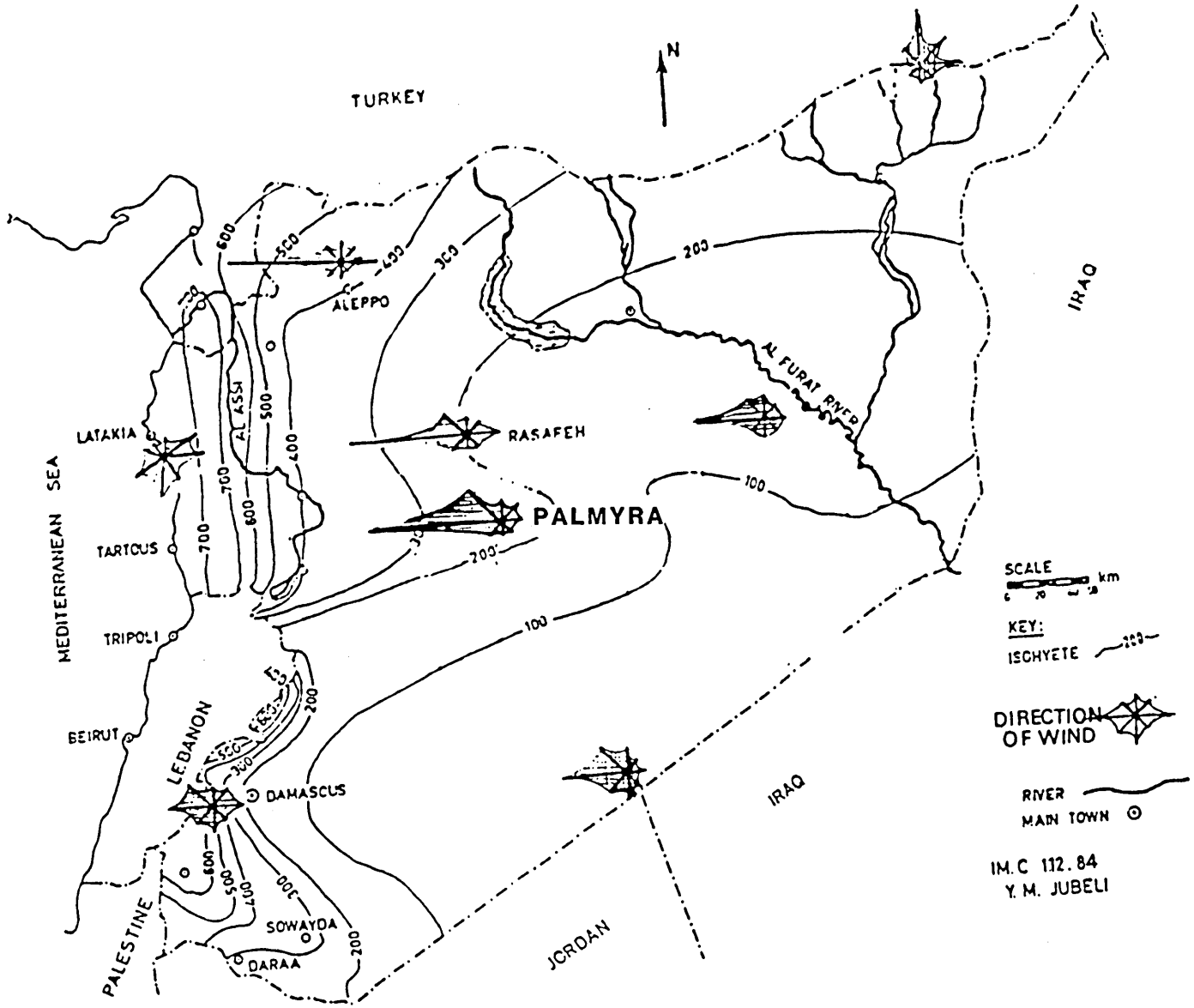


Fig.3.3 Rose diagrams of the winds.

Table 3.3 Atmospheric presure, hours of sunshine and average daily evaporation for the year 1981.

STATION	DAILY AVERAGE EVAPORATION (mm)	AVERAGE HOURS OF SUNSHINE	ATMOSPHERIC PRESSURE IN mbs	
			DEV. FROM MEAN	AVERAGE
Damascus	5.6	8.7	- 0.1	942.4
Palmyra	7.1	8.4	- 0.2	965.9
Lattakia	3.7	7.6	+ 1.3	1011.9
Aleppo	4.2	7.8	+ 0.8	967.6
Al-Kamishli	6.0	7.9	+ 0.1	959.0
Deir-ez-Zoor	5.7	8.3	- 1.2	986.2

Table 3.4 Precipitation and weather phenomena for the year 1981.

STATION	NO. OF DAYS WITH:					PRECIPITATION IN mm						
	DUST/ SAND STORMS	THUNDER STORMS	HAIL	SNOW	RAIN	MONTH	QUANT.	MONTH	DAY	QUANT.	% OF MEAN	YEARLY TOTAL
Damascus	6	9	0	0	42	Mar.	44.8	Mar.	25	29.2	144	168.9
Palmyra	7	10	3	0	43	Mar.	64.0	Apr.	15	20.9	144	185.3
Lattakia	0	46	0	0	87	Jan.	488.2	Jan.	26	56.4	87	1006.6
Aleppo	1	16	0	0	85	May	82.5	Nov.	11	27.0	119	399.1
Al-Kamishli	1	7	1	1	77	Mar.	102.7	Mar.	27	33.5	102	478.8
Deir-ez-Zoor	2	6	0	0	58	Feb.	52.7	Dec.	24	24.2	119	200.7

Table 3.5 Annual precipitation (mm), 1970-1981.

STATION	1970	1975	1979	1980	1981
Damascus	147.0	155.3	283.3	161.0	168.9
Palmyra	76.1	133.9	127.0	127.0	185.3
Lattakia	647.5	898.6	925.4	557.8	1006.6
Aleppo	182.1	306.6	322.6	334.2	399.1
Al-Kamshli	225.4	442.9	394.6	567.1	478.3
Deir-ez-Zoor	124.0	197.9	143.0	174.2	200.7

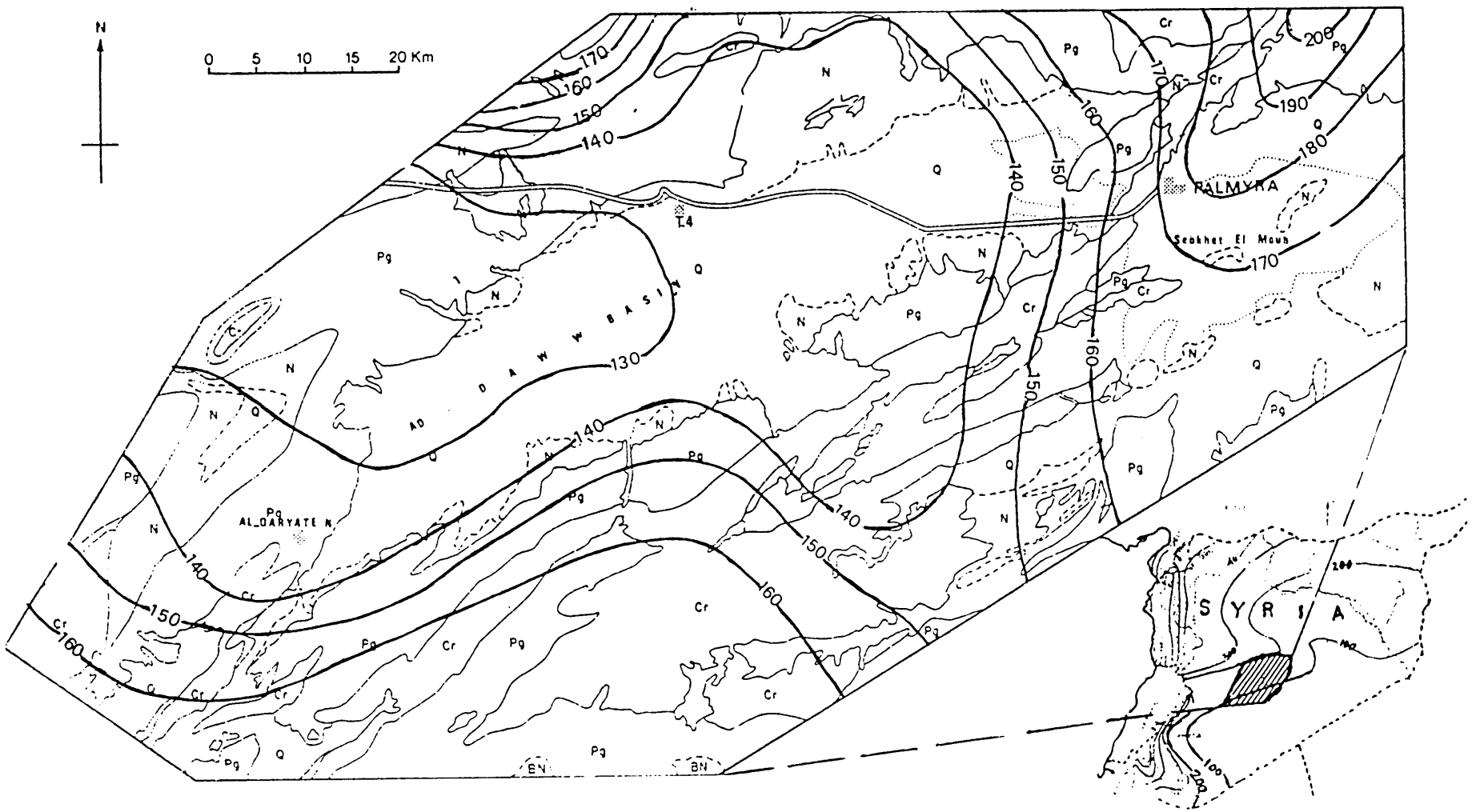


Fig.3.4 Isohytee of the Palmyrides and Syria.

3.3.5 Vegetation

Vegetation is typically stony desert and semi-desert grass and shrubs. In spring, the surface in the flat land and mountain sides changes to green steppe. Some permanent farms with olives, grapes and fruit trees, as well as oases of date palms, are found around the main settlements and near permanent springs and wells. Elsewhere vegetation is absent.

3.3.6 Animals

Except for the flocks of sheep, herds of goats and camels, the main animal species in the region are rodents, reptiles (especially snakes), birds, jackals, wolves, foxes and hyenas.

3.3.7 Population

The great majority of the people live in the main towns such as Palmyra and Al-Qaryatien. A few small villages are found along the four highways connecting Damascus and Homs with Palmyra and the phosphorite mining district. Miners live in two mining villages, namely Khneifiss and Ash-Sharqueh. Other settlements exist, the most important of which is the Tias village with the T.4 oil pumping station on the pipeline from Kirkouk (Iraq) to Banyas (Syria) and Tripoli (Lebanon).

3.4 The Geochemical Environment of the Palmyrides

3.4.1 General

The prevailing climate and topographical conditions favour subaerial surface and near surface weathering and erosion. Although weathering can be classified into three main types (namely, physical, chemical and biological), biological weathering is of very limited extent due to the scarcity of biological activity.

3.4.2 Physical Weathering

Field evidence leaves no doubt about the general effectiveness of thermoclastis (rock fracture) caused by solar heating then cooling. In fact, among the different agents of physical weathering acting in the area such as temperature, night frost and winds, the first is considered to be the main factor.The large daily ranges of temperature as well as the annual ranges (Tables 3.1 and 3.2) are responsible for the breakdown of the rocks by insolation processes whereby alternate heating and cooling are confined directly to the bare upper layers of the rock surfaces.

3.4.3 Chemical Weathering

Although the arid environment imposes constraints on the relative effectiveness of the chemical decomposition of the rocks, the limited amount of precipitation can still generate slow chemical changes. The main reactions involved are oxidation, hydration and hydrolysis. The limitations to chemical weathering in

the study area apply particularly to the complex reactions of hydrolysis, mainly due to the very short-lived contact between the water and the rocks caused by both the excessive evaporation or high relief. Such limitations however, do not seriously affect the hydrolysis of the carbonates (which dominate the area)

$$CaCO_3 + H_2O \longrightarrow Ca^{2+} + OH^- + HCO_3^-$$

Another limitation is the aggressiveness of weathering solutions, which tend to be weakly alkaline in reaction due to the said hydrolysis of carbonate.

Carbonation, on the other hand, is a very important process of chemical weathering of limestones and dolomites. The carbon dioxide of the atmosphere dissolved in rainwater can act as a weak acid, which converts calcium carbonate into soluble bicarbonate. This then is removed, causing decomposition of the carbonate rocks, and leads to the development of solution holes (sink holes or dolines). The continuous action of carbonation processes on and under the surface of the massive limestones has created many Karst features. It is worth mentioning that during this process the liberation of carbon dioxide increases the solvent power of the water and makes the reaction more vigorous.

Hydration is another conspicuous chemical weathering process in the region whereby anhydrite (calcium sulphate) takes up water, resulting in the formation of gypsum. This occurs in beds at certain horizons, and is accompanied by expansion which causes additional stresses within the rock. This is noticeable especially in the Triassic-Jurassic series as well as the younger evaporites.

Finally oxidation reactions, although slow, are very effective, the superficial uranium ochre of bright canary yellow minerals found at different depths indicates that oxidizing conditions extend more than 5 or 10m under the surface cover.

3.4.4 Combined effects of physical and chemical weathering in the Palmyrides

In general, the relative resistance of certain rock types under desert conditions differs from that in humid regions. Physical strength rather than chemical stability determines resistance to denudation. Therefore, the limestones and calcareous sandstones, normally subject to dissolution, are more resistant in the prevailing dry environment. Indeed, the removal of the different products of weathering from the mountain ranges is very fast, while the hillfoot is often the zone of waste accumulations. In contrast with evidence of the earlier humid periods, the present day rate of weathering is much reduced.

3.5 Erosion and Transport

3.5.1 General

Weathering products in any environment are very important as geochemical sample media. Among the weathering products mentioned by Rose et al. (1979) secondary U minerals, wadi sediment, overburden and water soluble products were used in this research.

3.5.2 The Effect of Wind

The movement of rock debris is subject to a variety of processes in which both erosive and transport effects are simultaneously active. The nature of the movement of particles by the wind can be distinguished as three types: suspension, saltation and surface creep.

Sandstorms which may rise hundreds of metres into the air are usually composed of very fine (dust) particles in the upper parts and of sand particles in levels near to the ground. Therefore, there is an erosive effect at the ground surface and a transport effect which extends over large areas and to considerable distances. Two main forms result: sand ripples (west of Palmyra); and sand ridges (west, southeast and east of Palmyra). The process of deflation of the finer constituents of the weathering products from the area probably accentuates the dominance of coarse waste. This results in what is termed stony desert Hammad (Fig.3.5).

The significance of the wind action to the present geochemical research is that it may cause dilution and/or depletion of any geochemical anomalies or it requires extreme care in sampling, sieving and retaining the appropriate fraction size.

3.5.3 The Effect of Rain Water

Rainfall, although very infrequent, is usually heavy or, indeed, extremely heavy during short periods of time. Track roads become impassable for a few days and asphalt roads are damaged. The

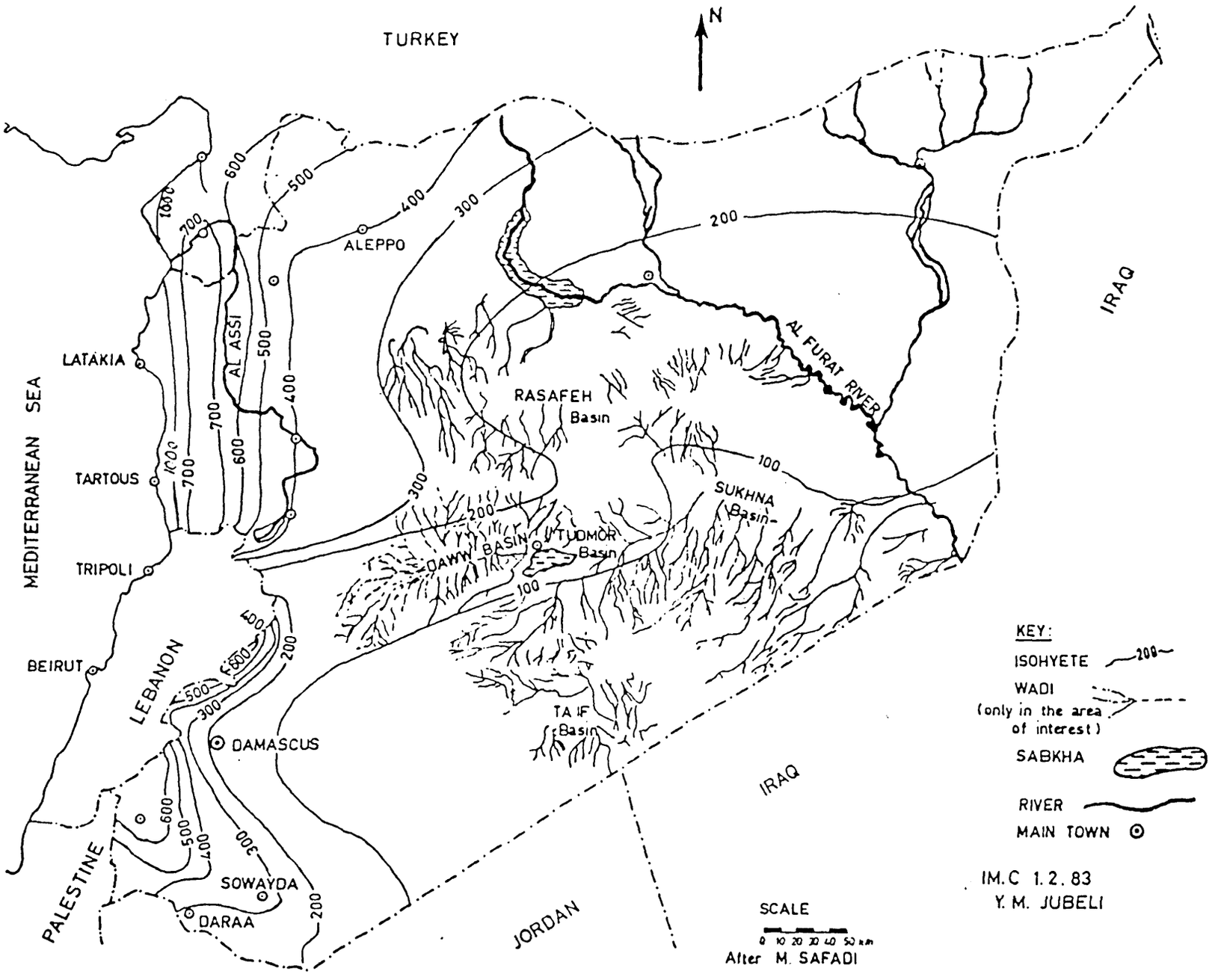


Fig.3.5 Pleistocene and recent drainage basins.

rate of rise of floodwater in normally dry watercourses is, in many cases, extreme, and have been termed streamfloods. They are rare and of short duration, but the amount of work in terms of transport and erosion of which they are capable is enormous. Fragments of all sizes up to great boulders may be carried until the flood subsides. The load is often transported out of the upland wadis and spread out as fans or cones at the upland margins. These floods constitute a significant agent of erosion in this environment at the present time, and their relative importance is greater than that of floods of humid temperate regions.

A second type of run off flow usually occurs in the flat lying areas which may be completely covered with a sheet of moving water (sheetflood). The main action of this type is transport. In this region the integration of the drainage patterns is so good that practically every sector can be assigned to one or another of the Pleistocene drainage basins (e.g. W.El Luweizeh is related to Sabekhet El Mouh basin; Al-Abyad, El-Jzel and Az-Zakarra to Ad-Dawwa (the deepest northeastern part of the Ad-Daww basin) as shown in Fig.(3.6).

3.5.4 Landslides

Very occasional landslide movements of catastrophic type can cause far more change than other movements. The escarpments west of Jabal Rmah, J.Aida and Sawwanet Ash-Shahba south of Palmyra and Jabal Antar northwest of Palmyra and various other places in the Palmyrides show a number of dislocations, which are probably slipped masses under gravitational effects along sliding surfaces.

Some of them are very large and probably displaced 30 to 50 m downslope.

3.5.5 Drainage

Permanent surface streams are absent in the Palmyrides region. However, the drainage is represented by dry valleys (wadis) and discharge hollows. The larger valleys in the uplands typically consist of narrow, V-shaped steep-sided valleys. Such valleys often have steep longitudinal gradients with a fairly regular down-channel increase in depth up to 8m and in some rare cases up to 25m. In the hilly areas, wadis are connected, close-branching and have clean, rocky channels in the headwaters, passing down-valley into gravelly and sandy floors. Drainage density and channel frequency are proportional to rock hardness. Close texture of first order rills are widely developed on soft marls and marly limestones especially west of J. El Bardeh and on the weak calcareous sandstones and clayey limestones all over the region. Many of the main wadis are confined to faults or fault zones under the plains.

3.5.6 Soil

Soils occur in the flat-lying areas as a brown and reddish variety, reflecting the oxidizing nature of the desert surface. In some localities a grey grassland type of soil has been found. The soil cover, however, is generally very thin with much rock debris. In Sabkhet El Mouh and the Ad-Daww basin a silty loam and silty-clayey soil attains important development and has an

alkaline pH.

Mountain ranges, especially those south of Jabal Hayyan, are practically devoid of any soil cover.

Aeolian sands can be found in the slopes of a few hills in the northeastern part of the Ad-Daww basin, and around the Sabkhat and Palmyra town.

3.6 Characteristics of the surficial geochemical environment of the Palmyrides

3.6.1 Principal features

The first principal feature of this geochemical environment is the formation of clastic rock cover composed of colluvium, alluvium, prolluvium and lacustrine deposits. The thickness and texture of this cover varies considerably from a few centimetres to about 4m in areas of high to moderate relief, and up to 20 to 30m in depressions and intermontane basins. The main dispersion mechanism for most of the elements is clastic, this type of dispersion is characterized by short paths and ubiquitous aeolian dilution.

Further, chemical, decomposition of the rock fragments takes place under conditions of abundant free oxygen. In such an oxidizing environment, leaching and redistributing of most of the elements may occur. The products of this leaching may be preserved in restricted soils, or may evaporate, precipitate or can travel downwards into the groundwater.

The second important feature of the geochemical environment of the Palmyrides is the formation of both veinlets and indurated crusts of calcrete (caliche) and gypcrete.These have been found in northeastern and southeastern parts of the Ad Daww basin and in the shallow channels of a few wadis in Om Jorn and J.Qal, and in part of the Ad-Daww basin adjacent to these areas. Elsewhere in the world (e.g. Yeellirie (Australia), Texas (USA) and the Namib Desert (Namibia)), such formations are hosts to uranium mineralization, and therefore some background on their occurrence is given below.

3.6.2 Formation of the duricrusts

Calcrete, gypcrete and, to a lesser extent, dolocrete are formed as horizons of lime enrichment and cementation under arid to semi-arid climatic conditions. Calcrete is generally formed near the surface above the water table as a residual horizon. Evolved profiles incorporate the various stages in upward succession in which laminar crusts may reflect several cycles of calcrete formation. The illuvial and pedogenic character of the calcrete is commonly indicated by a downward decrease in compactness and lime content, and by the occurrence of more soluble substances such as gypsum at greater depth (Fig.3.7).

3.6.3 Brief review of the factors of calcrete formation

Calcrete development and mode of formation has been the topic of many research workers. According to Blake (1902), one of the

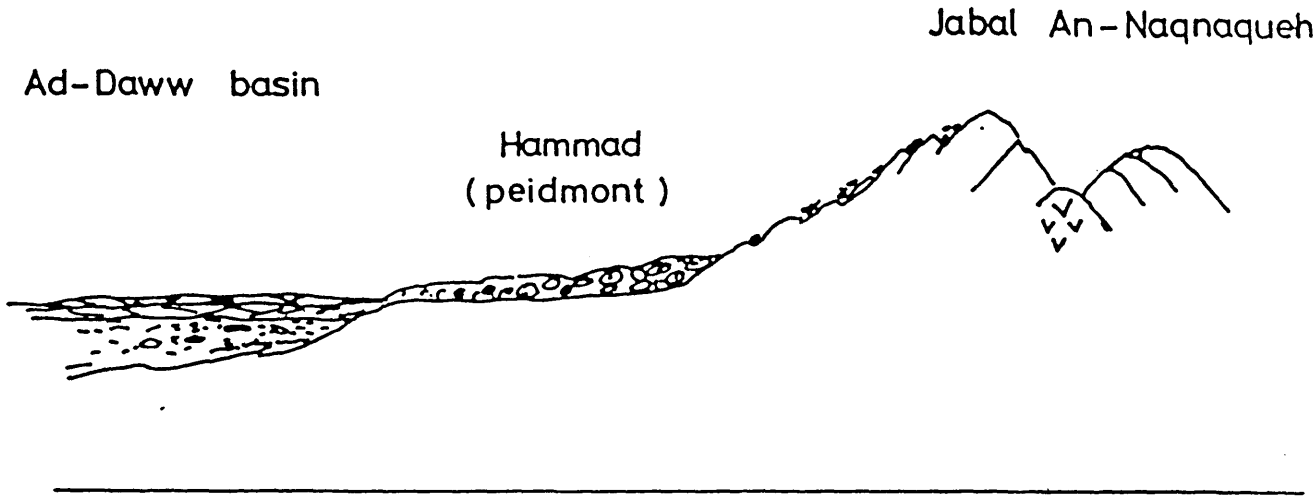


Fig. 3.6 Piedmont and stoney desert formation in parts of the Palmyrides Region.

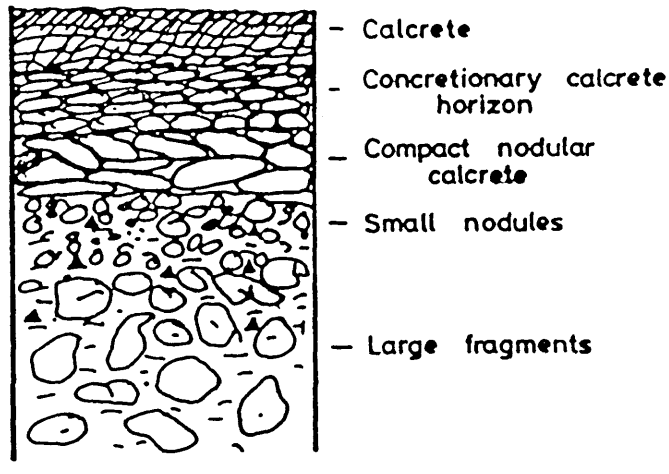


Fig. 3.7 Schematic Representation of Calcrete Profile.

first to apply the term caliche duricrusts, caliche was found as a result of the upward capillary flow under rapid evaporation of carbonate-rich waters within a generally dry regime. Regarding the effect of the annual amount of rainfall, Molls (1958) stated that if precipitation is high, $CaCO_3$ would then be leached out, producing only a very thin crust. Blank and Tynes (1955) however pointed out that calcrete was a deposit formed as a result of a process of in situ redistribution of $CaCO_3$ within a limestone formation, rather than one of addition of $CaCO_3$ from another source. Emphasizing the role of moisture, Watkins (1967) suggested an annual rainfall of 250 to 750mm for the formation of the duricrusts. Moreover, James (1972) noted that too little moisture allows only surface accumulation of carbonate while too much water causes considerable leaching of soluble materials. Goudie (1973) agreed with James on the mechanism of calcrete development and Read (1979) described the petrological constituents as accumulations of low-magnesium calcite associated with other secondary minerals. During the seventies Friedman et al. (1971), Kahte (1977) and Klappa (1979) added the role of biological factors whereby micro-organisms such as fungi, bacteria and algae are thought to play an important role in precipitation of calcareous and non-calcareous duricrusts.

Under these controls, calcrete, gypcrete and dolocrete occur in wide range of valleys, deltaic playa and lacustrine settings. They are characterized by groundwater transport and shallow subsurface precipitations of elements including V, K and U in association with authigenic carbonate and sulphate minerals under oxidizing and chemically complex regime (Carlisle, 1978, and 1984;

Butt et al. 1984; Otton, 1984; Mann and Deutschen, 1978; and Hambleton-Jones, 1976, 1984).

3.6.4 Classification of calcretes and U favourability

Netterberge (1969, 1978a) defined calcrete as pedogenic or non-pedogenic terrestrial material which has been cemented or replaced by calcium carbonate, however, Carlisle (1978, 1984) considered the non-pedogenic as the only one containing recoverable concentrations of U (economic calcrete). According to him a critical distinction must be made between two types of calcrete when U exploration is concerned.

1- Pedogenic calcrete such as: soilcaliche, crote calcare, kunkar, nari or caprock, which generated by ordinary soil forming processes and is not favourable for U mineralization.

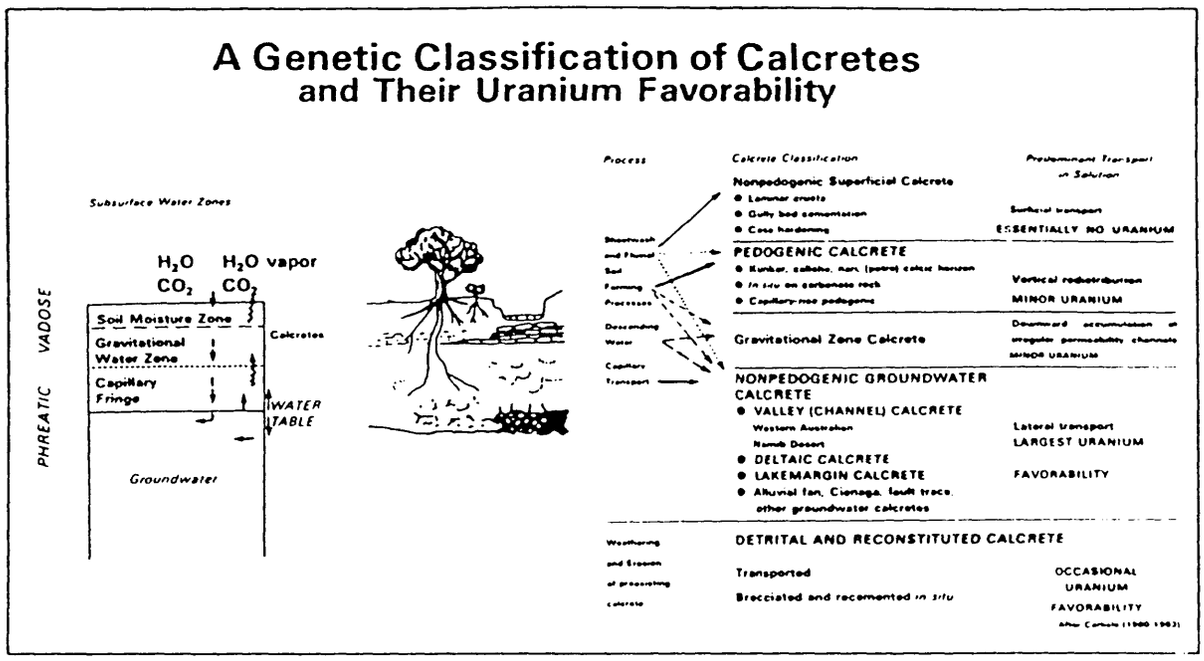
2- Non-Pedogenic = groudwater calcrete is generated mainly close to the water table from groundwater moving along low gradients. In most cases this type may contain appreciable amounts of recoverable U, hence Carlisle used the term economic calcrete. Based on the above criteria, a genetic classification is presented in Table 3.6 and Fig. 3.8, and the worldwide distribution of these calcretes is shown in Fig. 3.9.

3.6.5 Duricrusts of the Palmyrides

In the study area, gypcrete and calcrete formations were first reported by Technoexport (1967), during their studies of the

Table 3.6 Genetic classification of calcretes (from Carlisle, 1978).

Class	Process	Uranium favourability assuming a source
1. Pedogenic Calcretes	Authigenic cement concentrated vertically within a soil profile.	
a) Illuvial Calcrete	Precipitation of cement within the soil moisture zone after downward transport and evapotranspiration. Equivalent to calcic or petrocalcic horizon.	Very low to negligible.
b) In Situ Calcrete	Cement is derived from subjacent rock or sediment by insitu weathering.	Low.
c) Capillary rise pedogenic Calcrete	Rare variety derived by capillary rise from stagnant groundwater over a wide area without significant lateral transport.	Low.
2. Non-pedogenic Calcrete	Authigenic cement introduced to host by non-soil forming processes.	
a) Groundwater Calcretes	Externally derived cement from laterally moving groundwater, fluvial contributions may be large.	
I. Valley Calcrete		
i. Western Australian	Precipitation of cement within the soil moisture zone and/or capillary fringe by capillary rise from a shallow groundwater table, influenced by bedrock morphology.	High in areas of constriction and upwelling of groundwater. Destroyed by dissection and leaching.
ii. Namib Desert	Precipitation of cement within the capillary fringe or gravitational water zone from a changing water table.	
II. Deltaic Calcrete	Precipitation as in Ii. above but with lacustrine clays and hypersaline pore water causing groundwater to slow and approach the surface. Downdrainage $\pm$ of valley calcrete.	Low in mature, elevated deltas. High in recent deltas with zones of upwelling.
III. Groundwater Lacustrine Calcrete	Precipitation by a variety of processes. May be related to deltaic calcretes.	As above.
IV. Other Groundwater Calcrete	e.g. "Cienega" calcrete from groundwater seeps.	Unknown
b) Gravitational Water Calcrete	Deposition of authigenic cement from waters descending through the gravitational water zone with varying amounts of lateral transport.	Low to moderate. May facilitate carnotite reconcentration.



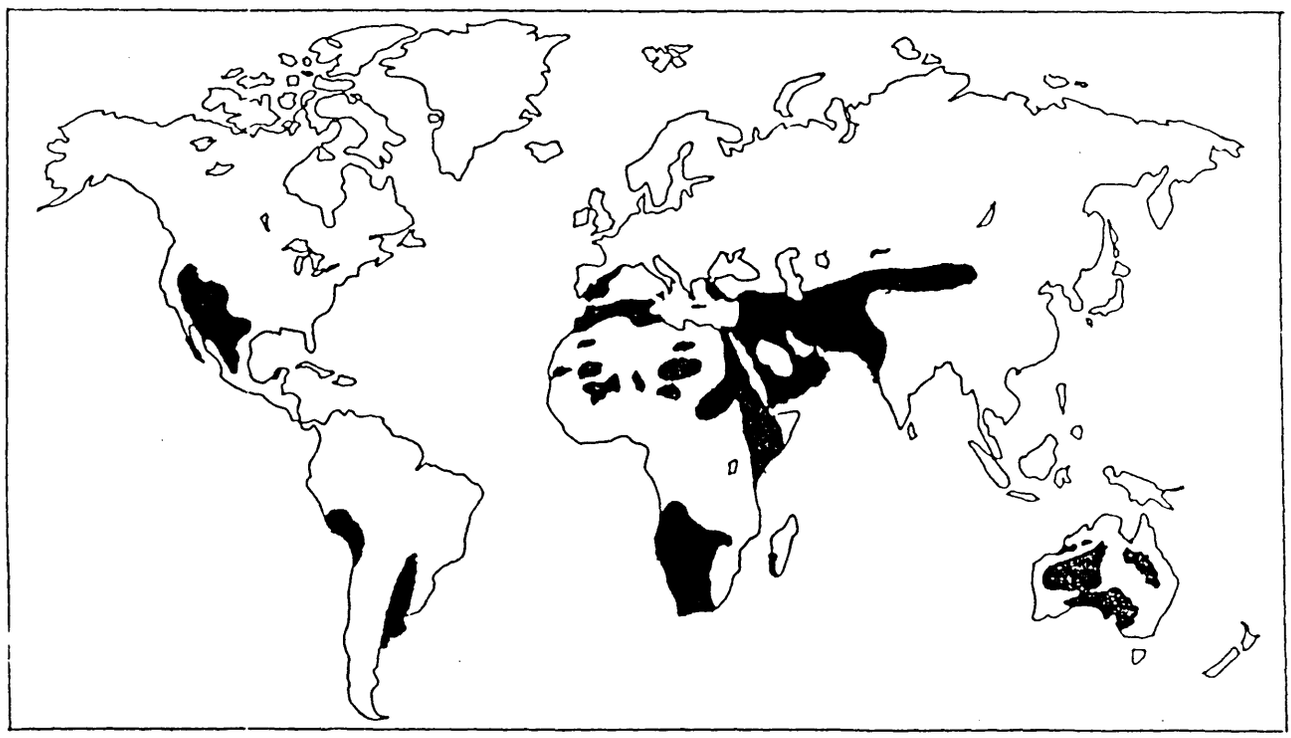


Fig.3.8 Genitic classification of calcretes , their U favorability and world wide distribution.

eluvial deposits of Syria. These crusts have been defined as a very compact (concrete) mantle, the thickness of which varies from 0.1 to 1.5m. The base of the crust is always separated from the bedrock by a fine-earthy pillow. The age of these duricrusts is mainly Lower Quaternary (Pleistocene).

In the course of the present survey, the calcrete and gypcrete crusts and veinlets seemed to be found in areas where the rain water is insufficient to induce significant downward leaching of materials, and upward movement of mineral solutions containing both calcium sulphate (gypsum) and calcium carbonate (calcite).

Evaporation of uraniferous solutions under these conditions plays a role in the concentration of uranium in these calcrete, gypcrete and similar crusts in the Palmyrides region.

CHAPTER IV

4. SAMPLING, ANALYSIS AND DATA PROCESSING

4.1 General

Geochemical prospecting in Syria is a recent development. Therefore an orientation (pilot) geochemical survey was considered necessary to overcome the difficulties arising from the lack of sufficient prior geochemical knowledge.

4.2 Sampling

4.2.1 The region selection and orientation survey

During the period mid-November to mid-December 1982 a preliminary survey aimed at defining a suitable region for further work was carried out; a certain amount of orientation work was incorporated in this survey and for convenience it is referred to as the orientation survey (although it is not solely orientation in the more conventional use of the word in exploration geochemistry. The choice of the field areas for this survey was based on the following criteria:

(a) accessibility to the area;

(b) availability of representative geological materials;

(c) the existence of known uranium mineralizations.

A total of 72 geochemical orientation samples of rocks, wadi sediments and residual detrital overburden was collected from two areas:(a) the Southern Palmyrides; and (b) Eastern Syria.

The latter region comprises mainly the northern parts of the Syrian desert, adjacent to the oil pipeline of the Iraq Petroleum Company (IPC), from the Palmyrides to the border with Iraq (see Fig.1.1).

A few mineralized localities as well as background areas were sampled. Planning of the sample collection was done on Syrian topographic maps of scale 1:50,000 with the help of geological maps of scale 1:200,000, Photogeological maps made by the B.R.G.M. (France) with an approximate scale of 1:50,000 were also used where coverage was available.

Wadi sediments were sampled up to 800m north and south of the intersections of a few major broad wadis with track roads running parallel to the oil pipeline. In general 80% of the materials collected were coarser than 2mm in size.A composite sample from each site was collected in a polythene bag, sealed with sellotape, numbered and placed in another numbered cloth bag.

Three items of equipment were used to sample the overburden as shown in Plate (5). These were a steel corer, 1.5m long, a hand auger and a hammer.

It is worth mentioning that a major part of the orientation field work was carried out under rainy and stormy weather conditions. This was unavoidable due to time constraints.

Sketch of the Steel Rod Corer.

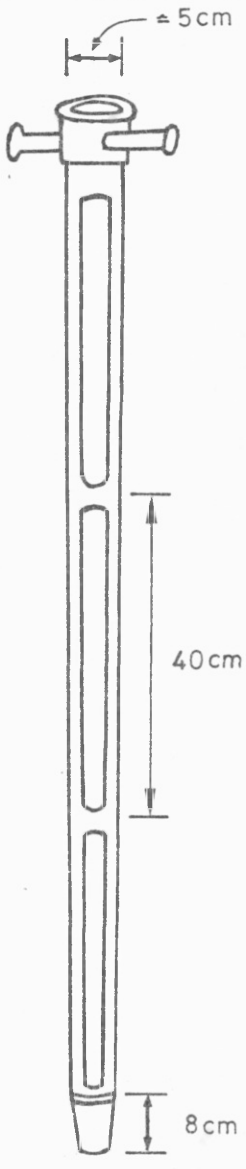






Plate 5 Sampling tools (steel corer, hammer and auger with three channel spectro_scintillometer for insitu radiometric measurements.

4.2.2 The reconnaissance survey

Following the execution of the orientation studies, a reconnaissance sampling programme was carried out during the period of mid-August to mid-October 1983 in the Southern Palmyride region, sampling mainly rocks. In addition, subordinate hydrogeochemical, detailed wadi sediment and playa sediment surveys were carried out.

The region was divided into three geological and physiographical provinces namely: the Palmyride Mountain ranges; the Ad-Daww basin; and the Sabkhet El Mouh playa. Each of these provinces has to be considered separately, because in each, different sample type was collected.

Nine traverses across the first two provinces were designed to be sampled as normal as possible to the general strike of the bedding. Rock samples along each of the nine traverses were collected and placed in polyethylene bags, which were in turn placed in cloth bags, with double labelling. The traverses were selected to cover the whole area and every effort was made to obtain samples representative of each lithological unit crossed by the traverse. Composite chip samples were taken from each wide but homogeneous unit; some mineralized horizons were also selectively sampled. Only five samples were collected from Jurassic, lower and middle Cretaceous sequences since they are of no interest to this study being older than any phosphorite formations.

Unequal intervals between sample sites were sometimes adopted in order to avoid sampling aeolian sands or other wind-deposited

materials.

Seventy-two samples were collected on a square grid from the third district, namely Sabkhet El-Mouh. The sediments were taken by hand auger and steel corer, generally from a depth of 30cm. A sampling density of one sample per $4km^2$ was obtained from this area. A few sites were selected to test the vertical variability of uranium dispersion in the uppermost one metre of the playa surface. To this end, samples were collected at a maximum of three different depths: 0 to 25cm; 40cm; and 80cm. At some sites a composite sample (grabs from various depths) was taken. The materials were taken into polyethylene bags and placed into cloth bags with double labelling. Plate (6) shows the dry surface and the uppermost vertical section of the playa.

Detailed wadi sediment sampling was carried out in one of the wadis draining the north-western side of Jabal Om Jorm. This area was found, during the orientation survey, to have a notable secondary uranium occurrence and the highest radiometric anomaly ever recorded in this region. A total of 43 samples was collected along a distance of 1250m, in order to investigate the response in the wadi sediment to uranium dispersion from a known mineralized occurrence.

Finally, a total of 33 groundwater and spring water samples of 500ml was collected in acid-rinsed, hard polyethylene bottles. On arriving at each well site, water was allowed to flow for five minutes to clear the pipes. A sample bottle was rinsed by filling, shaking and emptying it three times; then it was filled with water





Plate 6 The uppermost profile of the Playa surface showing various layers of clay, salt, loam, gypsum, sandy loam and sands (A), salty water and salt can be seen in (B).

which was millipore filtered at the site through a 0.45 μm cellulose nitrate filter. The pH of the water (and sometimes the temperature) were measured separately on water coming out of the pipes after sampling. The filtered water was acidified with 10ml of 10% HNO_3 Analar grade. The bottle was held upright so that all the air bubbles were dislodged, then it was capped, sealed with PTFE tape, and labelled prior to shipping. Sampling of the groundwater sites was carried out within relatively short time to minimize any temporal variations and, as was expected during the sampling period (August to October), no rainfall was experienced.

Finally it is worth mentioning that radiometric measurements were taken in each of the sampling sites. Vents of radioactive vapour emissions (400 C.P.S.) occur in the southwestern portion of J.Abou Rabah fold which is cut by nearly vertical calcite veins and cracks.

4.3 Physical preparation of samples for analysis

4.3.1 The orientation samples

Soil and wadi sediment samples were oven dried at 80°C then disaggregated in a porcelain dish and sieved through four different mesh size nylon sieves. The 500-250 μm (-30 to +60 mesh), 250-150 μm (-60 to +100 mesh), 150-90 μm (-100 to +170 mesh) and -90 μm (-170 mesh) fractions were taken into self adhesive plastic bags. The rock samples were crushed and pulverized in an agate tema-mill to pass a 90 μm (170 mesh) sieve. The mineralized specimens were split into two parts: the first was pulverized for total rock

geochemistry and X-ray diffraction mineralogical studies; the second was cut and prepared for scanning electron microprobe and mineralogical identification studies.

4.3.2 The reconnaissance samples

Rocks were crushed and pulverized in a similar way to the orientation samples. Wadi sediments were dried at 80°C and sieved through a nylon sieve with retention of the minus 30 mesh (500 μm). The playa samples were also oven dried at 80°C, then gently disaggregated and sieved under clean conditions. Some samples were sieved through three different mesh size sieves to test the distribution of uranium in those fractions, bearing in mind that no playa samples were collected during the orientation stage. Similarly, the soil and overburden samples were dried and sieved with retention of the minus 30 mesh fraction. No further preparation was needed for the ground water samples at this stage.

4.4 Instrumental analysis.

A wide selection of elements needed to be determined to meet the first two objectives of this study and also because of possible associations with uranium either in particular mineral phases or types of deposits. These elements, the way(s) in which they were analysed and the attendant detection limits are listed in Table (4.1). The sample preparation and/or decomposition for each analytical method is different.

TABLE 4.1 List of the elements determined, the methods of analysis and the detection limits.

ELEMENT	METHOD OF ANALYSIS	DETECTION LIMIT
Major Elements		
Al	ICPAES	5ppm
Ca	"	5ppm
Fe	"	4ppm
K	"	10ppm
Mg	"	10ppm
Mn	"	1.5ppm
Na	"	5ppm
P	"	4ppm
Ti	"	6ppm
Trace elements and REE		
Ag	ICPAES	1ppm
As	AAS + ICPAES (Hydride)	0.2, 0.05ppm
Ba	ICPAES	0.5ppm
Be	"	0.05ppm
Bi	ICPAES (Hydride)	0.02
Cd	ICPAES	0.5ppm
Co	"	1ppm
Cr	"	1ppm
Cu	"	1ppm
La	ICPAES + INAA	1, 0.2ppm
Li	ICPAES	0.3ppm
Mo	"	1ppm
Ni	"	1ppm
Pb	ICPAES + AAS	5ppm
Rb	ICPAES	20ppm
Sb	ICPAES (Hydride)	0.04ppm
Se	ICPAES (Hydride)	0.06ppm
Sr	ICPAES	0.5ppm
REE	INAA	0.02 - 0.2ppm
U	INAA + Fluorometry	0.02 - 0.2ppm
V	ICPAES	0.5ppm
Te	ICPAES (Hydride)	0.012ppm
Th	INAA	0.8ppm
Zn	ICPAES	1ppm

4.4.1 Total chemical extracion and ICP analysis

The quantitative determination of the total concentration of elements in the sample was desirable. This was achieved for Li, Na, K, Rb, Be, Mg, Ca, Sr, Ba, Al, La, Ti, V, Cr, Mo, Mn, Fe, Co, Ni, Cu, Ag, Zn, Cd, Pb and P by weighing 0.1g of sample powder into PTFE testtubes. A mixture of concentrated acids (HNO_3 2ml, $HCLO_4$ 1ml, HF 5ml, AR grade) was then added to dissolve the samples under elevated temperature using an aluminium heating block. After completion of the attack, the dry samples were removed and allowed to cool prior to leaching for one hour at 70°C in 2ml of 6M HCl. They were transferred into 15ml plastic tubes with de-ionised water, made up to a final volume of 10ml and mixed thoroughly. The solutions were then analysed by nebulization into an Applied Research Laboratories ARL 34000C Inductively Coupled Plasma Atomic-emission Spectrometer (ICP) at the Applied Geochemistry Research Group (AGRG) "Webb Laboratory", Imperial College. The results for the major and trace elements determined by ICP were stored in computer files.

4.4.2 Hydride generation and ICP analysis

For the determination of arsenic, antimony, bismuth concentrations in the samples, samples were first ashed with $Mg(NO_3)_2$ according to the method described by Pahlavanpour et al. (1980b). Simultaneous ICP determination of As, Sb and Bi was subsequently performed using the hydride generation method in which sample solution and tetrahydroborate solution were pumped into the hydride generator (peristaltic pump and a separation cell). The

hydrides of As, Sb and Bi were flushed directly by argon carrier gas to the ICP previously mentioned (Thompson et al.,1978). Hydride generated As was determined also by AAS along with Pb in some batches.

The hydride procedure was also applied for selenium determination by ICP. In this case Se was first taken into solution with HNO_3 and $HClO_4$, according to the method of Pahlavanpour et al. (1980a). The selenium concentrations were then determined the same way as described for As, Sb and Bi

4.4.3 Uranium and rare-earth elements analysis

Uranium is routinely measured in various geological materials by the following methods: delayed neutron counting (DNC) (MacMurdo and Bowman, 1977; Kunzendorf and Løvborg 1981); fluorimetry (Grimaldi et al.,1954; Danielsson et al.,1973; McElhaney et al.,1978; Volesky and Ratsimandresy,1979); laser induced fluorescence (Robbins,1978; Robbins and Castledine, 1979); gamma-ray spectrometry (Adams et al.,1971; Killeen,1979, 1982); X-ray fluorescence (Smith and Lynch,1969; James,1977); instrumental neutron activation analysis (INAA) (Gordon et al.,1968; Plant, 1971; Plant et al.,1976; Bowman 1977) and neutron activation with fission track counting (Fleischer et al.,1975; Reimer,1975; Ward and Bonder,1979). It has been shown in many investigations that INAA is a powerful, sensitive and sophisticated tool, and should rather replace DNC if simultaneous determinations of U , Th and rare-earth elements are required.

4.4.3.1 Principles of INAA

The principles of activation analysis were described in detail by Koch (1960); Lenihan and Thomson (1965) and Miland (1976). In general, the procedure involves the irradiation and bombardment of a sample with a flux of neutron particles, which upon interaction, convert the elements in the sample to various radionuclides. Each radioactive product then decays by radiating energy of a type (particle or ray), intensity and with a half-life that are all characteristic of the decaying radionuclides. These parameters permit the identification of the elements originally present in the sample.

4.4.3.2 Application of INAA in this study

Determination of uranium, thorium, hafnium , scandium, tungsten and the rare-earth elements in the present study was by INAA. The procedure took advantage of the development of low energy, high purity, 7mm thick and an active area of 300mm^2 germanium (Ge) detectors with energy resolution of about 550eV at 122 KeV full width half maximum (FWHM), to develop a programme for simultaneous determination of the said elements. This involves precisely weighing 200mg of homogeneous sample powder into high purity irradiation polyethylene capsules. Those are in turn inserted into polyethylene containers; 10 - 11 samples into one container, along with two multielement standards of known concentration, one in each container, to give good counting statistics (Henderson and Williams, 1981; Parry, 1981). The USGS reference NIM-G, G2, GSP-1, and AGV-1 (in powder form) were also

irradiated and counted to monitor the accuracy of the analysis. In a few cases, the reference materials GXR-4, soil-5 (IAEA) and HRM2 were also used.

Samples, standards and reference materials were irradiated simultaneously under a thermal neutron flux of $1.1 \times 10^{12} n.cm^{-2}s^{-1}$. in the core tube of the 100KW "Consort" Mark II reactor (based on the swimming pool type), at the University of London Reactor Centre. The said materials were irradiated for one week, and measurement of the gamma spectrum was performed after a decay time of 3 to 5 days (since the high activity immediately after such a long irradiation prohibits instant measurement of the sample).

The Nuclear Data (ND) 6600 system with linear amplifier ADC and an LS 1-12 Basid analysing system was used with 2048 channels assigned to each spectrum. A 12 position automatic sample changer housing the intrinsic germanium detector provides sufficient separation of most of the gamma-ray peaks of the REE along with uranium. This unit is linked to the Nuclear Data Computing system. Distance between the sample and the detector was always adjusted manually to define sample position in order to avoid dead time with the ADC beyond 10%. Measuring time on each sample was 5400 seconds (90 min.). After the final spectrum has been accumulated and written to disc, the results are computed on line by linking together several sub-routines including the peak search programme to correct for decay time and spectral interferences. The ND peak search programme calculates the area (A), background, and $counts.s^{-1}$.

The concentration of each element in a sample is given by the

following formula:

$$X_{Un} = X_{Std} \cdot \frac{A(Unknown)}{A(Standard)}$$

X_{Un} = concentration of the unknown element

X_{Std} = concentration of the element in the standard

A = measurement of the area

The computer programme calculates the element concentration and reports it as μg/g (ppm) in a special file. In the present study, the 106.3 KeV peak of ^{239}Np was considered to be the most accurate and interference free of the uranium gamma peaks, thus, it was used for U determination.

4.4.4 Fission-track radiography

A fission track registration following irradiation under appropriate thermal neutron flux (5.111×10^{16} $n.cm^{-2}.s^{-1}$) was performed on a number of samples. The procedure was similar to the application of this method by Bowie et al.(1972), which in turn was based on that of Kleeman and Lovering (1967). Uncovered polished thin sections of rocks and grain mounts 1 in x 1.25 in in size were cleaned and overlaid with Lexan polycarbonate film, secured with adhesive tape and marked by scratching onto the reverse sides of the overlays registration marks and sample number.

The prepared samples were then stacked alternately glass to glass and plastic to plastic in an aluminium container and sent to be irradiated at Aldermaston Atomic Weapons Research Establishment.

Under the said neutron flux, uranium ^{235}U atoms will split as follows :

$$^{235}U + {}^{1}n \longrightarrow {}^{236}U \longrightarrow {}^{94}Sr + {}^{140}Xe + 2{}^{1}n + Y$$

This type of phenomenon was used by Fleischer et al.(1965) for uranium detection. The fission fragments so induced will bombard the overlay films causing structural damage (tracks). After a "cooling off" period of several weeks the adhesive tape was removed and the adhesive spots on the Lexan films were cleaned by methanol prior to etching them in a solution of 6N NaOH at $90^{o}C$ over a waterbath for 5 to 7 minutes, in order to convert the invisible damaged areas into visible tracks. This was followed by binocular and microscopic studies and microphotographic mapping of the fission tracks. The necessary work was then carried out for the correct identification of specific features in the studied thin section with corresponding areas on the fission track registration.

4.5 Suitability of the data produced

The most important quality of field data is location. This was achieved by plotting the sample site onto an overlaid field map which was later transferred onto a sample location map. On the other hand, analytical data should be reliable enough that interpretation can be based on geological and geochemical considerations. This can be achieved by careful checking of the procedure and the results obtained, and by evaluating the sensitivity of the method and the accuracy and precision of the data. Usually exploration geochemists have been more concerned with

sensitivity and precision than absolute accuracy. However, in the long running projects both accuracy and precision must reach a reliable level (Garrett et al.,1980). The quality of the present analytical data was monitored throughout the work in terms of accuracy and precision.

Accuracy can be monitored by the repeat analysis of a suite of control reference materials. However, the term accuracy is used to denote the extent to which the mean of repetitive analysis approaches the true preferred concentration or accepted value of the standard reference material or analyte (Thompson,1983). These reference materials were included at random to make up 10% of each batch and were either in-house (for the major and trace elements determined by ICP) or both in-house and international reference materials (USGS and IAEA for uranium, thorium and the rare earth elements). Two drawback points concerning the reference materials need to be clarified here: firstly they are not of exactly the same mineralogy and composition as the samples; and secondly, the particle sizes are different to those of the samples.

However, the accuracy achieved in INAA was remarkably good, as is shown in Fig.(4.1). Only those batches of results that were in good agreement with the accepted values of the reference materials were used in this study, other batches being repeated to obtain reliable results. The accuracy of the ICP analytical data are based on the use of two house reference materials (Fig. 4.2 and 4.3). If the reported values for the control reference materials fell outside the acceptable limits for one or more elements, the batch was rejected and subjected to reanalysis, or the source of

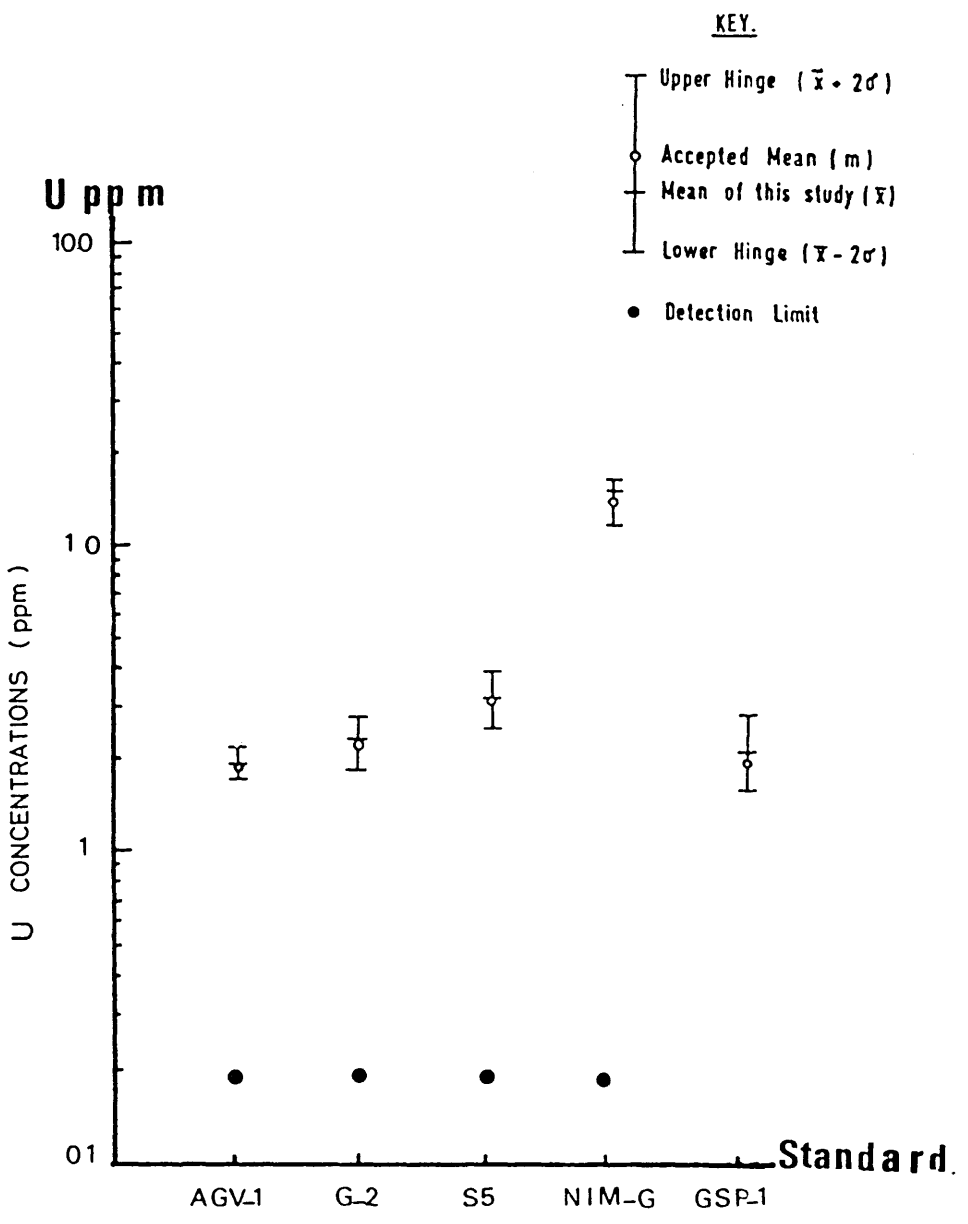


Fig.4.1 Accuracy of U determination by NAA.

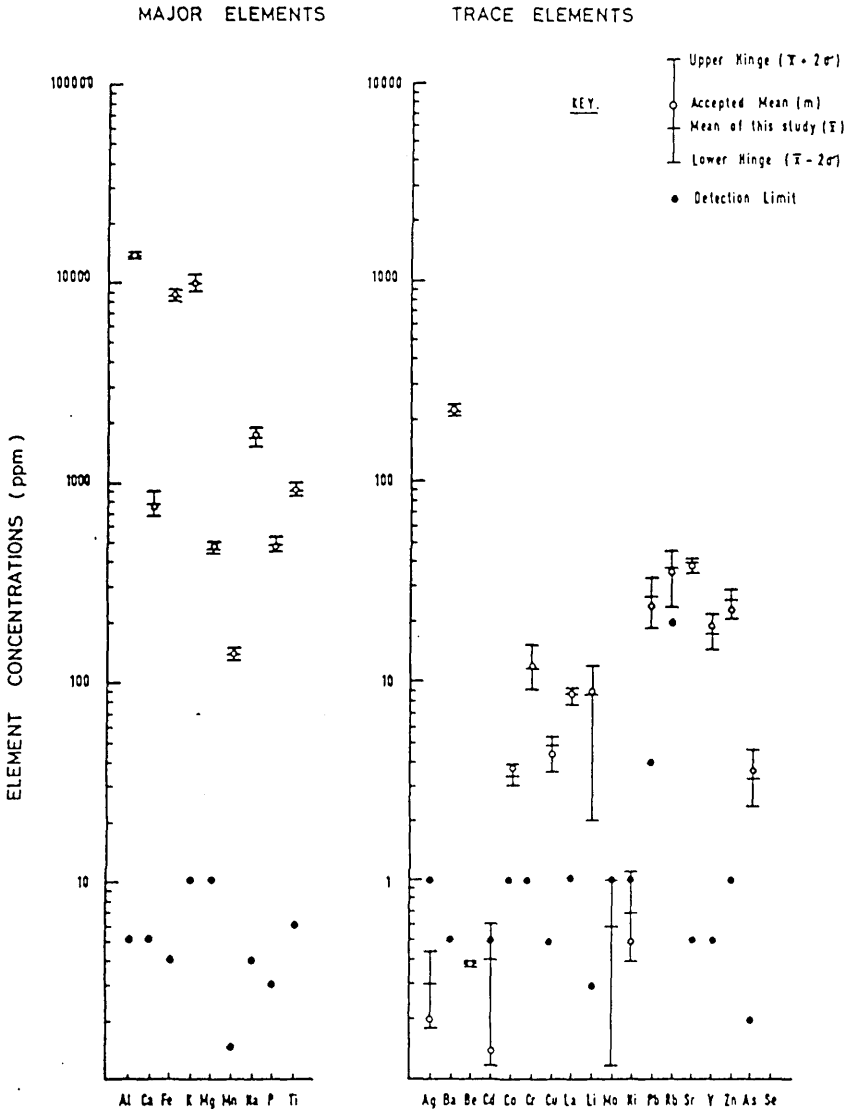


Fig.4.2 Shows the Accuracy of the Analytical Procedures of this Study compared to HRM1 Reference Control.

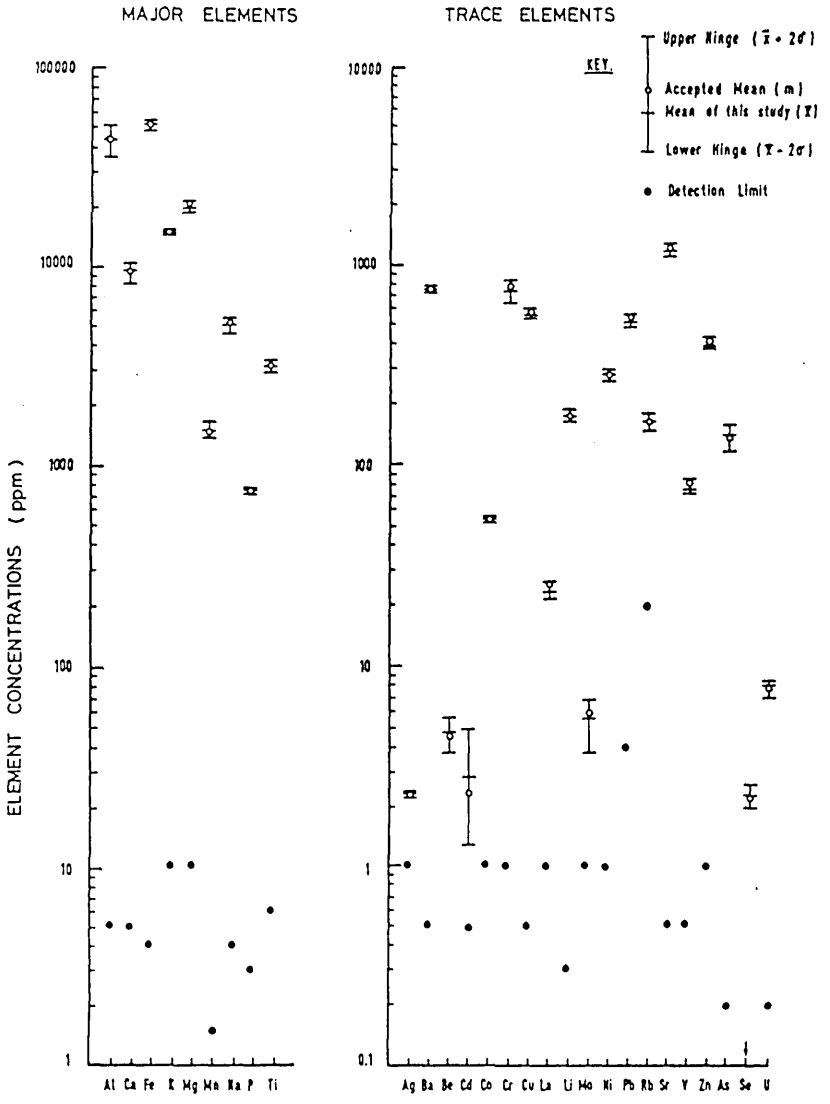
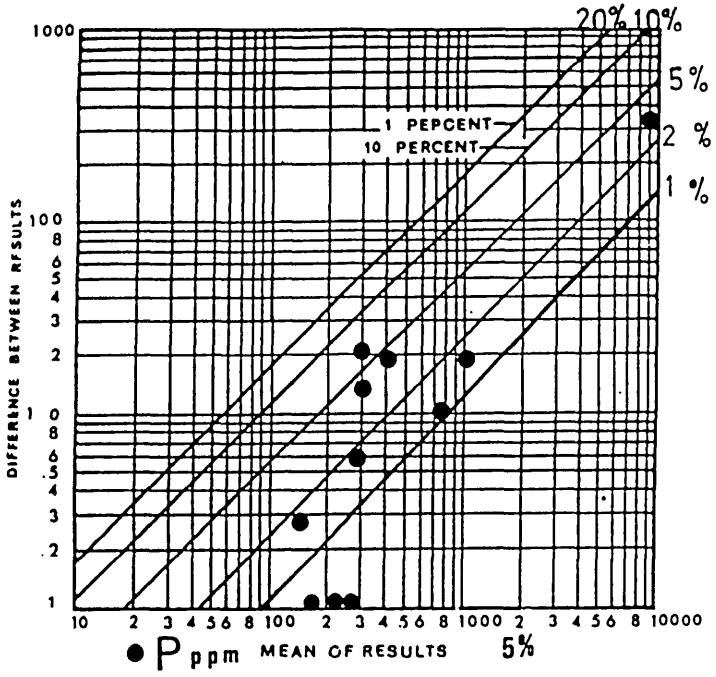


Fig.4.3 Shows the Accuracy of the Analytical Procedures of this Study compared to HRM2 Reference Control.

the errors was investigated and evaluated and the necessary corrections performed.

Precision is a numerical measure which indicates the analytical drift across the range of data obtained by the analysis of duplicates on a routine basis. Primarily, it monitors the whole error incurred in the sample preparation procedure such as weighing, attacking, leaching and diluting to volume, by comparing the values of duplicate analyses in the batches. It was found that precision varies as a function of proximity to detection limits, whereby precision improves as higher concentrations are present in the samples. In other words, precision refers to the spread of duplicate determinations around the mean as a function of the coefficient of variation. Therefore it is a factor of great importance in geochemical analysis. In each batch 10% of the samples were analysed in duplicate (the duplicates being included randomly within the batch) and a rapid test to monitor the precision was carried out using the special control chart based on the methodology of Thompson and Howarth (1973; 1976; 1978) and Howarth and Thompson (1976). If any batch of analysis shows significant deviation of results from the specified control levels (usually of 10% precision) it was rejected and re-analysed. Figures (4.4 and 4.5) demonstrate the precision control chart for major, trace and minor elements determined by ICP.Precision of INAA analytical data was also calculated and shows a level of 6% error in the case of uranium concentration levels in the orientation samples (Fig.4.6).

The accuracy and precision of ICP analyses were also



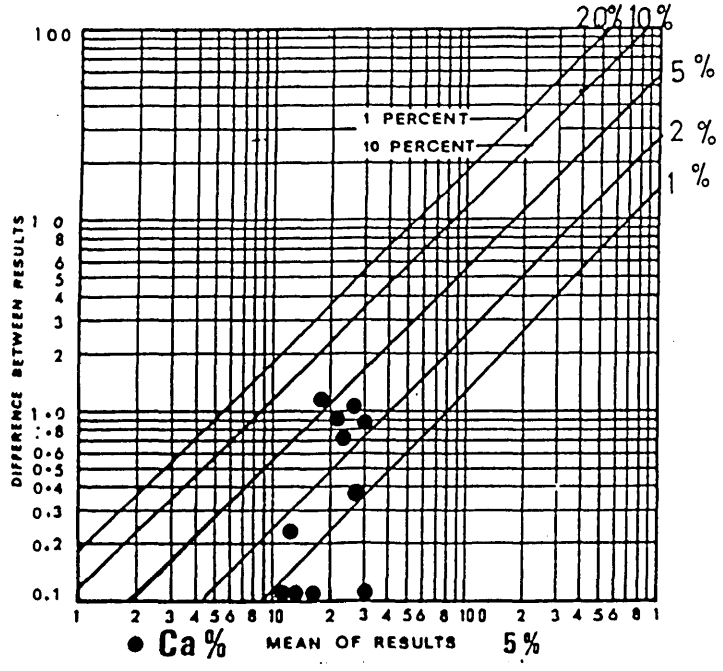
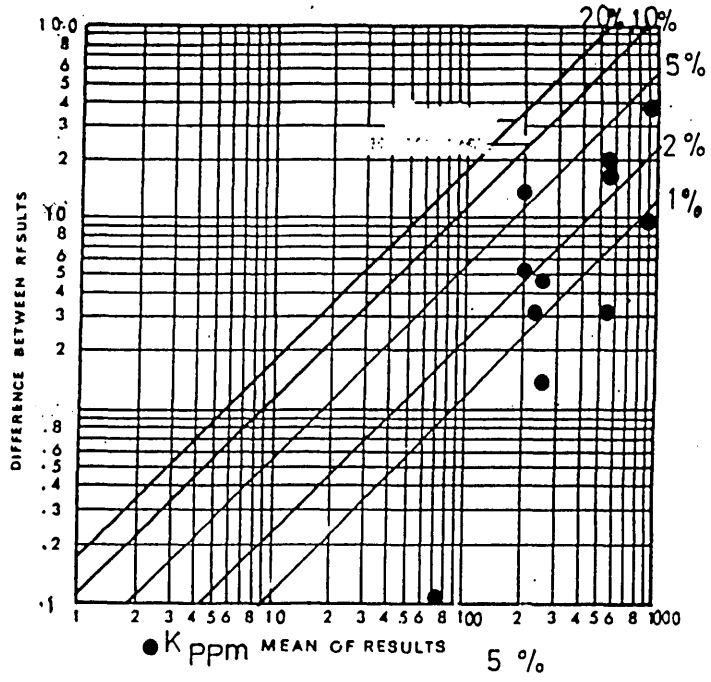


Fig.4.4 Precision of duplicate results for P and Ca.



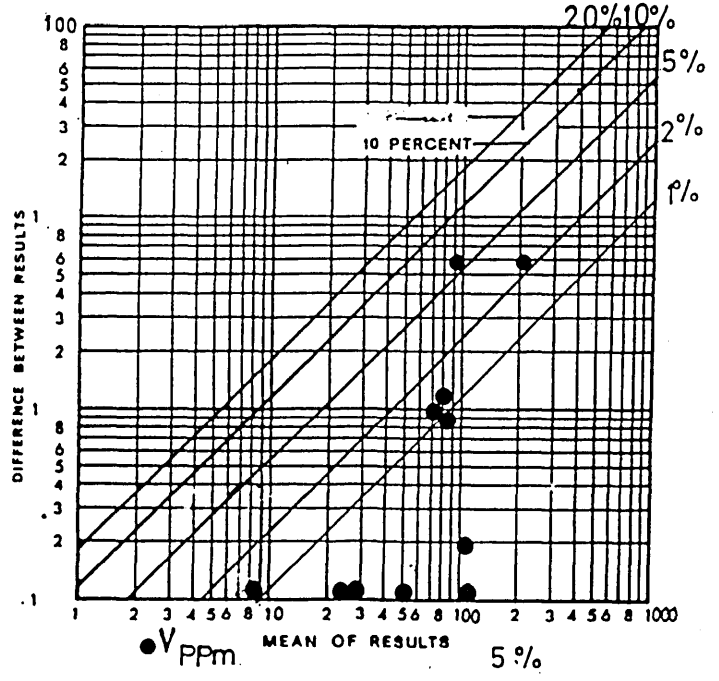


Fig.4.5 Precision of duplicate results for K and V.

monitored through QUTE, a scheme routinely used for the purpose by the Applied Geochemistry Research Group.

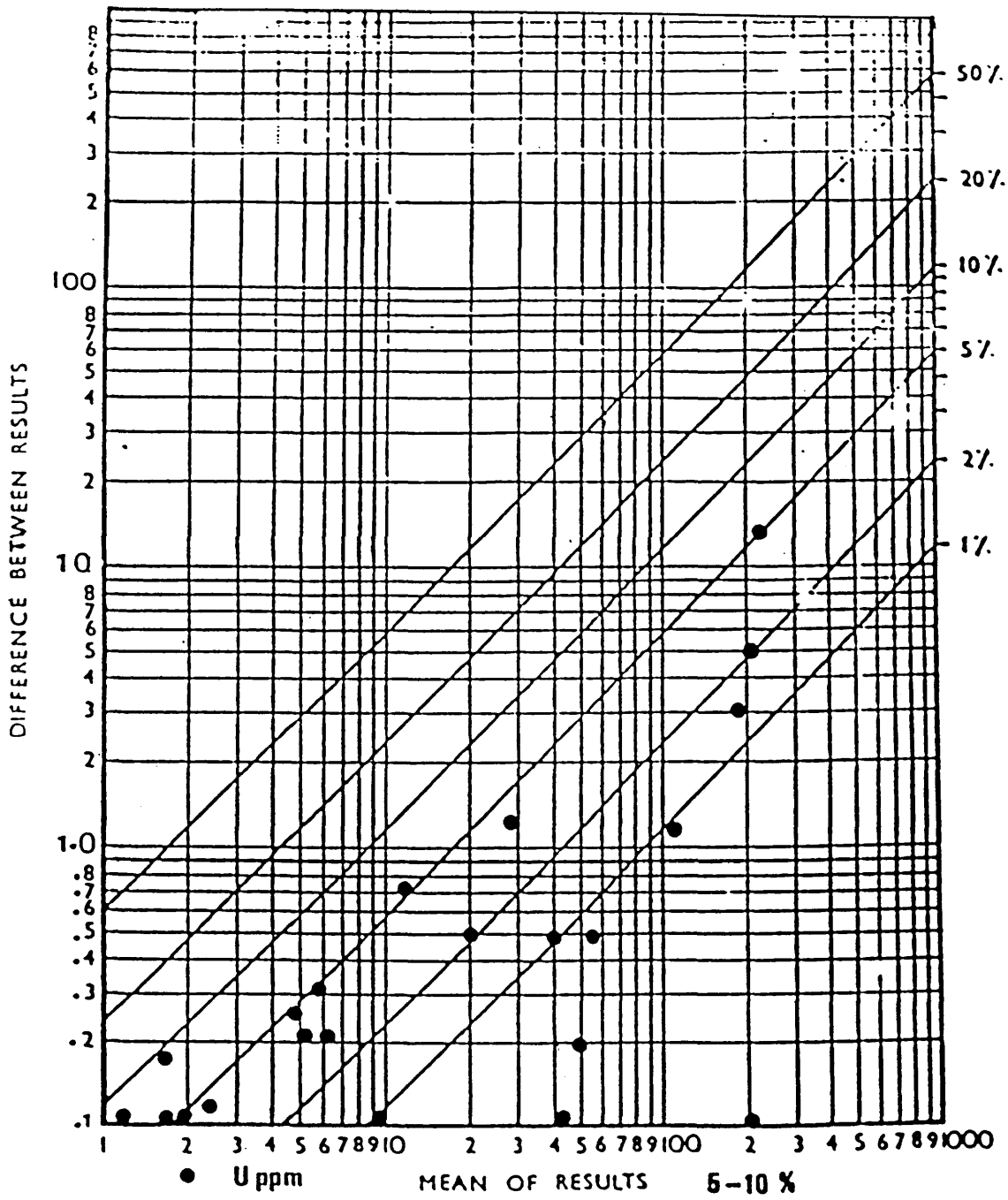


Fig.4.6 Accuracy of duplicate results for U.

CHAPTER V

5. REGION SELECTION AND ORIENTATION SURVEY

A very low density geochemical survey of the Palmyrides region and the eastern region of Syria (between Palmyra and the border with Iraq) was carried out with the triple objectives: discriminating the most promising region of the area for further reconnaissance; examining the mode of occurrence of U at known mineralized localities; and determining the optimum geochemical response from various sample media. This work is referred to collectively as the orientation survey.

5.1 Investigation of the optimum size fraction of the sediments and soil

According to Levinson (1974), the optimum size fraction for sediment to be analysed should be determined by an orientation sampling program within the study area before any reconnaisance program is undertaken. Therefore, the overburden and wadi sediment orientation samples were sieved to obtain the following four size fractions: 500-250 μm (-30 to + 60 mesh), 250-150 μm (-60 to + 100 mesh), 150-90 μm (-100 to +170 mesh), and -90 μm (-170 mesh). The distributions of uranium, major, minor, and trace elements incorporated in the four fractions were determined, and the results, shown in Fig. 5.1 demonstrate that, U, P, Se, V, Mo, La and, to a lesser extent, As, Zn and Cd concentrations in the coarse fractions are significantly higher than in the progressively finer fractions. This is attributed to a predominantly clastic dispersion

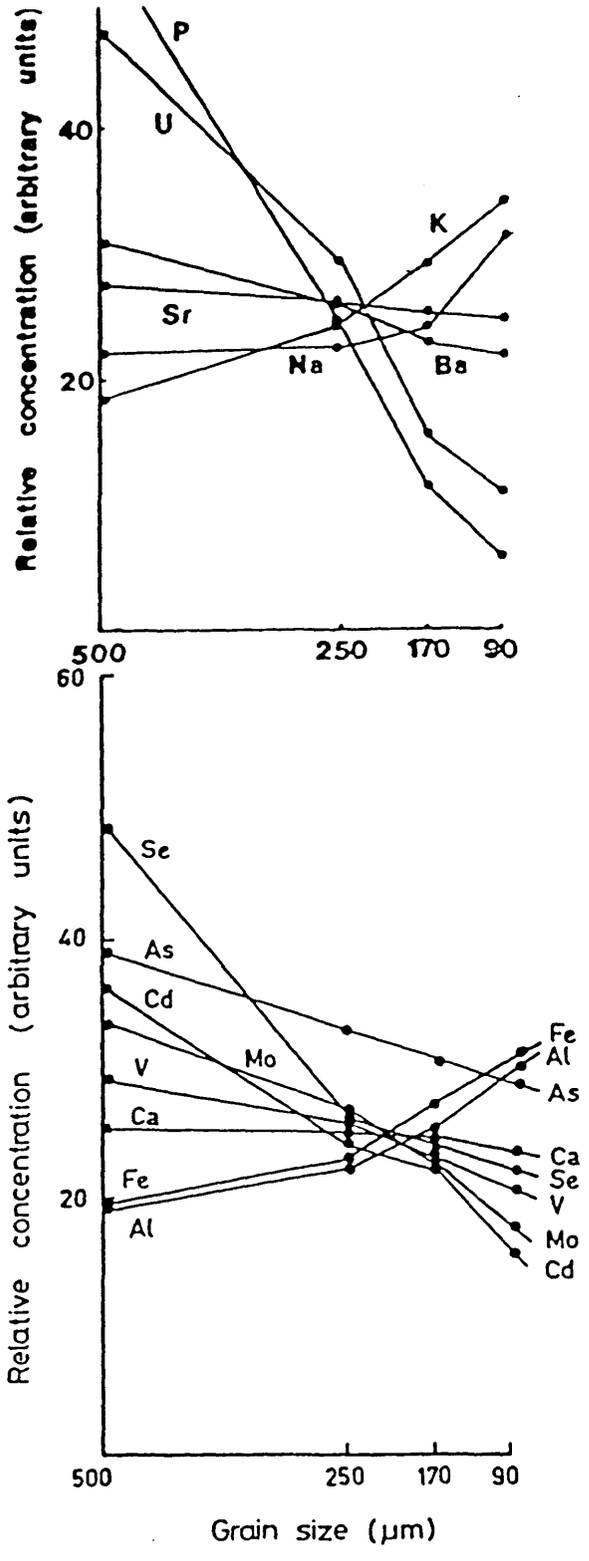


Fig.5.1 Relative concentrations of U and associated elements in different size fractions.

of these elements and/or the lack of effective adsorption of the foregoing elements on the fine fractions of clays and other colloids. Similar behaviour of uranium in the coarse fraction of sediments and clastic particles was noted by Rose (1977).

On the other hand, Li, Na, K, Mg, Al, Ti, Cr, Co, Mn, Cu and Ni tend to be concentrated in the fine fraction, suggesting some chemical breakdown in the dispersion processes, while Sr, Ba and Ca were uniformly distributed throughout the size fraction range.

5.2 Analysis of Uranium Minerals

5.2.1 General

No detailed optical and crystallographical measurements were intended in this stage of the work. However, the inadequacy of the existing descriptions of the uranium minerals which occur in the area and the initial lack of any analytical data led to adopt a general mineralogical and geochemical approach in order to determine and characterize the nature of the mineral occurrences. The approach includes the application of the scanning electron microscope, which is equipped with an energy dispersive electron microprobe for microchemical analysis (for more detail of the technique refer to Robinson and Nickel, 1979). An X-ray diffractometer was used to obtain X-ray powder diffraction interplanar spacing data. The combined data from these techniques are capable of characterizing the major features, phases, and perhaps the most likely mineral species in a specimen.

5.2.2 Sample preparation and analytical techniques

Four different mineralized samples from the Jabal Om Jorn and Jabal Tabaque areas were studied. Each sample was split into three representative subsamples. The first one was crushed using a tungsten carbide pestle and mortar, then pulverised in an agate Tema mill to pass through a 90 μm sieve. The powder was used for further chemical analysis. The analytical data are listed in Table 5.1.

The second subsample was prepared to be examined by backscattered SEM imagery with electron microprobe analysis. The samples were sliced exposing the mineralised particles before being coated with gold.

Corresponding polished thin sections were made from the third sample, then examined optically for choosing and marking accurately the phases of interest to be micro-chemically analysed. Tables 5.2 and 5.3 show results of the quantitative energy dispersive microprobe analysis of two different uranium minerals.

5.2.3 Scanning electron microscopy

The high atomic number of uranium and the extremely high resolution of the JEOL-733 scanning electron microscope used at Imperial College resulted in obtaining good quality SEM images, which demonstrate the crystal morphology, distribution, and relationships of the uranium minerals within each specimen (Fig.5.2). The quantitative microchemical analysis obtained by the

Table 5.1 Uranium contents in mineralized specimens measured by (NAA).

Sample N°.	C.P.S	Uppm	Location	Rock type
UM I	280	I96	J.Om jorn	Phosphorite
UM 2	200	II2	J.Om jorn	Phosphorite
THOI	280	I99	J.Tabaque	red shale
D527	350	230	J.Tabaque	organic limestone

Table 5.2 Microprobe analysis of U minerals; identification = carnotite group, formula $K_2(UO_2)_2V_2O_8.3H_2O$

15.00 kV TILT= .00 ELEV=40.00 AZIM= .00 COSINE=1.000

Spectrum: 27 A 1 SH02;D602

Last elmt by DIFFERENCE

ELMT	ZAF	%ELMT	ATOM.%	%OXIDE	FORMULA
NaK: 1	.747	.183	.560	.247	.177
MgK: 1	.779	.009	.027	.016	.009
AlK: 1	.902	.000	.000	.000	.000
SiK: 1	1.064	.145	.362	.310	.115
P K: 2	.990	.000	.000	.000	.000
S K: 1	1.382	.512	1.122	1.280	.356
K K: 1	1.392	4.812	8.642	5.796	2.740
CaK: 1	1.127	.163	.286	.228	.091
TiK: 1	1.097	.239	.351	.399	.111
V K: 2	1.147	9.686	13.353	17.293	4.233
CrK: 2	1.142	.049	.066	.072	.021
MnK: 1	1.050	.000	.000	.000	.000
FeK: 1	1.102	.046	.058	.059	.018
CuK: 1	1.133	.076	.084	.095	.027
ZnK: 2	1.252	.337	.362	.420	.115
SrL: 1	.999	.000	.000	.000	.000
MoL: 1	1.014	.000	.000	.000	.000
CdL: 1	.975	.000	.000	.000	.000
U M: 1	.831	71.522	21.100	81.137	6.689
BaL: 1	1.016	.000	.000	.000	.000
O K: 1	.000	12.219	53.627	.000	17.000
TOTAL		100.000	100.000	107.352	14.701

Table 5.3 Microprobe analysis of an unnamed urano-vanadate mica.

Spectrum: URANIUM GRAIN Y.JUBELI 14/2/84PASY

Last elmt by DIFFERENCE

ELMT	ZAF	%ELMT	ATOM.%	%OXIDE	FORMULA
NaK: 1	.755	.177	.590	.239	.146
MgK: 1	.776	.197	.621	.327	.154
AlK: 1	.895	.318	.904	.602	.223
SiK: 1	1.058	.917	2.498	1.961	.618
P K: 2	.969	.044	.110	.102	.027
K K: 1	1.403	.801	1.568	.965	.388
CaK: 1	1.161	1.303	2.489	1.824	.616
TiK: 1	1.124	.228	.364	.380	.090
V K: 2	1.173	9.486	14.253	16.934	3.525
CrK: 2	1.161	.165	.242	.241	.060
MnK: 1	1.066	.080	.111	.103	.028
FeK: 1	1.118	.256	.351	.330	.087
CuK: 1	1.151	.000	.000	.000	.000
ZnK: 2	1.273	.143	.167	.178	.041
SrL: 1	.995	1.790	1.563	2.116	.387
MoL: 1	.994	.000	.000	.000	.000
CdL: 1	.981	.000	.000	.000	.000
U M: 1	.835	67.954	21.851	77.089	5.404
S K: 1	1.356	.249	.595	.622	.147
BaL: 1	1.041	5.749	3.204	6.419	.792
O K: 1	.000	10.142	48.518	.000	12.000
TOTAL		100.000	100.000	110.432	12.733



Fig. 5.2 Scanning electron microscope photomicrograph showing platy uranium minerals and prisms of celestite from the Palmyrides region.

electron microprobe was of a great importance in distinguishing the mineral species, which are metamict and produce no distinguishable or useful diffractograms by the XRD method alone. Results of the SEM imagery are illustrated in Plate 7. Uranium minerals, found as enhedral tabular scales and laths, flattened, elongated and even curved in some cases with micaceous cleavage, probably simulate orthorhombic symmetry. The SEM images also show a peculiar combination of uranium minerals with celestite ($SrSO_4$) in all the samples studied, indicating the oxidising nature of the environment, and perhaps precipitation from solutions owing to evaporation.

5.2.4 X-ray photography and fluorescence

The yellow coating on the third subsample, which had been reported to be autunite, tyuyamunite and carnotite, was extracted carefully under the binocular microscope and collected as a pure a phase as possible. On a very clean glass slide, a drop of gum arabic or Durofix was then added to the powder to form a homogeneous spindle (a hair-like substance). The spindle was then placed at the centre of a Debye-Scherrer camera. This in turn was subjected to X-ray diffraction analysis using a Phillips PN 1050 diffractometer with Fe filtered Co K_α radiation (= 1.7889 Å) and 34KV.

Alternative identification based on the interplanar spacings, d(Å) measurements combined with the chemical results confirmed the existence of carnotite $K_2(UO_2)_2V_2O_8.1\text{-}3H_2O$, tyuyamunite

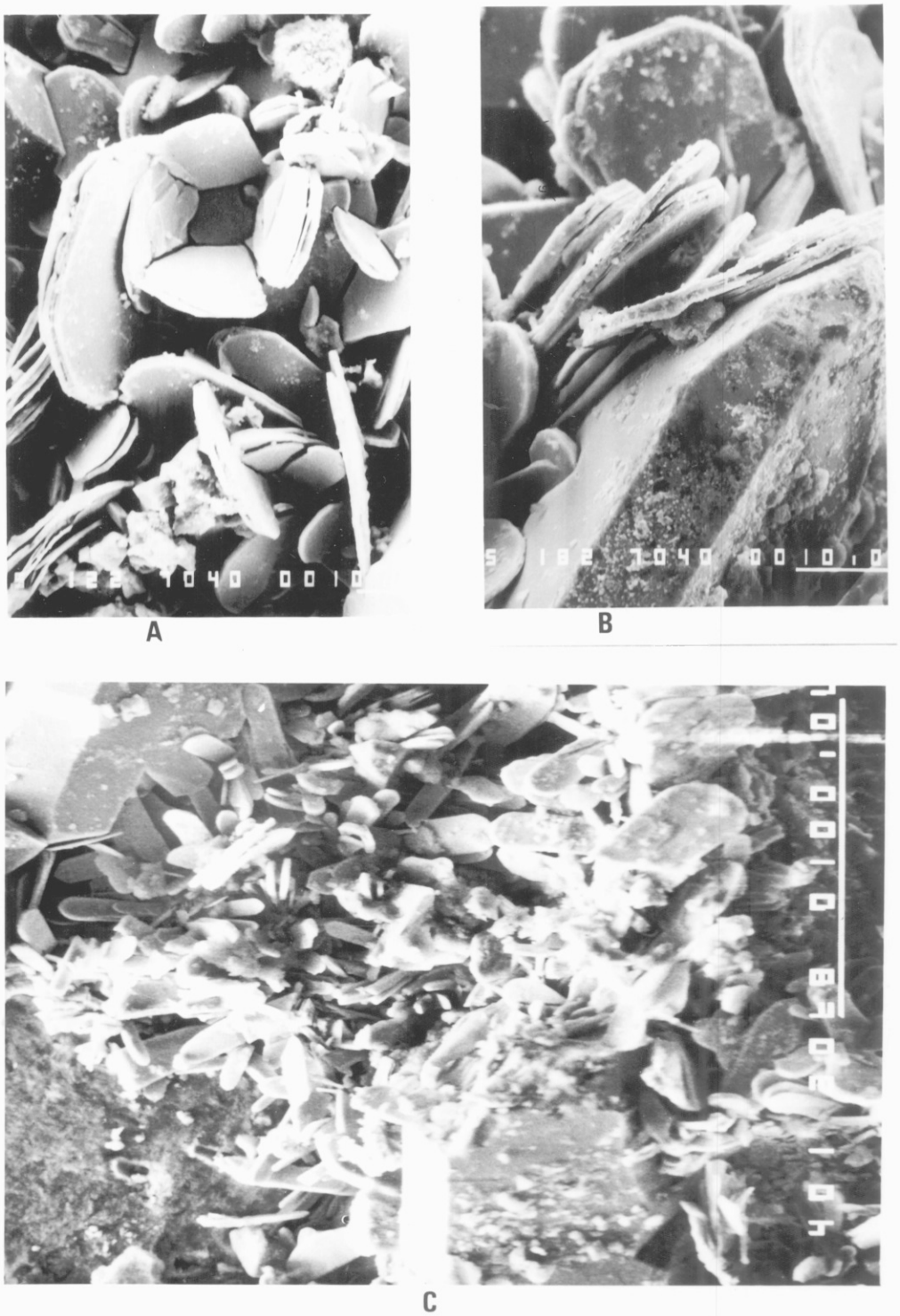


Plate 7 Scanning electron microscope images illustrating the crystal morphology of the uranium minerals (A) and their association with celestite B, C).

$Ca(UO_2)_2V_2O_8$, schroekingerite $NaCa_3(UO_2)(CO_3)_3SO_4F.10H_2O$, and metatyuyamunite $Ca(UO_2)_2V_2O_8.3\text{-}5H_2O$. No autunite was found at all. Photographs of the sample UM2 (J. Om Jorm) gave d(Å) data (Table 5.4) of which the three strongest lines are similar to those mentioned in the X-ray powder determinative tables under unnamed uranium vanadium hydroxide, lead uranyl $(UO_2)_3V_2O_8.(Pb_x).6H_2O$. It is worth noting that the microprobe analysis of the same mineral gave a chemical composition which confirms the general formula obtained by the X-ray diffraction method, but unfortunately the element lead was not included in the list of elements to be determined by the microprobe at the time. However, a qualitative XRF analysis of a spindle preparation of this mineral showed a distinct peak of Pb along with U and V peaks (Fig.5.3). Results of this analysis are shown in Table 5.5.

X-ray powder photography work was performed on a powder form of the same mineral using a Guinier focusing camera under the same XRD conditions of irradiation. After developing the film the X-ray photograph gave diffraction effects for two phases (multiple crystals). Nevertheless, after separating the d (Å) spacing pattern of the two phases the result was similar to that obtained by the Debye Scherrer camera. The first phase was found to be the unnamed U, V, Pb uranyl and the second phase was the strontium mineral celestite. This was interpreted as a result of impure sample consisting of a mixture of celestite and the unnamed uranium mineral.

This unnamed secondary uranium mineral has a chemical composition and the ratio of the main constituents similar to those

Table 5.4 Microprobe analysis of carnotite mineral .

Spectrum: U GRAIN 602

Last elmt by DIFFERENCE

ELMT	ZAF	%ELMT	ATOM.%	%OXIDE	FORMULA
SiK: 1	1.020	.788	1.461	1.686	.349
S K: 1	1.306	.464	.754	1 159	.180
K K: 1	1.312	6.875	9.157	8.282	2.188
CaK: 1	1.075	.933	1.213	1.306	.290
V K: 2	1.082	10.869	11.112	19.404	2.655
NaK: 1	.712	.111	.251	.149	.060
P K: 2	.940	.004	.007	.009	.002
U M: 1	.783	60.671	13.274	68.827	3.172
O K: 1	.000	19.285	62.771	.000	15.000
TOTAL		100.000	100.000	100.822	8.896

LIVETIME(spec.)= · 100

ENERGY	RES	AREA
2.5	129.08	58125

Table 5.5 Microprobe analysis of U mineral possibly schroekingerite; formula $NaCa_3(UO_2)(CO_3)SO_4F.10H_2O$

Spectrum: U GRAIN 602

Last elmt by DIFFERENCE

ELMT	ZAF	%ELMT	ATOM.%	%OXIDE	FORMULA
SiK: 1	.960	.838	.892	1.793	.200
S K: 1	1.166	4.494	4.188	11.223	.979
K K: 1	1.158	3.659	2.796	4.408	.653
CaK: 1	1.007	16.383	12.212	22.923	2.853
V K: 2	.949	5.630	3.302	10.050	.771
NaK: 1	.694	.000	.000	.000	.000
P K: 2	.864	.096	.092	.219	.022
U M: 1	.684	29.935	3.757	33.959	.878
O K: 1	.000	38.965	72.760	.000	17.000
TOTAL		100.000	100.000	84.575	6.364

of the mineral ferghanite. Frondel (1958) reported the formula for this mineral as (U_3O_8 77.00, V_2O_5 17.60, H_2O 10.75 and LiO_2 1.22), but noted a possible source of error in the oxide total. The same error was evident in the data obtained in the current research. The problem may be due to the number of oxygen atoms upon which the micro-chemical analyses were based in the calibration of the reference standards.

5.3 Fission track registrations

5.3.1 General

To investigate the controls on uranium minerals, an integrated petrological and geochemical procedure was used to facilitate the precise location of all uranium in some forty carbonate and phosphorite rocks and sediments from the orientation survey. The total uranium concentration was determined by INAA; results show a range of 1-230 ppm U. The fission track registration technique was applied to effectively locate, evaluate and identify the uranium distribution, and to compare the relative enrichment of uranium between and within different constituents of the sample.

5.3.2 Results and discussions

Differences in the concentration of the fission-tracks were found in isotropic and anistropic grains, ovulite, coprolite, glauconite, calcite grains and calcitic cements, collophane, apatite and other phosphate particles. Lexan plastic fission-track registration maps of the thin sections show that uranium follows

closely the presence of the phosphate grains (apatite, collophane, pellets and fish teeth) in many of the preparations (Plates 8 and 9), while in others, uranium occurs within microstructures and fissure-fillings of microcrypto crystalline varieties of grains and collophane mud (Plate 10).

In addition, undiscernable uranium phases occur most commonly as very dense, spotty, centred fission tracks locally reflecting increased levels of uranium, possibly of secondary origin (Plate 11). No uranium was found associated with either the calcite or the glauconite grains present in some thin sections (Plate 12). This seems, therefore, to be in agreement with the well established interpretation of uranium enrichment in the phosphorite as a result of isomorphous substitution of U^{4+} (ionic radius 0.97 Å) for Ca^{2+} (ionic radius 0.99 Å) in the phosphate minerals (Inglesrud et al., 1948; Thompson, 1953; McKelvey, 1956; Altschuler et al.,1958; Altschuler, 1980; Mott, 1983). However, such an interpretation should be used with caution when explaining the remarkable variation in uranium content within the same phosphorite horizon and from one phosphate grain to another. In some cases, this variation in uranium content can be explained in terms of the time for which the phosphate minerals were exposed to the source solution in which substitutions took place, or as a function of its uranium concentration.

It is more appropriate however,to relate uranium enrichment and variation to more than this type of process. To that end, other physio-chemical factors are believed to play a major role in the whole enrichment process. Some of these factors are: differential

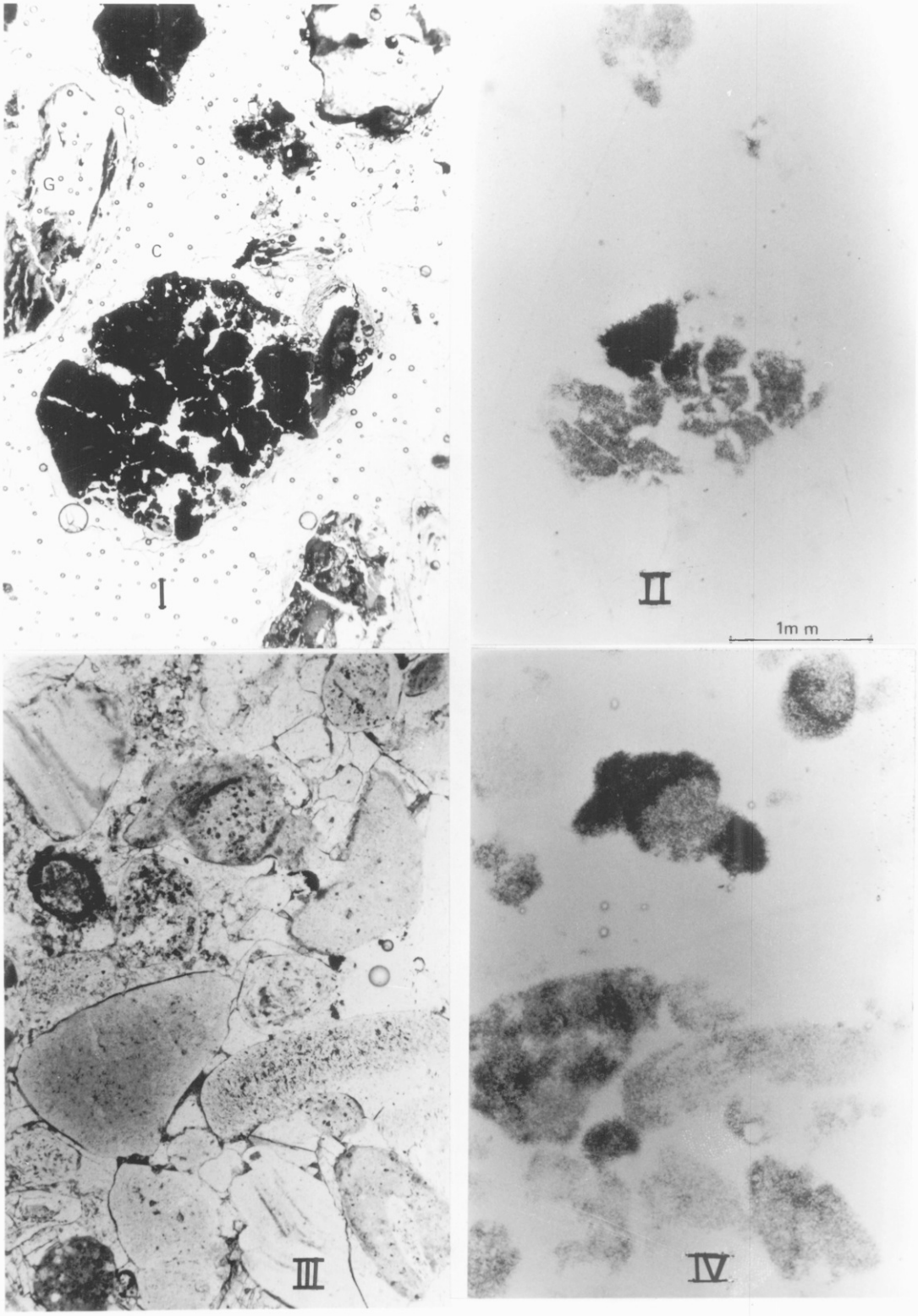


Plate 8 Photomicrographs of polished thin sections (I and III) and corresponding lexan fission track registrations (II and IV); showing phosphate particles and grains, glauconite (G) and calcite cement (C). Uranium occurs entirely with the phosphate grains and particles, no tracks are related to glauconite and calcite.

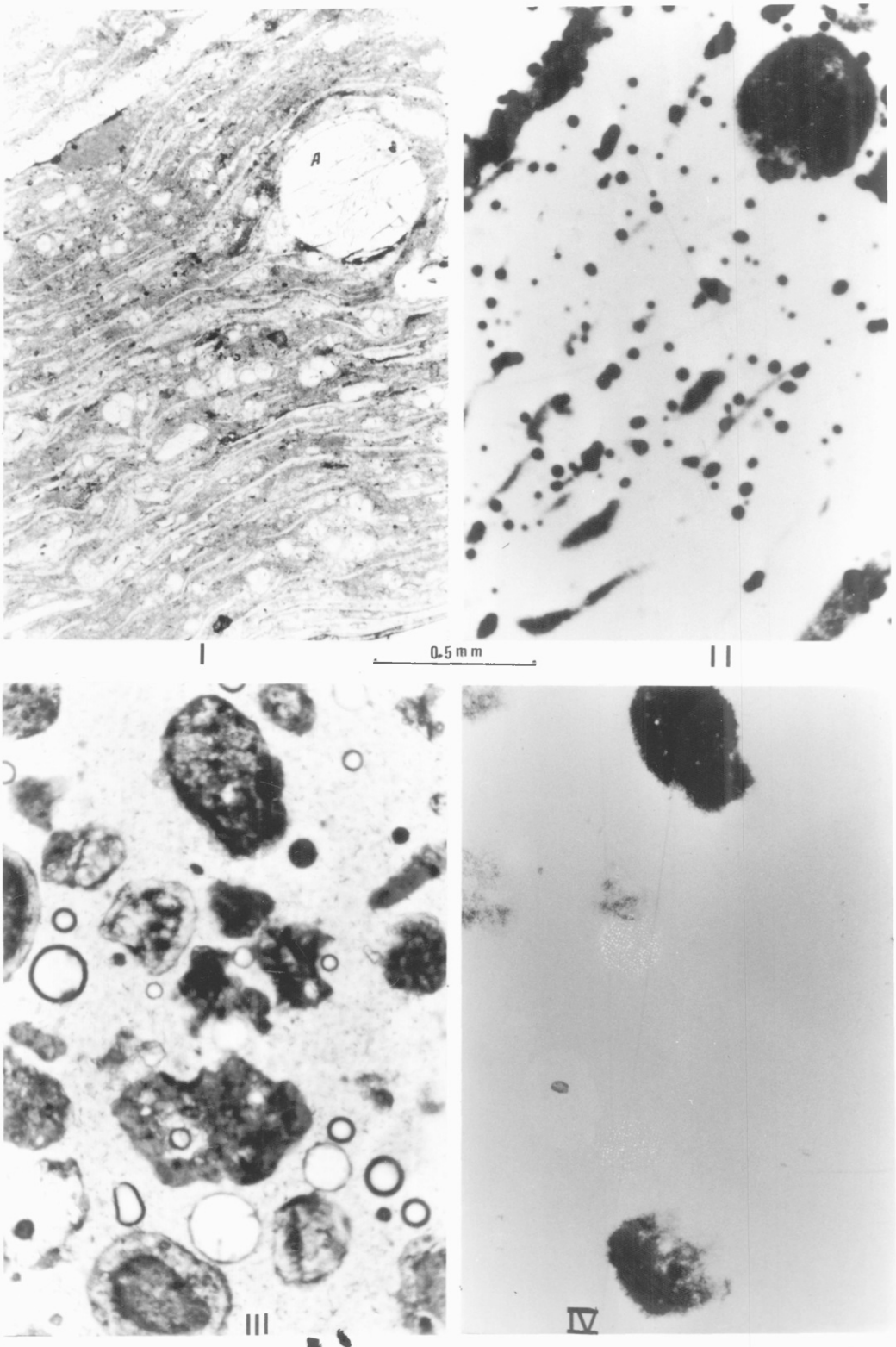


Plate 9 Photomicrograph of polished thin sections (I and III) and corresponding fission track registration (II and IV) showing dense tracks closely related to reworked (rounded) francolite grains; notic that uranium is not evenly distributed within and betwee the phosphate grain.



1mm

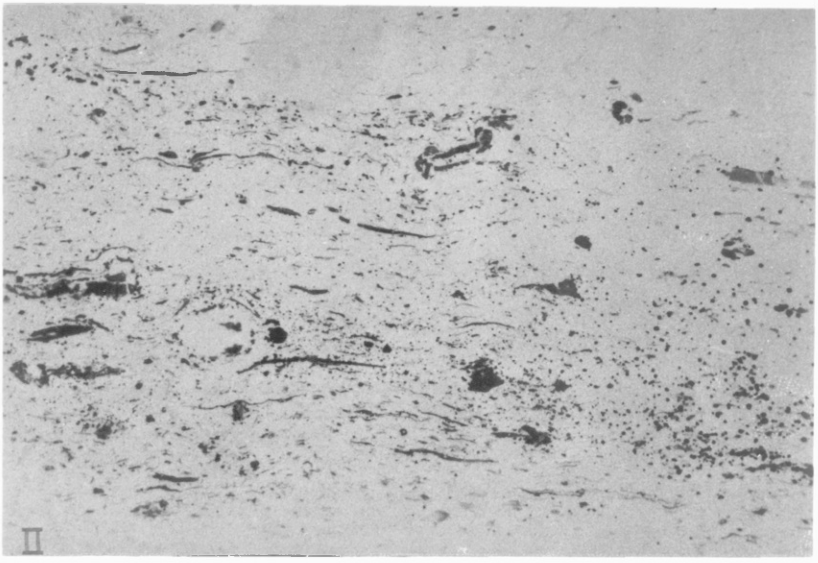
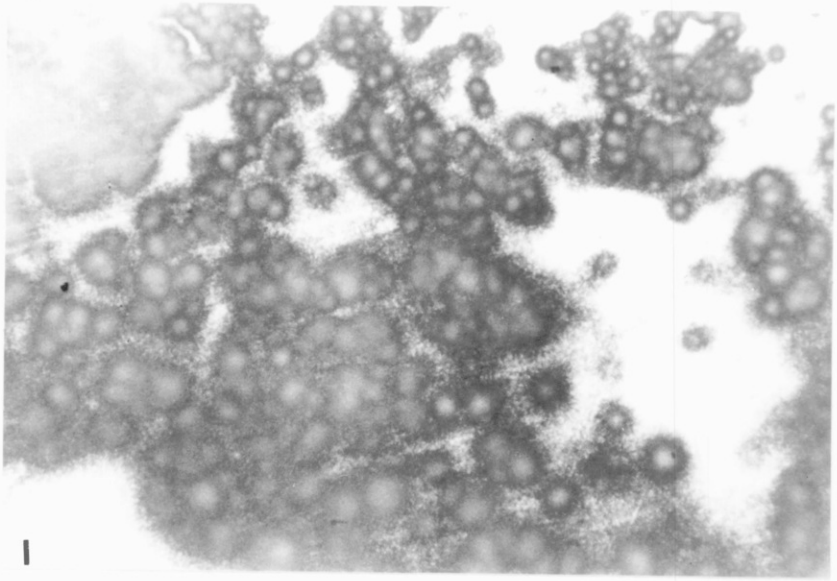
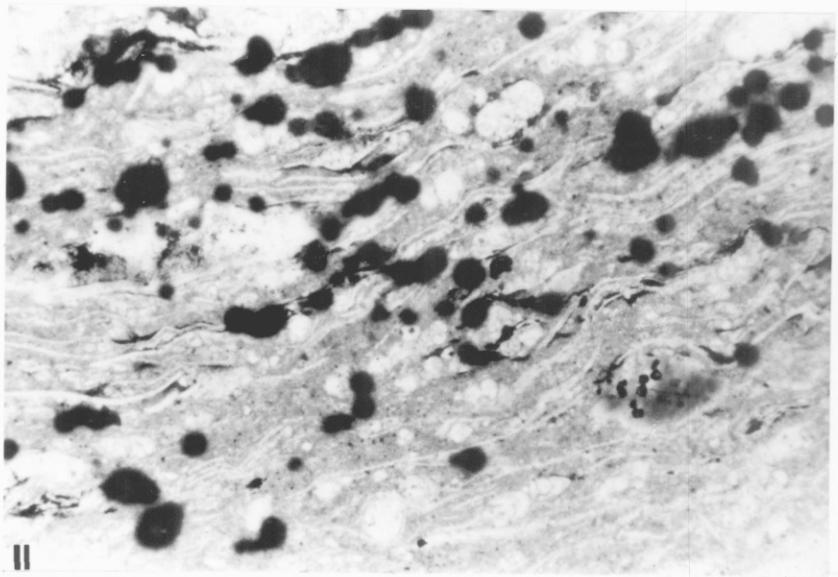


Plate 10 Photomicrographs of polished thin section (I) with offset superimposed lexan print to match the main textures of the rock. II is a fission track registration; the dense tracks reflect uranium enrichment in the microfractures filled with cellophane mud, the spotty nature of other track, show relationships with very small grains of phosphate minerals (apatite and/or francolite).

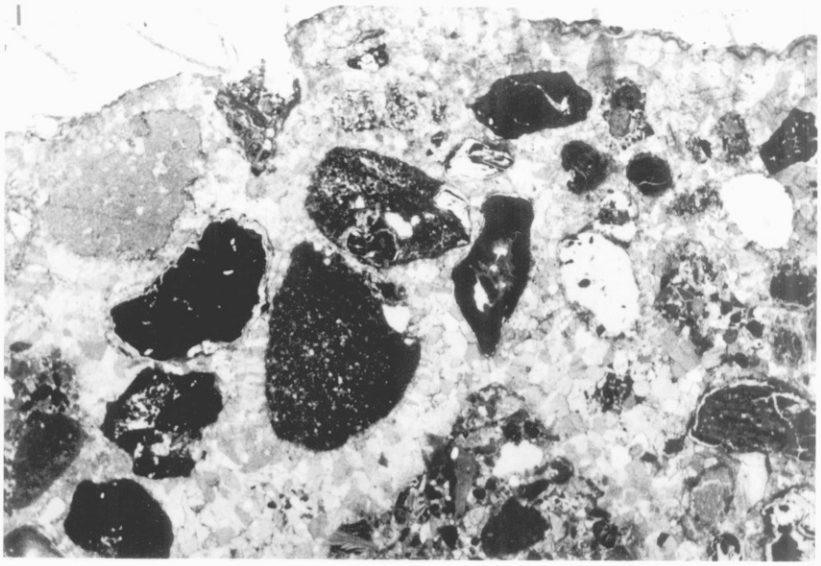


I



II

Plate 11 Photomicrographs of dense spotty centred U fission tracks registration (I) reflecting indiscernable uranium phase (possibly secondary U minerals). Notice that the centres of the rounded tracks are void of tracks. In II a lexan print is superimposed corresponding polished thin section with slight offset to illustrate the relationships between the tracks (black spots) and the crystallised phosphate grains, no uranium is related to the microlineations.



1 m m

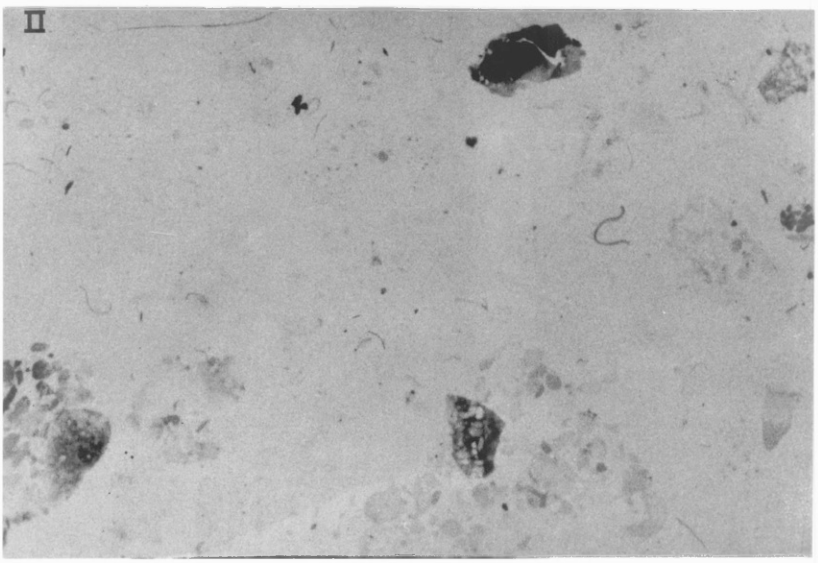


Plate 12 Matched photomicrographs of thin section of phosphatized glauconitic limestone (I, crossed Micols) and lexan fission track image (II) uranium is entirely related to reworked phosphorite grains, no tracks are associated with glauconite or the calcite cement.

absorption; preferential coprecipitation; replacement; and secondary enrichment. The abnormal levels of uranium in marine phosphorite can therfore be explained in terms of primary (syngenetic) and secondary (epigenetic) processes rather than relating them to a single mode of enrichment. In fact, part of the variation in uranium content is found to be associated with textural differences in the grains and within the rock (Plate 13). To elucidate these textural relationships, a study of the microphotographs helped to establish a relative timing of different diagenetic events in which uranium enrichment and depletion can be recognized. At least three periods of diagenetic history can be traced in the grain which is illustrated in Plate 14. First is a uranium-rich collophane mud, which is believed to be a primary phase. Later this was subjected to reworking and weathering during which detrital components were introduced and dilution occurred; this phase gives rise to a very poor pattern of fission-tracks in the overgrowth part, reflecting a low uranium concentration. This second stage was accompanied or directly followed by a third phase, which involved partial chemical leaching of uranium resulting in uneven distribution prior to redeposition. Other photomicrographs (e.g. Plate 9) shows a variety of reworked well crystallized francolite grains. Some are small, fissure-fillings and dissemminated in the matrix, others are bigger and perfectly rounded. The fission track registration of those grains and their microprobe analysis indicates that uranium correlates significantly with the reworked isotropic phase of phosphorite minerals. This further supports the possibility of different modes of uranium replacement.

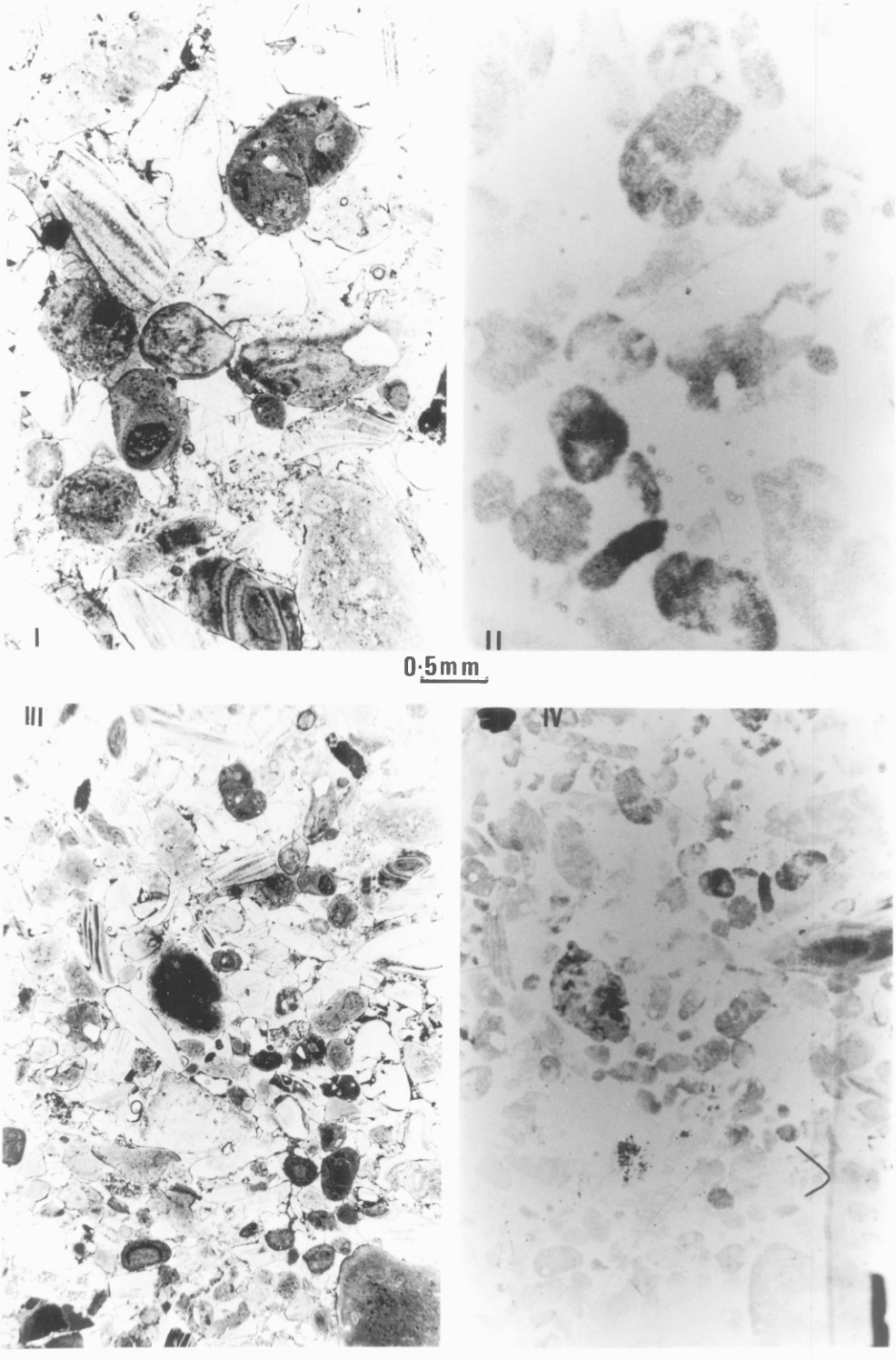
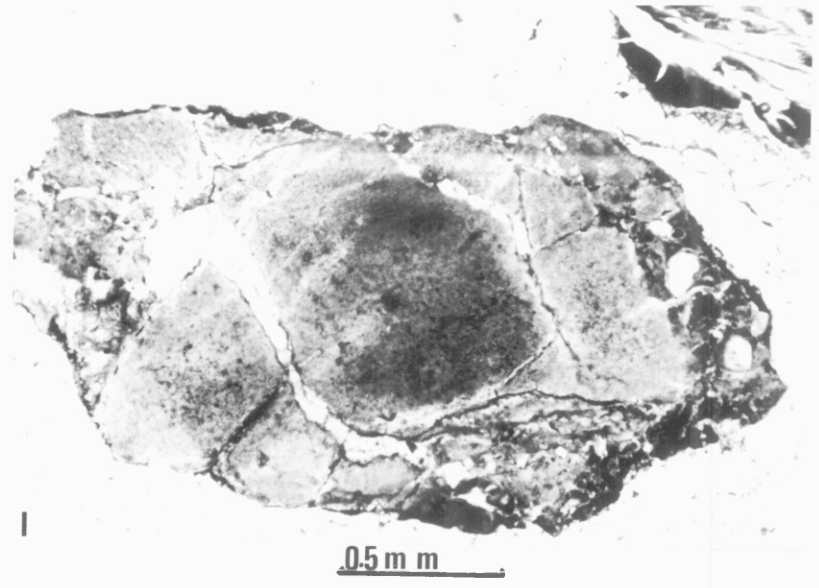
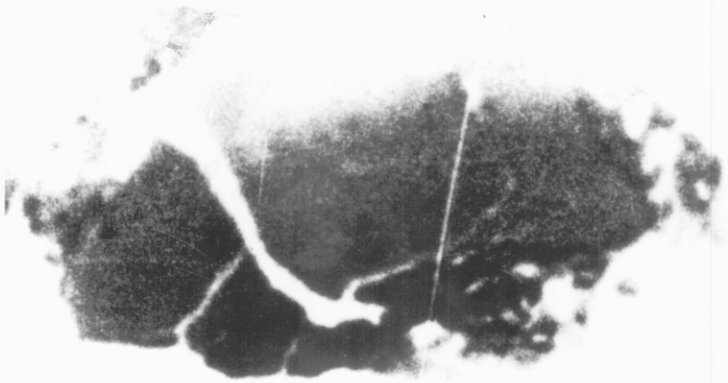


Plate 13 Matched thin section I, III and fission track image on lexan film (II, IV). Uranium distribution vary according to textural differences within the phosphate grains.





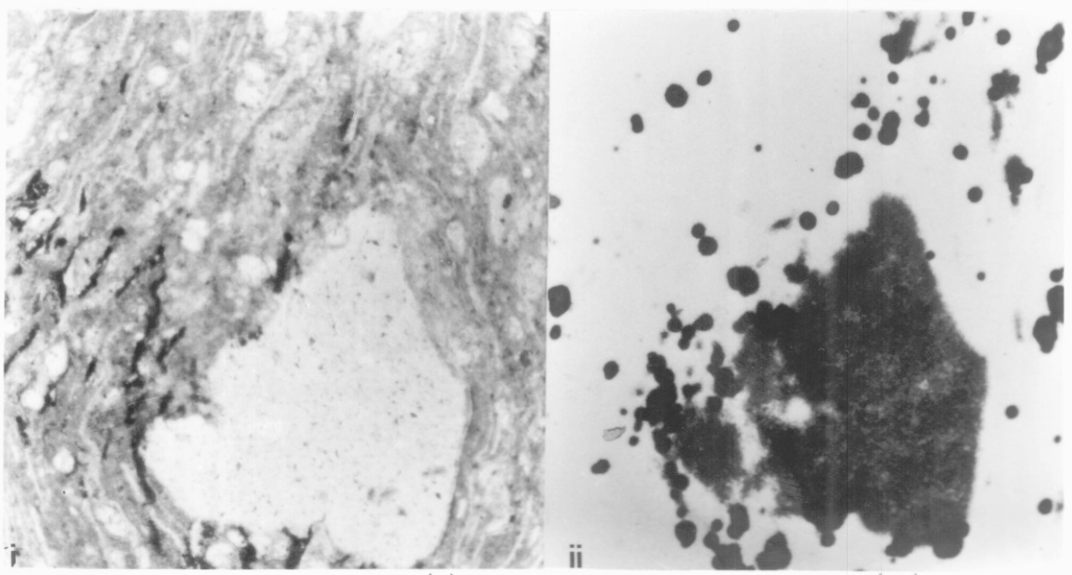


Plate 14 Matched thin section (I) and fission track registration (II), complex history of diagenesis can be drawn (refer to the text).

Another type of dense fission track was found to be related to secondary fractures and cracks (Plates 15, 16 and 17). In this case the combined SEM image, X-ray images and microprobe analysis, mineralogical and petrological studies showed that the fission tracks were generated by secondary uranium mineral grains precipitated from uranium-rich solution in a late stage of diagenesis (Plates 18 and 19 and Fig.5.4). The microphotos in these plates clearly show the brightness of the uranium minerals relative to other grains. Results of the microprobe analyses are listed in Table 5.5.

5.3.3 Reasons for variations in uranium content

Possible reasons for the observed variations in uranium content may be due to any combination of the following:

(1) - Change of the Eh-pH conditions in the depositional environment.

(2) - The content of carbonate, bicarbonate, phosphate, sulphate ions and organic matter.

(3) - The elemental species, particularly of uranium in the sea and interstitial (pore) waters.

(4) - Differences in temperature, turbulence and depth under which rocks were formed.

(5) - The stuctural framework and the texture of the rock.

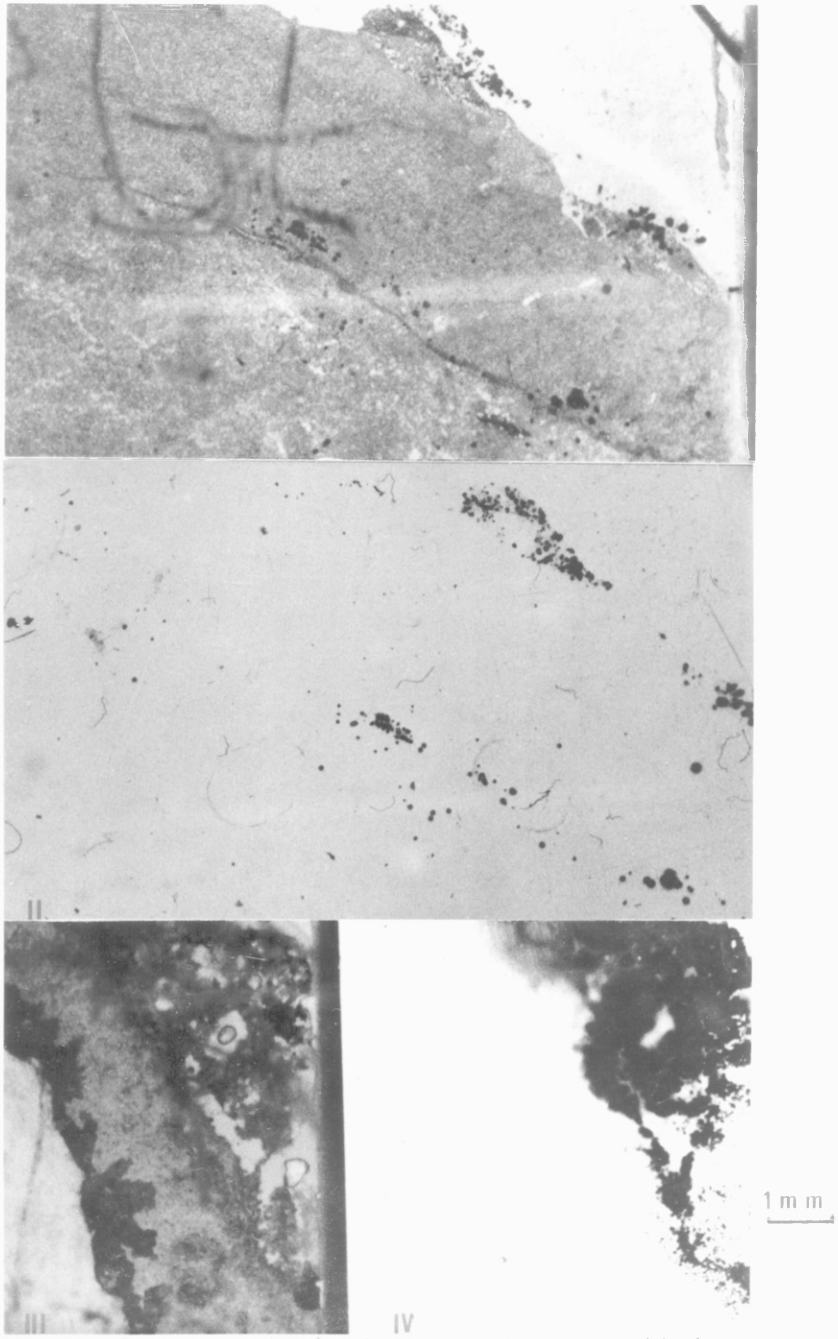


Plate 15 Photomicrographs of rock thin section superimposed by lexan print with a slight offset (I). This illustrate that the uranium tracks follow secondary fissures and microfractures. In (II, III, IV) the dense spotty centres of tracks are entirely related to the fractures and fissures and not to the rock constituents.

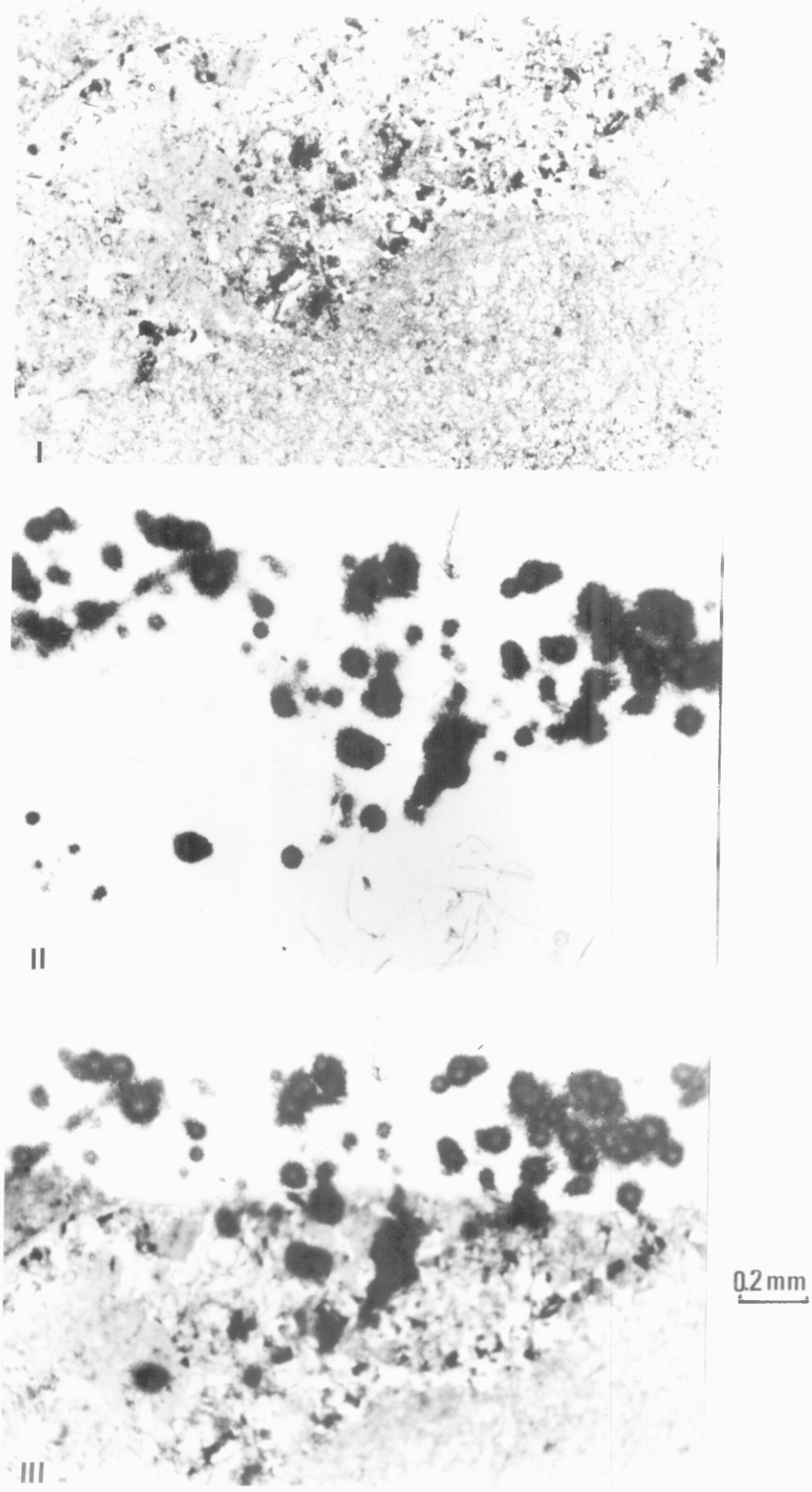


Plate 16 Matching thin section (I) and fission track registration (II), dense tracks are associated with secondary fractures filled with small uranium mineral grains (III).

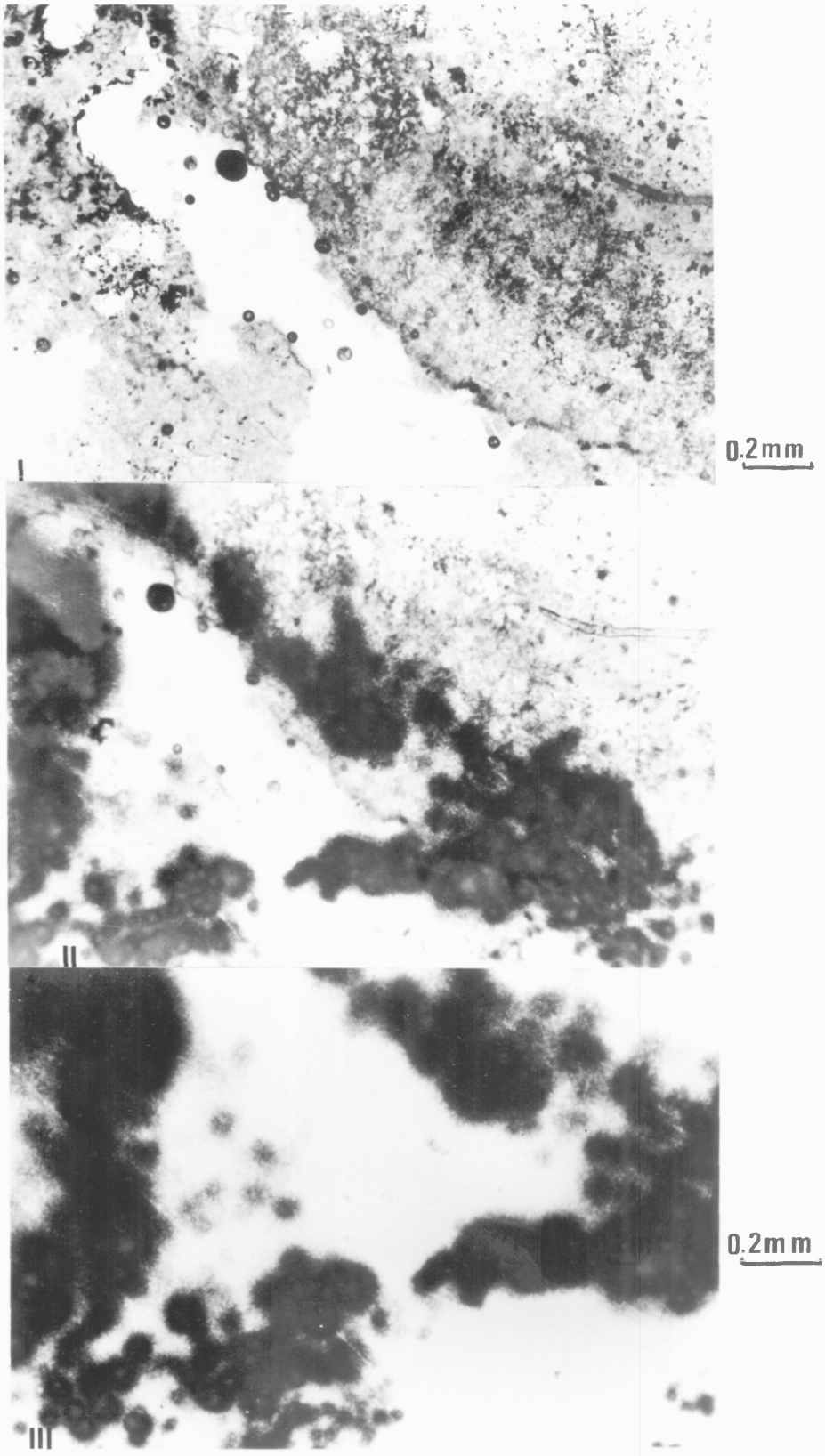


Plate 17 Photomicrographs of thin section (I) and the corresponding lexan print superimposed with slight offset (II). Secondary uranium minerals are formed by precipitation from U rich solution filling the available space III.

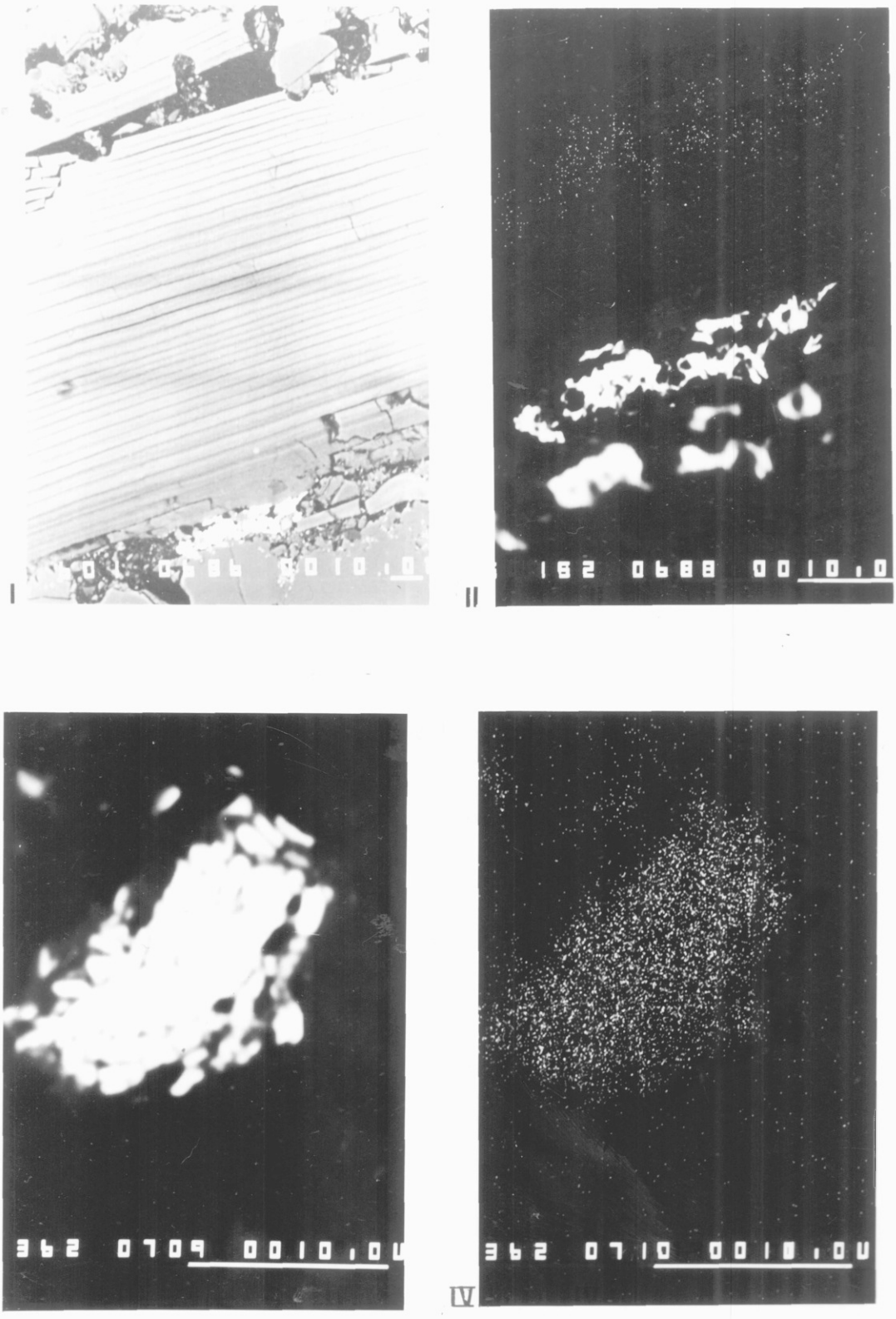


Plate 18 Photomicrographs of thin sections (I and III), bright uranium mineral are formed within bone microfracture (I) and in the matrix (III). In (II and IV) the X Ray electron images show the distribution of U in the corresponding grains.

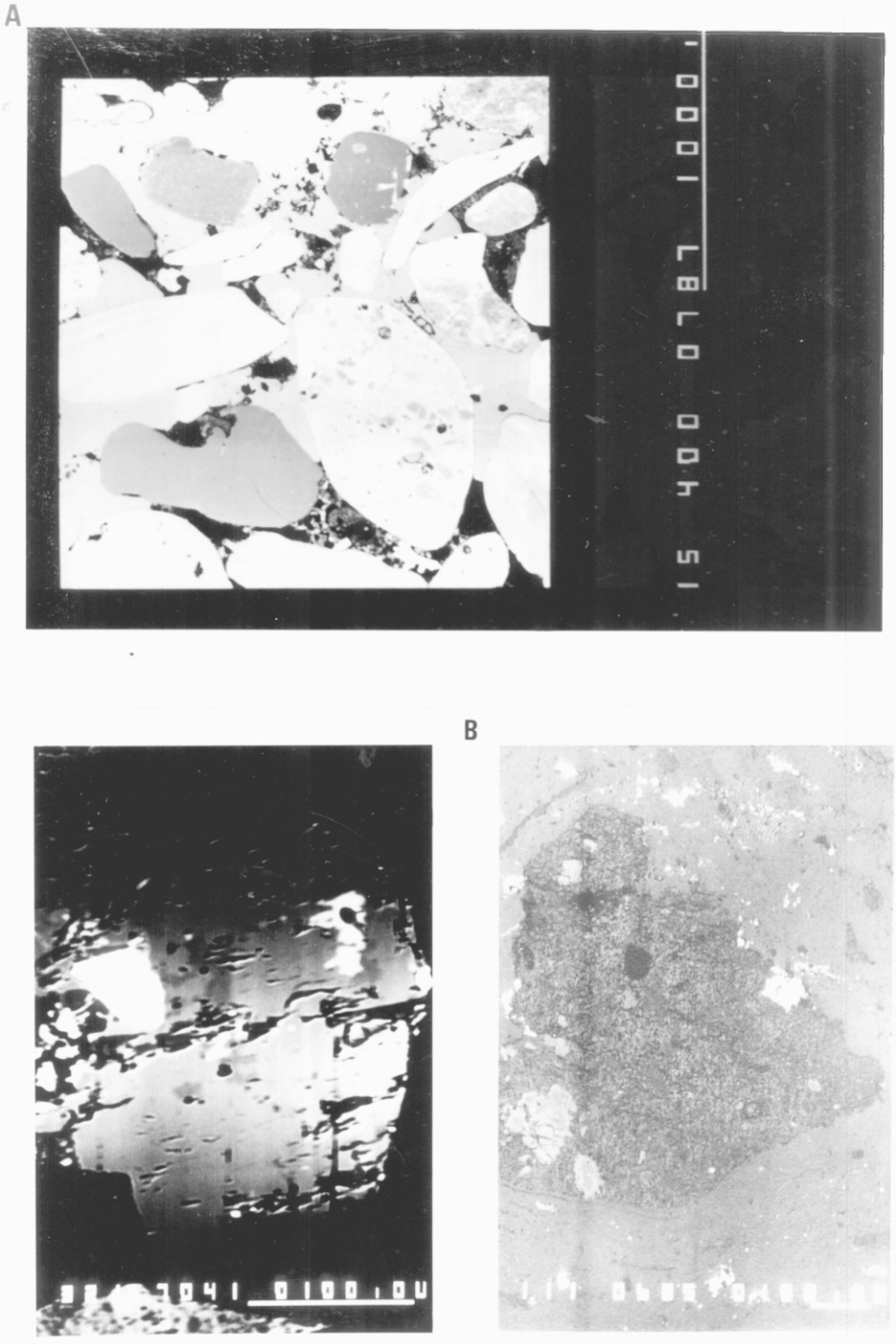


Plate 19 Photomicrographs of rock thin sections showing bright secondary uranium minerals within the pores and cement of the rocks. (A) Phosphorit, (B) Carbonite

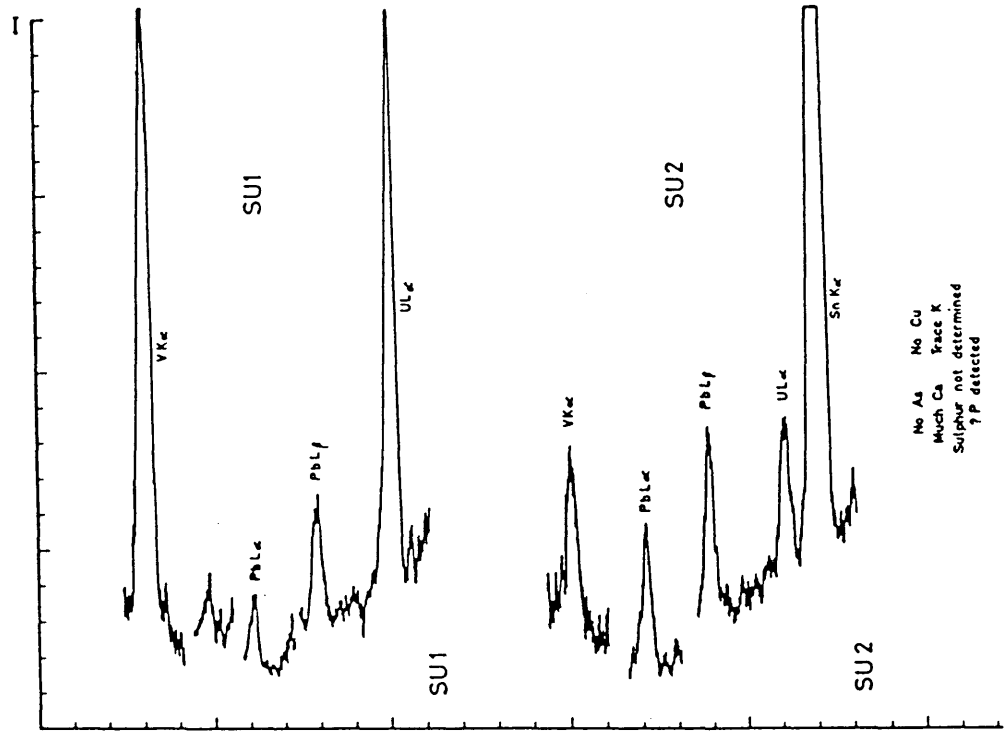


Fig.5.3 X-ray Fluorescence of Two Mineralized Specimens

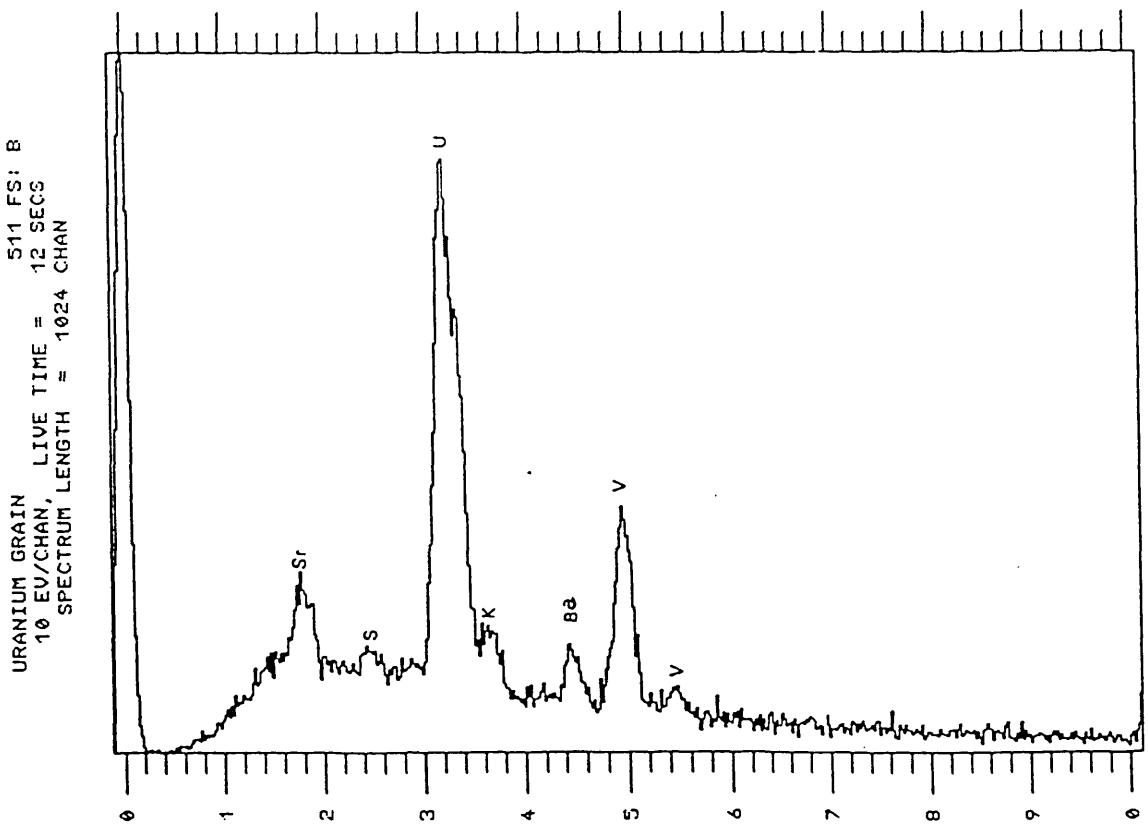


Fig.5.4 Microprobe analysis of U minerals.

(6) - The topography (relief) of the depositional environment.

(7) - The effects of hydrothermal fluids and other mineralized solutions.

(8) - Weathering, reworking and the role of ground and surface waters.

(9) - Rate of accumulation of phosphatic and other sediments.

Useful indications about the mechanism in which uranium was incorporated in the sample can be drawn from the fission track registrations and can be summarized in the following conclusions.

5.3.4 Conclusions of the fission track studies

(1) - The distribution of uranium in the samples studied is multimodal and is characterized by the following associations:

(a) - Uranium is primarily associated with various phosphate grains (ovules, coprolite, and pellets) and phosphate minerals (apatite or francolite, collophane mud, detrital collophanes, and hydroxy-fluorapatite).

(b) - The amount of uranium in these minerals seems to show conspicuous variations.

(c) - Uranium is primarily related to mud-like fissure fillings and pelletal grains.

(2) - Uranium enrichment is found to be related either to

syngenetic or epigenic events. The latter were accompanied, in some cases, by the formation of secondary uranium minerals in microfractures or within cement.

5.4 Geochemical results and region selection

5.4.1 General

Interpretation of the orientation geochemical data for uranium and associated elements comprised an investigation of the spatial distribution of the total data set of 72 samples to distinguish areas of interest, and statistical analysis of the data grouped according to sample type namely: wadi sediments, overburden and rock samples. Summary statistics of the geochemical data are presented in Table 5.6, and the whole data in Appendix 5.1.

5.4.2 Quality of the data

It is clear from Figures 4.5 to 4.7 that the accuracy of the analytical procedures in determining the major elements is ±5% and for uranium and most of the trace elements it is better than 10%. The precision, illustrated in Figures 4.8 to 4.10, is better than 5% for uranium, between 1 to 5% for major constituents and is 15 to 25% for most of the trace elements. The precision is still poorer in the case of Ag, Rb, Bi and Sb because these elements are consistently found at or below the instrumental detection limits; therefore they are excluded from further consideration. Selenium in the samples collected from the eastern region was generally below the ICP limit of detection, therefore it was also excluded from

Table 5.6 Summary statistics of the orientation samples.

U	N =	72	MEAN =	31.071	ST.DEV. =	55.5
HF	N =	72	MEAN =	2.6833	ST.DEV. =	2.16
AS	N =	72	MEAN =	2.9694	ST.DEV. =	2.05
CPS	N =	72	MEAN =	100.22	ST.DEV. =	62.8
TH	N =	72	MEAN =	3.1944	ST.DEV. =	2.06
P	N =	72	MEAN =	11533.	ST.DEV. =	23808.
ZN	N =	72	MEAN =	86.583	ST.DEV. =	89.9
CU	N =	72	MEAN =	19.300	ST.DEV. =	13.4
MG	N =	72	MEAN =	10058.	ST.DEV. =	10123.
CA	N =	72	MEAN =	225917.	ST.DEV. =	90352.
SR	N =	72	MEAN =	641.36	ST.DEV. =	622.
BA	N =	72	MEAN =	303.55	ST.DEV. =	354.
AL	N =	72	MEAN =	13120.	ST.DEV. =	10789.
LA	N =	72	MEAN =	13.861	ST.DEV. =	10.5
TI	N =	72	MEAN =	774.38	ST.DEV. =	631.
V	N =	72	MEAN =	92.118	ST.DEV. =	118.
CR	N =	72	MEAN =	41.834	ST.DEV. =	31.5
MO	N =	72	MEAN =	5.3531	ST.DEV. =	5.50
MN	N =	72	MEAN =	156.67	ST.DEV. =	159.
FE	N =	72	MEAN =	8823.2	ST.DEV. =	6610.
CO	N =	72	MEAN =	7.2915	ST.DEV. =	4.38
LI	N =	72	MEAN =	6.5773	ST.DEV. =	5.60
NA	N =	72	MEAN =	981.89	ST.DEV. =	1313.
K	N =	72	MEAN =	2874.4	ST.DEV. =	2367.

further discussion.

5.4.3 Data interpretation

5.4.3.1 Symbolic geochemical maps

Visual inspection of the spatial distributions of U, P, Th, Hf, Sr, V and the radiometric measurements (CPS) of these samples revealed some conspicuous variations of background values as well as anomalous values (Figures 5.5 to 5.11). In general the eastern area shows depletion of U, P, Sr, V and CPS relative to the Palmyrides region. An 8 ppm U threshold separates the two areas, except that one anomalous value of 205 ppm U occurs in the eastern area (related to a calcrete type rock in Wadi El Mourabbaa). In more detail, higher concentrations of U, P, Sr and V are confined to two areas of the Palmyrides region, namely, the mountain ranges and the Ad-Daww basin. This distribution pattern reflects a stong relationship with the mineralized occurrences as well as the abundance of phosphorite rocks.

Comparison of the spatial distribution maps for Th and Hf with those of U and P demonstrate marked differences in their dispersion patterns if the first two elements are compared to the second two. However, the enhanced levels of Th relative to U in the eastern region (where most of the samples collected were wadi sediments) may reflect differences in their geochemical behaviour in the secondary environment . The oxidation of U^{4+} to U^{6+} under very high free oxygen levels promotes the separation of Th and U, the latter being highly soluble and more mobile under these

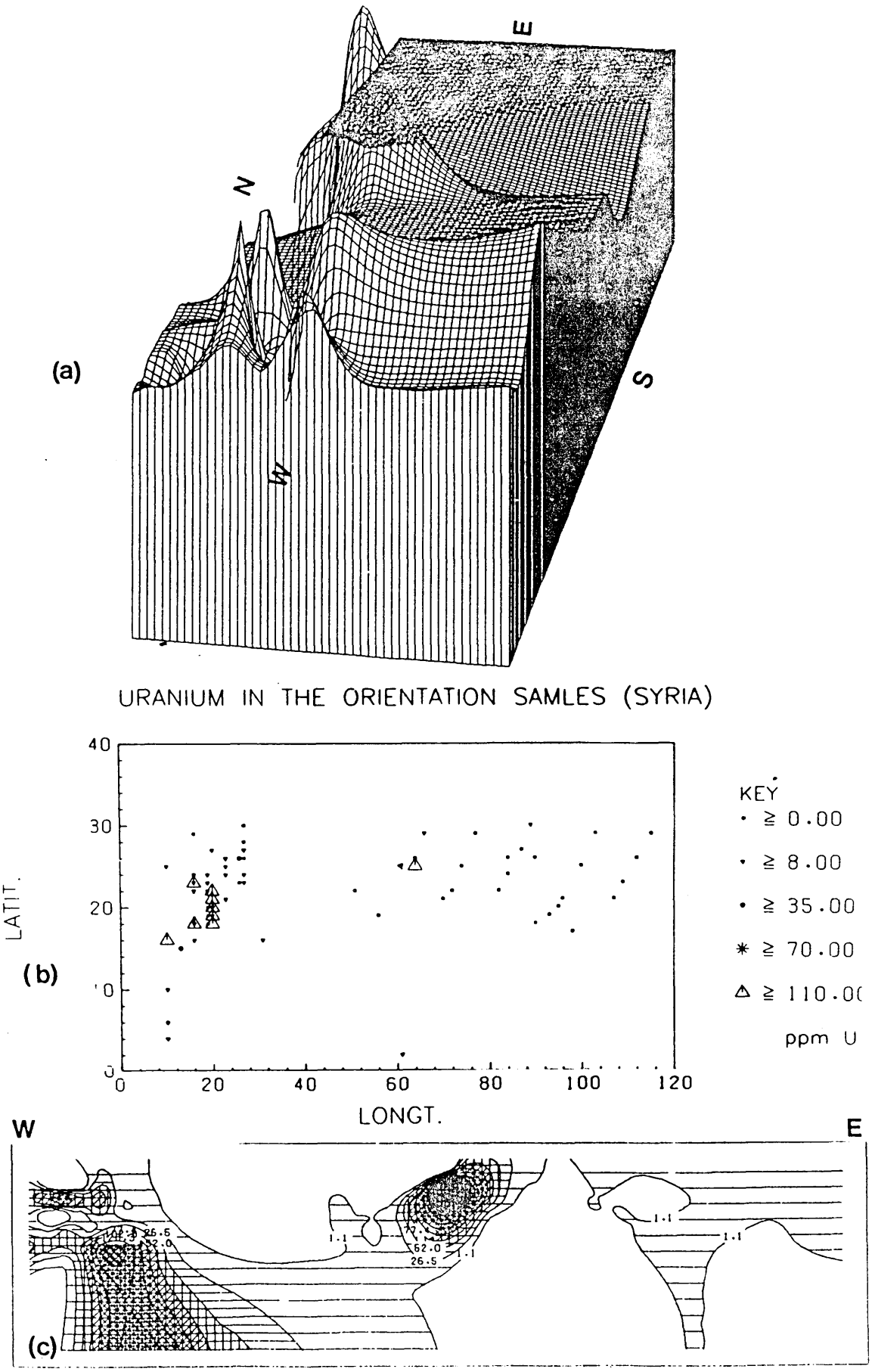


Fig.5.5 Spatial distribution of U in the orientation areas; solid surface (a), symbolic map (b),contour map (c).

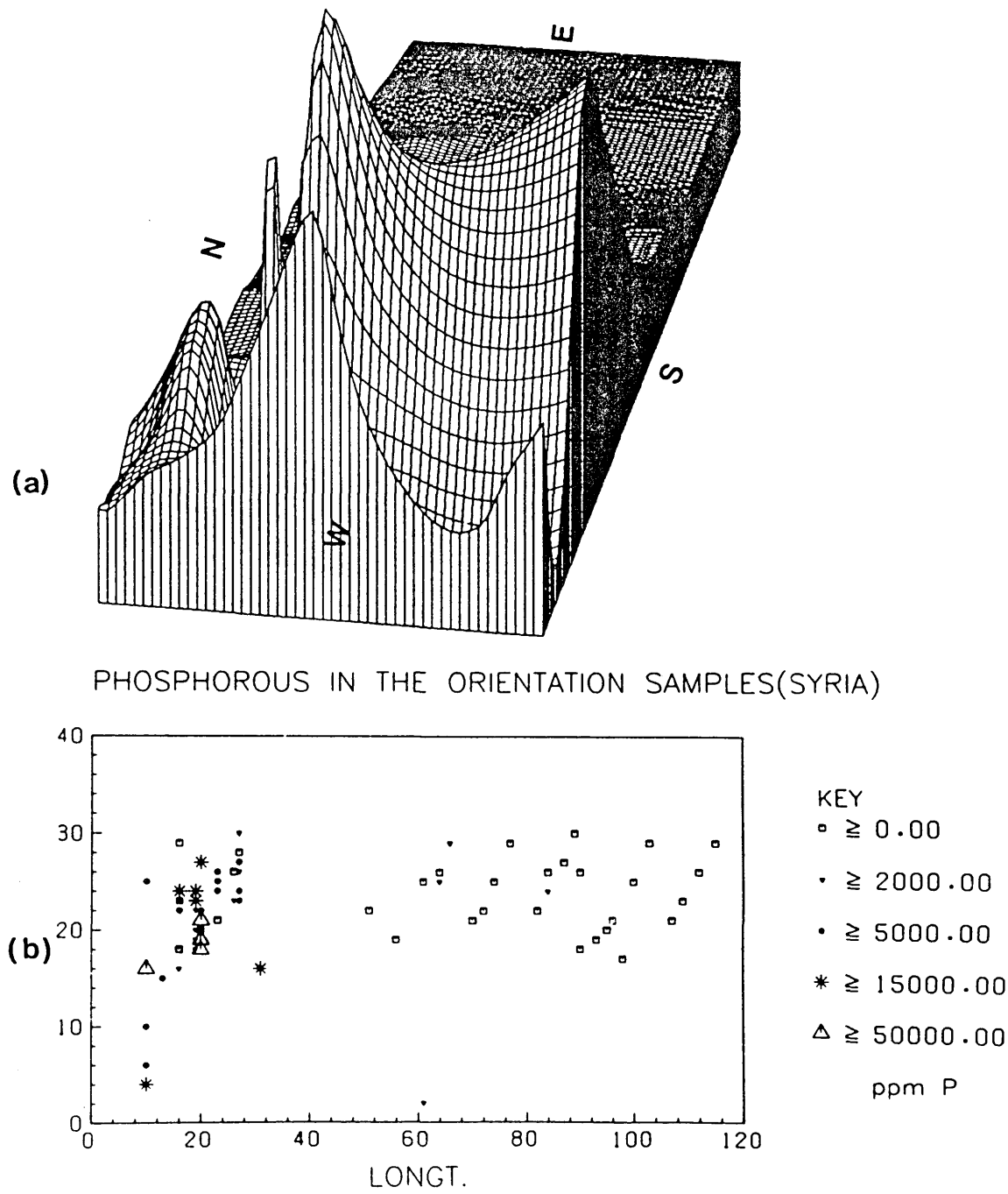


Fig.5.6 Spatial distribution of P in the orientation areas; solid surface (a), symbolic map (b).

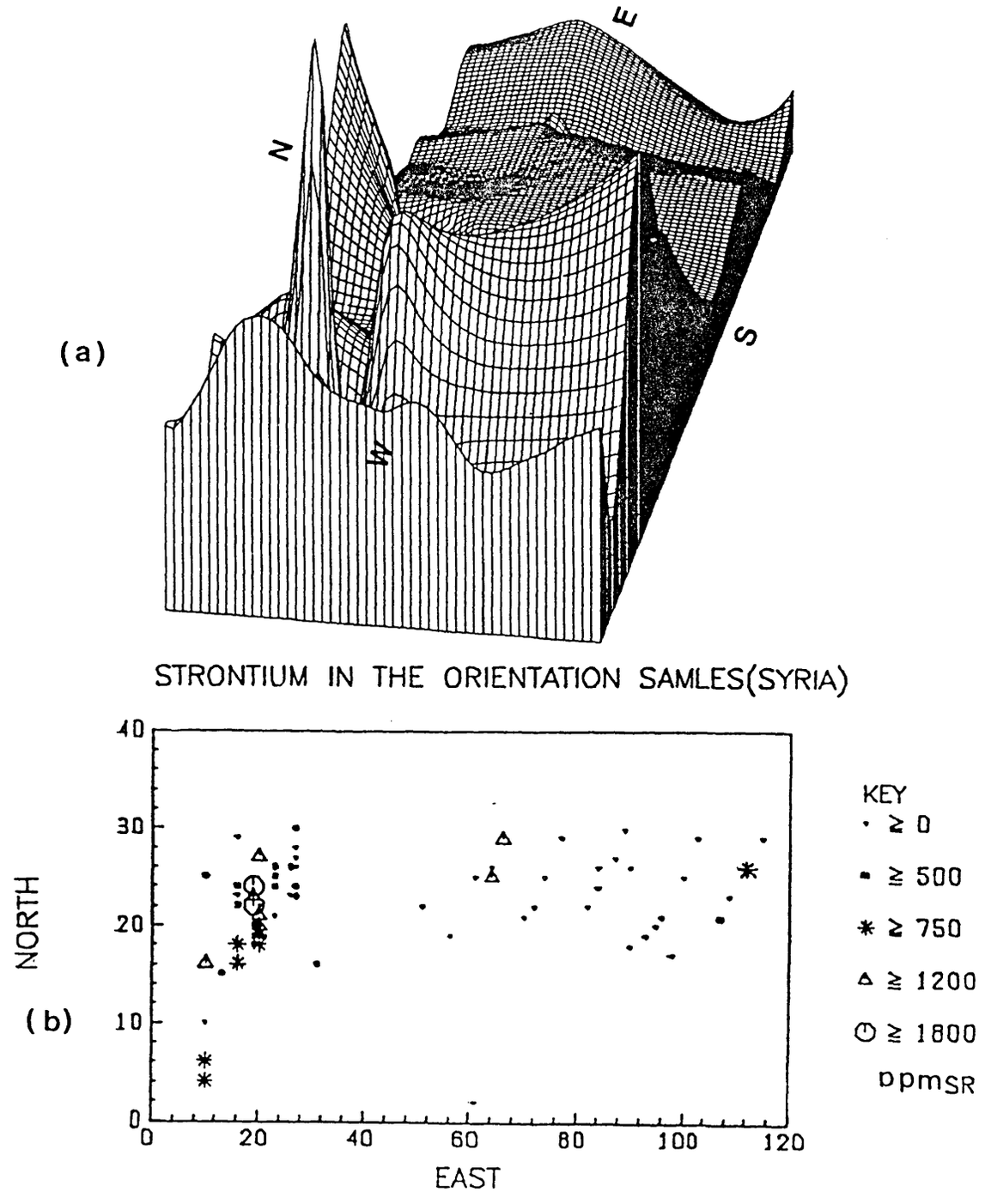


Fig.5.7 Spatial distribution of Sr in the orientation areas; solid surface (a), symbolic map (b).

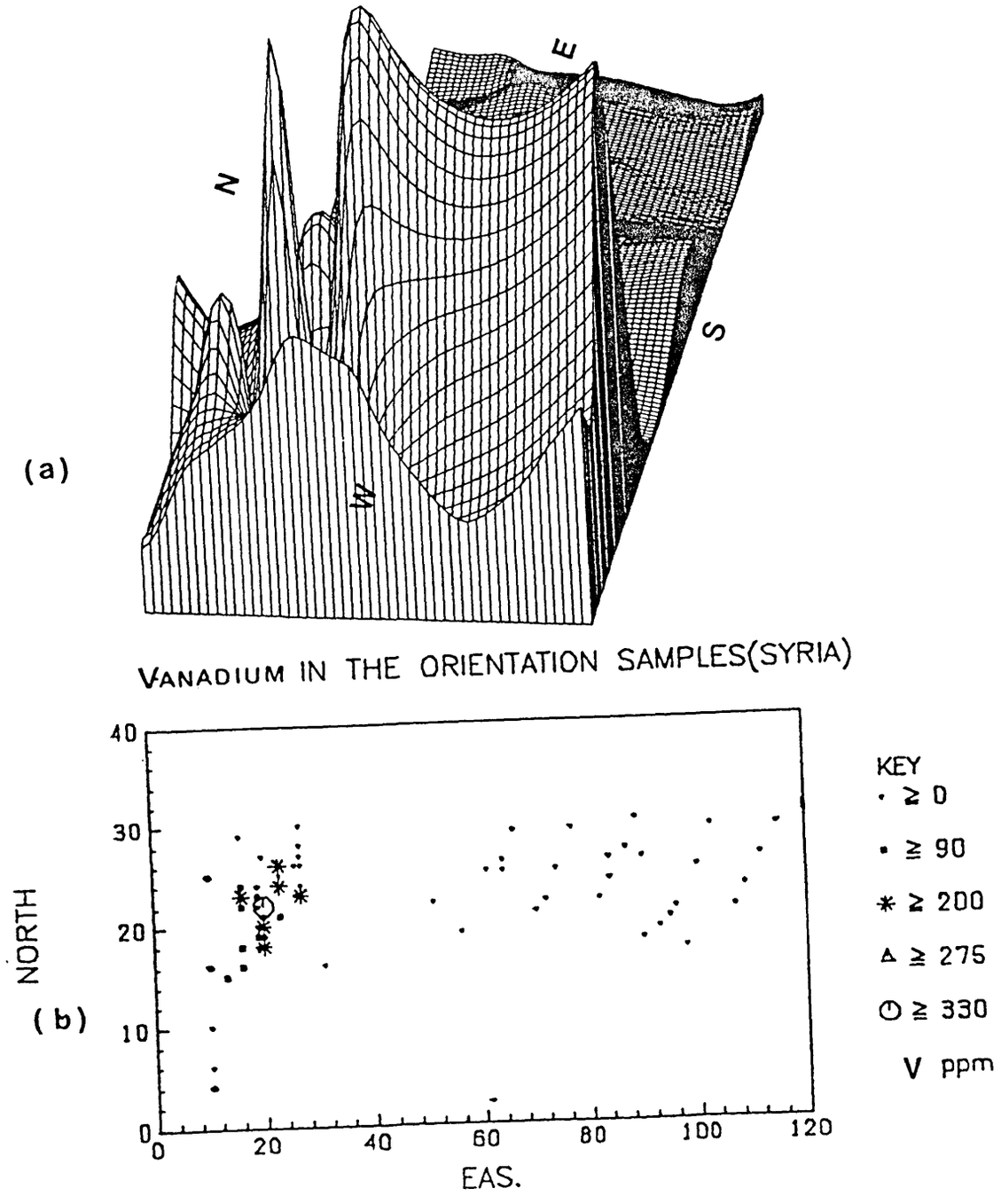


Fig.5.8 Spatial distribution of V in the orientation areas; solid surface (a), symbolic map (b).

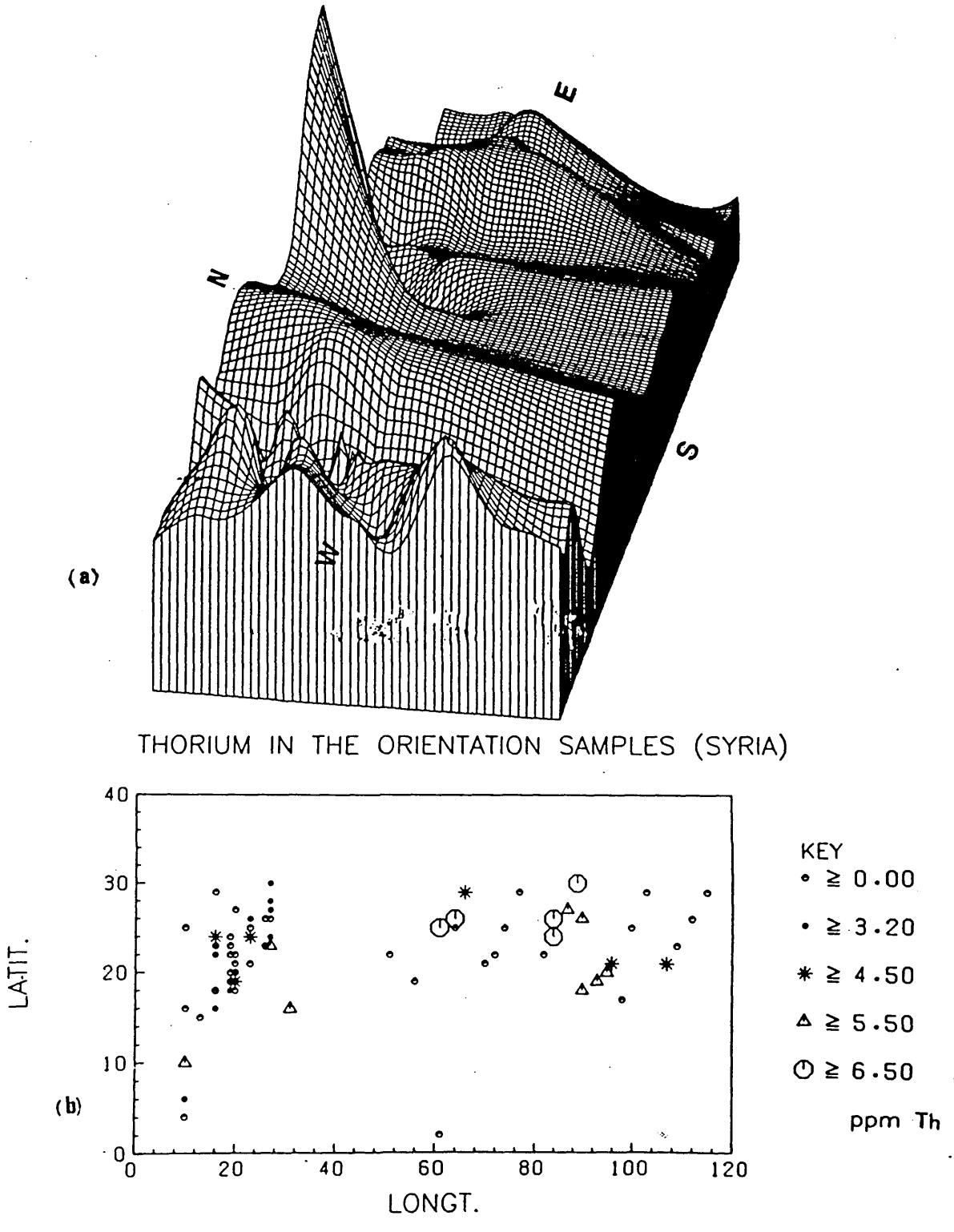
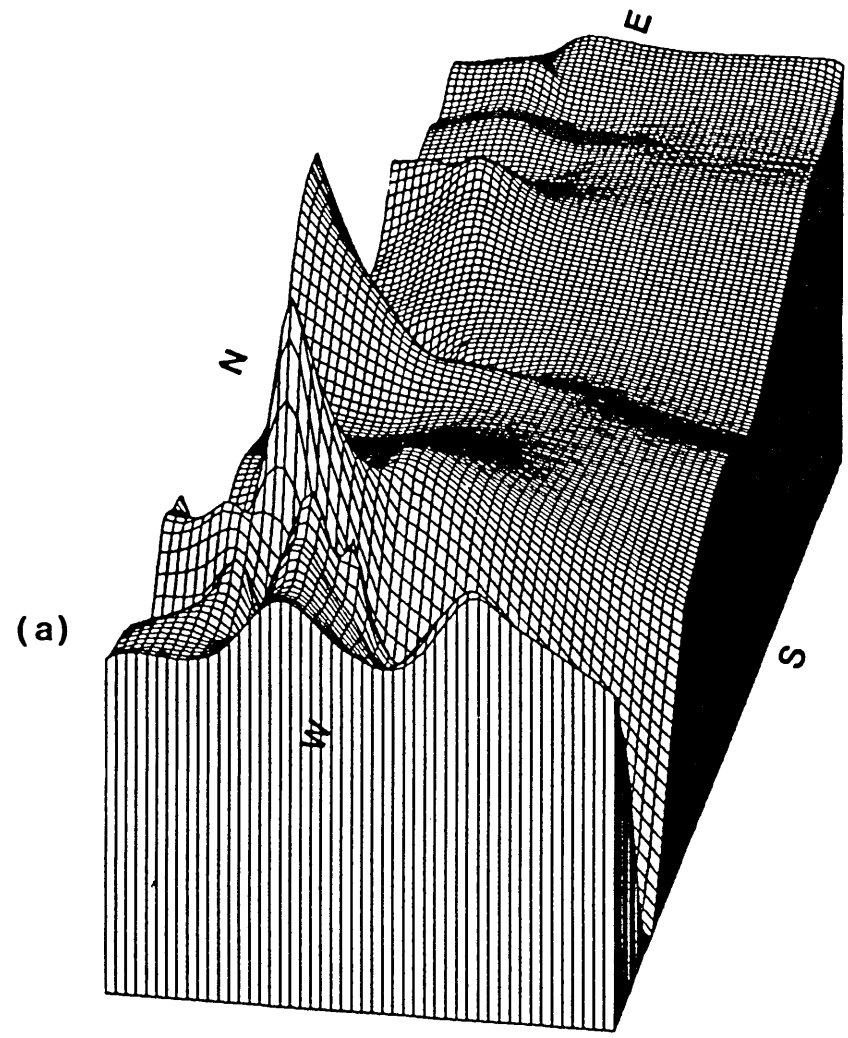


Fig.5.9 Spatial distribution of Th in the orientation areas; solid surface (a), symbolic map (b).



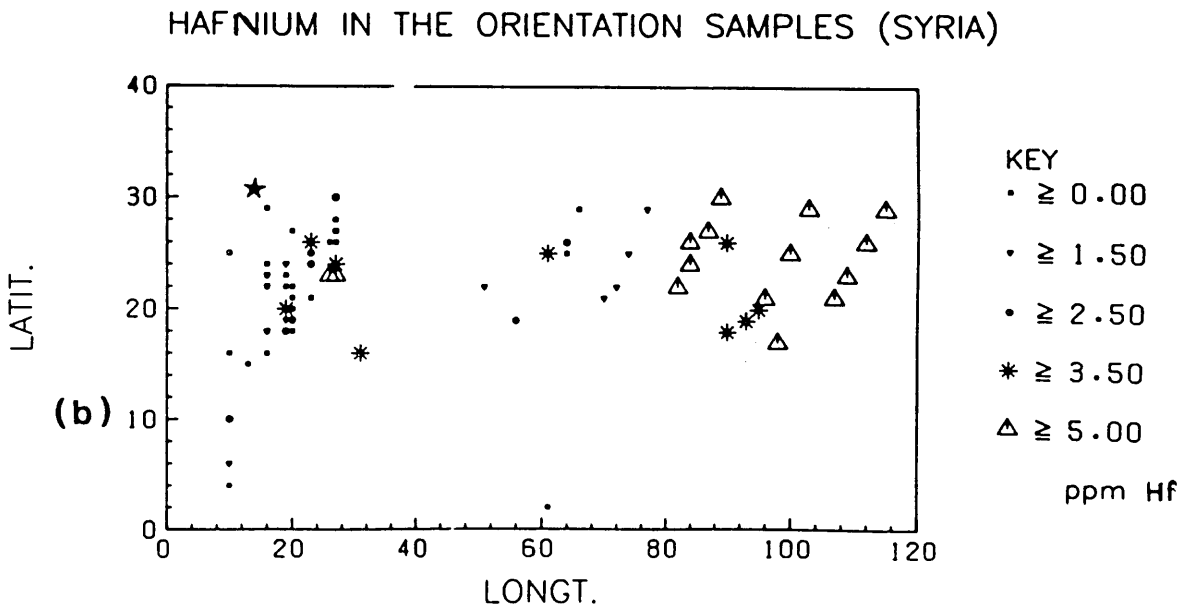


Fig.5.10 Spatial distribution of Hf in the orientation areas; solid surface (a), symbolic map (b).

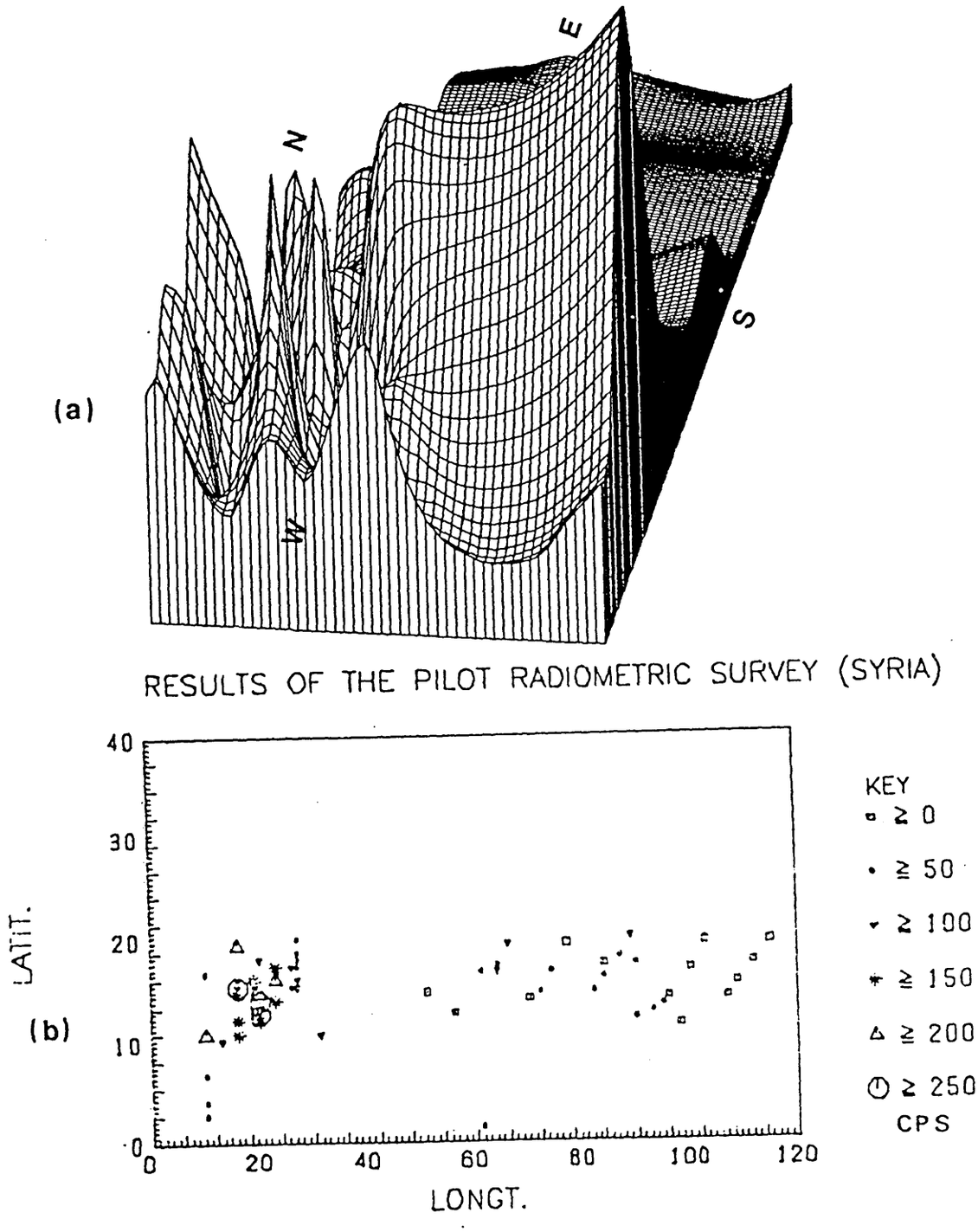


Fig.5.11 Spatial distribution of the CPS in the orientation areas; solid surface (a), symbolic map (b).

conditions, (Gabelman, 1977; Olade and Goodfellow,1978) resulting in its removal from the sediments possibly into the groundwater regime. The reported secondary uranium manifestations in the area probably have resulted from the precipitation of U from these enriched groundwaters. The paucity of the organic matter in the sediment, the lack of coprecipitation (scavenging) with Fe and Mn oxihydroxides and / or adsorption onto clay minerals (negative correlation between U and Fe, Mn and Al) further supports this interpretation and explains the observed low levels of U in wadi sediments of the eastern region. On the other hand, one must not forget that sampling of this area was carried out under heavy rain conditions which may possibly have flushed away the soluble U and left Th.

5.4.3.2 Boxplots

Boxplots of U, and other element concentrations are presented in Figures 5.12 to 5.15. These reveal that, relative to overburden and wadi sediment samples, the rock samples are enriched in U, P, Sr, Ca, V, Na, Cr and, to a lesser degree, rare earth elements (not presented). In contrast, the rock samples showed much lower mean concentrations of Th, Hf, K, Mg, Fe, Al, Ti and, to a lesser degree, Co and Cu (but wide concentration ranges). In the case of Th and Hf, this may indicate their incorporation in accessory resistate minerals, such as monazite, xenotime and zircon which are somewhat enriched in the wadi sediments. In the case of Fe, Al, Mg, Ti and K, the possible explanation of their concentration in the sediments and overburden is their susceptibility to hydromorphic dispersion, which has eventually led

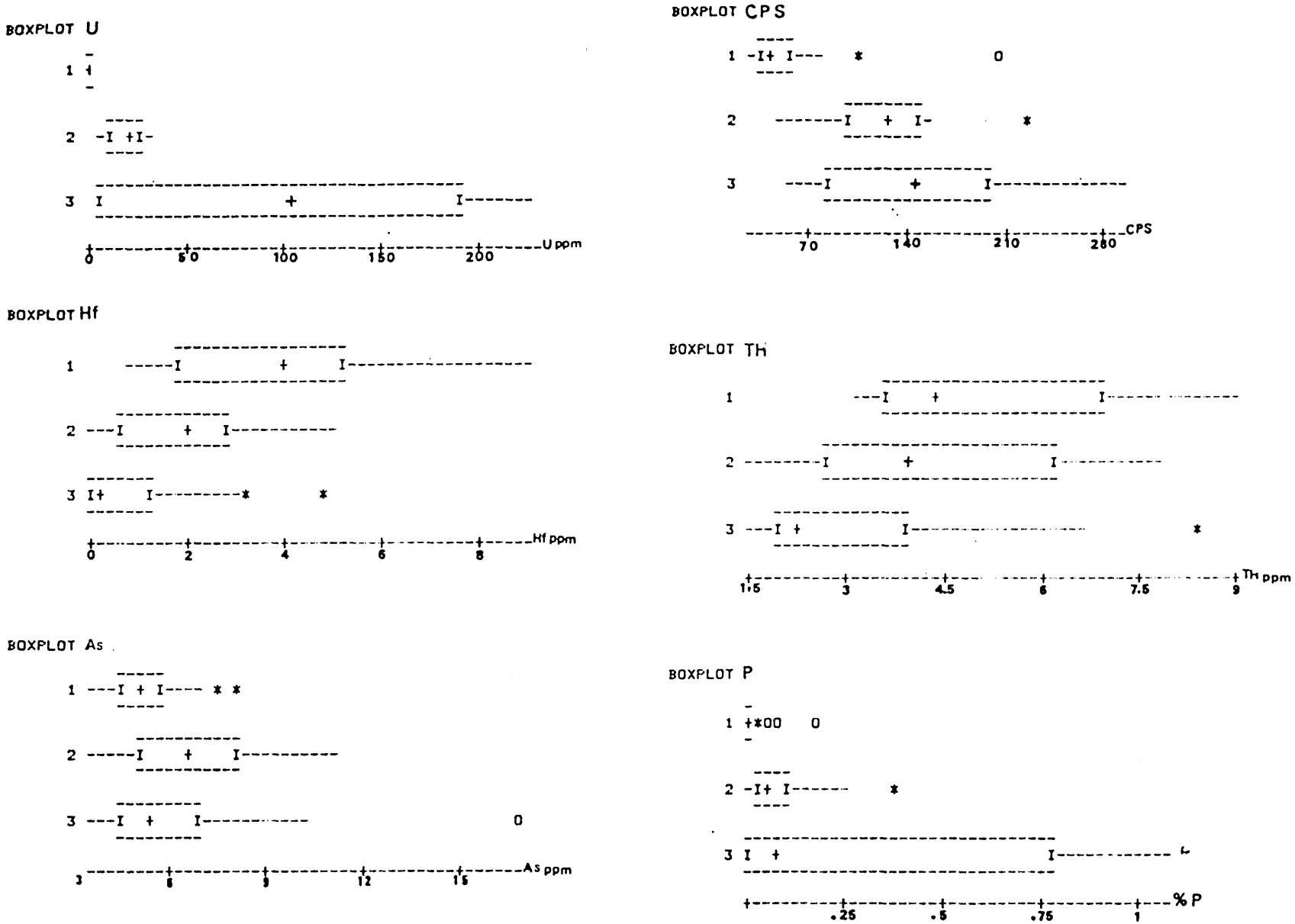


Fig.5.12 Boxplot of U, Hf, As, CPS, Th and P of the orientation survey by sample type. (1 = wadi sediments, 2 = overburden, 3 = rocks; asterisks indicate data beyond the mean plus or minus one standard error).

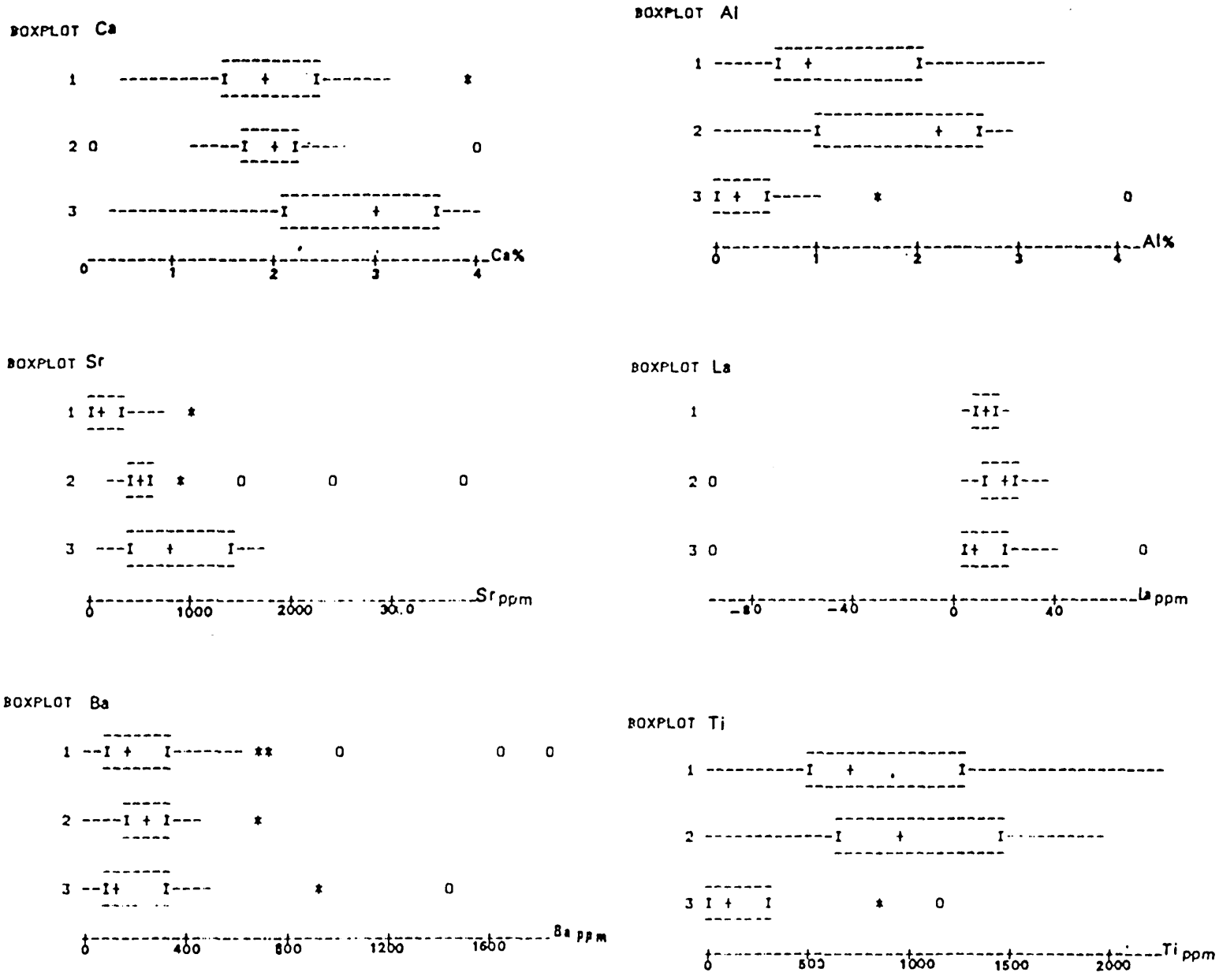
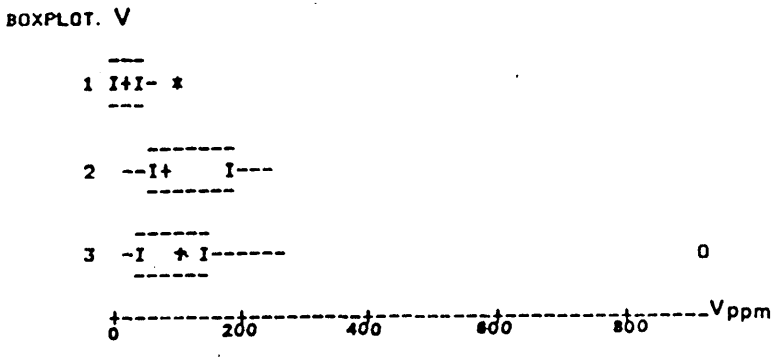
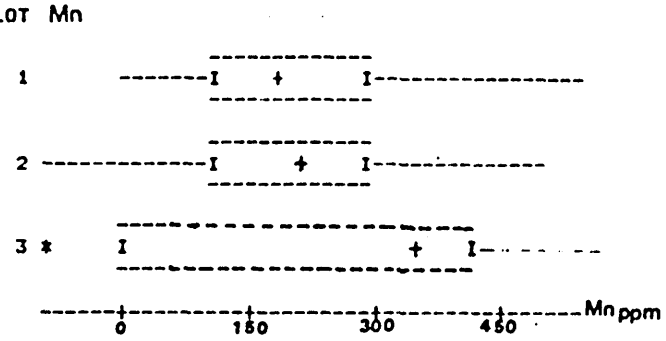
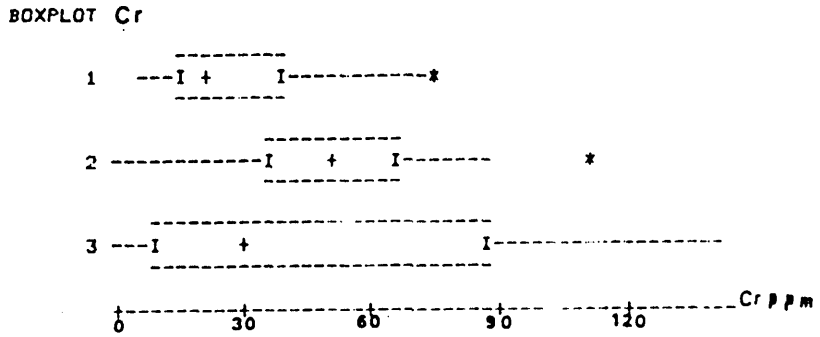
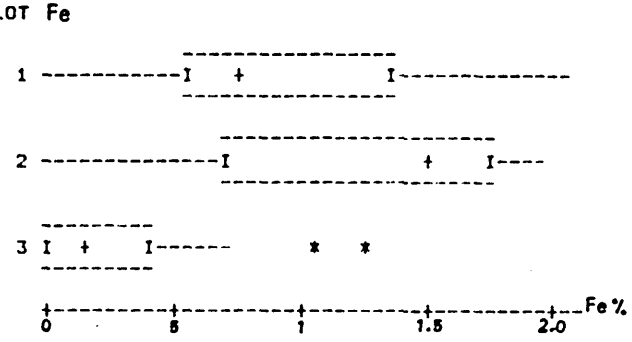


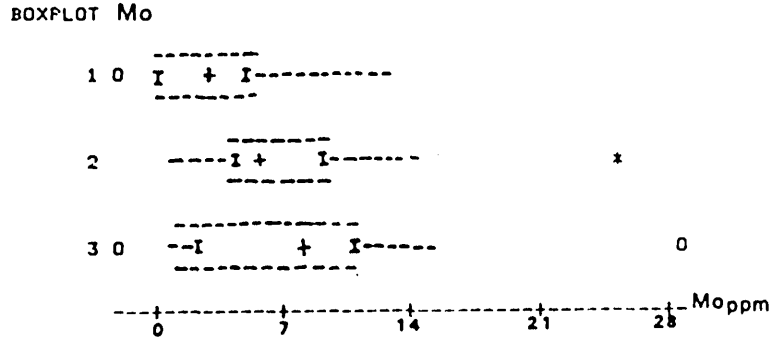
Fig.5.13 Boxplot of Ca, Sr, Ba, Al and Ti of the orientation survey by sample type. (1 = wadi sediments, 2 = overburden, 3 = rocks; asterisks indicate data beyond the mean plus or minus one standard error).











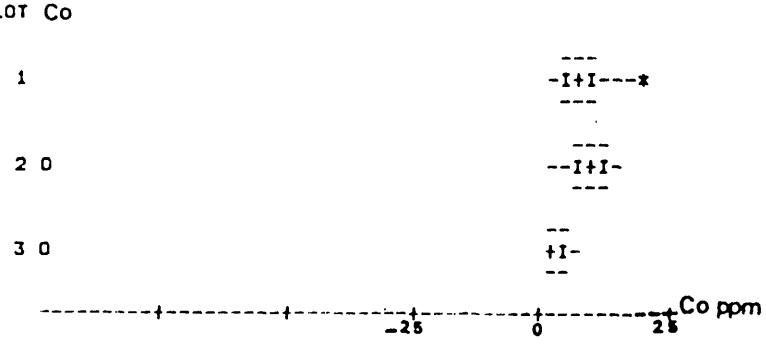
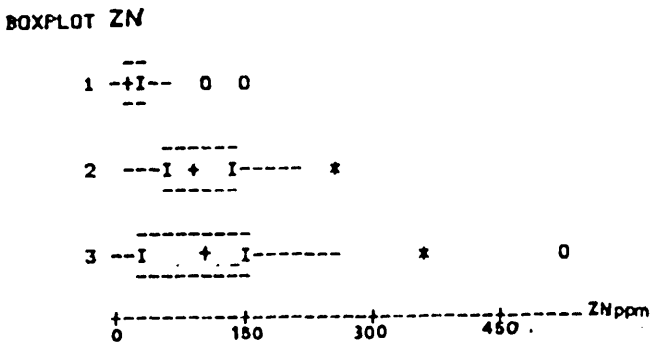
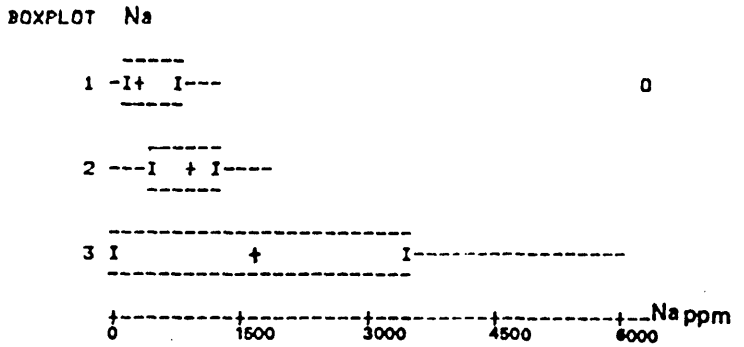
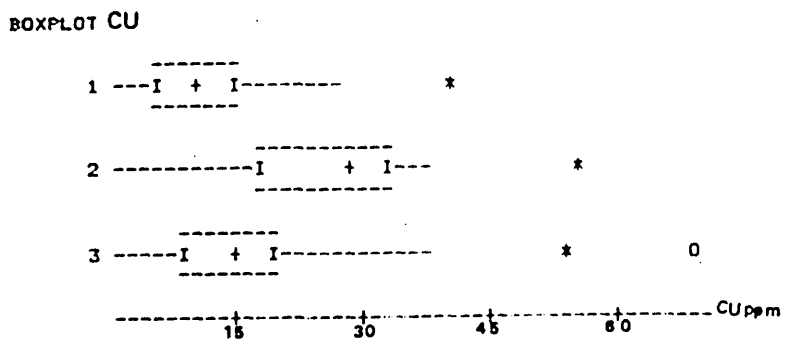
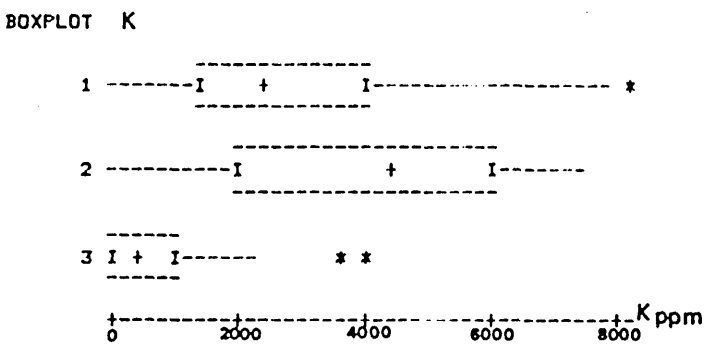


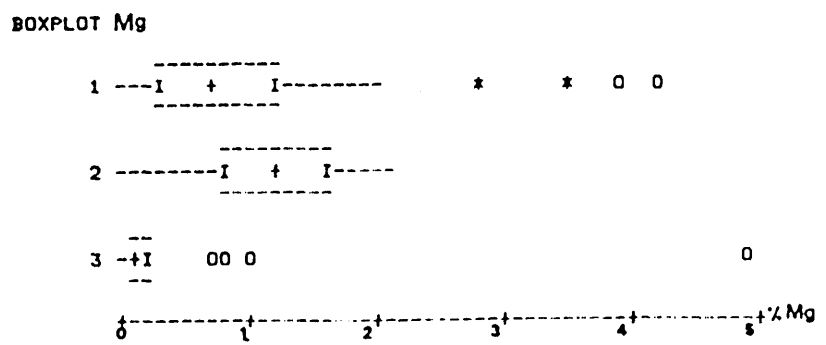
Fig.5.14 Box plot of means and ranges of Cr, Mo, V, Mn, Fe and Co in the orientation samples by sample type (1 = wadi sediments, 2 = overburden, 3 = rocks; asterisks indicate data beyond the mean plus or minus one standard error).











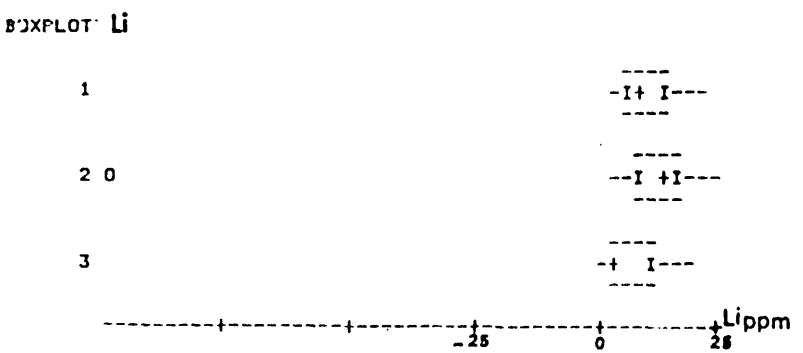


Fig.5.15 Box plot of means and ranges of Na, K, Mg, Zn, Cu and Li in the orientation samples by sample type (1 = wadi sediments, 2 = overburden, 3 = rocks; asterisks indicate data beyond the mean plus or minus one standard error).

to their accumulation in secondary clay minerals and other oxihydroxide forms. Therefore the higher Fe, Al, Ti, K and Mg values found in the detrital materials substantiate the interpretation that this association is a secondary environmental feature, which is closely associated with the bedrock.Arsenic, Mo, La, Ba, Li and Zn seem to have, more or less, uniform abundancies between the various sample types.

5.4.3.3 Histograms and frequency distributions

Frequency distributions of U and most other elements (eg. V, P and Sr) tend to show positively skewed distribution patterns. This indicates a possible lognormal distribution. Plotting the histograms of the log transformed values helped to mormalize their distributions (Figs. 5.16 and 5.17). In the case of U the histogram can be divided into three populations: the first represents the wadi sediment samples having, in general, the lowest U values; the second comprising mainly the overburden samples with some overlapping samples of both wadi sediments, from one side, and rocks from the other; and thirdly, another distinct group comprised mainly of phosphorite and mineralized rock samples. The cumulative frequency plot (Fig. 5.18) further demonstrates the presence of these U populations. Similarly the cumulative frequency plot of phosphorus shows two distinct populations, the first reflecting low phosphorus in a group of various lithologies and the second the phosphorite rocks in the region.

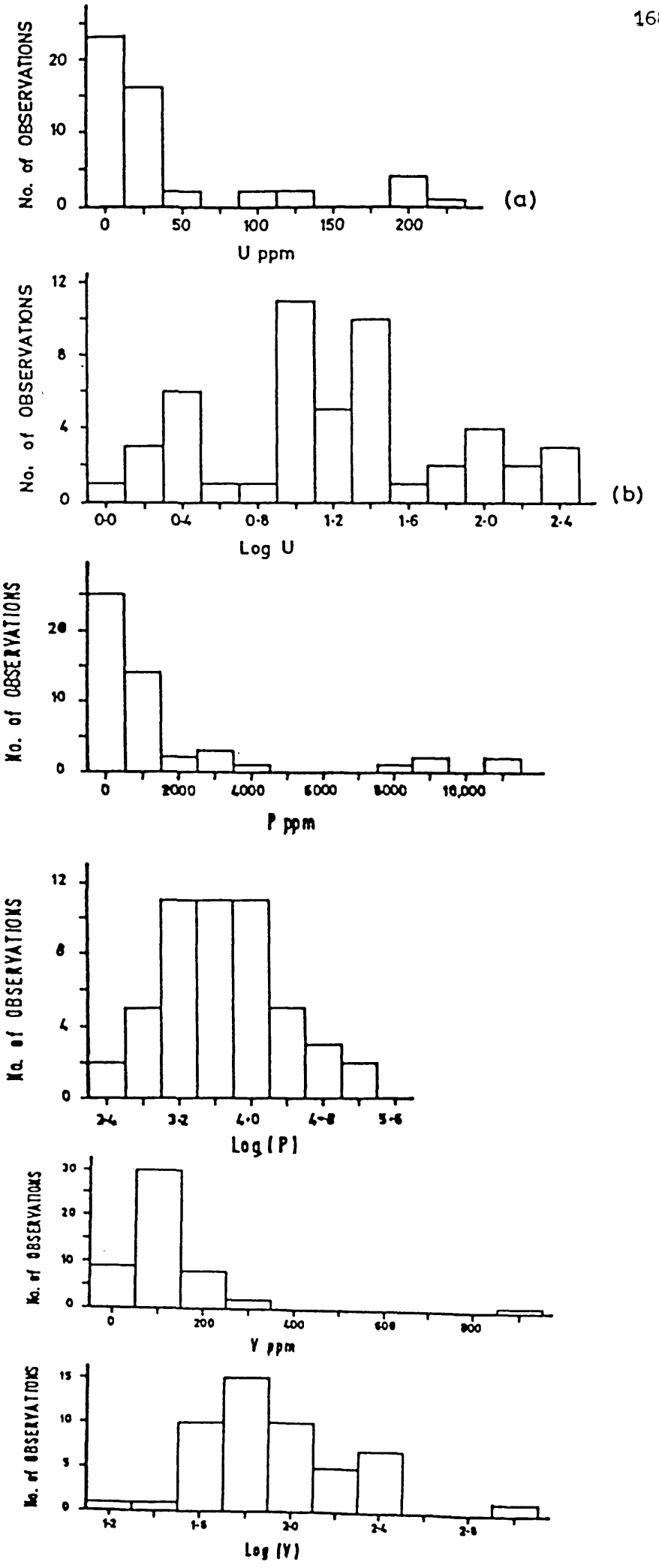


Fig.5.16 Histograms of U, P and V in the orientation samples.

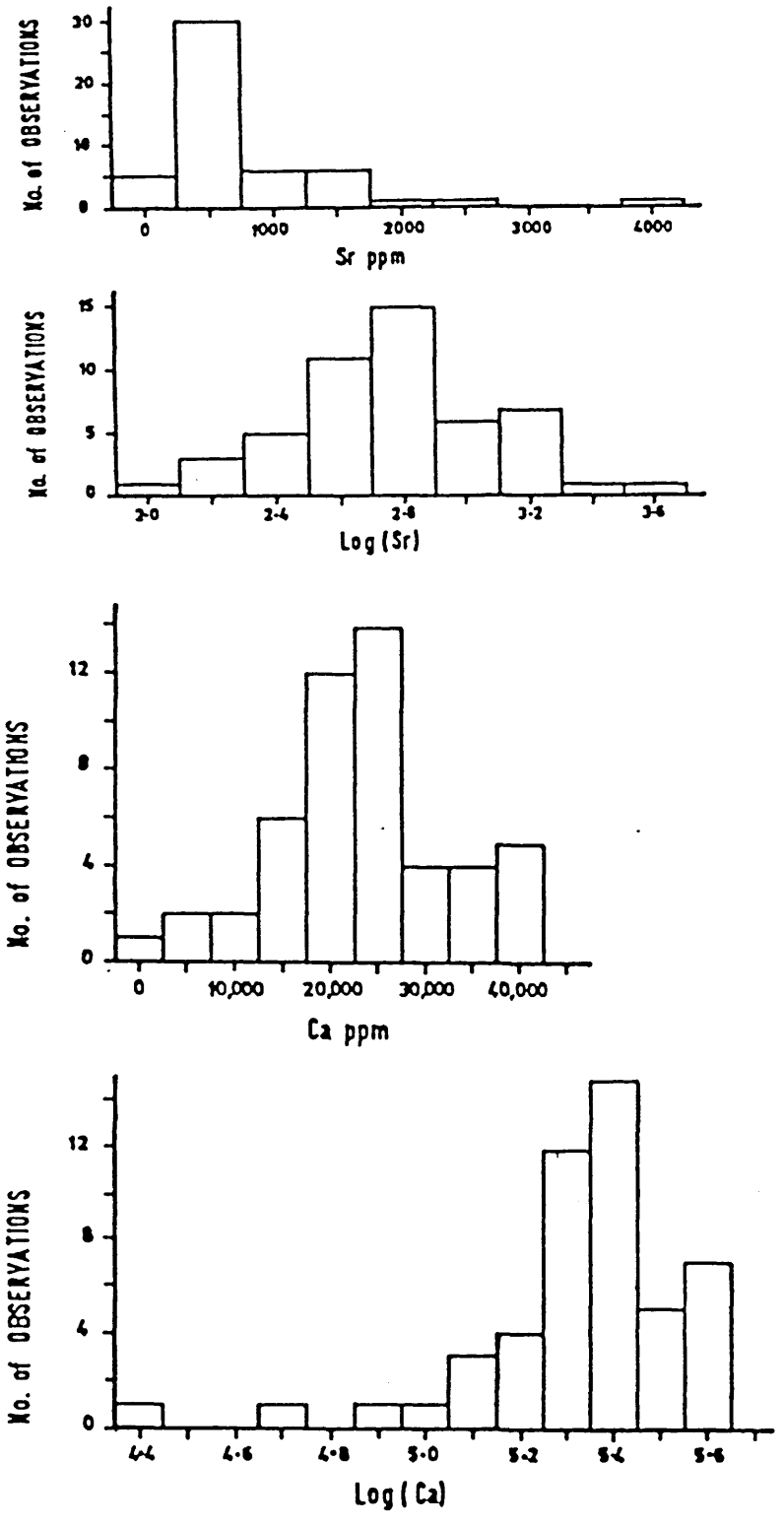


Fig.5.17 Histograms of Sr and Ca in the orientation samples.

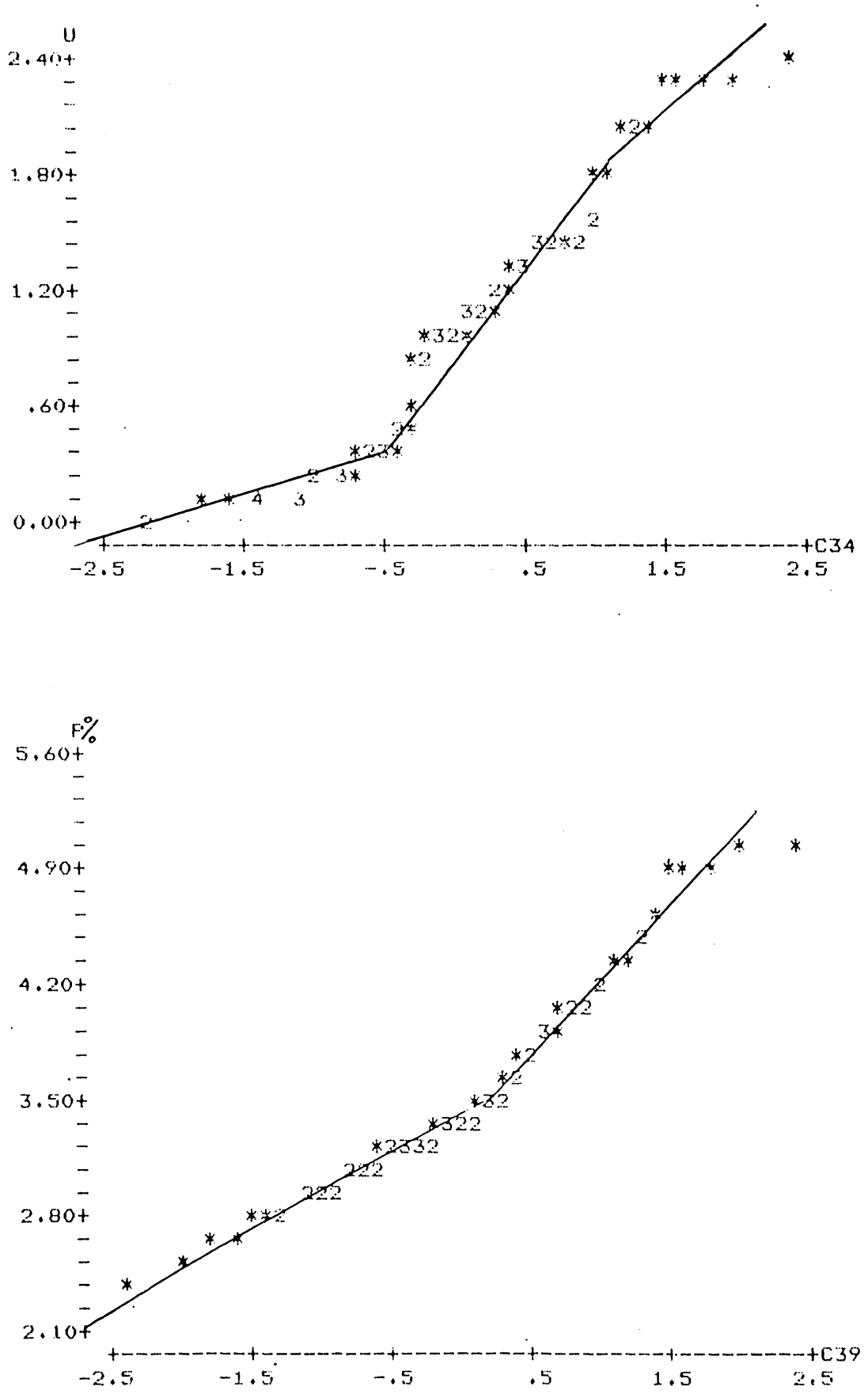


Fig.5.18 Normal Cumulative probability plot for U and P .

5.4.3.4 Interelement correlations

The standard Pearson correlation coefficient (Snedecor and Cochran, 1967; Kane et al., 1977), is only meaningful for normally distributed data. Therefore to evaluate the interelement relationships in the geochemical data, logarithms of all element concentrations were taken. Table 5.7 shows the correlation coefficients for 72 samples. Besides being significantly positively correlated with radiometric measurements (CPS), U is positively correlated at the 99% confidence level with Sr, V, Zn, P, Mo, Cu and As. In contrast U is negatively correlated with Hf, Th, Co, K, Fe, Al and Ti. The highest correlations for P are found with Zn, Cr, Sr, Na and Cu. Thorium is positively correlated with Hf, K, Fe, Al, Co, La, Ti, Na, Li and Cr, while it is negatively correlated with U and CPS indicting insignificant contribution to the radioactivity measurements of the region.

Among other correlations, Zn shows positive correlation with V, Cu, P, Cr, Mo, Sr, As and Na, and negative correlation with Hf, Mn and Th. No correlation was evident with the elements usually incorporated in the clay and the oxi-hydroxide minerals.

5.4.3.5 Variation diagrams

The scattergrams of U, Th and K against the measured radioactivities suggested that, perhaps the only significant relationship is between U and the radioactivity, both Th and K showed poor, if any, correlations (Fig. 5.19).

	U	HF	AS	CPS	TH	P	ZN	CU	MG	CA	SR	BA	AL
HF	-.624												
AS	.299	.109											
CPS	.836	-.543	.317										
TH	-.452	.719	.194	-.375									
P	.551	-.229	.491	.485	-.013								
ZN	.633	-.336	.606	.623	-.050	.748							
CU	.306	-.071	.568	.383	.189	.601	.778						
MG	-.276	.451	.359	-.171	.503	.127	.159	.495					
CA	.102	-.031	.252	.095	.055	.352	.335	.419	.245				
SR	.730	-.461	.266	.633	-.243	.683	.621	.557	.013	.225			
BA	.073	.187	.398	.048	.127	.323	.364	.383	.544	.017	.276		
AL	-.354	.522	.237	-.296	.610	.002	.138	.506	.768	.098	-.074	.422	
LA	.028	.283	.331	.121	.374	.489	.411	.628	.534	.317	.239	.358	.584
TI	-.329	.449	.197	-.254	.470	.034	.095	.482	.750	.256	-.087	.338	.805
V	.714	-.460	.557	.721	-.212	.530	.894	.650	.073	.131	.588	.274	.029
CR	.171	.113	.585	.216	.328	.720	.737	.788	.462	.452	.450	.467	.485
MO	.473	-.346	.428	.467	-.102	.399	.667	.653	.334	.033	.591	.484	.198
MN	-.486	.422	-.087	-.310	.319	-.385	-.232	.013	.627	-.213	-.377	.356	.771
FE	-.424	.537	.300	-.328	.616	.028	.148	.527	.835	.112	-.100	.503	.948
CO	-.387	.362	.163	-.239	.500	-.252	.128	.316	.605	-.421	-.171	.378	.754
LI	-.145	.291	.350	.064	.451	.056	.270	.417	.518	-.160	-.018	.368	.535
NA	.057	.188	.482	.149	.460	.636	.516	.662	.401	.460	.304	.163	.385
K	-.448	.533	.307	-.307	.642	-.035	.113	.510	.808	.028	-.135	.455	.899

	V	CR	MO	MN	FE	CO	LI	NA
CR	.516							
MO	.732	.443						
MN	-.233	.056	.011					
FE	.020	.523	.206	.769				
CO	.151	.323	.321	.644	.804			
LI	.227	.479	.297	.584	.588	.693		
NA	.323	.793	.280	-.057	.424	.138	.408	
K	.016	.484	.201	.669	.968	.632	.680	.424

Table 5.7 Correlation coefficient matrix of the orientation data.

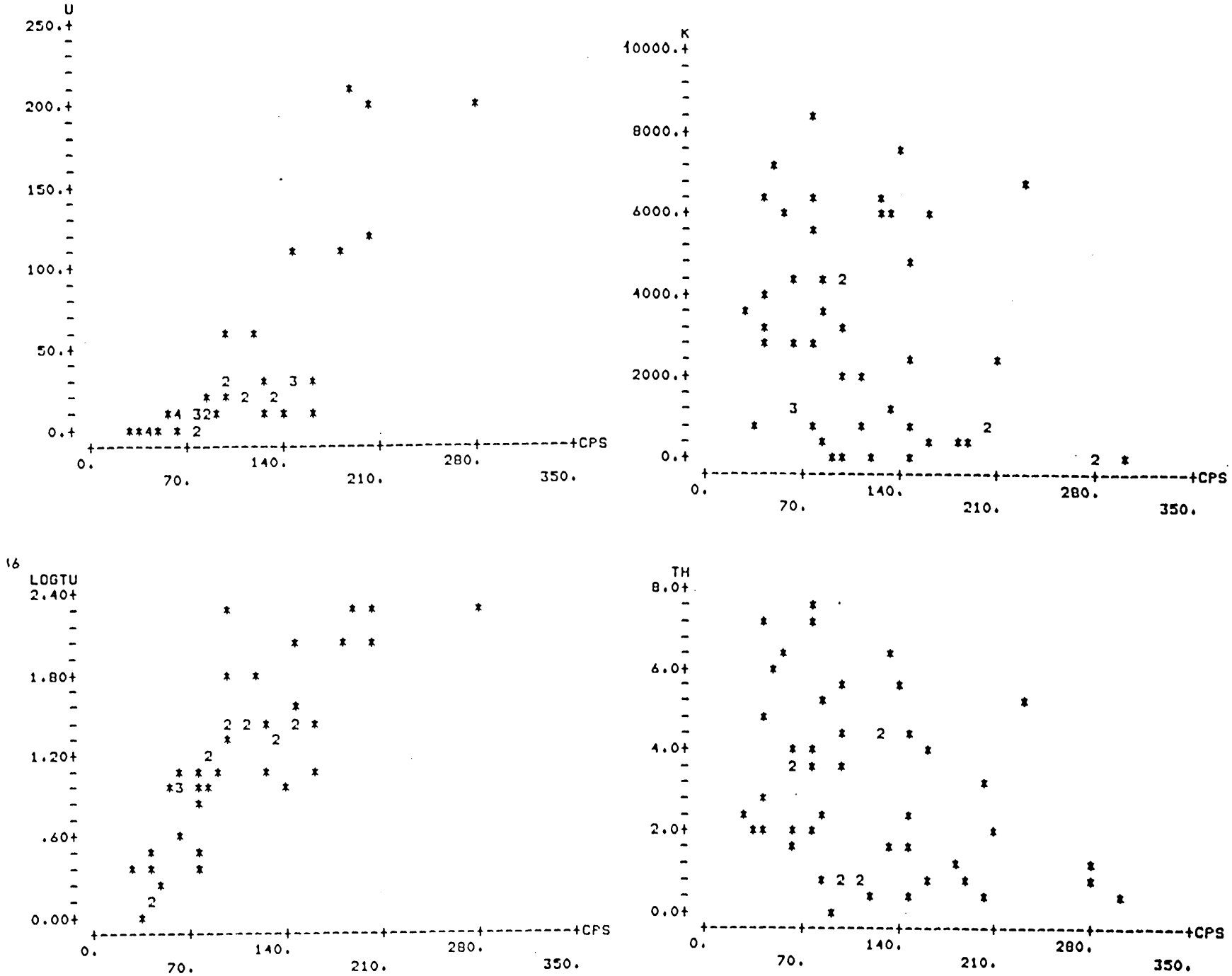


Fig.5.19 Scatterplots of U, Th and K Vs CPS

A scattergram of U content was plotted against percent P_2O_5 (Fig. 5.20), the result shows a strong linear relationship occurs only when P_2O_5 is less than 10%, while above that, the relationship becomes less obvious particularly for those samples containing above 20% P_2O_5. This, however, is in good agreement with the upper limit of linear relationship of 22% P_2O_5 found by Hunting (see Fig. 2.15)

5.4.3.6 Elemental ratios

Elemental ratios were used successfully by Simpson et al. (1979, 1982) and Plant et al. (1985) as geochemical criteria to recognize uraniferous granites. Many others used such ratios to minimize analytical variations, identify concentration levels of elements as petrogenic indicators and to smooth data (Govett, 1983). In the current work, ratios of U:P_2O_5 (an abbreviation for U x 10^4:P_2O_5%), U:Th, U:Hf and Sr:Ca were studied in an attempt to duscriminate between U-enriched phosphorite samples and other U enrichments not directly related to phosphorites, which perhaps might indicate U mineralization. From section 2.5.1 an average U:P_2O_5 ratio between 7 and 10 can be assigned for the U-enhanced Palmyrides marine phosphorite and a ratio of up to 30 may still indicate highly U enriched phosphorite samples. However, the results listed in Table 5.8 show a pattern of U:P_2O_5 ratios which is exceptionally high, ten samples 6, 7, 29, 31, 32, 35, 36, 40, 44 and 56 gave highly anomalous ratios ranging from 68 to 1562 which cannot be related to phosphorite; thus, these high ratios indicate another type of U enrichment. To clarify whether these exceptionally U-enriched samples may reflect the presence of the

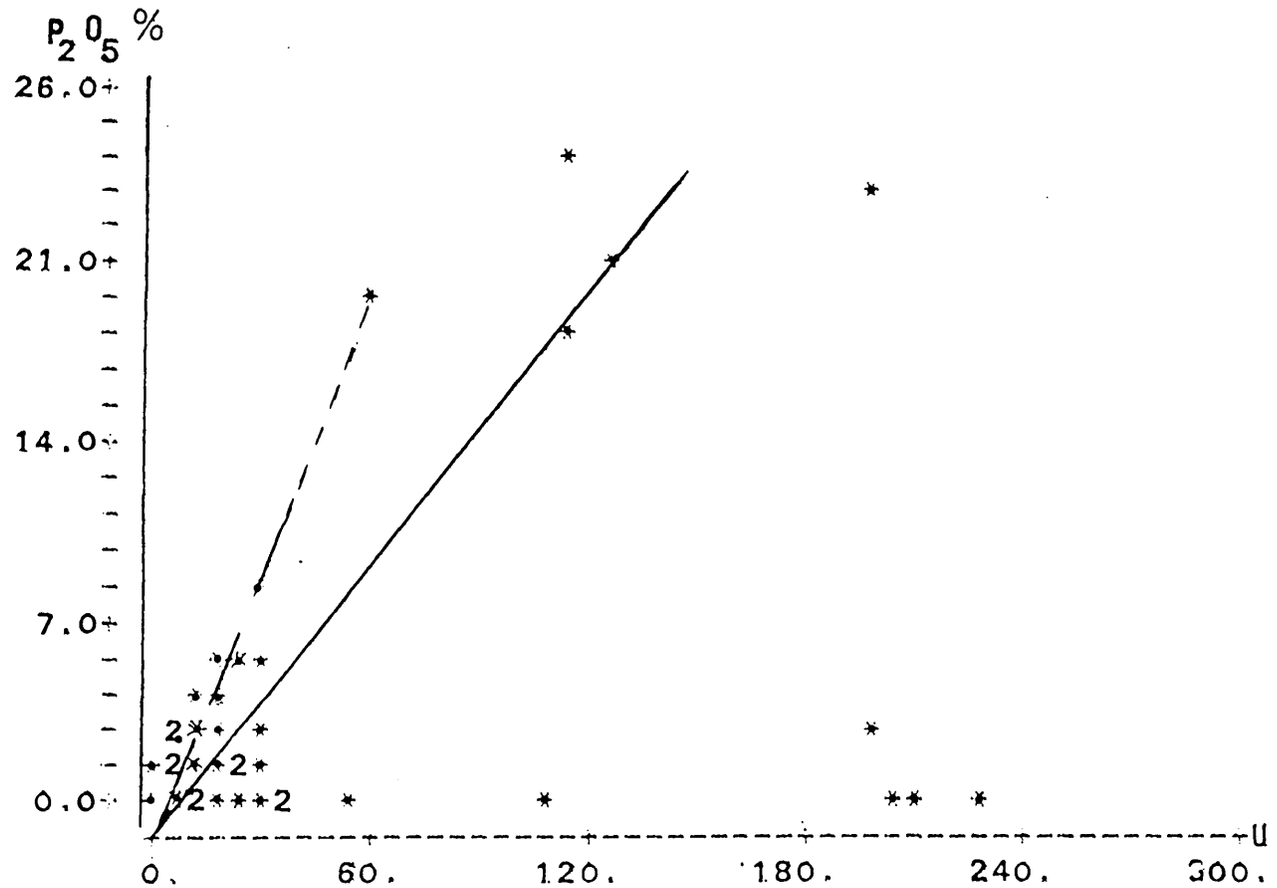


Fig. 5.20 Relationship of "P_2O_5" and "U" content in the orientation samples.

Table 5.8 Elemental ratios (P_2O_5 and Ca are in per cent, others in ppm).

C1 72	U/P2O5% 72	U/HF 72	U/TH 72	SR/CA% 72
1.	3.69	2.97	1.435	24.084
2.	8.70	3.20	2.667	25.238
3.	5.96	5.67	3.400	31.319
4.	19.93	15.71	15.714	165.217
5.	3.95	140.00	23.333	59.130
6.	247.05	58.32	44.320	64.844
7.	48.48	12.92	7.045	38.298
8.	5.10	24.42	5.426	28.571
9.	25.81	18.40	4.089	71.739
10.	8.21	.93	.355	17.791
11.	3.34	5.71	3.125	34.000
12.	6.28	2.80	1.400	15.417
13.	3.80	11.79	6.348	41.969
14.	4.48	13.80	6.571	30.058
15.	4.92	6.14	2.389	20.000
16.	10.27	48.83	8.371	26.429
17.	6.60	.44	.314	8.846
18.	15.65	1.00	1.286	24.725
19.	3.47	.76	.481	9.032
20.	9.66	.24	.286	17.596
21.	5.48	.59	.329	17.722
22.	6.05	1.24	.808	20.870
23.	7.40	.34	.287	14.333
24.	6.83	.21	.579	6.781
25.	9.11	.48	2.444	27.333
26.	8.78	2.12	1.750	25.833
27.	7.57	2.77	2.512	28.636
28.	7.18	1.82	1.500	29.091
29.	86.31	133.00	38.000	7.317
30.	3.02	3.13	5.882	22.682
31.	1582.50	383.33	575.000	9.148
32.	878.33	560.00	186.887	108.804
33.	3.88	120.00	30.000	35.143
34.	14.49	120.00	30.000	13.750
35.	623.82	330.00	165.000	247.828
36.	481.28	2070.00	285.714	243.838
37.	12.50	92.00	2.488	9.744
38.	5.84	87.88	41.000	47.027
39.	20.79	110.00	110.000	9.512
40.	342.81	341.87	256.250	58.148
41.	3.34	24.00	13.714	27.083
42.	2.87	17.08	10.843	29.730
43.	6.35	142.50	87.682	32.000
44.	90.13	1980.00	663.333	12.584
45.	4.51	186.67	112.000	50.968
46.	8.12	1960.00	217.778	54.194
47.	3.34	14.29	21.429	104.167
48.	38.84	12.92	7.045	24.862
49.	3.59	5.71	2.051	18.400
50.	8.84	5.71	3.529	40.370
51.	27.87	1.92	.641	28.750
52.	4.52	1.88	.867	27.841
53.	15.02	2.53	1.900	25.769
54.	41.41	5.00	6.667	24.800
55.	10.31	2.67	6.400	25.434
56.	68.32	165.00	8.250	80.768
57.	31.26	2.20	1.571	10.000
58.	7.67	.40	.400	7.720
59.	1.49	.20	.182	9.500
60.	3.99	.22	.407	4.781
61.	4.09	.70	.518	8.438
62.	3.84	.71	.625	12.273
63.	4.35	.74	.700	7.813
64.	8.01	.23	.467	17.800
65.	7.17	.21	.750	8.508
66.	11.59	.29	1.053	6.914
67.	15.65	.33	1.000	7.016
68.	4.83	.28	.850	5.581
69.	6.04	.29	.300	4.759
70.	7.32	.33	.267	14.088
71.	6.37	.36	.263	6.840
72.	11.92	.36	.283	6.286

resistate minerals zircon, sphene, xenotime or monazite, the ratios of U:Th and U:Hf were used to compare with corresponding U:P_2O_5 ratios. None of these highly anomalous samples seem to contain such enriched mineral phases. Therefore the ratio Sr:Ca was used to further investigate the possible source of high U:P_2O_5 values; this is because Sr is also known to be enriched in the phosphorite (Summerhayes, 1970, 1971), substituting for Ca in fracolite (McArthur, 1978, 1984), Sr is also highly enriched in calcretes along with U. Therefore comparing the ratios of Sr:Ca and U:P_2O_5 was expected to shed some light on the possibility for appropriate identification of these U anomalies. Only five out of the ten highly anomalous samples show equally high Sr:Ca ratios (samples 6, 32, 35, 36 and 56) which suggests non-phosphorite and possibly calcrete type of U enrichment. Sample 4 with Sr:Ca ratio of 165.2 and U:P_2O_5 ratio of 19.9 appears to be enriched in Sr and U, although it has not been clearly outlined by previous ratios; this sample could also be of a calcrete type. It is noteworthy that sample 31 which shows extremely high U:P_2O_5 ratio (1562.5) and very low Sr:Ca ratio (9.1) seems to reflect values consistent with it being a mineralized organogeneous limestone sample. This provides confidence in utilizing elemental ratios as a means of discrimination.

5.4.4 Wadi sediment data

The mean and standard deviation of elements in 34 wadi sediment samples are listed in Table 5.9. The frequency distribution of U suggested a bimodal distribution. Threshold value of 7 ppm separated the data into two populations, background and

Table 5.9 Summary statistics of the wadi sediments.

U	N =	34	MEAN =	3.1441	ST.DEV. =	2.86
HF	N =	34	MEAN =	3.9676	ST.DEV. =	2.06
AS	N =	34	MEAN =	2.3088	ST.DEV. =	.983
CPS	N =	34	MEAN =	56.206	ST.DEV. =	29.8
TH	N =	34	MEAN =	3.8088	ST.DEV. =	1.87
P	N =	34	MEAN =	2384.1	ST.DEV. =	2946.
ZN	N =	34	MEAN =	38.388	ST.DEV. =	22.0
CU	N =	34	MEAN =	13.112	ST.DEV. =	7.83
MG	N =	34	MEAN =	12358.	ST.DEV. =	12701.
CA	N =	34	MEAN =	207971.	ST.DEV. =	76900.
SR	N =	34	MEAN =	308.41	ST.DEV. =	215.
BA	N =	34	MEAN =	363.42	ST.DEV. =	471.
AL	N =	34	MEAN =	12881.	ST.DEV. =	9345.
LA	N =	34	MEAN =	10.868	ST.DEV. =	4.59
TI	N =	34	MEAN =	899.79	ST.DEV. =	647.
V	N =	34	MEAN =	39.279	ST.DEV. =	18.9
CR	N =	34	MEAN =	27.271	ST.DEV. =	15.7
MO	N =	34	MEAN =	2.9006	ST.DEV. =	2.69
MN	N =	34	MEAN =	208.02	ST.DEV. =	152.
FE	N =	34	MEAN =	9344.7	ST.DEV. =	5991.
CO	N =	34	MEAN =	7.8471	ST.DEV. =	4.57
LI	N =	34	MEAN =	8.0044	ST.DEV. =	5.32
NA	N =	34	MEAN =	649.03	ST.DEV. =	1065.
K	N =	34	MEAN =	3107.0	ST.DEV. =	2317.

anomalous (Fig. 5.21). In addition to U the skewness shown by histograms of P, Sr, Th, Mo and Ba indicates possible anomalies reflected by lognormal or even polymodal distributions while the histograms of Ca, Zn, Cu, V and As show close to normal distribution. Surprisingly, results of the correlation matrix (Table 5.10) suggested that uranium did not correlate with radiometric measurements (CPS) in the wadi sediment samples, instead, the highest possible correlation coefficient shown by U is with P (0.808). This may reflect better relationship between the two at their background concentration levels as was demonstrated in Fig. 5.20. Several other elements (Sr, Mo, Ba, As, Mg, V and Cu) correlate positively with U.

The following can be concluded from the wadi sediment orientation survey:

(1) - Variations in metal content in the wadi sediment reflect the presence of different phases as well as different behaviour in the secondary environment.

2) - The contrast between the background and the anomalous values was found to be low.

5.4.5 Overburden data

A summary of the means and standard deviations for 22 samples of overburden are presented in Table 5.11. Uranium concentrations range from 6.4 to 58 ppm; the histogram (Fig. 5.22) indicates that the distribution of U is bimodal consisting of two main populations

U

MIDDLE OF INTERVAL	NUMBER OF OBSERVATIONS	
1.	8	********
2.	14	**************
3.	5	*****
4.	1	*
5.	0	
6.	0	
7.	1	*
8.	2	**
9.	1	*
10.	1	*
11.	0	
12.	1	*

V

MIDDLE OF INTERVAL	NUMBER OF OBSERVATIONS	
10.	3	***
20.	5	*****
30.	6	******
40.	6	******
50.	7	*******
60.	4	****
70.	1	*
80.	2	**

AS

MIDDLE OF INTERVAL	NUMBER OF OBSERVATIONS	
.5	1	*
1.0	3	***
1.5	6	******
2.0	8	********
2.5	6	******
3.0	5	*****
3.5	0	
4.0	4	****
4.5	1	*

MO

MIDDLE OF INTERVAL	NUMBER OF OBSERVATIONS	
0.	11	**********
1.	1	*
2.	4	****
3.	5	*****
4.	3	***
5.	4	****
6.	1	*
7.	2	**
8.	3	***

P

MIDDLE OF INTERVAL	NUMBER OF OBSERVATIONS	
0.	11	**********
2000.	17	**********
4000.	2	**
6000.	1	*
8000.	1	*
10000.	1	*
12000.	0	
14000.	1	*

SR

MIDDLE OF INTERVAL	NUMBER OF OBSERVATIONS	
100.	6	******
200.	10	**********
300.	6	******
400.	3	***
500.	5	*****
600.	2	**
700.	1	*
800.	0	
900.	0	
1000.	0	
1100.	1	*

TH

MIDDLE OF INTERVAL	NUMBER OF OBSERVATIONS	
1.5	1	*
2.0	9	*********
2.5	5	*****
3.0	2	**
3.5	2	**
4.0	4	****
4.5	0	
5.0	2	**
5.5	0	
6.0	5	*****
6.5	1	*
7.0	1	*
7.5	2	**

Fig.5.21 Histograms of U, V, As, P, Sr and CPS in the wadi sediments.

U

MIDDLE OF INTERVAL	NUMBER OF OBSERVATIONS	
5.	1	*
10.	5	*****
15.	3	***
20.	3	***
25.	1	*
30.	5	*****
35.	2	**
40.	0	
45.	0	
50.	0	
55.	0	
60.	1	*

U

MIDDLE OF INTERVAL	NUMBER OF OBSERVATIONS	
0.	2	**
20.	4	****
40.	0	
60.	1	*
80.	0	
100.	0	
120.	4	****
140.	0	
160.	0	
180.	0	
200.	4	****
220.	0	
240.	1	*

Fig.5.22 Histograms of U in the overburden and rocks.

Table 5.10 Correlation coeffitients for U with other elements wadi,overburden and rock samples of the orientation survey.

	wadi sediment subgroup	overburden subgroup	rock subgroup
	U	U	U
HF	-.333	-.520	-.343
AS	.584	-.044	.397
CPS	.169	.148	.726
TH	-.116	-.320	-.479
P	.808	.111	.070
ZN	.688	-.048	.269
CU	.468	-.389	-.045
MG	.540	-.267	-.147
CA	.215	-.023	-.317
SR	.841	.090	.390
BA	.647	-.272	.300
AL	-.035	-.220	.175
LA	.029	-.237	-.061
TI	-.158	-.106	-.334
V	.486	-.057	.402
CR	.372	-.204	.055
MO	.727	-.097	.122
MN	-.228	-.207	.022
FE	.109	-.306	-.307
CO	.111	-.255	-.025
LI	-.033	-.275	.158
NA	-.118	-.150	-.175
K	-.049	-.327	-.356
	V	V	V
CR	.814	.514	.300
MO	.736	.626	.083
MN	.454	.360	-.174
FE	.765	.588	.047
CO	.747	.557	-.135
LI	.731	.499	-.163
NA	.280	.270	-.155
K	.722	.611	-.142

Table 5.11 Summary statistics of the overburden data.

U	N =	22	MEAN =	21.910	ST.DEV. =	12.5
HF	N =	22	MEAN =	1.8571	ST.DEV. =	1.45
AS	N =	22	MEAN =	3.4619	ST.DEV. =	1.87
CPS	N =	22	MEAN =	123.57	ST.DEV. =	40.0
TH	N =	22	MEAN =	3.3286	ST.DEV. =	2.02
P	N =	22	MEAN =	10180.	ST.DEV. =	9728.
ZN	N =	22	MEAN =	117.38	ST.DEV. =	66.5
CU	N =	22	MEAN =	26.976	ST.DEV. =	12.0
MG	N =	22	MEAN =	13293.	ST.DEV. =	7853.
CA	N =	22	MEAN =	210048.	ST.DEV. =	69418.
SR	N =	22	MEAN =	920.00	ST.DEV. =	831.
BA	N =	22	MEAN =	362.05	ST.DEV. =	374.
AL	N =	22	MEAN =	17883.	ST.DEV. =	10883.
LA	N =	22	MEAN =	16.565	ST.DEV. =	8.92
TI	N =	22	MEAN =	936.29	ST.DEV. =	587.
V	N =	22	MEAN =	120.43	ST.DEV. =	64.1
CR	N =	22	MEAN =	57.997	ST.DEV. =	33.9
MO	N =	22	MEAN =	8.2905	ST.DEV. =	4.34
MN	N =	22	MEAN =	188.72	ST.DEV. =	139.
FE	N =	22	MEAN =	12237.	ST.DEV. =	6666.
CO	N =	22	MEAN =	8.2800	ST.DEV. =	4.26
LI	N =	22	MEAN =	11.333	ST.DEV. =	5.69
NA	N =	22	MEAN =	889.67	ST.DEV. =	538.
K	N =	22	MEAN =	3940.0	ST.DEV. =	2345.

Summary statistics of the rock subgroup.

U	N =	16	MEAN =	102.60	ST.DEV. =	83.7
HF	N =	16	MEAN =	.95625	ST.DEV. =	1.40
AS	N =	16	MEAN =	3.5375	ST.DEV. =	3.35
CPS	N =	16	MEAN =	160.94	ST.DEV. =	74.7
TH	N =	16	MEAN =	1.8063	ST.DEV. =	2.00
P	N =	16	MEAN =	32766.	ST.DEV. =	43071.
ZN	N =	16	MEAN =	144.05	ST.DEV. =	144.
CU	N =	16	MEAN =	21.569	ST.DEV. =	18.5
MG	N =	16	MEAN =	2625.6	ST.DEV. =	2618.
CA	N =	16	MEAN =	286938.	ST.DEV. =	118655.
SR	N =	16	MEAN =	962.63	ST.DEV. =	580.
BA	N =	16	MEAN =	191.01	ST.DEV. =	227.
AL	N =	16	MEAN =	6090.0	ST.DEV. =	10559.
LA	N =	16	MEAN =	12.725	ST.DEV. =	19.0
TI	N =	16	MEAN =	178.19	ST.DEV. =	286.
V	N =	16	MEAN =	161.63	ST.DEV. =	218.
CR	N =	16	MEAN =	47.150	ST.DEV. =	42.4
MO	N =	16	MEAN =	12.290	ST.DEV. =	30.7
MN	N =	16	MEAN =	493.19	ST.DEV. =	1843.
FE	N =	16	MEAN =	2155.4	ST.DEV. =	2768.
CO	N =	16	MEAN =	4.0719	ST.DEV. =	7.96
LI	N =	16	MEAN =	5.2025	ST.DEV. =	4.82
NA	N =	16	MEAN =	1786.0	ST.DEV. =	2087.
K	N =	16	MEAN =	785.38	ST.DEV. =	1022.

best separated at 20 ppm. As all major sedimentary rock types present in the area, except phosphorite, have typical average background U concentrations (Rogers and Adams, 1970; Nichols, 1984; Tables 5.12 and 5.13) well below 20 ppm, the lower population thus comprises elevated background concentrations, whereas the upper population is definitely anomalous. There is good correspondence between the anomalous sites and the underlying organic-rich limestone of Palaeogene age, which is outcropping elsewhere in a hilly part of the eastern side of Ad-Daww basin. The field observations of these samples at the time did not reveal any visible mineralization and the relatively low levels of phosphorus excludes any possible phosphorite source. The possible interpretation therefore, is that the organic matter in these limestones may account for the enriched U levels, such type of enrichment is well known worldwide (Landais and Dereppe, 1985; Otton and Zielinski, 1985).

Results of interelement correlations (Table 5.10) revealed that no significant positive correlation between U and any of the variables is found, but U shows a significant negative correlation with Hf, Cu, Al, K and Ba. Thorium, however is positively correlated with Hf, Al, Mo, and K, and no significant negative correlations with Th are found. Phosphorus, on the other hand, is only positively correlated with Na.

The results described for the overburden geochemical data have led to the following conclusions:

(1) - Usage of overburden as a geochemical sampling medium seems to

Table 5.13 Typical concentrations of U in the natural environment. (from Nichols, 1984)

	U concentration	Remarks	Refer
Rocks	0.1–1.0 ppm	Basalts, tholeiitic and plateau, andesitic and alkali	1
	2 ppm	Av. in carbonate rocks of North America and Russian Platform	1
	2–4 ppm	Av. in Texas Gulf Coast (Tertiary) at the surface	2
	3.7 ppm	Av. for North America and Russian Platform	1
	2–15 ppm	Granites of U.S.A., U.S.S.R. and France	1
	3–20 ppm	Alkaline intrusives of U.S.S.R.	1
Waters	1–4 ppb	Sea water, worldwide	1
	0.5 ppb	Median of 155 stream water samples from Texas Gulf Coast*	2
	5.2 ppb	Median of 103 stream water samples from northwest Texas†	3
	0.7 ppb	Median of 75 stream water samples from Llano area, central Texas‡	4
	0.8 ppb	Median of 323 wells from Texas Gulf Coast*	2
	8.6 ppb	Median of 249 ground water samples from northwest Texas†	5
	0.6 ppb	Median of 49 wells from Llano area in central Texas‡	4
Stream sediments	1.1 ppm	Median of 463 samples from Texas Gulf Coast*	2
	1.7 ppm	Median of 161 samples from northwest Texas†	3
	1.2 ppm	Median of 95 samples in Llano uplift, central Texas‡	4
Plants	0.2–0.5 ppm	Median in ash of branches from 9 types of tree, Precambrian through Tertiary of Texas	(Table this p.

* Pleistocene through Eocene.
† Tertiary, Permian, Triassic and Cretaceous.
‡ Cretaceous, Permian, Devonian, Mississippian, Cambrian and Precambrian.

Table 5.12 Normal content of U in rocks.

Source: Rogers and Adams, 1970

Igneous Rocks	U	K
Ultramafic	0.003-0.1 ppm	
Gabbro-basalt	0.1-1	0.1-1%
Andesite	0.4-1.4	~1.3
Granitic	1-5	1-5
Alkalic Rocks		
Conway granite	15 ppm average	
Syenites - Russia	15-20	
Colorado Front Range	44 avg. to 140	
Sandstones		
Clean quartz sandstones	0.5-3 ppm	
Volcanic (andesitic) sandstones	0.5-1.3	
Arkoses	1.5 (est.)	
Limestones	2.2	
Shales		
Green, gray, and red	2-4	
Black Shales		
Marine (except geosynclinal)	20 ppm	
All black shales	8	
Chattanooga shale	80 (up to 350)	
Alum shale (Sweden)	170	

yield useful information only about the underlying bedrocks.

(2) - The localized nature of any anomaly found needs further detailed investigation in order to draw any useful results.

5.4.6 Bedrock data

A summary of the mean and standard deviation of the 16 rock samples involved in this orientation survey is presented in Table 5.12. Although, the relationships of U and associated elements could not be confidently quantified from such a small number of samples, results of the interelement linear correlation matrix (Table 5.10) point out that U is positively correlated with CPS, V, As and Sr at significant confidence limits (at 99% for the radiometric measurements and at 90% for V, As and Sr). No U correlation with P was found, while U shows negative relationships with Th, K, Hf, Ti and Fe. The uranium histogram (Fig. 5.23) shows several distinct populations which reflect the various lithologies of the region.

It can be concluded that, notwithstanding the very limited number of samples compared to the very large area, multielement bedrock geochemistry provided the best contrast between background and anomalous populations and a fundamental knowledge about the regional variation of the elements of interest and their concentration levels which is directly related to local variation in lithologies.

5.5 General conclusions of the orientation survey

(1) Among the data tested in this survey , rocks provide better geochemical contrast than both overburden and wadi sediments.

(2) The optimum size fraction for uranium determination in the detrital materials and other sediments is the 500-250 μm (-30 to +60 mesh) fraction.

(3) Strong to moderate interelement correlations exist between U and some trace elements, such as, As, Mo, V, Sr, Ba, Zn, P and Cu, whereas its correlation with P is only significant in samples representing background levels.

(4) Secondary enrichment of uranium is taking place in very thin duricrusts of calcrete and gypcrete.

(5) Using elemental ratios, such as those of U:P_2O_5, U:Th and U:Hf is a viable approach for identifying significant anomalies.

(6) Heavy rain and other climatic fluctuations may be responsible for variation in U content particularly in the eastern area (and possibly elsewhere in the region) by leaching U from the sediments into the groundwaters.

(7) Geochemical sampling of broad, low-lying wadis does not yield particularly satisfactory data, probably due to extensive mixing of sediment from various catchment areas.

(8) The Palmyrides region has overall higher uranium and associated element concentrations than the eastern region. Therefore it should be selected forthe reconnaissance survey.

(9) All uranium minerals found belong to the oxidizing types and mainly consist of carnotite, lyuyamunite, meta-tyuyamunite, an un-named (ferghanite-like) mineral and on rare occasions schroeckingerite. No autinite was found.

5.6 Recommendations for the reconnaissance stage

(1) The orientation survey recommended proceeding with the reconnaissance survey using rock geochemistry for all rock types and lithologies which are outcropping in the region; use of detrital overburden is only recommended in cases where rock outcrops are lacking (as is the case in the Ad-Daww basin).

(2) The leaching and incorporating of uranium into the hydrogeologic regime requires investigation during the reconnaissance stage of this research.

(3) Geochemical reconnaissance using the rapid wadi sediment sampling procedure is likely to be restricted to the V-shaped part of the wadis draining the mountain ranges, and should not be used in sampling other, lowerlying parts of the wadi. The size fraction which is recommended to be adopted for further work in which uranium dispersion in the secondary environment is of particular interest is 500-250 μm (-30 to +60 mesh) fraction.

(4) Priority would be given to the Palmyrides region for the reconnaissance survey. Investigation in other localities such as Wadi El Mourrabad, would be useful if still further work is carried out.

CHAPTER VI

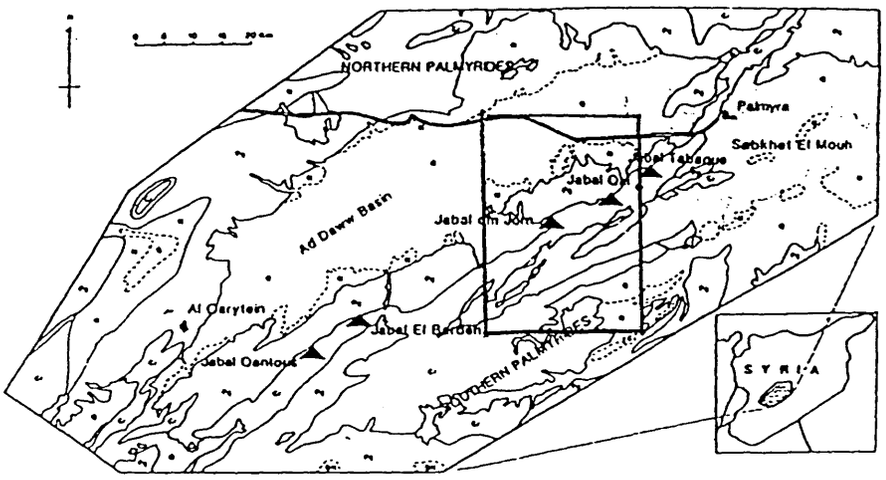
6. DRAINAGE SURVEY

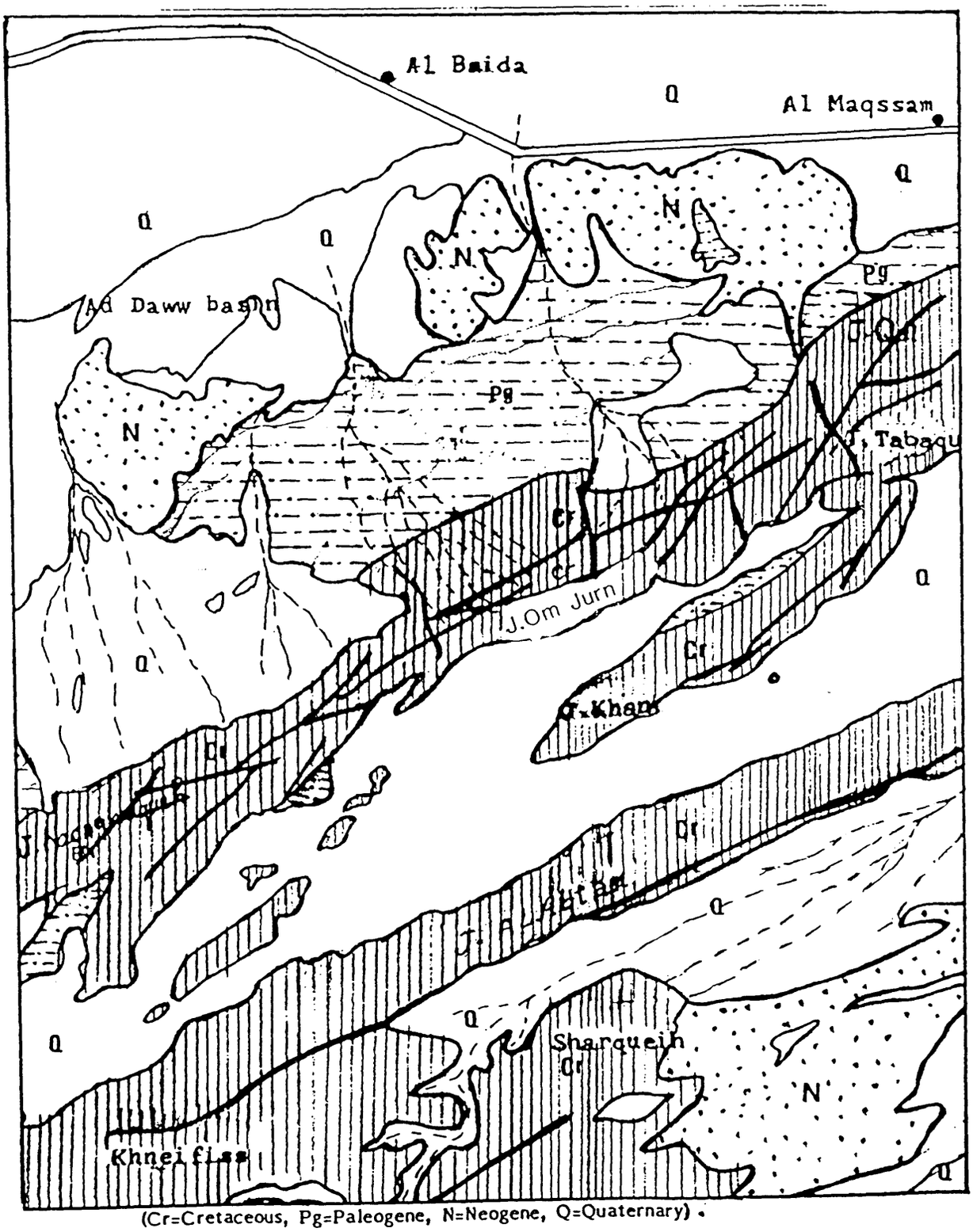
6.1 Detailed wadi sediment survey

In order to investigate geochemical dispersion in the surface drainage and to fulfil one of the recommendations of the orientation survey, a detailed wadi sediment survey was conducted in the Wadi Om Jorm drainage system where a uranium mineral occurrence had been found (see Section 5.2.2).

6.2 Location and geology

Jabal Om Jorn is one of the most faulted and complicated coffer folds of the Southern Palmyrides, situated between the An-Naqnaquiyeh range to the south and both J.Qal and J.Tabaque to the north (Fig. 6.1). Lower cretaceous rocks outcrop in its broken southeastern limb. The watershed is Cenomanian-Tuoronian dolomite and dolomitic limestones. Upper Cretaceous rocks of Coniacian (hard and soft carbonate), Santonian (thick bedded dolomitic limestone and dolomite with flint concretions) and Campanian (mainly limestone, organic limestone, phosphorite, brecciated chert and coquina) form the northwestern limb; they are dissected by strike faults with marked fault forking and distortions. In some places the dip of the beds in this limb is gentle (7° to 10° NW), while in others it is very steep, passing to upthrusted beds. The Maestrichtian formations, however, become rapidly flattened towards the Palaeogene hills farther west.





(Cr=Cretaceous, Pg=Paleogene, N=Neogene, Q=Quaternary).

Fig.6.1 Surface geology and location of wadi Om Jorm .

6.3 Wadi sediment geochemistry

6.3.1 Sampling and analysis

Samples were collected in a network of wadis draining the northwest flank of Jabal Om Jorn. At each site a composite sample of dry, inorganic sediment was collected within an area of about two square metres (Plate 20a). A total of thirty nine sediment samples were taken from the main channel and one sample from each of the three tributaries joining it, well above the confluences. Radiometric measurements taken along the wadi and its banks revealed the highest radiometric anomaly recorded in the region (5000 counts per second, using the SCINTREX GIS4 Scientillometer). This anomaly was confined to a small area on the left bank about 200m downstream from the headwater (Plate 20b).

Preparation and analysis of the samples were carried out as discussed in Chapter IV. Each sample was sieved with retention of the 500-250μm fraction as recommended by the size fraction orientation.

6.3.2 Results and discussion

6.3.2.1 Basic statistics and histograms

Summary of the geochemical data for the wadi Om Jorm sediments presented in appendix 6.1.







Plate 20 Various parts of wadi Om Jorn (a = general view; b = the upper part of the wadi showing outcrops of phosphorite (P), dolomite (D), and secondary U minerals (U); c = the lower part of the wadi.

After removal of highly anomalous values from the data, the MINITAB computer program was used to compute the basic statistics listed in Table 6.1. and frequency distribution of selected elements (Figs.6.2 and 6.3). The remaining 36 sediment samples from wadi Om Jorm contain between 4 and 50ppm U. These data have a bimodal distribution, and the population with uranium concentrations of 30ppm and upward is considered to be anomalous (Fig. 6.4).

Other elements which exhibit bimodal distributions are V, P, Mo, Zn, Cd, Cu, Ni, Mg, Ca, Al, La, Ti and to lesser degree As. The distributions of Se, Sr, Ba, and V decompose into background and anomalous populations at about 3ppm Se, 650ppm Sr, 450ppm Ba and 300ppm V. In many, but not all cases, anomalies of U, Se, Ba and V are found in the same sample. Spatial distributions of the samples with anomalous U, Ba, Se and Sr are shown in Fig. 6.5 while anomalous patterns of As, Zn, P, Mo, V, Cu, Ni and Cd are illustrated in Figs. 6.6 and 6.7. Anomalies of Sr, As and P (more than 7ppm As and 3.5% P) are also associated with U anomalies, as are several relatively high Mo, Zn, Cd, Cu and Ni concentrations (more than 24ppm Mo, 300ppm Zn, 25ppm Cd, 28ppm Cu and 85ppm Ni). The association of U with Ba and Sr in wadi sediments may owe something not only to mineralogy at source but also to the hydrodynamic similarity amongst the high density minerals in which these elements occur.

6.3.2.2 Correlation and cluster analysis

The interelement relationships expressed in correlation

Table 6.1 Summary statistics of wadi Om Jorn sediments.

U	N =	36	MEAN =	19.458	ST.DEV. =	11.7
AS	N =	36	MEAN =	5.8417	ST.DEV. =	1.97
SE	N =	36	MEAN =	2.1444	ST.DEV. =	1.57
P	N =	36	MEAN =	22869.	ST.DEV. =	12989.
LI	N =	36	MEAN =	7.1722	ST.DEV. =	2.94
NA	N =	36	MEAN =	635.00	ST.DEV. =	220.
K	N =	36	MEAN =	2319.2	ST.DEV. =	979.
RB	N =	36	MEAN =	5.7583	ST.DEV. =	13.9
BE	N =	36	MEAN =	.82167	ST.DEV. =	.290
MG	N =	36	MEAN =	37956.	ST.DEV. =	23130.
CA	N =	36	MEAN =	128167.	ST.DEV. =	93265.
SR	N =	36	MEAN =	473.42	ST.DEV. =	147.
BA	N =	36	MEAN =	249.71	ST.DEV. =	330.
AL	N =	36	MEAN =	12258.	ST.DEV. =	6245.
LA	N =	36	MEAN =	14.764	ST.DEV. =	5.20
TI	N =	36	MEAN =	228.75	ST.DEV. =	133.
V	N =	36	MEAN =	189.53	ST.DEV. =	116.
CR	N =	36	MEAN =	67.333	ST.DEV. =	25.7
MO	N =	36	MEAN =	19.414	ST.DEV. =	6.56
MN	N =	36	MEAN =	104.31	ST.DEV. =	46.0
FE	N =	36	MEAN =	7600.0	ST.DEV. =	3320.
CO	N =	36	MEAN =	5.0750	ST.DEV. =	1.66
NI	N =	36	MEAN =	56.294	ST.DEV. =	30.8
CU	N =	36	MEAN =	19.231	ST.DEV. =	9.58
AG	N =	36	MEAN =	.053611	ST.DEV. =	.262
ZN	N =	36	MEAN =	187.58	ST.DEV. =	129.
CD	N =	36	MEAN =	14.524	ST.DEV. =	10.8
PB	N =	36	MEAN =	15.309	ST.DEV. =	13.1

U

MIDDLE OF INTERVAL	NUMBER OF OBSERVATIONS	
5.	3	***
10.	8	********
15.	10	**********
20.	5	*****
25.	2	**
30.	2	**
35.	3	***
40.	1	*
45.	1	*
50.	1	*

AS

MIDDLE OF INTERVAL	NUMBER OF OBSERVATIONS	
3.	8	********
4.	1	*
5.	3	***
6.	9	*********
7.	9	*********
8.	3	***
9.	2	**
10.	1	*

SE

MIDDLE OF INTERVAL	NUMBER OF OBSERVATIONS	
0.	1	*
1.	12	************
2.	13	*************
3.	4	****
4.	4	****
5.	1	*
6.	0	
7.	0	
8.	1	*

P

MIDDLE OF INTERVAL	NUMBER OF OBSERVATIONS	
0.	1	*
5000.	4	****
10000.	6	******
15000.	3	***
20000.	2	**
25000.	8	********
30000.	5	*****
35000.	2	**
40000.	2	**
45000.	1	*
50000.	2	**

SR

MIDDLE OF INTERVAL	NUMBER OF OBSERVATIONS	
100.	1	*
200.	0	
300.	8	********
400.	7	*******
500.	9	*********
600.	8	********
700.	2	**
800.	0	
900.	1	*

BA

MIDDLE OF INTERVAL	NUMBER OF OBSERVATIONS	
0.	8	********
200.	19	*******************
400.	6	******
600.	1	*
800.	0	
1000.	1	*
1200.	0	
1400.	0	
1600.	0	
1800.	0	
2000.	1	*

V

MIDDLE OF INTERVAL	NUMBER OF OBSERVATIONS	
50.	8	********
100.	2	**
150.	9	*********
200.	7	*******
250.	2	**
300.	2	**
350.	2	**
400.	3	***
450.	0	
500.	1	*

MO

MIDDLE OF INTERVAL	NUMBER OF OBSERVATIONS	
8.	2	**
10.	5	*****
12.	3	***
14.	3	***
16.	0	
18.	0	
20.	1	*
22.	3	***
24.	9	*********
26.	6	******
28.	4	****

NI

MIDDLE OF INTERVAL	NUMBER OF OBSERVATIONS	
20.	4	****
30.	4	****
40.	10	**********
50.	2	**
60.	3	***
70.	4	****
80.	3	***
90.	2	**
100.	2	**
110.	0	
120.	0	
130.	0	
140.	2	**

Fig.6.2 Histograms of U,As, Se, P, Sr, Ba, V, Mo and Ni .

CU

MIDDLE OF INTERVAL	NUMBER OF OBSERVATIONS	
10.	9	*********
15.	12	************
20.	4	****
25.	4	****
30.	4	****
35.	1	*
40.	1	*
45.	0	
50.	1	*

ZN

MIDDLE OF INTERVAL	NUMBER OF OBSERVATIONS	
0.	1	*
50.	7	*******
100.	4	****
150.	9	*********
200.	4	****
250.	4	****
300.	1	*
350.	3	***
400.	1	*
450.	0	
500.	1	*
550.	1	*

CD

MIDDLE OF INTERVAL	NUMBER OF OBSERVATIONS	
0.	1	*
5.	9	*********
10.	13	*************
15.	2	**
20.	1	*
25.	4	****
30.	4	****
35.	0	
40.	1	*
45.	1	*

LI

MIDDLE OF INTERVAL	NUMBER OF OBSERVATIONS	
3.	4	****
4.	5	*****
5.	1	*
6.	5	*****
7.	4	****
8.	5	*****
9.	3	***
10.	4	****
11.	1	*
12.	4	****

NA

MIDDLE OF INTERVAL	NUMBER OF OBSERVATIONS	
200.	1	*
300.	4	****
400.	4	****
500.	0	
600.	9	*********
700.	7	*******
800.	8	********
900.	0	
1000.	1	*
1100.	2	**

K

MIDDLE OF INTERVAL	NUMBER OF OBSERVATIONS	
1000.	6	******
1500.	6	******
2000.	5	*****
2500.	7	*******
3000.	5	*****
3500.	3	***
4000.	4	****

MG

MIDDLE OF INTERVAL	NUMBER OF OBSERVATIONS	
10000.	6	******
20000.	6	******
30000.	9	*********
40000.	4	****
50000.	2	**
60000.	2	**
70000.	5	*****
80000.	0	
90000.	2	**

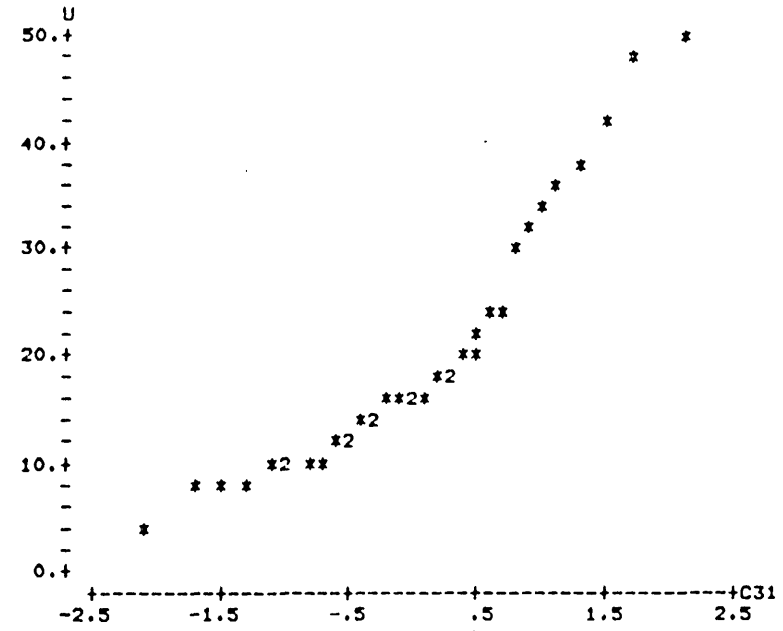
CA

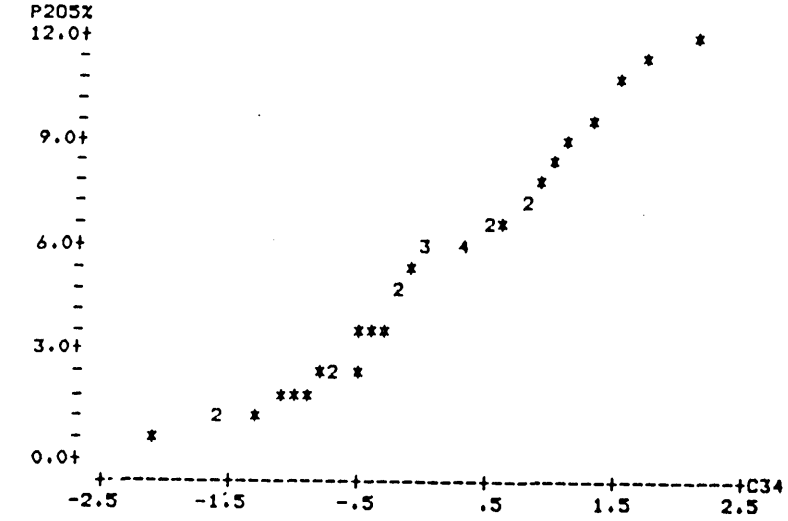
MIDDLE OF INTERVAL	NUMBER OF OBSERVATIONS	
0.	0	
40000.	15	***************
80000.	4	****
120000.	0	
160000.	0	
200000.	7	*******
240000.	8	********
280000.	1	*
320000.	1	*

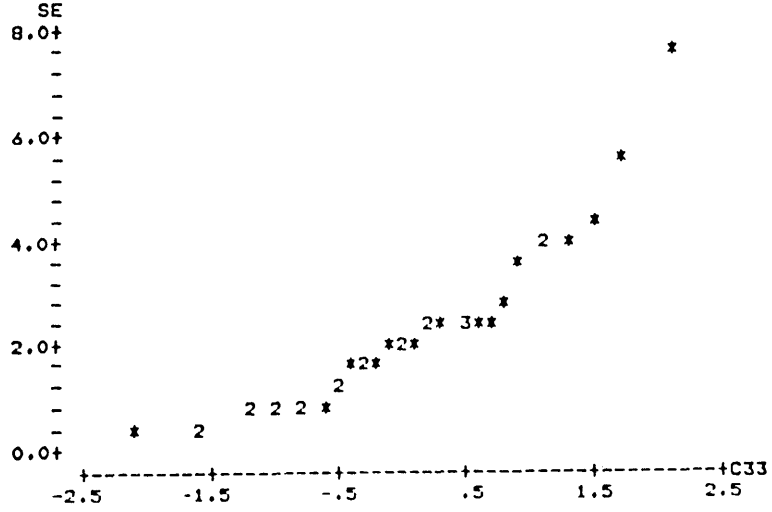
TI

MIDDLE OF INTERVAL	NUMBER OF OBSERVATIONS	
50.	2	**
100.	8	********
150.	5	*****
200.	5	*****
250.	4	****
300.	2	**
350.	5	*****
400.	2	**
450.	0	
500.	3	***

Fig.6.3 Histograms of Cu, Zn, Cd, Li, Na, K, Mg, Ca and Ti .







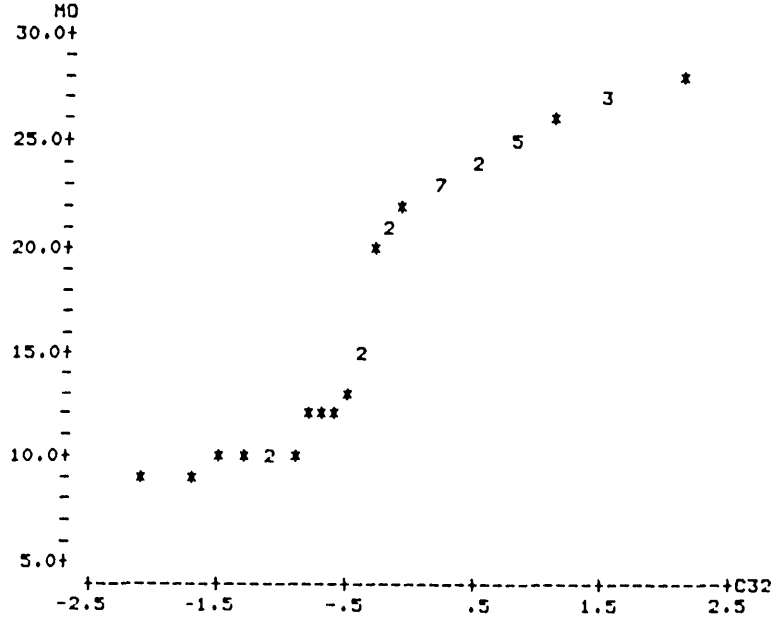


Fig.6.4 Normal cumulative probability plots of U, Se, Mo and P .

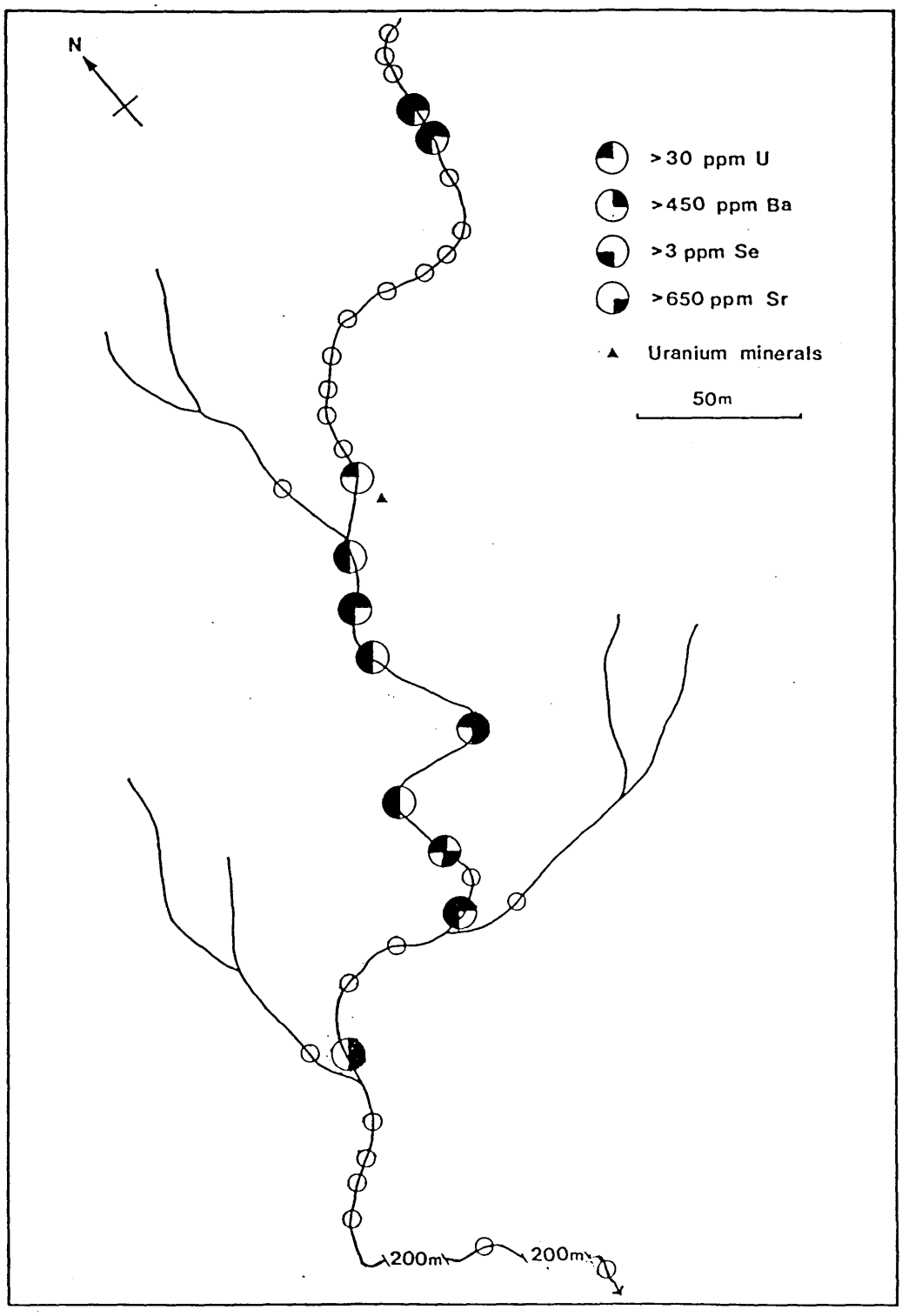


Fig.6.5 Geochemical dispersion patterns of U, Se, Ba and Sr in wadi Om Jorn .

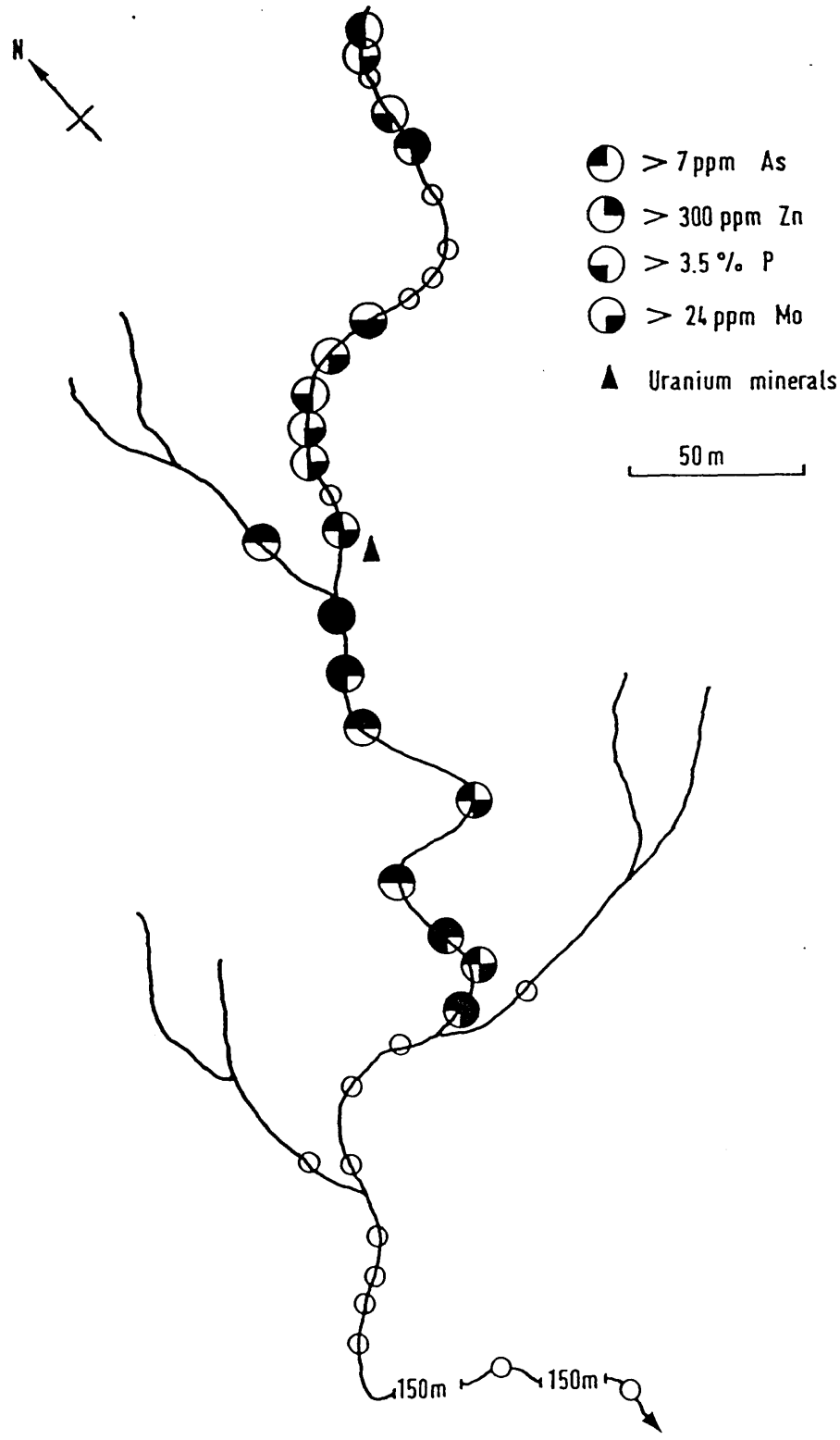


Fig.6.6 Geochemical dispersion patterns of As, Zn, P and Mo in wadi Om Jorn .

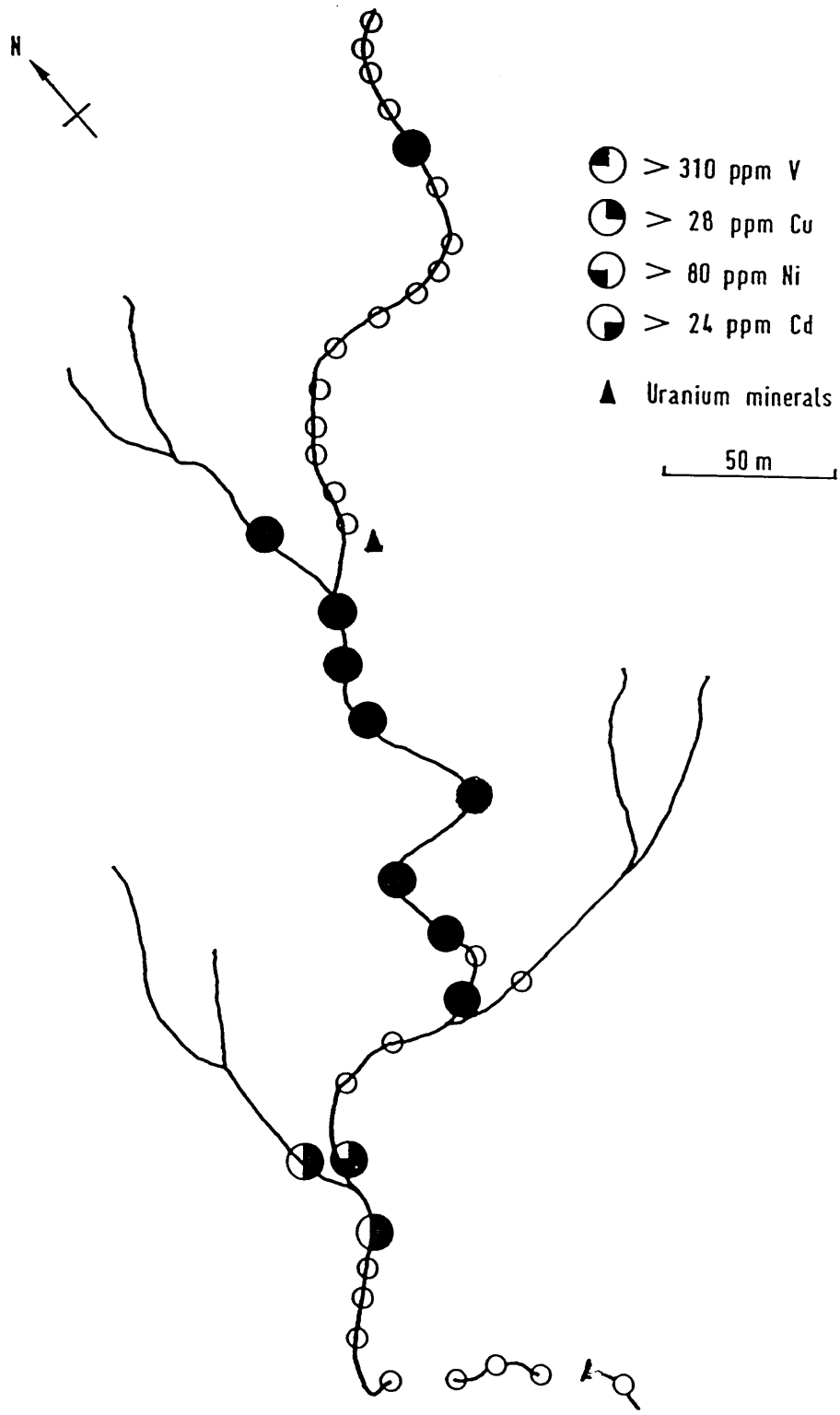


Fig.6.7 Geochemical dispertion patterns of V, Cu, Ni and Cd in wadi Om Jorn .

coefficients (Table 6.2) demonstrate that the highest linear correllation for U is found with Se, V, As, and P. Other significant positive correlations between U and La, Mo, Cd, Ni, Cu, Cr and to lesser degree Sr are also found.

To clarify the foregoing relationships between these variables, to identify unusual sample compositions and to define models for geochemical controls in the wadi sediments, the morphological representation of the data as Kleiner Hartigan trees was carried out (Kleiner and Hartigan, 1981). This method is based on hierarchical R-mode cluster analysis developed at Bell Laboratories, and improved in the Applied Geochemistry Research Group by Turner (AGRG, pers. comm.) The resultant dendograms of this clustering method form the basis for graphically representing the ordering of the variables in tree symbols.

Results of the R-mode cluster analysis show that U is most closely associated with Se and Ba (Fig. 6.8). A second group of elements comprising P and Mo and a third comprising As, Zn, in one hand and Cu, Cd, Ni and V in the other are weakly linked to the first two groups. A fourth group consisting of Sr, Na, Mn, Li, K, Al and Fe is dissociated from others, Calcium (at a very insignificant level) is linked to the first group, while Mg is separated from all other variables. Elements of the fourth group, reflect a secondary environmental feature (clay and oxihydroxid fractions) while Ca and Mg represent its carbonate nature.

After reducing the number of variables to only 10 (in order to minimize the effect of the large number of variables relative to

	U	AS	SE	P	LI	NA	K	RB	BE	MG	CA	SR	BA	AL	LA
AS	.611														
SE	.714	.654													
P	.717	.309	.613												
LI	.273	.508	.359	.488											
NA	.440	.526	.457	.641	.945										
K	-.063	.370	.117	.201	.906	.807									
RB	.197	.149	.303	.220	.209	.171	.145								
BE	.553	.727	.568	.645	.870	.917	.694	.238							
MG	-.476	-.748	-.518	-.272	-.601	-.604	-.476	-.262	-.693						
CA	-.026	.119	.263	.310	.284	.225	.302	.404	.204	-.117					
SR	.459	.496	.355	.516	.742	.807	.584	.269	.812	-.724	.127				
BA	.499	.259	.413	.403	.444	.538	.235	.434	.562	-.375	-.101	.594			
AL	.246	.473	.344	.521	.962	.894	.901	.217	.823	-.505	.377	.661	.317		
LA	.603	.417	.528	.860	.814	.914	.578	.257	.854	-.497	.296	.775	.596	.788	
TI	.051	.358	-.041	-.167	.239	.185	.230	-.005	.209	-.344	-.145	.374	.050	.192	.007
V	.707	.775	.620	.468	.589	.680	.320	.132	.813	-.667	-.146	.638	.641	.458	.635
CR	.485	.714	.447	.496	.813	.877	.673	.125	.931	-.651	.044	.835	.547	.744	.768
MO	.598	.610	.608	.698	.553	.614	.317	.080	.732	-.261	.206	.320	.307	.553	.653
MN	.034	.130	.083	.292	.806	.786	.789	.031	.595	-.452	.038	.652	.427	.761	.665
FE	.156	.481	.307	.424	.947	.858	.939	.209	.797	-.516	.392	.639	.281	.986	.716
CO	-.043	.294	.091	.223	.830	.744	.898	.153	.620	-.365	.332	.572	.184	.849	.548
NI	.539	.790	.556	.255	.541	.587	.349	.081	.731	-.661	-.124	.604	.558	.397	.477
CU	.478	.705	.399	.178	.555	.614	.396	.086	.716	-.670	-.205	.682	.640	.384	.478
AG	-.100	.371	-.073	-.286	.165	.124	.259	-.071	.194	-.312	-.078	.288	.018	.130	-.031
ZN	.411	.305	.336	.388	.089	.138	-.097	.109	.264	-.074	.038	.170	.195	.076	.270
CD	.535	.608	.411	.166	.397	.500	.192	.004	.590	-.618	-.340	.550	.596	.210	.399
PB	-.207	-.100	.061	.202	.266	.208	.311	.060	.157	.189	.471	-.081	-.081	.345	.187

	TI	V	CR	MO	MN	FE	CO	NI	CU	AG	ZN	CD
V	.226											
CR	.249	.816										
MO	-.080	.682	.630									
MN	.146	.334	.614	.113								
FE	.231	.413	.719	.498	.740							
CO	.272	.246	.602	.263	.734	.863						
NI	.292	.935	.786	.561	.291	.392	.280					
CU	.350	.907	.812	.431	.386	.383	.308	.954				
AG	.163	.196	.439	-.094	.222	.154	.170	.323	.398			
ZN	-.064	.319	.274	.501	-.133	.035	-.109	.255	.187	.143		
CD	.230	.891	.675	.363	.318	.178	.120	.882	.923	.320	.129	
PB	-.262	-.140	.028	.288	.162	.340	.305	-.151	-.216	-.224	.172	-.288

Table 6.2 Correlation matrix of the dranaige geochemistry.

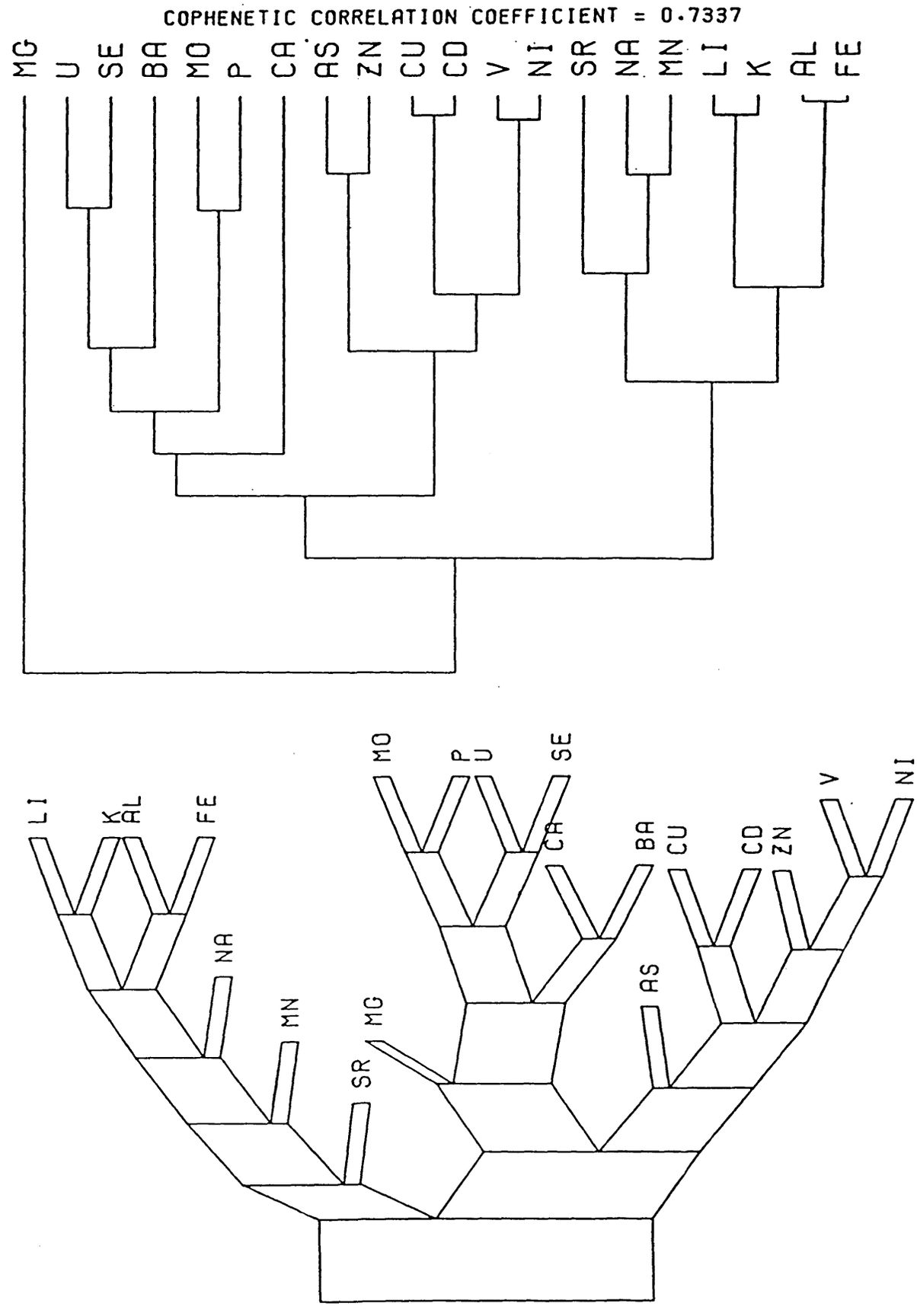


Fig.6.8 Cluster analysis of 20 variables of the drainage geochemistry.

the small set of 36 samples), the resultant tree and dendrogram (Fig. 6.9) show a similar grouping of elements representing the same four groups. Uranium is closely associated with Se and Ba in the first group, and As, V and Zn comprising a second group, is moderately linked to the first. Phosphorus and Sr, forming a third group are weakly associated with both the first and second groups, while Ca and Mg in the fourth group are dissociated from the rest. This, however, indicates the consistently strong association of U, Se and Ba with weaker but significant associations of U and V, Zn, Cd, Cu, Ni, Mo, P and Sr.

Different clustering was performed using various subsets of variables. Figure 6.10 illustrates a third clustering solution and the spatial distribution of trees (for each sample) along Wadi Om Jorm, and demonstrates clearly that the same type of grouping holds true.

6.3.2.3 Uranium anomalies

Anomalies of U and its closely associated elements occur in two parts of wadi Om Jorm (see Fig. 6.5). The first, two sample anomaly, about 30m downstream from the headwaters of the main drainage channel appears to reflect the presence of phosphatic limestone unit which outcrops on the left bank in this part of the wadi (see Plate 20). Although, high concentrations of P in the drainage system are found along this section of the wadi, there is no downstream dispersion of the U anomaly beyond its immediate source. This limited dispersion halo in such relatively steep part of the wadi channel and also the type of multielement associations

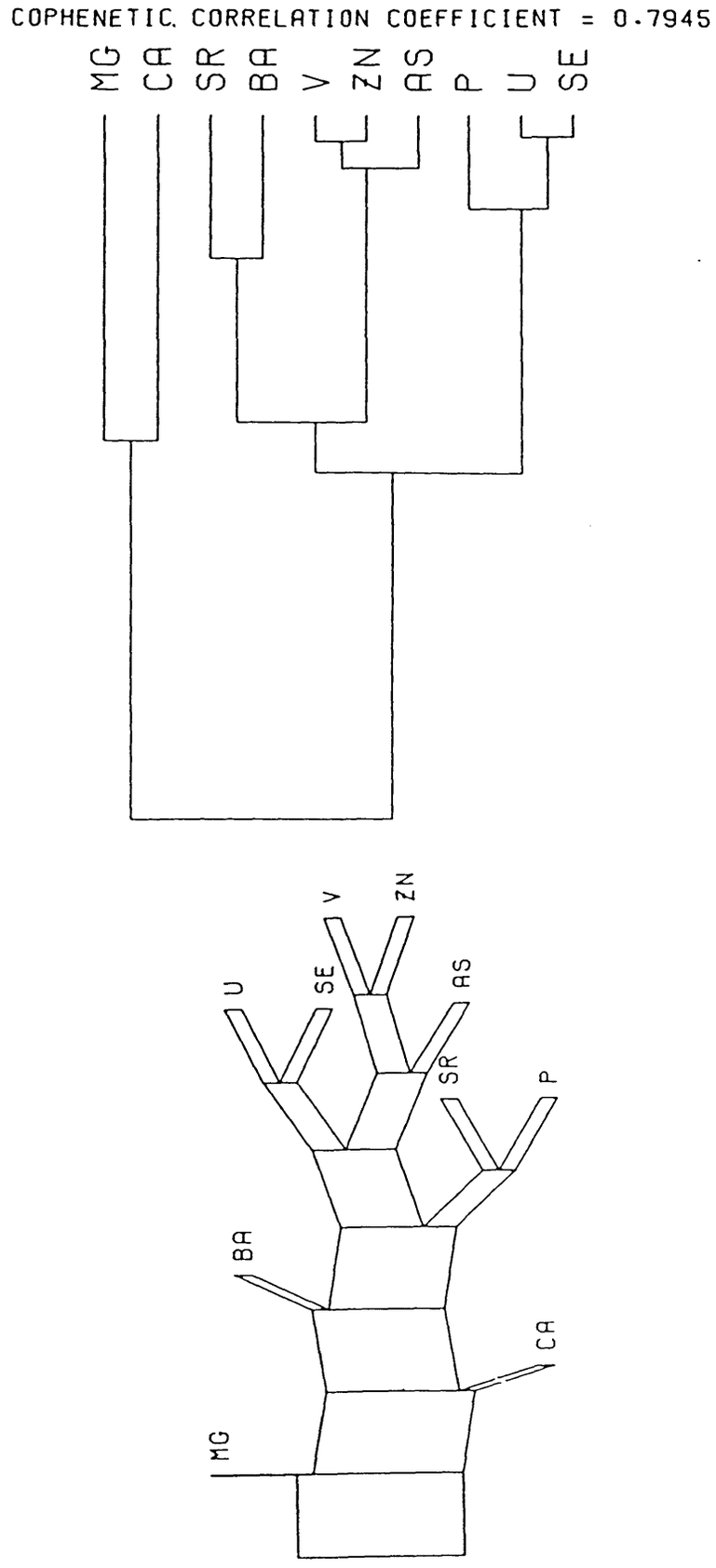


Fig.6.9 Cluster analysis of 10 variables of the drainage geochemistry.

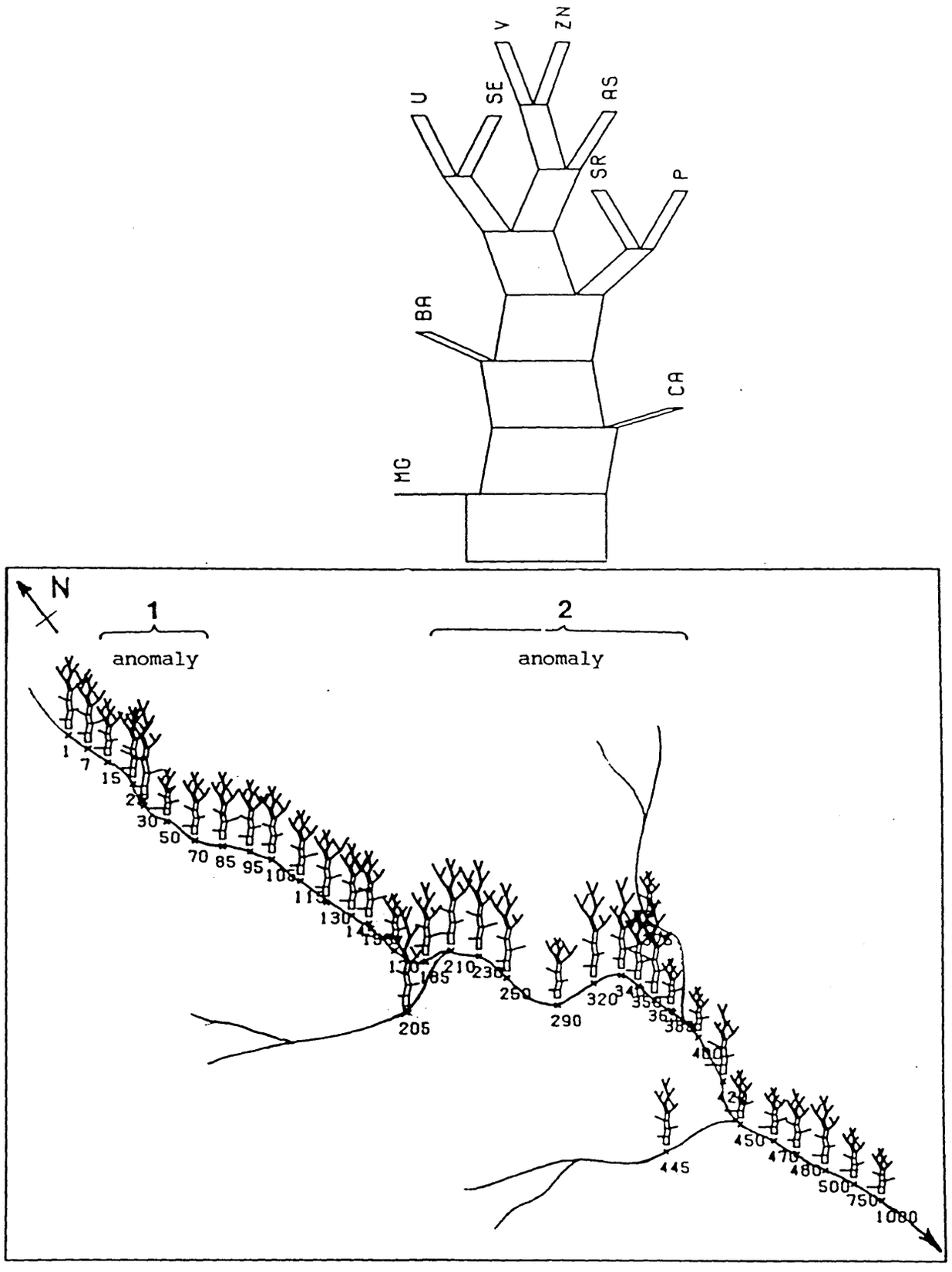


Fig.6.10 The Trees clustering pattern of the whole data set.

(U, Ni, Zn, V, Cd, Mo and Cu), do not support mechanical dispersion from the uraniferous phosphorite as a source for this U anomaly. Furthermore the highest P concentration is 100m farther downstream from this locality (sample 130 with 5.1% P). In addition, U enrichment in this anomalous area is, in fact, associated with the highest anomalies of Ba, Ni, Cu and Mo along with anomalous levels of As, Se, Cd, Zn and V. This multielement association indicates that the possible source is traces fo mineralization deposited from solution of hydrothermal origin circulating to the surface via fracture zones within the phosphate rocks. This interpretation is also supported by the local geology and the interelement correlation coefficient results, whereby the most significant positive correlations are found between V, Ni, Cu, Cd, Mo, Cr and As. This elemental association is most likely to be generated from subsurface source (magmatic or hydrothermal) rather than generated from a surficial one. Other support can be found in the spatial distributions of most anomalous elements which, in the majority of samples, are not related to P anomalies or associated with the highest P concentration.

About 200m downstream from the headwaters of the main wadi, in the vicinity of the first confluence, further anomalies emerge. Secondary uranium minerals occur on the rocks upstream on the left bank of the main channel near to this point. This second U anomalous train extends approximately 200m downwards and can be traced some further 200m downstream but are then lost as a result of catastrophic dilution by the sediments of two tributaries, which seem to drain unmineralized localities.

Such a short dispersion path is typical of the mechanical weathering and clastic dispersion which characterizes wadi Om Jorm drainage, networks and appears to prevail in all similar desert environments Leach (1977). The transport and redistribution of U and most of the associated elements (V, P, Ba, Cd, Se, Sr, Mo, Zn, Ni, As, Cu) farther from the secondary U mineral occurrences is largely controlled by such type of dispersion. However, this may explain the higher U concentrations in the coarse fraction discussed earlier.

As can be seen from the spatial distributions (Figs. 6.5-6.7), U anomalies in this part of the wadi are accompanied by V, Se, P, Zn, Cu, Ni, Cd, Mo, Sr and to a lesser degree La and As anomalies.

This association of elements and their dispersion trains indicate that the obtained anomalous levels are derived from a combination of more than one source, which collectively could provide the suite of elements and their anomalous contents involved in these patterns. However these probable sources are inferred to be as follows.

i) The mineralized outcrops which appears to provide an important parts of U, V, K and possibly Sr contents, mainly in a form of clastic fragments, because the carnotite group of U minerals are the least soluble (Langmuir, 1978), hence transport in solution is not expected to be an active process.

ii) The bedrocks which in addition to P, Ca, Mg, Na and Sr, their weathering products could provide variable amounts of trace elements (As, Se, Mo, V, Zn, La, Ba and leachable U) which

occur in exchangable and substitutional sites within these carbonate and phosphate rocks. Although the breakdown of these rocks may occur mechanically, it is equally possible to take place chemically (see chapter III). A clear sign of hydromorphic dispersion can be found in the above mentioned close association of Ba, Sr and U. Such association indicates that a significant part of the total Ba, Sr and U have been transported in solution as Ba^{2+}, Sr^{2+} and U^{6+} ions, which would react with the available SO_4^{2+} in solution and form a precipitate of Ba, Sr and U sulphates. Formations of U sulphates can be supported by the presence the in Om Jorm area of the mineral schroekingerite $NaCa_3(UO_2)(CO_3)_2SO_4F.10H_2O$ while the precipitation of Ba and Sr sulphates from solutions is well documented in the literature (Hawkes and Webb, 1962, p.361). This process shows that U is being leached out of the phosphate rocks (the most likely source of U at this site) and redistributed along the wadi channel.

iii) Additional supply of the elements Zn, Ni, V, Cd, Mo, As and Cu appears to be derived from a source of enrichment upstream of the first tributary and incorporated into the sediments in the main channel of wadi Om Jorn at the confluence point (site 205m downstream). This can be supported by the fact that the highest concentrations of Zn, 540 ppm, Cd, 39 ppm and V, 500 ppm, and elevated values of Sr, 630 ppm, Ni 136 ppm, Cu 36 ppm, As, 9 ppm are found in a sample taken in this first tributary on the right side of the main wadi channel (see Fig. 6.6 and 6.7). However, this may confirm the presence of an enrichment source within or beneath the dominant carbonate rocks in this catchment area which is also probably not

related to neither the mineralized occurrences nor to the phosphorite rocks. Therefore, this further supports the theory of a deep-seated source of enrichment.

To test this hypothesis, the total number of samples was divided into two populations. The first comprises sample sites 1 to 185, and includes the first uranium anomaly and the highest phosphorus concentrations. The second consists of all remaining sample sites. Separate R-mode cluster analyses, as discussed earlier, were performed on the two subgroups. Results for the first population (Fig. 6.11) show that U is closely associated with V, Zn and to a lesser degree with As, forming one group. Another group which includes Se, Ba and Ca, is moderately linked with the first at lower level, while a third group consist of P and Sr is very weakly linked at even lower level with both the first and second groups. Magnesium is dissociated from the whole. According to these results it is clear that the first uranium anomaly is not directly related to phosphorite outcrops along this section of the wadi but is probably more accurately interpreted as being a result of seepage along the fractures and other fault surfaces from subsurface magmatic or hydrothermal solutions (hot oxygenated groundwater can be included). In the second population (sample sites 205 to 1000) (Fig. 6.12), the first group of elements comprising V, Zn and As is most closely associated with Sr and Ba (representing a second group). Uranium however, is strongly associated with Se and P forming a third group which is weakly linked to the aforementioned groups. This may reflect the dispersion of U and associated elements from both the

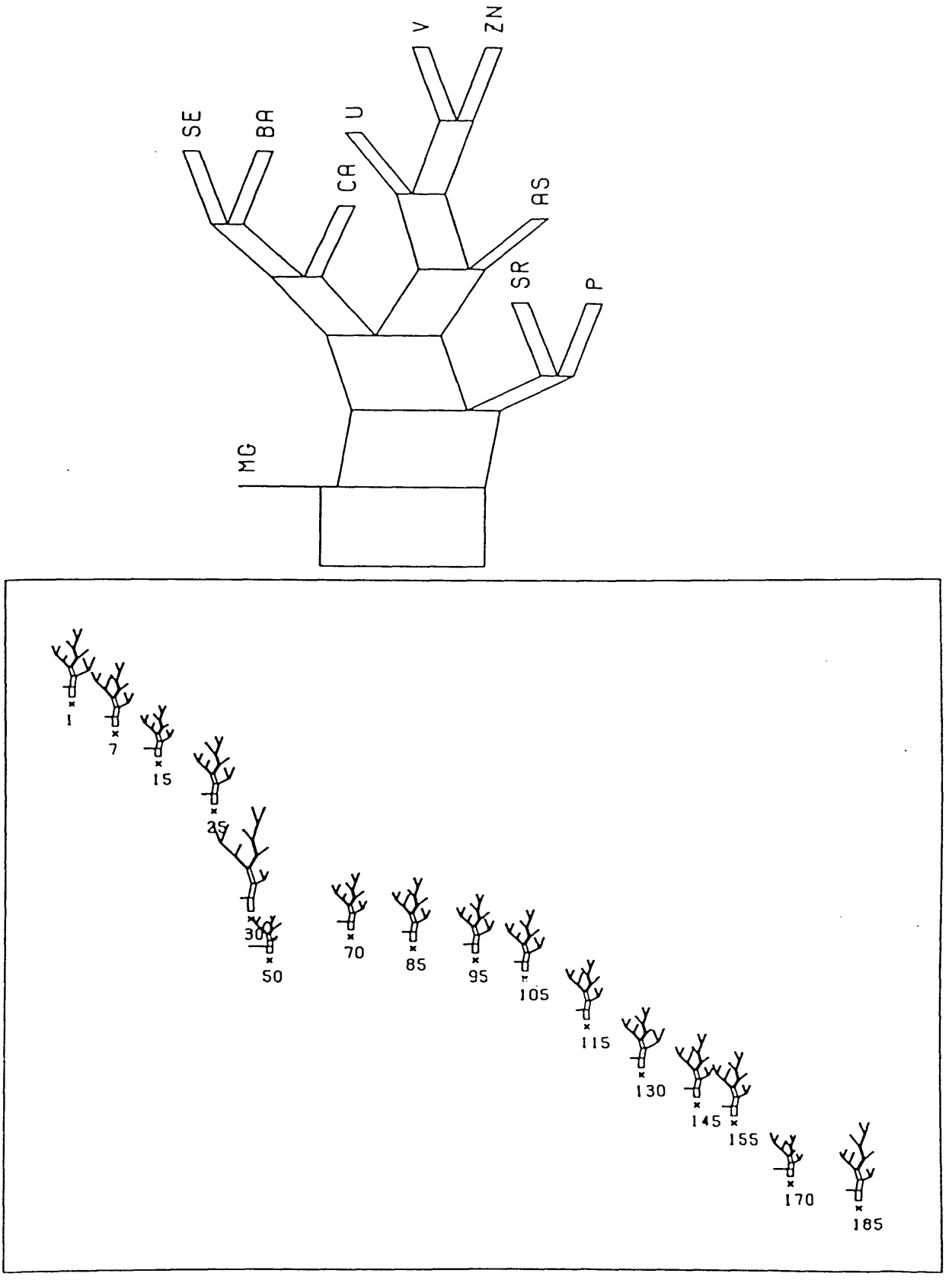


Fig.6.11 Cluster analysis of the upper section of wadi Om Jorn.

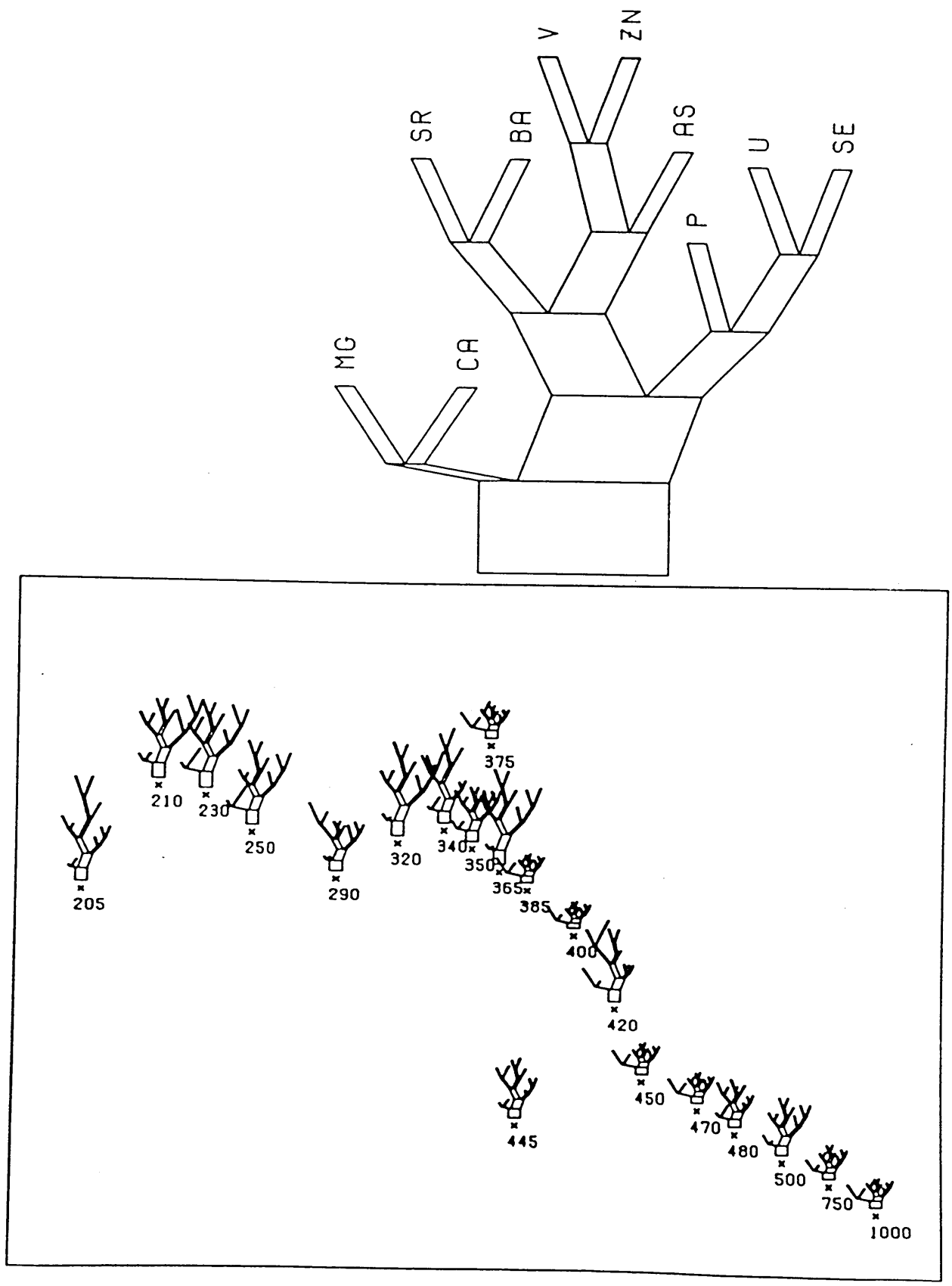


Fig.6.12 Cluster analysis of the lower section of wadi Om Jorn.

mineralized occurrences as well as the phosphate rocks. A fourth group with Mg and Ca representing the carbonate environment is dissociated from the others. Results of this clustering are consistent with the interpretation already given for the second uranium anomalies below the site 200m downstream.

6.3.2.4 Regression analysis

Multiple linear regression is the method most commonly employed in geology to describe the relationship of one element and/or variable to a number of other independent variables (Chapman, 1976). This is normally done by the classical least square method. An extension to this approach is known as stepwise multiple regression, in which variables are generally added sucessively to the regression equation (Dixon, 1973; Berk, 1973). However, Hoerl and Kennard 1980 showed that the estimation error of the regression coefficients is proportional to the sum of the inverse eigen values; therefore, the least square solution sometimes yields coefficients whose absolute values are too large and whose sign may reverse with negligible changes in the data (Howarth, 1984). They introduced a small constant K (the ridge constant) to the diagonal elements of the correlation matrix in order to form a biased estimator of the regression coefficients, which would have a smaller variance, thus producing overall better results. This achieves a reduction in the mean square error at the expense of a very small bias in the estimator (For more details about the use of ridge regression refer to Hoerl and Kennard, 1980; Howarth, 1984). The statistical significance of the regression solutions can be estimated by the F-test (Davis, 1973), from which

the corresponding F-ratio can be obtained. Acceptable solutions are those which give F-ratios above the corresponding critical value derived from tables.

Ridge regression was used to construct a model of estimating U levels of concentration and predicts its behaviour in terms of being dependent on independent estimators (predictor variables) of the drainage geochemical data. The regression model is based on a set of 20 variables of which U was regressed against 19 other geochemical variables. The choice of these elements aimed to represent all possible controls on the geochemical variations of U in the sediments such as:
the bedrock lithologies (P, Ca, Ba, Mg, Na), mineralization (U, V, K), adsorbant (Al, Fe, Mn, Ti) and the metalliferous fluids (Ni, V, Zn, Mo, Cu, Cd, Cr). Regression coefficients and associated statistics (R^2 and F-ratio of the regression line and the standard deviation of the residuals) for both the least square regression as well as the ridge regression are listed in Table 6.3. Attention is focused on the ridge trace (Fig. 6.13) which is a two dimensional graphic procedure for portraying the complex relationships in this multivariate data. From this figure, it can be seen that P, As, V and Mo are the best positive predictors, whereas Mn, K and Fe are the negative predictors. The suite of positive predictors confirm the foregoing interpretation that U behaviuor in the wadi sediments is largely controlled by;
(i) mineralizarions (fluids and secondary U minerals represented by V, Mo and As), and the phosphate lithology (represented by P), no significant influence of the carbonate lithology on the U levels of concentration was revealed by this regression analysis. The

Table 6.3 Regression coefficient of wadi Om Jorn sediments.

STANDARDIZED ESTIMATORS	RIDGE CONSTANT .00	.02	.04	.06	.08	.10	.15
AS	.5388	.5608	.4866	.4335	.3939	.3630	.3092
SE	.0678	.0818	.0976	.1089	.1169	.1227	.1316
K	-.5498	-.1852	-.1767	-.1738	-.1716	-.1695	-.1647
MG	-.1438	.0054	-.0093	-.0230	-.0337	-.0421	-.0561
CA	.0109	.0293	.0289	.0277	.0263	.0251	.0223
SR	-.5187	-.2232	-.1656	-.1284	-.1018	-.0817	-.0483
BA	.0994	.0886	.0690	.0545	.0439	.0360	.0235
AL	-.7915	-.2402	-.2015	-.1823	-.1696	-.1601	-.1432
LA	.6194	.2888	.2309	.2005	.1809	.1669	.1442
TI	.2379	.1802	.1694	.1598	.1514	.1441	.1294
V	.3026	.1546	.1181	.1043	.0981	.0952	.0931
CR	.6548	.1731	.1267	.1049	.0913	.0818	.0666
MO	-.2050	-.1126	-.0667	-.0374	-.0169	-.0017	.0236
MN	-.0154	-.1050	-.1182	-.1276	-.1350	-.1409	-.1507
FE	.3326	-.1864	-.1842	-.1772	-.1704	-.1642	-.1516
NI	-.5543	-.2714	-.1894	-.1448	-.1158	-.0950	-.0616
ZN	-.0789	.0481	.0491	.0454	.0418	.0388	.0338
CD	.0995	.3492	.3555	.3465	.3353	.3243	.3006
P	.0000	.0000	.0000	.0000	.0000	.0000	.0000
AVERAGE VIF	61.62	12.58	8.13	6.19	5.06	4.32	3.21

	MLR ESTIMATOR	STD. ERROR	RIDGE ESTIMATOR	STD. ERROR
INTERCEPT	3.7975		1.5042	
AS	I 1.0089	.41705	I .63257	.26362
SE	I -.11583	.11601	I .26793E-01	.99123E-01
K	I -.18932	.75421	I -.16272	.28272
SR	I -.99919	.68652	I -.10141	.35800
BA	I .23202	.90608E-01	I .13073	.80140E-01
AL	I .56909	.82436	I .17807E-02	.22846
LA	I -.23015	.70481	I .63299E-01	.34281
TI	I .79168E-01	.99396E-01	I .71581E-01	.91519E-01
V	I -.15155E-01	.41835	I .75251E-01	.20076
CR	I .70146	.69415	I .15760	.29770
MO	I -.80825	.44658	I -.12240	.24668
MN	I -.50739	.47404	I -.40700	.26501
FE	I -.57868	1.0960	I -.11041	.27233
CD	I .70727E-01	.28462	I -.35745E-01	.15041
P	I .68136	.30672	I .28560	.15762

ANALYSIS OF VARIANCE % RIDGE

SOURCE OF VARIATION	SUM OF SQUARES	DEGREES OF FREEDOM	MEAN SQUARES	F-RATIO
REGRESSION	1.48	15	.10	6.1576
RESIDUAL	.32	20	.02	
TOTAL VARIATION	1.80	35		

MULT. R-SQUARED = .8220 STD. ERROR OF EST. = .1264
VARIANCE OF ERROR TERM = .0160

RIDGE TRACE

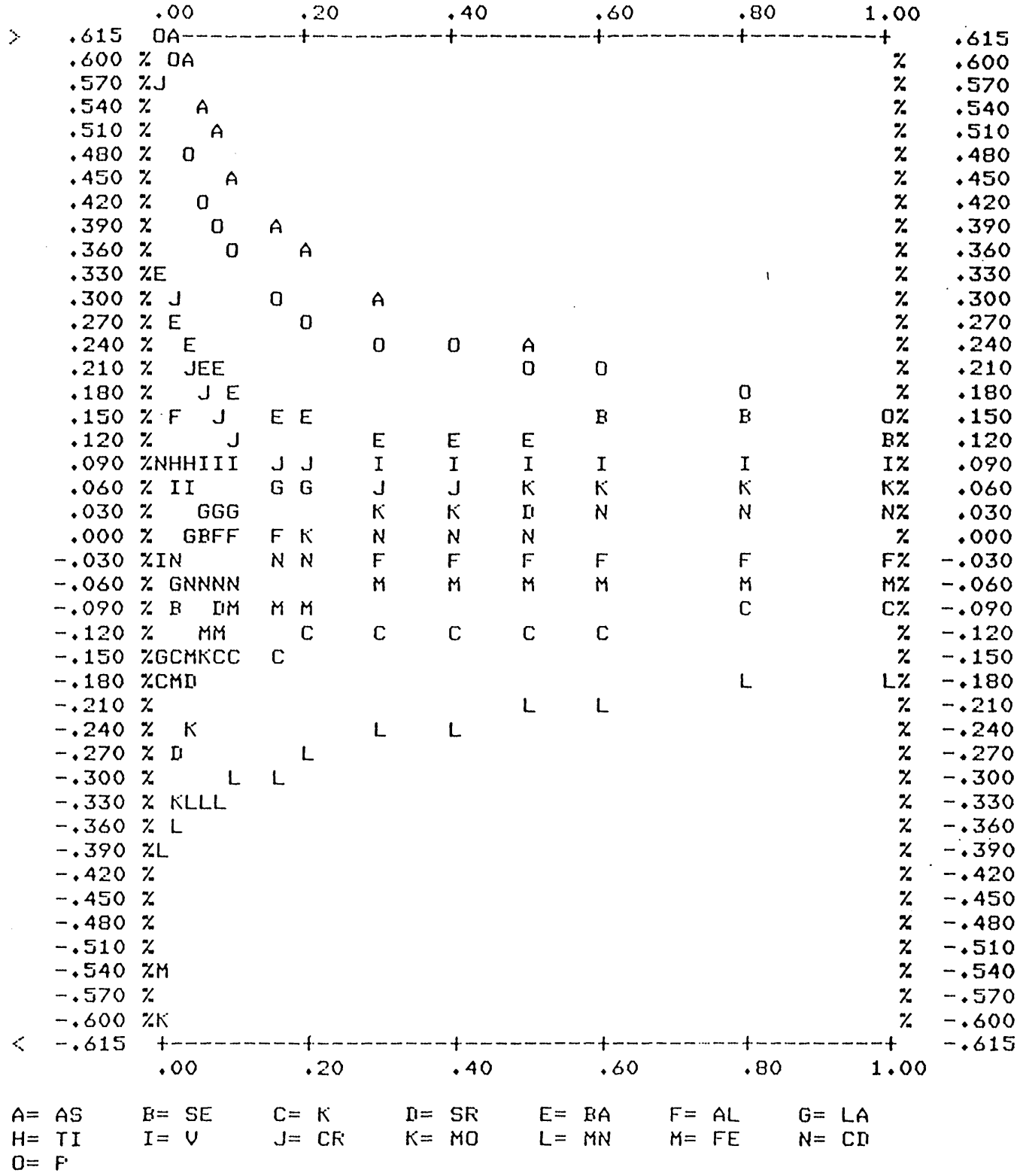


Fig.6.13 Ridge trace for a regression model of U Vs 15 other geochemical variables in the wadi geochemistry.

antipathetic relationship between U and Mn and to a lesser degree Fe is in good agreement with the results of correlation and cluster analysis. Moreover this suggests that adsorption onto Fe-Mn hydroxides does not play any significant role in modifying the relationship of U dispersion in its secondary (wadi sediments) and primary (bedrocks and mineralizations) environments.

The pattern of U residuals is almost identical to its spatial distribution pattern, and it outlines the same two U anomalous areas.

Finally, in the surface drainage systems of humid regions, U derived from mineralization tend to be dispersed in aqueous solutions and adsorbed by organic matter and/or secondary Fe, Mn oxides (Rose and Keith, 1976). In the arid Ad-Daww region, U dispersion appears from the foregoing discussion to be predominantly clastic. Any U passing into solution is unlikely to be adsorbed by organic matter, which is virtually absent from the unpopulated parts of the Palmyrides region. In addition, no correlation between U and Fe, and a very low negative correlation between U and Mn, suggests that secondary Fe, Mn oxihydroxides do not act as a significant U precipitation barrier or scavengers. Furthermore, lack of significant correlation between U and Al, Na and K suggests that adsorption onto clay minerals is unlikely.

6.4 Conclusions

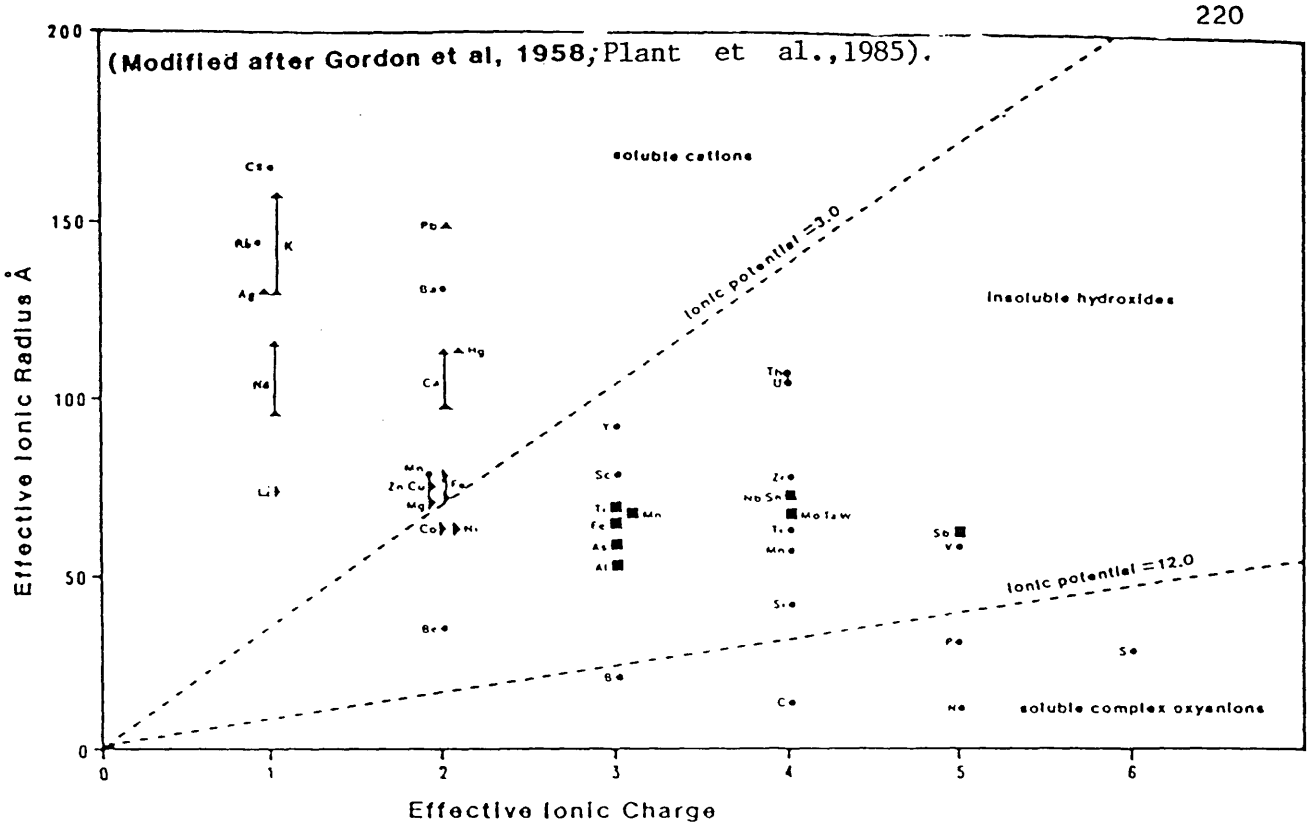
From the results described above five main conclusions can be drawn as follows.

1) Anomalous patterns are not found in the wadi after it has left its V-shaped channel on the western flank of Jabal Om Jorm and descended into the lowlands of Ad-Daww basin.
2) This survey has shown that U is dispersed beyond the phosphorites in the studied area and U anomalies have been detected in the drainage system.
3) As a sampling medium for locating source areas, wadi sediments are suitable provided samples are collected in the main drainage channels and above each confluence in wadi networks directly draining mountain slopes, because anomalies cannot be readily recognized in the wadis on lowland areas.
4) Applying the multielement geochemical approach, it was possible to select a suite of elements including U, Se, P, V, Mo, As, Zn, Cd, Ba and Sr that could define the anomalous areas, despite the relatively small number of samples involved.
5) Some of the peculiar elemental associations such as Zn, V, U, Mo, Cu, Cd, Ni and As require further detailed study, because they possibly indicate subsurface magmatic activity and deep rooted taphrogenic events accompanied perhaps by low temperature metalliferous hydrothermal solutions.

7. HYDROGEOCHEMISTRY OF THE PALMYRIDES

7.1 General

The research work has indicated the possibility that U in part of the investigated region was leached out of bedrock, and perhaps, has been incorporated into the groundwater regime. A hydrogeochemical survey is therefore potentially useful for identifying element migration in solution. Elsewhere, hydrogeochemistry has been effectively used both in detailed mineral exploration as well as in reconnaissance surveys (De Voto, 1984). Groundwaters have a particular value in U exploration especially in the arid regions where there is little surface water, because aqueous solutions are involved in both the formation of U ores and their subsequent alteration (Giblin and Snelling, 1983). They provide also a medium that can carry a signal away from the ore leading to detection of concealed ore (Giblin, 1985). According to Dall Aglio (1971), the uranyl ion and not uranic U^{6+} is the stable ion in an oxidizing surficial environment. This is because the uranyl ion has a much lower ionic potential value than U^{6+} which leads to the formation of many soluble uranyl complexes with most common anions. Hence it shows higher mobility than that expected from U cation mobility alone (Fig. 7.1).



Eugster's Classification of Ore Forming Elements:

- BOCs (bivalent octahedral cations)
- ALKs (cations capable of occupying alkali positions)
- LHCs (large highly charged cations)

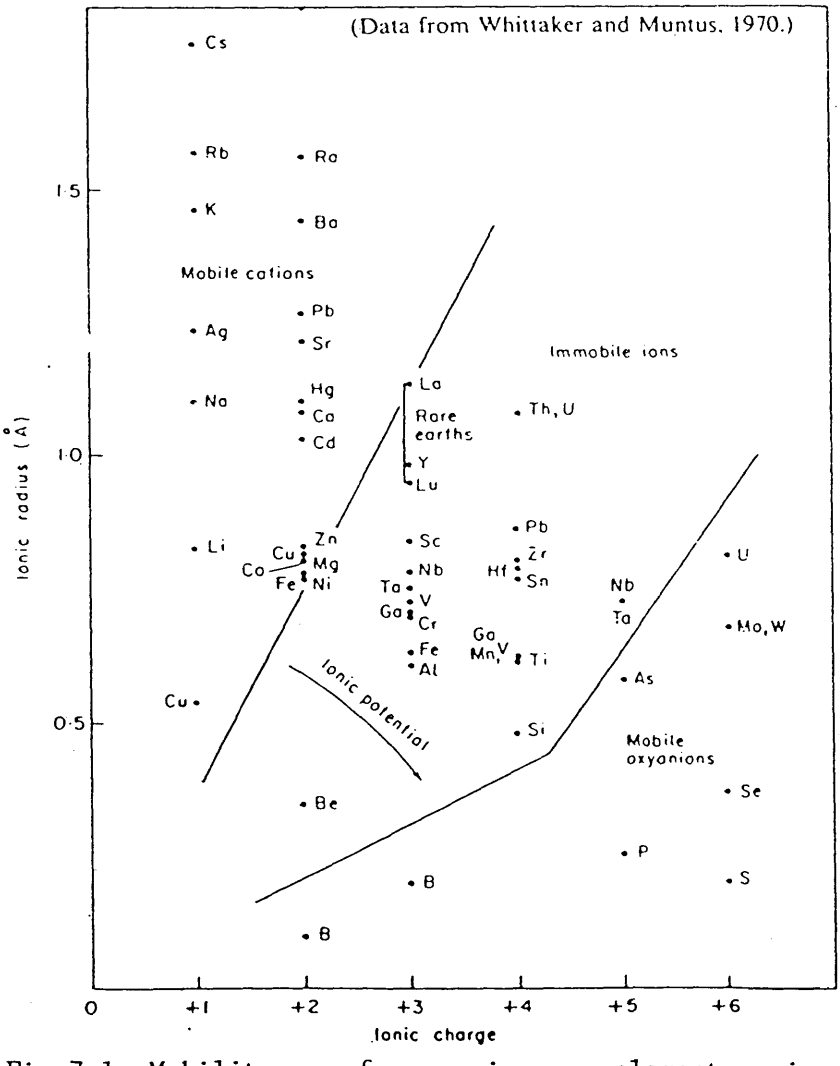


Fig.7.1 Mobility of various elements in the surface environment (from Rose et al.,1979

7.2 Sample location and geology

7.2.1 Sample location

The sample locations for thirty groundwaters collected from the Palmyrides region are shown in Fig. 7.2. Three more samples were taken from outside of the surveyed area as controls and for comparative reasons. The geographic distribution of the groundwater samples is uneven and the density is generally low. Because wells are highly scattered, a systematic grid system of sampling was not possible. The majority of the water samples were obtained from the Ad-Daww basin along the main Homs-Palmyra road. Depth, pH and temperature were the only measurements taken in the field as equipment was not available for conductivity, Eh or total dissolved oxygen measurements.

7.2.2 Geology

The general geology of the region was discussed in Chapter II and the main features relevant to hydrogeochemistry are outlined in a simplified lithostatigraphic column illustrated in Fig. 7.3. During Triassic and Jurassic times, permeable formations of evaporite and dolomite prevailed. Cretaceous formations of ferrugenous sandstone, dolomitic limestones and dolomites dominate the period up to Coniacian times. These outcrops formed the main body of both the Northern and Southern Palmyrides mountains. During Santonian, Campanian and Lower Maestrichtian times, formation of marly limestones, phosphorite, chert, detrital limestones and coquina, are deposited mainly on the flanks of these mountains. In the region, the lack of persistent clay layers between the

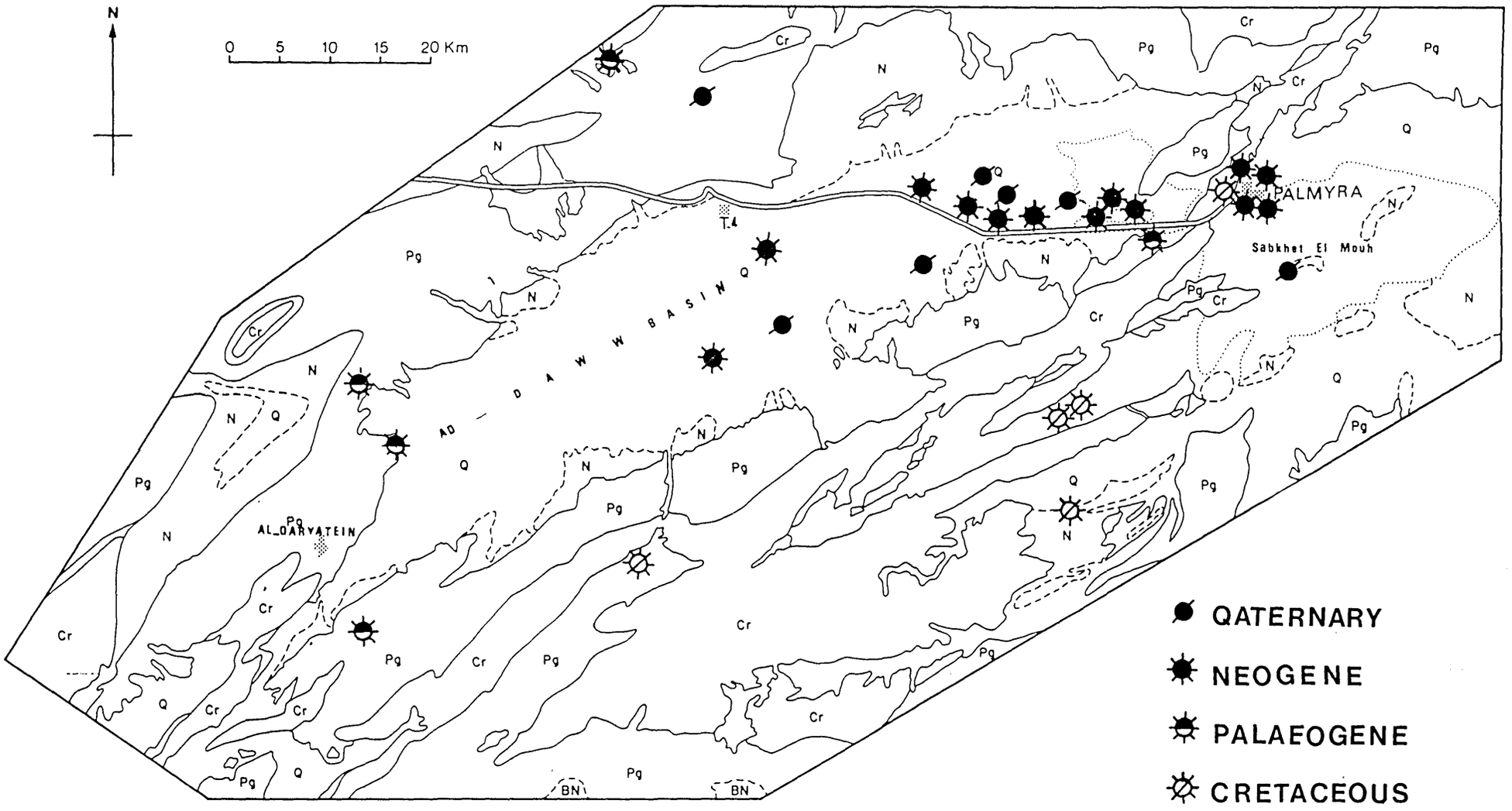


FIG · 7·2 Sample location in relation to surface geology

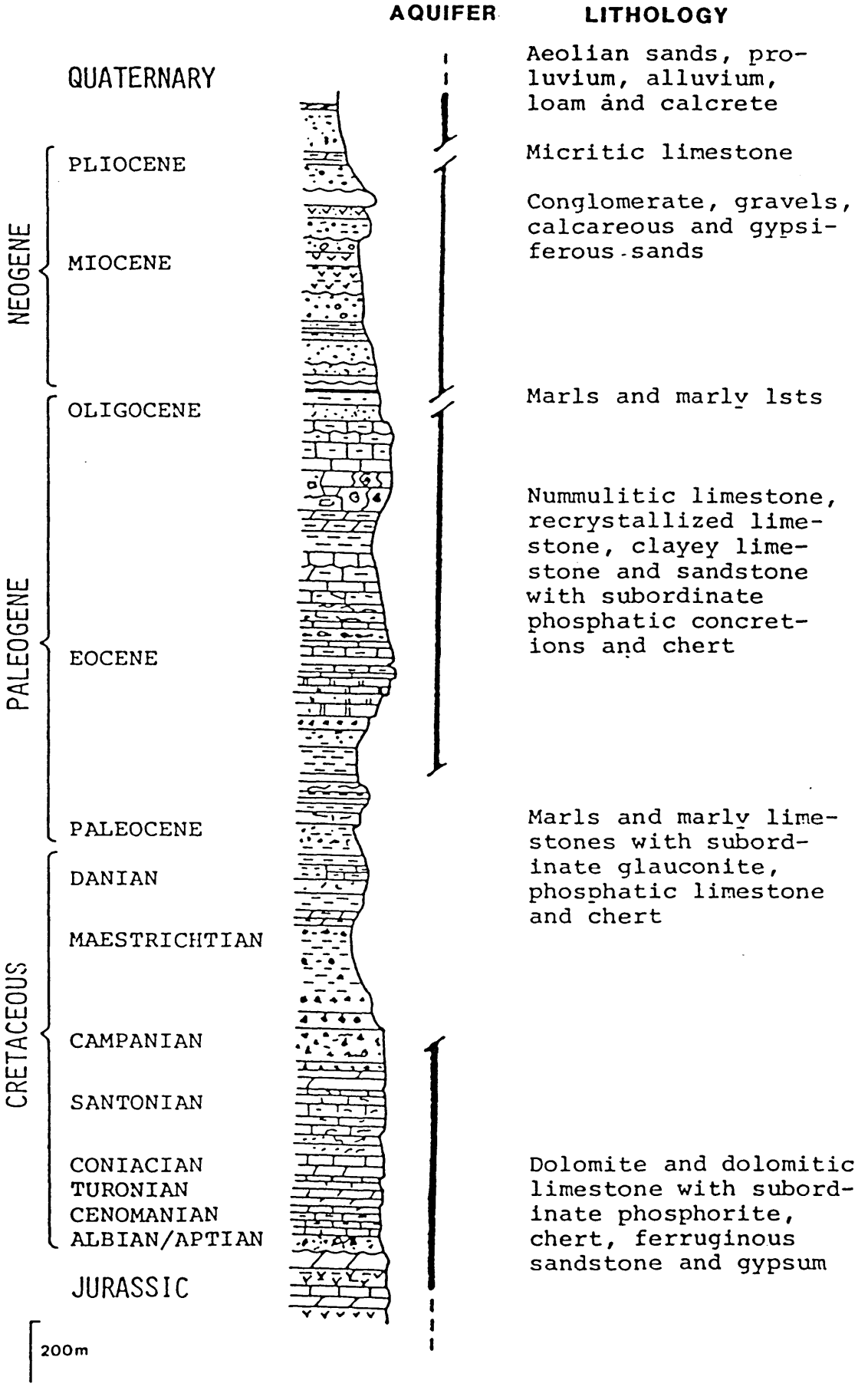


Fig.7.3 The Palmyrides aquifers in relation to the lithostratigraphic column .

Cretaceous Series and the rocks below them makes it possible to have a hydraulic connection resulting in one aquifer. A thick monotonous series of impervious marls dominated the period of Maestrichtian to Palaeocene times. These marls acted as a major aquiclude, separating the Cretaceous aquifer from the remaining permeable Palaeogene formations. These Palaeogene rocks are encountered in the hills surrounding the Ad-Daww basin, and are mainly represented by marly and glauconitic limestones, chalky limestones intercalated with flint nodules and chert bands of Lower Eocene age followed by Middle and Upper Eocene limestones. The Oligocene sandstones, silts, sandy limestones and micritic clayey limestones mark the end of the Palaeogene. In Neogene times, continental conditions prevailed; permeable terrigenous materials derived by erosion of pre-existing rocks along with autochthonous carbonates and lacustrine sediments were deposited. A complete section of these hydrologically important Neogene formations consists of :

- red quartzitic sands and sandstones.
- white quartz sandstone and carbonate-cemented conglomerates.
- greenish sandstones with clay cement.
- green to brownish clay with intercalations of brownish gypsum and sandstones.
- micritic, red to brown limestones with quartz and flint nodules.
- conglomerate and gypsum bands.

The Quaternary sediments consist mainly of highly permeable clastic fragments and aeolian sands. Both the Neogene and Quaternary formations are highly permeable with locally disrupted

permeability between Upper Pliocene and Lower Pleistocene caused by very fine grained Neogene lacustrine limestones.

7.3 Hydrogeology

7.3.1 The aquifers

Groundwater in the region can be attributed to four aquifers as follows

(1) - Cretaceous aquifer with medium to high permeability.

(2) - Palaeogene aquifer (contain more than one water horizon) with low to medium permeability.

(3) - Neogene aqifer with high to medium permeability.

(4) - Quaternary aquifer with high permeability.

The four aquifers in Fig. 7.3 are not necessarily fully isolated from one another along the whole region; this holds true particularly in the case of aquifers (3) and (4). However, some of the hydrogeologic units usually include several hydraulically connected water levels. Each of the foregoing aquifers is represented in the suite of the 30 groundwater samples acquired.

The main controls on the configuration and character of the hydrological flow systems of the Palmyrides are, geology, topography, tectonics and climatic conditions. Lithology on the other hand determines the hydrogeological properties of the rocks.

7.3.2 The hydrologic system

Mifflin (1968) recognized four zones in a typical groundwater system:

1 - Zone of recharge;

2 - Zone of lateral flow;

3 - Zone of increasing groundwater potential;

4 - Zone of discharge.

In the Palmyrides flow system, recharge takes place in the high parts of both Palmyrides mountain belts, especially where the outcrops of Upper Cretaceous dolomite and limestones are strongly fissured and fractured along the axes of the anticlines. Due to the extensive outcrops of folded carbonate and chert rocks and the well developed system of faults and joints, the recharge is caused by direct infiltration. This, from the writers point of view, affects mainly the recharge flow of the Upper Cretaceous aquifer and to a lesser extent perhaps the Palaeogene one. Direct infiltration through the unconsolidated sediments of various origin permits the recharge of both Neogene and Quaternary aquifers. A third method of recharge is by runoff surface water through recharge wadis; among these, Wadi El Abyad (NW Palmyra) constitutes the largest hydrographic basin ($660km^2$) in the northern Ad-Daww depression. Khouri (1973) reported a subsurface flow of fresh water in the alluvium cover of this wadi resulting from 1972 thunderstorms.

7.3.3 The water flow

Lateral flow is determined by lithology, aridity and fault

systems. It occurs in a northeasterly direction parallel to the axes of the main Palmyrides folds. Kouri and Droubi (1981) studied the groundwater movement in the fractured carbonate rocks of the eastern Mediterranean Sea. Using isotope data they suggested a possible connection between the deep aquifers of the Palmyrides with the Damascus basin and Anti-liban mountains (Fig.7.4). However, the flow system is more complicated in the northern segment of the region than it is in the southern part; the groundwater movement occurs in more than one direction. It follows north to south-southwestern trends in the extreme northeastern corner of the region towards Sabkhet El Mouh and along the subsurface flows of the major wadis running from the southern flanks of the Northern Palmyrides mountains towards the northern part of Ad-Daww basin (e.g.wadi El Abyad). This can be supported by the observed southern introduction of saline waters in El Baida-Maqssam area (Khouri and Agha, 1979). There is also an important west to east groundwater movement mainly along regional and local faults and major fractures.

The zone of increasing groundwater potential seems to be situated in the southeastern part of Ad-Daww basin (J. El Bardeh) and the extreme northeastern corner of the region. Discharge zones, on the other hand, are represented by the two major depressions of Ad-Daww basin and Sabkhet El Mouh playa. Other discharge points may be found along the main plunging anticlines where they meet with the topographic surface if the hydraulic conditions are suitable. Discharge through capillary action, evaporation and pumping centres is significant, particularly in dry periods and irrigation seasons. It is worth noting that a belt of discharging hot springs smelling

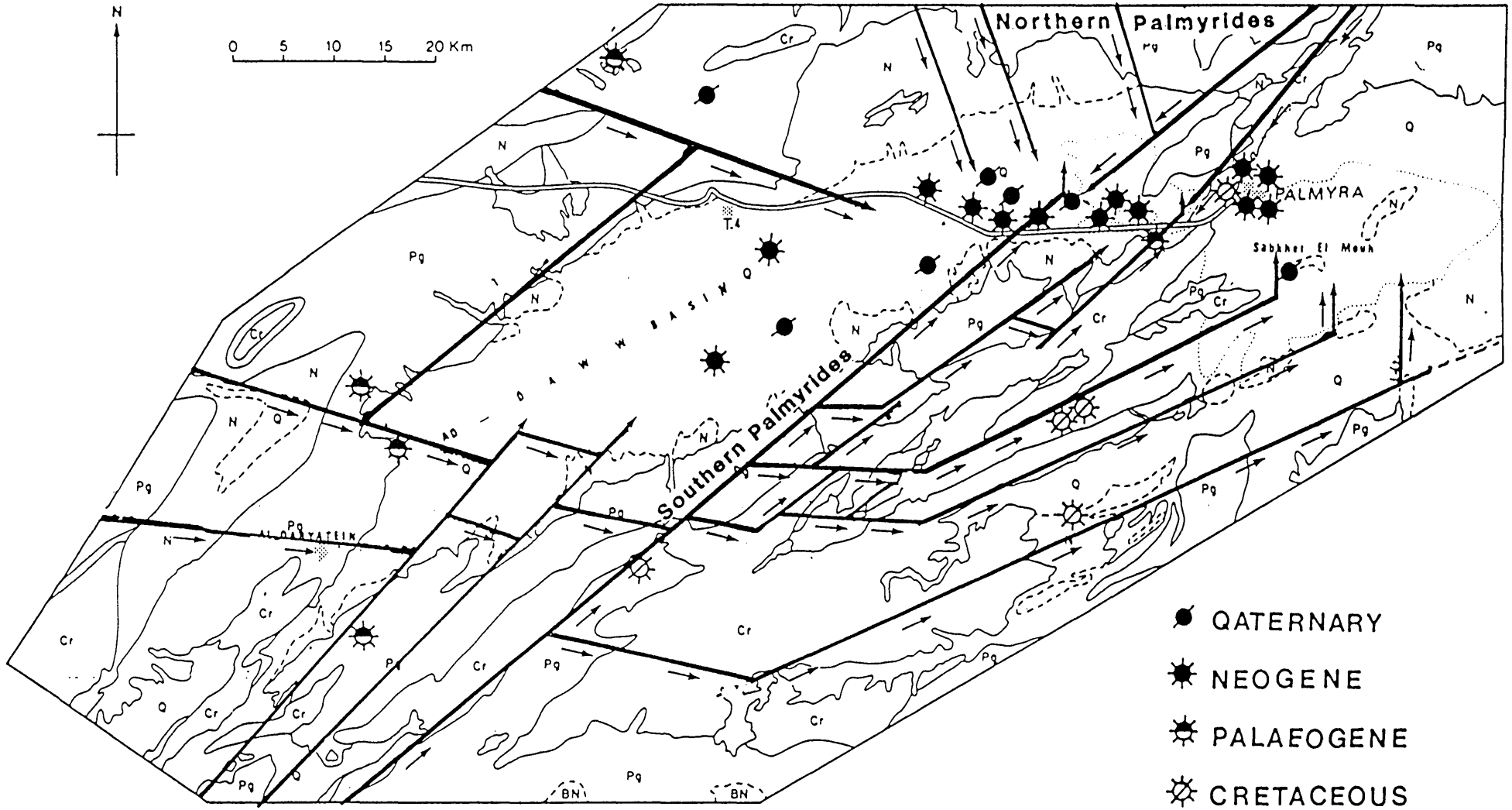


Fig.7.4 Direction of the groundwater movement in the region.
in relation to the sample location (modified after Khouri and Droubi, 1981).

of H_2S is running across the region from J.Abou Rabah through Palmyra towards the extreme northeastern corner (As-Soukhneh) parallel to the northeasterly trending Southern Palmyrides faults zone.

Finally, palaeoclimatic dates (Keiser et al., 1973) suggest that the region has witnessed two pluvial periods.
1 - north pluvial period from 25000 to 19000 years BP.
2 - Neolithic pluvial period from 8300 to 3600 years BP.
During these periods, the groundwater flow system was slightly different, the discharge zone was more extensive and lakes were existent over many parts of the region.

7.4 Methods of analysis

A total of 33 major and trace elements was measured in the groundwater samples. Most of the methods used are those described in Chapter 4, but U and F in water comprises a special case.

Fluoride was determined by specific ion electrode (SIE) using selective electrode Orion Model 7409 and WGPYE pH/mv meter. Samples must fall above pH5 to avoid complexation by hydrogen ions and below pH7 to avoid hydroxide interference. Addition of TISAB (total ionic strength adjuster) to samples and standards adjusted the pH to between pH5 and 5.5.

Uranium was determined by three methods. The first, developed by the author (Jubeli and Parry, 1986) involved epithermal neutron

activation using the ^{239}U Υ-ray of 74.7 Kev (at Imperial College Reactor Centre, Silwood Park). Gamma-ray spectrometric measurements were made upon the solid residue obtained by freeze-drying 50ml of each sample. The second method was by the conventional neutron activation analysis (INAA) with ^{239}Np at gamma ray of 106.4 Kev. The third method was uranium determinations by laser-induced fluorescence (Robbins, 1978; Robbins and Casteldine, 1979) using an AU-3 Uranium analysis which was kindly and generously provided by the British Geological Survey (BGS). The three techniques yielded results in close agreement (Fig. 7.5, and Table 7.1). The measurements of U were fairly accurate and the precision of duplicates was better than 10% (Fig. 7.6).

7.5 Results and discussion

7.5.1 General characteristics

The flow system and lithology are the two main factors that determine the water chemistry in the region. The chemical data in Appendix 7.2 shows that the groundwaters collected from the Palmyrides range in pH from 7.3 to 8.0. They have a content of dissolved solids (Na + K + Mg + Ca) ranging from 56 to 3335 mg/l. The composition of most tends towards alkaline, and Na^+ is usually the predominant cation (Fig. 7.7). These findings are consistent with earlier hydrochemical studies (Faradzhev, 1966; Khouri, 1973) which additionally showed that the greater part of the study area has stagnant chloride water, typical of a closed basin with a low precipitation to evaporation ratio. Agha and Droubi (1983), reached similar conclusions by plotting the major cation and anion data on

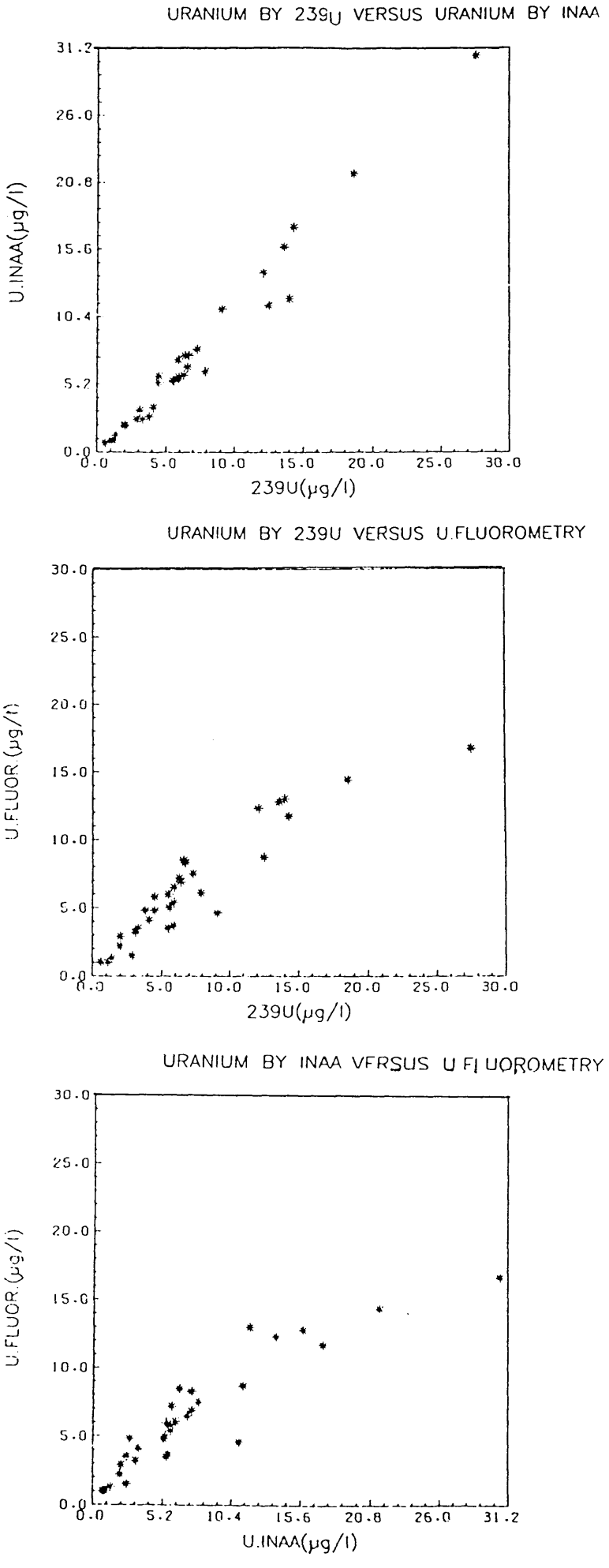


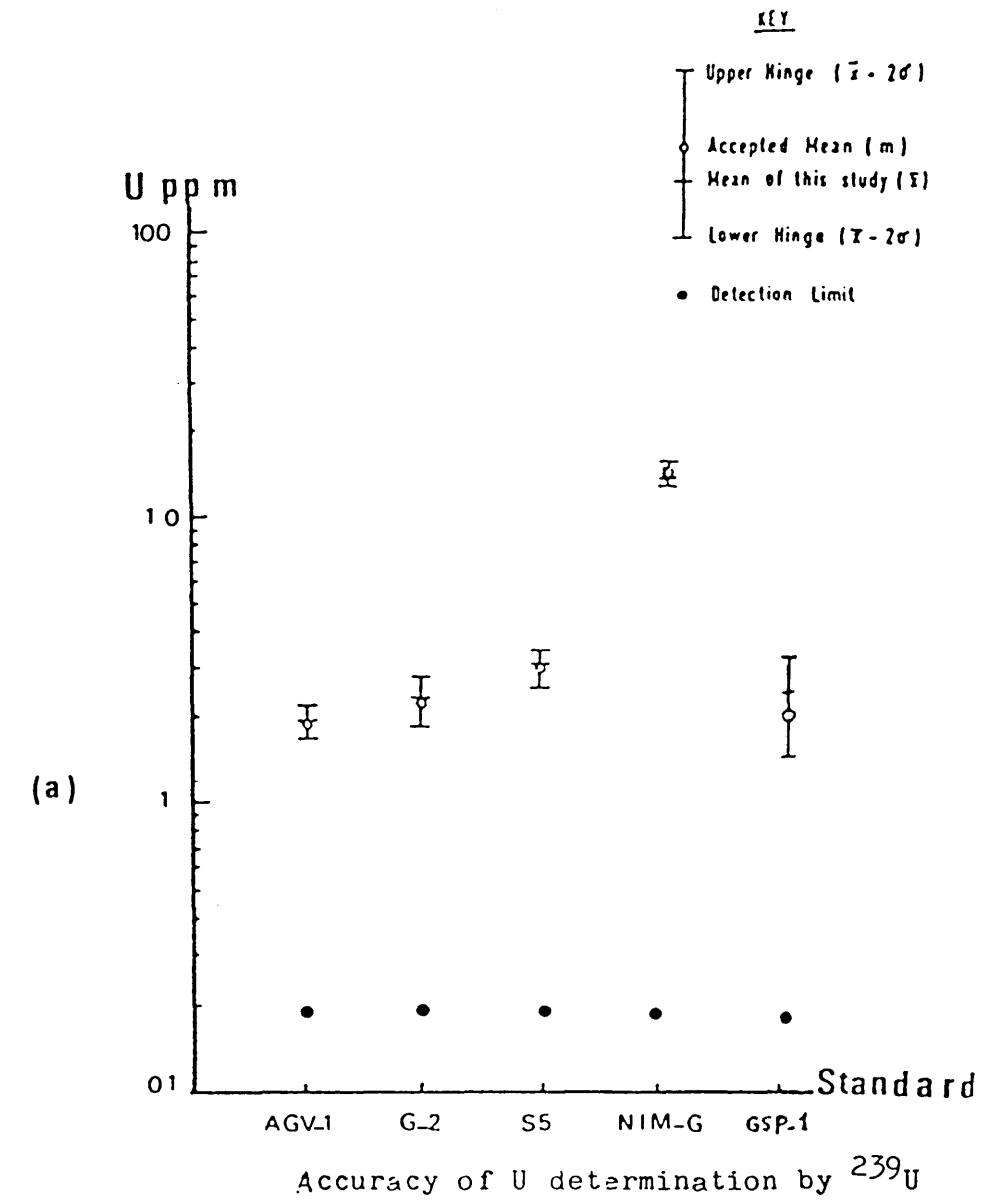
Fig.7.5 The relationship of U contents measured by various techniques .

Table 7.1 Uranium concentration in the groundwaters.

COLUMN	239U	U.INAA	U.FLUO
COUNT	33	33	33
ROW			
1	9.4000	9.7000	4.6000
2	6.6000	6.7000	4.8000
3	.9000	.7000	1.0000
4	5.5000	5.2000	3.8000
5	7.1000	7.8000	5.0000
6	18.0000	23.1000	11.7000
7	7.5000	7.4000	6.9000
8	3.0000	3.9000	2.9000
9	18.4000	25.0000	14.4000
10	8.5000	8.4000	8.5000
11	15.0000	15.3000	12.3000
12	8.4000	8.4000	7.5000
13	6.5000	6.0000	6.0000
14	4.1000	4.0000	4.8000
15	3.8000	4.0000	3.5000
16	1.9000	1.9000	2.2000
17	6.6000	6.2000	6.5000
18	5.5000	5.9000	3.5000
19	5.5000	5.6000	3.7000
20	2.0000	1.5000	1.3000
21	8.0000	8.0000	7.2000
22	15.2000	15.3000	12.8000
23	4.0000	3.9000	3.2000
24	1.2000	1.2000	1.5000
25	15.2000	19.6000	13.0000
26	24.5000	29.3000	16.7000
27	15.6000	16.6000	8.7000
28	9.5000	9.4000	8.3000
29	6.6000	6.4000	6.1000
30	7.3000	7.3000	5.4000
31	.9000	.9000	1.0000
32	4.3000	4.0000	4.1000
33	.8000	.8000	1.0000

Correlatio coeffcient of U measured by the three methods.

	239U	U.INAA
U.INAA	.987	
FLUO	.962	.945



Accuracy of U determination by ^{239}U

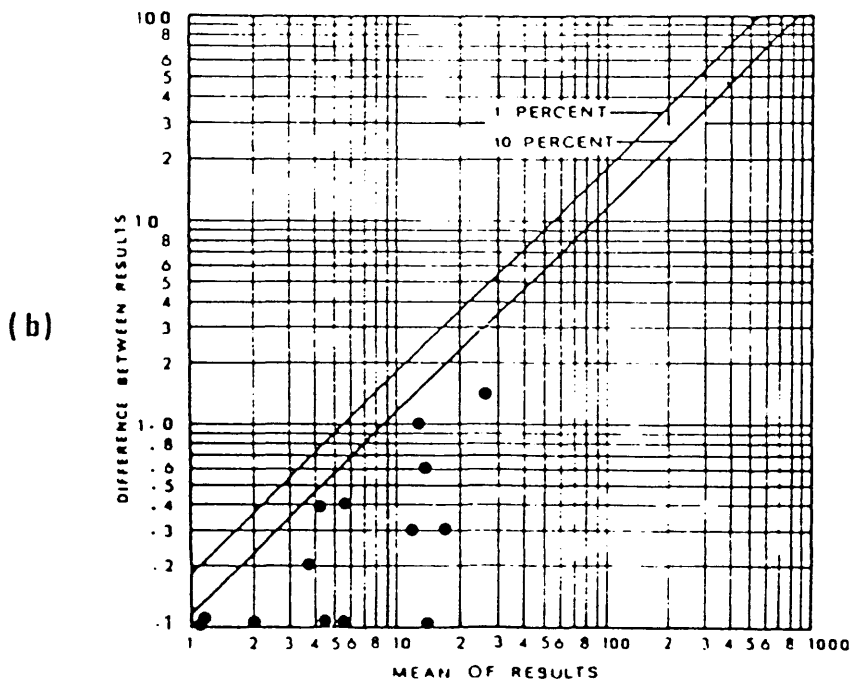


Fig.7.6 Accuracy (a) and precision (b) of U determination by the ^{239}U (NAA).

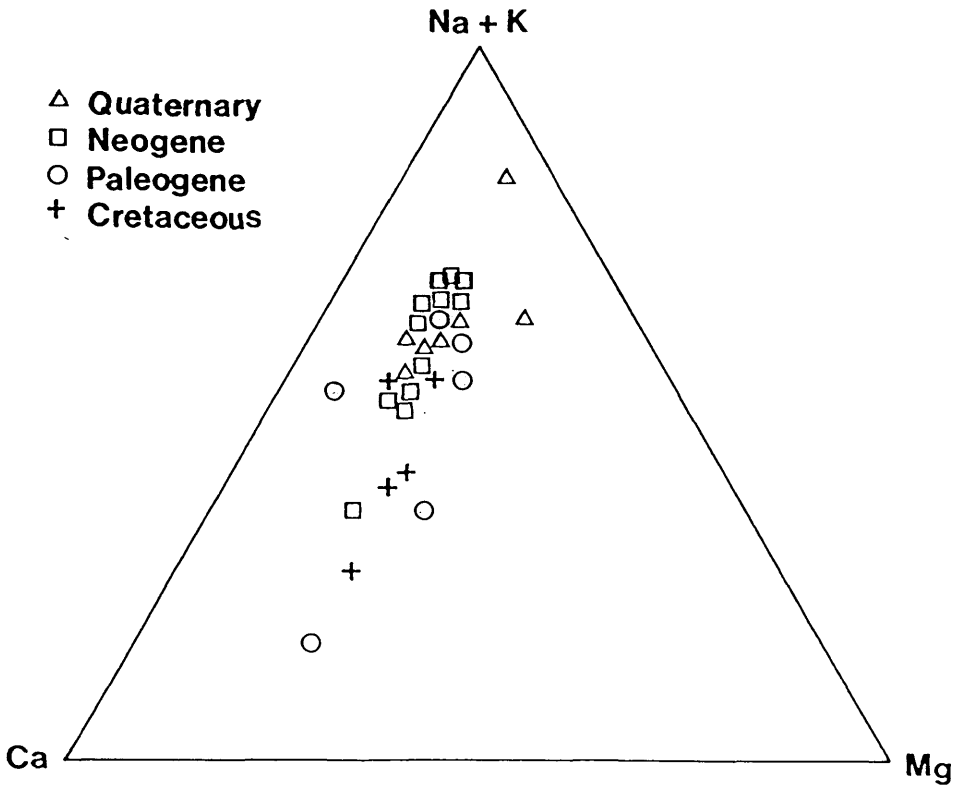


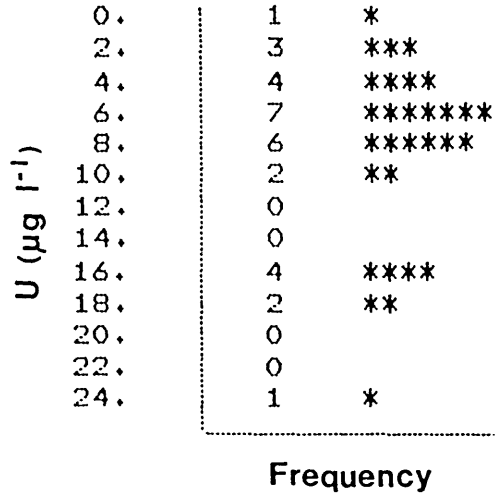
Fig.7.7 Ternary diagram of the major alkaline elements in the Palmyrides hydrogeochemistry.

a Piper diagram for groundwater obtained mainly from the northern part of the Ad-Daww basin (El Baida-Maqssam area). Moreover, they reported an increase in salinity towards the topographically lowest part of the basin, the so called "Ad-Dawwah", situated a few kilometres north of the Homs-Palmyra road in El Maqssam area. Using the solubility index (SI), they explain the high salinity of the groundwater in the vicinity by the dissolution of halite (NaCl) and gypsum ($CaSO_4.2H_2O$). Their calculations for the solubility indices for these salts showed that the waters of El Baida-Maqssam area are saturated with respect to halite and gypsum. It is worth noting that potassium concentrations in these waters were found to be relatively low by both Hale and Jubeli (1985) and Agha and Droubi (1983). Since evaporation tends to increase K as well as all other major cations present in the water, the observed salinity, seems better explained in terms of dissolution of evaporite (gypsum)and surface salts (halide) which contain no K.

High concentrations of several trace elements relative to their typical abundances in groundwaters was found. Elements so enhanced include U, Se, Sr, As, Mo, P and S. This, however, might be a result of aridity, whereby evapotransportation causes increases of elemental content in general.

7.5.2 Frequency distribution

Dissolved U in the samples range from 1 µg/l to 25 µg/l. The histogram and Q_nQ_n plots (Fig. 7.8) clearly constitute two populations separated at about 12 µg/l. The lower population comprises typical background concentrations of U, and the upper



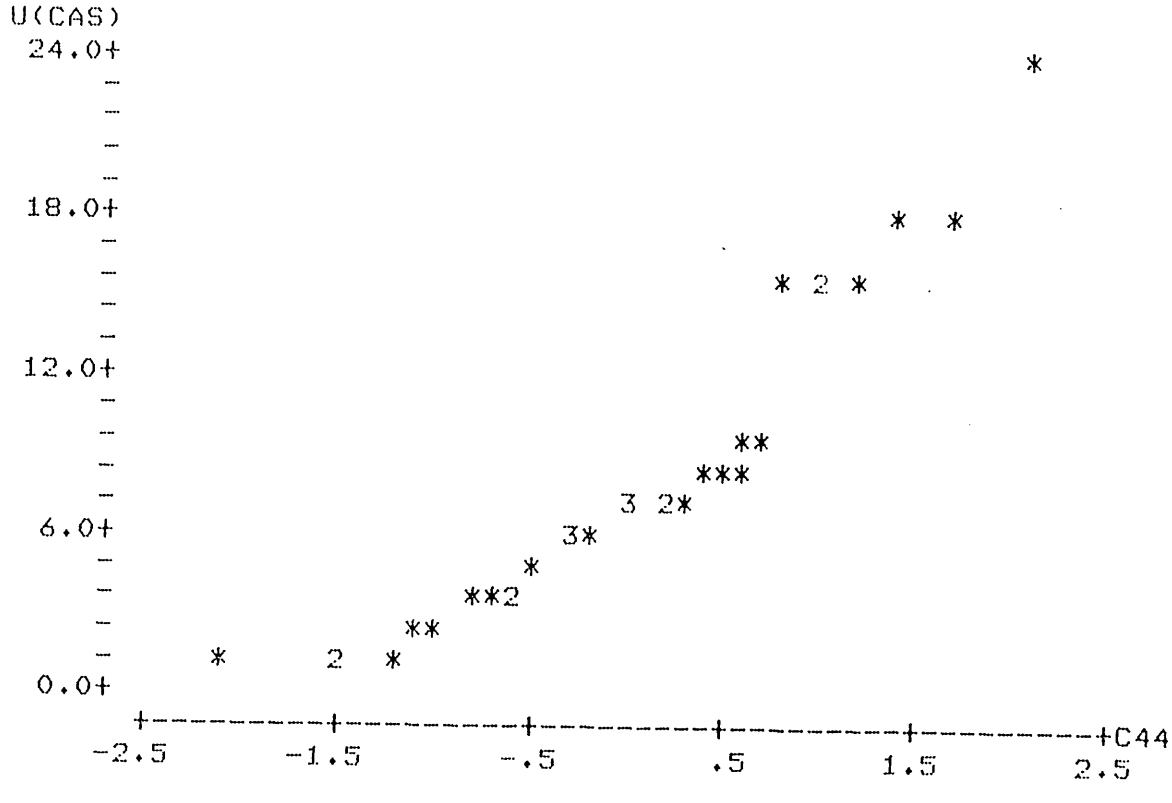


Fig.7.8 Histogram and QQ plot of U in the groundwaters .

population is seven samples which are anomalous in U content. Each sample in the anomalous population is enriched and possibly anomalous in at least one and usually several other trace and major elements. The maximum concentrations these attain are 2268 mg/l Na, 900 mg/l S, 730 mg/l Ca, 370 mg/l Mg, 230 mg/l K, 3.5 mg/l P, 250 µg/l As, 51 µg/l V, 14 µg/l Se and 101 µg/l Mo.

In general there is a marked skewness of element frequency distributions (except for U), log-transformation of the data proved unsuccessful in normalizing the distributions, but power transformation appeared to be more appropriate (Mancy and Howarth, 1980). This tool is particularly helpful in multielement geochemistry since each element may be optimized with single parameter transformation without risking deleterious effect of overall transformation (Howarth and Earl, 1979). The parameter for basic statistics of the geochemical data are listed in Table 7.2.

7.5.4 Interelemental correlation

The computed correlation coefficient matrix for the power transformed data (Table 7.3) is usually less sensitive to outliers. It showed that U is significantly positively correlated with Mo, Sr, V, and Se at the 99% confidence level and with P and TDS at the 95% level. Lopatkina (1964) has shown that, in humid regions, chemical weathering of uranium-bearing host rocks yields waters in which there is a linear correlation between U content and total dissolved solids (TDS). The same relationship does not necessarily hold in arid regions (Rose, 1977), but chemical weathering may have been significantly more active in the region during the two earlier

Table 7.2 Summary statistics of the hydrogeochemical data.

U	PPB	N =	33	MEAN =	7.7970	ST.DEV. =	5.82
SE	PPB	N =	33	MEAN =	6.4894	ST.DEV. =	12.0
F	PPM	N =	33	MEAN =	1.5606	ST.DEV. =	.874
AS	PPB	N =	33	MEAN =	56.152	ST.DEV. =	55.2
LI	PPB	N =	33	MEAN =	45.061	ST.DEV. =	48.3
SR	PPM	N =	33	MEAN =	7.4786	ST.DEV. =	5.14
BA	PPB	N =	33	MEAN =	28.061	ST.DEV. =	36.5
V	PPB	N =	33	MEAN =	20.424	ST.DEV. =	12.8
MO	PPB	N =	33	MEAN =	38.485	ST.DEV. =	20.7
CO	PPB	N =	33	MEAN =	7.8788	ST.DEV. =	4.32
NI	PPB	N =	33	MEAN =	26.515	ST.DEV. =	37.8
CU	PPB	N =	33	MEAN =	7.4242	ST.DEV. =	6.18
ZN	PPB	N =	33	MEAN =	279.52	ST.DEV. =	395.
CD	PPB	N =	33	MEAN =	5.0000	ST.DEV. =	3.99
P	PPB	N =	33	MEAN =	256.27	ST.DEV. =	683
S	PPM	N =	33	MEAN =	213.97	ST.DEV. =	210.
NA	PPM	N =	33	MEAN =	446.88	ST.DEV. =	544.
K	PPM	N =	33	MEAN =	22.400	ST.DEV. =	38.8
MG	PPM	N =	33	MEAN =	111.75	ST.DEV. =	90.7
CA	PPM	N =	33	MEAN =	209.00	ST.DEV. =	165.
SI	PPM	N =	33	MEAN =	6.4152	ST.DEV. =	5.09
TDS.PPM		N =	33	MEAN =	790.03	ST.DEV. =	764.

Table 7.3 Correlation matrix of the hydrogeochemical data.

	U	SE	F	AS	LI	SR	BA	V
SE	.602							
F	.334	.109						
AS	.328	.298	.430					
LI	.195	-.086	.576	.357				
SR	.682	.348	.662	.409	.733			
BA	-.048	.026	-.309	-.160	-.311	-.280		
V	.618	.283	.338	.538	.281	.474	.129	
MO	.720	.444	.569	.420	.482	.721	-.054	.566
CO	.382	.074	.334	.190	.306	.400	-.113	.383
NI	.015	.097	.055	-.236	.053	.039	.050	-.011
CU	.068	.096	-.024	.165	.128	.160	.015	.042
ZN	.408	.154	.534	.585	.631	.629	-.112	.528
CD	.263	.025	-.030	-.053	.302	.321	-.303	.153
P	.502	.359	.567	.061	.161	.485	.040	.109
S	.401	.305	.533	.284	.830	.863	-.236	.260
NA	.509	.051	.485	.379	.855	.824	-.095	.541
K	.200	-.058	.341	.264	.796	.589	.059	.334
MG	.499	.206	.526	.325	.858	.882	-.268	.407
CA	.460	.328	.517	.286	.729	.859	-.352	.199
SI	.050	-.025	.062	.245	.519	.314	.016	.359
TDS	.493	.138	.502	.341	.875	.880	-.202	.448

	MO	CO	NI	CU	ZN	CD	P	S
CO	.364							
NI	.311	-.105						
CU	.090	.572	.025					
ZN	.545	.316	-.039	-.032				
CD	.082	.316	-.087	.186	.073			
P	.522	.290	.145	.039	.215	-.032		
S	.604	.385	.198	.303	.596	.331	.420	
NA	.618	.502	-.005	.239	.663	.362	.269	.819
K	.470	.385	.163	.300	.564	.101	.217	.765
MG	.581	.486	.075	.269	.578	.469	.316	.909
CA	.549	.435	.082	.356	.545	.330	.697	.903
SI	.031	.298	.026	.309	.251	.296	-.208	.447
TDS	.613	.507	.055	.297	.646	.407	.312	.922

pluvial periods. This perhaps contributed to the observed association between U and TDS (effectively Na + Ca + Mg since K is by comparison present generally in very low concentrations as mentioned earlier).

7.5.4 Cluster analysis

Hierarchical cluster analysis of the hydrogeochemical data was performed applying the approach discussed in Chapter 6. The dendogram for 22 variables (Fig. 7.9) indicates that: uranium is closely associated with Mo, V, and Se; this group has a low order association with As, Zn on one side and S and F in the other; a second major group (embracing two subgroups) comprises, K, Cd, Ca, Sr, Li, Ma, Na, Si and Sr and a third group, comprising P, TDS, Cu and Co, is weakly connected with a fourth group consisting of Ba and Ni.

Reducing the number of variables to only 13 the dendogram shows the following four groups as illustrated in Fig. 7.10.

(1) U, Sr, Se and V;

(2) S, Ca, Mo, Mg and As;

(3) Na and F;

(4) K and P.

When cluster analysis was performed on the power transformed data, the dendogram presented in Fig. 7.11 indicated that U, Mo, V and Se are closely associated, the highest correlation being between U and Mo. This association is also being joined at a significant level by As and Zn from one side and F and P on the

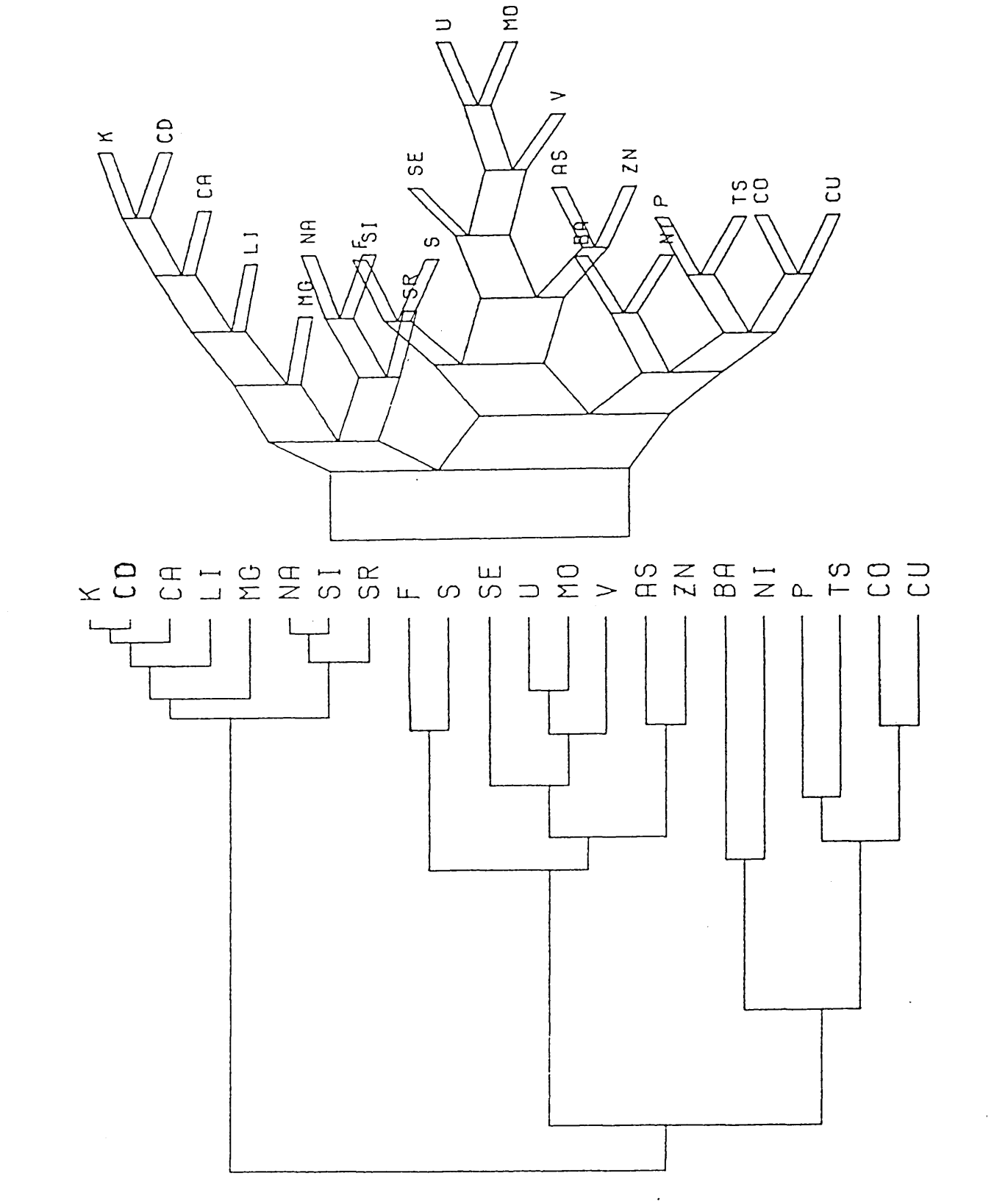


Fig.7.9 Cluster analysis of 22 hydrogeochemical variables.

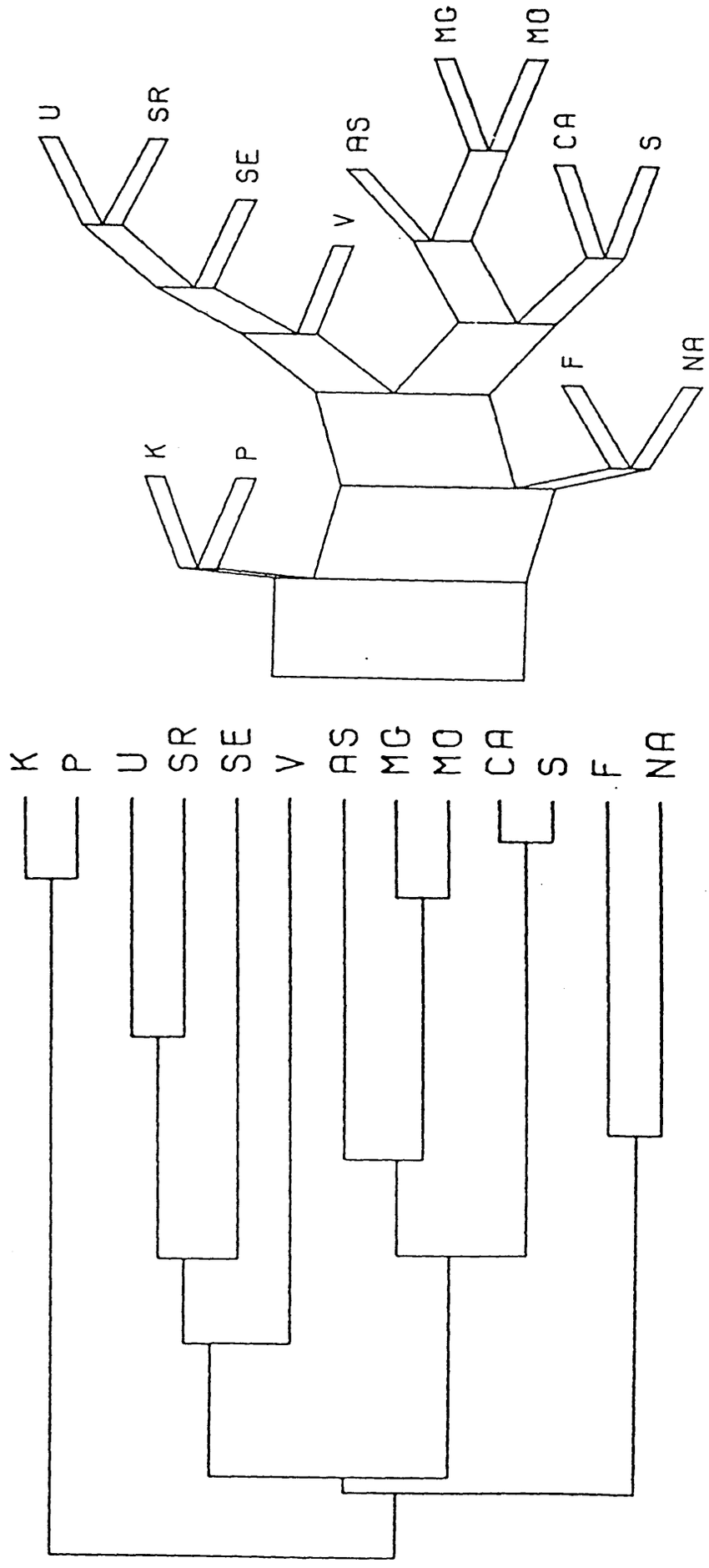


Fig.7.10 Cluster analysis of 13 hydrogeochemical variables.

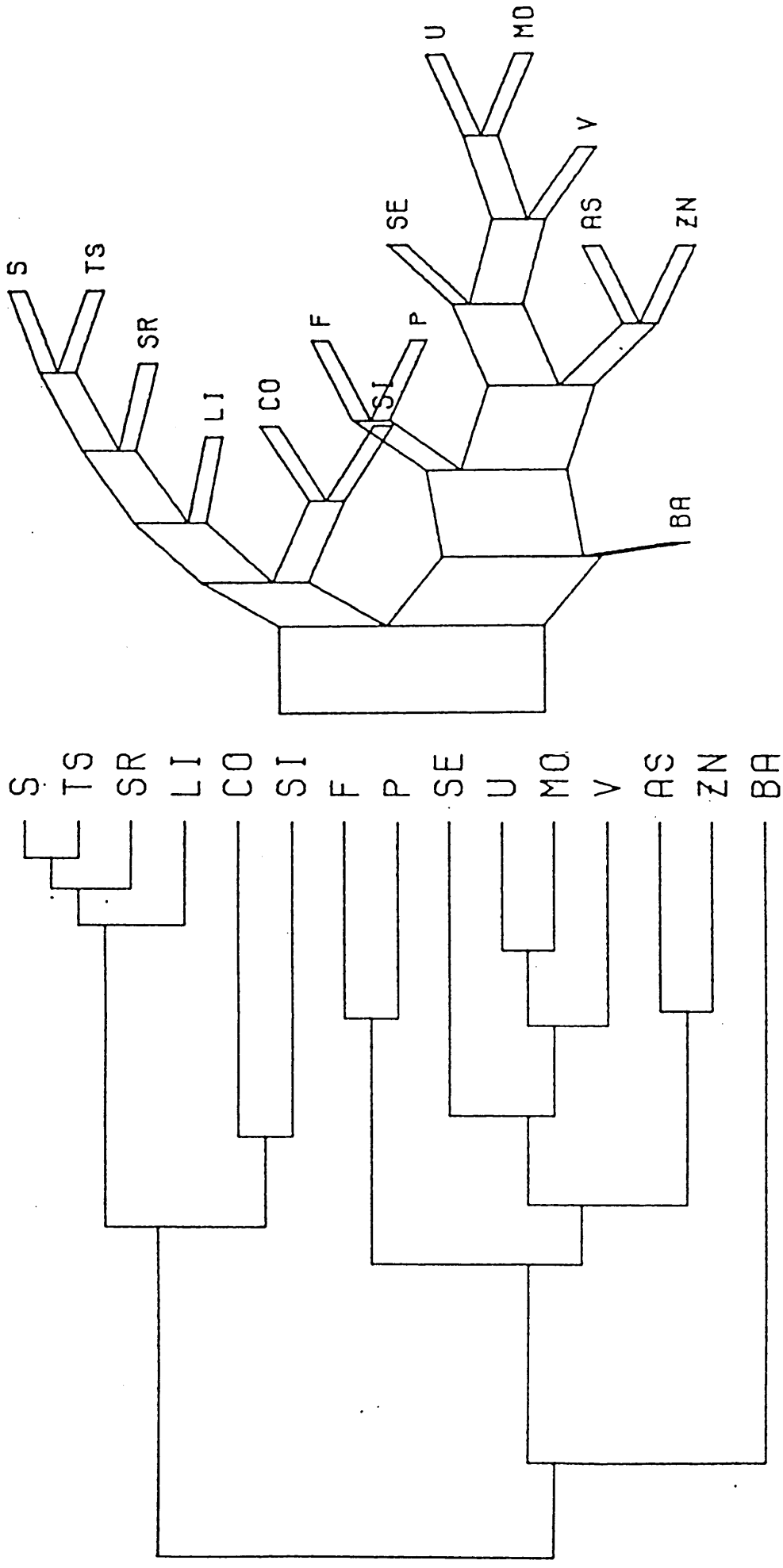


Fig.7.11 Cluster analysis of 15 hydrogeochemical variables.

other, forming one major group. Total dissolved solids, S, Sr and Li are also closely associated in one cluster, which in turn are joined by Co and Si to form a second major group. Barium stays isolated from the two major groups. This leads to a tentative conclusion that the foregoing associations between U, Mo, V, Se, Sr and to a lesser degree As is persistent and no significant association of U with P, F and S can be found.

Thermodynamic calculations by Langmuir (1978) show that U is soluble partly as uranous, uranyl fluoride and uranyl sulphate complexes at low pH and is soluble mainly as uranyl phosphate complex in the pH range 4 to 7.5 (see Fig. 1.4). At higher pH, U is soluble as one of these uranyl carbonate complexes: dicarbonate $UO_2(CO_3)^{2-}_2$; and tricarbonate $UO_2(CO_3)^{4-}_3$ in increasing order of solubility. Anderson (1985) reported that U^{2+} in groundwaters follows its thermodynamically predicted behaviour. As the Palmyrides groundwaters are slighlty alkaline having pH 7.3 to 8.0 it is evident that uranyl carbonate complexes predominate and the observed lack of close association of U and P, F and S is consistent with the thermodynamic data.

The close association of U and V, however, lends support to the possible existence of soluble uranyl vanadate complexes analogous to uranyl phosphate complexes (Langmuir, 1978). The lack of enough reliable data for the calculations of saturation status and solution-mineral equilibria has hindered the use of these tools as exploration indicators (Langmuir and Chatham, 1980). Nevertheless, Se, Mo, V and As in groundwaters were considered by many workers to be helpful pathfinders (c.f. Dyck, 1975; Nichols et

al., 1977; Cadigan and Felmlee, 1979; Rose and Kormer, 1979). Moreover, the U, Mo, V and Se association revealed in the Palmyrides groundwaters has also been reported in groundwaters from areas of known U deposits (where Ra, Rn and As sometimes constitute additional members of the association) (Arendt, 1978; Rose and Wright, 1980). Other data from the Shirley Basin and Pennsylvania indicated the same typical zoning sequence of these elements as in Fig. 7.12, which is known in sandstone roll front U deposits (King and Austin, 1965, Hareshman,1972; and Chester, 1984). Thus the significance of the Palmyrides hydrogeochemical data in pointing out a possible U accumulations must not be ignored.

7.5.5 Ridge regression

Ridge regression was performed on the standardized hydrogeochemical data using a computer programme developed by Howarth (1984). This programme was run several times (with different subsets of variables) to eliminate variables with the least predictive power.

The first ridge regression utilising 19 of the analysed elements (Table 7.4) shows the classical least square solution to occur where $K = \emptyset$ and the VIF = 51.4. If this solution is employed, Se, V, Zn, Na, Mo and P are the strongest positive predictors and As and potassium are by far the strongest negative predictors. With a small increase in the ridge constant, however, several of these estimators show a rapid decrease in their predictive importance particularly, As and K (Fig. 7.13).

When the number of variables is reduced to 12 (combining Na +

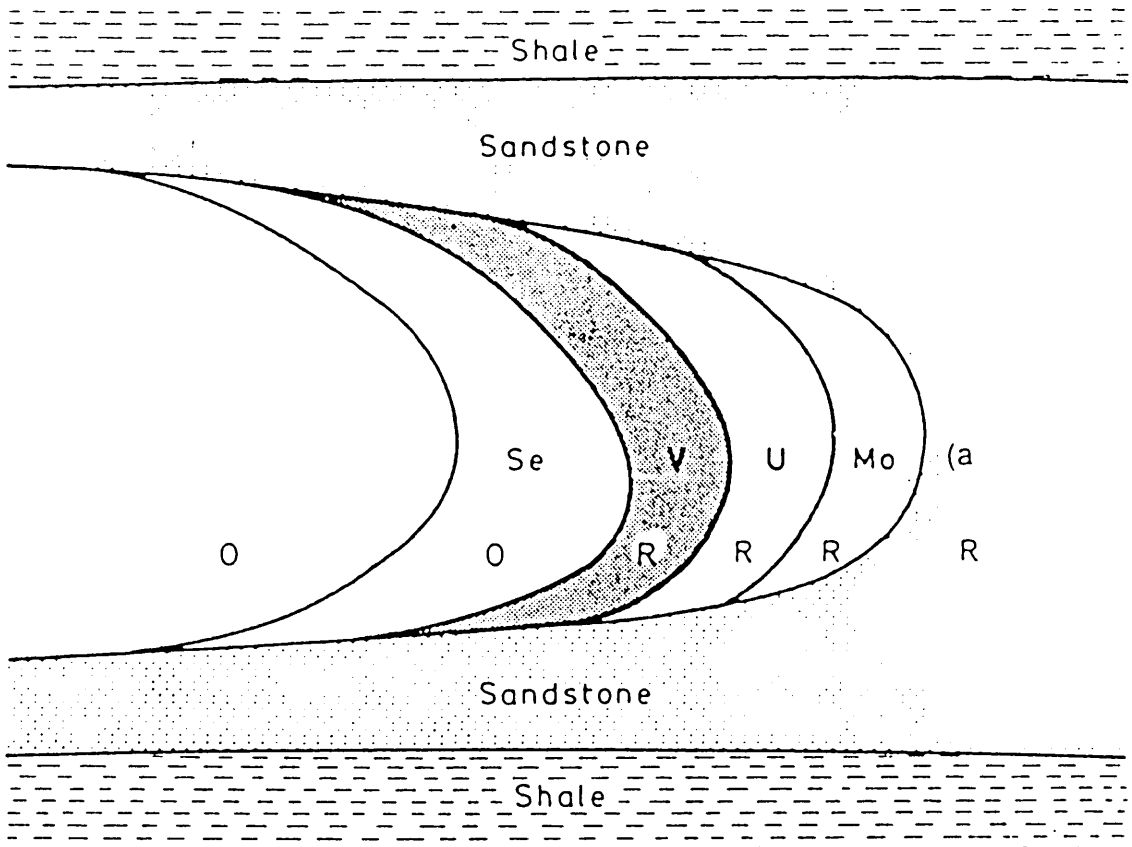


Fig.7.12 Zonation of Roll-Front type of U deposit (from Chester, 1984).

Table 7.4 Standardized estimators and regression coefficients.

STANDARDIZED ESTIMATORS

	RIDGE CONSTANT						
	0.00	.02	.04	.06	.08	.10	.15
K	-.3322	-.2639	-.2269	-.2026	-.1849	-.1713	-.1470
MG	.0140	.0103	.0071	.0048	.0033	.0024	.0017
CA	-.0691	-.0541	-.0487	-.0456	-.0431	-.0410	-.0359
SR	.2720	.2339	.2086	.1906	.1771	.1666	.1481
NA	.2562	.1890	.1578	.1392	.1266	.1173	.1022
AL	-.0325	-.0188	-.0126	-.0090	-.0066	-.0048	-.0020
V	.2891	.3016	.3024	.2997	.2958	.2912	.2794
AS	-.3911	-.3577	-.3284	-.3038	-.2829	-.2651	-.2299
MO	.2336	.2160	.2097	.2058	.2027	.1998	.1934
MN	.0308	.0334	.0331	.0321	.0310	.0299	.0273
FE	-.1015	-.1013	-.0964	-.0911	-.0861	-.0816	-.0725
NI	.0614	.0462	.0363	.0292	.0239	.0198	.0130
ZN	.2663	.2522	.2371	.2234	.2113	.2006	.1788
P	.1427	.1360	.1313	.1278	.1251	.1229	.1188
S	-.1392	-.1258	-.1173	-.1109	-.1057	-.1012	-.0923
SI	.1334	.1390	.1401	.1393	.1375	.1351	.1284
SE	.3287	.3504	.3611	.3669	.3699	.3711	.3693
F	-.1347	-.1186	-.1079	-.0995	-.0925	-.0864	-.0738
MAXIMUM VIF	51.44	19.03	12.34	9.27	7.47	6.27	4.51

STANDARDIZED ESTIMATORS

	RIDGE CONSTANT						
	.20	.30	.40	.50	.60	.80	1.00
K	-.1303	-.1075	-.0917	-.0797	-.0700	-.0552	-.0442
MG	.0023	.0047	.0074	.0100	.0123	.0162	.0192
CA	-.0312	-.0231	-.0164	-.0109	-.0062	.0010	.0063
SR	.1360	.1209	.1116	.1050	.1001	.0928	.0875
NA	.0928	.0817	.0753	.0710	.0680	.0639	.0611
AL	-.0001	.0023	.0039	.0050	.0058	.0067	.0072
V	.2679	.2476	.2306	.2163	.2040	.1841	.1685
AS	-.2036	-.1661	-.1400	-.1206	-.1053	-.0827	-.0666
MO	.1875	.1769	.1678	.1598	.1529	.1413	.1319
MN	.0249	.0209	.0176	.0149	.0126	.0090	.0063
FE	-.0657	-.0562	-.0497	-.0449	-.0412	-.0356	-.0315
NI	.0088	.0043	.0022	.0011	.0005	.0001	.0000
ZN	.1621	.1380	.1214	.1093	.1001	.0870	.0781
P	.1158	.1114	.1079	.1048	.1019	.0965	.0917
S	-.0855	-.0753	-.0680	-.0623	-.0577	-.0506	-.0453
SI	.1215	.1089	.0983	.0897	.0824	.0712	.0630
SE	.3640	.3494	.3334	.3177	.3030	.2768	.2546
F	-.0638	-.0485	-.0371	-.0284	-.0214	-.0110	-.0038
MAXIMUM VIF	3.54	2.50	1.94	1.59	1.35	1.04	.84

RIDGE TRACE

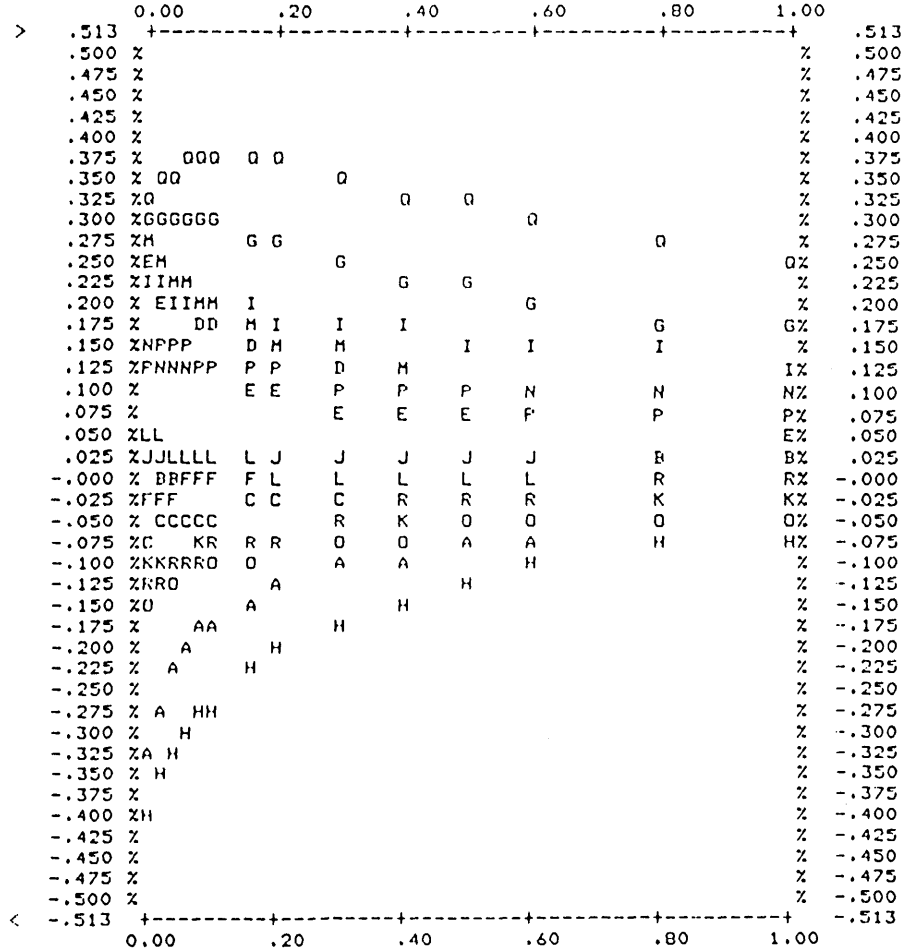


Fig.7.13 Ridge trace for regression of U Vs 18 variables in the hydrogeochemistry.

RIDGE TRACE

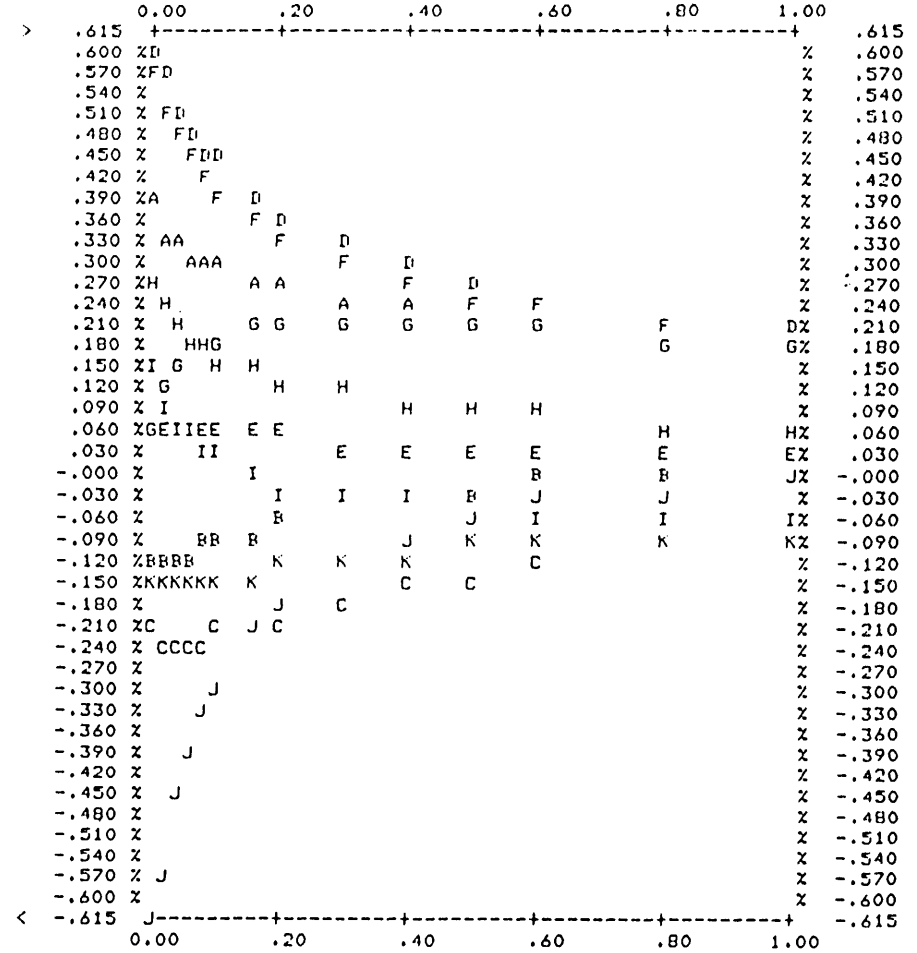


Fig.7.14 Ridge trace for regression of U Vs 11 variables in the hydrogeochemistry.

K + Mg + Ca as TDS and adding pH and AQ = aquifer), the ridge trace (Fig. 7.14) indicates that if the least square solution (K = Ø) had been accepted, S and As would have been the strongest negative predictors and Sr, Mo, Se, TDS and V (in decreasing order) are the strongest positive ones. However, adding an optimum ridge constant (0.1 to 0.2) indicates that As and pH are the most stable negative predictors, while the predictivity of Sr, Mo and Se continued to be of the same order, but the importance of V predictivity became more than that of the TDS. Therefore, when applying the ridge regression one has to consider the stability of the predictors as well as the importance of their predictivity.

After excluding both pH and AQ, the ridge regression solution obtained (Fig. 7.15) showed that Si, As and F are the most stable negative predictors, while S shows a lesser negative predictivity. Strontium, Se, V, Mo, P and Na, on the other hand, are found to be the strongest positive predictors of U content. It is worth noting also that TDS decreased sharply from being the strongest positive predictor at K = Ø to a low predictor when adding the optimum K constant used for this regression equation (K = 0.15). The regression line produced in this case gave the best goodness of fit. Thus, this regression can be considered a good estimator of U content in the hydrogeochemical data of the investigated area. The statistical significance of this regression line was tested using the two parameters mentioned earlier, namely R^2 and F-ratio. As can be seen from Table 7.4 and the corresponding ridge trace (Fig. 7.15), the R^2 value approached one (R^2 = 0.918) indicating a good fit, and the value of F-ratio (14.7) fell well above the critical value of F = 4.70 at the 99% confidence level

```
          0.00        .20        .40        .60        .80       1.00
>    .666  K---------+---------+---------+---------+---------+     .666
     .650 %                                                  %    .650
     .619 %A                                                 %    .619
     .588 %                                                  %    .588
     .556 % A                                                %    .556
     .525 %  A                                               %    .525
     .494 %D  A                                              %    .494
     .463 % D  AA                                            %    .463
     .431 % I       A                                        %    .431
     .400 %  D        A                                      %    .400
     .369 %  ID             A                                %    .369
     .338 %    D                  A                          %    .338
     .306 %   I D                          A     A           %    .306
     .275 %    I   D                                   A     %    .275
     .244 %    EI  E E     E      E                          A%   .244
     .213 %I  E    I       D           E     E               %    .213
     .181 %GKE     F I     F      F    F     F         E     E%   .181
     .150 % GGGGG  G G     G      G    G     D         F     F%   .150
     .119 %  K             I      I          G         G     G%   .119
     .087 %   KK                          I     I     I     I%   .087
     .056 %E   K  K K     K      K    K     K     K   K     K%   .056
     .025 %                                                  %    .025
    -.006 %                                  C     C     H%   -.006
    -.038 %J               C      C    C     B     J     J%   -.038
    -.069 % JJJJJ  J J     J      J    J     J               %   -.069
    -.100 %   BCC                H                          %   -.100
    -.131 % CCC            H                                %   -.131
    -.163 %C                                                %   -.163
    -.194 %          H                                      %   -.194
    -.225 %                                                 %   -.225
    -.256 %        H                                        %   -.256
    -.288 %                                                 %   -.288
    -.319 %                                                 %   -.319
    -.350 %     H                                           %   -.350
    -.381 %                                                 %   -.381
    -.413 %    H                                            %   -.413
    -.444 %                                                 %   -.444
    -.475 %   H                                             %   -.475
    -.506 %                                                 %   -.506
    -.538 %                                                 %   -.538
    -.569 %  H                                              %   -.569
    -.600 %                                                 %   -.600
<   -.616  HH-------+---------+---------+---------+---------+    -.616
          0.00        .20        .40        .60        .80       1.00

 A= SE     B= F      C= AS     D= SR     E= V      F= MO     G= P
 H= S      I= NA     J= SI     K= TDS
```

ANALYSIS OF VARIANCE % RIDGE

SOURCE OF VARIATION	SUM OF SQUARES	DEGREES OF FREEDOM	MEAN SQUARES	F-RATIO
REGRESSION	427.75	10	42.78	14.7097
RESIDUAL	37.80	13	2.91	
TOTAL VARIATION	465.56	23		

MULT. R-SQUARED = .9188 STD. ERROR OF EST. = 1.7053
VARIANCE OF ERROR TERM = 2.9080

Fig.7.15 Optimum ridge regression of U in the hydrogeochemical data.

(Davis, 1973). Therefore, the corresponding ridge regression solution was accepted as significant, and preferred as it has the highest R^2 value.

The present application of the ridge regression suggested that U concentrations in the Palmyrides waters are essentially a function of their Se, Mo, Sr, V, P and TDS contents.

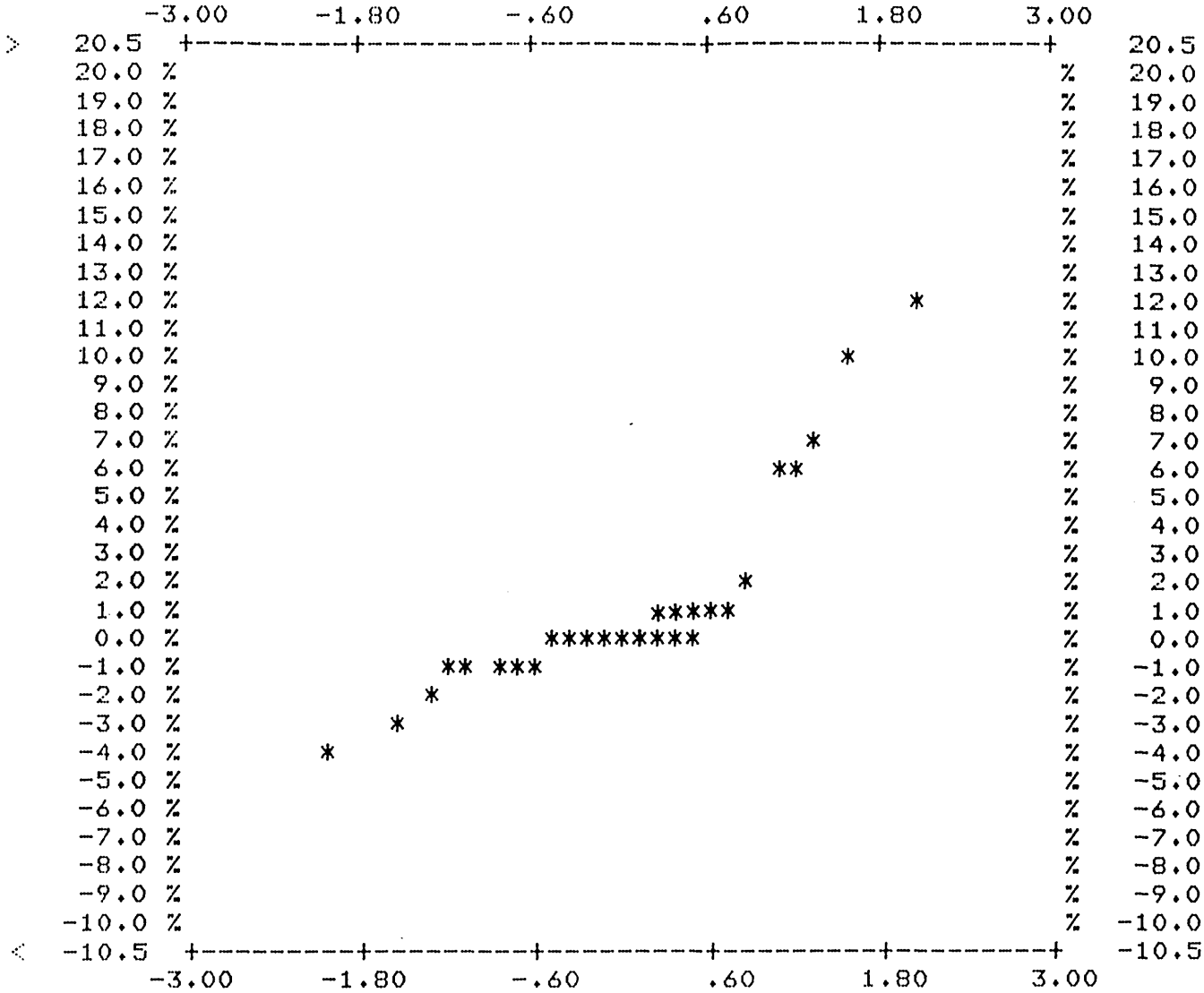
The residual probability plot obtained from this ridge regression is presented in (Fig. 7.16).

7.5.6 Boxplots

Examination of the hydrogeochemical data by aquifer was performed using the subroutine Boxplot within MINITAB. This graphic presentation is particularly useful for comparing the distribution of U and other elements between the four aquifers. The body of the box includes the median (marked by +) and the upper and lower quartiles of the data (25% and 75%); the whiskers extend to the outermost data values that are still not beyond the hinges (1.5x the difference between the quartiles); individual values lying beyond these limits may be considered outliers and are shown individually by asterix or O (Howarth, 1984).

The Boxplot of uranium in the data reveals that the highest median U content and the widest U concentration range is found in the Neogene aquifer (Fig. 7.17). Similar distributions are shown by Mo, TDS, S, Ca and to a lesser degree Sr and V (Fig. 7.17 - 7.18). Of the seven samples with anomalous U concentrations, all but one

RESIDUAL PROBABILITY PLOT



SMALLEST RESIDUALS		LARGEST RESIDUALS	
16	-3.96205	25	11.80511
3	-3.18539	26	9.85389
18	-2.47330	27	7.37446
29	-.90339	22	5.85567
17	-.77286	11	5.77360
24	-.62834	6	1.89951
4	-.60029	28	1.28012
1	-.56782	13	.98078
7	-.54043	12	.78652
20	-.49186	15	.43227
10	-.32595	9	.21907
23	-.31992	2	.20742
14	-.31666	30	.12276
8	-.15117	19	-.08548
21	-.11537	5	-.10891

Fig.7.16 Residual probability plot of U in the groundwaters.

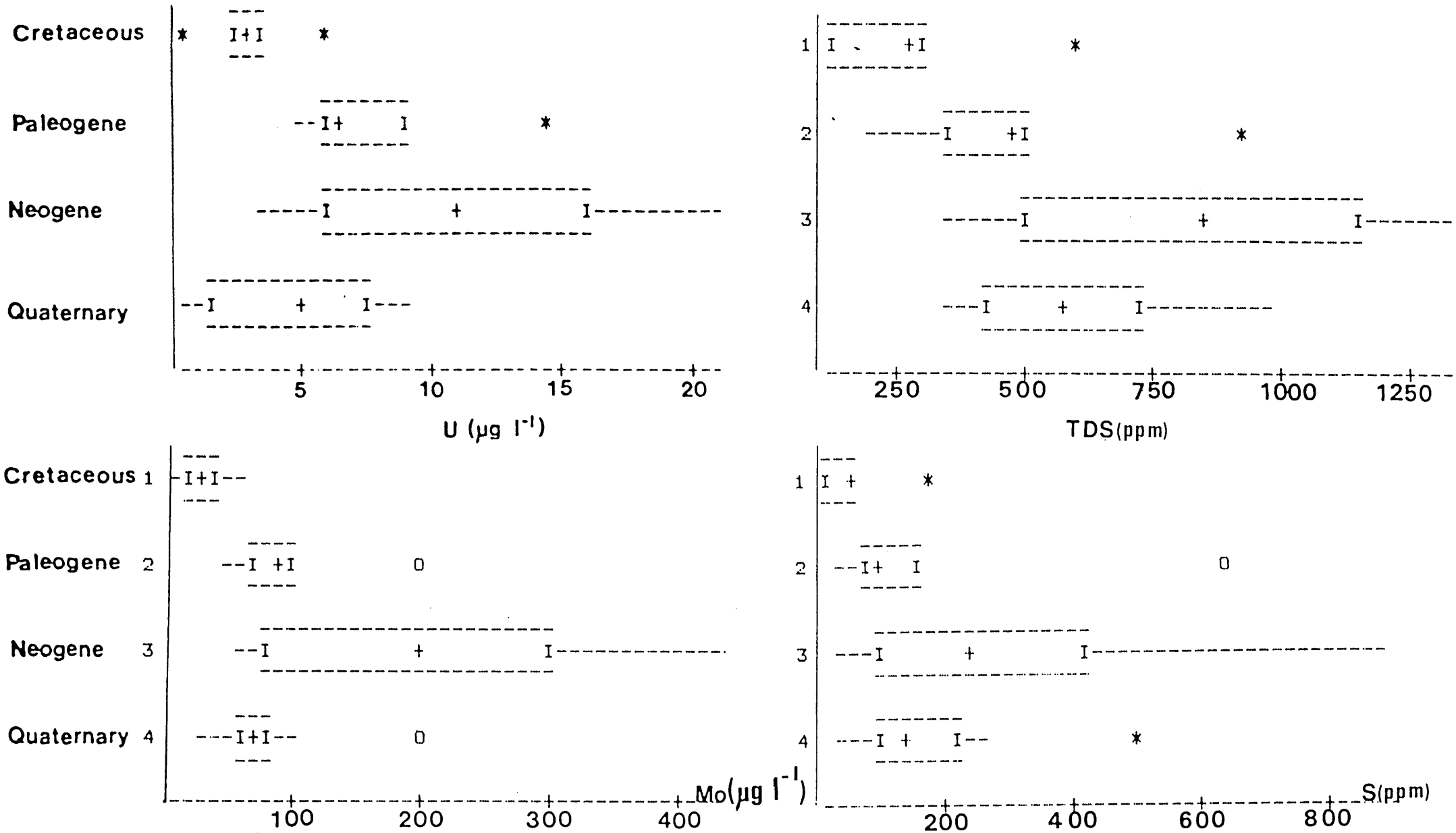


Fig.7.17 Boxplot of U, TDS, Mo and S of the hydrogeochemistry.

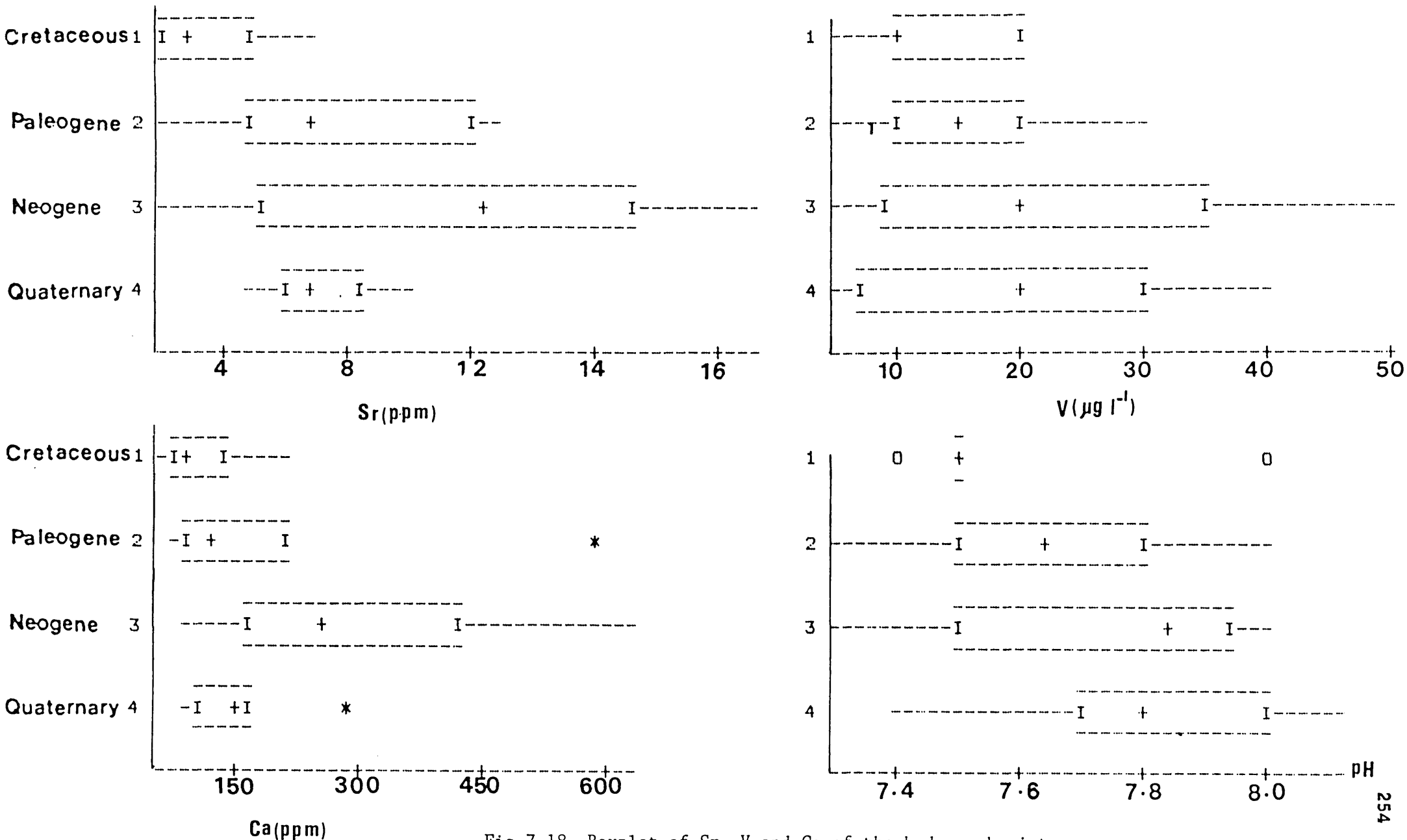


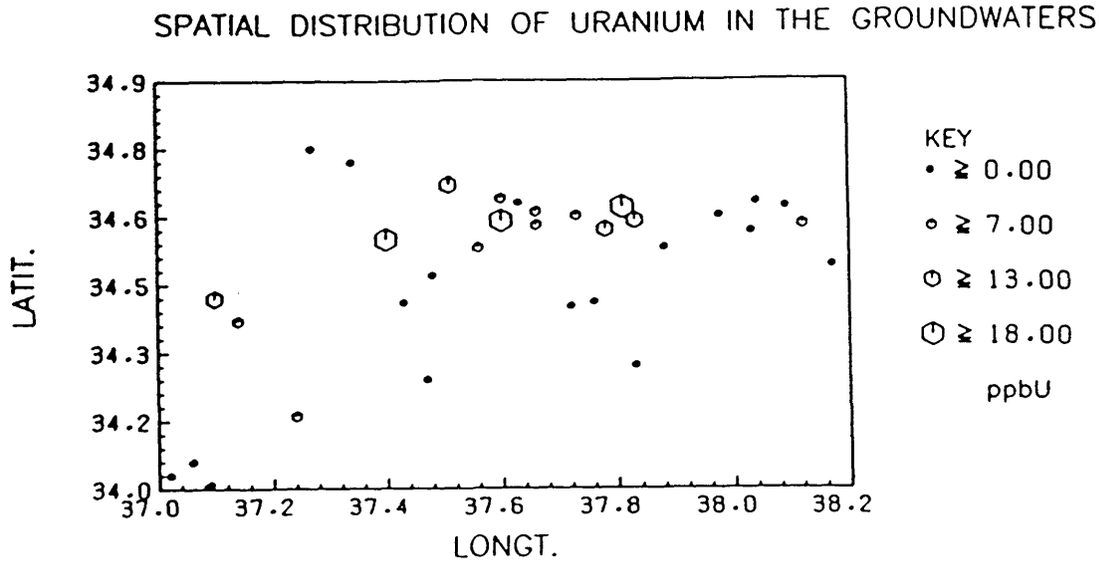
Fig.7.18 Boxplot of Sr, V and Ca of the hydrogochemistry.

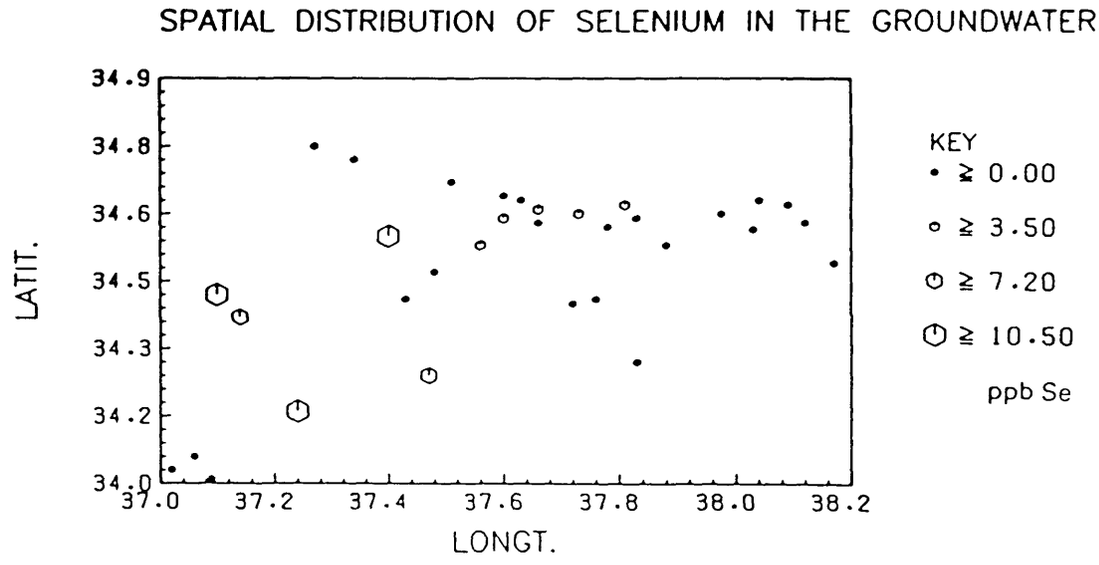
are from the Neogene aquifer (the remaining anomalous sample being associated with high Se at one sample location in the Palaeogene aquifer).

7.6 Spatial distribution of U and associated elements

7.6.1 Symbolic distribution

Symbolic spatial distribution plots for U and elements known for their association with U in aqueous complexes or in mineralized occurrences of the sandstone, unconformity or calcrete types are shown in Figs. 7.19-7.20. Study of the distribution patterns showed that F, V, Sr, As and, to a lesser extent, Mo anomalies either coincided with or occurred in close proximity to uranium anomalies, Selenium anomalies occur further west in the region, accompanied by anomalous U and Sr contents, coinciding with a major lineament interpreted as a trend of a main regional fault. This spatial relationship could be of great importance in indicating the two sides of a roll front (if such a front does exist in the region) namely the oxidized and the reduced zones. Chester (1984) illustrated the likely zonations of a roll front (Fig. 7.12); however, the similarity of the spatial distribution of the foregoing anomalies with that illustrated in Chester's graph. Studying these patterns, may help in obtaining a clear idea of how far these hydrogeochemical haloes extend and whether the source of the anomalies can be traced.





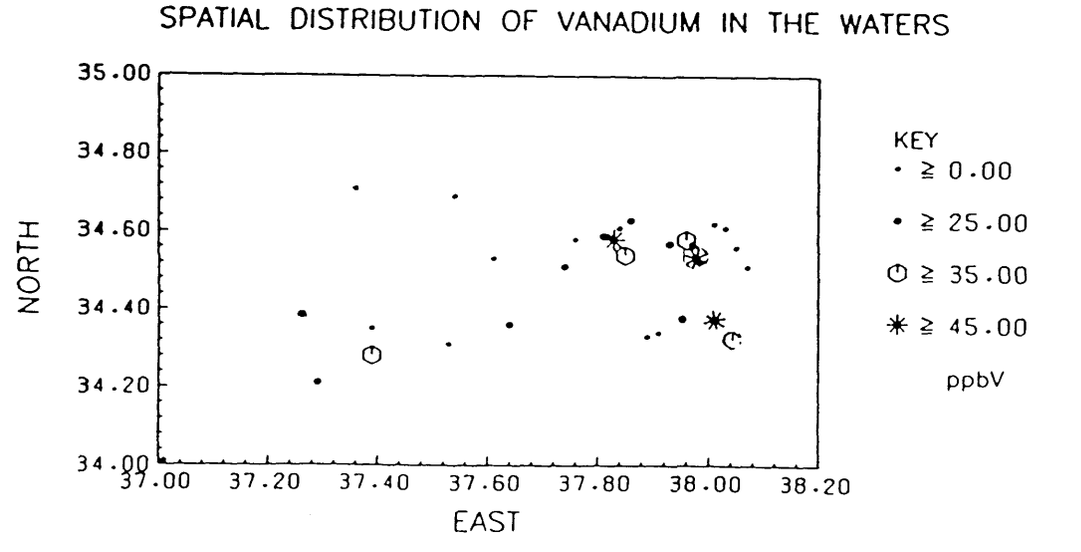


Fig.7.19 Spatial distribution of U, Se and V in the Palmyrides hydrogeochemistry.

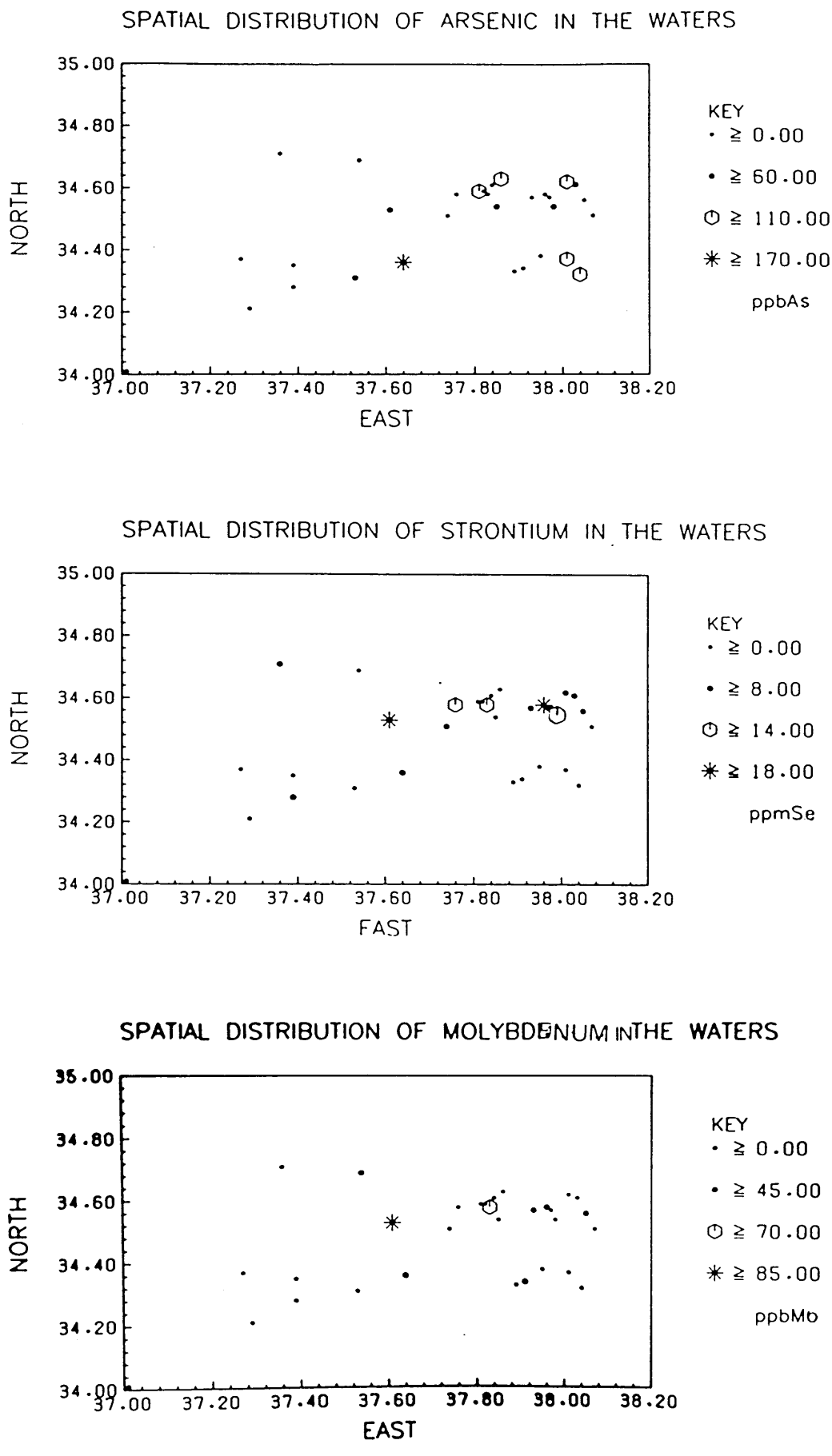


Fig.7.20 Spatial distribution of As, Sr and Mo in the Palmyrides hydrogeochemistry.

7.6.2 Uranium anomalies

In terms of spatial distribution, U anomalies occur as two clusters to the west of Palmyra along the Homs-Palmyria road. The first anomaly is centered at sample sites 26 and 6 in the vicinity of El Maqssam, about 20km west of Palmyra. Strong anomalies of V, Mo, Sr, F, P, Ca and to lesser degree As can also be found in this locality. The second U anomaly is centred at sample sites 11 and 9 situated 8km southwest of T.4 about 35km west of Palmyra. This anomaly is surrounded by weakly anomalous U halo, running along the western edge of Ad-Daww basin and including sample sites 22, 21 and 1. These two anomalous U clusters are distinctly separated by a group of background waters trending northeast-southwest coincident with the position of a rise in the pre-Neogene impervious base which has been detected by gravity measurements (Agha, 1976). It appears that U and its associated elements have accumulated in partially separated basins to the west and east of this uplift (Fig. 7.21 and Fig. 7.22).

The fate of U in these two anomalous areas seems to be of interest. That is because observed changes in colour of the Neogene sandstone from red to green could reflect reduction of Fe^{3+} to Fe^{2+}, thereby emphasizing the potential for a possible reaction of the U enriched solution with a reducing component. This might result in restricting its further movement and perhaps yielding some U accumulations. In this respect, the persistent association of U, V, Mo, Se, As, Sr and S in the anomalous areas can also be accounted for largely by reduction of the oxidizing solutions carrying these elements. In addition, the presence in the same area

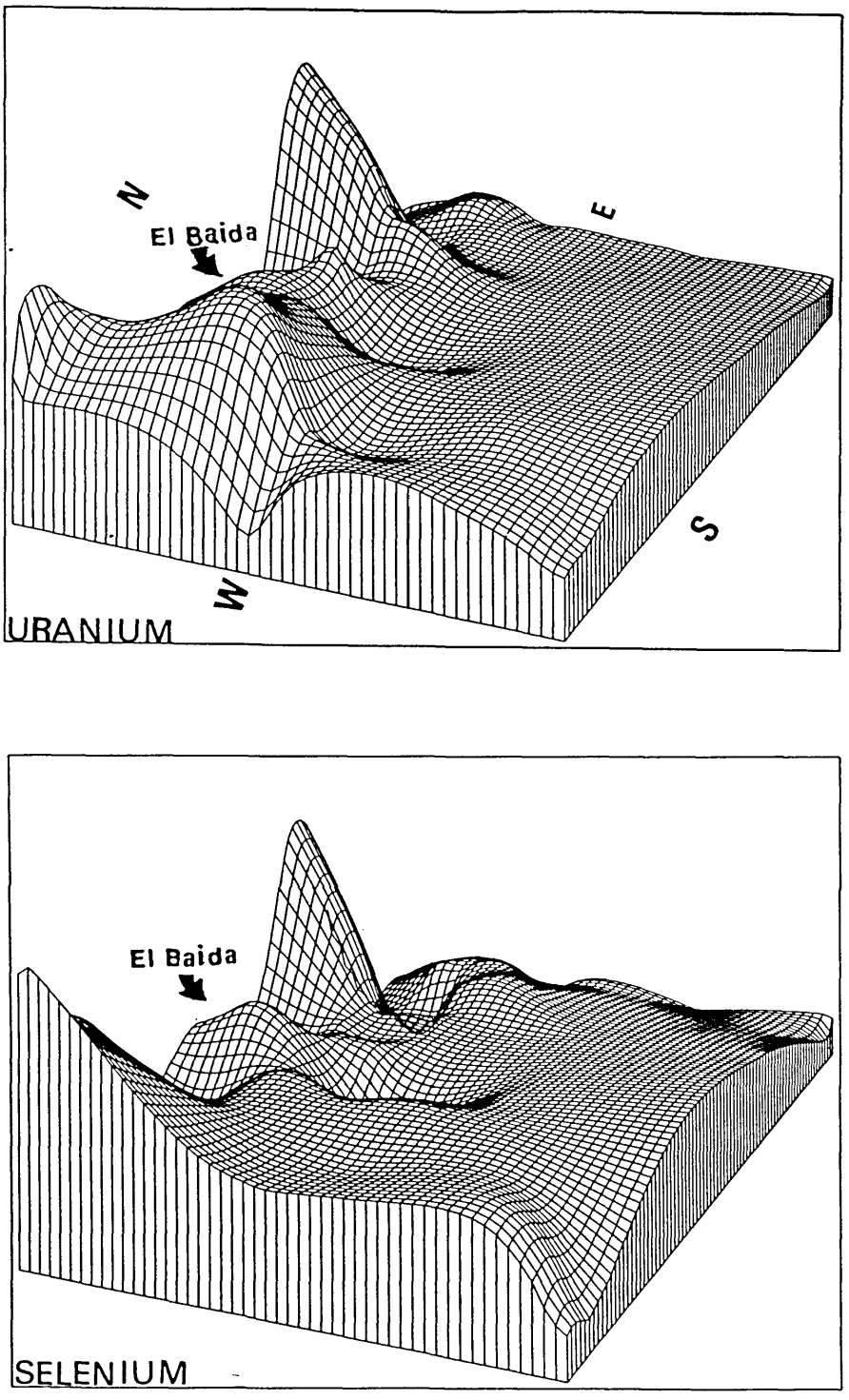


Fig.7.21 Solid surface distribution of U and Se in the Palmyrides hydrogeochemistry.

SELENIUM

URANIUM

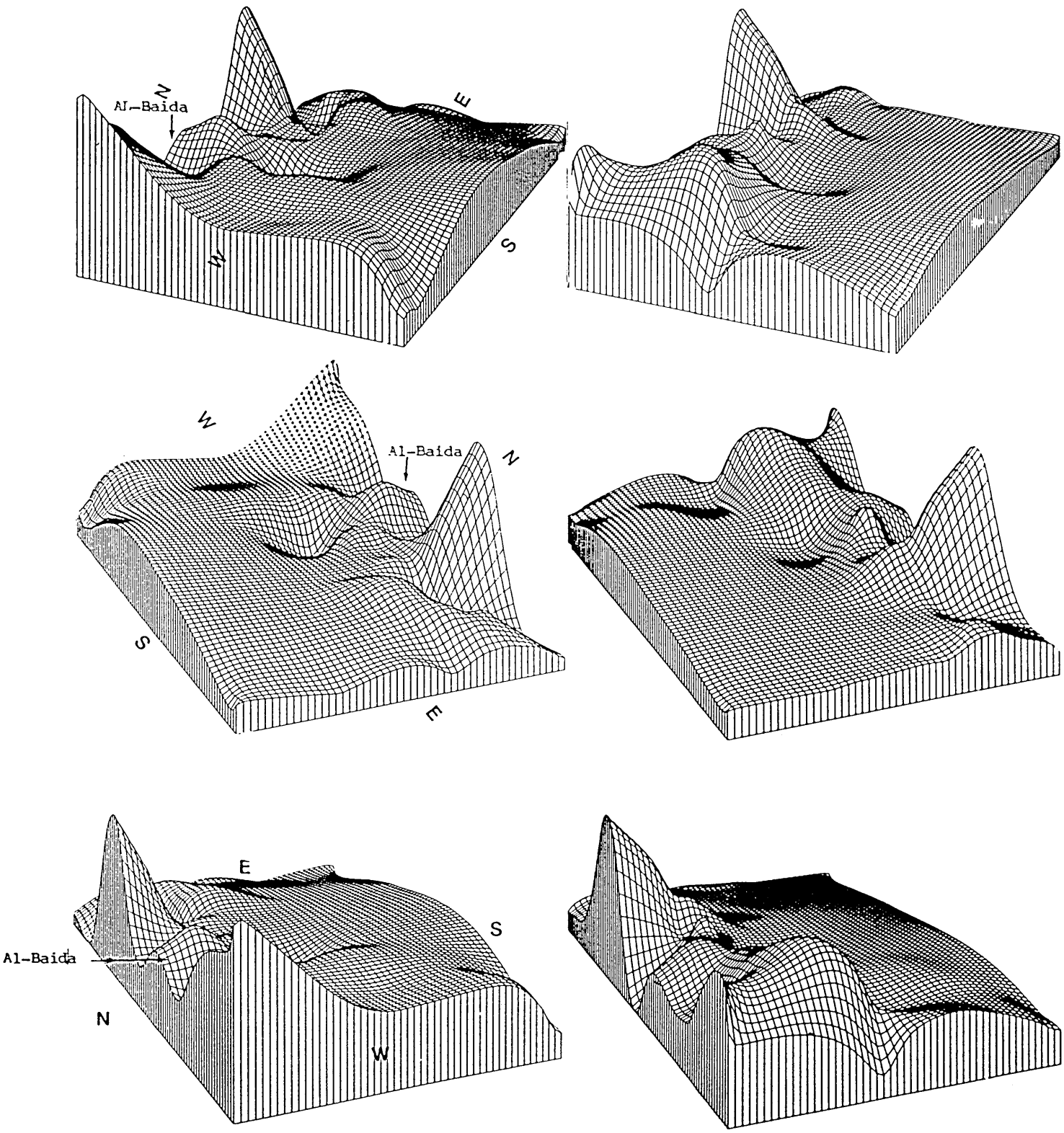


Fig.7.21 Solid surface distribution of U and Se in the Palmyrides hydrogeochemistry.

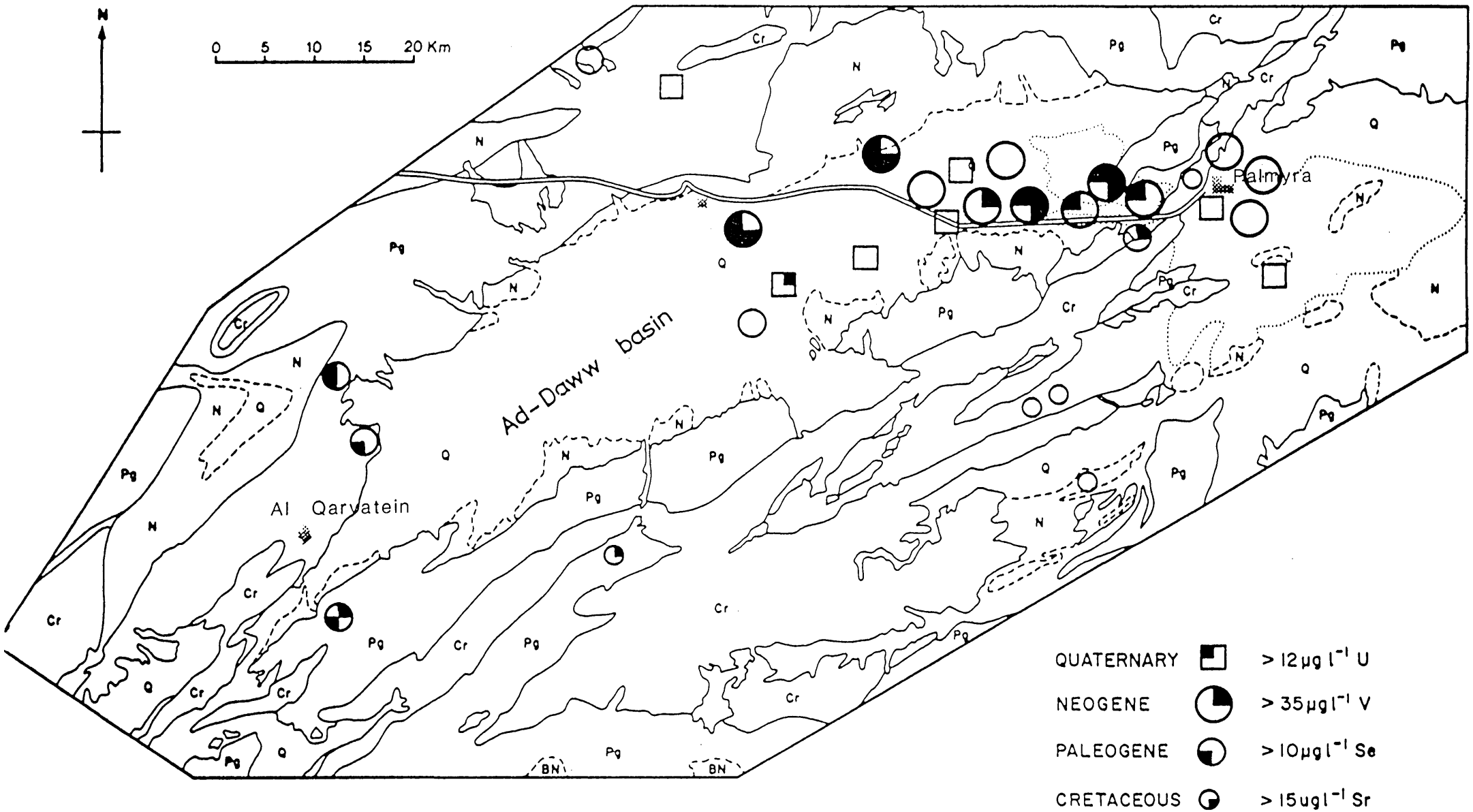


Fig.7.22 Areal distribution of U, V Se and Sr anomalies in the Palmyrides.

of both anomalous U and V is thought to be responsible for the widespread (although always minor) occurrences of secondary urano-vanadate minerals. However, this further suggests that these mineral occurrences (carnotite, tyuyamunite and meta-lyuyammunite) may be associated with locally reducing environments (Nach et al., 1981) or that the groundwaters became saturated with respect to saturation indices of the mineral concerned. The incorporation of K in the formation and precipitation of the mineral carnotite $[K_2(VO_4)_2(UO_2)_2.3H_2O]$ might account for the observed low levels of K content in the Palmyrides groundwaters. Thus variations in the concentrations of K, V, U and to lesser degree Ca require careful consideration.

It is worth noting here that the absence of autunite suggests the possible complexing of uranyl ions by vanadate rather than by phosphate. The notable association of U and Sr in the Palmyrides environment which was mirrored in the U mineralogy and wadi sediment geochemistry (Hale and Jubeli, 1985) has not been reported as such elsewhere. Nevertheless, Barbier et al. (1980) recorded during their sulphur isotope work in the uraniferous calcretes of Somalia that Sr is present in the calcrete as celestite (and not as carbonate). Therefore, the similar association of the two elements (U and Sr) observed in the present work may reflect the possible formation (at the present time) of uraniferous calcrete.

In the pH range that was found in the region, V, Sr and maybe F, being mobile and abundant in the phosphate and carbonate domains, are possible indicator elements (Deering et al., 1983). The potential use of other elements such as Mo, Se and As is

feasible although other workers (Langmuir and Chatham, 1980) reported that they are less useful than U and V which, according to them, offer the same general information as the saturation indices of the most common U minerals in the oxidizing groundwaters.

7.7 Model of U enrichment

Based on the foregoing results and discussion, a model to explain these accumulations of U is illustrated in Fig. 7.23. The model emphasize the role of a possible Jurassic diapiric evaporite dome forming during Upper Palaeogene times, perhaps rising until recent times, causing unconformity between the permeable Neogene sediments and the less permeable Palaeogene series.

From Chapter III, it is inferred that the interaction between physical and chemical weathering has controlled the fragmentation, disaggregation and comminution of the outcropping rocks in the region. Thus cones of debris of carbonate rocks as well as fragments of phosphorites and clayey limestones enriched in U and its associated elements have accumulated. This has promoted reaction between the falling rain and the rock debris, causing breaking of the chemical bonds and disordering the crystal lattices. Additional reactions with running water might occur along the transport path. The predominant carbonate rocks of the region have produced carbonate complexes and alkaline waters which promote the mobilization of U from its source rocks by increasing its solubility (Cathelineau, 1985; Dyck, 1974). The efficiency of the leaching procedure increases with time and reducing fragment size. Migration of the leachate into the groundwater took place

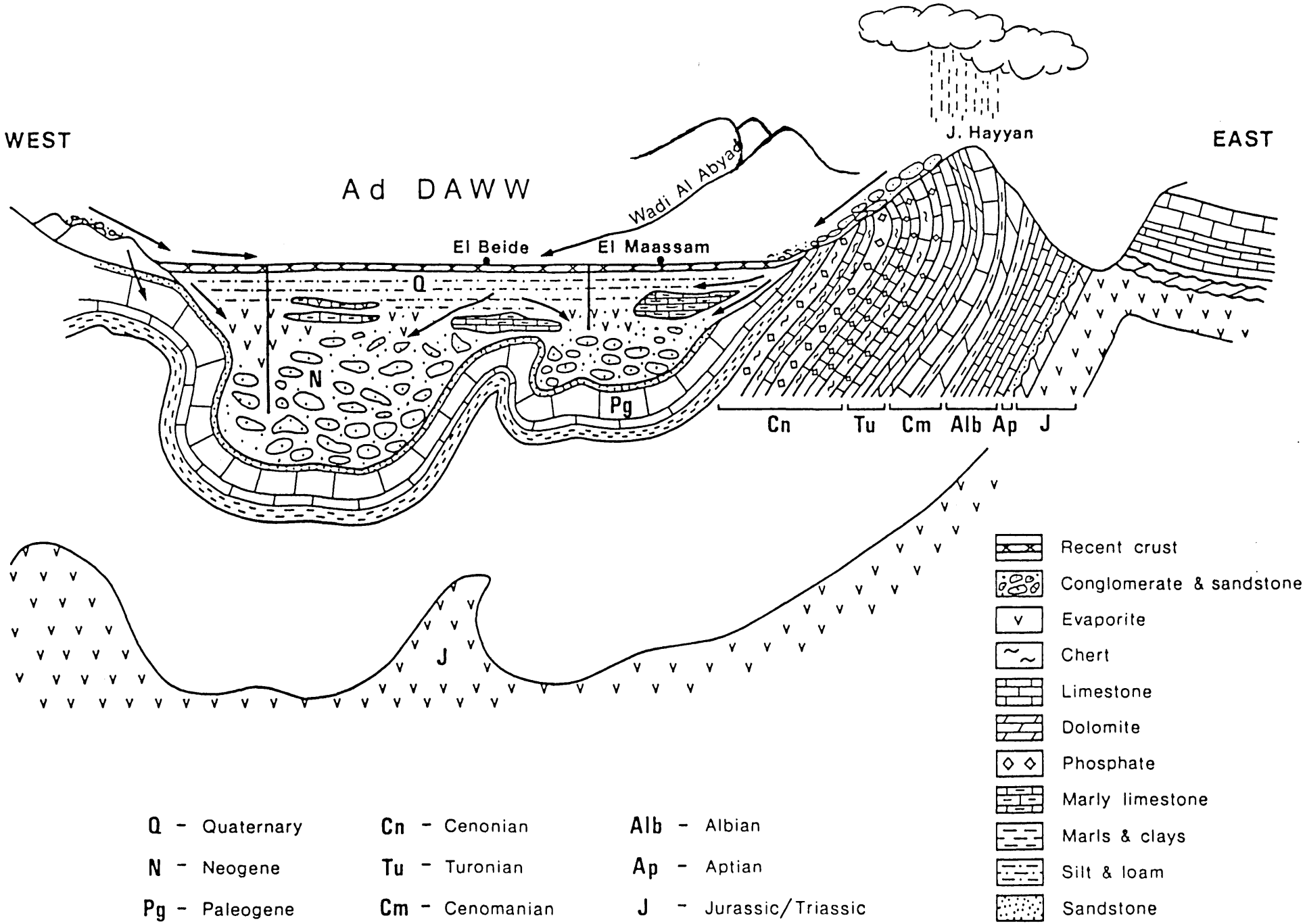


Fig.7.23 An explanatory model of U enrichment in the Neogene-Quaternary aquifer of the region.

through the permeable cover, and fissures.

For the resultant soluble elements, two possible behavioural pathways can be suggested.

1) In the absence of suitable reductants or absorbents, U and its associated elements may remain soluble in these carbonate-rich alkaline groundwaters as complexes, such as UO_2^{2+}, VO_2^{+}, $H_2VO_4^{-}$, $H_2VO_4^{2-}$, MoO_4^{2-} and Se^{5+} or Se^{4+}. These species would not be prone to precipitation or adsorption in the sediments with which they came into contact (Cameron and Hornbrook, 1975; Naurice, 1977; Langmuir, 1978). While this would maintain U concentrations in solution in the groundwaters, this U may be dissipated and diluted along the flow system, such that its ultimate dispersion is only of geochemical and not economic interest.

2) The second possibilty depends on the structure and geometry of the post Palaeogene aquifers, especially that of the Neogene which shows significant U enrichment. Here, in the two partially separated zones (caused by the said topographic rise of the impervious Palaeogene base), groundwaters tend to stagnate, leading to zones of restricted oxidation. This in turn may cause enrichment and possible precipitation of U, V, Mo, Sr, As and Se. As can be seen from Fig. 22, the presence of calcium sulphate (gypsum) and other carbonaceous and clay-cemented rocks in the Neogene could contribute to establishing locally reduced environments. The most probable reducing agent in this

environment is H_2S, generated by sulphate reducing bacteria. Eventually, this could cause U reduction, precipitation and accumulation near the unconformity or elsewhere in the Neogene sediments. This is further suggested by various field observations and indications of H_2S odour and sulphur precipitation, which are not lacking in the region (Technoexport, 1966). However, one must also consider that the flow system of the groundwater in this aquifer does not support multiple cycles of precipitation and dissolution; therefore, accumulation of significant quantities of precipitated U by repetition of this cycle is only a remote possibilty. Ultimately the significance of any U accumulations in terms of size is doubtful.

7.8 Conclusions

(1) - Although the sample site distribution and sample density of the groundwater survey were sub-optimal, the work showed that hydrogeochemistry is a useful approach in U exploration in this arid region and well water a suitable sample medium.

(2) - Multielement geochemical data proved advantageous in locating areas of interest and aided the interpretation of U results.

(3) - Uranium, V, Se, Mo, Sr and K are possible U indicators in the Palmyrides hydrogeochemistry.

(4) - The Neogene aquifer seems to be of particular importance with respect to U enrichment in the groundwaters.

(5) - Aquifer recharge is extremely limited under the present climatic conditions. Therefore, U and its associated elements

were, for the most part, leached into the groundwaters prior to the onset of aridity, although the current dispersions of these elements both hydrogeochemical and clastic suggests that there may be contemporary contributions.

Chapter VIII

8. Geochemistry of Sabkhet El Mouh (Playa Sediments)

8.1 Introduction

The discovery by Jones (1970) of an economic U deposit in playa lake sediments, and the discovery of the Yeelirrie U deposit in Australia in 1972, has focused exploratory attention on the playa environments (Mann, 1979; Butt, 1984; Briot and Fuchs, 1984).

In a review of the term playa, Reeves (1968) used it to refer to intermittently flooded low area of a basin, with no climatic or genetic restriction implied. Shearman (1978), however, used the Arabic word sabkha to describe flat salt-crusted deserts which occur either inland far away from the sea (continental sabkha) or along the coast in semi-arid and arid parts of the world (coastal sabkha). According to Shearman, the distinction between the two is that the groundwaters appear to be essentially terrestrial in the inland sabkha and are largely marine-derived in the coastal type. With respect to surficial U-deposits, Toens and Hambleton-Jones (1984) referred to the term playa as flat and generally barren portions of arid basins of usually internal drainage that periodically floods and accumulates detrital and/or evaporitic sediments. They classified the playas into three types.

Type 1.Circular topographically controlled playas with fairly steep sides having floors well below the regional elevation.

Type 2. Elongated playas coinciding with palaeo- or choked-drainage channels in which the conditions can be either oxidising or reducing.

Type 3. Floor playas, which are large and irregular in size and are usually not significantly depressed below the surroundings.

Anomalous radioactivity is well known in lacustrine sediments deposited in these closed basins, and U mineralized occurrences are widely distributed in the playas of Australia (Butt and Mann, 1984; Gamble, 1984); South Africa (Richards, 1975; Levin, 1978); Europe (Bowie et al., 1973; Ziegler, 1984); North Africa (Briot, 1984; Mokaddem and Fuchs, 1984), throughout the western United States (Carlisle, 1980; Otton, 1984) and Canada (Culbert et al., 1984). The possibility that uraniferous deposits are associated with saline waters and sabkha processes was suggested by Reeves (1978) and Benson and Leach (1979).

However, the use of playa sediments for mineral explorations in general and U exploration in particular is still in its infancy (Boyle, 1984; Pagel, 1984). A geochemical investigation of U in the playa sediments was reported by Leach et al. (1980), who summarized the conditions that would make some playas more favourable than others for the accumulation of U as follows:

(1) the presence of precursor carbonate-rich saline lakes;

(2) nearby uranium-rich source rocks;

(3) restricted groundwater discharge into the playa;

(4) localized precipitation mechanisms or phases in the playa;

(5) large drainage basin and adequate precipitation;

(6) stability of a hydrologically closed basin for a long period of time.

Farrell (1984), using the coarse loam fraction of the playa sediments, concluded that, although this sampling medium is not a panacea, it is one for consideration in an integrated exploration programme in the arid landscape.

Considering the foregoing cases it was felt that the geochemical environment of sabkhat El Mouh seems to fulfil most of the above mentioned conditions. Therefore, the present playa sediment geochemical reconnaissance was carried out in the region.

8.2 Objectives of the playa Geochemistry

The aims of conducting this investigation are:

(1) to establish primary information about the general level of abundance of U and other elements measured in the sediment;

(2) to pinpoint the major controls on the dispersion pattern of these elements, particularly what controls U dispersion within the sabkha;

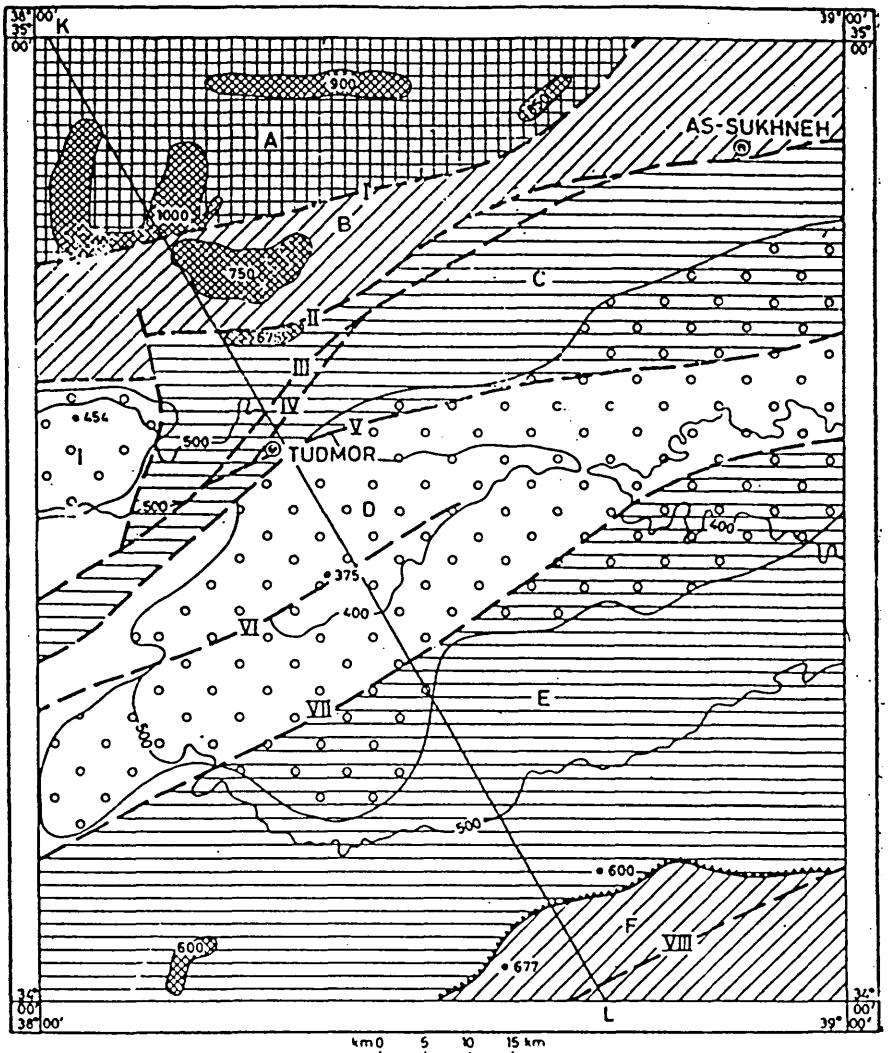
(3) to shed some light on the applicability of this sampling median for uranium exploration in the region.

8.3 Description of the area

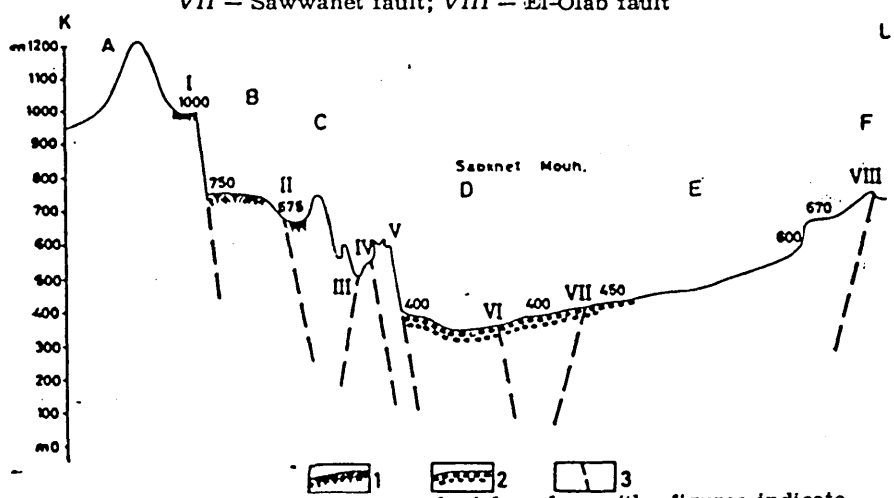
The studied area lies approximately between 38°06' and 38°40' East and between 34°25' and 34°36' North. Palmyra town occupies the extreme northwestern corner of the Sabkha, which extends tens of kilometers eastwards and southwards. The whole area is situated in a tectonic trough and bounded in the south by the northwesterly trending Sawwaneh fault. Depression of the basin floor and elevation of the surrounding mountains and plateaux indicates that tectonic activities began in the area in Neogene times and are still evolving at present (Fig. 8.1).

Waters that drained into the sabkha formed a lake during the pluvial period of the Pleistocene, which filled with lacustrine deposits derived from the active denudation of the surrounding rocks. At present, the sabkha receives runoff waters from the northern and northwestern slopes by two major wadis (W. Thaniyet Arak and W. Az zouqaq) in addition to other secondary ones. The southern and southwestern slopes receive waters also via a few main wadis (W. Qasser El Hallabat, W. Lewizeh, W. Habashi and W. Tlool Halwoush). Normally pools of both runoff and groundwater occupy much of the central part (except in the case of a succession of drought seasons). Small saline pools occur throughout the dry part of the sabkha, and some of these have been commercially exploited on a small scale for their salts, the source of which is surface and interstitial waters (see Plate 6).

The surface of the sabkha supports no vegetation, while the neighbouring piedmont alluvial fans are covered by a sparse growth



1 — the most uplifted step (block *A*) with absolute elevations of the ancient Pleistocene surfaces of 850-1000 m; *2* — steps (blocks *B, F*) with absolute elevations of ancient Pleistocene surfaces of 670-750 m; *3* — steps (blocks *C, E*) with absolute elevations of ancient Pleistocene surfaces of 500-675 m; *4* — steps (blocks *D, I*) with absolute elevations of Pliocene surfaces of 375-500 m; *5* — relics of proluvial Lower Pleistocene deposits; *6* — areas of the present-day distribution of lacustrine-continental Pliocene deposits; *7* — main tectonic sutures; *8* — scarp; *9* — direction of the schematic profile (Fig. 29). *I* — Matnet fault system; *II* — As-Safra fault; *III* — system of faults of the northern slope of El-Mazar; *IV* — As-Satih system of faults; *V* — Arak system of faults; *VI* — El-Abtar fault; *VII* — Sawwanet fault; *VIII* — El-Olab fault



1 — relics of ancient Quaternary proluvial surfaces (the figures indicate absolute elevation in metres); *2* — Pliocene surfaces of the basins (the figures indicate absolute elevation in metres); *3* — main tectonic sutures; *A* — *F* — main tectonic steps (blocks), forming the modern structure

Fig.8.1 Schematic diagram and profile of Sabkhet El Mouh.

of plants typical of desert terrains. A small oasis is found in one of the hills situated within the sabkha and projects 8 to 10m above its surface. On the extreme northwestern corner, cultivated land and palm trees can be found, especially in the vicinity of Palmyra (see Plate 4). The sabkha margin supports the most salt-tolerant halophytic shrubs, forming a distinct border and marking the change to sandy, less saline overburden. Moving east and southeastward the sabkha grades into a stony desert without any marked break in topography.

8.4 Sampling and Geology

8.4.1 Sampling

Sampling of the playa sediments was carried out on a grid, as discussed in Chapter IV. Lines approximately 12km long, 2km apart sampled at intervals of 2km gave a density of one sample per $4km^2$. A total of 72 playa sediments was collected in this survey. The sediments are a complex interbedded mixture of loam, sandyloam, silt, clays, organic matter, gypsum and other evaporites, particularly halite and mixed salts. Field inspection of the sediments indicates changeable surface conditions (shifts in salinity, CO_2, temperature and other factors). This has led to mineralogically heterogeneous layers (see Plate 6). Very many episodes of fluctuations during depositional periods can be traced, which could help in reconstructing the geochemical environment that prevailed during sabkha formation; a mixture of both clastic and chemical precipitation components occurs all over the area.

8.4.2 Geology

Sabkhet El Mouh consists of several beds of flat-lying Neogene and Quaternary alluvial and lacustrine sediments that underlie the dry surface. Along the northern and western sides Mesozoic and Tertiary rocks outcrop. They are represented by rocks of the late Cretaceous (mainly limestones, phosphorites, chert and dolomites) overlain by the Palaeogene series of marls, glauconitic limestones, chalky limestone, carbonates and sandstones. The southern edge is bounded by low hills and plateaux of Neogene sandstones, conglomerates and micritic lacustrine limestones which are covered with Quaternary sands, conglomerates and clays. A ridge of Upper Cretaceous and Lower Palaeogene hills intrudes the midwestern side of the sabkha, while other smaller and isolated Neogene hills striking in a northeastward direction stand 10 to 20m higher than the present surface in more than one locality (Fig. 8.2).

Much of the dry surface is veneered by polygons of a mixture of surficial salts and clays (see Plates 4 and 6). Buried beneath the salt-crusted surface is a sequence of laminated brown to reddish clays and carbonated silts, sands, crystalline gypsum and debris of old alluvial fans and lacustrine deposits. The core of the sabkha is composed of Pliocene lacustrine formations whose thickness is estimated from the isopach-lithological maps to be 80m (Technoexport, 1966). Aeolian sands and debris are found on the periphery mainly along the eastern edge of the sabkha basin. The sands produces characteristic forms such as cumulose knolls, up to 2m high.

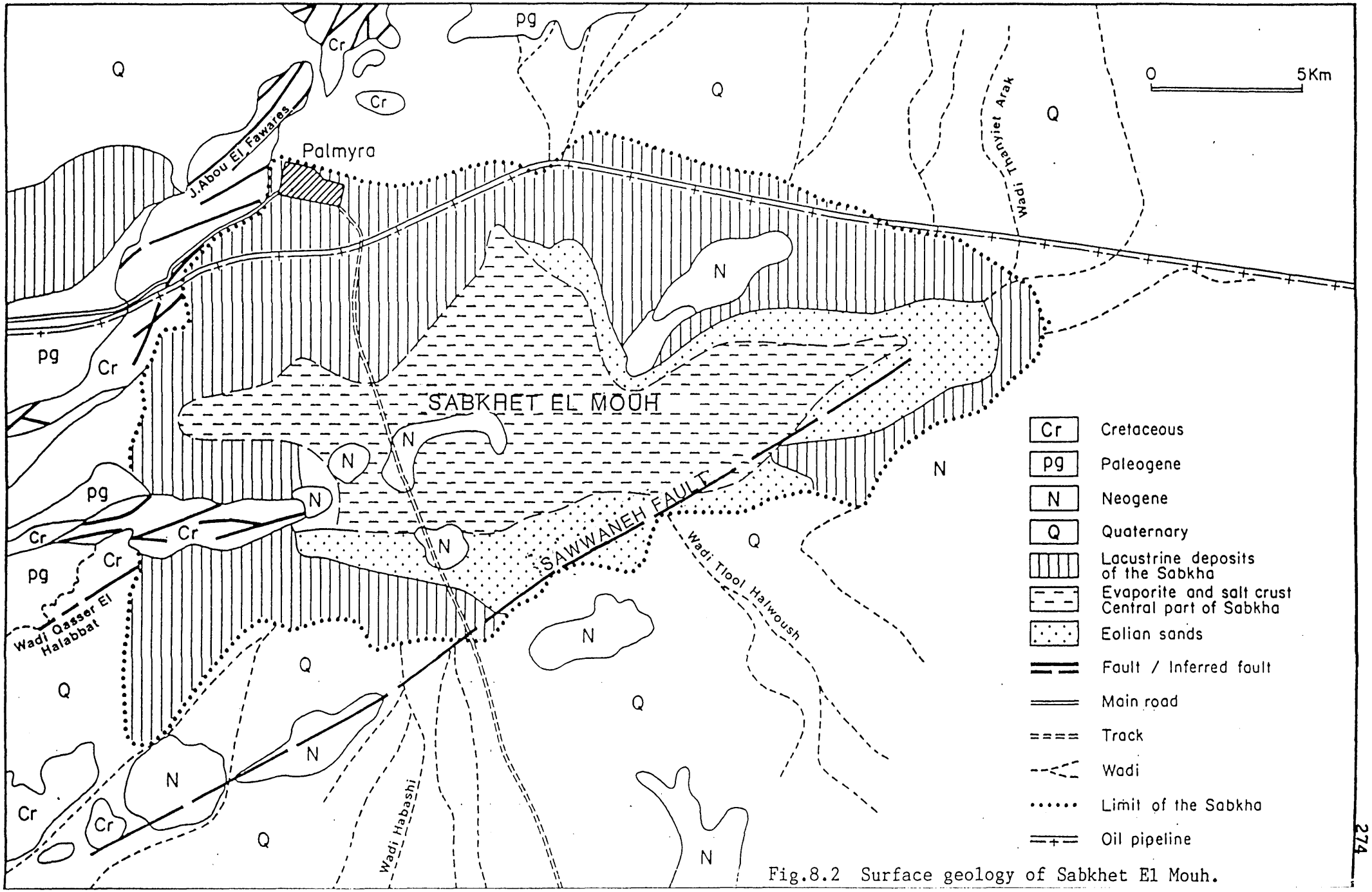


Fig.8.2 Surface geology of Sabkhet El Mouh.

8.5 Analysis and data control.

Because no playa sediments were included during the previous orientation work, a preliminary size fraction orientation was carried out using 25 out of the 72 collected playa samples. These samples were seived to obtain the following three fractions for analysis : 500-250 μm; 250-90 μm; and -90 μm. The data for U, major and trace elements showed that the finest size particles (-90 μm) contained the highest concentrations of elements (Fig. 8.3). It is worth noting that the -250 μm fractions constitutes 70 to 80% of the sample (which is not unexpected).

Inspection of the elemental abundance in 10 samples which were collected from four sample sites at three different depths (section 4.2.2) indicates that, in general, U, As and to a lesser degree Sr show a slight increase with depth. Vanadium and Mo contents are enhanced in the intermediate depth, P and Ti contents are highest at the surface while most other elements show little or no variation.

Multielement analysis of the 72 sediment samples was therefore carried out on the -90 μm fraction using as previously discussed NAA, ICPAES and AAS methods. Evaluation of the quality of the produced analytical data was based on reference control samples and duplicate analysis system (as described earlier). Precision (estimated at the 95% confidence level on the basis of duplicate determinations was better than 6% for major elements and better than 10% for other elements.

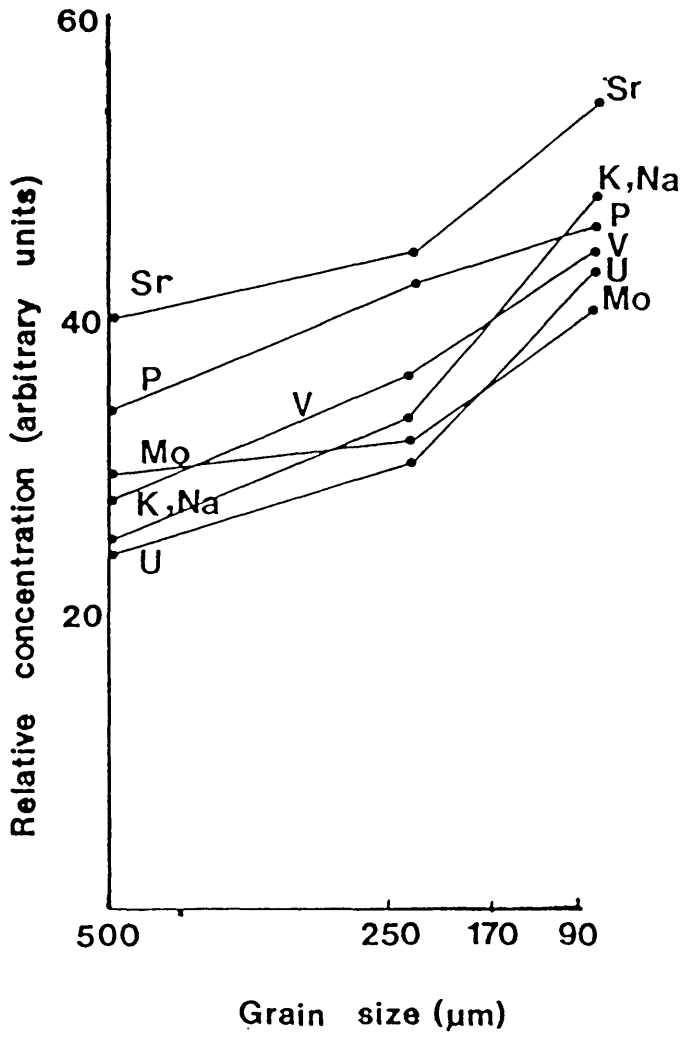


Fig.8.3 Relative concentrations of U, Sr, V, Na, K and P in different size fractions of the sabkha sediments.

8.6 Results, discussion and interpretation.

8.6.1 Element abundance

The statistical parameters of the determined elememts which were consistently above the detection limit are listed in Table 8.1 while the whole data is presented in Appendix 8.1. Relative to other sediments of the region (wadi sediments and overburden), playa sediments show generally higher Mg, Ti, Al, Fe, Rb and Li concentrations and the maximum Na (10.4%) and Sr (1.8%) and to a lesser degree K (1%) content in the region. The concentration levels of Ba, Mo, P and As are generally lower; the remaining elements show no marked differences.

Uranium concentrations range from 1 to 56.7 ppm with a median of 3.7 ppm which is nearly the same as the median U concentration in Winnemucca basin (3.9 ppm, in Leach et al., 1980) where U occurences are known. A nearly identical median was reported also by Leach et al. (1980) from Sevier Lake playa (3.8 ppm U) and Cave Valley playa (3.8 ppm U) which do not contain any known U occurences. This demonstrates the need to seek other factors rather than univariate statistics in order to assess whether or not the observed U concentrations may reflect mineralizations or U occurences. The maximum concentrations shown by other elements in sabkhet El Mouh are 115 ppm V, 100 ppm Zn, 79 ppm Li, 53 ppm Rb, 15 ppm Mo, 6.6 ppm As, 3 ppm Se, 88 ppm Cr, 600 ppm Ba, 700 ppm Mn, 2900 ppm P, 3500 ppm Ti, 3% Fe, 4.4% Al, 8.6% Mg and 22% Ca.

Table 8.1 Summary statistics of the sabkha geochemistry.

C.F.S	N =	72	MEAN =	118.79	ST.DEV. =	93.3
U	N =	72	MEAN =	6.6639	ST.DEV. =	7.49
AS	N =	72	MEAN =	3.7250	ST.DEV. =	1.09
SE	N =	72	MEAN =	.75417	ST.DEV. =	.458
P	N =	72	MEAN =	1606.0	ST.DEV. =	508.
ZN	N =	72	MEAN =	57.917	ST.DEV. =	20.6
LI	N =	72	MEAN =	28.838	ST.DEV. =	13.9
NA%	N =	72	MEAN =	2.2951	ST.DEV. =	2.10
K%	N =	72	MEAN =	.68371	ST.DEV. =	.238
MG%	N =	72	MEAN =	4.0607	ST.DEV. =	1.77
CA%	N =	72	MEAN =	8.6778	ST.DEV. =	5.19
SR	N =	72	MEAN =	2243.8	ST.DEV. =	3157.
BA	N =	72	MEAN =	207.88	ST.DEV. =	104.
AL%	N =	72	MEAN =	2.6503	ST.DEV. =	1.17
LA	N =	72	MEAN =	15.861	ST.DEV. =	5.87
TI	N =	72	MEAN =	2147.9	ST.DEV. =	813.
V	N =	72	MEAN =	61.322	ST.DEV. =	21.5
CR	N =	72	MEAN =	52.113	ST.DEV. =	17.9
MO	N =	72	MEAN =	8.5444	ST.DEV. =	2.19
MN	N =	72	MEAN =	332.03	ST.DEV. =	151.
FE%	N =	72	MEAN =	1.8522	ST.DEV. =	.734
CO	N =	72	MEAN =	12.588	ST.DEV. =	4.48
NI	N =	72	MEAN =	47.938	ST.DEV. =	17.1
RCU	N =	72	MEAN =	21.136	ST.DEV. =	6.64
RB	N =	72	MEAN =	16.991	ST.DEV. =	16.7
BE	N =	72	MEAN =	.87194	ST.DEV. =	.369
AG	N =	72	MEAN =	.12583	ST.DEV. =	.396
CD	N =	72	MEAN =	1.3268	ST.DEV. =	.570
PB	N =	72	MEAN =	14.285	ST.DEV. =	5.36

8.6.2 Single element frequency distribution

For each element a frequency histogram was constructed before and after log transformation of the geochemical data. An almost perfect normal (non transformed) distribution is shown by Mo, Mg, Cr, Cd, Mn, Zn, V, Ca, Li and to a lesser degree Ti and Al (Fig. 8.4). Whereas the radioactivity measurements expressed in counts per second (CPS) and the remaining elements including U seem to be log normally distributed. Figure (8.5) clearly shows a comparison between the log transformed and the raw (nontransformed) distribution of (CPS) and U as an example. Visual inspection of the U frequency distribution and its probability plot (Fig. 8.6) indicates that U data display a bimodal distribution in which two populations are separated by a threshold at about 10ppm. The lower one (63 samples) constitutes background values, while the upper population is relatively anomalous (9 samples). The concentrations of other elements such as Sr and K also show anomalous values (Fig. 8.7).

The bimodal distribution of U and perhaps Sr are probably a reflection of the heterogeneous nature of their source and/or occurrence within by different phases, especially in the case of Sr which shows much wider range (0.03 to 1.86%). One possible explanation is that a source rock rich in these two elements has contributed or been incorporated unevenly into the playa sediments (e.g. phosphorite fragments brought along the drainage channels), but even the highest Sr contents in the phosphorite of the region do not lend any support to the phosphorite choice. Therefore, the most likely alternative source (in this type of geochemical

V

MIDDLE OF INTERVAL	NUMBER OF OBSERVATIONS	
10.	1	*
20.	2	**
30.	8	********
40.	6	******
50.	9	*********
60.	7	*******
70.	16	****************
80.	13	*************
90.	8	********
100.	1	*
110.	0	
120.	1	*

MO

MIDDLE OF INTERVAL	NUMBER OF OBSERVATIONS	
4.	2	**
5.	3	***
6.	7	*******
7.	9	*********
8.	14	**************
9.	13	*************
10.	11	***********
11.	7	*******
12.	3	***
13.	2	**
14.	1	*

AS

MIDDLE OF INTERVAL	NUMBER OF OBSERVATIONS	
1.5	2	**
2.0	4	****
2.5	10	**********
3.0	9	*********
3.5	8	********
4.0	15	***************
4.5	11	***********
5.0	10	**********
5.5	1	*
6.0	1	*
6.5	1	*

MG

MIDDLE OF INTERVAL	NUMBER OF OBSERVATIONS	
0.	1	*
10000.	2	**
20000.	8	********
30000.	19	*******************
40000.	17	*****************
50000.	9	*********
60000.	6	******
70000.	7	*******
80000.	2	**
90000.	1	*

Fig.8.4 Histograms of V, Mo, As and Mg in the sabkha geochemistry.

U.PPM

MIDDLE OF INTERVAL	NUMBER OF OBSERVATIONS	
0.	8	********
5.	50	**********
10.	6	******
15.	3	***
20.	3	***
25.	1	*
30.	0	
35.	0	
40.	0	
45.	0	
50.	0	
55.	1	*

LOG U

MIDDLE OF INTERVAL	NUMBER OF OBSERVATIONS	
0.0	1	*
.2	2	**
.4	11	***********
.6	30	******************************
.8	16	****************
1.0	4	****
1.2	5	*****
1.4	2	**
1.6	0	
1.8	1	*

CPS

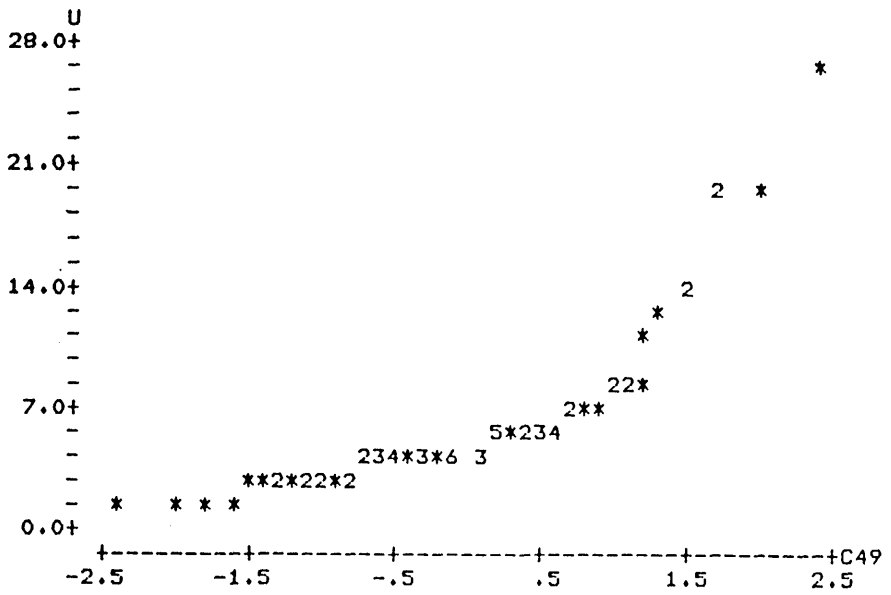
EACH * REPRESENTS 2 OBSERVATIONS

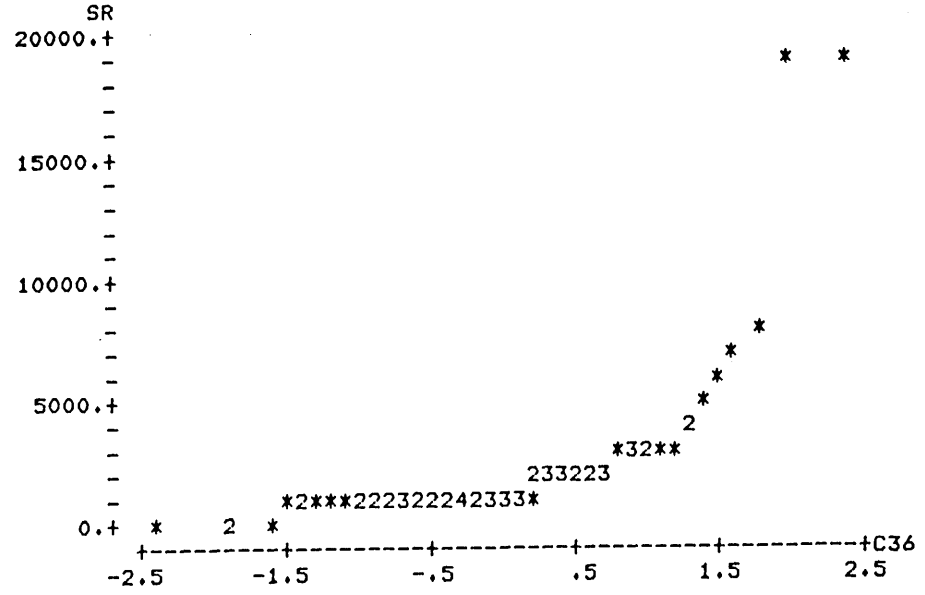
MIDDLE OF INTERVAL	NUMBER OF OBSERVATIONS	
0.	3	**
100.	62	**********
200.	3	**
300.	2	*
400.	1	*
500.	0	
600.	0	
700.	0	
800.	1	*

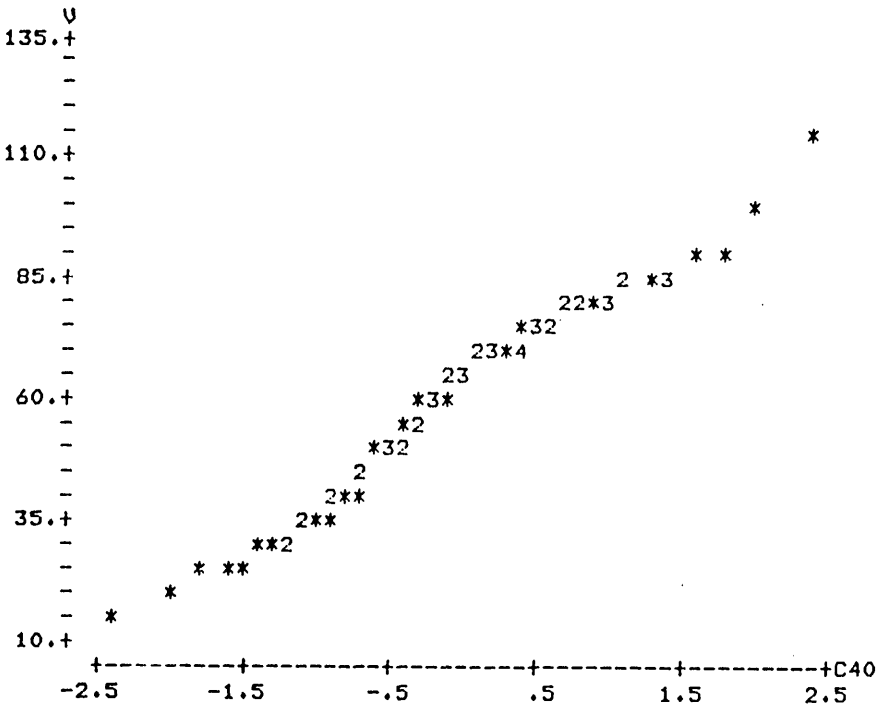
LOG CPS

MIDDLE OF INTERVAL	NUMBER OF OBSERVATIONS	
1.6	1	*
1.7	4	****
1.8	6	******
1.9	15	***************
2.0	21	**********
2.1	13	*************
2.2	6	******
2.3	2	**
2.4	2	**
2.5	0	
2.6	1	*
2.7	0	
2.8	0	
2.9	1	*

Fig.8.5 Histograms of U and CPS of the sabkha geochemistry.







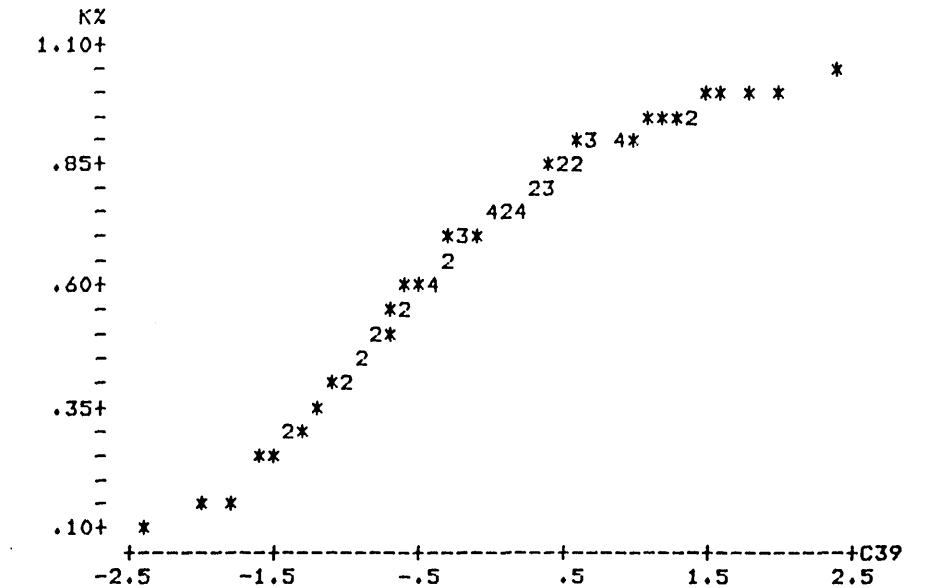


Fig.8.6 Normal probability plots showing bimodal distributions.

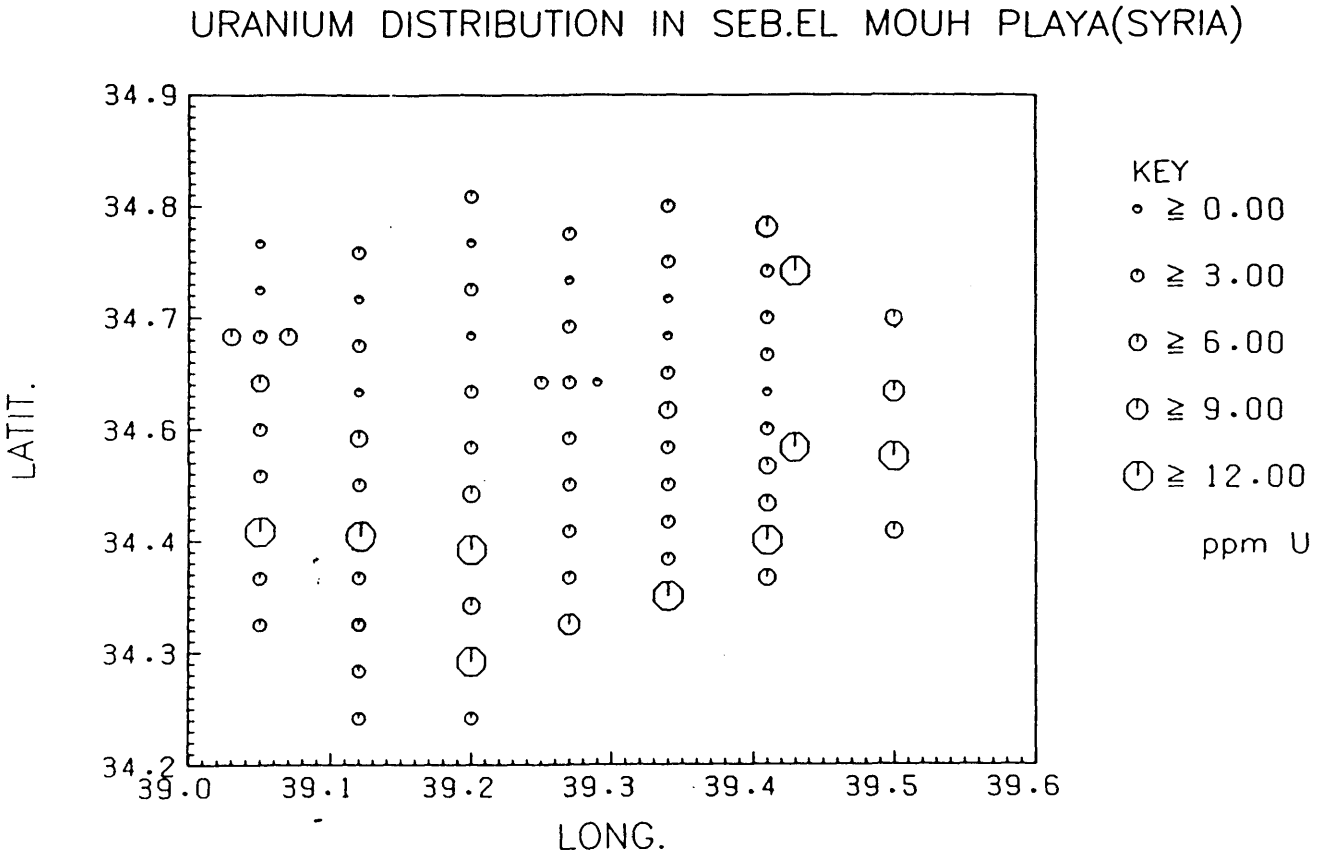
Fig.8.7 Normal probability plots of Sr and K showing

environment) could be the contribution of a calcrete component, the presence of which in some playa samples can explain the large standard deviations of Sr and U. Otton (1984) describing the surficial U deposits in the U.S.A. reported even wider ranges of 0.5 to 5% Sr and 27 to 450ppm U. He attributed that wide range of concentrations of both elements to the presence of dense calcrete or calcrete lenses which resulted from the interaction of the playa sediments with weakly saline groundwaters close to the surface rather from pedogenic processe alone.

Similar geochemical changes (but maybe on a smaller scale) within Sabkhet El Mouh sediments cannot be ruled out. Such processes might cause the noticeable large variations in the concentrations of U and Sr, and a greater attention must be given in future exploration to the area or areas with high Sr and U contents.

8.6.3. Spatial distribution of selected elements

Areal distributions of U, Sr, P, As, V, Mo, Mg, Ti, Fe and K are illustrated in Figs. 8.8 to 8.12. This simplistic approach shows that U anomalies are confined to two locations. The first consists of three samples situated near the western side of the Sabkha and spatially related to the elongated Cretaceous and Palaeogene hills which occur in that part of the sabkha; this perhaps may reflect a genetic relationship. The second is an anomaly of 7 samples trending from the southern edge towards the northeastern corner of the Sabkha, coinciding with the continuation of drainage channels (wadis) running parrallel or along the



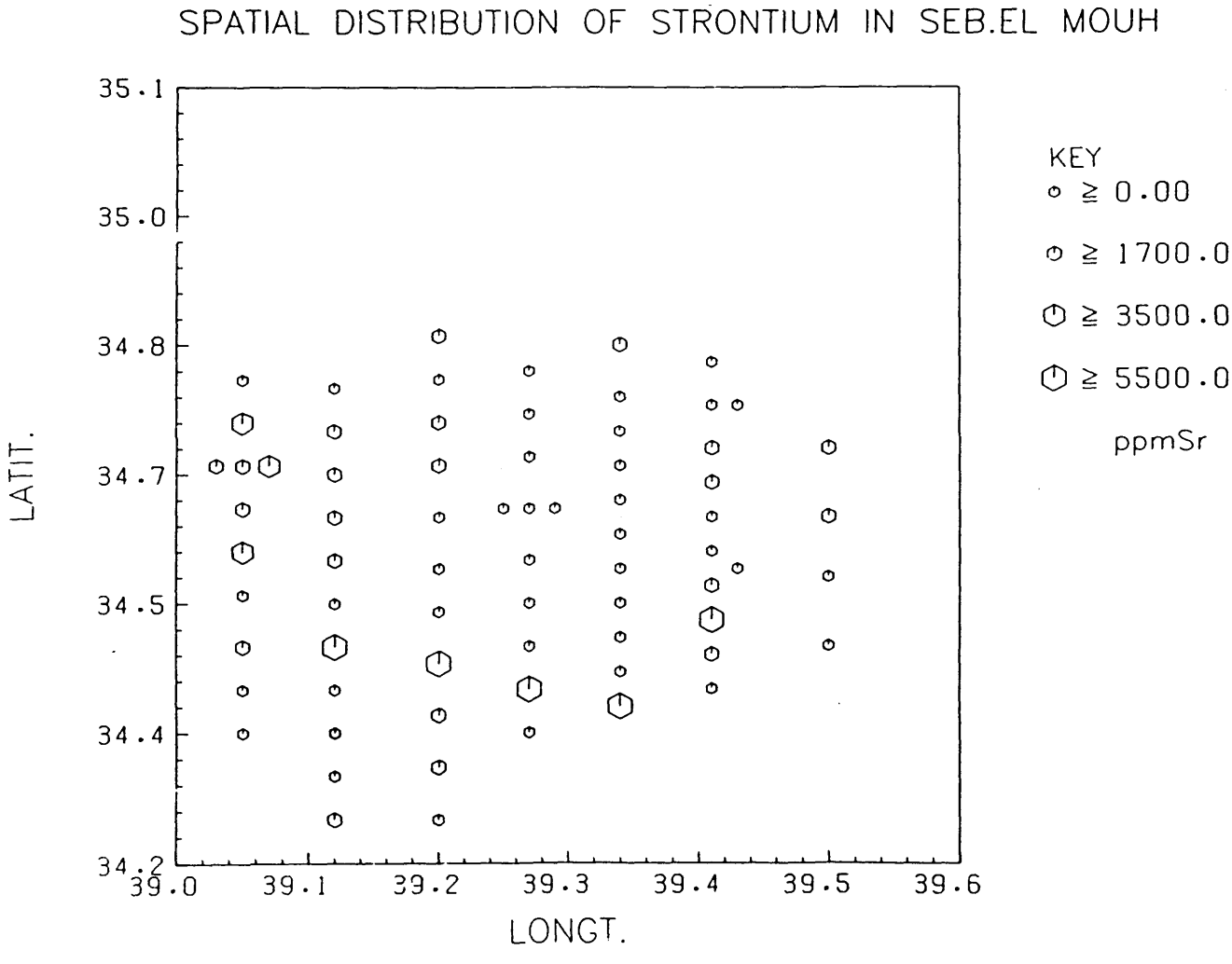
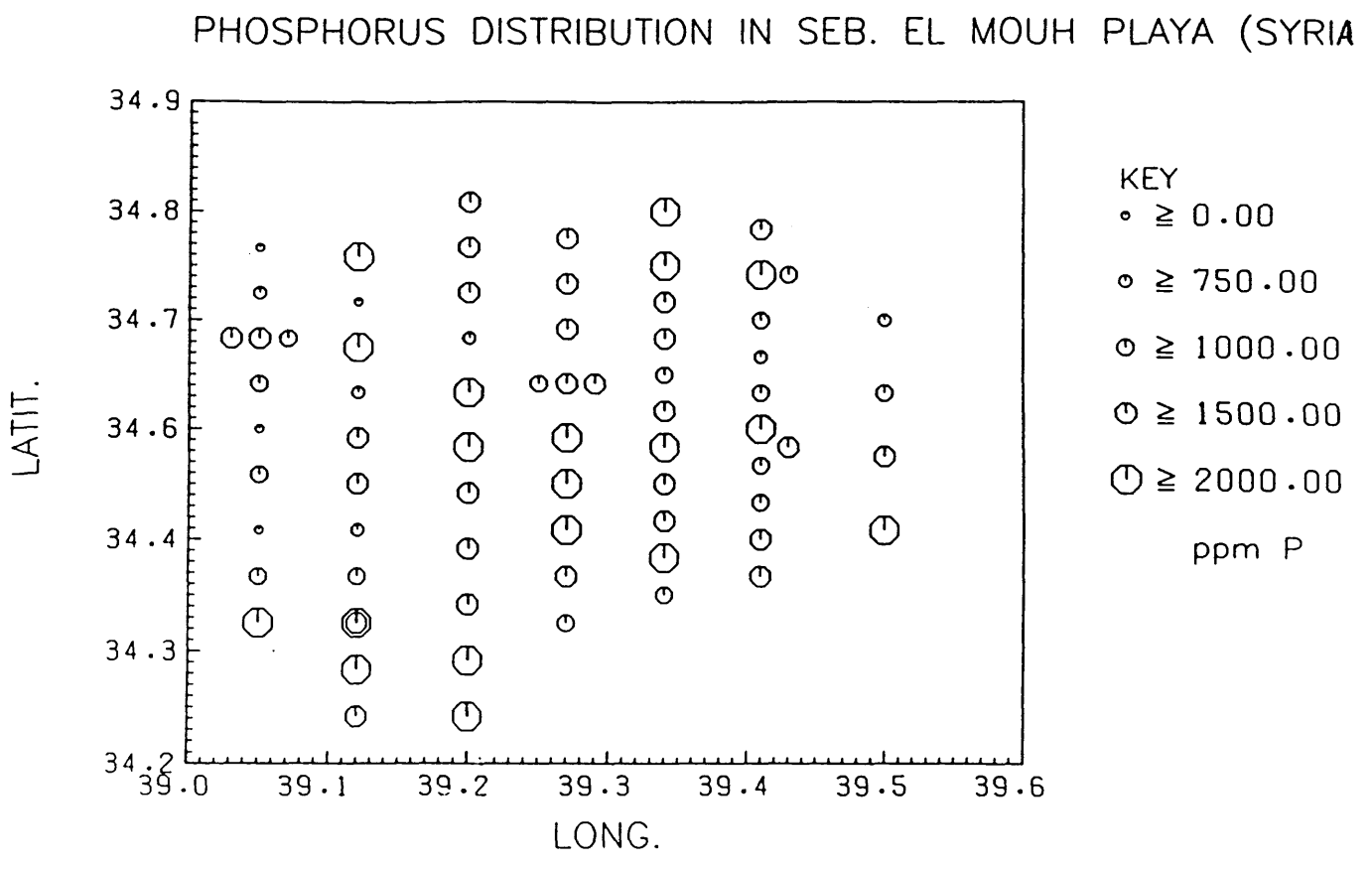


Fig.8.8 Symbolic areal distribution of U and Sr in the sabkha sediments.



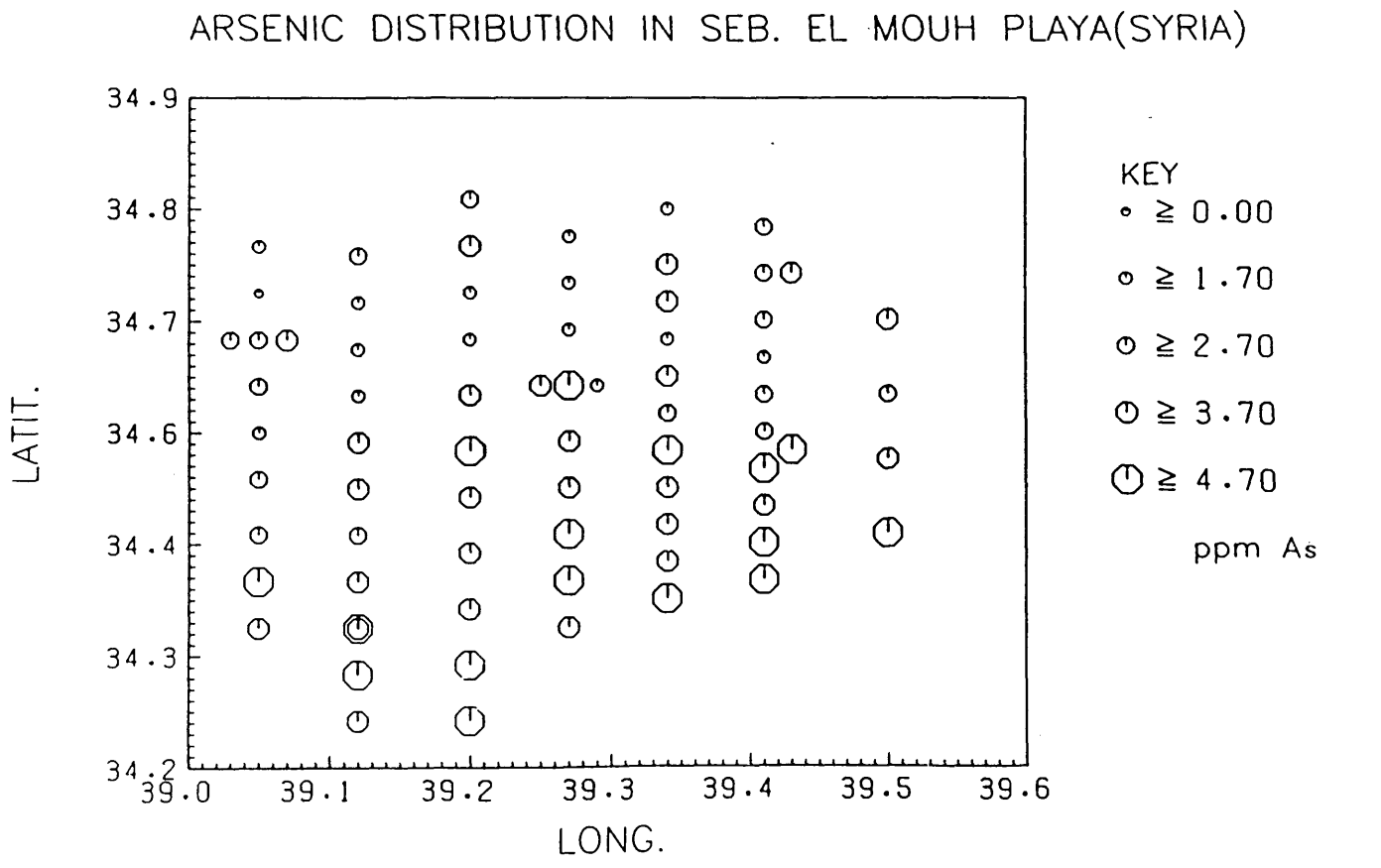
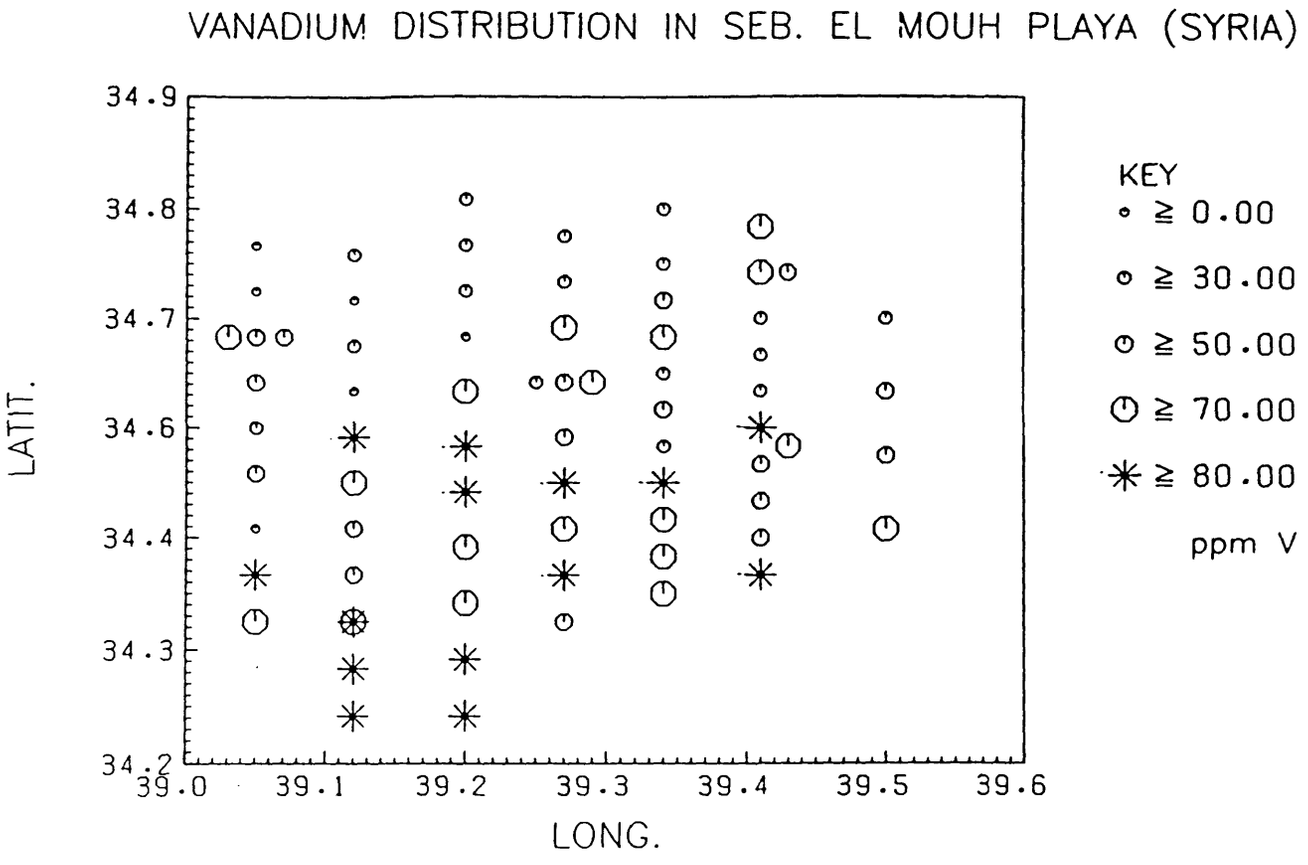


Fig.8.9 Symbolic areal distribution of P and As in the sabkha sediments.



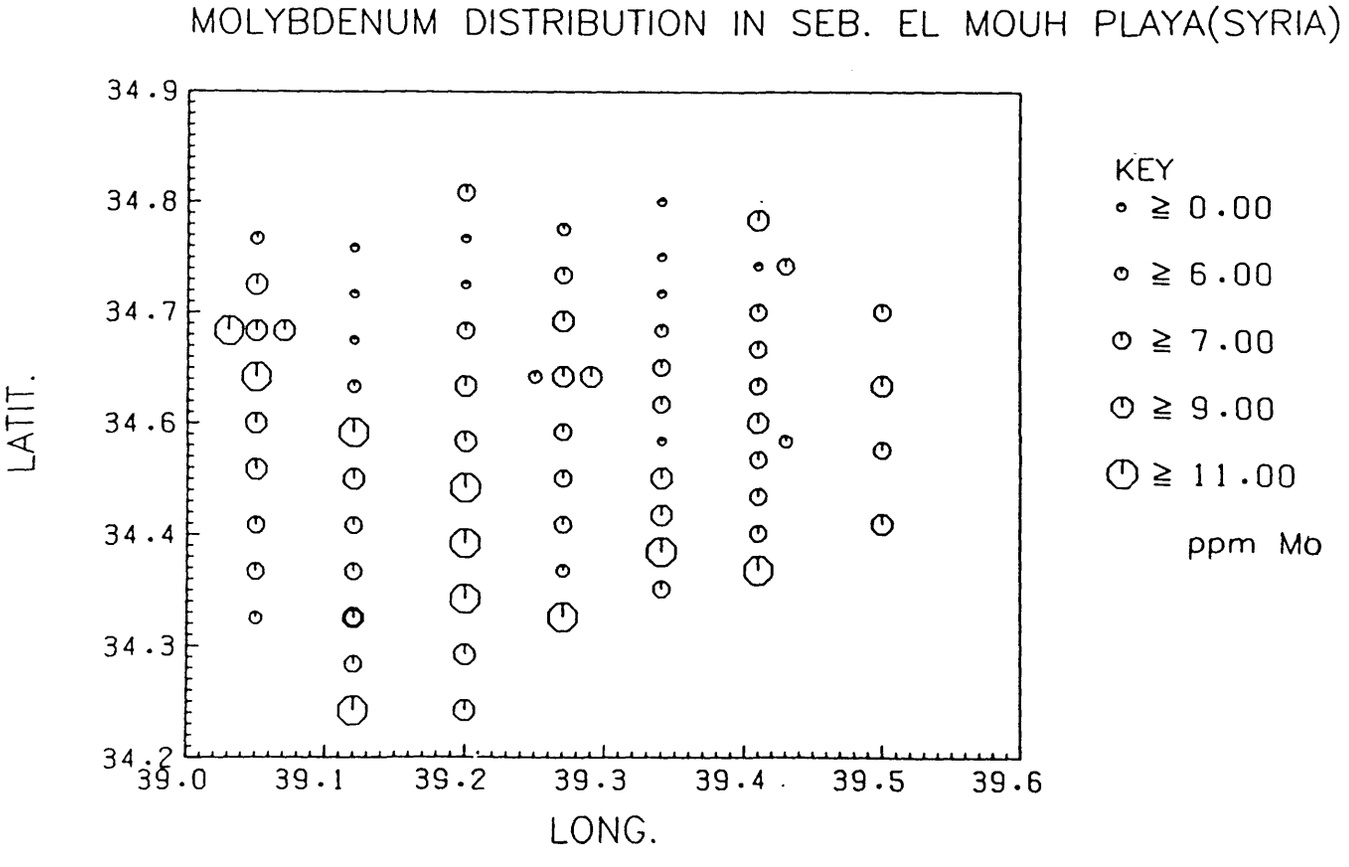
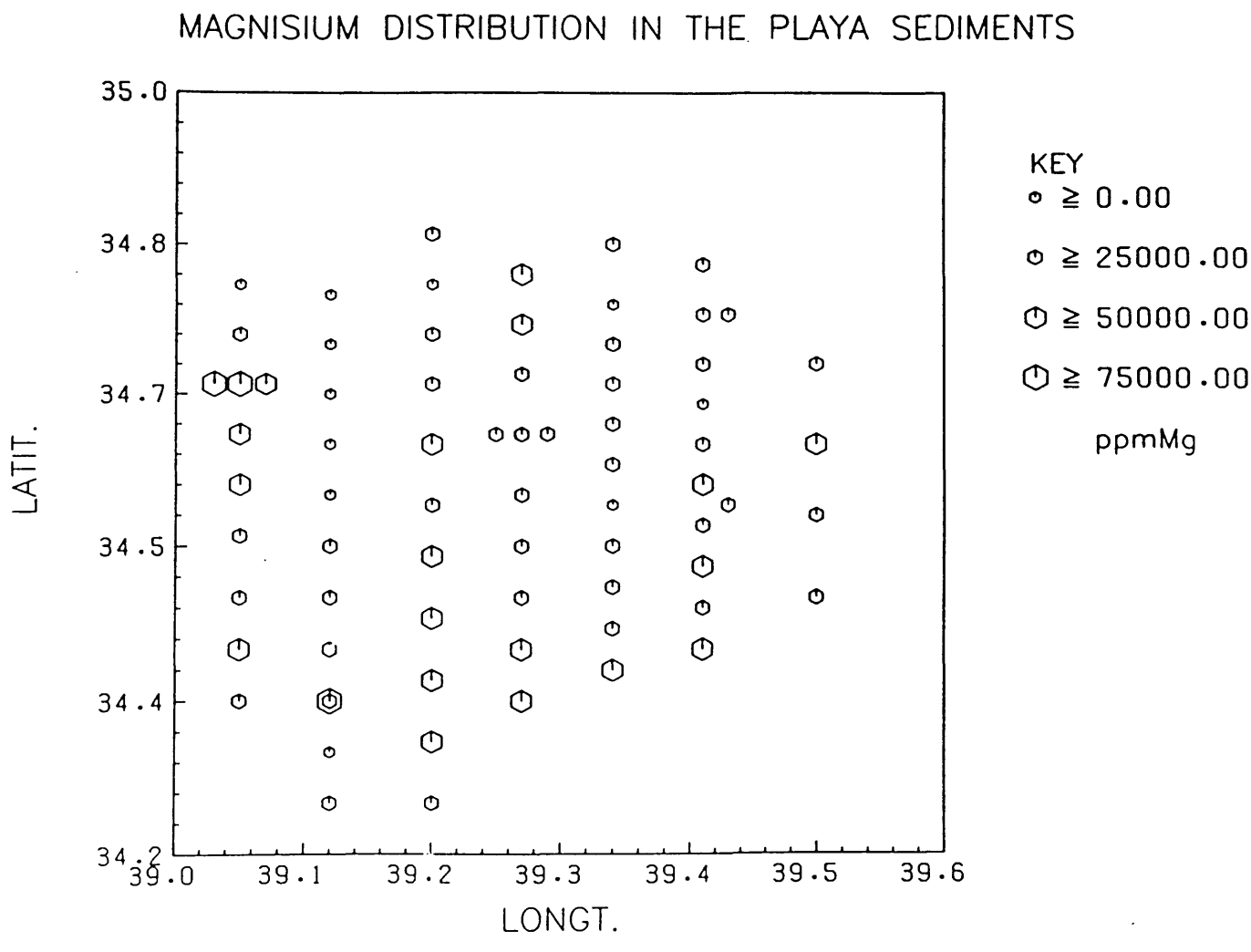


Fig.8.10 Symbolic areal distribution of V and Mo in the sabkha sediments.



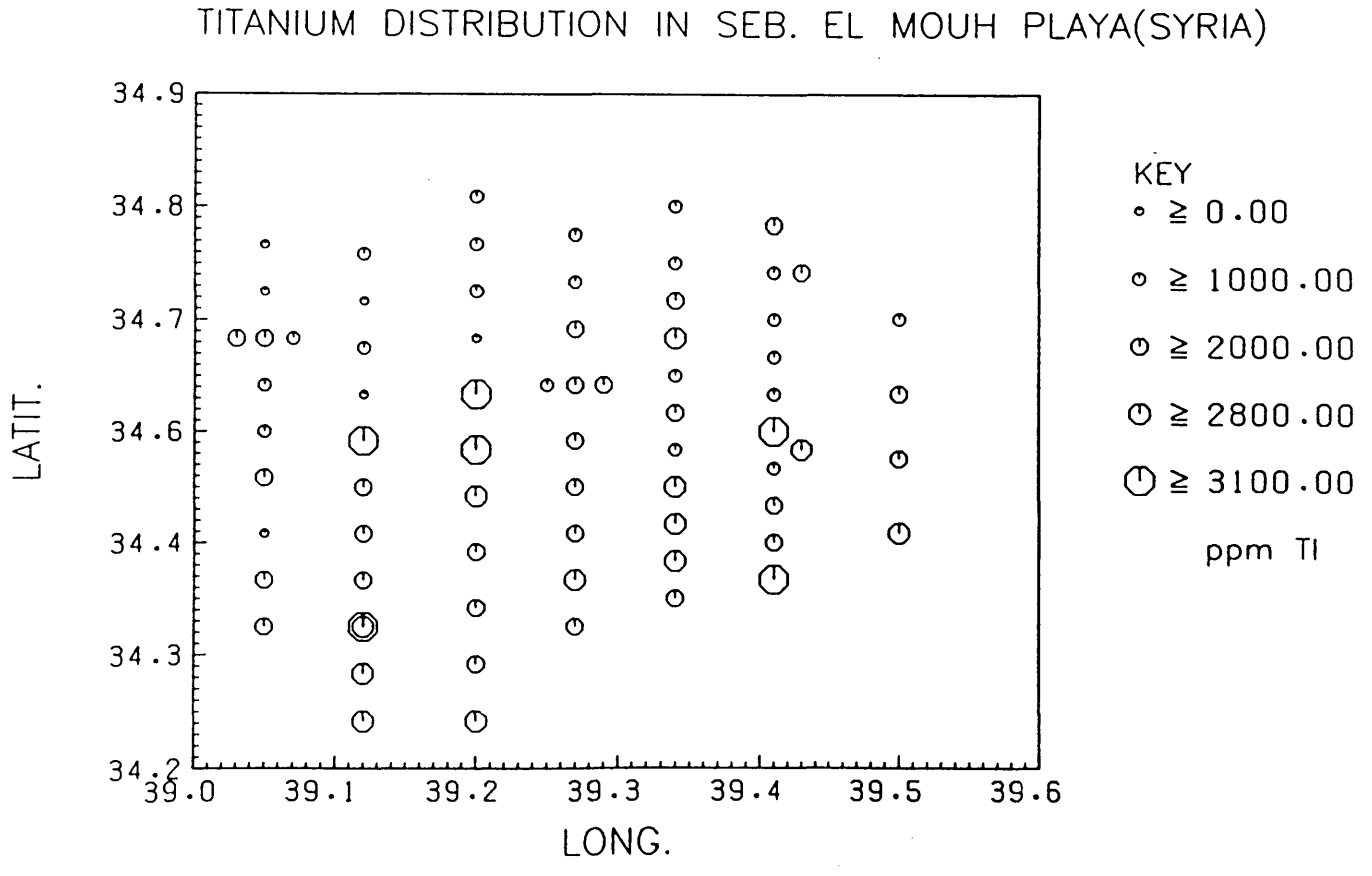
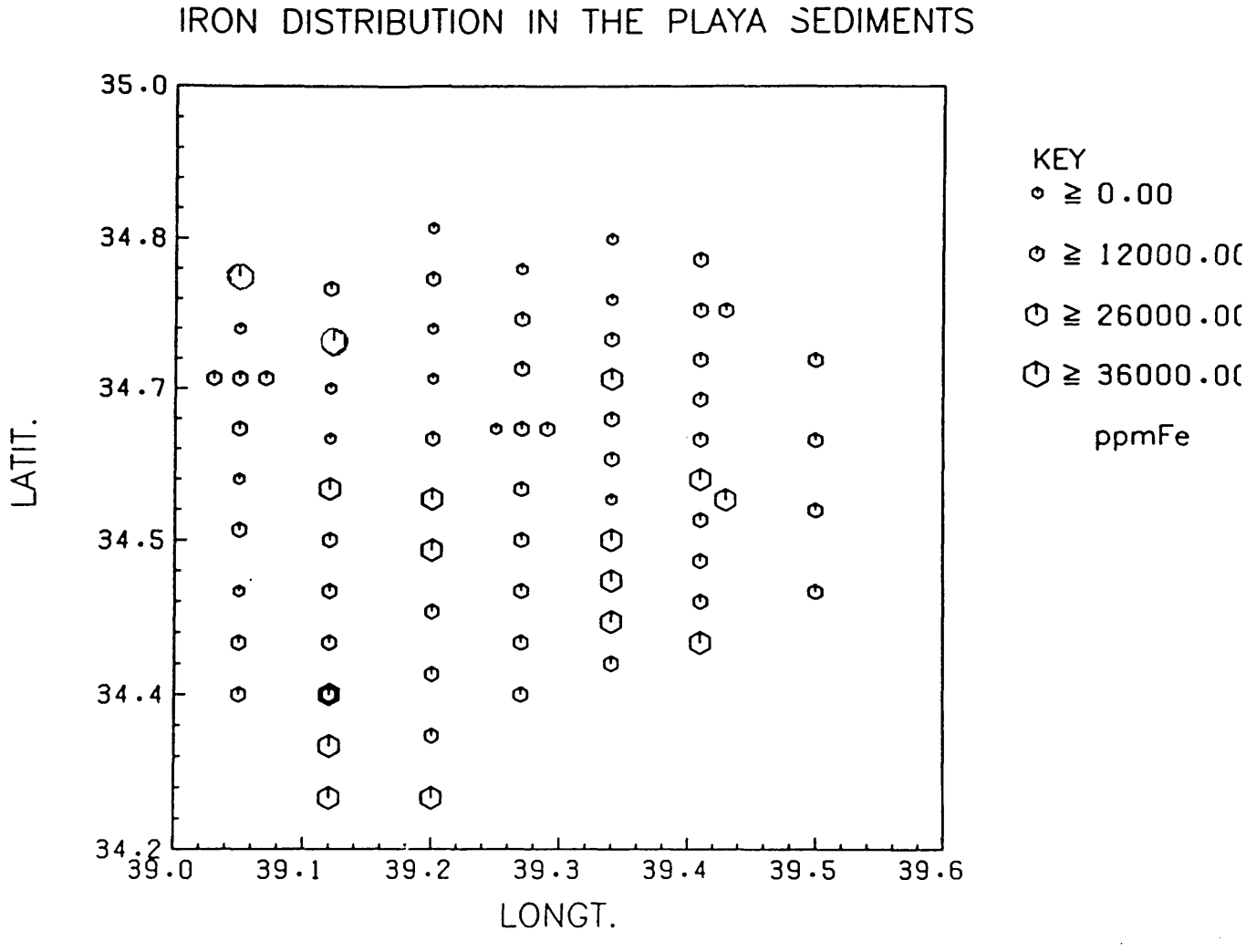


Fig.8.11 Symbolic areal distribution of Mg and Ti in the sabkha sediments.



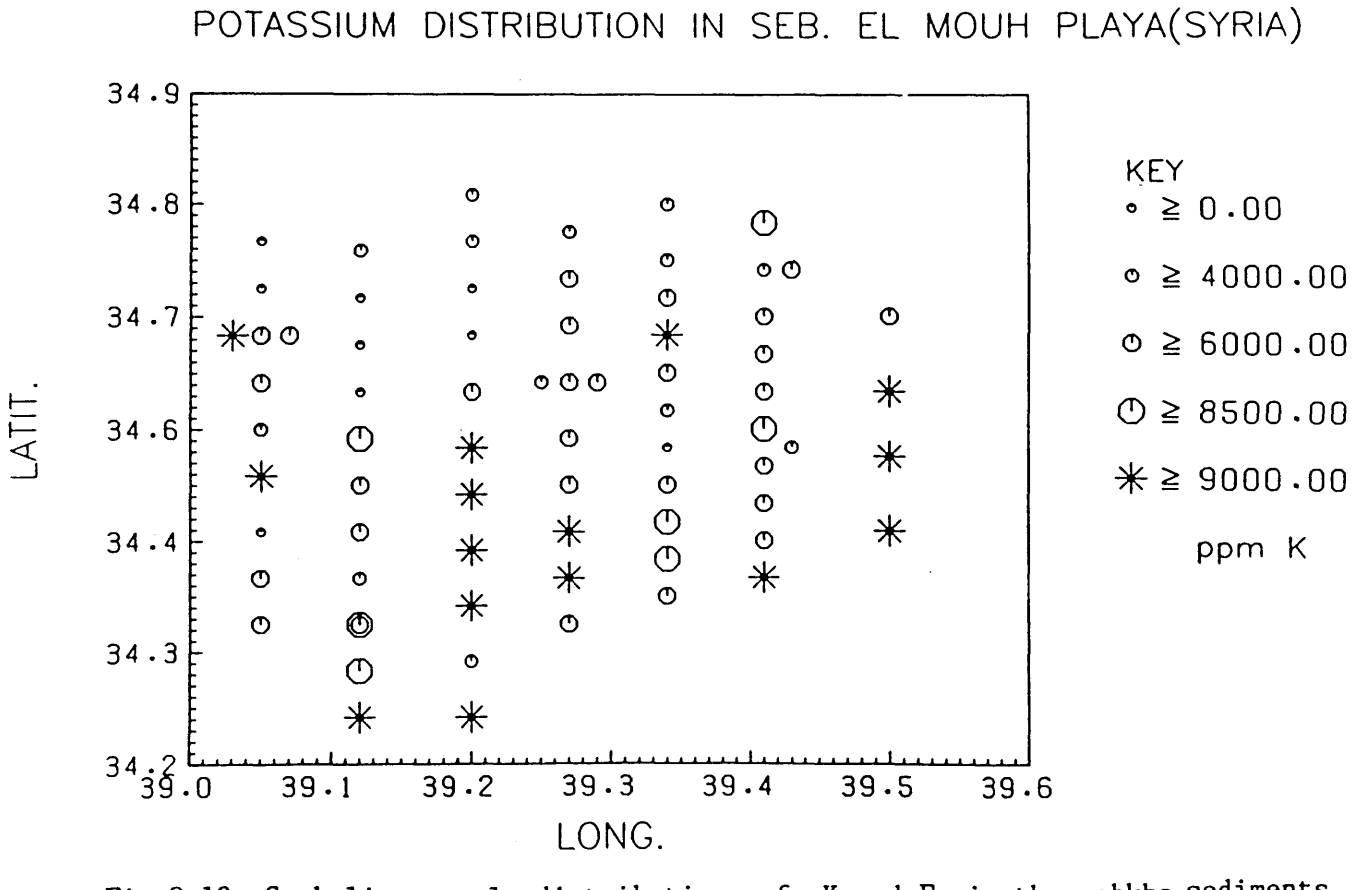


Fig.8.12 Symbolic areal distribution of K and Fe in the sabkha sediments.

Sawwaneh fault (see Fig. 8.2). The rest of the Sabkha, particularly its north and northwestern parts are void of U anomalies and occupied by only background values.

The highest Ca and Ag concentrations (22% and 2ppm respectively) are associated with the first anomalous U site along with anomalous Sr, supporting a possible derivation of these elements from the Cretaceous and Palaeogene carbonate rocks and phosphatised clayey limestones. These rocks are known to have enhanced average of U contents, therefore it is possible that the groundwaters may react with the rocks leading to chemical breakdown and leaching of these elements. Fluctuations in the groundwater level due to the climatic conditions may cause upward capillary migration of the leachate. Reprecipitation due to evaporation on or near the surface could explain the observed anomalies in this part of the sabkha.

Anomalies of As, Sr, Mo, and to lesser degree V are associated with the second site of anomalous U values. The distribution patterns of these elements are presented as three dimensional solid surface (Figs. 8.13 to 8.17) in which the anomalous trends extend diagonally from the southern edge to the northeastern side of the sabkha. The source of U and its associated elements in this trend especially As is most likely to be influenced by the detrital influx which is discharged into the sabkha by the above mentioned wadis (Fig. 8.18). The marly limestone, chert, phosphalized limestones and dolomitic debris that result from denudation of the catchment areas may reflect a source of enrichment in these elements, possibly as a result of active

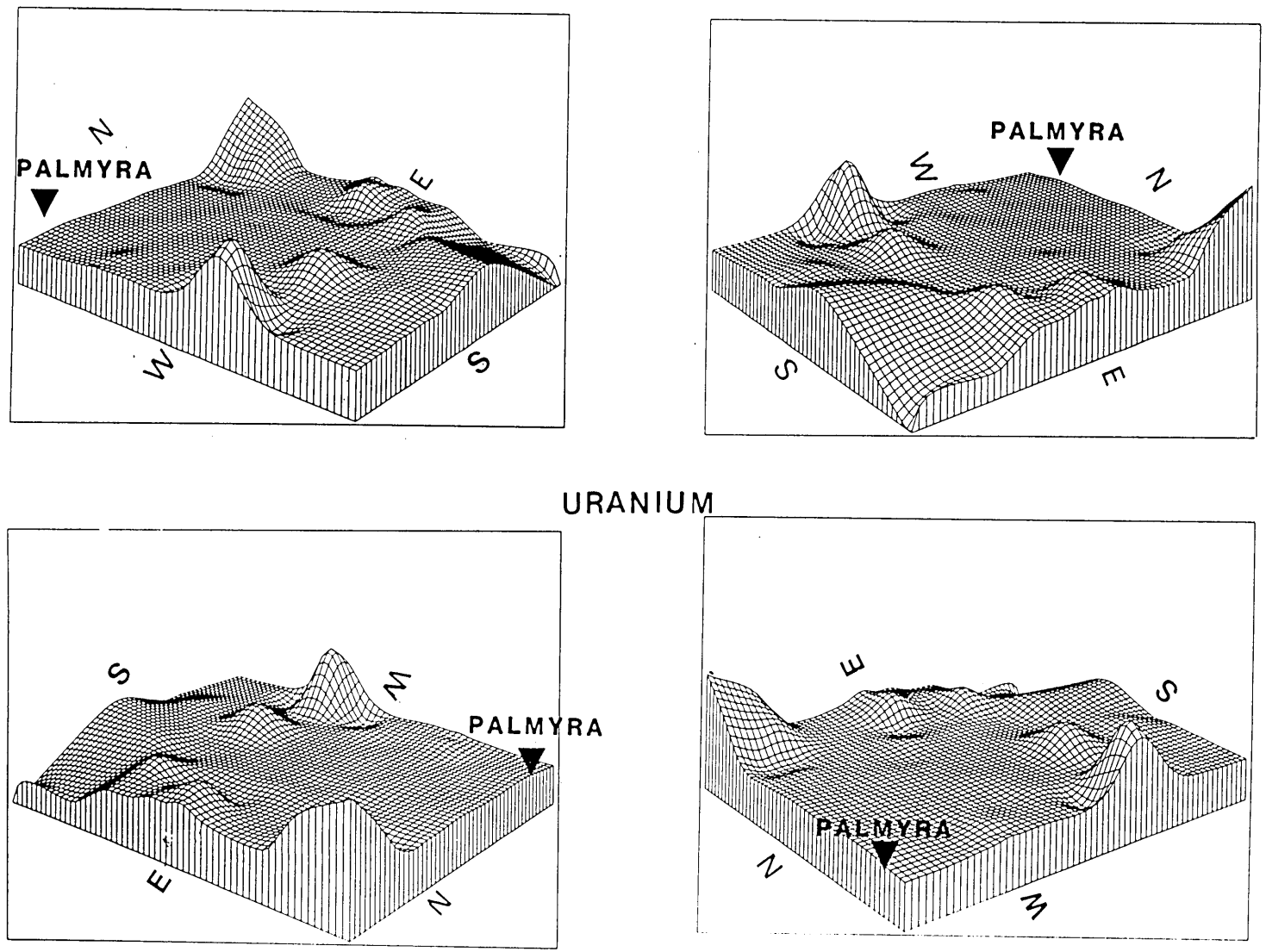


Fig.8.13 Solid surface distribution of U in the sabkha.
(notice that the distribution is viewed from four angles).

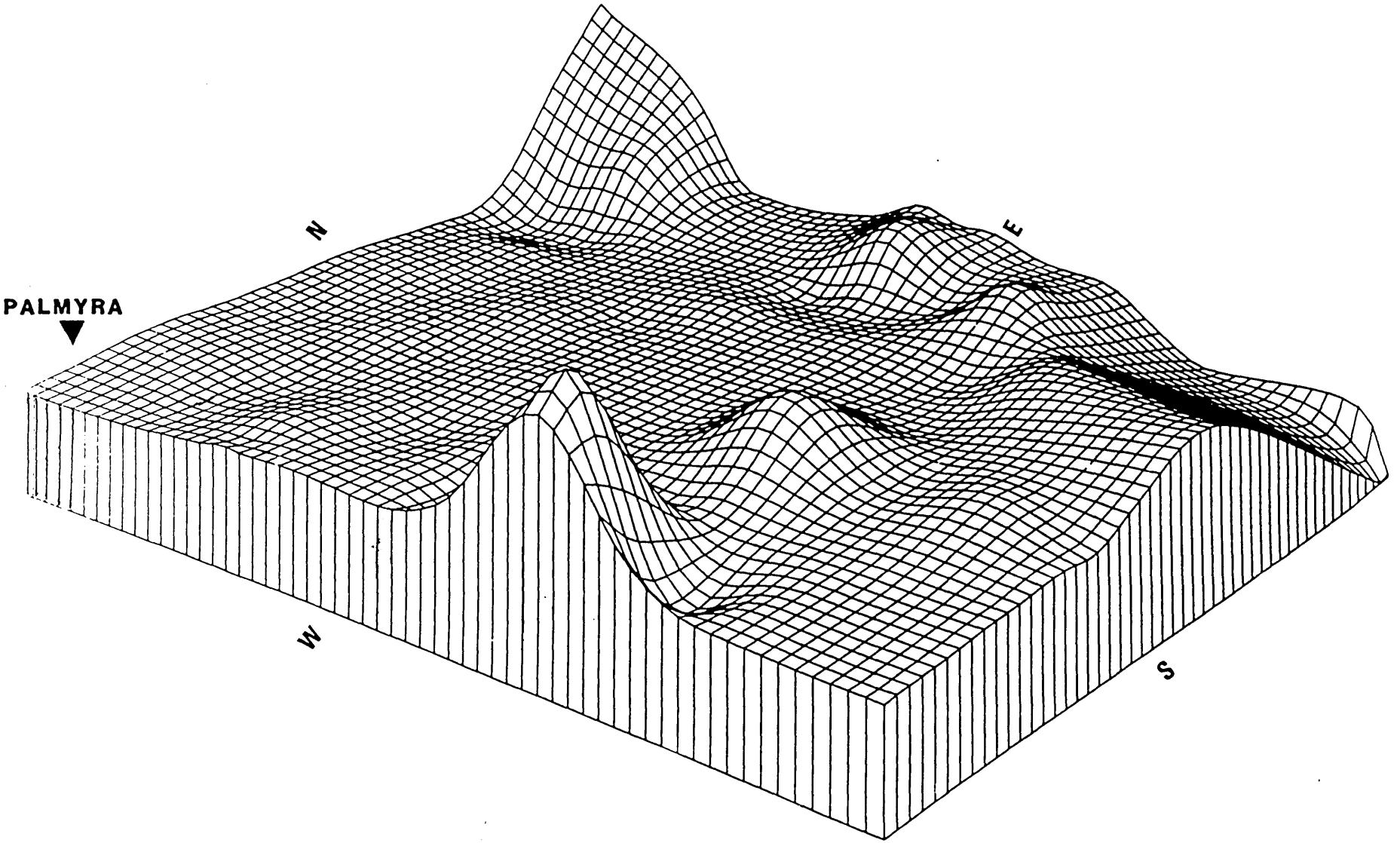


Fig.8.13 Solid surface distribution of U in the sabkha.

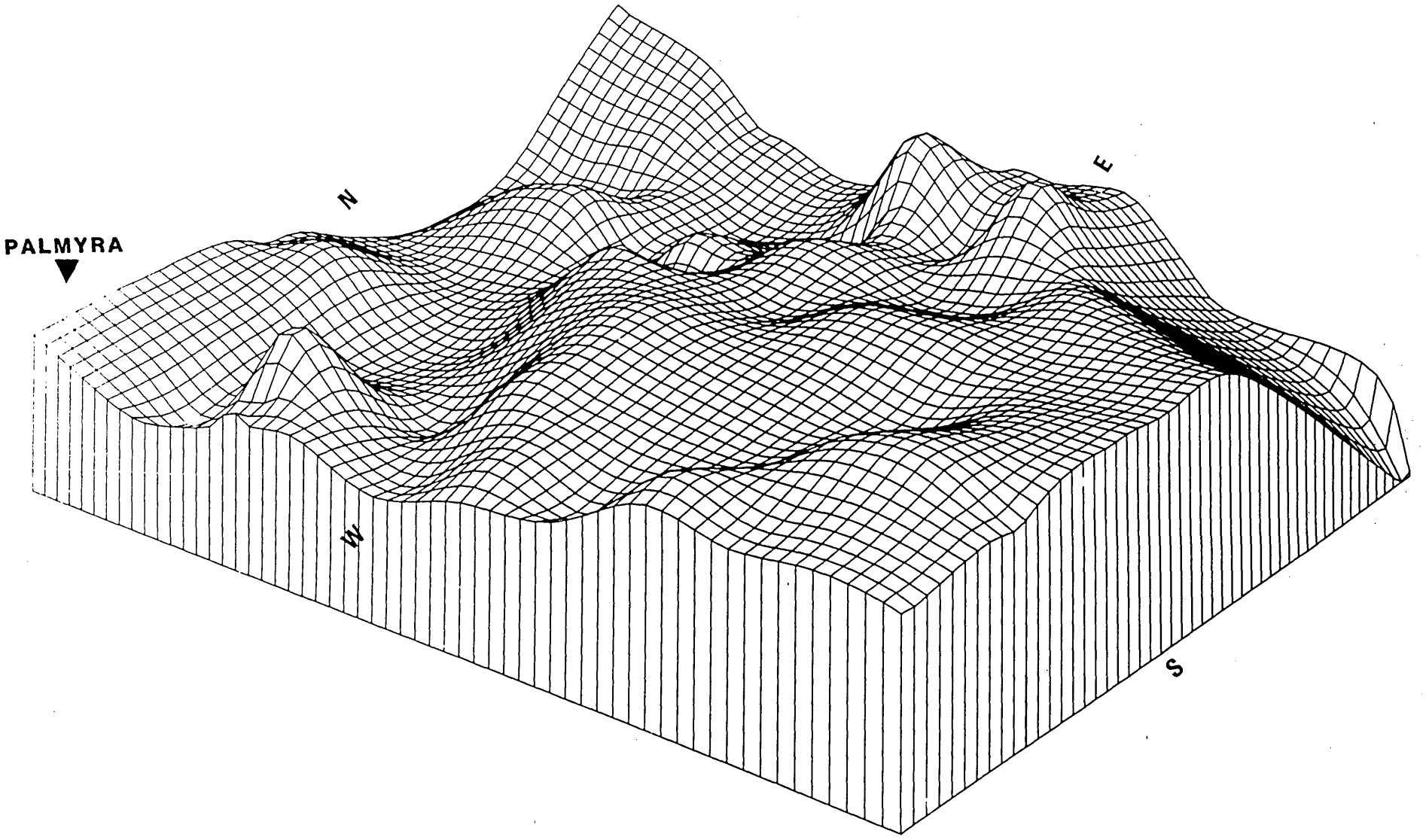


Fig.8.14 Solid surface distribution of As in the sabkha.

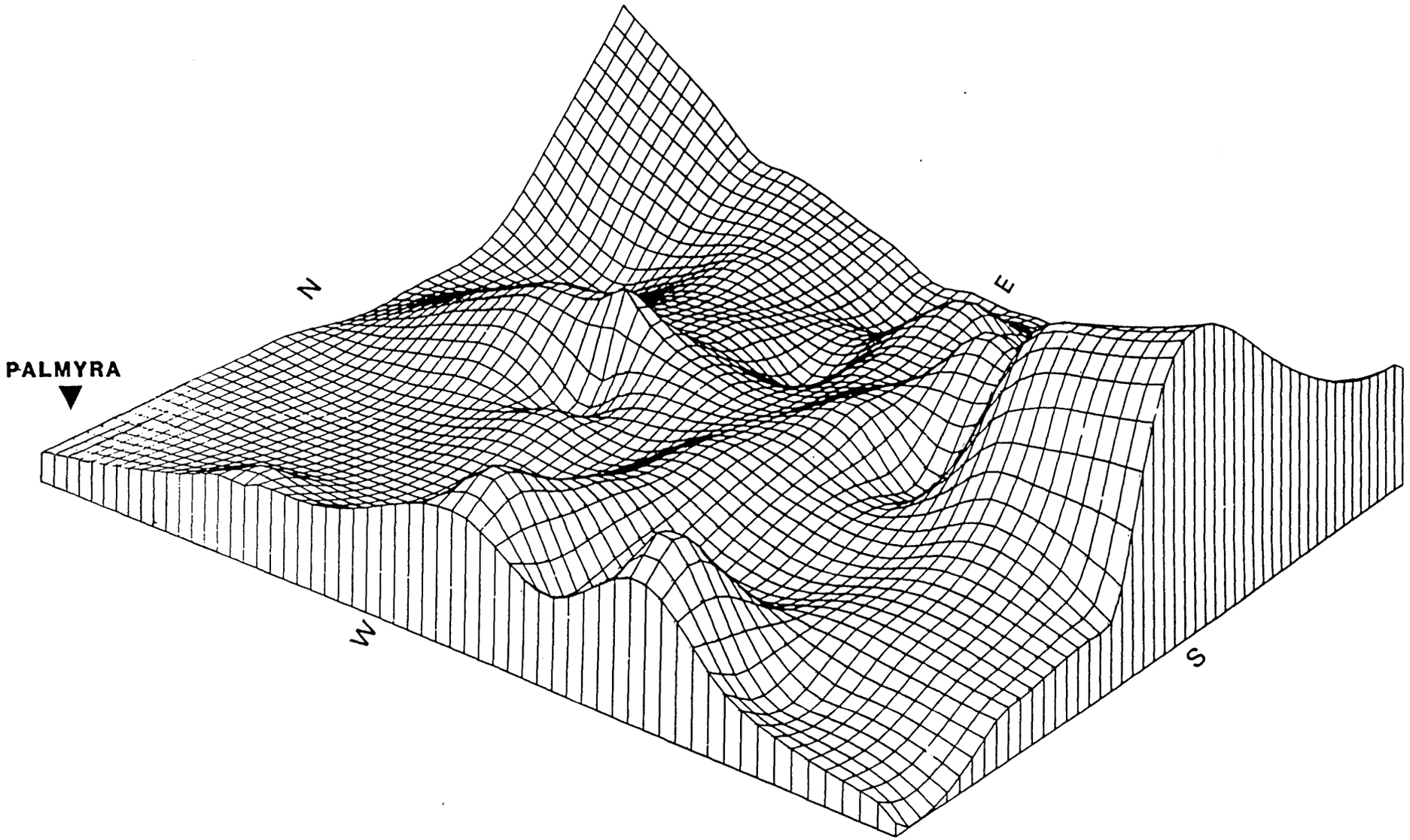


FIG.8.15 Solid surface distribution of Sr in the sabkha.

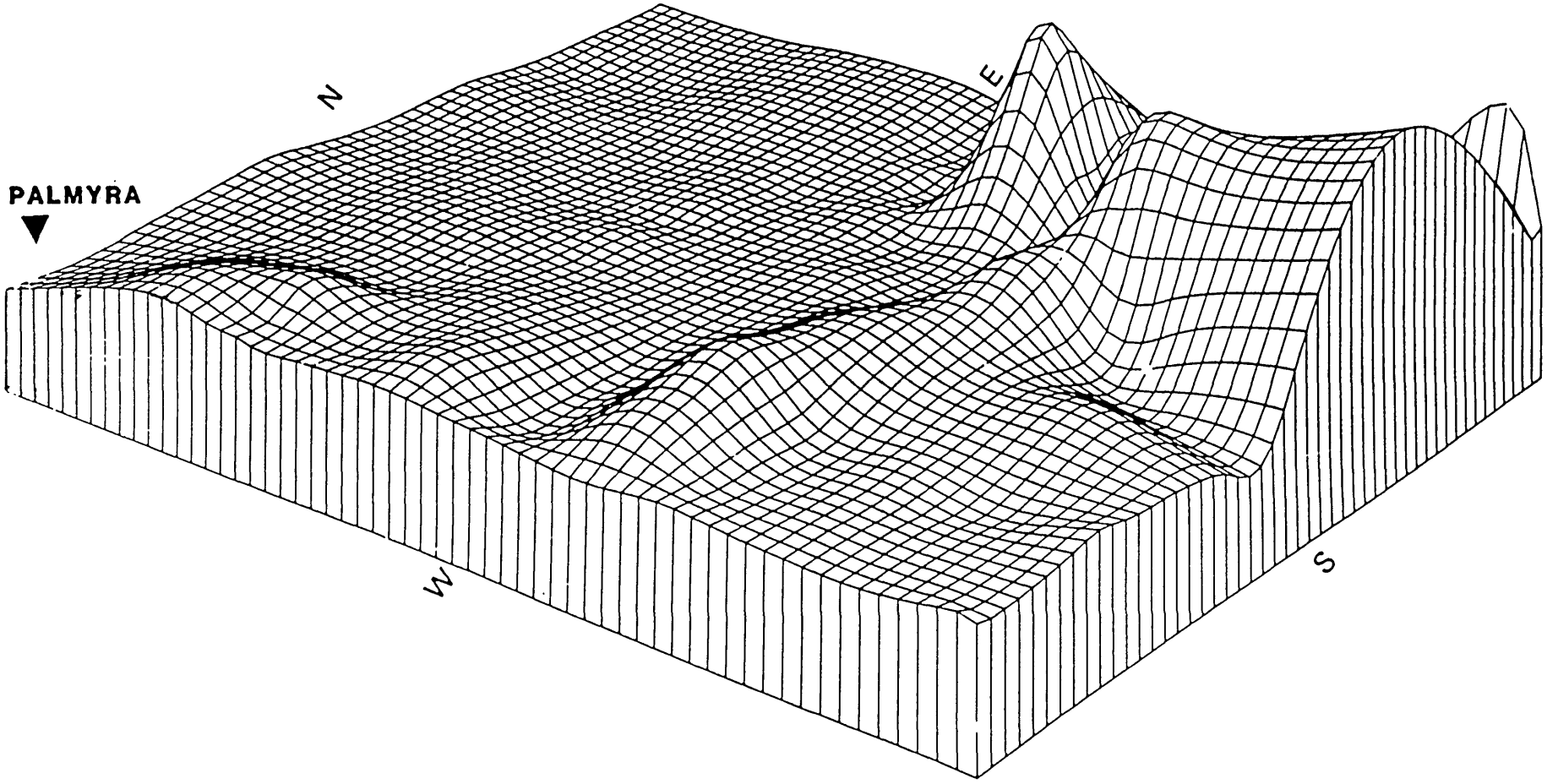


Fig.8.16 Solid surface distribution of Mo in the sabkha.

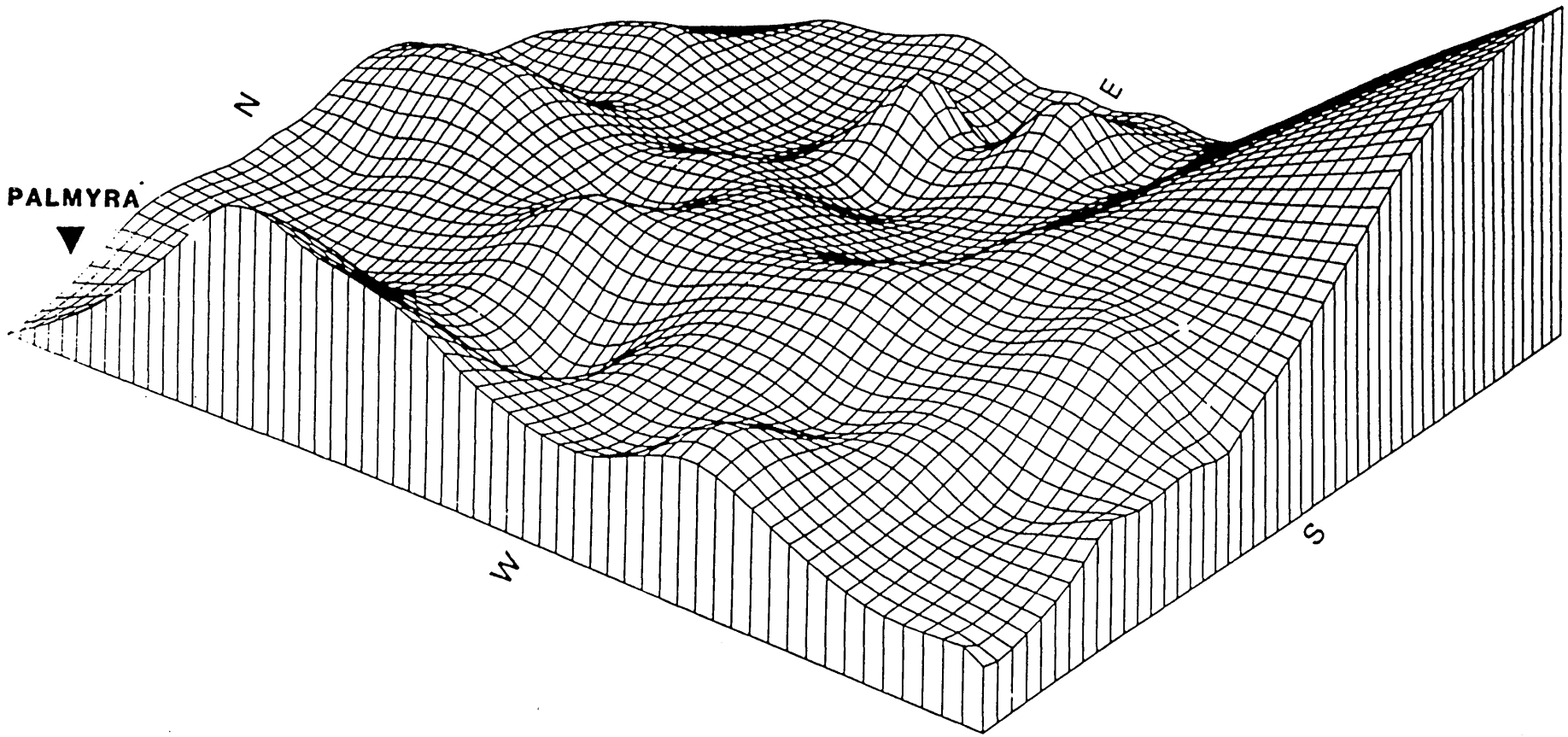
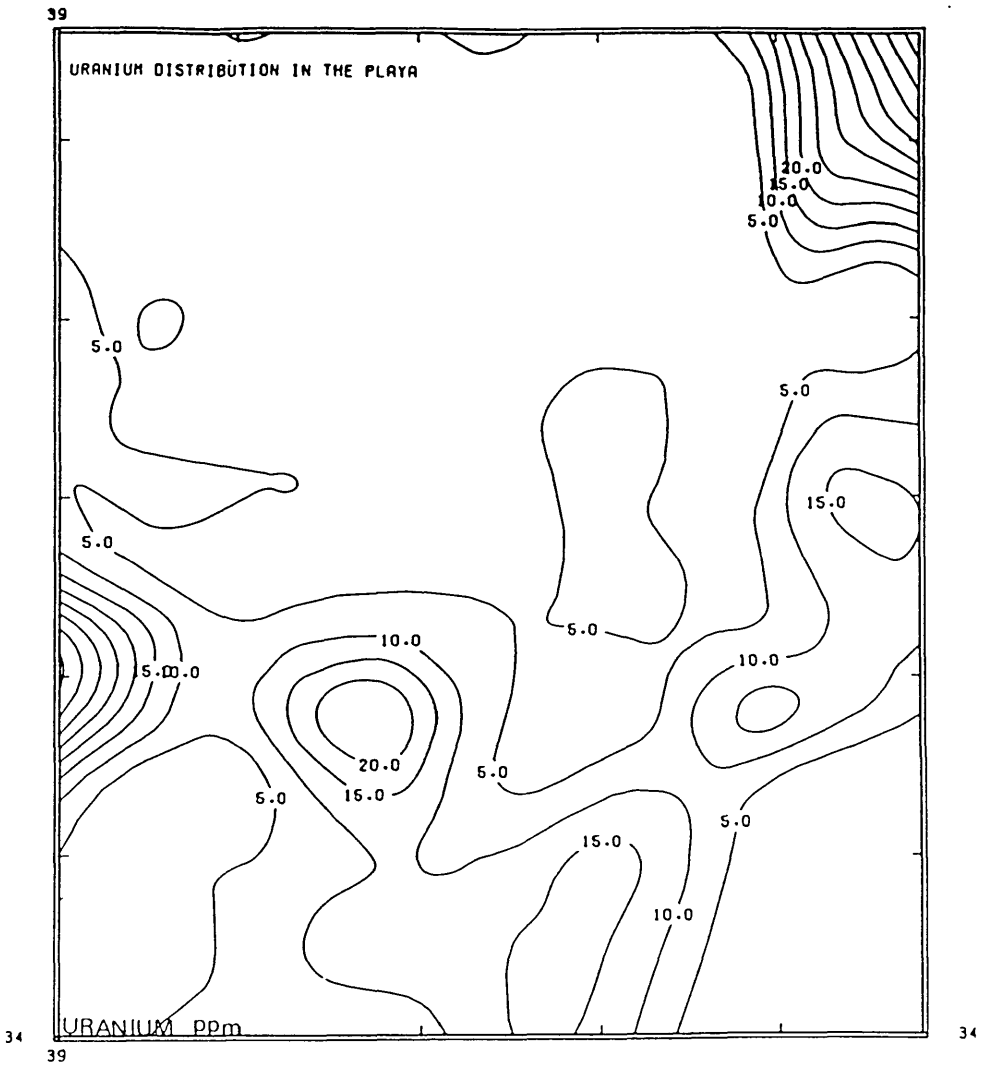


Fig.8.17 Solid surface distribution of V in the sabkha.



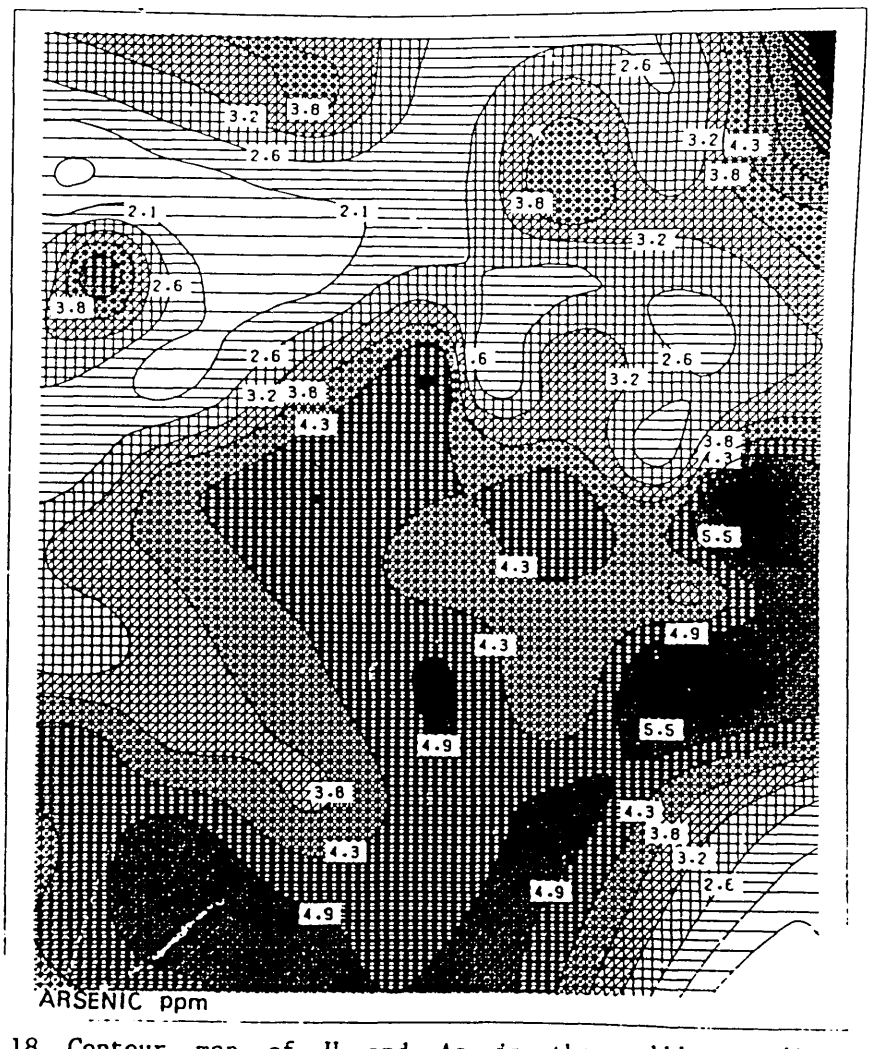


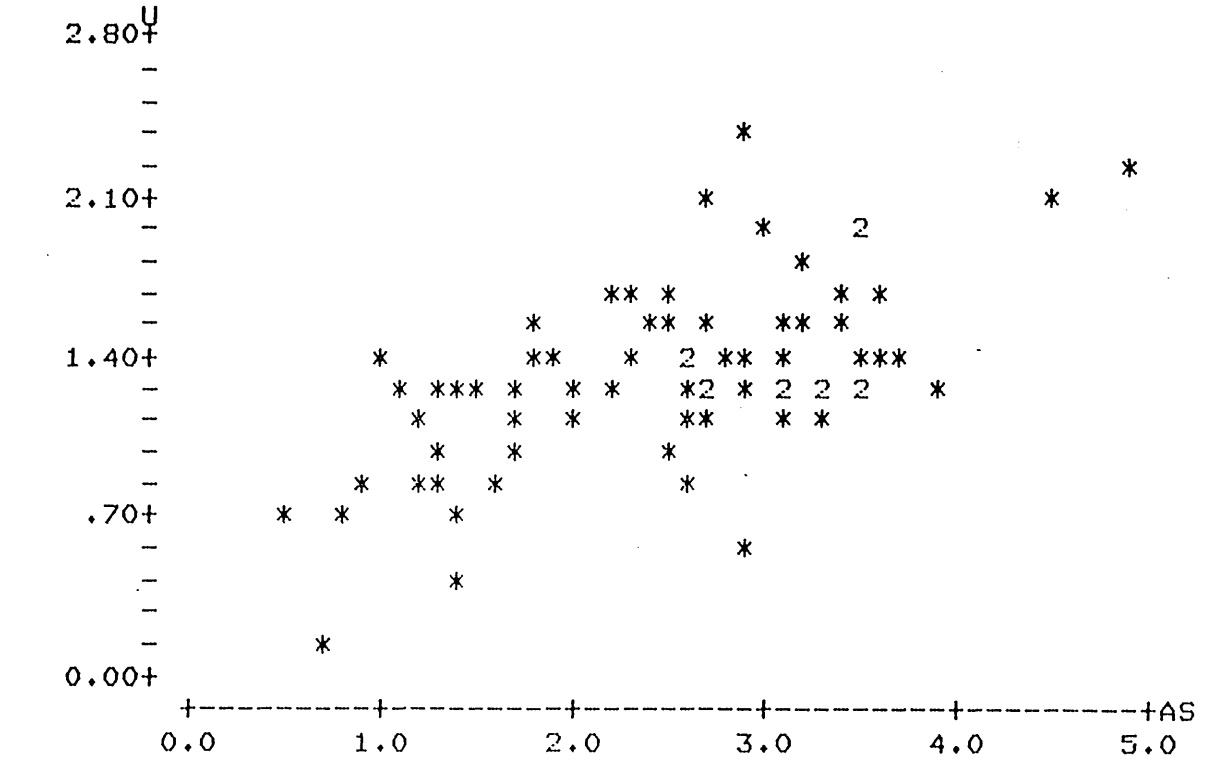
Fig.8.18 Contour map of U and As in the sabkha sediments

physio-chemical processes such as those leading to duricrust formation or enrichments on or near surface compositional changes.

8.7 Multivariate analysis of the data

8.7.1 Inter-elements relationships

The correlation coefficients for every pair of variables found to be always above the detection limit were computed. The linearity of the relationships, can be tested by plotting the variables of the corresponding pair against one another (Fig. 8.19). Inspection of the first column of the correlation coefficient matrix (considering the 99% confidence level) has revealed that U is moderately positively correlated with As, Mo, Mg, Cu and V (>.3). The highest correlation at this confidence level is found between Fe, Ti, Co, Zn, Al, Mn, La, Cu, V, Cr, K, Ni and to a lesser degree As and Li. These relationships clearly illustrate the affinity of these elements towards clays and Mn and Fe oxy-hydroxide complexes. Such components seem to play a major role in the geochemistry of sabkhet El Mouh. However, at a lower confidence level (95%), U shows acceptable correlation coefficients with the above mentioned elements (Fe, Ti, Co, Zn, Al, Mn, La, Cu, V, Cr, K, Ni and As). A second significant relationship is found between P, Ba, Zn, La, Cr, V, Ti, Be, Fe, Cu, Mn, Co and to a lesser degree Cd, As and K. Geochemically, this association represents the phosphorite input into the sabkha, possibly as a product of complex processes of erosion, tranportation, deposition and diagenesis. A third group of elements comprising Li, Ni, V, Mg, K, Al, Ti and Nb reveals a significant interelationship which seems



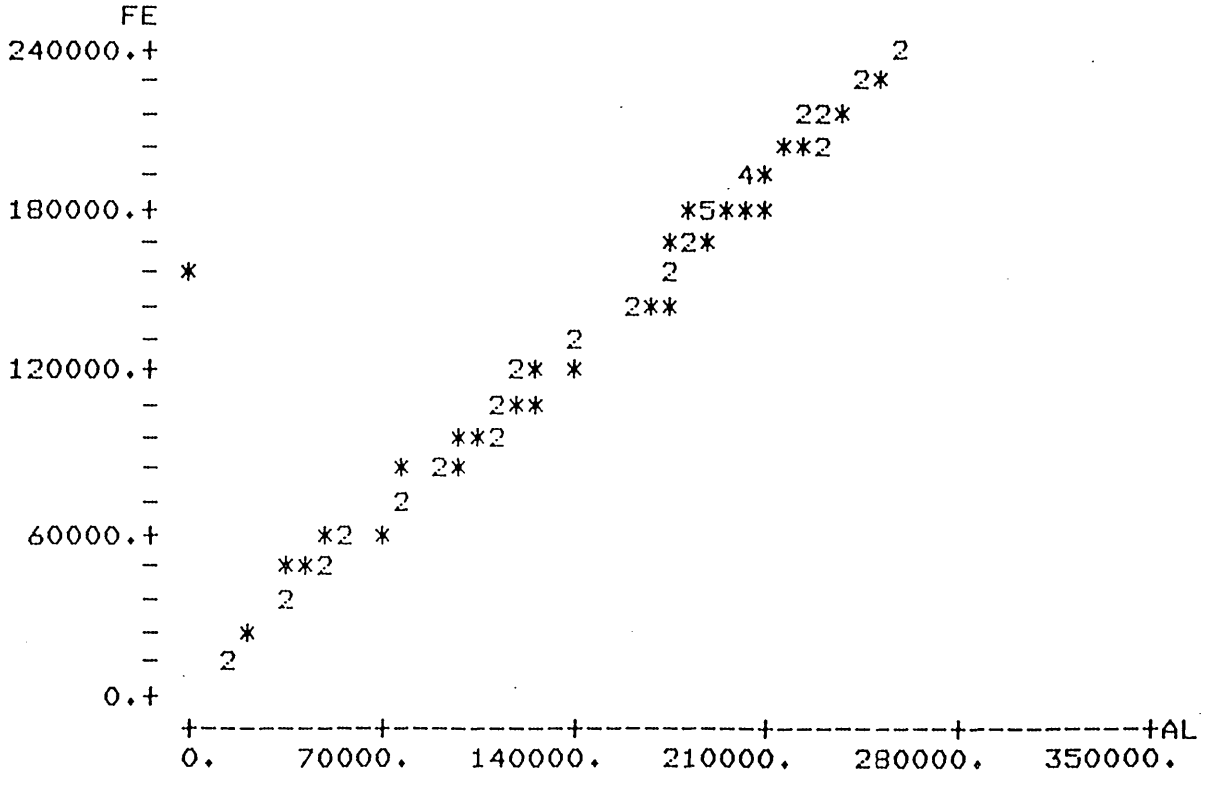


Fig.8.19 Scatterplots showing very good linear relationship between Al and Fe and less obvious one between U and As.

to indicate the influence of the salts and other evaporite phases present in the playa sediments.

Comparable results were achieved following a Box-Cox power transformation of the geochemical data. The correlation coefficients (Table 8.2) revealed similar interelement relationships with slightly improved reliability of the Pearson correlations.

8.7.2 Cluster analysis

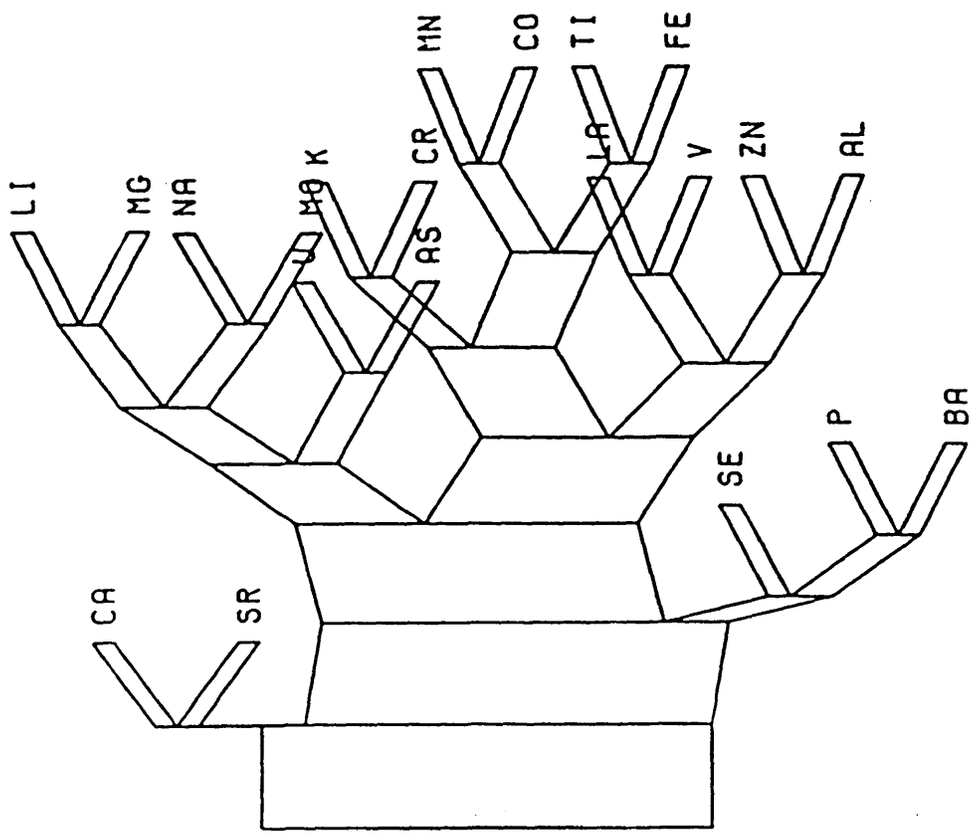
In order to investigate the structure of the geochemical data of these sediments, a second multivariate technique was used. The hierachical R-mode cluster analysis based on the Kleiner-Hartigan representation (trees) was performed. This application falls in the data exploration and hypothesis testing category (Ball, 1971). The dendrograms were examined to determine not only variables that are related to one group (correlation) but also to obtain an insight into the mutual relationship between the various groups (Park, 1966; Cormack, 1971; and Howarth, 1984). The dendrogram (Fig. 8.20) from clustering 21 of the measured variables in the playa sediments reveals five principal clusters or groupings: (1) U, As; (2) Mo, Na, Mg, Li; (3) Fe, Ti, Co, Zn, Al, Mn, La, V, Cr, K; (4) P, Ba, Se; and (5) Ca, Sr.

As can be seen from the dendrogram, U and As, although forming a distinct cluster group, also show a close relationship with the second group (Mo, Na, Mg, Li) at a significant level. The third cluster demonstrates the highest similarity level and the

	U	AS	SE	P	ZN	LI	NA	K	MG	CA	SR	BA	AL	LA	TI
AS	.546														
SE	.005	-.063													
P	.064	.351	.294												
ZN	.289	.551	.037	.611											
LI	.347	.387	-.106	.155	.559										
NA	.212	.179	-.036	-.063	.346	.485									
K	.299	.463	-.029	.304	.769	.661	.470								
MG	.381	.145	-.025	.041	.275	.653	.534	.412							
CA	.004	-.116	-.244	-.254	-.065	-.064	-.318	.098	-.107						
SR	.052	-.188	-.160	-.281	-.284	.010	-.300	-.129	.041	.286					
BA	.185	.399	.171	.719	.490	.297	.138	.276	.123	-.207	-.440				
AL	.267	.528	.003	.489	.935	.600	.372	.804	.239	-.020	-.189	.439			
LA	.308	.519	.081	.586	.914	.623	.387	.769	.342	-.065	-.317	.624	.893		
TI	.298	.578	.002	.519	.948	.638	.404	.825	.325	-.066	-.315	.534	.939	.951	
V	.366	.605	-.016	.528	.916	.696	.363	.746	.387	.011	-.227	.556	.880	.896	.921
CR	.332	.574	.045	.536	.894	.522	.253	.780	.224	-.035	-.240	.398	.847	.849	.909
MO	.373	.216	-.119	-.049	.543	.523	.504	.639	.514	.150	.108	-.056	.601	.557	.584
MN	.285	.520	-.030	.463	.914	.699	.512	.801	.416	-.090	-.309	.501	.910	.913	.944
FE	.314	.576	-.007	.499	.963	.630	.419	.821	.294	-.066	-.313	.496	.959	.941	.986
CO	.319	.554	-.003	.461	.944	.662	.393	.818	.335	.006	-.282	.471	.939	.937	.976

	V	CR	MO	MN	FE
CR	.837				
MO	.531	.521			
MN	.881	.809	.648		
FE	.923	.904	.597	.947	
CO	.922	.890	.621	.952	.976

Table 8.2 Correlation matrix of the Box-Cox transformed data of the sabkha.



CLUSTER ANALYSIS

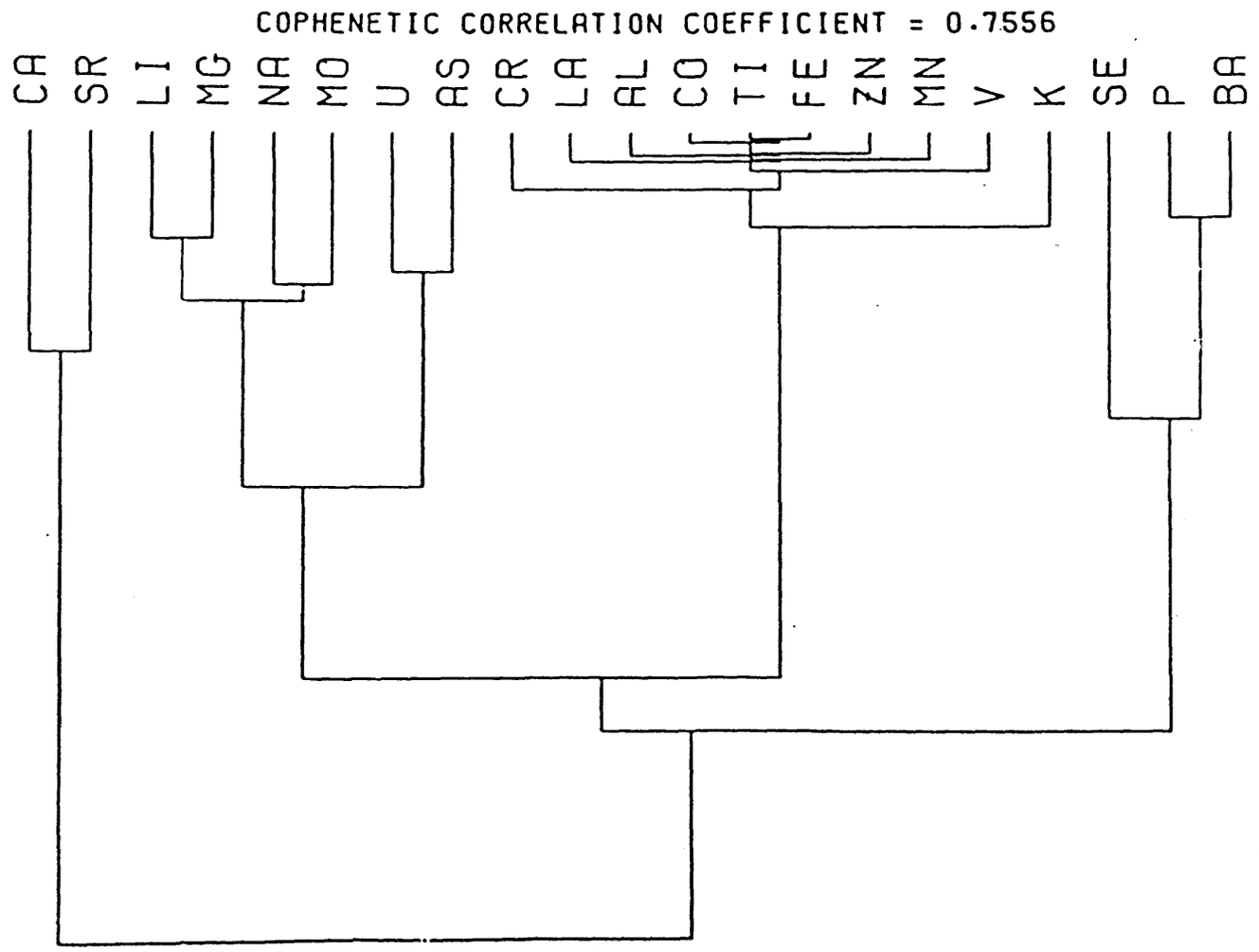


Fig.8.20 Dendrogram showing R-mode cluster analysis of 21 geochemical variable of the sabkha.

most significant one. It is clear that the first two clusters join this group at a low level of similarity, indicating insignificant association with it. However, the third group seems to be the most dominant effect in the geochemistry of the playa. The fourth group has no significant association with other groups; this was also the case of group five. It is suggested that the elements in group four may indicate a phosphorite association and those of group five a carbonate origin; whereas group three represents Fe-oxy-hydroxide and/or clay fractions. Group two reveals typical alkaline salt component and group one seems to indicate chemical precipitation from a leachate solution owing to evaporation. Thus, it was felt that the elements in each of the five clusters seem to reveal either their mutual geochemical affinities or reflect the effects of interacting natural processes related to their incorporation into the sediments (provenance, erosion, transportation, deposition and diagenesis).

8.7.3 Principal Component and Factor Analysis

The distribution of the compositional and textural components of the sediments govern the concentration of the elements in the sample (Dahlberg and Griffith, 1967, Calvert, 1976). Therefore the variability of the elements may reflect the differential influences of underlying natural causes and processes which produced the sample under consideration. Other aspects such that related to measurement error may also contribute to the variability of the element content (Read and Dean, 1972). In order to estimate the relative importance of these various components in controlling the abundance of a particular element, and to clarify the relationship

between variables, principal component and R-mode factor analysis may be used (Nichol, 1973; Garrett, 1983; Zhou, 1984).

The approach is to find a linear transformation of the set of observed variables which provides a set of derived theoretical variable vectors termed principal components. Although, the pincipal component matrix has as many new vectors as original variables, it may reveal the degree of complexity and the cause and effect of the natural system by smaller number of dimensions or orthogonal axes (components) required to express a high proportion of the variability of a particular data set. The remaining components often represent a negligible fraction of the total data variance and can be ignored. These components usually are viewed in terms of geological, geochemical or other underlying processes, and may reveal associations and contrasts between the variables which are the most important aspects contributing to data interpretation.

The procedure usually uses the correlation matrix to calculate eigenvectors and eigenvalues (details are described by Cooley and Lahens, 1962; Harman, 1976; and Joreskog et al., 1976). The loadings of each of these vectors onto an eigenvector constitute a column of the principal component matrix. The sum of the squares of these loadings is equal to the corresponding eigenvalue. Rotation of the principal components by a method of rotation (e.g. Kaiser varimax) generates the "factors". Practically, only those components with eigenvalues close to one (Kaiser's criterion, cited in Child, 1970) account for the largest data variance, and hence can be selected as model factors.

A substantial list of limitations to this approach was discussed by Matalas and Reiher (1967), however, the distinctive characteristic of reducing the dimensionality of the data set and providing a better angle for viewing the geochemical data, so obtaining insight into the underlying pattern of relationships, makes this technique widely acceptable. In addition, the factor scores themselves may be used as input for further analysis.

8.7.3.2 Application of the method

In this study, R-mode factor analysis with two subsets of 20 and 13 variables was applied in order to investigate the controlling factors of U distribution in the playa sediments. A log transformed robust correlation was used to compute the principal components matrix (eigenvectors and eigenvalues) utilizing the computer program BPCA2 (Mancey, 1980). Only the first few eigenvalues were near to or greater than one, and therefore their corresponding components were considered for varimax rotation in the factor analysis. However models with 4, 5, 6 and 10 factors were investigated, their results are summarized in Table 8.3, which lists only variables with loadings greater than 0.3. Each factor solution provides;

1) the factor loadings which are a measure of the correlation between the variables involved and the underlying component (factor);
2) the communality of the variables which is a measure of the amount of variance of each element explained by the factor model chosen, and calculated as the sum of squares of the values in the appropriate row of the principal component matrix;

Table 8.3 Summary of factor loadings for 4, 5, 6 and 10 factor models.

No. components		10	6	5	4
% variance explained		96.2	87.8	83.7	80.8
Associations in each component factor	1	Ti, Fe, Zn, Cr, Co, Mn, La, K, Al, P, Li, Ba, As.	Fe, Al, Ti, Zn, Cr, Mn, La, V, K, Li, As, U	Ti, Fe, Zn, Cr, V, Co, La, Mn, K, Al, P, Li Ba, As.	Fe, Ti, Zn, Al, Co, Cr, Mn, K, Li, P, Ba, As, U
	2	Ba, P, Se, Mg, Na.	Sr, Ca, Na.	Ca, Se, P, Ba.	Ba, Sr, P, Mo, U.
	3	Sr, Ca, Mg, Se.	Mg, Li, Na, Mo.	Na, Mg, Mo, Li, Mn.	Na, Ca, As, U, Mg.
	4	U, As, Ca, Na.	U, As, Sr.	U, As.	Ca, U, Mo, Sr.
	5	U, Sr.	Se.	Sr, Ba, Al.	
	6	Ca, As, U, Sr.	Ba, P, Mo.		
	7	Mg, Ba.			
	8	Ba.			
	9	-			
	10	Li.			

3) the eigenvalues which are a measure of the original variance explained by a particular factor (expressed as a percentage) which should equal the sum of the squares of the factor loadings;
4) factor scores which are an indication of the weighting of each rotated factor on individual samples.

In accordance with usual practice (Howarth, per commu, 1985), rotated components are subsequently called "factors". However, in the discussion of the results, both the components ("factors" before rotation) as well as the factors (after varimax rotation) are considered and discussed.

8.7.3.3 Results and interpretation

The constraints on the choice of a particular factor model perhaps may ensure that only the appropriate factors which adequately explain some of the controlling processes of Sabkhet El Mouh geochemistry are extracted. However, the optimum numbers of necessary factors has been approached in different ways by different workers (Jeffers, 1965). From the various possible solutions obtained, factor models 6 and 5 have been chosen to establish some relationships either with geological situations and known lithotypes or with physio-chemical processes of the playa environment.

Tables 8.4 and 8.5 report the principal components and the factor loadings for the six factor model. The six factors in this model explain 88% of the total variance generated by the 20

Table 8.4 Loadings of six components for a principal component analysis of the sabkha geochemistry.

TABLE OF COMPNT LOADINGS

	FACT 1	FACT 2	FACT 3	FACT 4	FACT 5	FACT 6
U	-.5325	-.3054	-.4714	.3860	.2299	-.2061
AS	-.6618	.0818	-.1113	.3598	.4868	-.2320
SE	-.0306	.3141	-.6682	.0310	-.6080	-.2197
P	-.6672	.5930	-.1334	.0386	-.0641	.1543
ZN	-.9599	.0870	.0871	.0292	-.0600	-.0550
LI	-.8265	-.3355	-.0805	-.0476	-.0104	.1689
NA	-.6118	-.3574	-.0724	-.5490	.0455	.0173
K	-.9226	-.1592	.0593	-.0453	-.0771	-.0254
MG	-.4867	-.4895	-.3435	-.2627	.0224	.3886
CA	.1471	-.3167	.3868	.6608	-.3477	.2795
SR	.2763	-.6661	-.3732	.2913	-.0375	.1081
BA	-.5415	.5674	-.1796	.1038	.1317	.4297
AL	-.8199	.0781	.2333	-.0517	-.2132	-.1761
LA	-.9183	.1369	.0091	.0771	-.1055	.0793
TI	-.9867	.0399	.0500	.0079	-.0096	-.0050
V	-.9648	.0128	.0507	.1230	.0235	.0581
CR	-.9454	.0699	.0561	.0930	-.0345	-.0961
MO	-.5772	-.5800	.1977	-.0569	-.1718	-.1984
MN	-.9812	-.0323	.0778	-.0499	-.0157	.0213
FE	-.9860	.0220	.0846	.0070	-.0119	-.0536

VARIANCE ACCOUNTED FOR BY COMPNTS.

COMPNT	VARIANCE PERCENT	CUM VAR
1	56.0372	56.0372
2	11.4916	67.5289
3	6.3792	73.9080
4	6.1351	80.0432
5	4.5187	84.5619
6	3.5952	88.1570

Table 8.5 Loadings of six factor model for factor analysis of the sabkha ageochemistry.

BASED ON RETAINED COMPNTS
1 NUMBER OF ROTATION AND VARIANCE AT EACH STEP

0	.1974304
1	.2948251
2	.3241391
3	.3348721
4	.3380038
5	.3386835
6	.3387869
7	.3387997
8	.3388014
9	.3388014
10	.3388014
11	.3388014
12	.3388014

NEW ROTATED FACT LOADINGS

****

	FACT 1	FACT 2	FACT 3	FACT 4	FACT 5	FACT 6
U	-.3190	-.2678	-.1496	.0326	.8036	-.0257
AS	-.4901	.0946	.1750	-.1303	.7266	.2294
SE	.0024	.0252	-.9716	-.0828	.0256	.1133
P	-.5489	.0760	-.2164	-.1559	.0508	.6806
ZN	-.9207	-.0948	-.0168	-.0732	.1729	.2276
LI	-.7028	-.5358	.0561	.0277	.2073	.0720
NA	-.5321	-.5828	.0947	-.3932	-.0481	-.1494
K	-.8801	-.2875	.0158	-.0433	.1611	.0584
MG	-.2732	-.8516	.0066	-.0489	.1031	.0469
CA	-.0060	.0790	.1040	.9334	-.0564	-.1249
SR	.3753	-.4565	-.1176	.3948	.3381	-.3521
BA	-.3278	-.0551	-.0414	-.0713	.0999	.8561
AL	-.8952	.0319	-.0529	-.0661	-.0143	.0468
LA	-.8452	-.1442	-.0789	.0015	.1504	.3485
TI	-.9144	-.1791	.0176	-.0882	.2036	.2451
V	-.8745	-.1851	.0556	.0180	.2654	.2822
CR	-.8985	-.0714	-.0290	-.0533	.2494	.2067
MO	-.6628	-.3137	.0838	.1081	.0900	-.4651
MN	-.9161	-.2432	.0557	-.0903	.1584	.1954
FE	-.9333	-.1493	.0301	-.0927	.2044	.1956

VARIANCE ACCOUNTED FOR BY COMPNTS.

COMPNT	VARIANCE PERCENT	CUM VAR
1	47.1958	47.1958
2	10.1074	57.3032
3	5.5356	62.8387
4	6.4509	69.2897
5	8.4401	77.7298
6	10.4273	88.1570

---

variable data set (N=72). The remaining 12% of the variance is explained by a group of 14 factors, which thus have been neglected. The communality of all the elements proved to be good, regardless of the factor model used; this indicates a consistent analytical variance.

The first component factor explains the highest percentage of the total variance (56%). It is characterized by very strong negative loadings on Ti, Fe, Mn, V, Zn, Cr, K, La, Li and Al, and significant loadings on P, As, Mo, Mg and U. The large loading of this element association reveals that the main underlying control expressed by this factor is a combined effect of Fe-Mn oxy-hydroxide complexes and clay fraction geochemistry of the sediments which influences the behaviour of nearly all the elements involved in this association including the closely related U and As. At this stage, this factor perhaps is able to provide a feasible explanation for the close relationship between U and As that was found by using other techniques (cluster and correlation analysis). Hence, such association cannot be attributed to the presence of any U arsenate components in the sediments (due to the generally low level of As content 6.6 ppm), the possible interpretation therefore, is that these two mobile elements (U and As) may be coprecipitated under the effect of the dominant Fe oxy-hydroxide and clay controls shown by the element association in this component. It is well known that the Fe distribution is the main control on that of As in the near surface environment (Hawkins et al., 1980; Moon, 1983) and it can greatly influence the fixation of U (Samama, 1984). Therefore the strong loadings of Fe, Ti, Al and Mn in this component can at least account for a portion of U

and As concentrations in one phase of their close association.

After rotating this component however, the resulting factor 1 shows the same characteristics as component 1, but it explains slightly less of the total variance (49%) and shows generally lower loadings especially on Mg, which became insignificant to this factor.

The three dimensional solid surface areal distribution of the factor scores is presented in Fig. 8.21. The highest scores are found in the extreme northwestern corner of the sabkha (near Palmyra). These high values extend in southeasterly direction across the sabkha plain and seem to meet with another trend having generally lower but still significant scores. This second trend starts from the southern side of the sabkha and strikes northeastwards.

In view of the elemental association of this factor and its spatial, geomorphological and geological relationships, it is suggested that the underlying controls which were expressed in the pattern shown may indicate a secondary surficial (supergene) processes possibly influenced or contaminated by agricultural components derived from the land used in the immediate vicinity of the northwestern part of the sabkha (see section 8.3). The irrigation waters may interact continuously with the sediments leading to the formation of clays and Fe-Mn oxy-hydroxides. These, then will act as scavengers of those elements significantly loaded in this factor. Such important fixation processes greatly affect the dispersion patterns of the trace elements including U in the

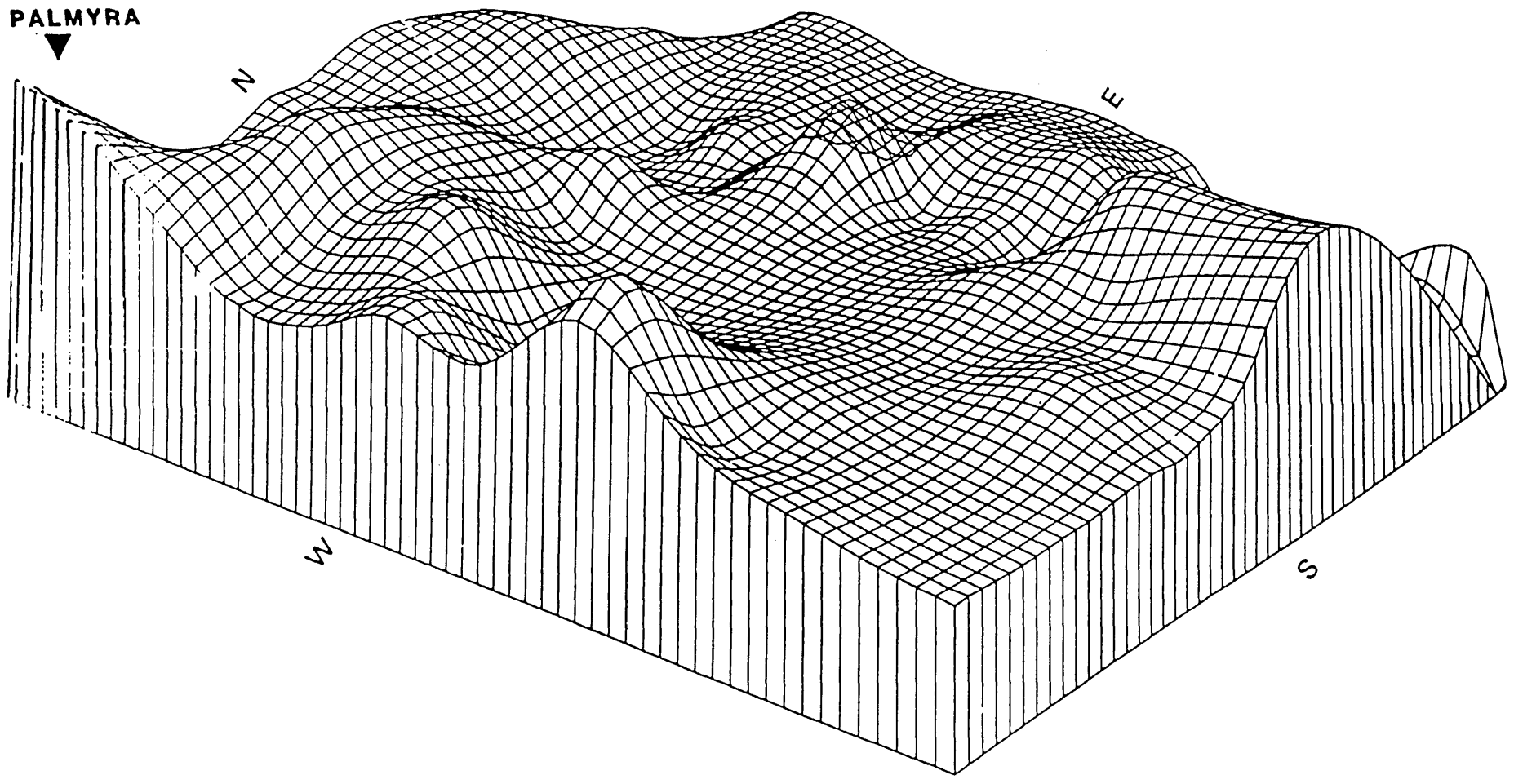


Fig.8.21 Solid surface distribution of the scores of factor 1 association of the sabkha sediments.

sabkha geochemistry. The high proportion of the data variance explained by these natural physio-chemical processes speaks of their prominent role in the sorption, coprecipitation and removal of U and its closely associated elements from solutions.

Investigation of the relationships between Ca and Sr from one side (which usually represents the carbonate component in the sediments) and the main factor association (Fe, Ti, Mn, Al, K, CO) on the other, has revealed an antipathetic relationship (Fig. 8.22). Using this contrasting relationship derived from analysing factor 1, it is perhaps feasibl to suggest that carbonate rocks do not contribute into this factor to any extent. Such indication lends further support for a supergene surficial origin of factor 1. Although the exact timing for an effect of this type upon the sediments is not clearly known, there is no doubt that it can be held responsible for most of the compositional changes and textural variations in the playa sediments, possibly immediately after their deposition since the Neogene times leading to the formation of lacustrine marls and clays which may account for the large proportion of the fine fraction in those sediments as stated earlier.

The second component accounts for 11.5% of the total variance and indicates significant positive loadings on P, Ba and to a lesser degree on Se and significant negative loadings on Na, Li, Ca and to a lesser degree on U. In general, this pattern reveals a definite resemblance to the geochemical signature of phosphorite of the region, indications of which seems to be reflected in these playa sediments. Such an interpretation can find its support not

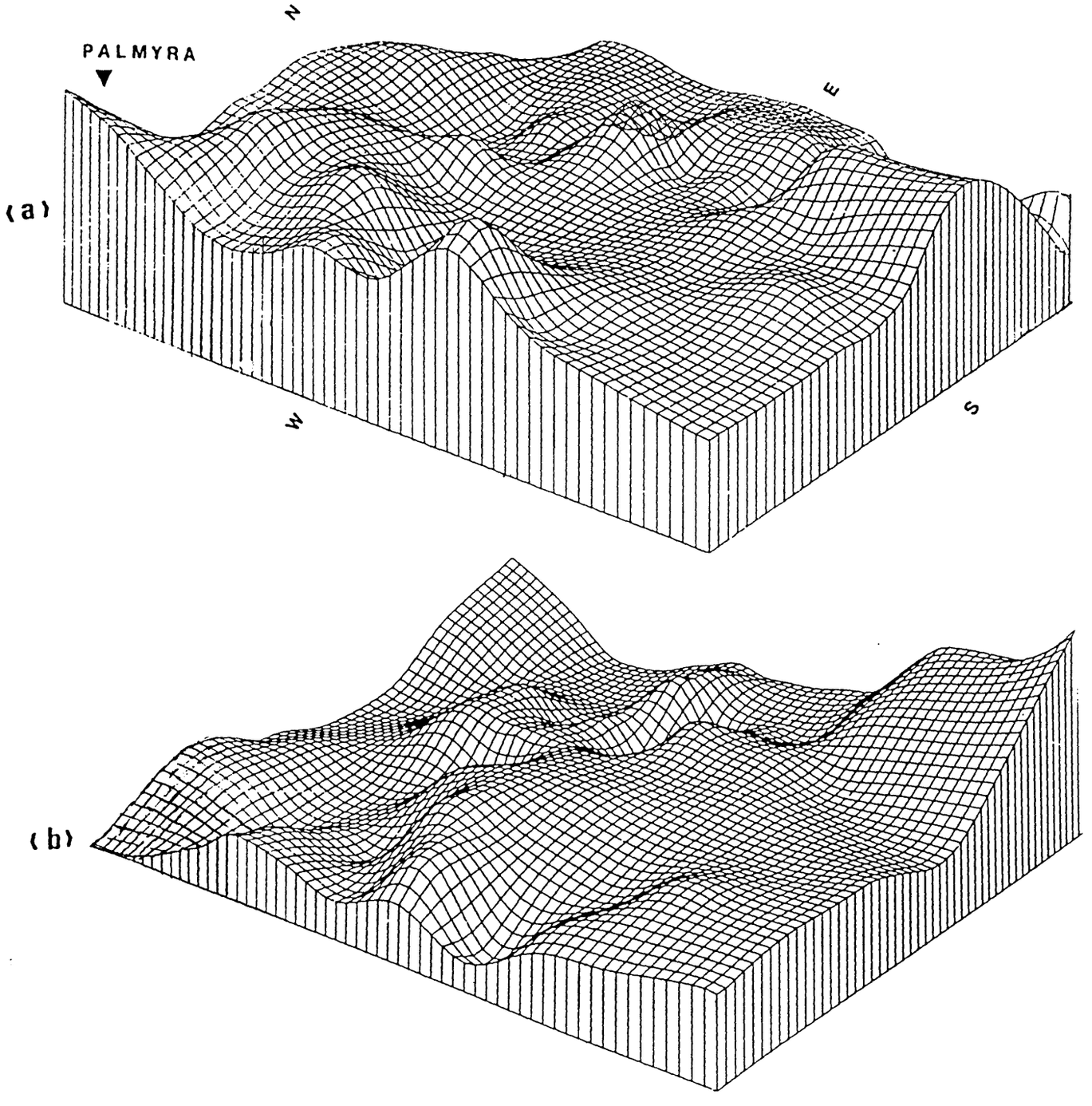


Fig.8.22 Solid surface distribution of the scores of factor 1 association of the sabkha sediments (a), compared to Ca distribution (b).

only by the geochemistry but also by the geological information as well as findings of previous chapters.

After rotation this second component association is downgraded to factor 6 explaining then only 3.6% of the total variance with strong loadings on P, Ba, Mo and Sr. The solid surface areal distribution of the factor scores (Fig. 8.23) seems to compare well with that of P which further supports a phosphorite influence in this factor.

However, factor 2 which resulted after rotation expresses 10% of the variance and is significantly loaded in Mg, Na, Li and Sr representing perhaps the salt and other evaporitic components which are widespread in sabkhet El Mouh. Additionally a dolomitic component can possibly be inferred into this factor by considering the dolomitic input from the catchment area as well as indications of H_2S and S in a few sample sites (reduction?) and the relatively high Mg content (section 8.6.1). Watson (1983) reported (from other sabkhas elsewhere in the world) that dolomite is more common, whereas Shearman (1963) suggested that dolomitization in the sabkha can occur at the expense of its aragonite and calcite constituents. Therefore, factor 2 can be attributed to both evaporitic and dolomitic controls.

The areal distribution of the factor 2 scores is presented in Fig. 8.24; the pattern indicates a general even enhancement all over the sabkha with exception of its southeastern part.

The third component explains 6.4% of the total variance and

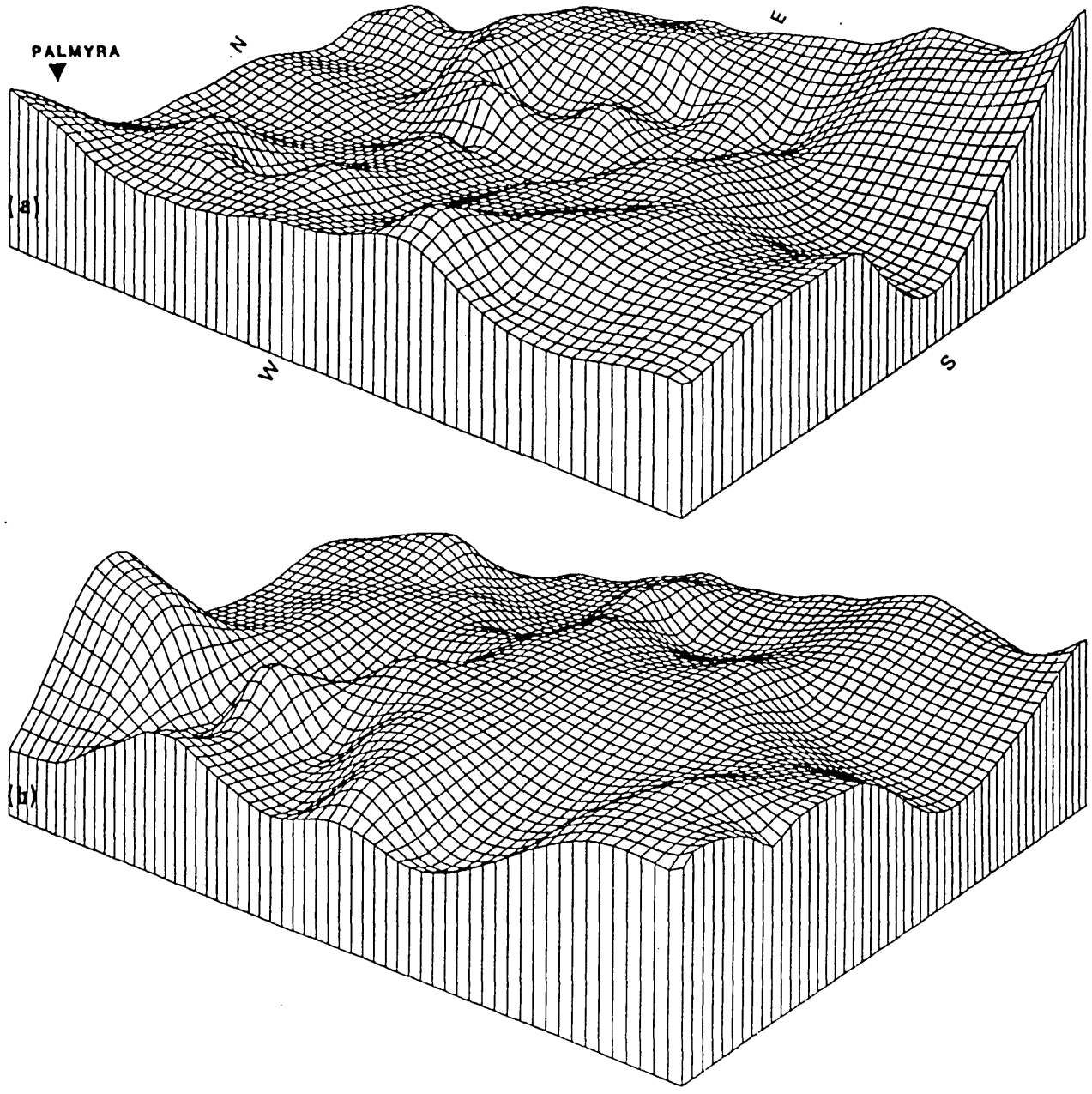


Fig.8.23 Solid surface distribution of the scores of factor 6 (a) compared to P distribution (b) in the sabkha sediments.

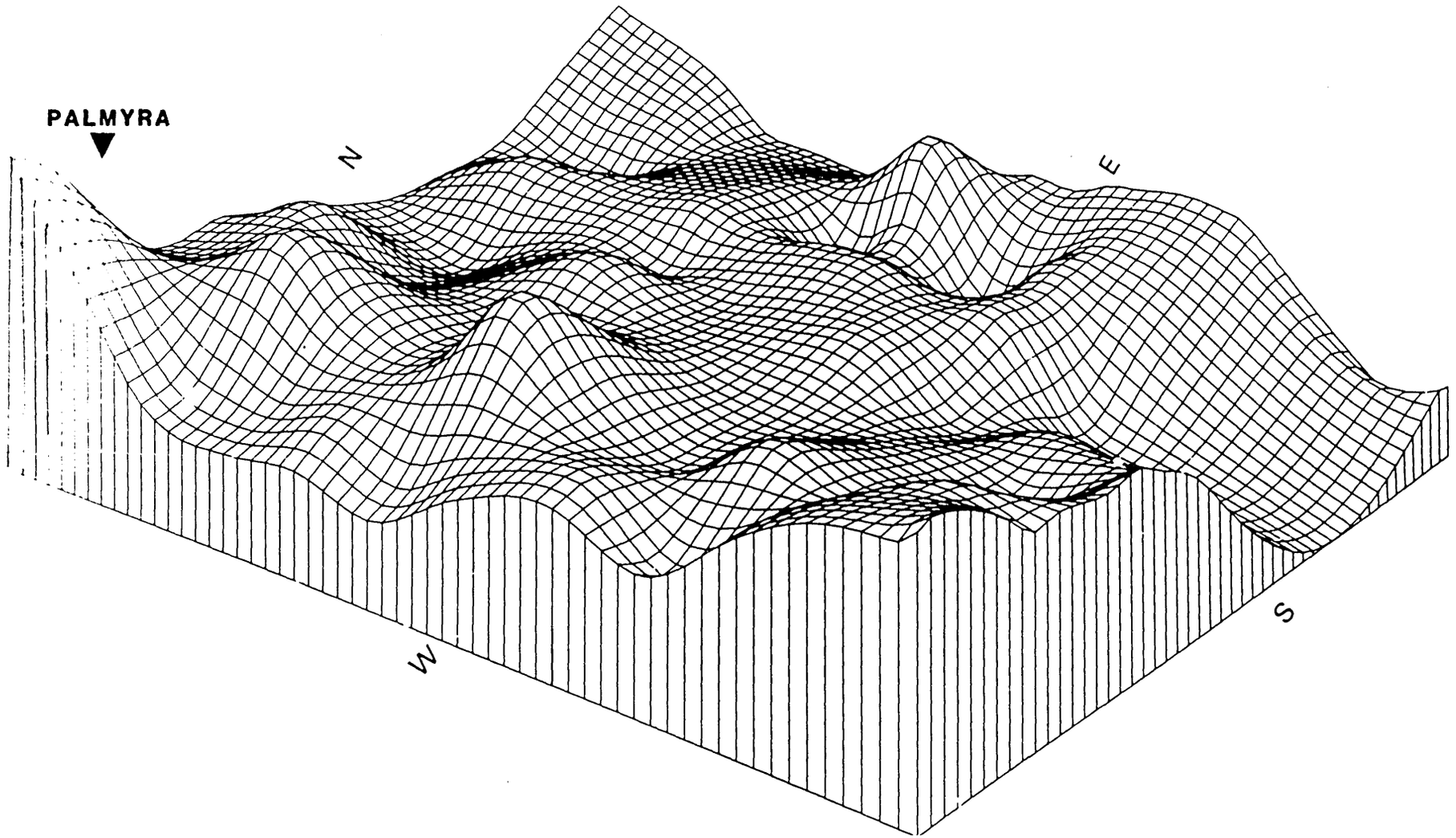


Fig.8.24 Solid surface distribution of the scores of factor 2 association in the sabkha sediments.

shows relatively high negative loadings on Se and to a lesser degree on Sr, U and Mg of one end and low positive loadings on Ca at the other. Upon rotation it produces factor 3 which is characterized by only strong negative loadings on Se. However due to the generally low concentration of Se in the playa sediments. This factor can not be interpreted in terms of geochemistry or geology. Consequently this factor is uninterpretable and can be ignored.

In component 4, which accounts for 6.1% of the data variance, the association Ca, U, As and Sr is positively loaded while Na shows contrasting negative loadings. Such a component can reflect geochemically a carbonate lithotype association. However after rotation factor 4 reveals only strong positive loadings on Ca and to lesser degree on Sr. Accordingly, it is more appropriate to consider this factor as representative of a Ca and Sr sulphate component (gypsum and anhydrite), in which Sr is possibly substituting for Ca in either sulphate or carbonate minerals (Britsch; 1971). Another possible interpretation is that both Ca and Sr can form a calcrete duricrust.

The areal distribution of the factor scores is presented in Fig. 8.25; it shows various levels of distribution especially in the extreme southeastern and northwestern corners, this pattern favours the gypsum anhydrite and duricrust interpretation.

Component 5, which explains 4.5% of the total variance, shows moderate negative loadings on As and negative ones on Se. However, after rotation factor 5 reveals characteristics of strong positive

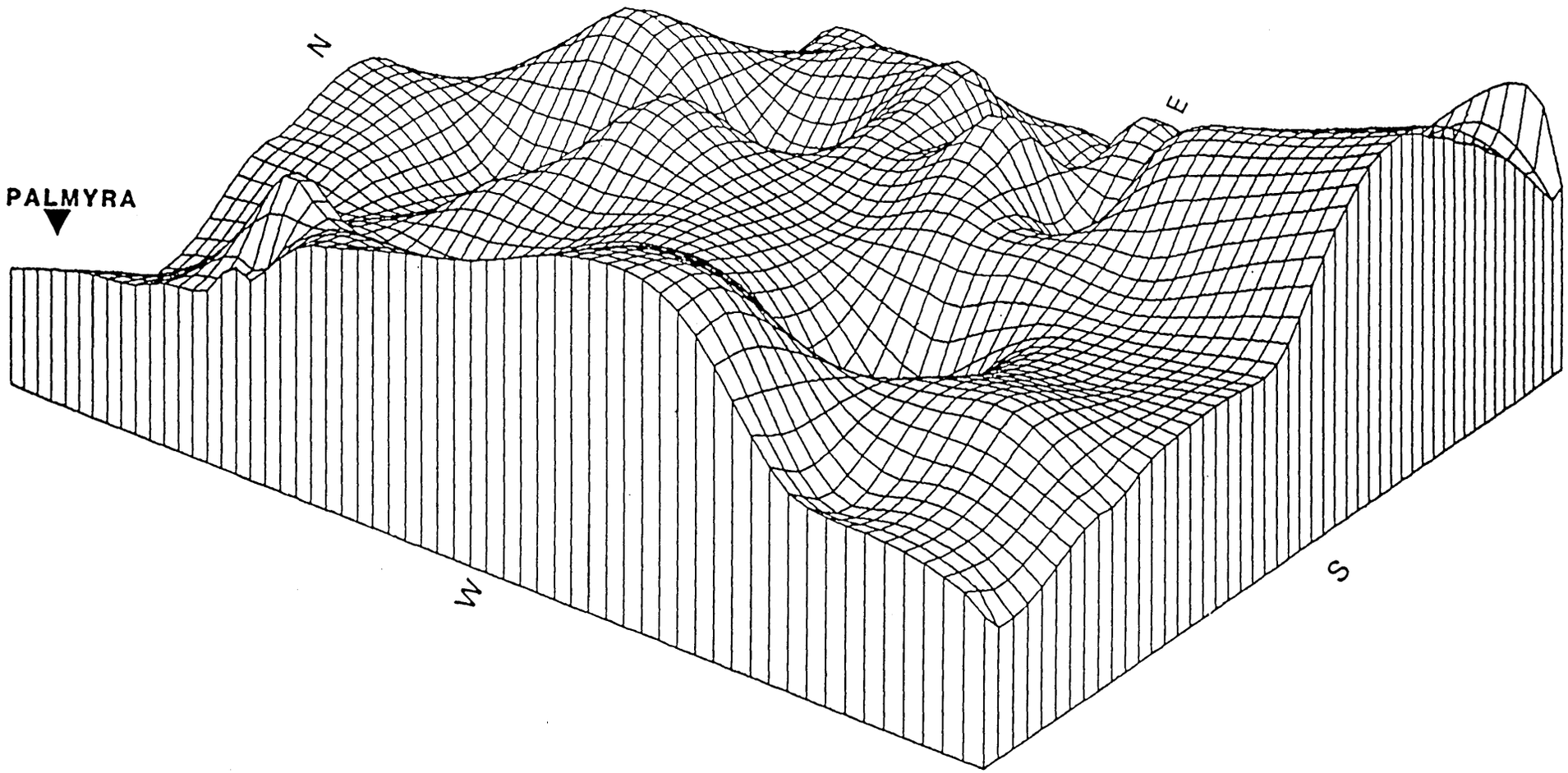


Fig.8.25 Solid surface distribution of the scores of factor 4 association in the sabkha sediments.

loadings on U and As and significant positive loadings on Sr. Both U and As seem to show their highest loadings in this factor (0.80 and 0.70 respectively), confirming a good geochemical association between them in the playa environment. Their association in other factors (although with lower loadings) may indicate that they are present in the sediments in more than one phase. However, factor 5 seems to express certain geochemical affinity as well as reflecting U and As concentration in Sabkhet El Mouh. The areal distribution of the factor scores (Fig 8.26) corresponds closely with the spatial distribution of both U (Fig. 8.13) and As (Fig. 8.14). It is worth noting at this stage that, comparing the distribution of factor 5 with that of factor 1 reveals some sort of similarity in the southern edge of the sabkha and striking differences in the northeastern and northwestern corners. This further suggests that the processes controlling the distribution of U in the sabkha are diverse, and each may account for part of the U content in the sediments. However, the good accordance between factor 5 and the distribution of U in general may permit the interpretation of factor 5 as a U concentration factor. Also, it coincides with the areal distribution of V and Sr, making it an interesting factor for follow-up investigations.

In order to liberate most of the factors from the possible masking effect of factor 1 (56% of the total variance), the elements which showed strong loadings on this factor were excluded prior to rerunning the PCA2 program. The remaining 13 elements gave the factor loadings shown in Table 8.6, which explain 81% of the total variance by only five factors instead of six as in the previous case.

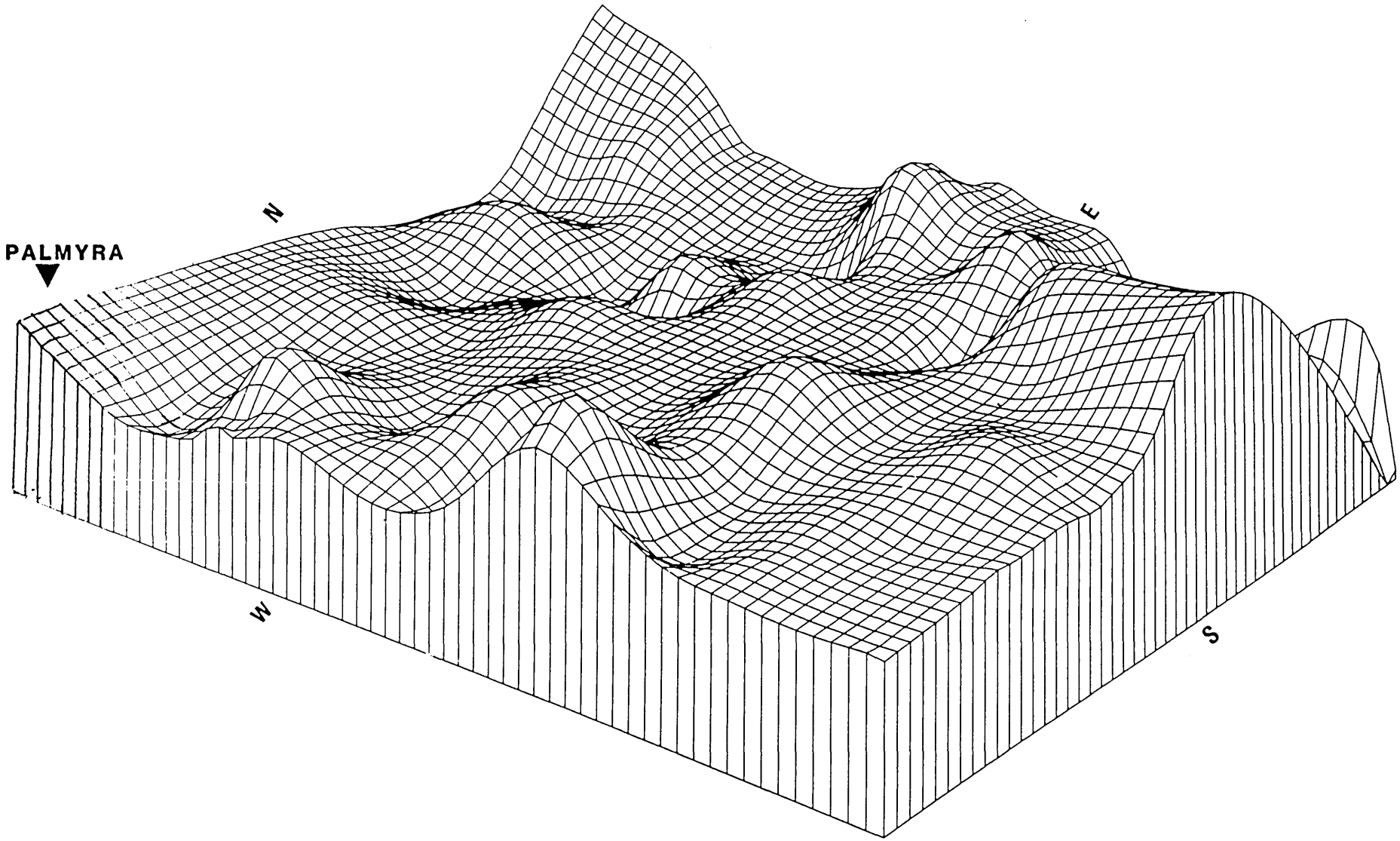


Fig.8.26 Solid surface distribution of the scores of factor 5 association in the sabkha sediments.

Table 8.6 Loadings of five factor model for factor analysis of the sabkha geochemistry.

1 NUMBER OF ROTATION AND VARIANCE AT EACH STEP

0	.2097082
1	.4428224
2	.4505342
3	.4506845
4	.4506860
5	.4506860
6	.4506860
7	.4506860
8	.4506860

NEW ROTATED FACT LOADINGS

	FACT 1	FACT 2	FACT 3	FACT 4	FACT 5
U	-.2690	.0533	.8696	-.0820	.0285
AS	-.2172	-.4664	.7297	.1922	-.0585
SE	.0657	-.1347	-.0243	-.9159	-.0722
P	-.1765	-.8548	.1038	-.2464	-.0780
LI	-.8287	-.2392	.2510	-.0191	.0474
NA	-.8293	-.0623	-.0351	.0849	-.3416
K	-.7938	-.4323	.1828	.0336	.0618
MG	-.7536	.1030	.1859	-.1787	-.1319
CA	.0414	.1606	-.0066	.0799	.9462
SR	-.0854	.7314	.3000	-.2568	.2113
BA	-.0688	-.8006	.2143	-.1732	-.0618
V	-.6561	-.6069	.3484	.0492	.1132
MO	-.7756	.0849	.1456	.1880	.2011

VARIANCE ACCOUNTED FOR BY COMPNTS.

COMPNT	VARIANCE PERCENT	CUM VAR
1	29.0258	29.0258
2	21.5767	50.6025
3	13.1610	63.7635
4	8.6457	72.4093
5	8.8674	81.2767

The largest variance, 29%, is accounted for by factor 1, which is characterized by a strong association of Na, Li, K, Mg, Mo and V. Clearly this factor represents the presence of salt and other evaporitic components in the sediment. It is worth noting that this factor was not brought out as clearly by the previous six factor model, thus illustrating the existence of masking effects in the data represented by the above discussed Fe-oxi-hydroxide and clay fractions.

Factor 2 explains 21.5% of the variance, and indicates the consistent association of P, Ba, Sr, V and As which, as discussed earlier, resembles the phosphorite geochemistry. Thus, this factor can account for the phosphorite component of the sediments.

The third factor accounts for 13.2% of the data variance, and is characterized by significant loadings on U, As, V and Sr. This association invokes the interpretation that factor 3 is an indicator of the presence of some sort of mineralizing solutions or at least a U concentration factor which is not related to processes that can be described solely in terms of adsorption or colloidal precipitation.

The addition of V to the association of U, As and Sr in factor 3 after eliminating what seems to be a masking effect in the data is of special significance. This is because V represents a major compositional constituent of all the secondary uranium minerals encountered in the region, outside the sabkha (section 5.2), and also because V plays an important role in the process

involving the fixation of U in calcrete and other surficial environments and of being partially responsible for the localization of carnotite mineralizations (Boyle, 1984). This finding may further justify the elimination of the elements which account for the masking effects despite their strong presence in the data in order to perhaps enhance or clarify weaker controls in the geochemical data, hence improving its interpretation. However, factor 3 explains a still higher proportion of the data variance, and with U and As being the major contributors to this factor, the enhancement obtained as a result of elimination of Fe, Mn and Al provides further support to the previous interpretation that U is being partially coprecipitated with or adsorbed onto clays and Fe-hydroxides and partially present in other forms. One of these forms may be inferred from the association of factor 3 as being a reprecipitation of U, V, Sr, As and possibly Mo out of an oxidized leachate solution along its route either within the wadi channels or along the fault zone beneath. This may occur due to changes in the redox states or can be caused by evaporation of groudwater rich in these elements.

Factor 4 is only loaded on Se, and, such a factor has no interpretation. Factor 5 explains 8.8% of the data variance and is exclusively positively loaded on Ca and negatively on Na, therefore the best possible interpretation of factor 5 is that it indicates the gypsum rather than the carbonate component in the sediments.

Notwithstanding the foregoing major controls or factors, the existence of additional but minor processes cannot be ruled out. However, PCA and FA define those basic processes and controls that

have evolved the present pattern of the playa geochemistry. Studying the results in the light of factor models 6 and 5, it can be suggested that some factors can be considered lithological factors (2, 4 and 6 in model 6 and 1, 2 and 5 in model 5), others may represent secondary surficial processes (1 in model 6), whereas others (5 in model 6 and 4 in model 5) may express geochemical associations or affinities and may be considered as element concentration factors. Lastly, a few may not have any possible interpretation (3 in model 6 and 4 in model 5).

It is worth noting that the distribution patterns of the factor scores (multivariate data) instead of the univariate data clearly enhances the chances of defining areas of interest, which can then be pointed out on the basis of indicative element associations rather than single element enrichment.

8.7.1 Regression analysis

The relative importance of the major and trace element composition of the playa sediments as possible predictors of the behaviour of U in this environment can be established by application of multivariate regression analysis. Based on reasons given previously the ridge regression technique has been used.

It is apparent from Table 8.7 and Fig. 8.27 that of all 20 variables used, As followed by Mo and V have the strongest positive influence on the behaviour of U in these sediments. On the other hand, K and P are the most stable negative predictors of U. Iron changes from being the strongest positive predictor to a very low insignificant predictor, moving from the least square solution

Table 8.7 Standardized estimators and the regression coefficients for U Vs 19 variables of the sabkha geochemistry.

72 SAMPLES INPUT
DATA MATRIX % 72 OBSERVATIONS 20 VARIABLES

		RIDGE CONSTANT					
	0.00	.02	.04	.06	.08	.10	.15
STANDARDIZED ESTIMATORS							
AS	.5587	.5387	.5225	.5085	.4953	.4826	.4531
SE	.1230	.1266	.1219	.1168	.1118	.1072	.0970
P	-.2082	-.2158	-.1956	-.1807	-.1689	-.1591	-.1402
ZN	.1872	.2334	.1814	.1505	.1295	.1141	.0887
LI	-.0297	-.0678	-.0797	-.0805	-.0776	-.0733	-.0617
NA	.0673	.0294	.0109	.0009	-.0049	-.0086	-.0129
K	-.1710	-.1911	-.1857	-.1751	-.1642	-.1539	-.1321
MG	.2264	.2049	.1997	.1948	.1900	.1855	.1749
CA	-.0177	-.0190	-.0181	-.0166	-.0151	-.0136	-.0103
SR	.2005	.1883	.1882	.1862	.1836	.1809	.1743
BA	.3271	.2321	.1982	.1773	.1622	.1503	.1284
AL	-.0001	-.0291	-.0376	-.0424	-.0453	-.0473	-.0496
LA	-.2234	-.2133	-.1885	-.1672	-.1496	-.1352	-.1082
TI	1.3889	-.4260	-.2678	-.1975	-.1570	-.1304	-.0912
V	.2868	.3036	.2773	.2528	.2325	.2158	.1847
CR	.5683	.2779	.1870	.1411	.1133	.0948	.0679
MO	.3114	.2953	.2847	.2745	.2649	.2559	.2356
MN	-.2572	-.2179	-.1688	-.1372	-.1156	-.1000	-.0745
FE	.6502	.0395	.0198	.0150	.0130	.0119	.0106
MAXIMUM VIF	242.38	35.35	19.33	13.35	10.22	8.29	5.64

Table 8.8 Standardized estimators and the regression coefficients for U Vs 11 variables of the sabkha geochemistry.

		RIDGE CONSTANT					
	0.00	.02	.04	.06	.08	.10	.15
STANDARDIZED ESTIMATORS							
AS	.6811	.6426	.6153	.5932	.5740	.5567	.5193
SE	.1968	.1945	.1905	.1858	.1809	.1761	.1647
P	-.3591	-.3248	-.2885	-.2634	-.2445	-.2294	-.2012
ZN	.2385	.2278	.1605	.1177	.0896	.0703	.0420
MG	.2872	.2266	.2064	.1944	.1858	.1789	.1658
AL	-.1919	-.1787	-.1718	-.1616	-.1511	-.1414	-.1208
LA	.5789	.3661	.2707	.2162	.1808	.1558	.1171
TI	-1.5138	-.6141	-.3848	-.2743	-.2091	-.1661	-.1039
V	-.2175	-.1452	-.1067	-.0812	-.0628	-.0489	-.0254
CR	.4806	.3381	.2806	.2457	.2210	.2021	.1690
MO	-.1624	-.1166	-.0966	-.0848	-.0766	-.0704	-.0596
FE	.7803	.1436	.0726	.0501	.0400	.0346	.0285
MAXIMUM VIF	86.17	26.43	15.94	11.48	8.99	7.40	5.15

Table 8.9 ANALYSIS OF VARIANCE % RIDGE

SOURCE OF VARIATION	SUM OF SQUARES	DEGREES OF FREEDOM	MEAN SQUARES	F-RATIO
REGRESSION	2.57	19	.14	4.9978
RESIDUAL	1.33	49	.03	
TOTAL VARIATION	3.90	68		

MULT. R-SQUARED = .7192 STD. ERROR OF EST. = .1495
VARIANCE OF ERROR TERM = .0224

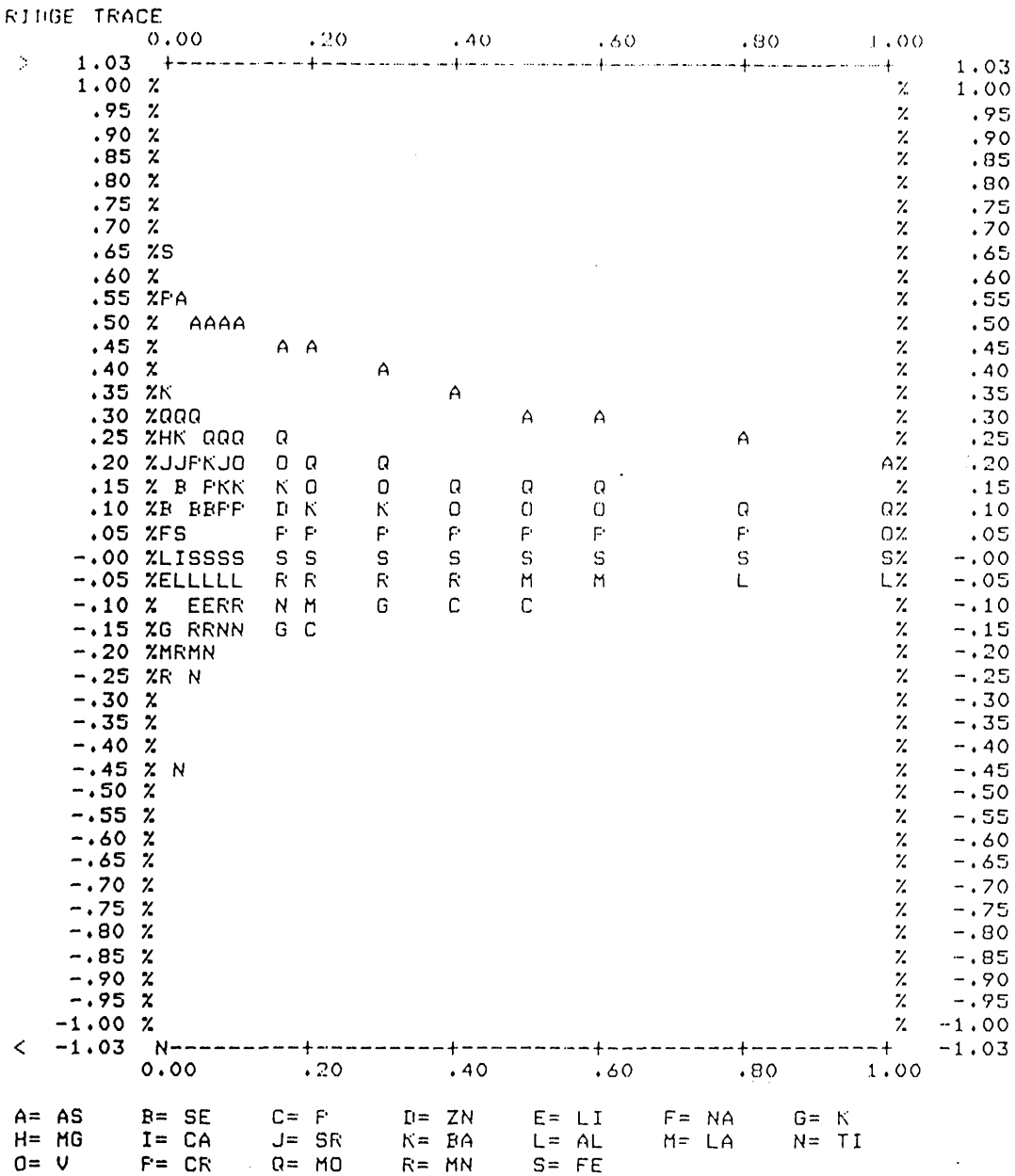


Fig.8.27 Ridge trace of U regression Vs 19 geochemical variables in the sabkha sediments.

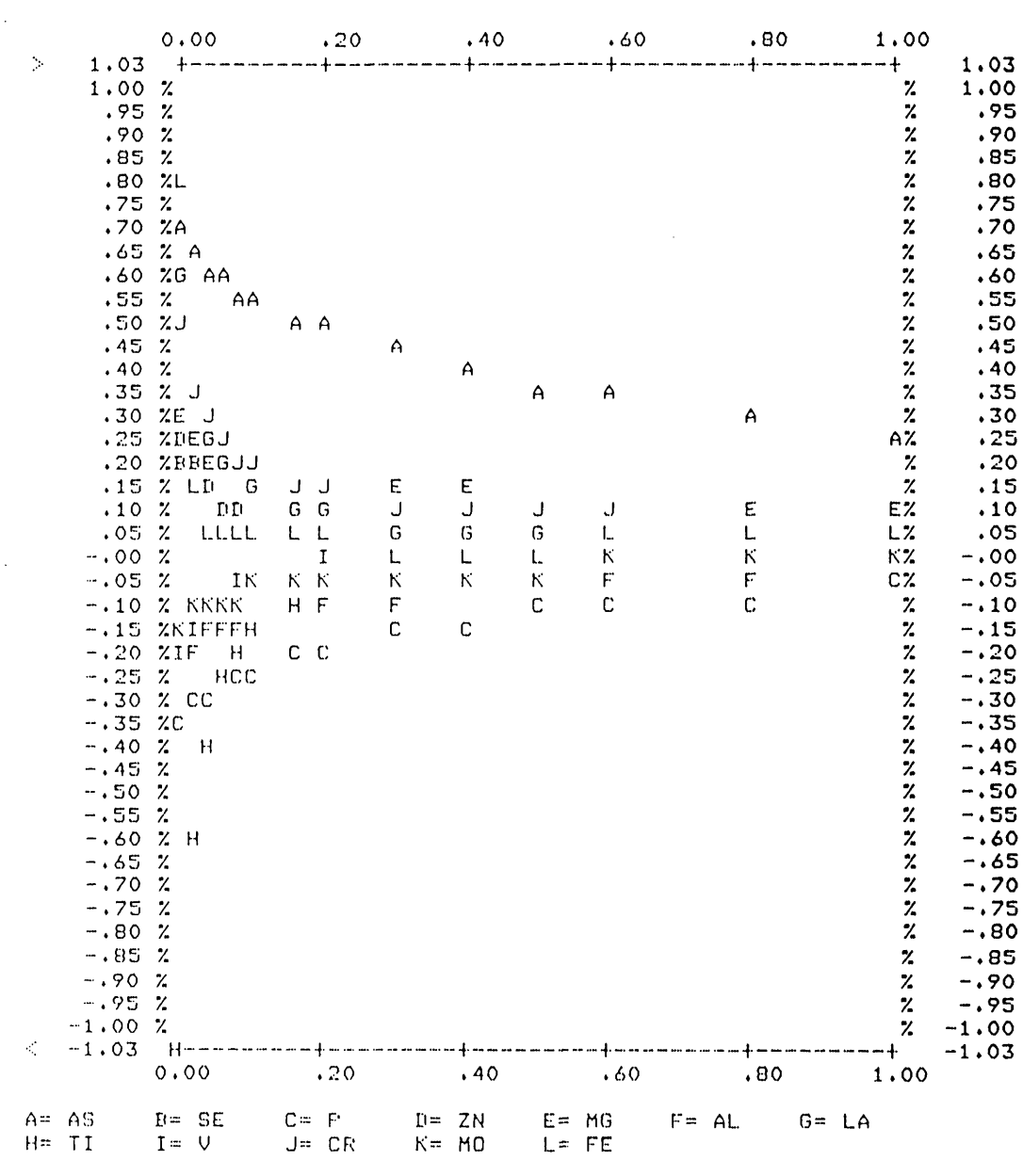


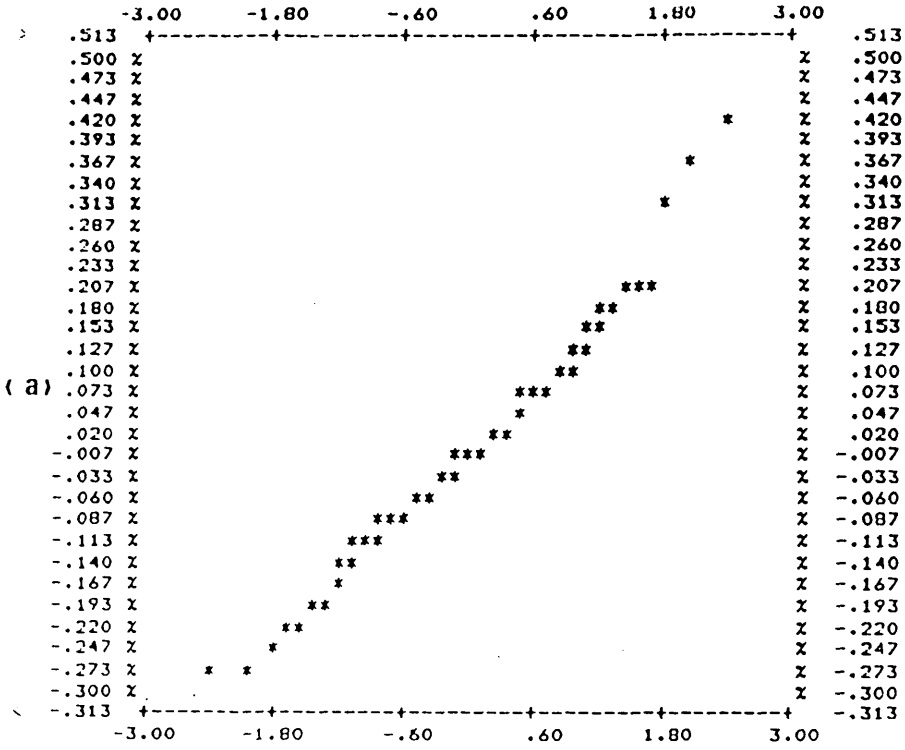
Fig.8.28 Ridge trace of U regression Vs 11 geochemical variables in the sabkha sediments.

(when the ridge constant is zero) to a small ridge constant (K=0.02). Similar unstable behaviour is shown by Cr, Ba and Mg (among the positive predictors) and Ti and Mn (among the negative ones), indicating that they cannot be considered as good U predictors. In addition to being stable, the predictivity of As, Mo, V, P and K has been confirmed in a second regression of U as a dependent variable against only 12 of the independent variables. Results of this regression are summarized in Table 8.7 and Fig. 8.28. According to this solution, Sr can also be identified as a good U predictor in the geochemical environment of Sabkhet El Mouh.

Parameters measuring the significance of this regression (R^2 and F-ratio) are presented in Table 8.7, the F-ratio (4.99) is greater than the critical value of the F-distribution at the 99% level for the corresponding degrees of freedom (F=2.3; Davis, 1973). Therefore the above regression solution is significant. The probability plot of the U residuals resulting from fitting this regression equation is shown in Fig. 8.29a along with the plot of their redistribution into the whole data set (72 samples), this also outlines the presence of anomalous U samples (Fig. 8.29b)

Considering the foregoing regression results in the light of the findings of other multivariate techniques used earlier, U and its stable predictors seem most likely to be derived from one source, whereas the unstable predictivity of Fe, Al, Mn, Ba and Ti clearly confirm earlier interpretations that these elements have a minor control on U behaviour, especially in the anomalous samples, while they may show close association with U in its background values. The exact mechanism for such an association, however, is

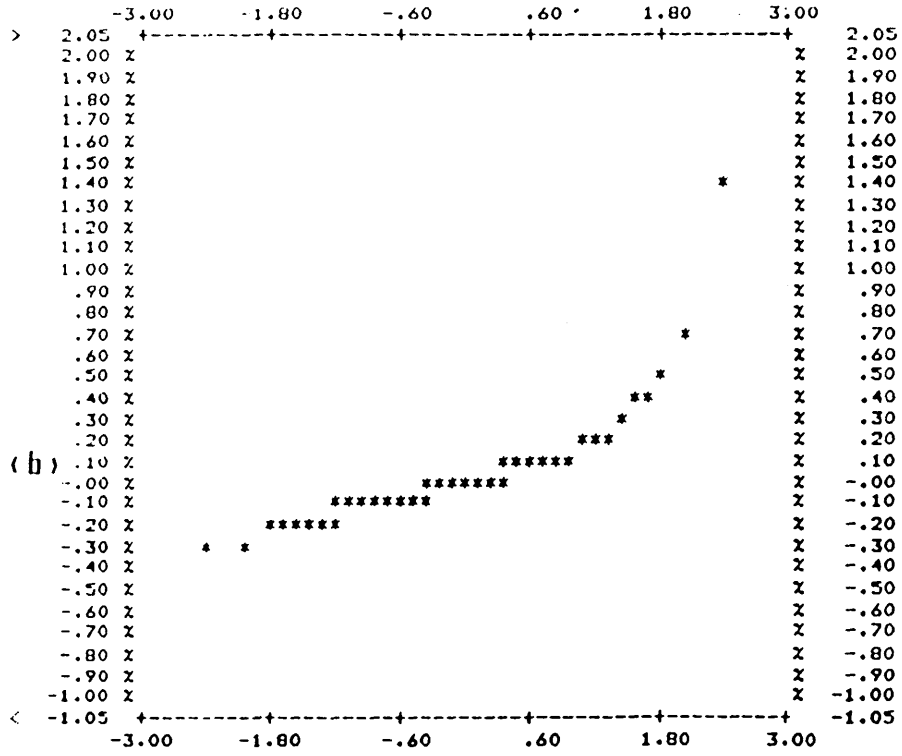
RESIDUAL PROBABILITY PLOT



(a)

SMALLEST RESIDUALS		LARGEST RESIDUALS	
8500	-.28145	8600	.42006
7400	-.27548	4700	.35423
5700	-.24963	9000	.32034
6500	-.23228	4500	.21421
5400	-.20747	7100	.20955
6100	-.19038	2600	.20584
6700	-.18869	5600	.18235
663000	-.17640	6600	.17564
4900	-.13846	3300	.14713
3200	-.13539	2700	.14558
4000	-.11394	2900	.13344
3100	-.11368	5200	.11848
8300	-.11294	8900	.10588
5900	-.11221	7800	.10257
8200	-.09719	3700	.09501

RESIDUAL PROBABILITY PLOT



(b)

Fig.8.29 Normal probability plot of U residuals in the sabkha sediments.

unknown or unclear, but all the indications which are discussed above (especially factor 1) promote similarities with those of sorption, ion exchange and coprecipitation mechanisms reported by Culbert et al., (1984) during their studies of the surficial U deposits of Canada and by many others (Borovec, 1981; Michel et al, 1982; and Samama, 1984) in their explanation of the close relationships of U and Fe-hydroxide and clay complexes. It should be stressed however, at this point that investigating the distribution of anomalous U samples shown by the regression and factor analysis indicates that they do not coincide with the main trend of Fe, Ti, Mn and Al association. Hence, U anomalies are not directly related to scavenging or adsorption mechanisms and therefore can be classified according to Jubeli (1981) as true anomalies.

In general, it can be said that using the geochemical derivatives of the multivariate techniques has shed some light on discriminating between more than one phase or pattern of element distributions and thus may aid the selection of areas of interest.

8.8 Conclusions

Taking into account all the foregoing investigations, discussions and results, the following conclusions regarding the geochemical behaviour of U and its associated elements in Sabkhet El Mouh samples can be drawn.

1) Multielement playa geochemistry has indicated that surficial as well as other processes have been continuously acting upon, and changing the lacustrine and alluvial deposits that have filled

the sabkha. Some of these processes have weakly enriched U in the playa sediments.

2) About one seventh of the samples reveal enhanced U concentrations. However, no secondary U minerals were found. Instead geochemical evidence for coprecipitation on clays and Fe-hydroxides and redistribution due to evaporation was supported by the various multivariate statistical techniques used in the study to achieve its aims.

3) The geochemical data also reveals enhanced levels of Mg, Sr, Li and other alkalis reflecting Mg-salts, dolomite and other evaporitic components.

4) In general, there are indications of elemental variations along the wadi channels particularly where they discharge their alluvial loads into the sabkha. This is markedly evident in its northeastern corner as well as its southern side. It seems likely therefore, that processes such as erosion, leaching and migration, transportation, deposition and diagenesis are relatively active, and can be held responsible for the observed variations. Other variations are caused by reactions of the sediments with the hydrologic regime due to the fluctuations of the groundwater table.

5) Compositional variations in depth were only evident in a few samples. Although no definite conclusion can be drawn due to the very limited number of samples involved, results of this work suggest that a more condensive investigation along this line should precede further surveying.

6) Using multivariate techniques and to a lesser degree univariate ones, it was possible to point out potentially favourable locations for further detailed U exploration (e.g. the area extending from the southern edge of the sabkha towards its northeastern corner).

CHAPTER IX

9. LITHOGEOCHEMISTRY OF THE PALMYRIDES.

9.1 Introduction

The principles of whole rock geochemistry in mineral exploration and various primary halos were usefully discussed by Beus and Grigorian (1977); Govett (1983); Koval (1984) and Smee and Bailes (1986).

Lithogeochemical methods can be used in reconnaissance (regional) as well as detailed (local) surveys (Boyle, 1984; Nurmi and Isohanni, 1984). The effectiveness of the methods in outlining geochemical provinces whose rocks contain higher than normal amounts of particular element(s) (e.g. U, Au, Cu, Mo, Pb, Zn and Sn or W provinces) is well documented (Boyle, 1982; Simpson and Plant, 1984).

Several workers, using lithogeochemical studies, have discussed the distribution of U in rocks as a guide to recognition of uraniferous regions. Darnley et al. (1977) suggested that direct rock sampling and analysis provides the ultimate control on regional studies of U distribution. Simpson et al. (1977) using lithogeochemistry coupled with lexan fission track analysis showed that U is enriched in the Hercynian granites of southwest England relative to the Caledonian granites of Scotland. They concluded that U occurs in primary mineral phases such as apatite, monazite, sphene and zircon. Their work demonstrates the importance of the

mineralogical control on U behaviour. In a later work, Simpson et al. (1979) suggested that U enriched granitic magmas are derived from subcontinental lithosphere underplated onto pre-existing basement; U mineralization in the crust occurs as a result of the interaction of the epizonal meteoric water with U-rich and volatile-rich magma. Watson and Plant (1979) added to this model the role of deep seated faults and magmatic activities to explain the U enrichment in the Old Red sandstone of the Orcadian basin of Scotland which reflects both regional and local factors. Plant et al. (1980) and Simpson et al. (1982) proposed the terms "metalliferous" and "mineralized" granites to distinguish intrusions with a high primary magmatic concentration of U and other metals from those associated with metalliferous mineralization as a result of water-rock interaction. In their discussion of high heat production granites and their role in forming U provinces, Simpson and Plant (1984) concluded that the development of U mineralization associated with granites depends on magma emplacement in adequately hydrous environments and that their model can be applied to understanding the genesis of U mineralization, thus enabling reliable exploration criteria to be established and targets identified. In more recent work Simpson et al (1985) and Simpson and Hardely (1985) reported high U potential in the Bushveld complex and concluded that U has been reconcentrated by sedimentary processes into younger formations such as the Karoo sequence. Plant et al. (1985) demonstrated through detailed lithogeochemical work using the lithophyle elements (U, Th, Rb, Cs and K), the incompatable elements (Ba, Mo and Li), and the REE the ability to discriminate three different suites of Caledonian granites. They also described the

redistribution of U, Th, K, REE and other elements from primary to secondary and hydrothermally altered sites. Also, they modelled criteria for the recognition of weathered and hydrothermally altered granites.

Very many publications during the last three decades demonstrate the application of a lithogeochemical approach in U exploration, mostly in intrusive and extrusive igneous rocks, metamorphic rocks and sandstone-type sedimentary rocks (Boyle, 1982; Govett, 1983; IAEA, since 1970 to 1985). Roll-type or basal-type U deposits are also associated with U-rich igneous rocks (Roshold et al. 1973; Stuckless and Nkomo, 1978; Boyle, 1985).

However, except for studies of U in phosphate rocks (McSwiggen et al., 1986; Molt and Drever, 1983 and Jeanmaire, 1985), and U in calcrete-type U deposits, very little lithogeochemical exploration work in carbonate rocks have been reported (Rose and Wright, 1980). The main problem in the use of carbonate rock geochemistry for U exploration is the variable composition and the variable amount of impurities. Furthermore, the U content of pure carbonate is usually very low (less than 4ppm U). Bell (1963) has reported that U content of carbonates varies considerably with the content of impurities such as clays, organic matter and phosphates.

9.2 Aims of lithogeochemistry in this study

Application of lithogeochemistry as an exploration method was used to achieve the following objectives.

a) to define regional geochemical trends in outcropping rocks;
b) to establish elemental patterns associated with U, recognizing their responses petinent to its enrichment i particular lithostratigraphical units or rock types, and whether any of these patterns can be used to locate U mineralization;
c) to delineate areas of mineral potential.

9.3. Surface geology and the phosphorite rocks

9.3.1 Surface geology

The region is underlain by a thick series of marine sediments which range in age from Triassic through Oligocene as a result of many sedimentary cycles. These marine sediments were then overlain by alluvium, lacustrine and other continental formations of the Neogene and Quaternary. A major unconformity is found between the lower Neogene (Miocene) and upper Palaeogene (Oligocene) series. The general distribution and apparent thickness of the whole sedimentary sequence are reflected in the surface geology of the region (Fig. 9.1), and the simplified lithostratigraphical column (Fig. 9.2).

The oldest outcrops are those of evaporite, dolomite and dolomitic limestone rocks of Triassic and Jurassic age, encountered in the core of most of the Palmyrides mountains. These mountains consist mainly of Cretaceous rocks while the surrounding hills and plateaux are formed of Palaeogene rocks. The basins and synforms are filled with Neogene deposits and covered by Quaternary proluvium, alluvium and windblown sands and debris.

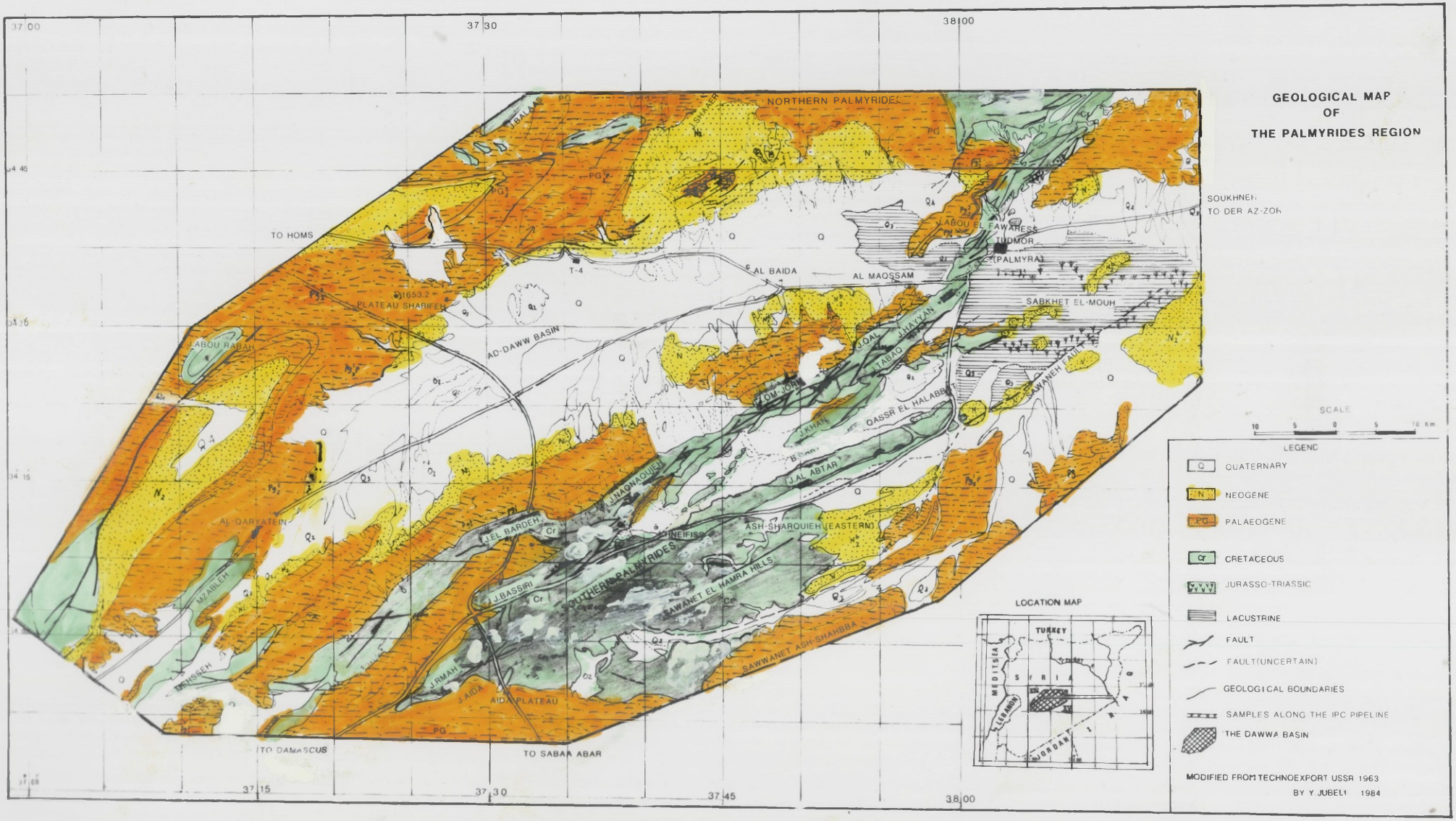


Fig. 9.1 Surface geology of the Palmyrides region.

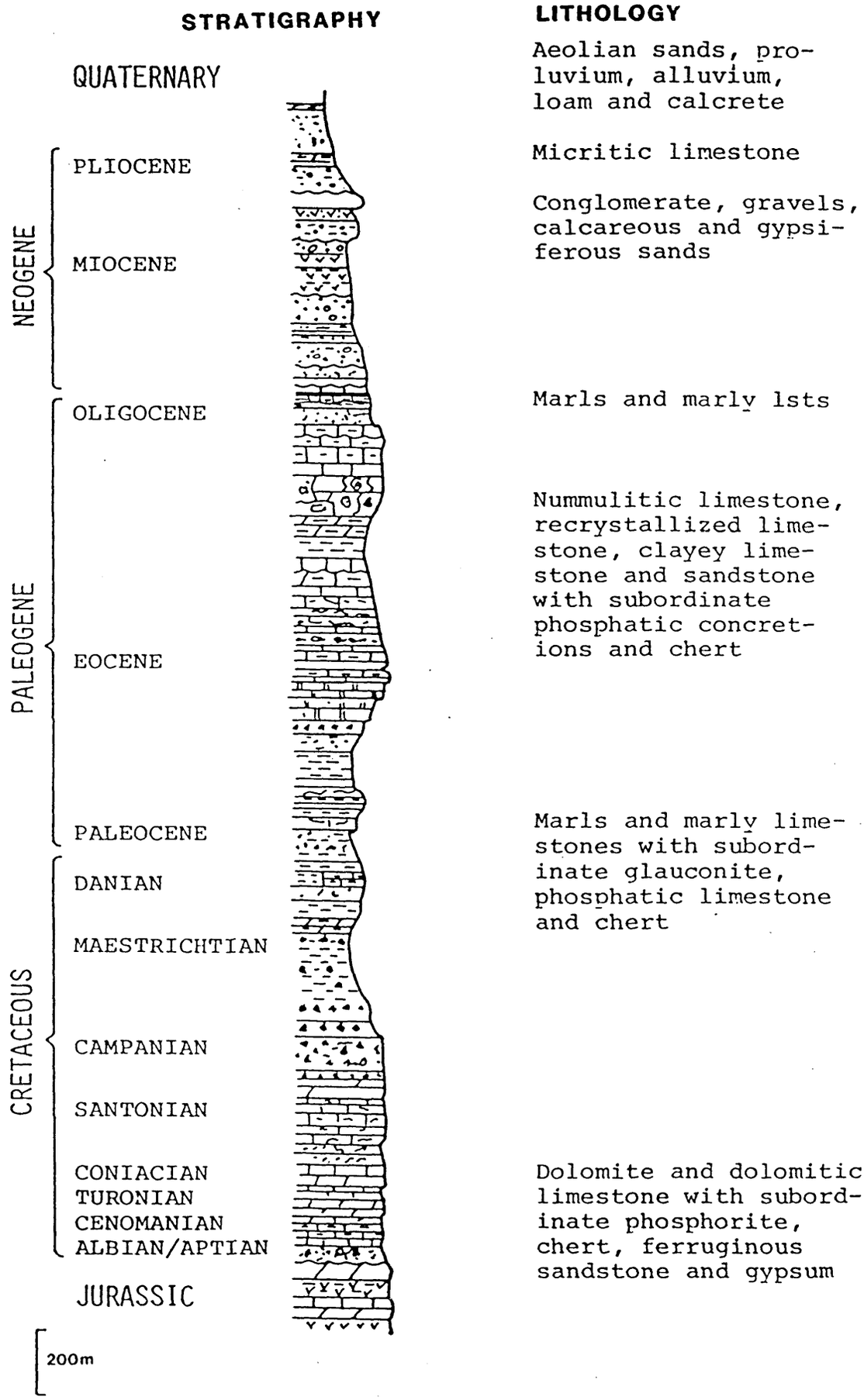


Fig.9.2 Simplified lithostratigraphic column.

9.3.2 The Palmyrides mountain belts

The three main mountain belts in the Palmyrides region, namely, northern, central, and southern were traversed. The watershed in the northern belt is made of Turonian dolomite and dolomitic limestones, whereas the limbs are made of Upper Cretaceous and Lower Palaeogene marly limestone, chert, phosphorite and marls. A few important wadis are present, draining the southern limb, such as Az Zakarra, El Jzel, Al Dalil, Jhar valley and W. Er-Khieme.

The central belt consists of mainly Palaeogene rocks except the case of J. Abou Rabah where the strongly deformed Upper Cretaceous rocks are outcropping.

The southern belt is a chain of narrow, linearly streched anticlinal echelon-like folds. The common features of which were discussed earlier. The body of the mountains is made of Middle Cretaceous carbonate rocks, and the flanks are made of Upper Cretaceous carbonate, phosphorite, chet and marls.

9.3.3. The basins

The two basins discussed in Chapters VII and VIII form the major synform of the region: Ad-Daww basin separates the two northern and southern Palmyrides, and the Sabkhet El Mouh basin which occupies the area south and southeast of Palmyra.

9.3.4 Phosphorite deposits of the Palmyrides.

Platform type marine sedimentary phosphorite of granular and mixed texture are widely distributed in the area. The commercially workable deposits are confined to the Upper Cretaceous (Campanian-Maestrichtian).

There are at least two major Campanian phosphatic beds nearly everywhere in the Palmyrides, but the total number varies in different sections from 6 to 12. The thickness of the beds varies widely from 0.4m to more than 12m.

The Maestrichtian sequence is made up of marls, marly limestone, glauconitic limestone, varigated clay, phosphate with oysters, intercalations of chert bands and lenticular flints. There are commonly 3 to 8 phosphate beds, which may increase to 13 to 20. In surface outcrops these beds noticeably differ from the Campanian ones by their whitish colour, clayey matrix and by yeilding to weathering. Both carbonate and siliceous varieties of phosphorites are found.

Danian and Palaeocene sequences contain a few single horizons of concretionary phosphorite. However, only at Ghadir El-Hamel do the Danian formations incorporate thin laminae of granular phosphate.

The Lower Eocene formations contain, at the base, non-persistent phosphorite beds alternating with limestone and glauconitic limestone. Younger Lower Eocene series of Jabal

Sawwanet Ash-Shabha contain three granular phosphorite beds, each 0.1 to 0.7m thick with a lower P_2O_5 content ranging from 6 to 15%.

9.4 Uranium content of the Palmyrides phosphorite.

Uranium was analysed in a few phosphorite samples during the geological mapping by Technoexport workers (USSR). Results gave a range of 10 to 105 ppm uranium. On the other hand uranium in some phosphorite samples taken by Western Knapp Engineering (USA) from the main phosphorite formation in Ghadir El Hamel and Er-Kheime deposits was chemically analysed by the Battelle Memorial Institute (Ohio, USA) in 1963. Their results gave a range of 23 to 130 ppm uranium. Estimations of U_3O_8 content in the phosphorite was determined by Liaschenko and Tatarnikov (1968). These results showed a range of 30 to 160 ppm U_3O_8 with an average U_3O_8 concentration of 100 ppm at the Khneifiss deposit and 65 ppm at the Eastern deposit. Moreover, Hunting (1975) reported uranium in the phosphate samples listed in Table 9.1 which was determined by neutron activation analysis at the Atomic Weapons Research Establishment reactor at Aldermaston. The range of uranium concentrations is 25 to 136 ppm, not greatly dissimilar from earlier results. The above reported results indicated that the content of uranium in the Syrian phosphorites is similar to that recorded for most marine phosphorite, not only from neighbouring countries (Al-Bassam et al. 1983; Reed and Saadi 1971) but also from others in the Mediterranean and North African phosphorite (McArthur; 1974) and other world-wide phosphorite formations (Gulbrandsen, 1966; Cook, 1974; De Voto and Stevens, 1980).

Table 9.1 Geochemical data on U and P_2O_5 in the palmyrides phosphorites (from Hunting, 1975).

Location	Sample number	R/hr in situ	ppm U	P_2O_5
Khneifiss	1C	75	103.5	32.06
	2C	75	107.0	33.13
	3C	75	109.0	32.47
	24C	85	114.5	32.90
	4C	100	130.5	35.65
	4D	-	124.0	34.65
	21C	110	136.0	34.71
	5C	100	105.0	29.71
	5D	-	114.0	29.90
	19C	100	87.0	30.50
	22C	80	103.5	28.64
	23C	55	73.0	24.08
Eastern A	33C	40	52.0	30.87
	34C	40	59.5	31.76
	35C	40	58.5	30.45
	27C	45	45.0	23.67
	6C	45	27.5	25.55
	7C	--	33.0	33.50
	6D	35	34.5	30.97
	31C	--	40.0	29.51
	31D	35	36.0	33.04
	7D	--	34.0	32.49
	32C	30	19.0	13.63
	32D	--	23.5	16.54
	9C	60	64.5	32.40
	28C	30	16.5	23.49
	29C	60	60.5	34.97
	30C	40	30.5	24.33
	25C	50	49.0	20.94
	25D	--	99.0	27.77
	26C	45	66.0	27.34
Eastern B	38C	40	51.5	28.23
	39C	40	49.0	28.19
	12C	50	63.0	20.23
	AN3C	--	83.0	25.23
	AN4C	--	108.5	30.73

(from Hunting, 1975)

9.5 Sample locations and analysis

9.5.1 Sample location

Sampling methodology was discussed in Chapter IV. Nine traverses across the Palmyrides region were sampled by collecting surface rock chips and unconsolidated Quaternary rocks from outcrops as unweathered as possible. The traverses were numbered sequentially in multiples of hundreds 100, 200, 300....etc., and within each travers samples were also numbered sequentially starting at 1 from the southeastern end. As shown in Figs. 9.3 and 9.4, sampling was undertaken at varying intervals depending on the stratigraphic and lithologic units sampled. A total of 467 samples was taken from: all main lithostratigraphical units (405 samples); a separate group of 57 phosphorite samples was collected from the phosphorite mines and other major deposits within the limits of the surveyed region (Khneifiss, Eastern (Ash-Sharqueih), Al-Abtar and Central phosphorite deposits). The aim of the latter sampling was to compare the phosphorite U and P contents with those phosphate rocks taken along the traverses, as well as with some of those reported earlier by other workers. (Five grab samples which were collected for their high radiometric measurements not included in the systematic investigations). The flow diagram (Fig. 9.5) illustrates all these rock groups.

The spatial distribution of the samples along each traverse could be related to a typical representative geological cross-section, trending SE to NW, transecting the main geomorphological, stratigraphical and lithological units found in

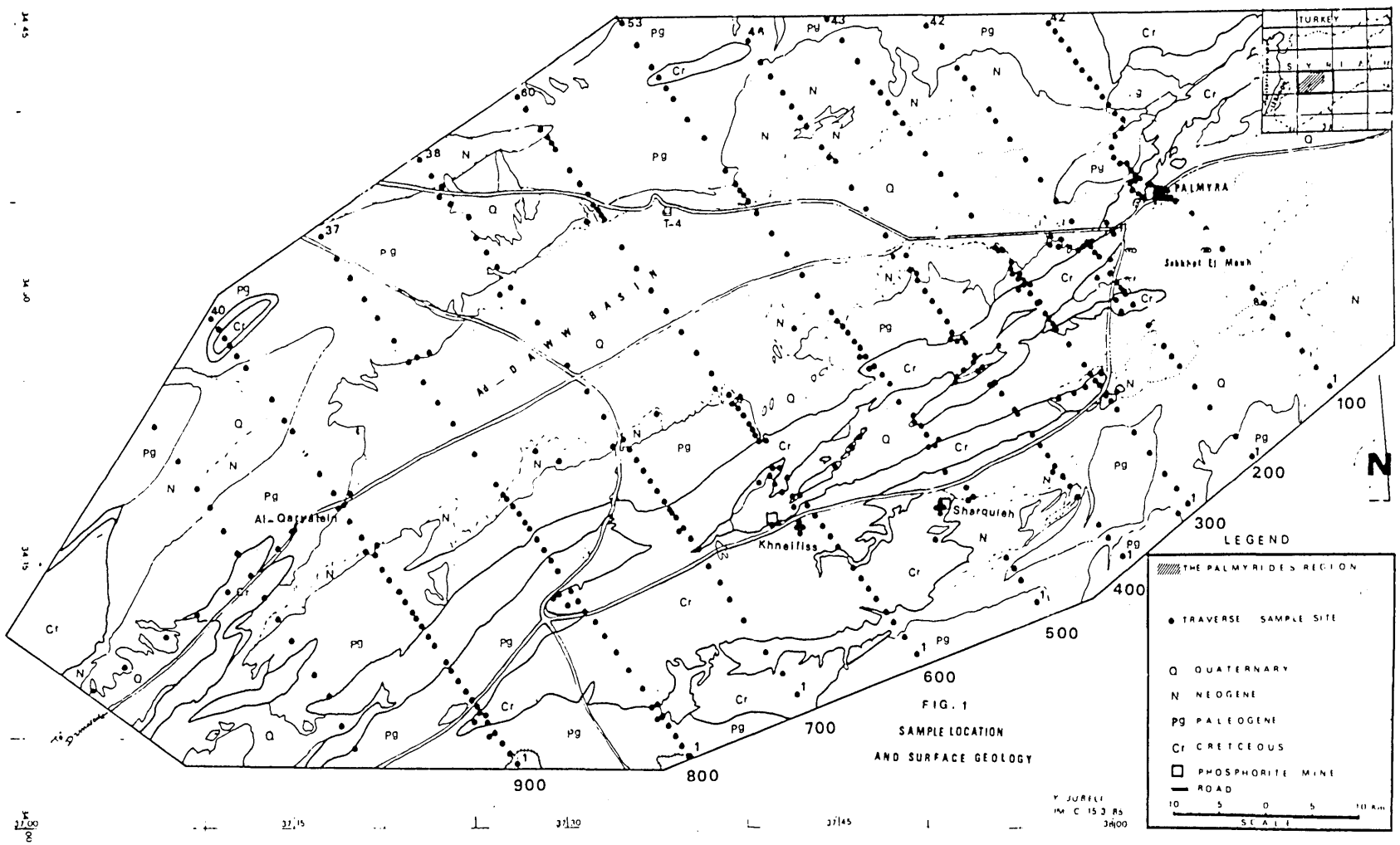


Fig.9.3 Sample location in relation to surface geology.

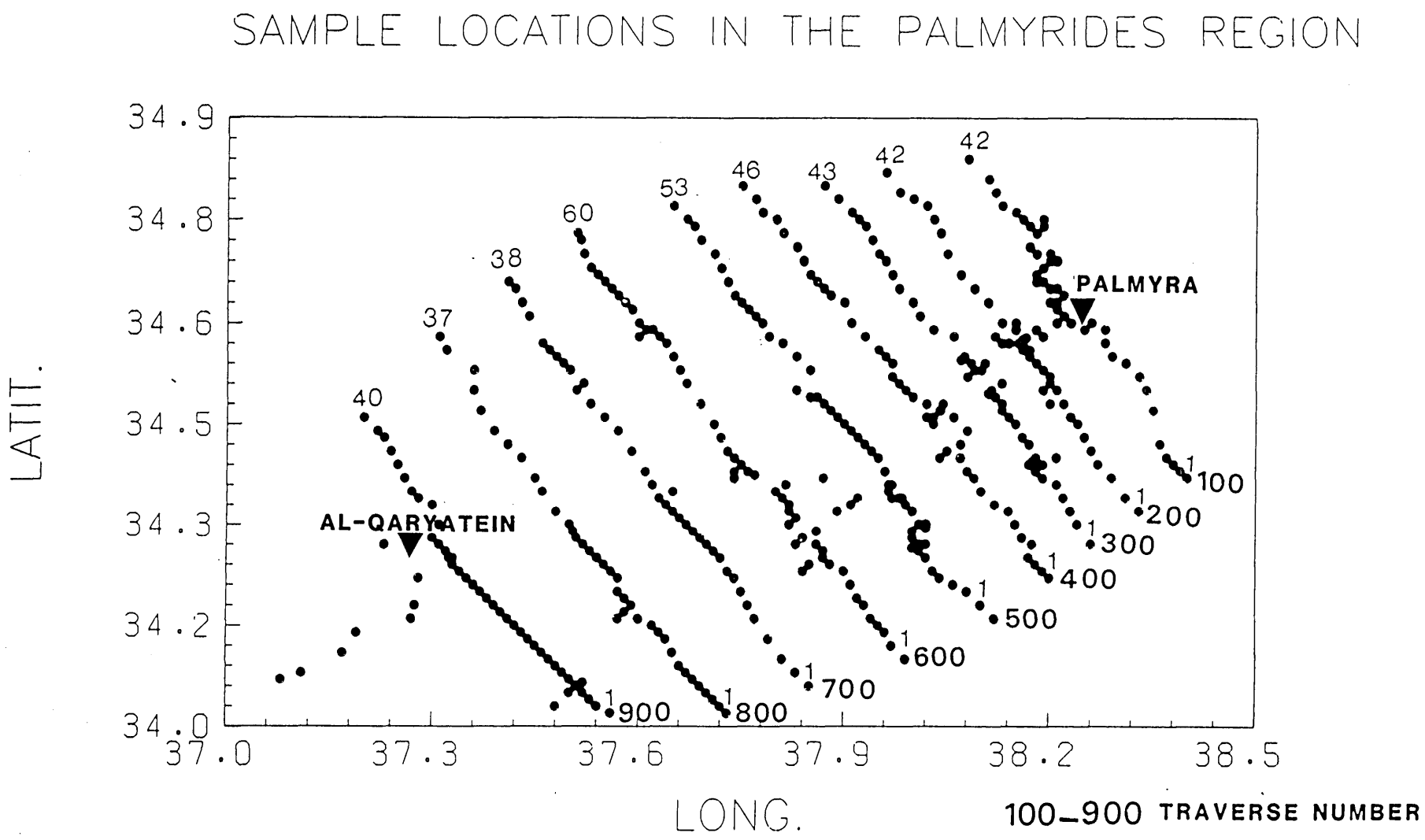


Fig.9.4 Sample location in each of the nine traverses.

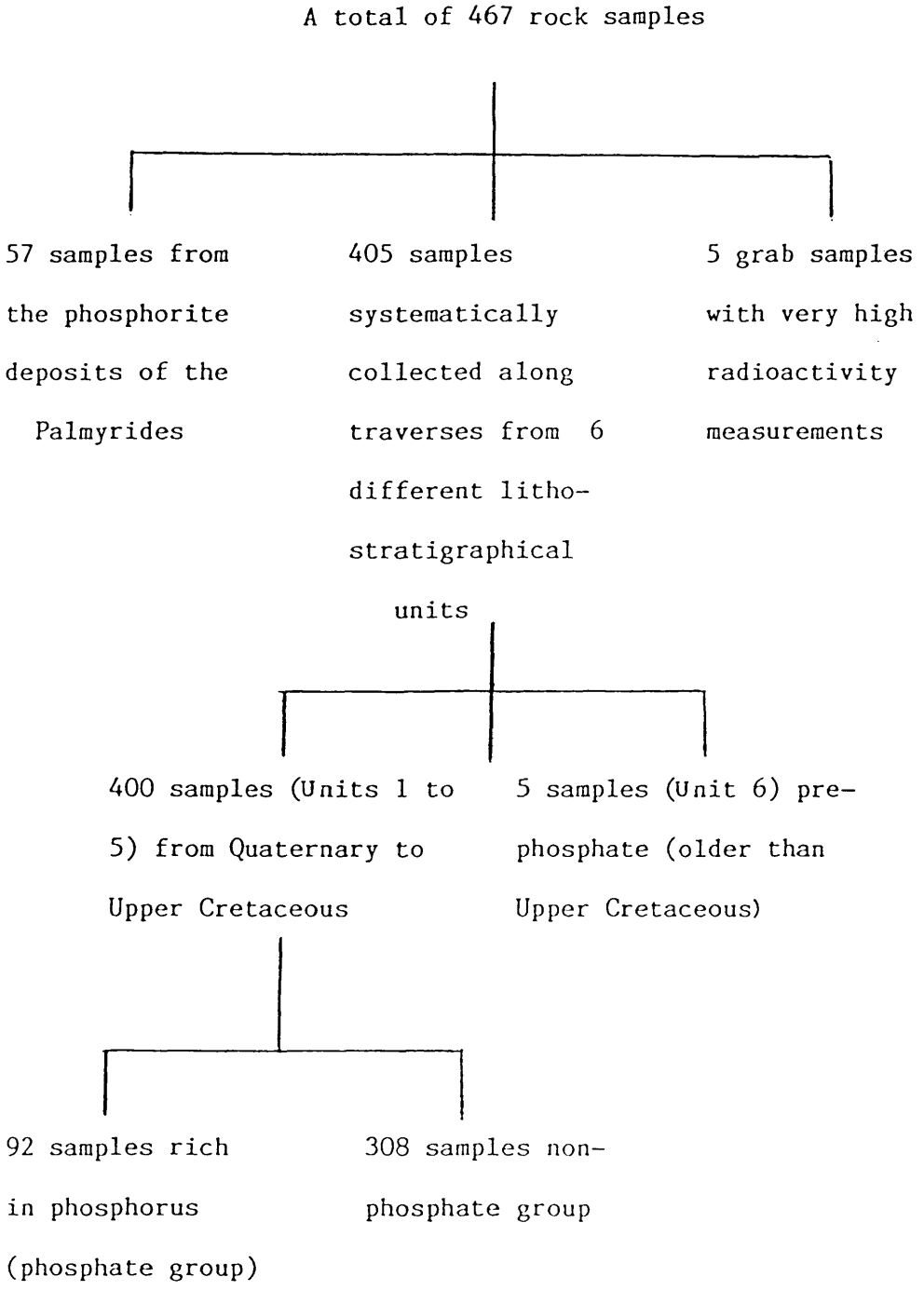


Fig.9.5 Flow diagram of the sampling scheme.

the region and outlined in Fig. 9.6 and Table 9.2. This section coincides more or less with traverse 600, therefore, distribution of elements in this traverse could provide a general guide to the geochemistry of the above mentioned units.

9.5.2 Analysis and data control

Samples were crushed, ground and sieved through 90 μm nylon sieve, then the fine material was analysed with determination of: 25 major and trace elements by nebulization ICPAES; and hydride generations and ICP determination of As, Sb, Bi and Se. Uranium, Th and La and other REE were measured by neutron activation analysis using both, the ^{239}Np peak at 106.6KeV and the ^{239}U γ-ray at 74.7 KeV (Parry and Jubeli, 1986). The precision for U in the rocks ranges from 1 to 5%, while it is slightly poorer for Th ranging between 5 to 10% (Fig. 9.7), perhaps due to Gd and Sm interferences. Elements such as Rb, Be, Ag, Bi and Sb show very low concentrations in a relatively large number of samples; therefore, they are not reported here.

9.5.3 Petrography and mineralogy

Detailed petrographical, biostratigraphical and mineralogical studies of the major rock units of the region were carried out as part of a recent geological mapping of selected cross-sections over the entire territory of the Palmyrides (Mouty et al. 1983). Except for a limited X.R.D., electron microprobe analysis and optical and scanning electron microscopy, no further detailed petrographical or mineralogical studies were attempted in the present reconnaissance

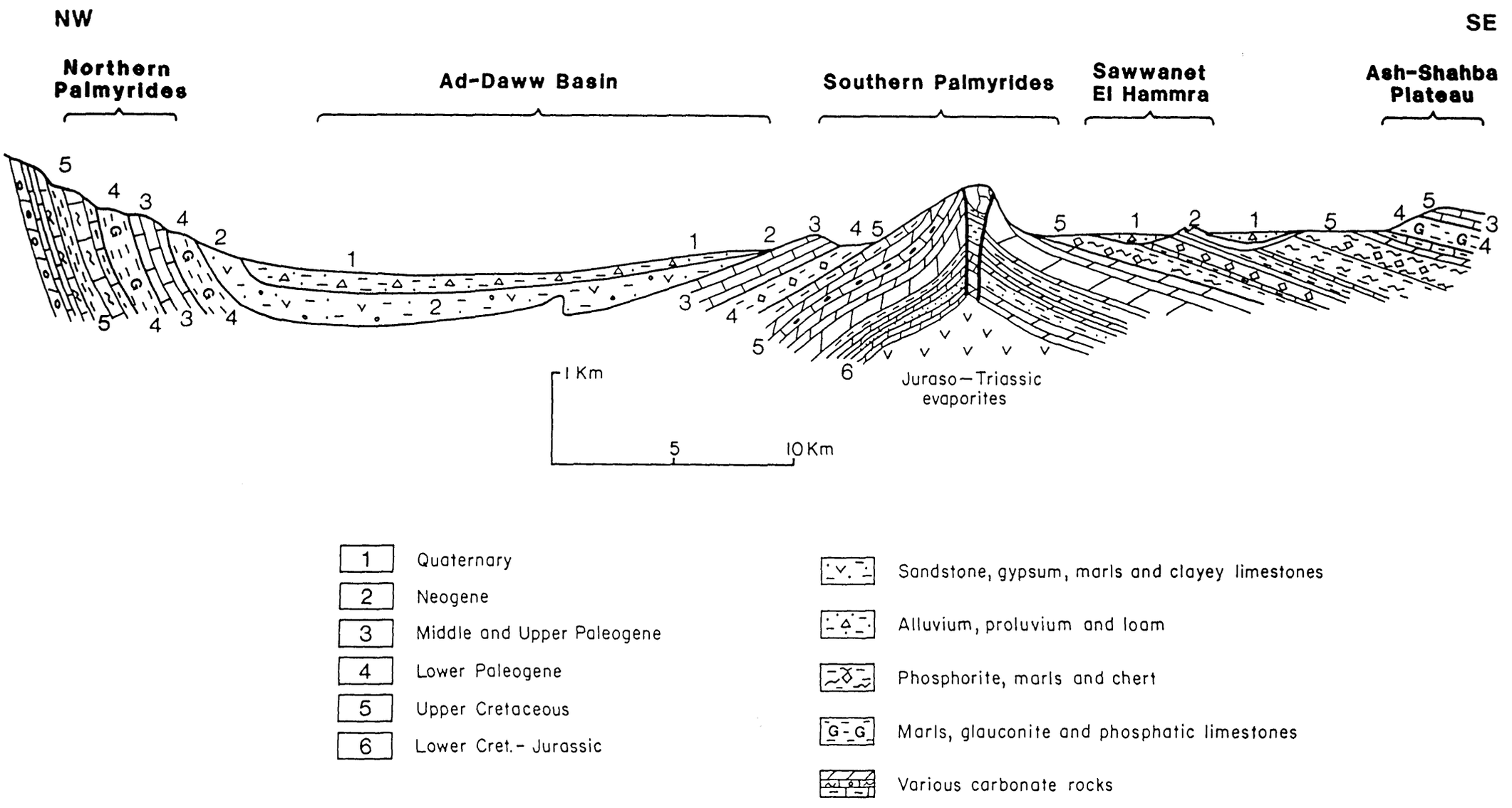
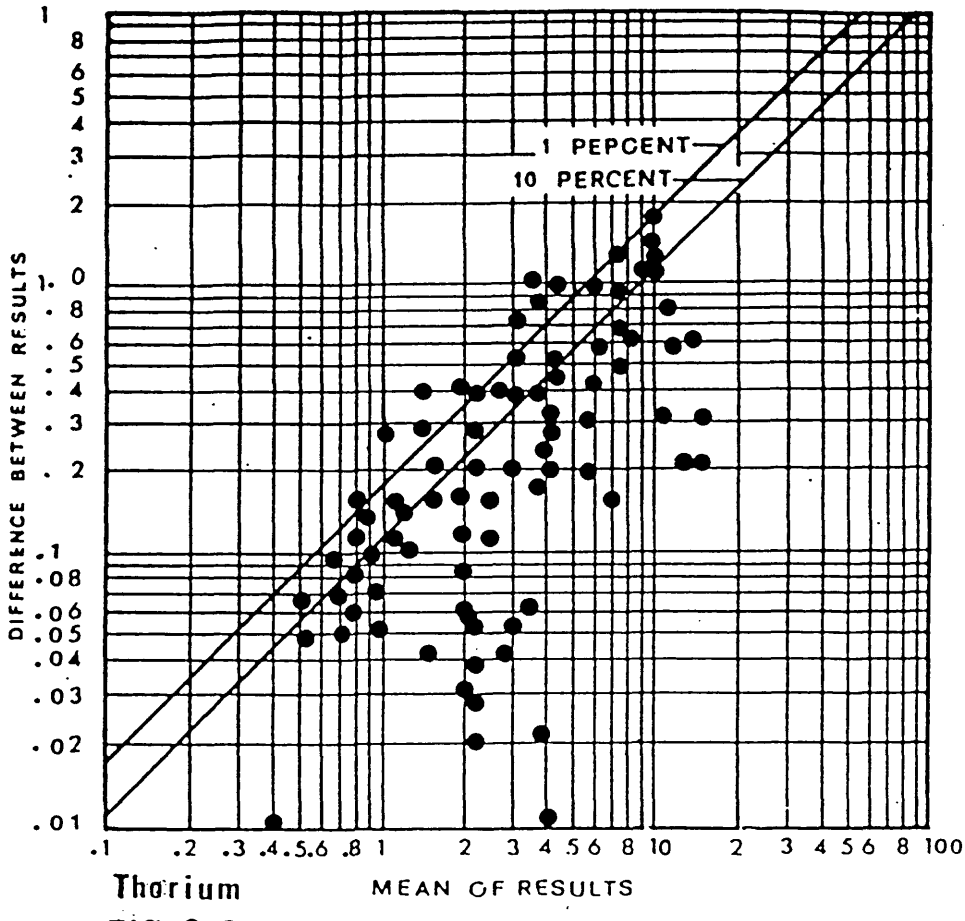


Fig.9.6 A typical geological cross-section of the region coinciding with traverse 600.

Table 9.2 The major lithosratigraphic units in the region.

UNIT NO.	SYSTEM		SERIES	LITHOLOGY
1.	Quaternary		Recent U. Pleistocene M. Pleistocene L. Pleistocene	Poorly cemented proluvial, alluvial, aeolian sands with lacustrine deposits, poorly sorted conglomerates and duricrusts.
2.	Neogene	Upper	Pliocene	Conglomerates, siltstone, marls, dolomitic limestones, sandstones, gypsum, marls, gravels, clays, sandstones, limestones and gypsum, quartzous sands and micritic lacustrine limestones with nodules of flint.
		Lower	Miocene	
3.	Paleogene	Upper	Oligocene	Sands and quartz sandstones, clays, marls, sandy limestones, nodular and bedded flints replaced laterally by algal limestones.
		Lower	U. Eocene M. Eocene L. Eocene	Recrystalline limestone, clayey and chalky limestone, micritic and glauconitic limestone, chert, nodular phosphates and phosphatic limestones and marly limestones with flints and chert beds.
4.			Paleocene	Limestones, clayey limestones, glauconitic rocks and calcareous limonitic concretions and phosphate nodules.
5.	Cretaceous	Upper	Danian	Marls, glauconitic clays and marly limestones with flints
			Maestrichtian	Marls, marly and clayey limestones, phosphorites* and phosphatic marly limestones, cherts, limestone and poorly sorted conglomerates with glauconitic and phosphatic grains.
			Campanian	Marly limestones, phosphorite*, phosphatic marly limestone, limestone, coquina limestone, micritic limestone, nodular flints and chert beds.
			Santonian	Limestones, flints, dolomitic limestone and dolomite.
			Coniasian	Massive dolomite with polycypods, limonitic limestone and nodules of flints and sandstones.
6.		Middle	Turonian	Dolomite, ammonitic dolostone and marly limestones with thin beds of dolomite.
			Cenomanian	Massive dolomite, clayey dolomitic limestone, layered dolomite, dolomitic limestones and limestones.
		Lower	Albian	Clayey dolomitic limestone, dolomite and gypsiferous marls.
			Aptian	Sands, sandstones and ferrogenous clayey marls.
	Triassic-Jurassic			Evaporite, evaporitic marls and dolomites.

* = Workable deposits.



Fig·9·6

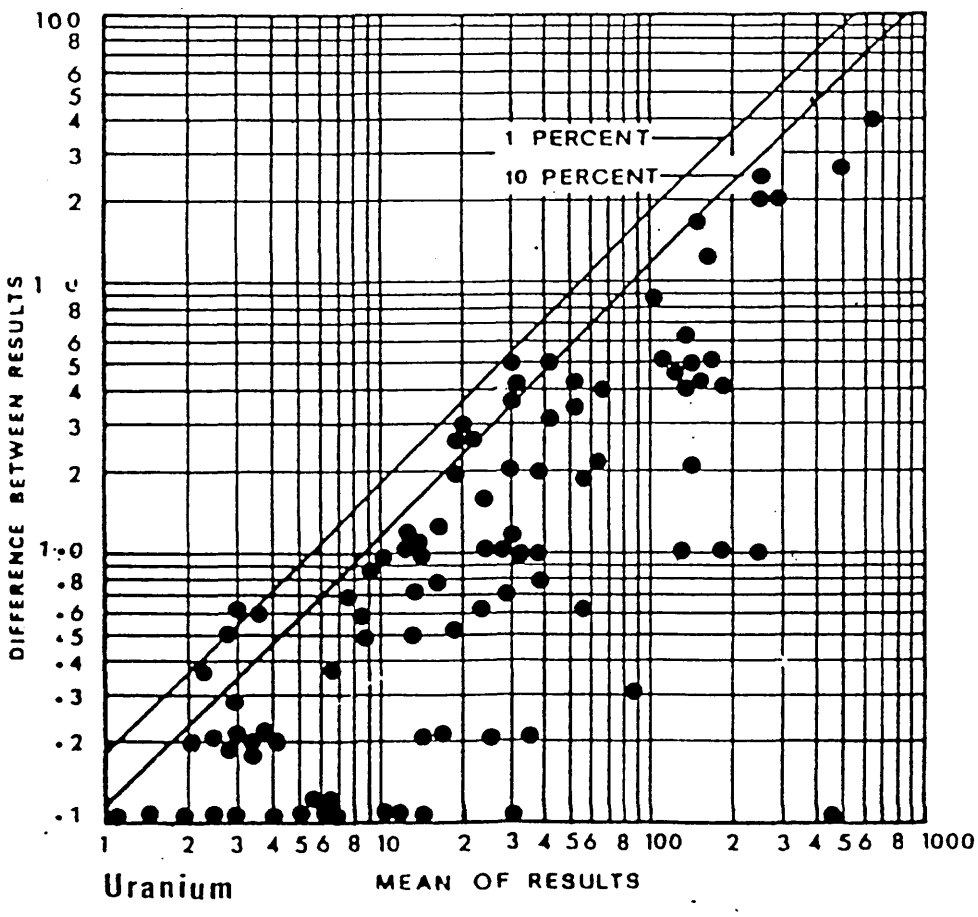


Fig.9.7 Precision of duplicate measurements of U and Th of the lithogeochemistry.

In a set of duplicate measurements on many samples where for each sample the precision of measurement is 10 per cent at the 95 per cent confidence limit (i.e. $\sigma/\mu = 0.05$) the indicated proportion of points will fall above the diagonals. The scale of the means must be 10 times greater than the scale of the differences.

work.

9.6 Statistical and areal distribution of the lithogeochemical data.

9.6.1 Statistical parameters.

Summary statistics of the lithogeochemical traverse data for all 405 samples is given in Table 9.4, whereas the geochemical data is presented in Appendix 9.5. Compared with the average values of common sedimentary rocks (see Table 5.13), the mean content of U, Sr, Ni, Se, V, Mo, Zn and Cr seems to be high. Lower than average contents of Mn, Fe, Na, Pb, Li, Rb, Be, Ag, Bi and Sb are found. The most striking characteristics, however, are some extremely high standard deviations shown by the data distribution for Ni, Zn, Cd, Se, U and P, and to lesser degrees Mo, V, Na and gamma radioactivity (counts per second). This reflects marked variations in the concentrations of these variables in various rock types.

The frequency distributions of nearly all elements except Ca reveal very skewed patterns (Fig. 9.8). However, log-transformation of the data failed to remove the skewness. Stem and Leaf frequency distributions of these data have been adopted to display patterns of selected elements to best advantage of separating groups of samples (Fig. 9.9 to 9.15).

CPS
18 OBSERVATIONS ABOVE THE LAST CLASS.

MIDDLE OF INTERVAL	NUMBER OF OBSERVATIONS	
0.0	0	
10.0	0	
20.0	0	
30.0	2	**
40.0	7	*******
50.0	8	********
60.0	19	*******************
70.0	26	**************************
80.0	34	**********************************
90.0	31	*******************************
100.0	32	********************************
110.0	24	************************
120.0	23	***********************
130.0	22	**********************
140.0	15	***************
150.0	18	******************
160.0	13	*************
170.0	11	***********
180.0	10	**********
190.0	9	*********
200.0	8	********
210.0	4	****
220.0	5	*****
230.0	5	*****
240.0	1	*
250.0	4	****
260.0	0	
270.0	2	**
280.0	5	*****
290.0	0	
300.0	5	*****
310.0	3	***
320.0	5	*****
330.0	0	
340.0	1	*
350.0	0	
360.0	2	**
370.0	1	*
380.0	0	
390.0	0	
400.0	5	*****
410.0	2	**
420.0	1	*
430.0	1	*
440.0	3	***
450.0	1	*
460.0	0	
470.0	1	*
480.0	2	**
490.0	0	
500.0	1	*
510.0	0	
640.0	2	**
650.0	1	*
660.0	0	
670.0	0	
680.0	2	**
690.0	0	
700.0	2	**
710.0	0	
720.0	0	
730.0	1	*
740.0	0	
750.0	4	****
760.0	1	*
770.0	1	*
780.0	0	
790.0	0	
800.0	0	
810.0	2	**
820.0	0	
830.0	0	
840.0	0	
850.0	1	*
860.0	0	
870.0	0	
880.0	1	*
890.0	0	
900.0	1	*
910.0	1	*

U
EACH * REPRESENTS 5 OBSERVATIONS

MIDDLE OF INTERVAL	NUMBER OF OBSERVATIONS	
0.0	175	**********************************
10.0	111	**********************
20.0	38	********
30.0	27	******
40.0	8	**
50.0	9	**
60.0	5	*
70.0	6	**
80.0	2	*
90.0	2	*
100.0	4	*
110.0	1	*
120.0	3	*
130.0	1	*
140.0	3	*
150.0	1	*
160.0	0	
170.0	1	*
180.0	0	
190.0	2	*
200.0	1	*
210.0	0	
220.0	2	*
230.0	0	
240.0	0	
250.0	1	*
260.0	0	
270.0	0	
280.0	0	
290.0	1	*
300.0	0	
310.0	0	
320.0	0	
330.0	1	*
340.0	0	
350.0	0	
360.0	0	
370.0	0	
380.0	0	
390.0	0	
400.0	0	
410.0	1	*
420.0	0	
430.0	0	
440.0	0	
450.0	1	*
460.0	1	*
470.0	0	
480.0	0	
490.0	1	*
500.0	0	
510.0	0	
520.0	0	
530.0	0	
540.0	0	
550.0	0	
560.0	0	
570.0	0	
580.0	0	
590.0	0	
600.0	1	*

Fig.9.8 Histograms of U and CPS in the Palmyrides lithogeochemistry.

STEM-AND-LEAF DISPLAY OF CPS
LEAF DIGIT UNIT = 10.0000
1 2 REPRESENTS 120.

```
     2   +0T  33
    23   +0F  44444444444555555555
    68   +0S  6666666666666666666666666667777777777777777
   133   +0.  888888888888888888888888888888888888888888889999999999*
   194    1*  00000000000000000000000000001111111111111111111111111111*
  (42)    1T  22222222222222222222222222233333333333333
   174    1F  44444444444444555555555555
   148    1S  66666666666667777777777777777
   119    1.  8888888999999999
   103    2*  00000111111
    92    2T  222333333
    83    2F  5555
    79    2S  77
    77    2.  88888
    72    3*  00000111
    64    3T  22222
    59    3F  4
    58    3S  667

          HI   40,  40,  40,  40,  40,  41,  41,  42,  43,  44,  44,
               44,  45,  47,  48,  48,  50,  64,  64,  65,  68,  68,
               70,  70,  72,  75,  75,  75,  75,  76,  77,  81,  81,
               85,  88,  90,  91, 100, 118, 120, 140, 140, 147, 148,
              157, 158, 180, 185, 210, 223, 223, 240, 260, 280, 400,
```

STEM-AND-LEAF DISPLAY OF U
LEAF DIGIT UNIT = 1.0000
1 2 REPRESENTS 12.

```
    40   +0*  000011111111111111111111111111111111111111
   138   +0T  22222222222222222222222222222222222222222222222222222222222*
   190   +0F  44444444444444444444444444444444444444455555555555555555
  (38)   +0S  66666666666666666666667777777777777777
   182   +0.  88888888899999
   168    1*  000000000000001111
   150    1T  222222222233333
   135    1F  444444444445555555
   117    1S  666677777
   108    1.  88899
   103    2*  0000111
    96    2T  22333333
    88    2F  445
    85    2S  66677
    80    2.  8888899999999
    67    3*  00001
    62    3T  22
    60    3F  45
    58    3S
    58    3.  99
    56    4*  001
    53    4T  33
    51    4F  55

          HI   48,  48,  49,  51,  52,  52,  53,  55,  58,  58,  58,
               60,  66,  67,  68,  68,  69,  70,  81,  84,  85,  85,
               98, 101, 104, 104, 110, 121, 123, 124, 130, 136, 137,
              140, 153, 167, 186, 188, 198, 216, 223, 253, 286, 326,
              405, 453, 461, 493, 602
```

STEM-AND-LEAF DISPLAY OF TH
LEAF DIGIT UNIT = .1000
1 2 REPRESENTS 1.2

```
    17   +0*  12222333444444444
    57   +0.  555555555666666667777777777777888888888
   108    1*  000000000000000000000011111222223333333334444444444
   153    1.  555555555555556666666777777777778888888889999
   194    2*  00000000000000000000001222333333333444444
  (38)    2.  55555666666677777777778888888889999999
   178    3*  000000001223333344444
   156    3.  555666666667777778800009999
   128    4*  000000000001111122223333 44
   101    4.  55555555666777888888
    83    5*  00000000111122222334
    63    5.  555588899
    54    6*  0044
    50    6.  55888
    45    7*  0013
    41    7.  55
    39    8*  004

          HI   90,  90,  90,  90,  94,  96, 100, 100, 100, 100, 100,
              108, 110, 110, 114, 119, 120, 120, 120, 120, 120, 131,
              136, 138, 138, 143, 152, 163, 165, 167, 177, 183, 191,
              194, 200, 343
```

STEM-AND-LEAF DISPLAY OF AS
LEAF DIGIT UNIT = .1000
1 2 REPRESENTS 1.2

```
    18   +0*  011222223333444444
    35   +0.  55666677888888899
    58    1*  000000111122233333333444
    78    1.  55556667777788888889
    94    2*  0000123333334444
   110    2.  5556667777889999
   133    3*  000000000012223344444444
   168    3.  555555555666666667777777777888999
  (46)    4*  000000000000001111112222222222333333333344444444
   196    4.  566666677777777777788888888899999999
   161    5*  000000000011111112333334444
   135    5.  55556677889999
   121    6*  00000012233333444
   104    6.  5555556667788899
    88    7*  0000114
    81    7.  5577799
    74    8*  0011134444
    64    8.  6667778
    57    9*  00002224
    49    9.  78
    47   10*  00000
    42   10.  5
    41   11*  00000
    36   11.  78
    34   12*  0

          HI  123, 123, 125, 128, 130, 130, 136, 140, 143, 145, 150,
              150, 152, 154, 170, 173, 180, 180, 190, 190, 260, 260,
              295, 330, 330, 330, 340, 420, 460, 500, 500, 540, 660,
```

Fig. 9.9 Stem-and-Leaf display pattren of U,CPS,Th and As of the Palmyrides lithogeochemistry.

STEM-AND-LEAF DISPLAY OF SR
LEAF DIGIT UNIT = 10.0000
1 2 REPRESENTS 120.

```
  11     0   36777888999
  28     1   00222223445577899
  50     2   000011133455667889999
  95     3   00133333444445555556666666677777778888899999999
 154     4   000111112333333334444555555566666666667777777788889999999*
 199     5   00000011222333334444444455556666777777777099
(28)     6   00111123335555556666777888888
 183     7   0002222333557888999
 163     8   001133346667799
 148     9   11222333445555778899
 127    10   1344444579
 117    11   01112334455667899999
  96    12   11112223444455680
  79    13   11233444556788999
  62    14   00011234589
  51    15   12245569
  43    16   27
  41    17   003559
  35    18   2225
  31    19   11334
  26    20   0
  25    21   000
  22    22   0000

       HI   260, 260, 270, 280, 280, 330, 330, 340, 380, 390, 420,
            440, 450, 450, 460, 510, 550, 550
```

STEM-AND-LEAF DISPLAY OF SE
LEAF DIGIT UNIT = .0100
1 2 REPRESENTS 0.12

```
  48     0   11111111111111112222222333344444555556666777777 8
  72     1   000000000000000000000000
 100     2   00000000000000000000000000000
 126     3   000000000000000000000000000
 161     4   0000000000000000000000000000000000
 193     5   00000000000000000000000000000000
(28)     6   0000000000000000000000000000
 189     7   000000000000000000000000000000
 160     8   00000000000000000000000
 135     9   000000000000000
 118    10   000000000000000
 101    11   00000000
  93    12   0000000000
  83    13   0000000
  76    14   000
  73    15   000000000000
  61    16   00000000
  53    17   000
  50    18   0
  49    19   000
  46    20   0000000

       HI    220,  220,  230,  250,  250,  260,  260,  260,  270,
             270,  300,  300,  300,  320,  390,  460,  480,  570,
             600,  600,  700,  890,  950, 1000, 1000, 1200, 1250,
            1300, 1460, 1500, 1700, 1900, 2300, 2400, 2400, 2500,
            3460, 5300, 6300
```

STEM-AND-LEAF DISPLAY OF BA
LEAF DIGIT UNIT = 10.0000
1 2 REPRESENTS 120.

```
  35    40* 00111111111222222222333333334444444
  67    40. 55555555566666667777778888889999
 107     1* 000001111222222222222233333334444444444
 138     1. 555566666667777777788888899999
 187     2* 00000111111111222222222233333333344444444444444444
(35)     2. 5555555666667777777777888888889999
 188     3* 000000000011111222333344444
 162     3. 555555666666677777777888888889
 131     4* 000111111111222233344444
 108     4. 5555555666788999
  92     5* 000000111222344
  77     5. 666677889
  68     6* 0122344444
  58     6. 556667889
  49     7* 122
  46     7. 55670
  41     8* 114
  38     8. 57888

       HI    95,  96,  96,  96,  97,  97,  97,  97,  98,  98, 102,
            102, 103, 106, 112, 118, 118, 125, 136, 141, 149, 157,
            160, 160, 161, 169, 180, 193, 230, 230, 260, 260, 280,
```

STEM-AND-LEAF DISPLAY OF P
LEAF DIGIT UNIT = 100.0000
1 2 REPRESENTS 1200.

```
  80     0   000011111111111222222222223333444444444455555556666666666*
 168     1   00000000001111112222222222222233333333334445555555555555555*
(55)     2   00111111122222222333333333344444445555666677777888889999
 187     3   000011123333444445555566677888899
 154     4   0012334445567778
 138     5   0000023344667899
 122     6   112345667799
 110     7   34468
 105     8   0223568
  98     9   00122336
  90    10   0445566
  83    11   8
  82    12   16
  80    13   4
  79    14   0
  78    15   3
  77    16   34
  75    17   5

       HI    195,  196,  197,  199,  200,  210,  210,  220,  230,
             230,  230,  240,  240,  250,  260,  260,  260,  260,
             280,  280,  290,  290,  310,  310,  340,  340,  340,
             380,  510,  510,  520,  520,  550,  560,  560,  590,
             600,  610,  620,  620,  660,  670,  770,  807,  820,
             820,  840,  880,  900,  908,  910,  910,  910, 1000,
            1023, 1030, 1070, 1090, 1090, 1120, 1140, 1140, 1160,
            1210, 1300, 1310, 1320, 1330, 1340, 1340, 1420, 1450,
            1560, 1560
```

Fig.9.10|Stem-and-Leaf display pattern of Se,Sr,Ba and P of the Palmyrides lithogeochemistry.

STEM-AND-LEAF DISPLAY OF K
LEAF DIGIT UNIT = 100.0000
1 2 REPRESENTS 1200.

```
  61    +0* 00000000000000111111111111112222222333333333333333444444444*
 103    +0. 55556666666666667777788888888889999999999
 143     1* 000000000000011111111222222222333333344444
 170     1. 555555557777777777788888999
 188     2* 000001111222223334
(27)     2. 555556666667777777888889999
 195     3* 0000011222334444
 179     3. 555566667788888999999
 157     4* 00112233344444
 143     4. 55566777888889999
 126     5* 000001112233334444444
 105     5. 555555666666789999999
  85     6* 00112223333344
  71     6. 55555677889
  60     7* 000001112223344
  45     7. 5667789
  38     8* 0001244
  31     8. 566689
  25     9* 01244
  20     9. 67799
  15    10* 0222
  11    10. 56
   9    11* 1
   8    11.
   8    12* 2

       HI  123, 142, 145, 151, 160, 200, 230
```

STEM-AND-LEAF DISPLAY OF V
LEAF DIGIT UNIT = 1.0000
1 2 REPRESENTS 12.

```
  20     0  24466666777777888999
  35     1  001333367788999
  62     2  00111112233334446666778889
 104     3  000011122223344444445555777788888888999999
 144     4  011122222223334444555566677788889999999
 179     5  000011112333333445556667777789999999
(36)     6  000000022223333444455556666667889999
 195     7  000011111111222222222223334445555556666666777888888999999
 139     8  11122222222344444456666666788899
 108     9  000112333334445556677 9
  86    10  0122333335666789
  70    11  11244445888
  59    12  45558
  54    13  011
  51    14  67
  49    15  469
  46    16  346

       HI  181, 184, 194, 195, 198, 198, 210, 210, 210,
           210, 220, 230, 240, 250, 250, 250, 260, 270,
           280, 330, 330, 360, 380, 420, 430, 430, 450,
           470, 480, 490, 540, 690, 700, 700, 750, 770,
           880, 930, 930, 970, 1080, 1890, 6700
```

STEM-AND-LEAF DISPLAY OF MO
LEAF DIGIT UNIT = .1000
1 2 REPRESENTS 1.2

```
  38     0  00000000000000000000000000000000000
  72     1  000112222233344444555677777899999
 137     2  000111111112222222233333333334445555556666666777777777778*
 183     3  000001111111111233334444445555666677777888899
(36)     4  00000001111222234444445666777889999
 191     5  000011111233334455556677888099999
 159     6  001122333455566777888999
 134     7  000012233333444556608888899
 106     8  00001112233444667888 9
  84     9  0011223333344456699
  65    10  0446777788
  55    11  02345
  50    12  3599
  46    13  05566
  41    14  0199
  37    15  146

       HI  181, 182, 183, 192, 199, 200, 210, 210, 220,
           230, 240, 240, 250, 260, 280, 300, 340, 350,
           370, 400, 440, 450, 480, 610, 670, 720, 720,
           720, 720, 820, 880, 880, 1020, 1250
```

STEM-AND-LEAF DISPLAY OF CD
LEAF DIGIT UNIT = .1000
1 2 REPRESENTS 1.2

```
  46    +0* 00000000000000000000000000000000000000000000000
  98    +0. 55555555666666667777888888888888888888999999999999
 155     1* 000000000011111111111111222222222233333344444444444444444
 196     1. 555555555556666666777778888888889999999
(29)     2* 000011111112222223333333444 4
 185     2. 55555566666666777777889999999999999
 151     3* 00112233344
 140     3. 55677788888999
 126     4* 11111223344
 115     4. 55666677899
 104     5* 0122233333344
  91     5. 5567788
  84     6* 00014
  79     6. 6777778889
  69     7* 12334
  64     7. 889
  61     8* 00000
  56     8. 55
  54     9* 44
  52     9. 88
  50    10* 233
  47    10.
  47    11* 0

       HI  115, 116, 124, 124, 124, 125, 126, 126, 128,
           129, 140, 141, 157, 163, 188, 196, 210, 210,
           210, 260, 310, 330, 350, 350, 390, 430, 430,
           430, 470, 480, 520, 610, 750, 960, 960, 1150,
           1180, 1200, 1330, 1820, 1900, 1900, 2400, 3200, 3300,
           3800
```

Fig. 9.11 Stem-and-Leaf display pattern of V,K,Mo and Cd of the Palmyride lithogeochemistry.

```
STEM-AND-LEAF DISPLAY OF LI
LEAF DIGIT UNIT =   1.0000
1 2 REPRESENTS 12.

 48  +0*  000000000000000000000000000001111111111111111111
 95  +0T  222222222222222222222333333333333333333333333333
140  +0F  444444444444444444444444455555555555555555555
191  +0S  666666666666666666666777777777777777777777777777
(29) +0.  88888888888888888999999999
190   1*  000000000000000000111111111111111111
153   1T  222222222222223333333333333333
124   1F  444444444444444555555555555555
 92   1S  66666666666666777777777
 66   1.  888888888999999999999
 45   2*  000111111111111
 30   2T  22233333333333
 16   2F  44555
 11   2S  66
  9   2.  99

     HI  40, 42, 44, 44, 48, 78, 80
```

```
STEM-AND-LEAF DISPLAY OF NA
LEAF DIGIT UNIT = 100.0000
1 2 REPRESENTS 1200.

 80   +0* 00000000000000001111111111111111122222222222233333333333333*
144   +0. 55555555555555555666666666667777777777777888888888888888899*
(78)   1* 00000000000000000000111111111111111122222222222222223333*
188    1. 555555555566666666667777777777088889999999
145    2* 0000112222333344
129    2. 555556666667777778888999999
102    3* 00001112333444
 88    3. 55566777789999
 74    4* 000111
 68    4. 567888
 62    5* 00112233
 54    5. 66777799
 46    6* 01222

     HI   63,  63,  64,  65,  65,  67,  68,  70,  71,  74,  75,
           76,  78,  80,  83,  88,  93,  93, 106, 107, 109, 115,
          117, 119, 119, 123, 126, 141, 147, 148, 149, 149, 157,
          158, 220, 230, 290, 460, 530, 590, 600
```

```
STEM-AND-LEAF DISPLAY OF MN
LEAF DIGIT UNIT =  10.0000
1 2 REPRESENTS 120.

161   +0* 00000000000000000000000000000000000000000000000111111111*
(72)  +0. 55555555555556666666666666666677777777778888888888888888*
177    1* 00000000000001111112222233344444
143    1. 555566666677777789999999
120    2* 001122222333334444
102    2. 55566666677777788808889999
 75    3* 000000000011111222333333444
 47    3. 5555566666677777888
 28    4* 000122224
 19    4. 5788
 15    5* 23
 13    5. 6

     HI   57,  58,  58,  60,  62,  64,  68,  73,  73,  75, 101,
          118
```

```
STEM-AND-LEAF DISPLAY OF FE
LEAF DIGIT UNIT =1000.0000
1 2 REPRESENTS 12000.

 61   +0*  00000000000000000000000000000000000000000000111111111111111*
113   +0T  22222222222222222222223333333333333333333333333333
164   +0F  44444444444444444444444444455555555555555555555555
(42)  +0S  66666666666666666666777777777777777777777
204   +0.  88888888888888889999999999999999999999
164    1*  00000000000011111111
144    1T  2222222223333333333
125    1F  444444444444444555555555555
 97    1S  66666666666666666777777777
 72    1.  888888888888889999999
 52    2*  00011111111111
 38    2T  22222222222333333
 21    2F  4444555
 14    2S  677777
  8    2.  8888
  4    3*  01

     HI  37, 77
```

Fig. 9.12 Stem-and-Leaf display pattern of Na,Li,Mn and Fe of the Palmyrides lithogeochemistry.

```
STEM-AND-LEAF DISPLAY OF MG
LEAF DIGIT UNIT =1000.0000
1 2 REPRESENTS 12000.
      49  +0*  0000000001111111111111111111111111111111111111111
     100  +0T  22222222222222222222222233333333333333333333333333
     142  +0F  44444444444444444444444455555555555555555
     178  +0S  66666666666666666777777777777777777
    (31)  +0.  88888888888888889999999999999
     201   1*  000000000001111111111111111
     173   1T  22222222222222233333333333333333
     140   1F  44444444445555555555555
     115   1S  66666666666666666677777777777777
      83   1.  888888899999999
      68   2*  0001111
      61   2T  2222333333
      51   2F  4444455
      44   2S  667777
      38   2.  89
      36   3*  0001111
      29   3T  3333
      25   3F  45

          HI   36,  38,  39,  40,  42,  43,  44,  47,  48,  50,  51,
               53,  54,  54,  60,  61,  63,  79,  101,  105,  106,  108,
               119
```

```
STEM-AND-LEAF DISPLAY OF CA
LEAF DIGIT UNIT =**********
1 2 REPRESENTS 120000.

      1  +0*  1
      6  +0T  22223
     12  +0F  444555
     13  +0S  7
     14  +0.  9
     20   1*  001111
     34   1T  22222223333333
     56   1F  4444444455555555555555
     97   1S  66666666666666666666777777777777777777777
    145   1.  88888889888880888888899999999999999999999999999
    169   2*  00000000111111111111111
   (42)   2T  22222222222222222223333333333333333333333333
    199   2F  444444444445555555
    180   2S  66666666666666666677777777
    152   2.  888888888999999999999
    129   3*  000000001111111111111111
    104   3T  2222223333333333
     88   3F  44444444445555555555555
     65   3S  66666666666677777777777777
     39   3.  8888888899999
     26   4*  000000000000011111111
      5   4T  222
      2   4F  44
```

```
STEM-AND-LEAF DISPLAY OF TI
LEAF DIGIT UNIT = 100.0000
1 2 REPRESENTS 1200.

     77  +0*  00000000000000000000000000000000000000000000000000000000000000*
    141  +0T  22222222222222222222222222222222223333333333333333333333333*
    202  +0F  44444444444444444444444444444555555555555555555555555555*
   (37)  +0S  66666666666666666677777777777777777
    171  +0.  88888889888889999999999999
    145   1*  000000000000001111111111
    120   1T  22222223333333333333
     98   1F  4444444445555555
     82   1S  666666666777777
     67   1.  8888888999999
     54   2*  0000111111
     44   2T  22222333
     36   2F  444444455555
     24   2S  6666677777
     14   2.  8999

          HI   31,  31,  32,  32,  33,  34,  34,  35,  50, 132
```

```
STEM-AND-LEAF DISPLAY OF CR
LEAF DIGIT UNIT =   1.0000
1 2 REPRESENTS 12.

     35    0  000011222334444455666777778888999999
     76    1  00000001111122223333333333334555666788999
    118    2  011111222233333455555666666667777888999999
    169    3  000011122222222344444444455556666777888888888899999
   (41)    4  00112222333444445555566677777888899999999
    200    5  000111111113333444455555567788888888999999
    159    6  000000001112222333344444455566667777889
    120    7  00000112356666677777789999
     93    8  000011112333344557899
     73    9  0123345556778
     60   10  112233344478899
     45   11  001125679
     36   12  46889
     31   13  0445778
     24   14  336788

          HI  158, 161, 163, 166, 166, 173, 177, 177, 180, 182, 182,
              210, 210, 230, 270, 280, 300, 680
```

Fig. 9.13 Stem-and-Leaf display pattern of Ca,Mg,Ti and Cr of the Palmyrides lithogeochemistry.

STEM-AND-LEAF DISPLAY OF ZN
LEAF DIGIT UNIT = 1.0000
1 2 REPRESENTS 12.

```
 15     0   134556777778899
 50     1   00000111222223445556777777788888889
 67     2   02233344456666889
102     3   00011222244444455555566666677888889
141     4   000000001122223333444455555677778888999
201     5   0000000111111222222333344444455555566666777788888888888999*
(32)    6   00011123333334444444566667889 99
177     7   01111112234455555567777768888888999
144     8   0001233345666667789 9
124     9   000111112233333344777 99
101    10   01134579
 93    11   1245
 89    12   0045778
 82    13   04558899
 74    14   0124677088
 64    15   79
 62    16   44667
 57    17   789
 54    18   1

      HI   188,  188,  190,  193,  200,  200,  200,  200,  200,
           210,  210,  210,  210,  220,  220,  230,  230,  230,
           240,  250,  260,  260,  260,  280,  280,  350,  350,
           370,  420,  430,  460,  510,  510,  530,  570,  620,
           640,  650,  660,  710,  730,  750,  770,  870,  960,
           960, 1090, 1750, 1840, 1940, 1940, 1950, 8100
```

STEM-AND-LEAF DISPLAY OF CU
LEAF DIGIT UNIT = 1.0000
1 2 REPRESENTS 12.

```
  2   +0*   01
 14   +0T   222222333333
 42   +0F   44444444555555555555555555
 64   +0S   6666666666677777777777
 81   +0.   88888888999999999
107    1*   00000000000000001111111111
127    1T   22222222222333333333
161    1F   44444444444444444555555555555555555
195    1S   66666666666666777777777777777777777
(31)   1.   88888888888888889999999999999999
184    2*   000000000011111111111
163    2T   22222222333333333333
142    2F   44444444444445555555555555
115    2S   66666666677777777777
 95    2.   8888889999999
 82    3*   000111111111111
 67    3T   2222333
 60    3F   444455
 54    3S   67
 52    3.   8999
 48    4*   000000
 42    4T   333
 39    4F   45
 37    4S   677
 34    4.   89

      HI   51,  53,  54,  55,  55,  57,  57,  58,  58,  60,  60,
           60,  61,  61,  64,  65,  67,  67,  70,  70,  76,  78,
           78,  85,  86,  87, 108, 147, 165, 170, 220, 450
```

STEM-AND-LEAF DISPLAY OF AL
LEAF DIGIT UNIT =1000.0000
1 2 REPRESENTS 12000.

```
 50   +0*   00000000000000000000000001111111111111111111111
 80   +0T   22222222222222222223333333333
115   +0F   44444444444444444445555555555555555
161   +0S   66666666666666666667777777777777777777777777
194   +0.   88888888888888888889999999999
(31)   1*   00000000000011111111111111111
185    1T   22222222222233333333
165    1F   444445555
156    1S   666666677777777777
130    1.   8888899999
128    2*   0000111111111
115    2T   22222222222222233333
 95    2F   44444455555555
 81    2S   6666677777777
 68    2.   88888888099999
 54    3*   00000000000011111
 38    3T   2223333
 31    3F   4444444455
 21    3S   677
 18    3.   8999
 14    4*   001
 11    4T   22233
  6    4F   4
  5    4S   7

      HI   49, 49, 49, 67
```

STEM-AND-LEAF DISPLAY OF LA
LEAF DIGIT UNIT = 1.0000
1 2 REPRESENTS 12.

```
 31   +0*   00000000000000000001111111111111
 55   +0T   22222222222222233333333
 83   +0F   44444444445555555555555555555
118   +0S   66666666666666677777777777777777777
157   +0.   88888888888888888899999999999999999999
198    1*   00000000000000000000000001111111111111
(15)   1T   222223333333333
197    1F   44444444444445555555555555555555
164    1S   66666666666677777777777777777777777
128    1.   88888888888889999999999999
 99    2*   000000000011111111111
 77    2T   2222222233333333333
 55    2F   444444455555555555
 37    2S   66666777
 29    2.   88899
 24    3*   000011
 18    3T   2223
 14    3F   4555
 10    3S   77
  8    3.   8

      HI   41,  42,  57,  65,  81,  98, 135
```

Fig. 9.14 Stem-and-Leaf display pattern of Cu,Zn,Al and La of the Palmyrides lithogeochemistry.

```
STEM-AND-LEAF DISPLAY OF PB
LEAF DIGIT UNIT =    1.0000
1 2 REPRESENTS 12.

 45    +0* 000000000000000000000000000000000000000000000000
 82    +0. 555555556666777777777888808888999999
125     1* 00000000000111111111111122222333334444444
178     1. 555555555555566666666667777777778888889999999999999
(33)    2* 000000111111222222222333344444444
199     2. 555555555555666666666666777777088088999999999
153     3* 000000000000111112222222222333334444444444444
107     3. 555555555566666666666667777777708888888808889999999
 53     4* 00000011111112222233444
 30     4. 55555566677770
 16     5* 0123
 12     5. 58
 10     6* 0
  9     6. 88

      HI   77,  87,  96, 108, 143, 196, 240

STEM-AND-LEAF DISPLAY OF CO
LEAF DIGIT UNIT =     .1000
1 2 REPRESENTS 1.2

 14     0  00000000000000
 41     1  00111122333344456677788889
 87     2  001111222222223333344445666666677778888899999
137     3  000111111122222222233344455566666677777788808899999
180     4  00000111111222222223333345556667708808889999
(28)    5  000011123333355556666678899
202     6  11111122222334445566667777880888
171     7  00112244555556666667799999
146     8  11113444567889
132     9  001222234566677999
114    10  00011133445666788 8
 96    11  000111123333444566788999
 72    12  033455666679
 60    13  02466788899
 49    14  0125666899
 39    15  01122336778
 28    16  011233444
 19    17  024
 16    18  5
 15    19  0129
 11    20  0
 10    21  0

      HI  220, 230, 240, 320, 350, 620, 640, 700, 720

STEM-AND-LEAF DISPLAY OF NI
LEAF DIGIT UNIT =    1.0000
1 2 REPRESENTS 12.

 15    +0* 022222233333444
 36    +0. 55555556666678899999
 60     1* 000001122222223333344444
 83     1. 555566677777777888888889
104     2* 00011112222222333344
123     2. 5555566666777788899
149     3* 011111112222222223333333444
184     3. 555555666667777888888888999999999
(30)    4* 000001111112222222233333334444
196     4. 555555556666777777788888999999
166     5* 000001111111122333333444444
138     5. 555566666677777777888888888999
109     6* 000001111223444
 94     6. 556667889
 85     7* 000011111122233444
 67     7. 555667788999
 55     8* 02333344
 47     8. 5567788
 40     9* 0122344
 33     9. 6789
 29    10* 3
 28    10. 6
 27    11* 2
 26    11. 6

      HI  118,  119,  121,  125,  128,  131,  137,  150,  170,
          179,  194,  195,  196,  196,  198,  200,  200,  210,
          210,  210,  210,  250,  300,  460, 9700
```

Fig. 9.15 Stem-and-Leaf display pattern of Co,Pb and Ni of the Palmyrides lithogeochemistry.

9.6.2 Single element areal distribution

Only the salient features of the areal dispersion patterns of U, CPS, Th, As, Se, P, Sr, V, Mo and K are descibed below, their selection is based on the significance to U exploration and the finding of earlier chapters.

9.6.2.1 Uranium.

Concentrations of U in the Palmyrides rocks range from 0.8 ppm to over 600 ppm, their spatial distribution (Fig. 9.16) reveals contrasting areas within the overall region. High values (>=120 ppm U) form three main trends.

The first, a central trend is coincident with part of the southern Palmyrides range of mountains between the J. Bassiri-El Bardeh axis and J. Abou El Fawaress, northeast of Palmyra. Most of the anomalous levels of U show a close relationship with the phosphate and phosphorite rocks of the Campanian, Maestrichtian and Eocene. Individual highly anomalous values, however, occur in non-phosphatic Cretaceous rocks such as samples 710 and 711 (J. El Bassiri) and 527, 330 and 119 (J. Om-Jorm, J. Qal-Tabaque and J. Abou El Fawaress respectively). Sample 710 was taken from a fault zone, and its X-ray diffractogram (Fig. 9.17) shows that it consists mainly of low temperature quartz with minor clay phases. The striking feature of this sample (and to a lesser degree all the above mentioned non-phosphate ores) is extremely anomalous levels of trace elements; up to 1% Ni; 0.87% Zn, 0.67% V, 0.06% U, and the highest concentrations of Cu (450 ppm), Cr (230 ppm), Cd (75 ppm),

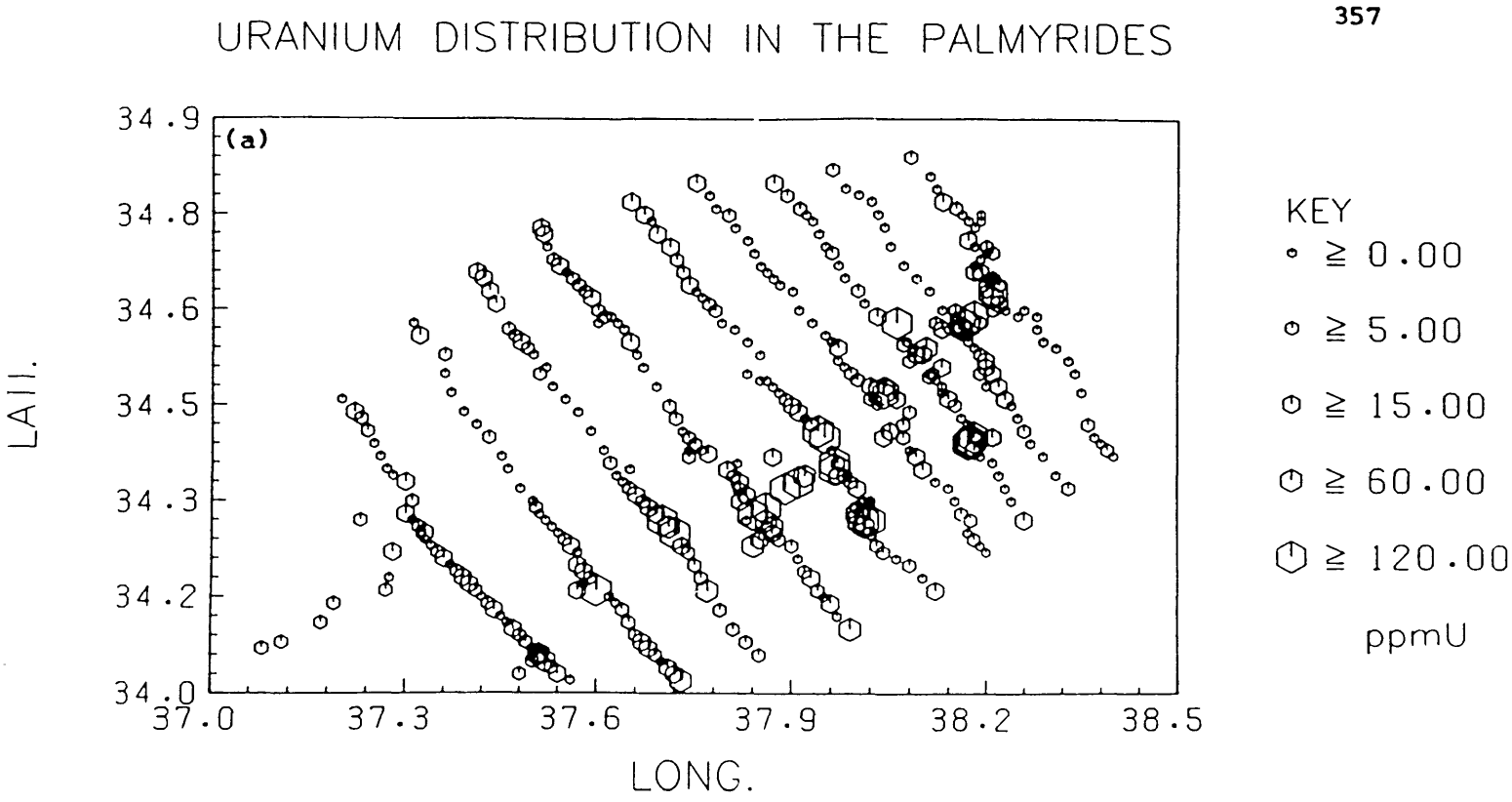
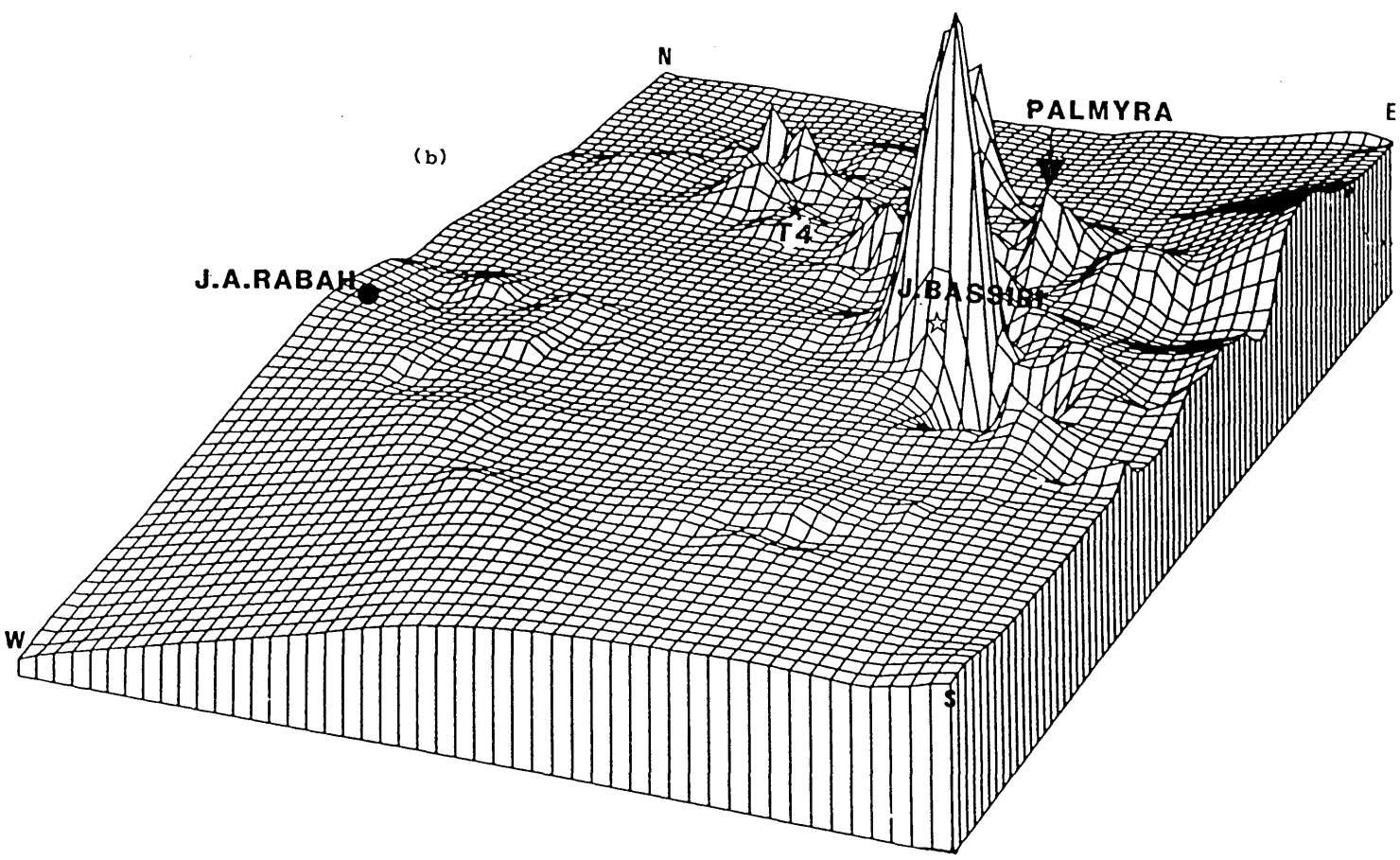


Fig.9.16 Symbolic areal distribution of U in the region(a); Solid surface(b).



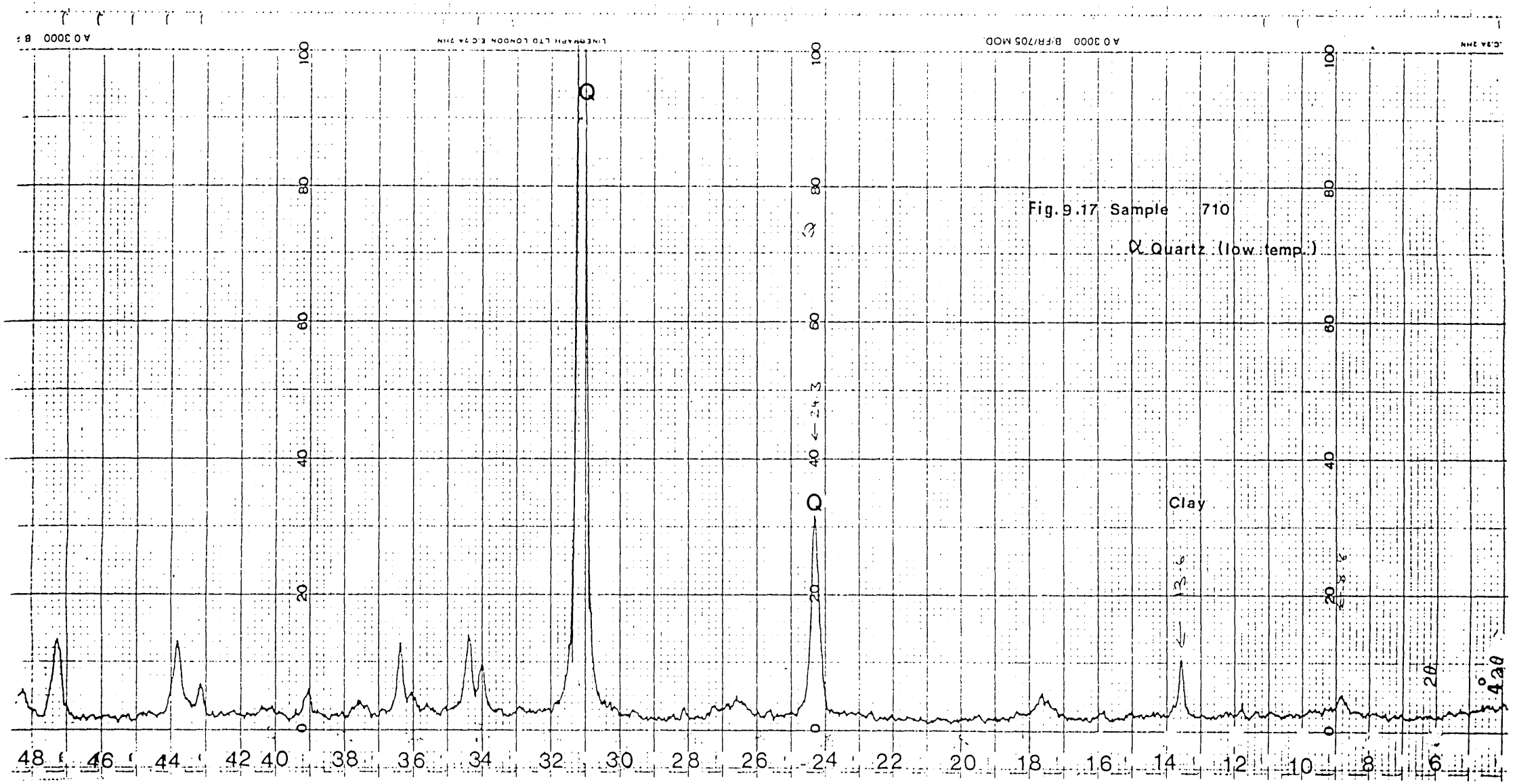


Fig.9.17 X-ray diffractogram of sample 710.

Se (63 ppm) and Mo (48 ppm). Among other relatively abnormal elements are Pb (53 ppm), Be (8 ppm) and Ag (3.7 ppm). In contrast elements such as Mn (12.7 ppm), Na (470 ppm) and Ca (5.8%) are relatively very low. Scanning electron microscopy, electron microprobe and other optical polished-thin section examination revealed the presence of Cu, Zn and Mo mineralizations along with secondary U mineral grains (Plates 21 to 23). The field relationship and descriptions indicate that most of these samples fall in fault zones spatially coinciding with the intersection of NE to SW and NW to SE striking faults. It should be noted that most of the mineralized specimens studied for their U minerals were collected from similar sites.

In addition to being geochemically interesting the elemental association in these sites is similar to that described in the first anomalous site of Wadi Om-Jorn drainage geochemistry (see section 6.4). The element assemblage and the element concentration levels clearly support earlier interpretation of being generated from a subsurface source. The most likely one is solutions moving along deep faults towards the surface; however, the possibility that they were derived from subsurface igneous activity of mafic composition (Basaltic?) cannot be ruled out. The local geology provides further support for such an interpretation, because there are no other surface rocks in the vicinity which might provide these high levels and types of anomalies. The same trace element association (Ni, V, Mo, Cu, Zn, U, Mo, co and Ag) was reported by Sopuck et al. (1983) during their lithogeochemical work in Saskatchewan to migrate upwards along fault structures towards the top. Furthermore, Strand (1983) suggested that such concentrations

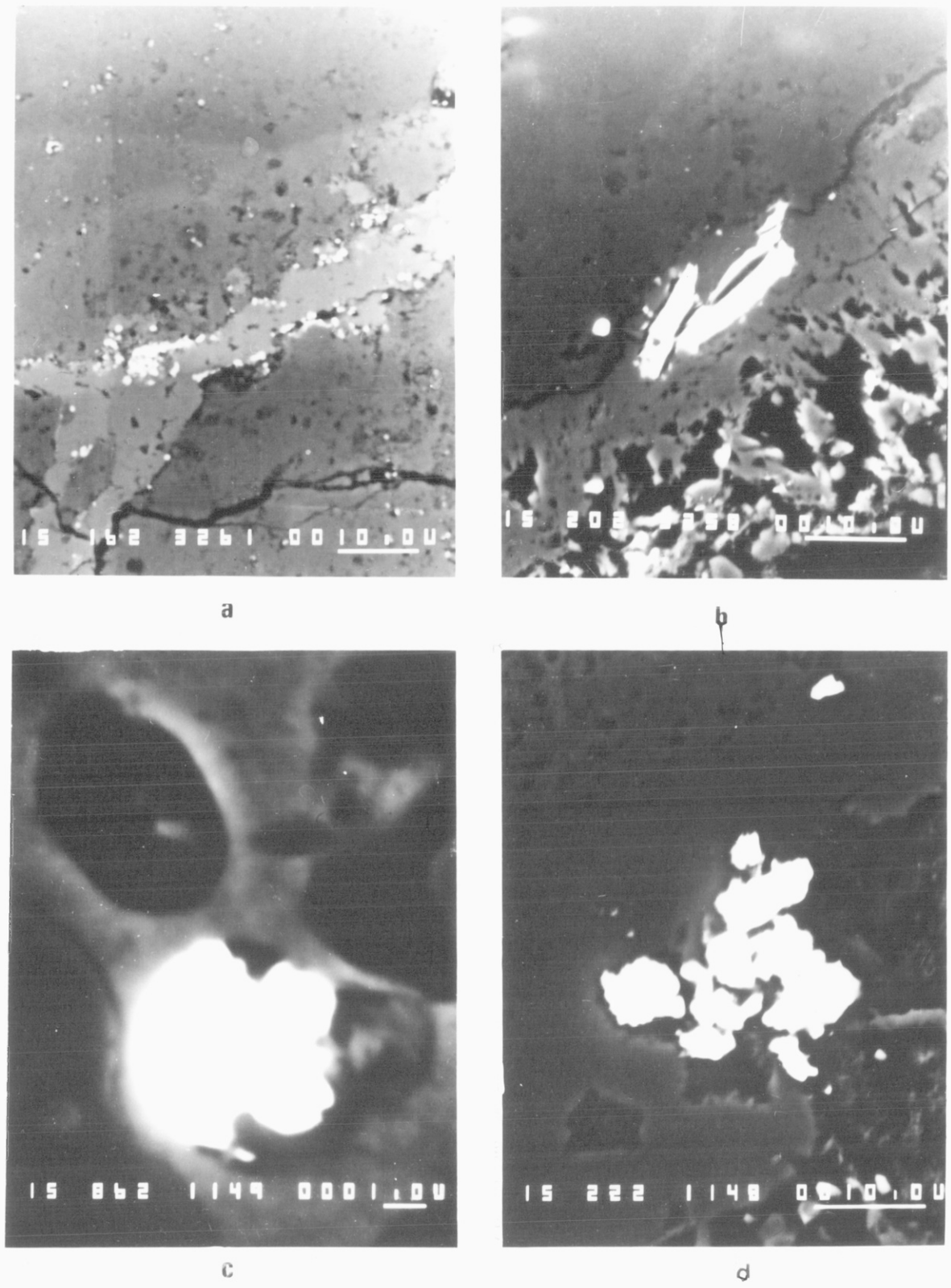


Plate 21 Backscattered photomicrograph showing U, Zn, Fe, Cu, Ba and Mo mineralization in a quartz vein of sample 710. (a=Cu-Zn mineralization in a microfissure; b=U and Pt minerals ; c= Pt grain ; d== Cu,Zn and Mo sulphides).

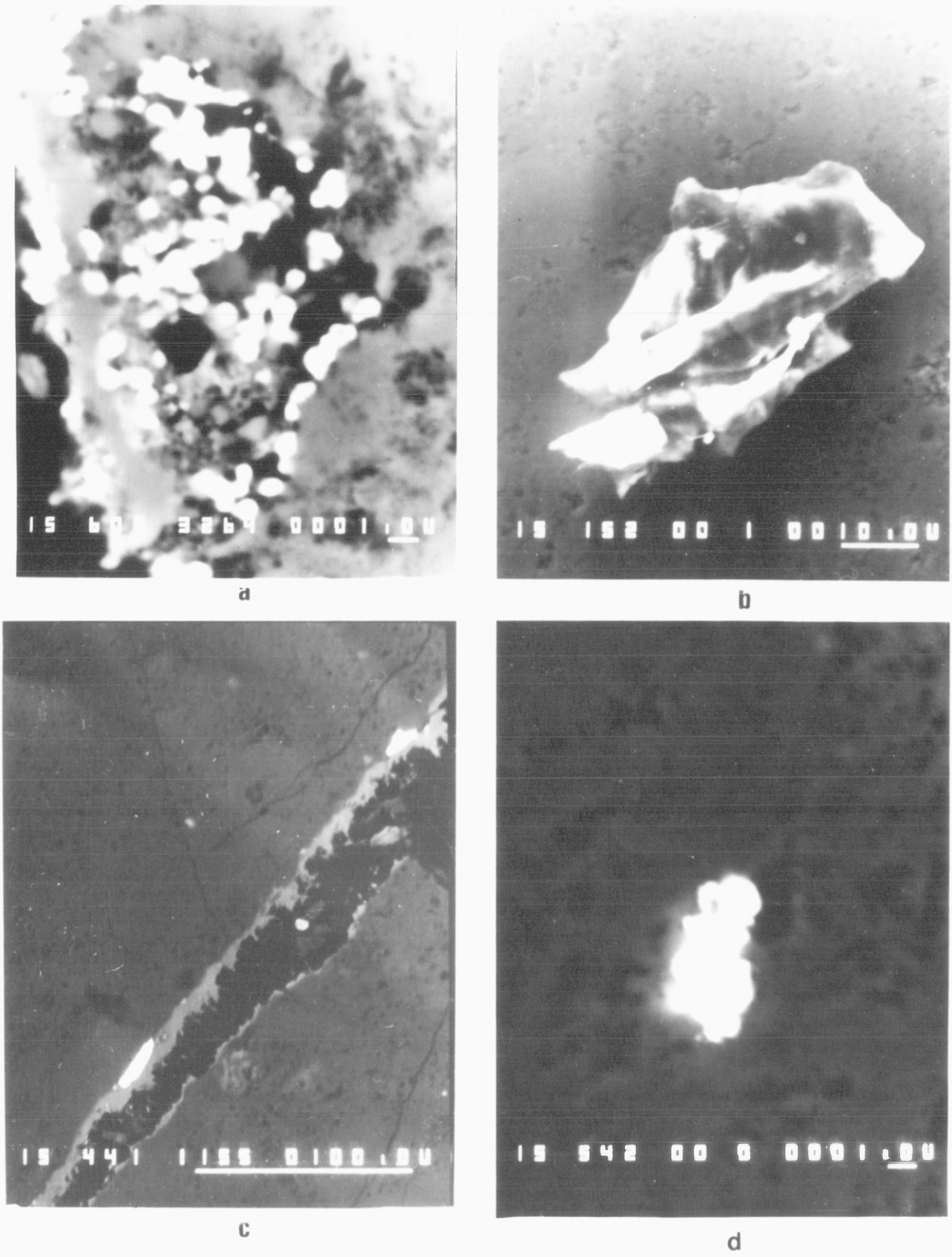


Plate 22 Backscattered photomicrograph showing U, Pt, Zn, Cu and Fe mineralizations and high temperature zinc-phosphate and barium minerals in sample 119 and 121.

(a=Ba-Zn-Cu-Fe and Mo mineralization; b=MoS_2; c=carnotite; d=chalcopyrite).

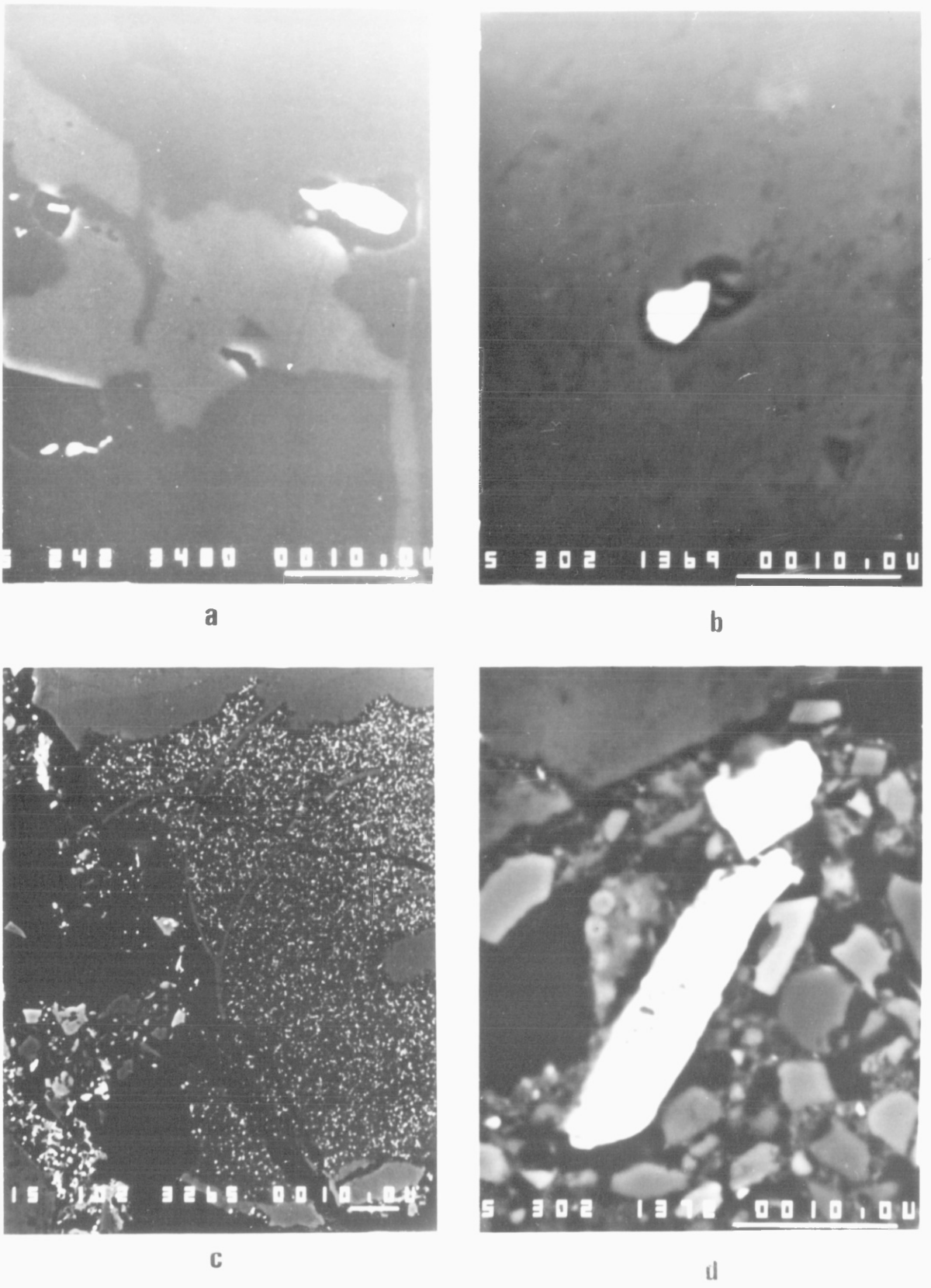


Plate 23 Backscattered photomicrograph showing U, Pt, Zn, Cu and Fe mineralizations and high temperature zinc-phosphate and barium minerals in sample 119 and 121.
(a-pyrite; b-Pt grain; c-U-Ba and Zn minerals; d-Cu,Fe sulphides).

cannot be produced by simple sedimentation of detritus.

The second trend in the distribution pattern of U is of moderately high values along the western boundary of the region. It is formed by clusters of samples at the northwestern end of most of the traverses which are underlain by mainly clayey and marly carbonate rocks of Palaeogene age. There are as well some weaker anomalous values over rocks of Neogene age, especially upper Miocene and Pliocene fluvial and lacustrine rocks. However, these latter anomalies occur only in few of the traverses, such as 100, 500 and 600 suggesting that they are not controlled by lithology but also by other depositional conditions. The clay fraction in these Neogene rocks perhaps accounts for the enhanced U levels. On the other hand, their location along the regional lineament found in the western side of Ad-Daww basin, and in somewhat structurally disturbed sites, must also be taken into consideration. In general, there is a great deal of uncertainty as to whether any diffusion of mineralizing fluids moving via these ancient taphrogenic lineaments ever took place along this trend, leading to its becoming relatively enriched in U. However, because of the direction of the groundwater movement away from this trend towards north and east (see Fig. 7.4), the likelihood of generating significant accumulations is doubtful due to the lack of any cyclicity or reconcentrating. Instead, dilution by groundwater destruction and flushing away of existing concentrations by oxidation could prevent (in the presence of carbonate anions) any fixation processes. The low U levels in the permeable Oligocene sandstones and the younger Neogene sediments (1 to 3.4 ppm) relative to other less permeable Palaeogene rocks averaging (10 ppm U), are perhaps, resulted from

the oxidizing groundwater circulation which seems to have a decreasing effect on U content of the permeable rocks by oxidizing, and then dispersing it elsewhere. The highest U content in the western trend (70 ppm) is found in dark grey marly limestone rocks of Lower Palaeogene age. Judging from the colour and texture, these rocks are less permeable in addition to being higher in carbonaceous and organic matter. Therefore, interpretation of U levels in this trend seems to be controlled by far more complicated factors than those can be inferred from the areal distribution pattern in Fig. 9.16, indicating the importance of additional geological, lithological and environmental information in order to obtain satisfactory intepretation. More detailed investigations to establish the underlaying controls are needed.

The third trend is located along the eastern boundary of the region and is formed by moderate to weakly anomalous values found in restricted numbers of samples. Usually they comprise only the first sample of each traverse except for traverses 700 and 800 where more than one sample falls within this trend, can be considered anomalous. It is noteworthy that these samples are spatially related to the two sides of Wadi Ghadir El Hamal, especially along the Ash-Shahba plateau where there are lower Eocene marls, marly and clayey limestones that are occasionally phosphatized and glauconatized.

Uranium dispersion in the above mentioned three trends seems to be influenced by the following controls;

i - the presence of phosphate rocks.

ii - fault zones and other structural lineaments.

iii - the groundwater regime and other surficial environmental conditions.

In Fig. 9.18 the three dimensional solid surface areal distribution of U in the Palmyrides region is viewed from four different angles to illustrate fully its pattern and without obscuring lower peaks by much higher ones.

Two additional items of information can be drawn from this figure. The first concerns the clear depletion in U content shown in the western side of the region south of J. Abou Rabah; and the second is that in the eastern trend of U anomalies, The values are seen to be decreasing southwards.

9.6.2.2 Radioactivity (CPS)

Measurements of the radioactivity of the rocks, are expressed in gamma ray counts per second (CPS) for each sample site; the measurements were made by Scintrex GIS 4 portable spectro-scintillometer. The symbolic areal distribution of the gross-count radiometric measurements is presented in Fig. 9.19, and the solid surface distribution is shown in Fig. 9.20. Inspection of the radioactivity pattern reveals great similarities with that of U. Few exceptions can be found particularly in the northern sector of Tudmor (Palmyra), and along the two eastern and western boundaries of the region, and these are best illustrated in the solid surface distribution (Fig. 9.20). The anomalous radioactivity in the northern vicinity of Palmyra is related to Quaternary lacustrine sediments and Recent (Holocene) rock debris. The

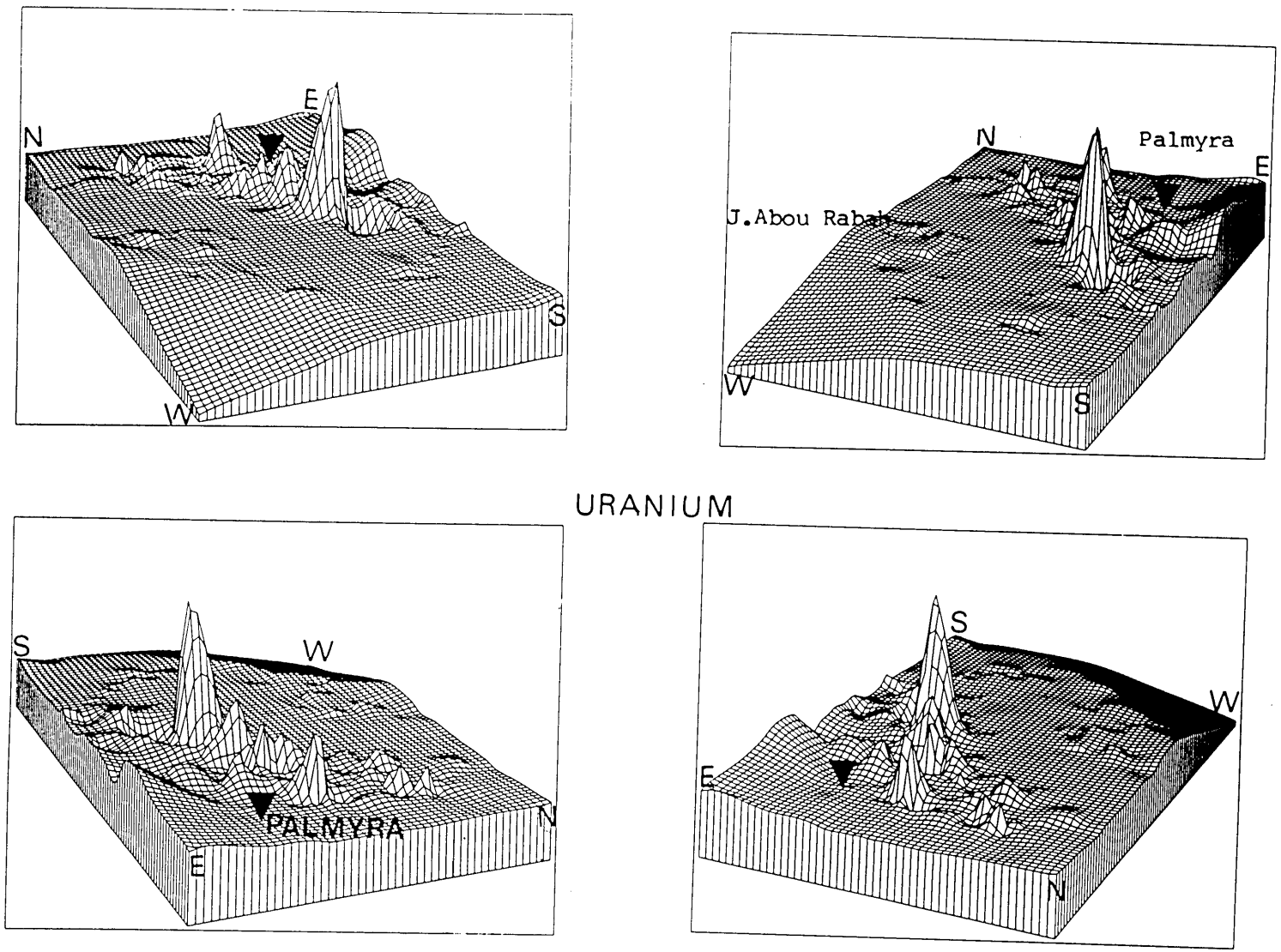


Fig. 9.18 Solid surface distribution of U in the region(viewed from four different angles).

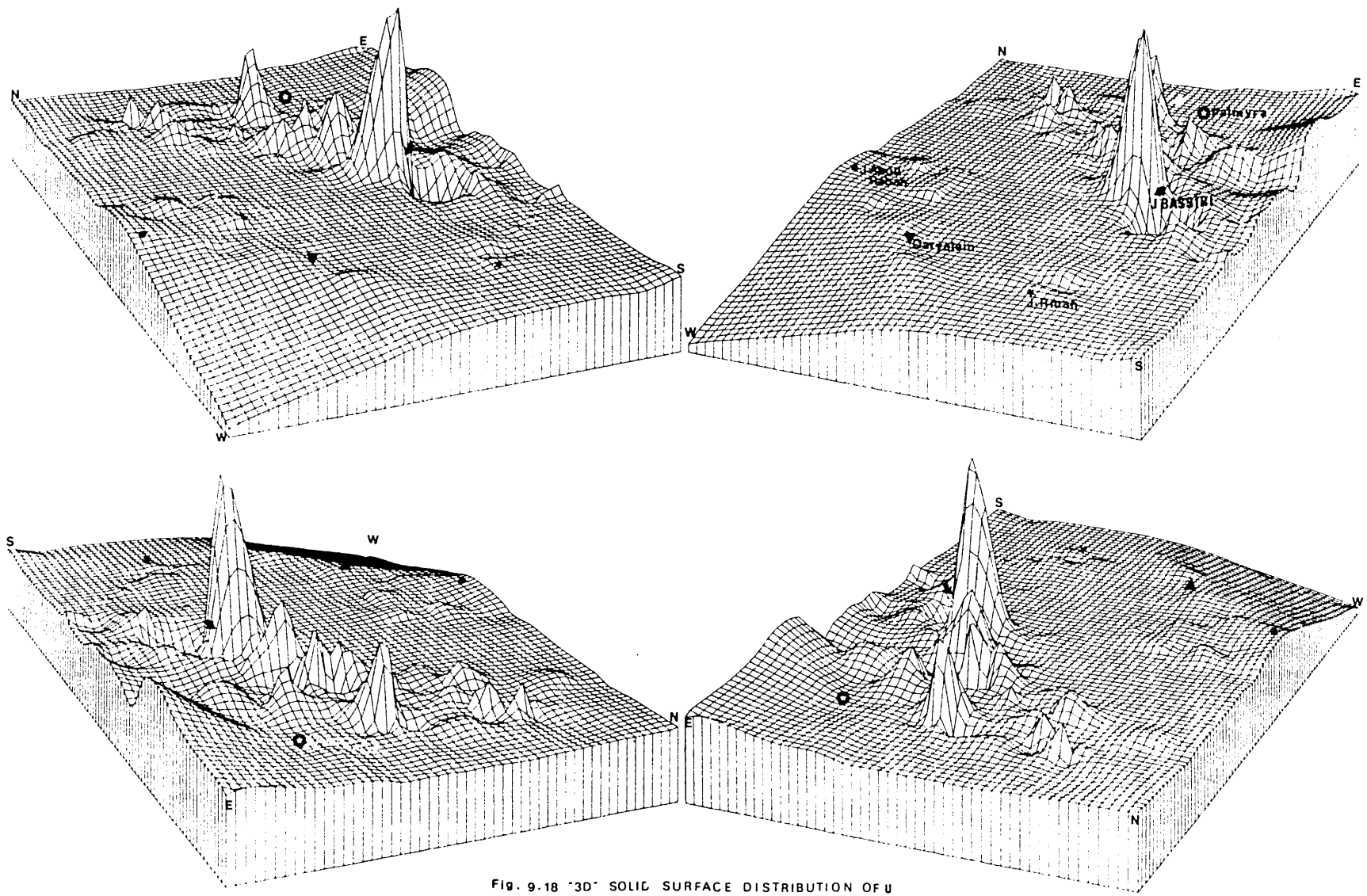


Fig. 9.18 "3D" SOLID SURFACE DISTRIBUTION OF U

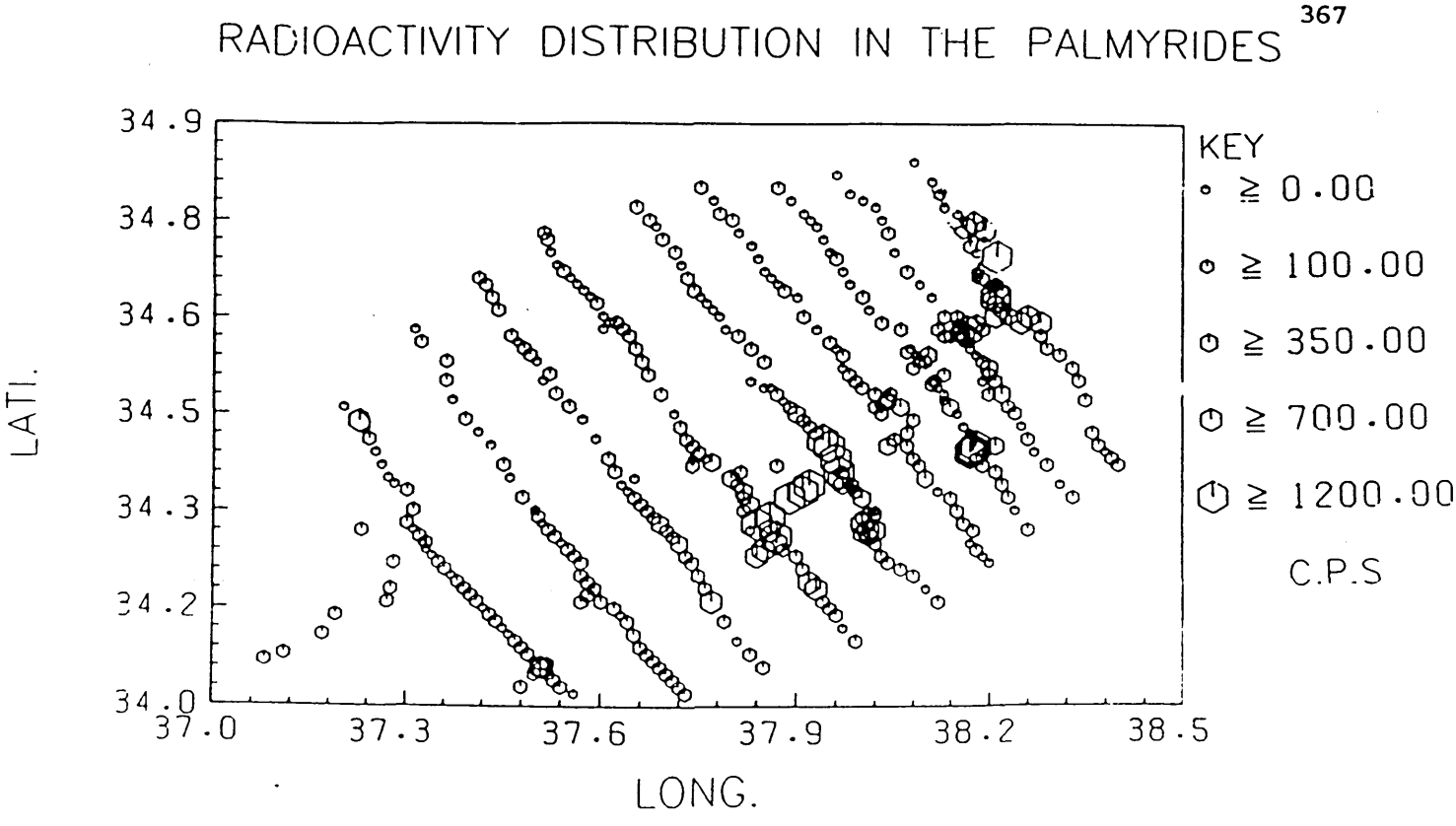


Fig.9.19 Symbolic areal distribution of CPS in the region.

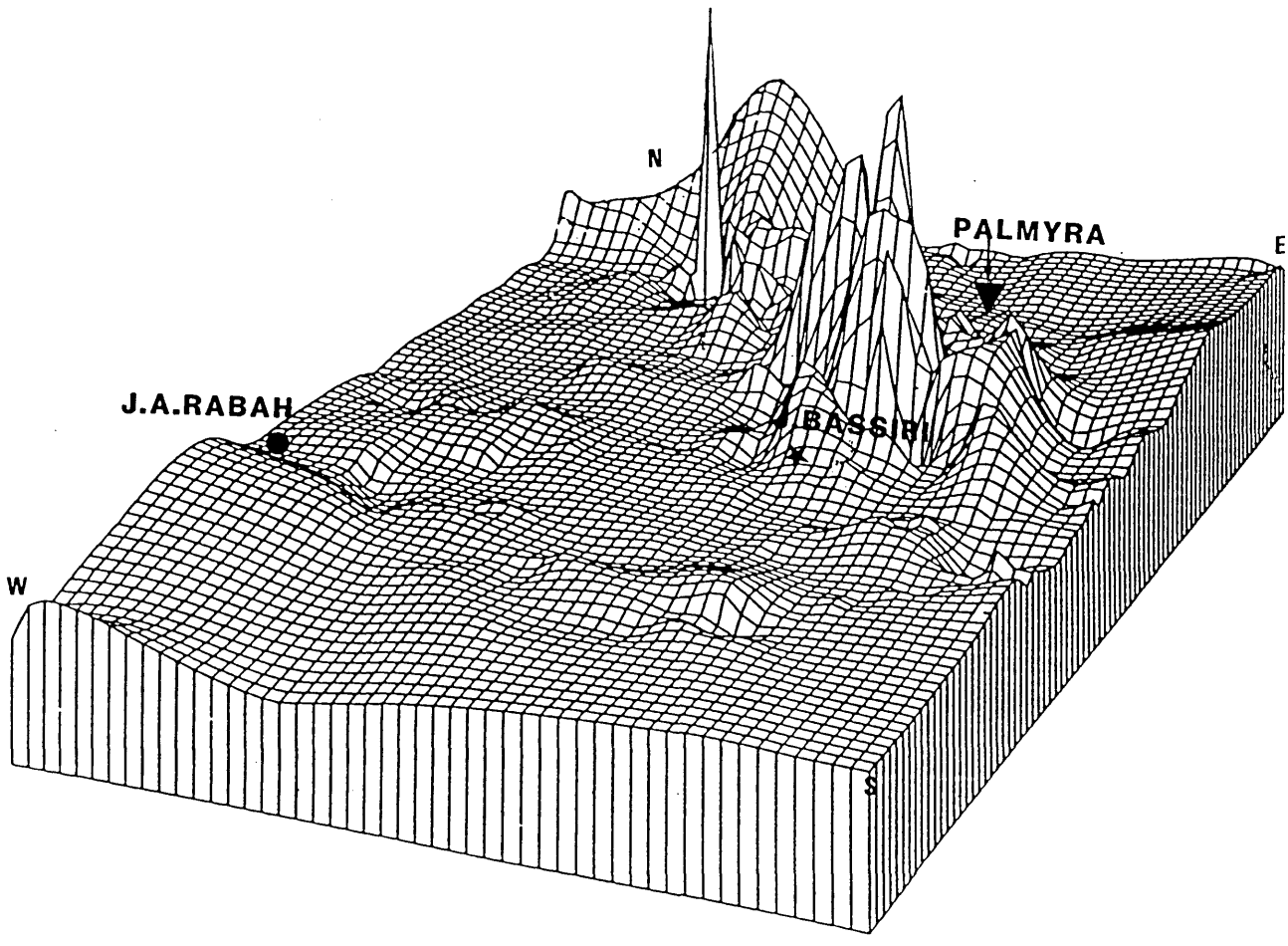


Fig.9.20 Solid surface distribution of CPS in the region.

scintillometer measured a total count of 1460 CPS, 2300 CPS and again 1460 CPS from three sites, while their calibrated background was 67 CPS. Accordingly a high equivalent U was expected from the samples collected from the corresponding localities, but surprisingly, neutron activation analysis from these sites yielded very low U concentrations ranging from 1.3 to 3 ppm. Although the Th content of these samples is weakly to moderately anomalous such Th concentrations cannot explain such high radioactivities, neither can they be explained in terms of the K content which is, more or less similar to most other sample sites. Therefore a great deal of uncertainty is related to the interpretation of this anomaly, and whether it represents some sort of contamination, or being caused by other reasons is not fully understood. It should be noted that in a few other cases, high radioactivity measurements (up to 4000 CPS) in J. Abou El Fawaress yielded 223 ppm U, while 410 CPS measured at the site of sample 710 reflects a U content of 602 ppm, similar cases were encountered outside the present lithogeochemical systematic sampling. Taking into consideration the finding of the present orientation survey as well as the conclusion made by Atfeh and Faradzhev (1965) and Hunting (1975), that, the radioactivity of the region is mainly controlled by the U content and not Th or K contents, and bearing in mind the above mentioned examples, it can be said that, although radiometric measurement can outline areas of interest for U exploration, its inconsistancy in terms of quantitative equivalent U content must be kept in mind when converting gamma-ray measurements into U concentrations. A weaker radioactivity response relative to corresponding moderate U anomalies along both the eastern and western margins of the region can also be seen. This reflects the presence of the Palaeogene and

Neogene rocks. Comparing the two solid surface patterns for U (Fig. 9.18) and radioactivity (Fig. 9.20), it is evident that the latter shows much less depletion in the southwestern corner than the former.

Elsewhere the radiometric high values are controlled by or associated with phosphate rocks and faulted areas.

9.6.2.3 Thorium

The concentration of Th in the Palmyrides varies between 0.1 to 34.3 ppm. The principal features of its areal distribution are shown in Fig. 9.21 and the solid surface Fig. 9.22. Compared to U and CPS patterns, a strong displacement of the very high Th anomalies towards west and to lesser degree south is clearly shown especially in Fig. 9.22.

Two trends of anomalous values (>=16 ppm Th), are running nealy parallel to each other from south-southwest towards north-northeast, the fartherwest of them seems to follow the lineament of the western side of Ad-Daww basin, and nicely coinciding with the boundary between the Neogene and Palaeogene rocks. In addition, a minor trend striking E-W across the hills of Sawwanet El Hammra south and south west of Khneifiss is outlined by moderately high Th levels (6 to 16 ppm). Although the phosphate lithologies, in general, show moderate to high levels of Th, the highest values seem to be related to structural features rather than to lithologic ones, and almost all very high anomalies coincide with the NE-SW, E-W and NW-SE striking faults. The

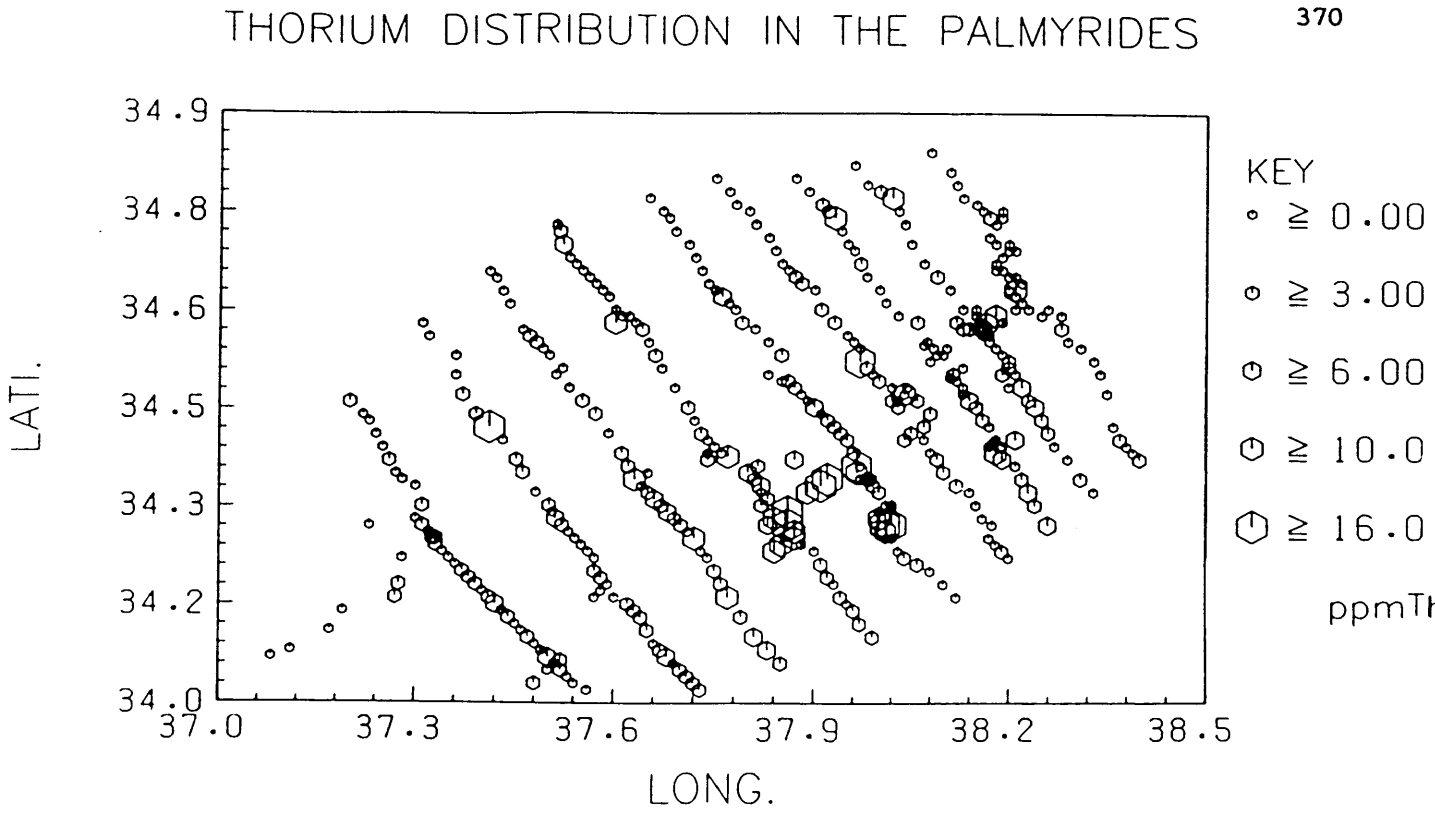


Fig.9.21 Symbolic areal distribution of Th in the region.

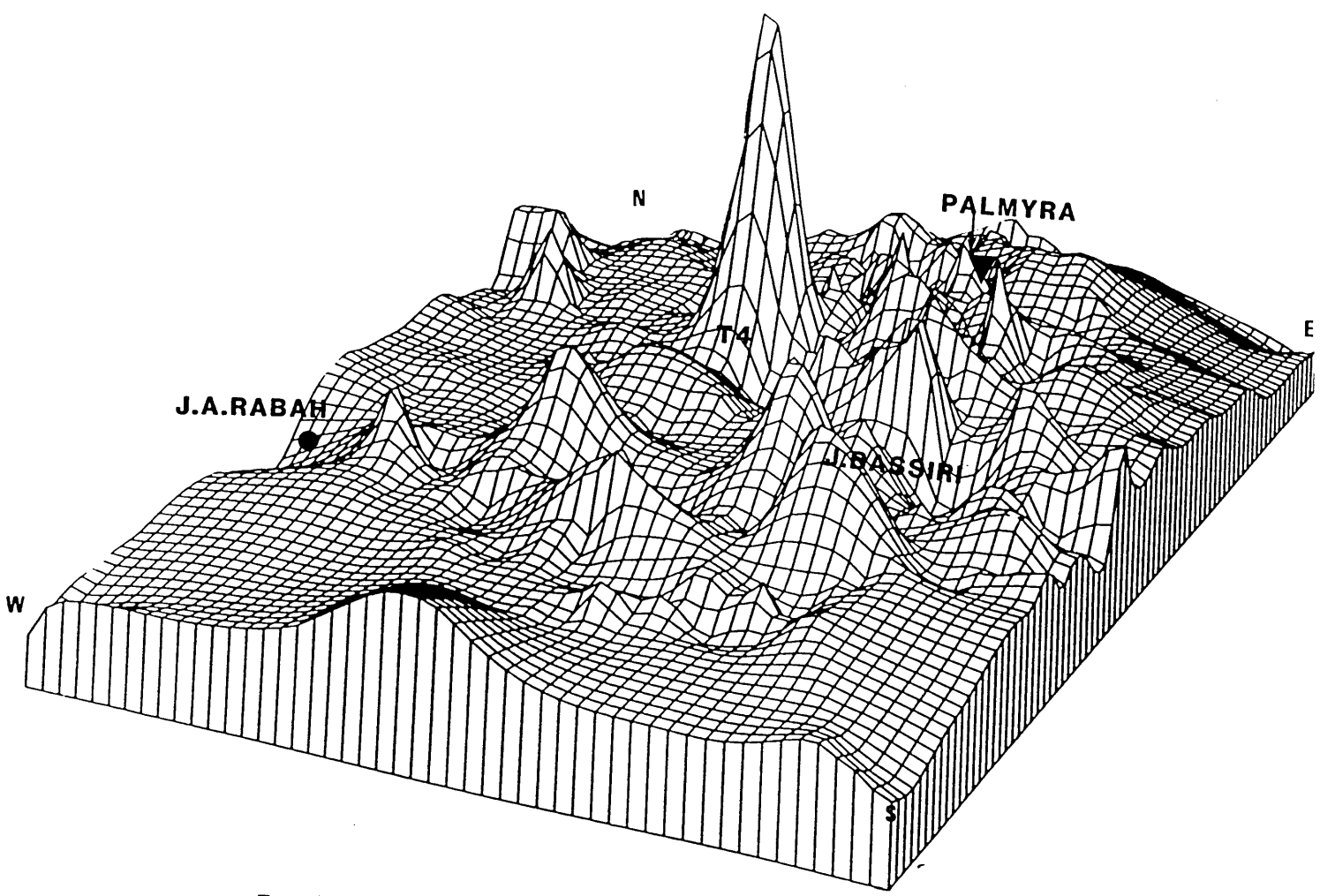


Fig.9.22 Solid surface distribution of Th in the region.

unconformity contacts of the Neogene with the older rocks in both sides of Ad-Daww basin and within the central part of its northern margin, are particularly enriched in Th. Furthermore, a weak to moderate Th anomaly occurs along the southern margin of Sabkhet El Mouh coinciding with the Sawwaneh fault (see Fig. 8.2), others can be seen along the lower part of traverse 700 below the fault controlled sample 710. These features are better seen in the solid surface distribution (Fig. 9.22).

The distribution pattern of Th suggests that the main controls of its primary dispersion are structurally related, and to lesser degree the phosphate lithologies.

9.6.2.4 Arsenic

The spatial distribution of As (Fig. 9.23) demonstrates a considerable difference between the eastern and western halves of the region. The divide can be inferred along the western edge of the southern Palmyrides mountains. Arsenic concentrations range from very low (0.01 ppm) to relatively high (66 ppm) levels. High and moderately high values (25 to 66 ppm) occur over Upper Cretaceous rocks in close relation to phosphate and marly-clayey limestone lithologies particularly along the flanks of these mountains.

A series of sample sites with relatively enhanced As contents (>=15 ppm) are found over the Lower Palaeogene rocks especially in the southeastern parts of traveses 900, 800, 600 and to a lesser degree 400, as well as of samples close to site 710 in traverse

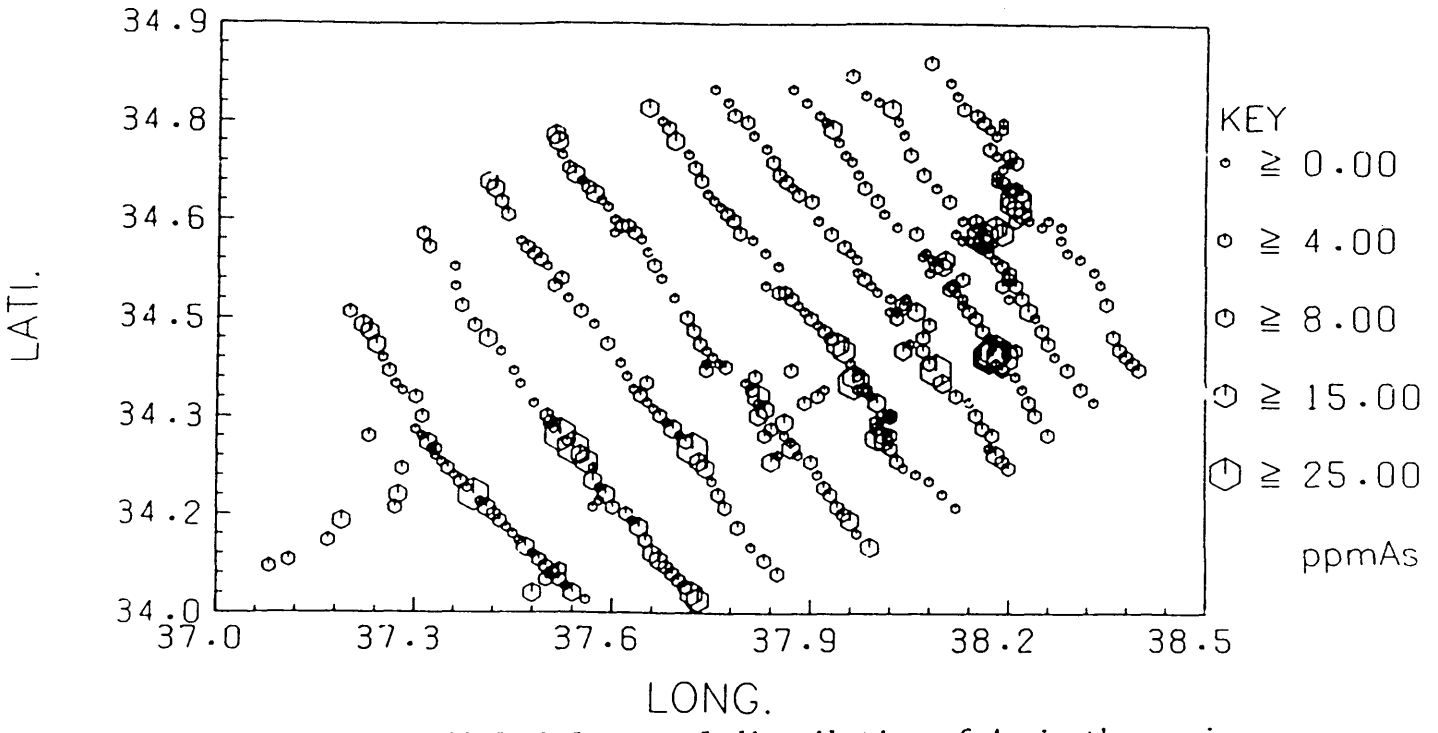


Fig.9.23 Symbolic areal distribution of As in the region.

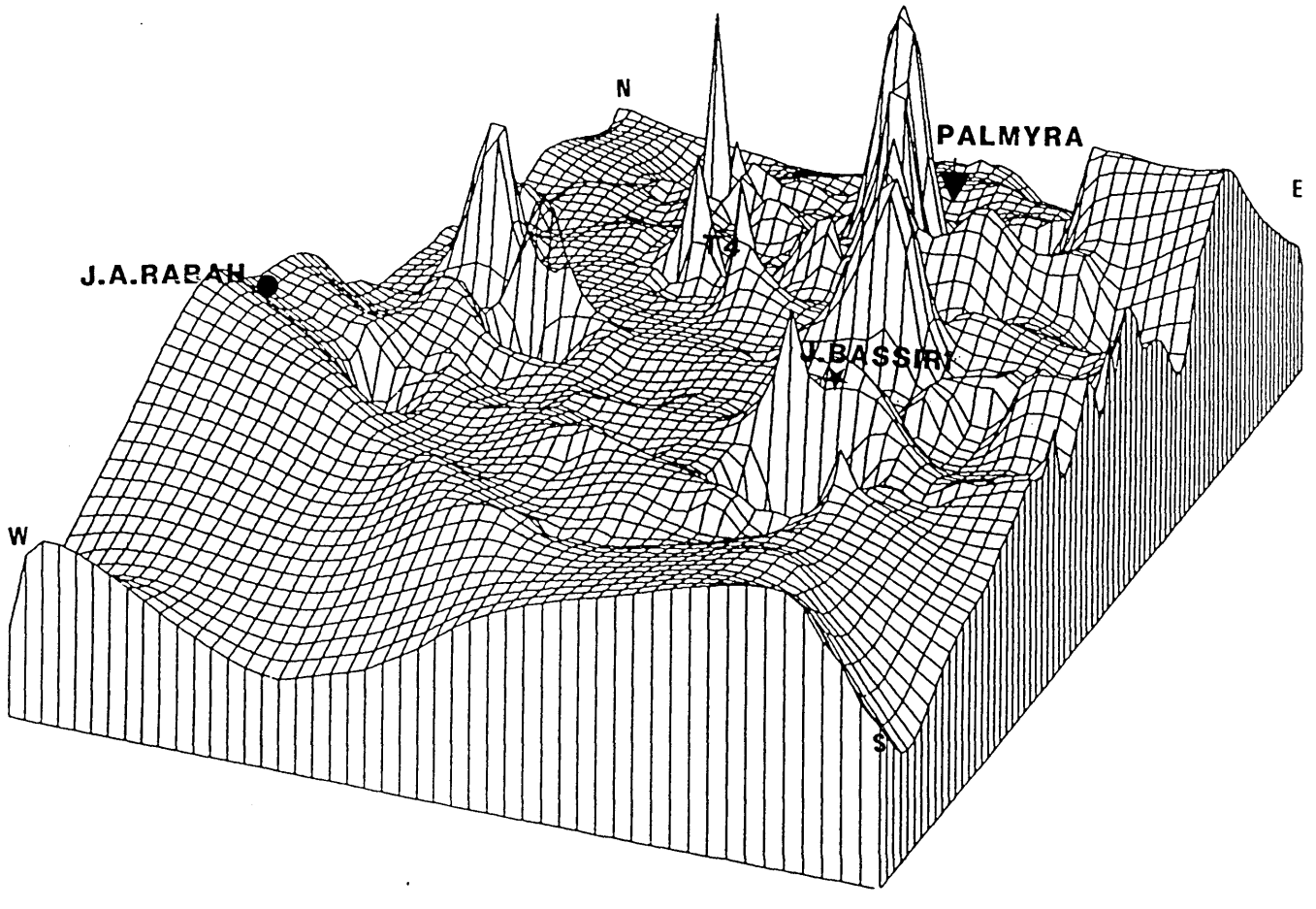


Fig.9.24 Solid surface distribution of As in the region.

700. The Quaternary rocks all over the region are generally low in As and almost void of anomalous levels. Very few weak to moderate anomalies, however can be found in the Lower Neogene formations particularly along the regional lineament at the western side of the Ad-Daww basin. A cluster of three moderately anomalous values of As (15 to 25 ppm) occurs over the area of J. Abou Rabah at the western margin of the region, while anothe cluster which consists of the highest value (66 ppm) and a few moderately highs is found in the extreme northeast corner of the ad-Daww basin, and is related to the Upper Cretaceous rocks of the western flank of J. Abou El Fawaress. These two clusters can be seen clearly in the solid surface distribution (Fig. 9.24).

Low levels of As are encountered over the Cretaceous hills that are located between traverse 500 and 600, along Wadi Qasser El Halabbat where samples gave very high U, Th and radioactivity levels. Except for these samples, however, the regional distribution of As seems to reflect underlying lithological control and to a lesser degree structural one, with phosphate and clayey carbonate rocks of Upper Cretaceous and Lower Palaeogene are being characterized by high As levels. The peaks of As in Fig. 9.24 reflect both controls and outline the features of the primary dispersion of As in the Palmyrides region.

9.6.2.5 Selenium.

The areal distribution of Se is presented in Fig. 9.25. It is clear that a small number of samples show Se concentrations higher than 12 ppm, therefore can be considered highly anomalous. Except,

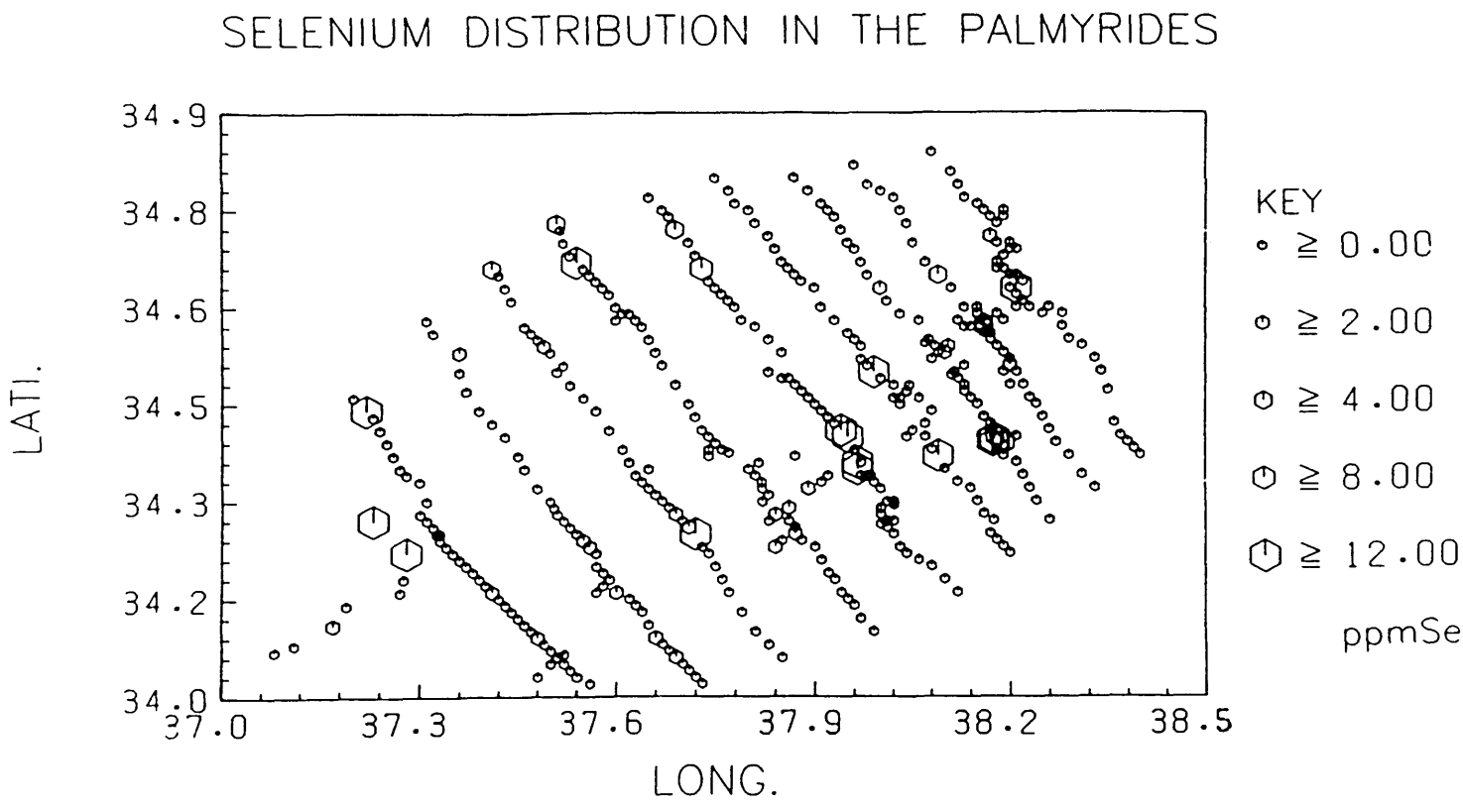


Fig.9.25 Symbolic areal distribution of Se in the region.

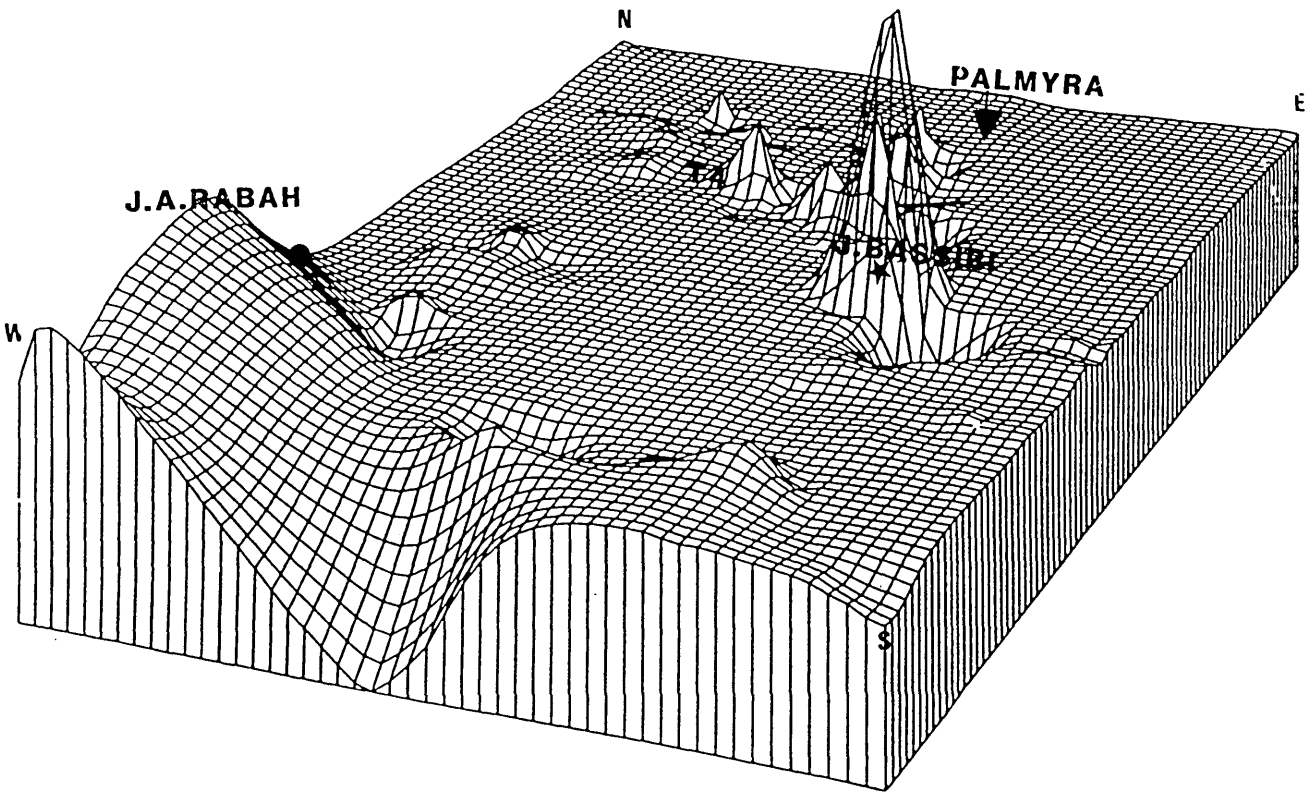


Fig.9.26 Solid surface distribution of Se in the region.

however, for those high values related to sites along previously mentioned fault zones, other scattered Se anomalies are restricted to rocks of Cretaceous and Lower Palaeogene formations that also are being affected by faults and fractures. Therefore the areal extent of anomalous Se levels that can be seen in Fig. 9.26 is generally small.

The longest trend of high values is found on traverse 500 closely related to the range of J. Om-Jorn and extending northeastwards across J. Qal, J. Tabaque and J. Hayan. It should be pointed out that this trend is not continuous, but it is made of individual Se highs that are spatially related to intercepting NE-SW and NW-SE trending faults. Therefore, it is evident that the major peaks in the solid surface distribution pattern (Fig. 9.26) coincide with structurally controlled locations.

A short E-W trend of moderate to high Se values (8 ppm), can be recognized in the northern third of Ad-Daww basin close to J. Tyas in the vicinity of T-4 oil pumping station on the road (Tudmor-Homs). Geochemically speaking, this trend is very interesting because it coincides nicely with similar trends of anomalous Se in the groundwater data that was detected during the present hydrogeochemical survey (see section 7.6 and Fig.7.21). Taking the scale difference into consideration, comparison of the solid surface distributions of Se in the groudwaters (Fig. 9.27) and the lithogeochemical data (Fig. 9.26) suggests that, the E-W trend in both figures reflect the significant role of the interaction between the groundwaters and their aquifer rocks. Furthermore, an intermittent weakly anomalous Se trend running

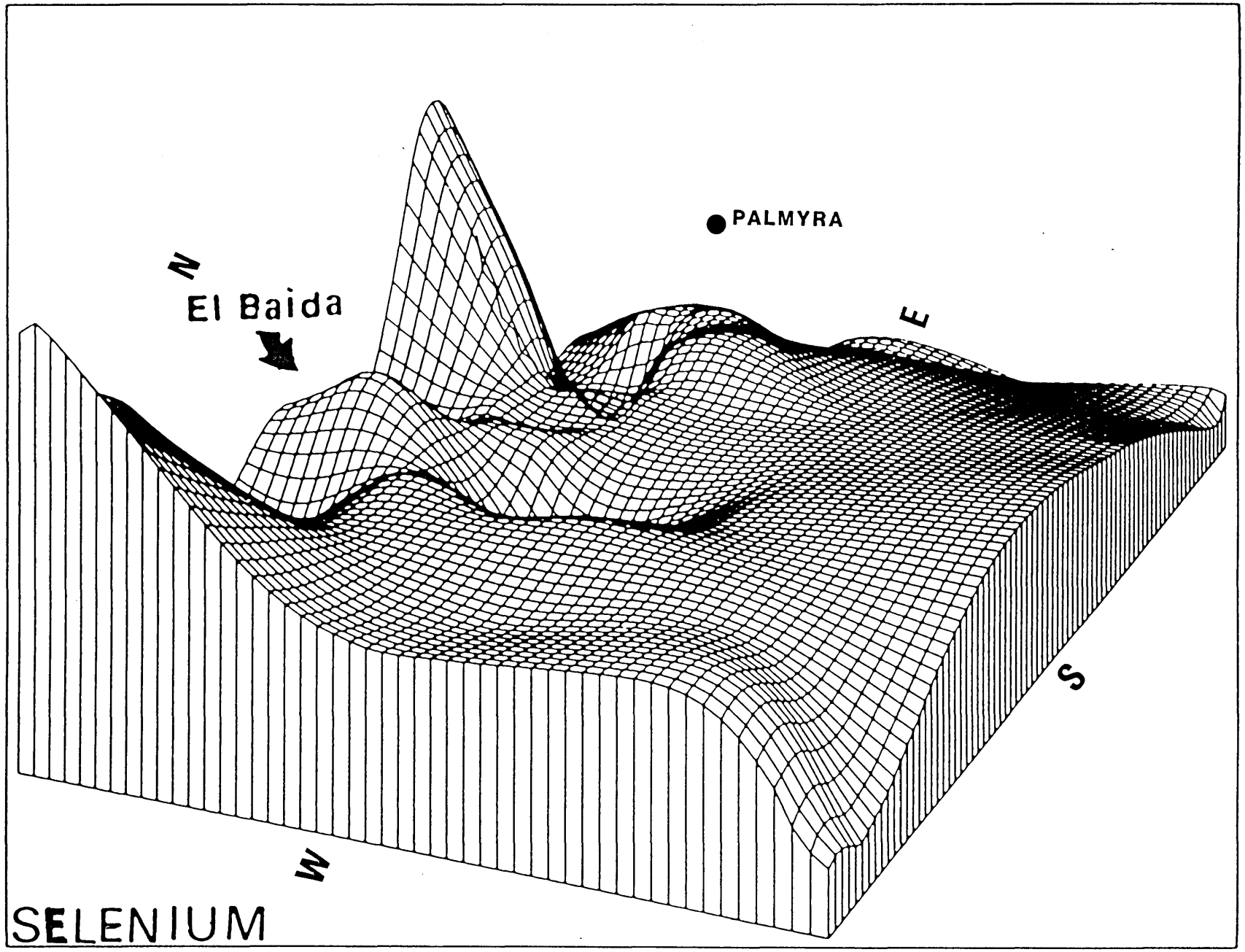


Fig.9.27 Solid surface distribution of Se in the hydrogeochemistry.

parallel to the regional lineament in the western side of Ad-Daww basin, can be inferred to coincide with the unconformity contact between Neogene and Palaeogene rocks. This discontinuous trend includes moderate Se concentrations in samples taken from J. Tyas, much weaker Se levels from samples of Sharifeh hills and others moderately anomalous Se levels in the vicinity of J. Abou Rabah. It should be stressed, however, that similar extent of the hydrogeochemical Se anomalies along the above mentioned regional lineament were discussed previously in Chapter VII and can be seen in Fig. 9.27.

From the foregoing characteristics of the primary dispersion pattern of Se, it can be said that the major controls of its distribution are structurally related to faults and regional lineaments, and more probably it is also affected by the groundwater circulation to a certain extent.

9.6.2.6 Phosphorus.

The distribution pattern of P (Fig. 9.28) reflects the presence of phosphorite and phosphate rocks in the region. However, almost all values >= 8% P (18.3% P_2O_5) are found in Upper Cretaceous (Campanian-Maestrichtian) rocks, while values in the range of 5 to less than 8% P are found over Lower Palaeogene phosphatized carbonate rocks.

The pattern of anomalous P starts in the vicinity of J. Rmah and Wadi Ghadir El Hamal in the southeastern part of the region, and their values intensify along a trend striking northeastwards,

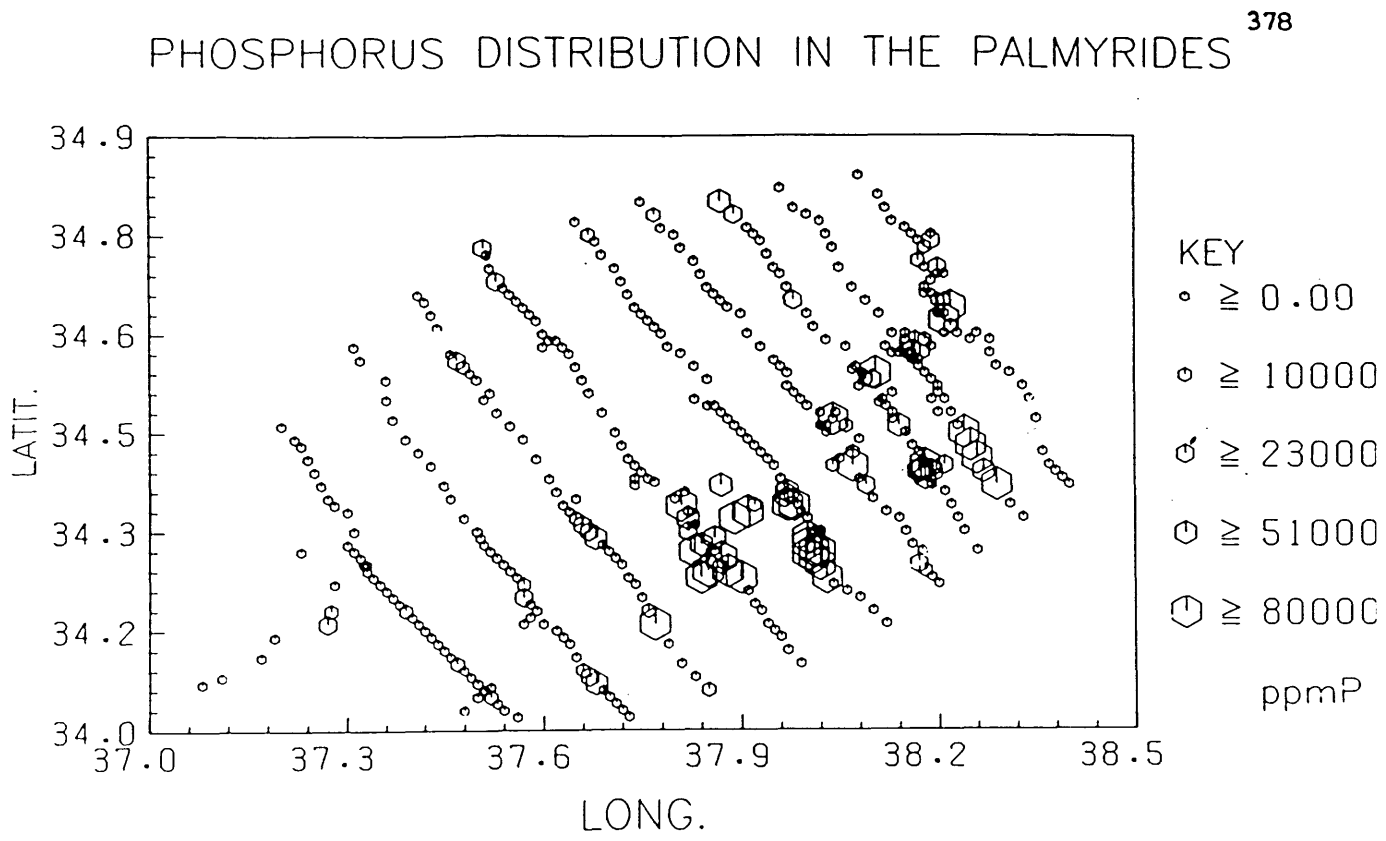


Fig.9.28 Symbolic areal distribution of P in the region.

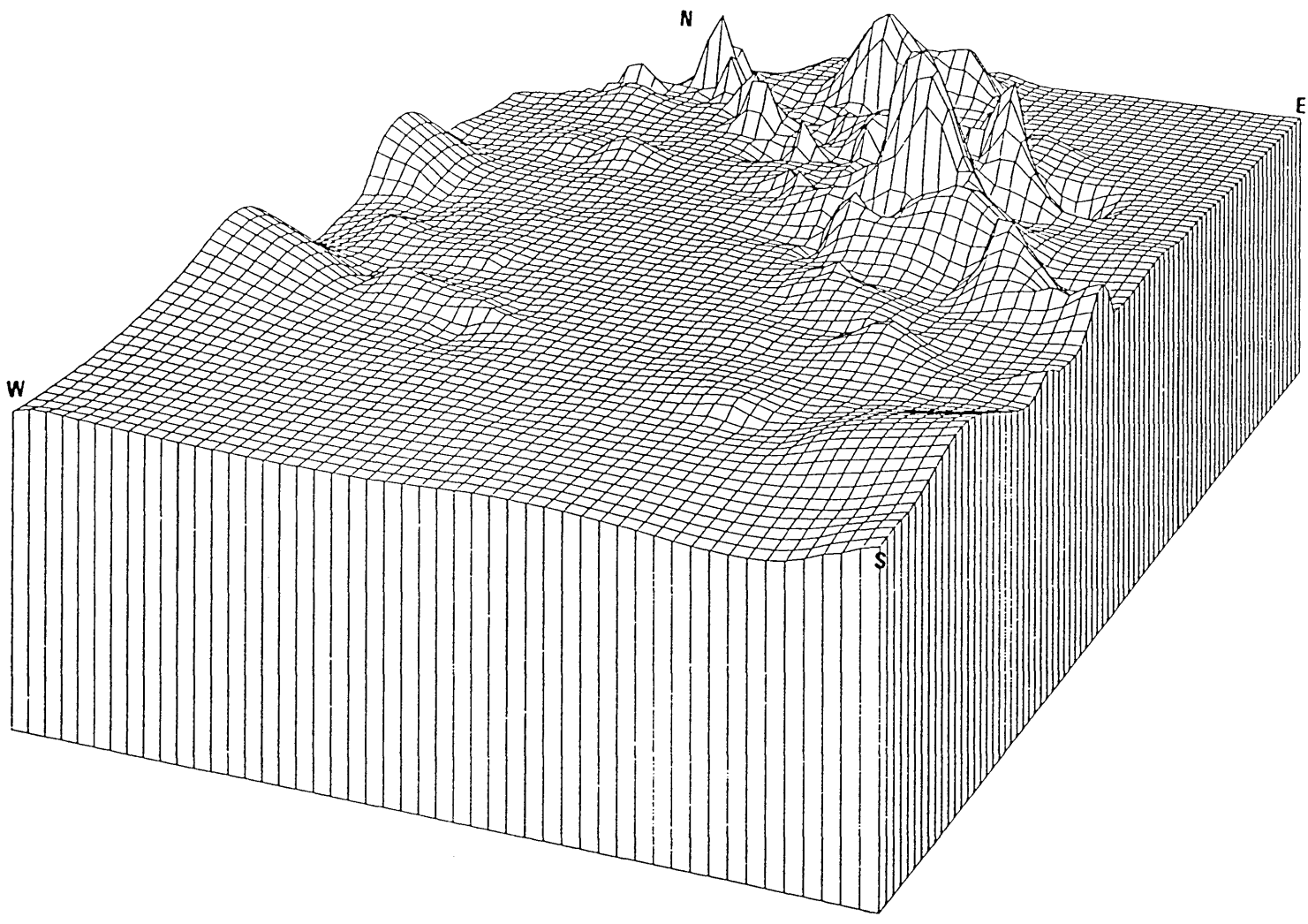


Fig.9.29 Solid surface distribution of P in the region.

especially over known phosphorite deposits such as those in the Khneifiss and Ash-Sharquieh areas. This trend coincides spatially with the southern Palmyride mountains, however, a cluster of high P values occur at the lower part of traverse 200 further east of the mountains and south of Sabkhet El Mouh. In this locality the rocks are either lacustrine and clastic sediments of Neogene age, or marly limestones and marls of the Palaeogene sequence, both are, however, in contact with the Upper Cretaceous phosphate and phosphatized carbonate by the well marked southern Palmyrian zone of faults. Therefore, the above mentioned cluster over these rocks seems to be influenced by P remobilization either singenetically or epigenetically due to later processes that took place along the fault. In addition the solid surface distribution (Fig. 9.29) shows a smaller cluster of high P levels occuring further west of the main Neogene-Cretaceous fault contact, the P anomaly here is confined to the extreme northern end of Jabal Al Abtar. The brecciated nature of the phosphate rocks, and the enhanced levels of their U and radiometric measurements relative to similar phosphates in the area suggest a strong effect of the Sawwaneh-Abtar fault on the behaviour of all these variables including P.

As mentioned in the geology (Chapter II), rifting and sea floor oscillation characterize the marine sedimentary environment of the late Cretaceous period in the Palmyrides. The major phosphorite deposits and other phosphatization occur within a carbonate dominant sequence, contemporaneously to the Neo-Tethys plate tectonism in the Middle East region. The rapid and narrow variations in the slightly alkaline pH condition can account for

the alternating beds of phosphorites, limestones, phosphatic carbonates and carbonates. It is relevant to stress that these tectonic activities and environmental effects are the major controls of the primary dispersion of P in the region and can be considered the main underlying causes for phosphorite precipitation.

9.6.2.7 Strontium.

The areal distribution pattern of Sr (Fig. 9.30) is characterized by relatively high background levels 1000 to 1500 ppm. Such values are located mostly in the Ad-Daww basin and over the main plateaux. All lithologies including the phosphates and Quaternary formations show distinct variations in Sr content with concentration values ranging from 39 to 5500 ppm. However, high anomalies of Sr (concentrations greater than 3500 ppm) are encountered mainly over the phosphorite formations of the Upper Cretaceous and Lower Palaeogene, the gypsum horizons of the Neogene sequence, the duricrusts of the Quaternary formations and to a lesser degree the carbonates of the Palaeogene system. Moderately high values (>= 3000 ppm Sr) are spatially related to Sabkhet El Mouh margins as well as to faulted zones (samples 710, 711, 712, 121). Hale and Jubeli (1985) reported a distinct association of celestite ($SrSO_4$) with secondary U minerals in the region. Hence the presence of disseminated celestite in samples of similar fault-setting to sample 710 may explain an enrichment in Sr within these faulted areas. Strontium concentration towards the top of a carbonate layer was suggested by Vinogradov and Borovik-Romanova (1945) on the basis of their work in Kazan, later such enrichment

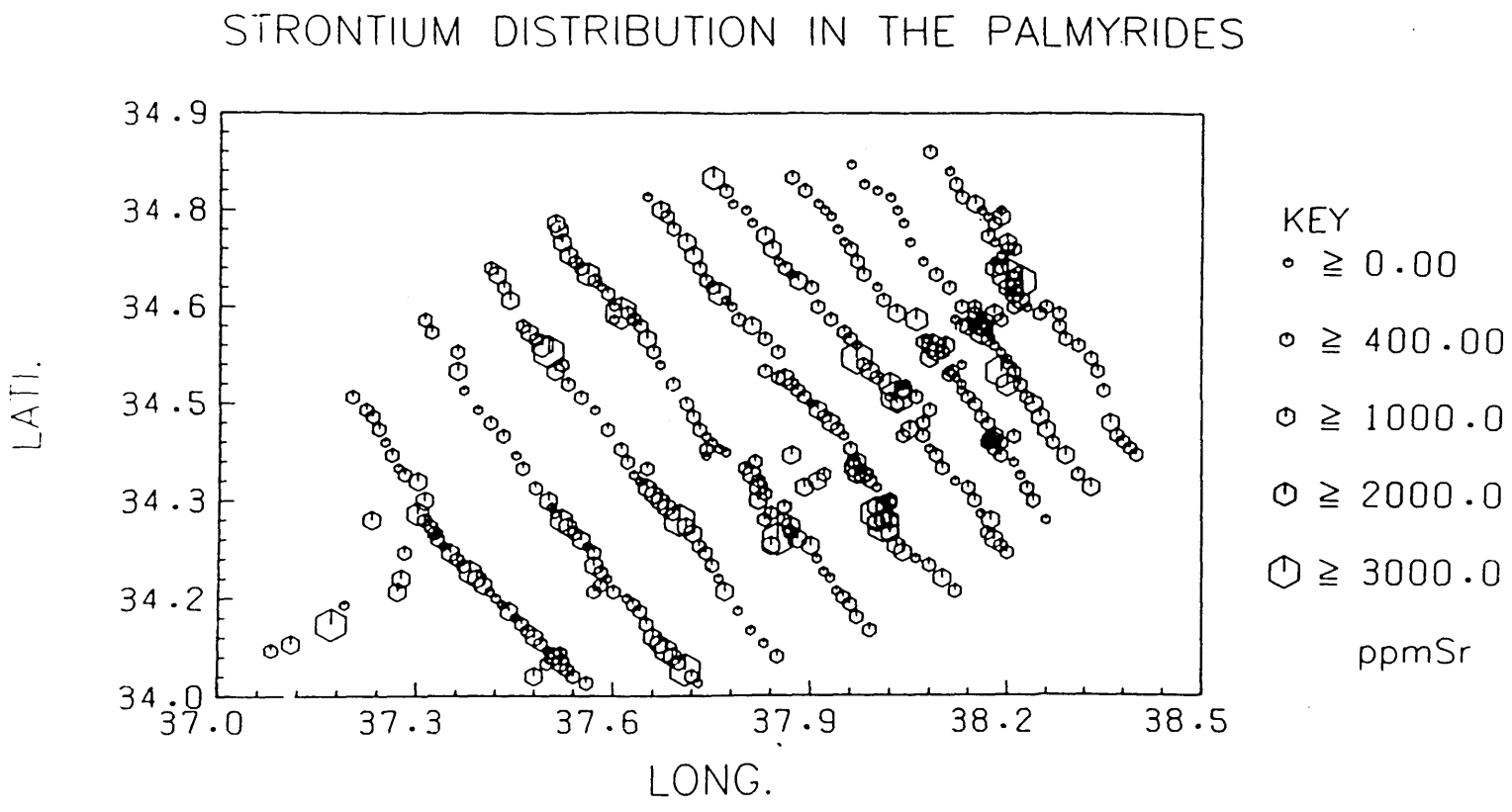


Fig.9.30 Symbolic areal distribution of Sr in the region.

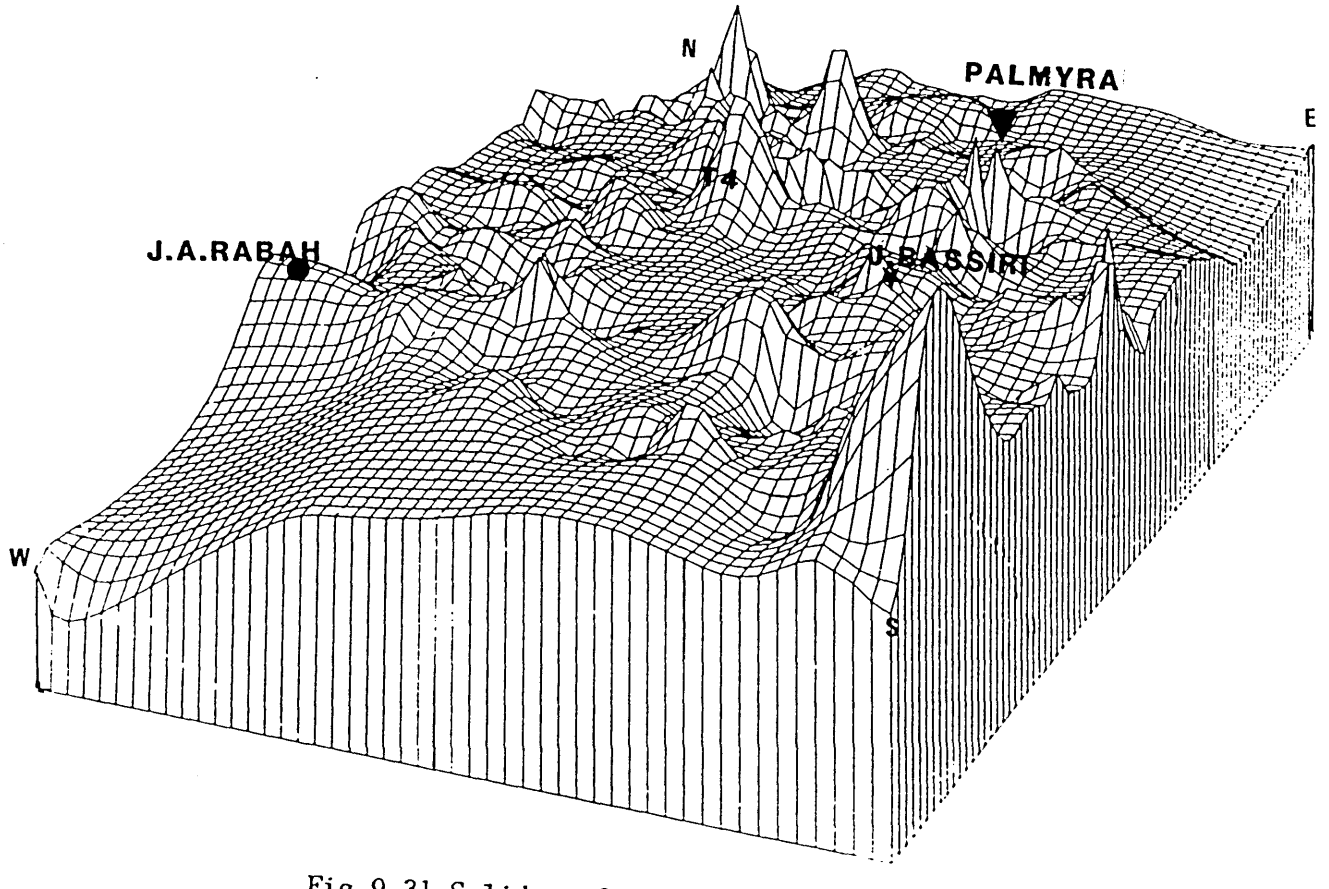


Fig.9.31 Solid surface distribution of Sr in the region.

was related to climatic and formation of calcrete, due to interaction with saline waters (Otton, 1984). Similar processes are inferred to be responsible for the observed Sr enrichment in the western vicinity of Sabkhet El Mouh, the northern part of Ad-Daww basin and the plateaux of Aida and Ash-Shahba in the southeastern side of the region. Whereas the enrichment within the phosphate rocks is restricted only to areas where perhaps interaction took place between phosphatic solutions and clayey limestones acting as scavengers for the concentration of Sr (Frondel, 1958). Such areas, however seem to suffer faulting and fracturing.

The major anomalous peaks of Sr in the solid surface distribution (Fig. 9.31) outline all above mentioned areas and reflect the underlying processes that control the lithogeochemical dispersion pattern of Sr. Climatic and environmental conditions exhibit a significant control particularly in the central north and south, aridity, as well as, the resulted variations in groundwater levels (discussed previously) and other sedimentary environments have been playing a major role in producing the present pattern of Sr distribution. Structural features of major faults and regional lineaments can also be considered as important, and enhanced levels of Sr in the phosphate rocks could perhaps indicate a weaker lithological control.

9.6.2.8 Vanadium

The distribution of vanadium in the Palmyrides rocks (Fig. 9.32) displays a distinctive contrast of concentration between the southern Palmyrides mountains and elsewhere in the region.

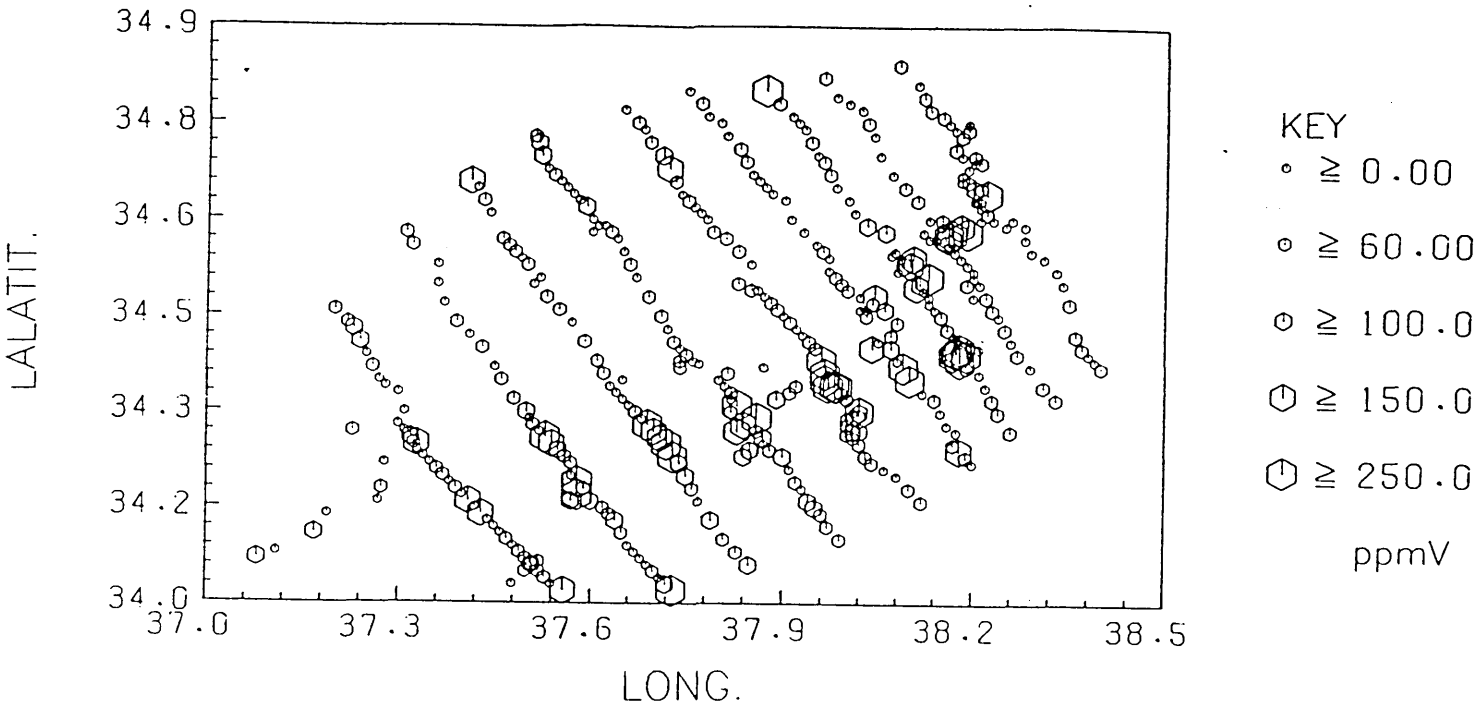


Fig.9.32 Symbolic areal distribution of V in the region.

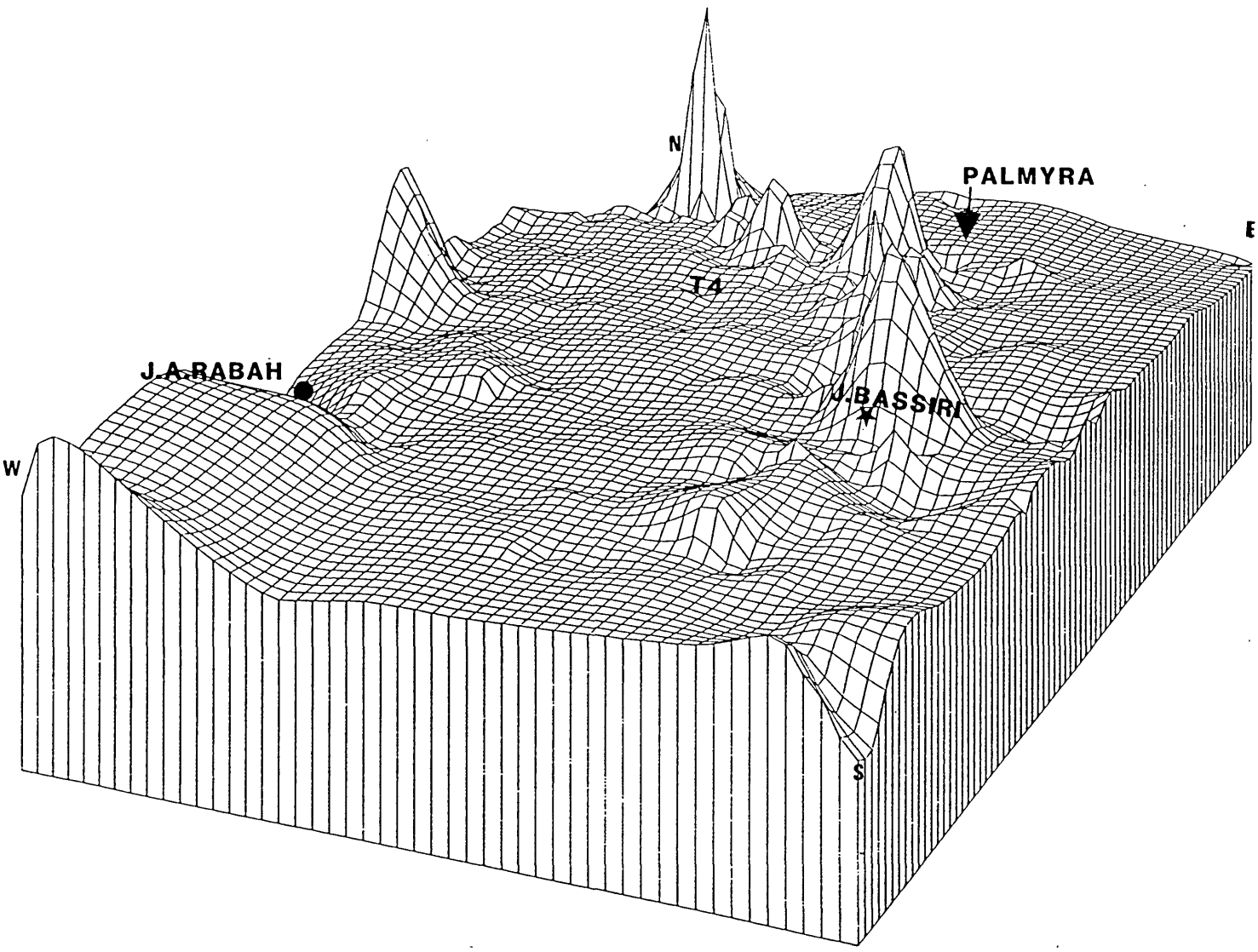


Fig.9.33 Solid surface distribution of V in the region.

Extensive areas of high V levels (>=160 ppm) can be distinguished along the eastern side of Ad-Daww basin, in good agreement with V distribution in the hydrogeochemical survey of the region (chapter VII). This further supports the interpretation that the dispersion halo of V appears to be more extensive than that of U. The majority of V anomalies (>=160 ppm) are closely related to phosphorites, Lower Palaeogene clayey glauconitic carbonates and especially fault zones. A few scattered moderately high values are found along the extreme western and eastern margin of the region, the eastern ones are closely related to small outcrops of volcanic rocks just outside the surveyed area. Moreover, a small cluster of 5 samples centered around sample 710 deserve particular attention due to:-

a) its extremely high V concentrations (0.1% to 0.67%); and
b) the enhanced levels of an association of Ni, Zn, Cu and Mo, the significance of which has been discussed through the finding of diseminated mineralizations along this faulted location.

The remaining parts of the region are generally void of V anomalies. This is better illustrated in the solid surface spatial distribution of V (Fig. 9.33).

Both lithological and structural controls are equally important in their influence of the dispersion pattern of V in the region. The first control is displayed mainly by the phosphorites and glauconitic limestones of the Upper Cretaceous and Lower Palaeogene respectively, while the circulating solutions through fault and fracture conduits lead to further enrichments, even with the said lithologies, and emphasizes the structural control.

In general, the distribution pattern of V is similar to that of U (although larger in its areal extent along the eastern side of Ad-Daww basin), and in some respect it is similar to a few other elements, particularly Mo, Zn, Cd, Cu and to a lesser degree Ni.

9.6.2.9 Molybdenum

The main features of the areal distribution of Mo are illustrated in Fig. 9.34. There is a 7ppm display of a regional background level. High values of Mo occur over the phosphate domains especially in the Khneifiss area, and to a lesser degree near to faulted zones. However, there is a marked concentration of high Mo levels over the Palaeogene rocks in fact, the highest anomaly (125 ppm) occurs in the mid western side of the region over predominantly clayey limestone rocks of Lower Palaeogene age. These anomalies are better illustrated in the solid surface distribution (Fig. 9.35). In this figure both positive and negative (below background) Mo levels of concentrations can be seen. The lower than background values (depletion) are confined to very small areas in the extreme southeastern corner as well as the northern limb of J. Abou Rabah in the lower part of the western side of the Palmyrides region. As mentioned earlier, the primary dispersion pattern of Mo, in general, is similar, although smaller in areal extent, to that of V and perhaps to U. Hence, the distribution pattern of Mo in the region seems to be controlled by the phosphate lithologies, impurities in the carbonate rocks and the regional structural features. The anomaly in the western side is also outlined by the V pattern and requires further investigation.

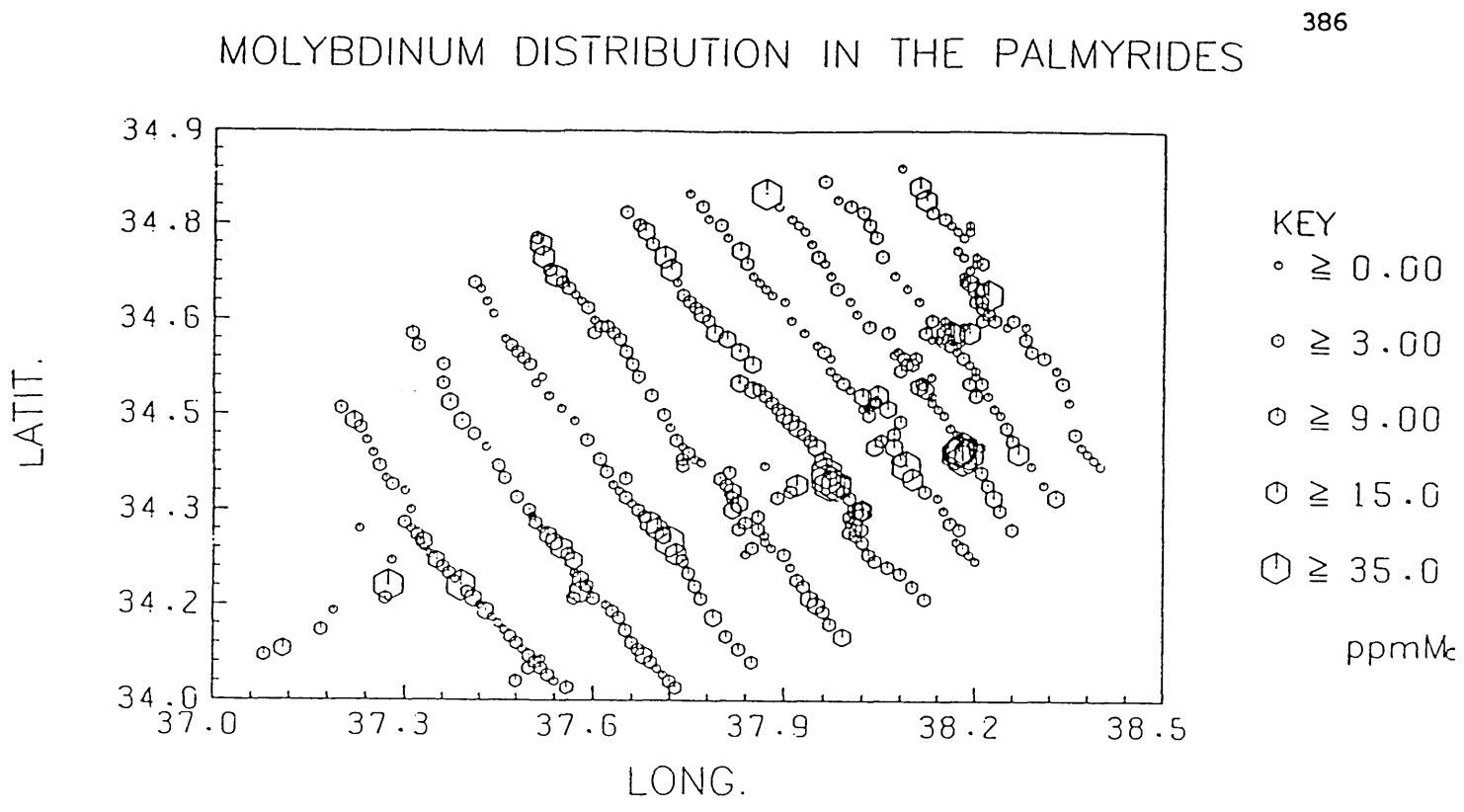


Fig.9.34 Symbolic areal distribution of Mo in the region.

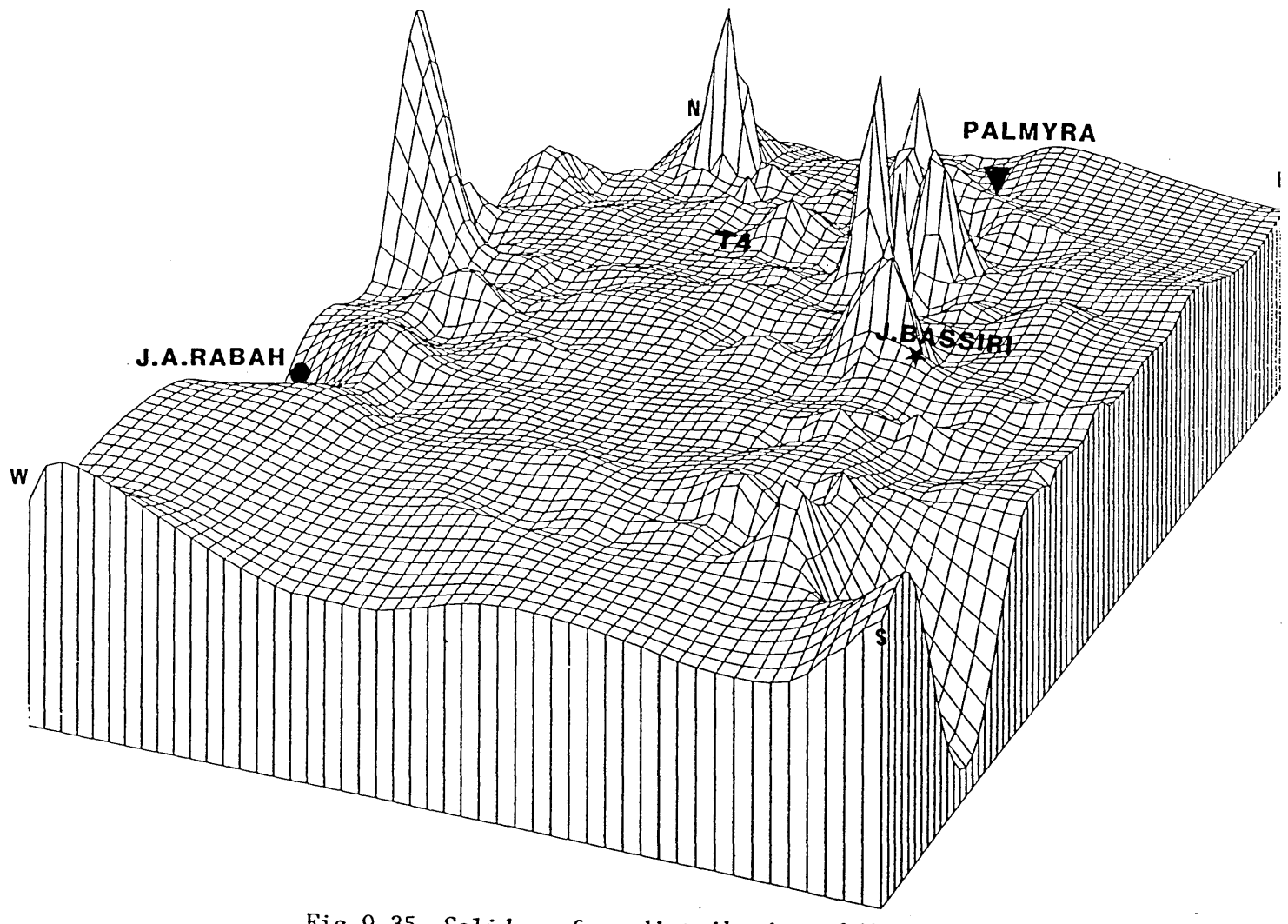


Fig.9.35 Solid surface distribution of Mo in the region.

9.6.2.10 Potassium

Potassium shows very low levels of concentration in the phosphate rocks of the Palmyrides, and is an essential element in all the secodary U minerals found in the region. Concentrations of K in rocks of this study range from 20 to 23000 ppm. Anomalous levels greater than 1.2 percent coincide to a large extent with clayey glauconitic limestones and marls of the palaeogene rocks. Other high values, 1.2 to 2.3 per cent K, can be seen in the areal distribution pattern (Fig. 9.36), and the solid surface pattern (Fig. 9.37). The highest K values (2 to 2.3%) are related to a small cluster of samples taken from J. Bassiri along with sample 710 where scanning electron microscopic examinations and probe analysis shows disseminated carnotite group minerals [$K_2O(UO_2)_2V_2O_8$-$3H_2O$] within the matrix of these samples, as well as precipitated along microfractures (see Plates 21 and 22). It should be noted also that moderately high levels of K (1 to 1.2%) are encountered in the southeastern part of Palmyra and within sabkhet El Mouh. The pattern of K highs clearly outlines areas of non-phosphate lithologies and in general it follows E-W trends. Furthermore, several highs are confined to the two eastern and western sides of the region.

Apparently, the major lithological controls of the primary dispersion pattern of K are represented by rocks of clayey limestones, glauconite and marls, however, the good spatial correlation with faults indicates also the significance of the structural control.

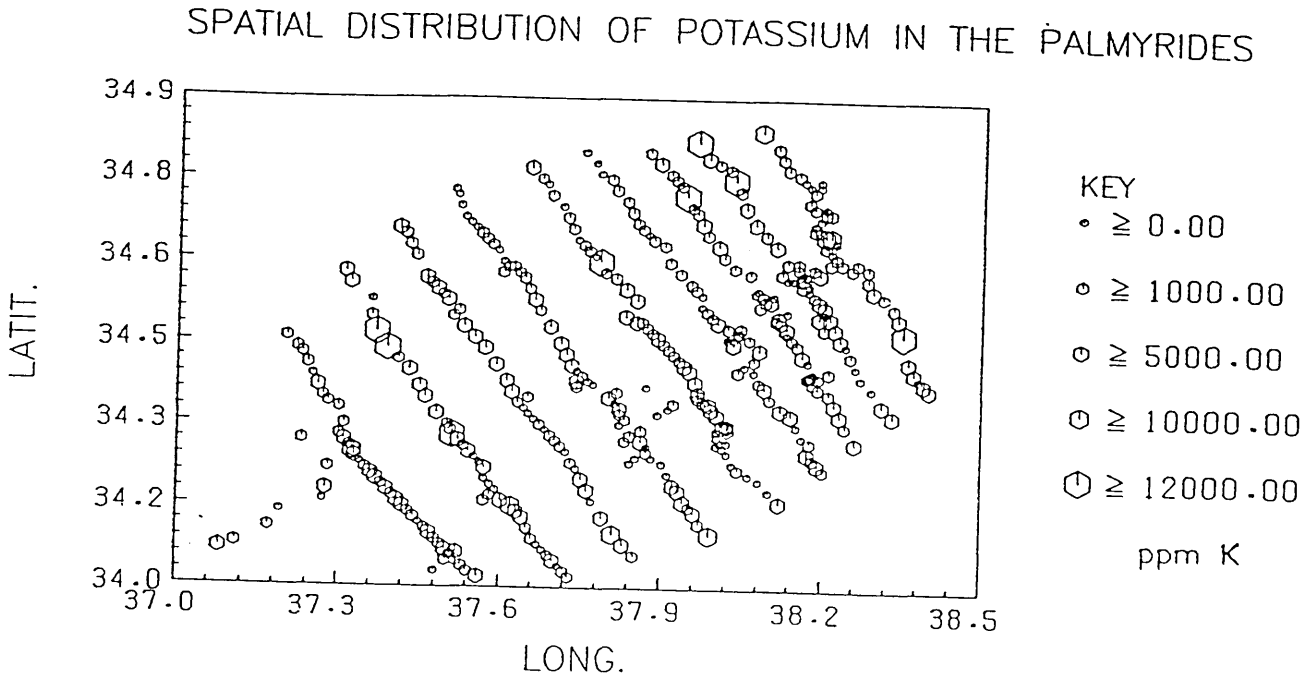


Fig.9.36 Symbolic areal distribution of K in the region.

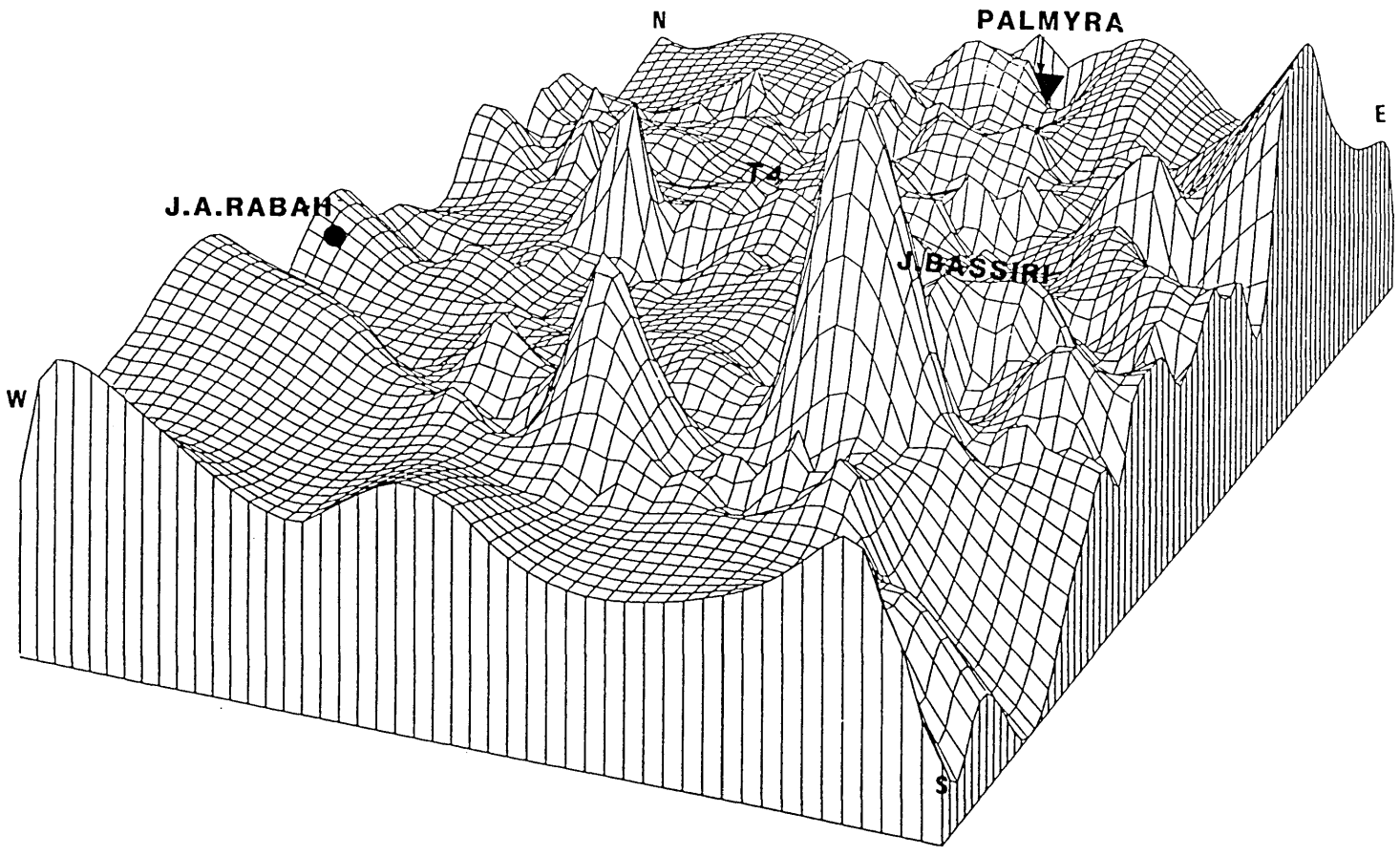


Fig.9.37 Solid surface distribution of K in the region.

Finally the similarities between the highs of the solid surface distribution patterns of K, V and U can be used to outline areas for further U exploration and/or predicting areas of occurrences of secondary U minerals.

9.7 Lithological studies

9.7.1 General

The 405 systematic lithogeochemical samples includes 5 samples of pre-Senonian (Upper Cretaceous) age, this samll number of samples prohibited further extensive geochemical investigations, therefore, the behaviour of U in this group will only be discussed as part of U distribution in various lithostratigraphical units of the region. Further investigations, however, of the geochemical data of the 400 remaining samples were carried out by separating the whole geochemical data into two subsets on the basis of their P content. The first consists of 92 samples of phosphate rocks that shows P concentrations equivalent or above 3.4% P_2O_5 hence will be called phosphate group. It is worth noting that if the P_2O_5 content exceeds 18%, then the rock will be considered as true phosphorite (Bushinsky, 1964; McArthur, 1974). Accordingly 308 samples are found to be nonphosphates, and comprises the second group. It should be also noted that, it is extremely difficult to attempt the above separation depending only on the field and microscopic observations of such very fine grained samples.

9.7.2 Geochemistry of the two main rock groups

Summary statistics for the two phosphate and non-phosphate geochemical data sets is presented in Table 9.4 along with that of the phosphorite deposits, a group of fault controlled samples and the 405 total data set for comparison.

Relatively, the phosphate group shows the following characteristics;

(a) U, Th, Sr, Se, As, V, Cr, Mo, Ni, Cd, Zn and P are greatly enriched, their standard deviation is also higher than corresponding ones of the nonphosphate group and the total set which suggests greater variation of their contents within the phosphate group.

(b) elements such as K, Li, Co, Ti, Al, Fe, Mn and Mg are depleted and show less variations than in other groups.

(c) the elements Na, Ba, Pb and to lesser degree Cu are, in general, unchanged.

Despite the fact that the nonphosphate group of rocks is made of a wide variety of rock types (see Table 9.2) the standard deviations for most of the elements are greater in the phosphate group; this indicates the great impact and influence of the phosphate minerals and grains on the behaviour of other elements, particularly with respect to trace element geochemistry.

Comparing the geochemistry of the two groups of rocks, it is believed that apart from P which by itself is of a little exploration value (at least for the present work), other elements

Table 9.4 Summary statistics of all the rock groups compared to the whole data set.

ELEMENTS	Samples of all traverses N = 405		Phosphates and phosphatic limestone N = 92		Non-phosphatic samples N = 308		Samples of the phosphoric deposits N = 57		Samples from fault zones N = 20	
	$\bar{X}$	S.D	$\bar{X}$	S.D	$\bar{X}$	S.D	$\bar{X}$	S.D	$\bar{X}$	S.D
U ppm	26.40	65.20	89.70	116.00	8.20	9.00	112.10	120.00	266.50	143.00
C.P.S	250.00	417.00	654.00	718.00	127.30	83.00	890.10	816.00	1593.00	975.00
Th ppm	3.60	3.70	6.10	5.10	2.90	2.90	8.10	5.40	9.30	6.20
As "	5.90	7.30	11.20	12.40	4.00	12.70	12.70	14.20	23.60	19.00
Se "	1.60	5.30	4.10	9.80	1.00	2.60	4.60	9.30	14.00	17.70
Li "	10.60	9.00	6.50	5.60	12.00	9.50	4.90	4.70	5.80	4.10
Sr "	891.00	818.00	1241.00	851.00	776.10	713.00	1475.60	1009.00	1566.50	1364.00
Ba "	380.00	396.00	330.00	409.00	391.20	387.00	412.70	446.00	395.10	504.00
La "	14.50	12.10	20.30	16.30	12.50	7.30	27.20	23.10	35.40	32.70
Ti "	934.00	1035.00	384.00	353.00	1107.50	1119.00	287.10	314.00	407.80	36.00
V "	119.00	366.00	273.00	717.00	65.50	50.00	231.80	339.00	782.80	1464.00
Cr "	60.70	56.00	96.00	56.00	46.30	32.20	121.80	92.20	160.60	142.00
Mo "	7.80	16.10	15.50	22.90	5.40	5.40	19.10	29.60	41.10	39.40
Mn "	147.80	174.00	55.90	94.60	172.70	174.00	28.40	29.30	32.60	34.00
Co "	7.80	8.40	4.60	3.90	8.70	8.50	4.10	4.20	4.60	2.70
Ni "	75.00	464.00	170.00	1007.00	47.60	34.80	63.10	82.10	584.8	2149.00
Cu "	24.50	30.60	35.00	52.00	20.70	14.20	32.50	40.90	77.20	106.00
Zn "	146.20	464.00	344.00	899.00	76.30	98.80	316.40	497.00	983.10	1781.00
Cd "	9.50	40.00	29.50	62.00	3.30	7.30	36.90	80.50	84.00	115.00
Pb "	25.40	21.50	28.90	27.00	24.00	19.60	26.80	33.50	29.90	30.00
P %	1.50	3.10	5.30	4.80	0.38	0.57	7.77	3.98	4.20	4.00
Na %	0.30	0.61	0.33	0.32	0.30	0.69	0.38	0.27	0.32	0.21
K %	0.35	0.32	0.18	0.18	0.41	0.34	0.12	0.16	0.15	0.14
Mg %	1.34	1.35	0.80	0.75	1.48	1.67	0.89	1.15	0.90	1.10
Ca %	24.70	9.00	29.90	7.70	23.10	8.70	31.80	6.60	28.60	8.80
Al %	1.40	1.10	0.89	0.91	1.60	1.19	0.73	0.97	1.19	1.10
Fe %	1.00	0.80	0.56	0.56	1.10	0.85	0.46	0.48	0.15	0.31

C.P.S = Radioactivity; N = Number of samples;
$\bar{X}$ = Arithmetic mean; S.D = Standard deviation.

of interest such as U, V, Mo, As, Se, Zn, Sr, Cd and to lesser degree Ni, Cr and K show considerable contrast between the two groups of rocks. It is worth noting however that major elements such as Fe, Ca, Al, Ti, Mg and Na and minor elements such as Mn, Co and Li show significantly smaller variances in both the phosphate and nonphosphate groups. In the light of the above observation concerning the higher variances within the phosphate rock, the smaller variances of these elements clearly indicate that the detrital influx (which is represented by the elements Fe, Al, Ti, Co, Li and Mn), into the environment of phosphatization and/or phosphorite formation was very weak, this, however, explains their smaller variances shown by the phosphate group. In general, the observed variances in trace and other elements contents can be controlled and be explained by any of the following (notwithstanding the significance of various phosphate minerals in this respect):

i - different chemical and mineralogical composition of the rocks.

ii - surface processes (weathering) and groundwater movement (interaction and alterations) past and present.

iii - tectonisms and other structural influences on the primary dispersion of elements and their distributions.

Therefore although a high proportion of the variance is due to lithological factors (primary dispersion), the possibility that part of the variations in the elements concentrations of these surface rocks, including rocks of the phosphate and nonphosphate groups, can be attributed to weathering despite the fact that as unweathered rocks as possible were sampled.

9.7.3 Distribution of U and its associated elements in the phosphate group.

The areal distributions of U, Th, As and Se in the phosphate group of samples, show both positive and negative anomalies that can be recognized in Figs. 9.38 to 9.41. Comparing these patterns with corresponding patterns of these elements in the total data set (Figs. 9.18, 9.22, 9.24 and 9.26), and bearing in mind the interpretation that the Lower Palaeogene rocks on the eastern side of the region are more enriched in their U content due to higher clays, phosphate grains and perhaps organic matter impurities, relative to Upper Palaeogene, Neogene and Quaternary rocks situated further west, the two U patterns display major differences along the eastern and western margins, but, as expected, show similarities over the Southern Palmyrides mountains. Although the trend of positive U anomalies in Fig. 9.38 is in good agreement with the geographical distribution of known phosphate rocks in the region, the marked enhancement of the two highest peaks, relative to other phosphate samples is probably due to U enrichment that took place via the well known fault conduits found in these locations.

The striking similarities of the distribution pattens of Th, As and Se between the two data sets, further emphasize the great role that the phosphate lithologies have been playing in the primary dispersion of these elements in the region. It is of a great importance, however, to stress that faults and other taphrogenic lineaments are perhaps the major underlying controls of almost all these elements content even within the phosphate rocks

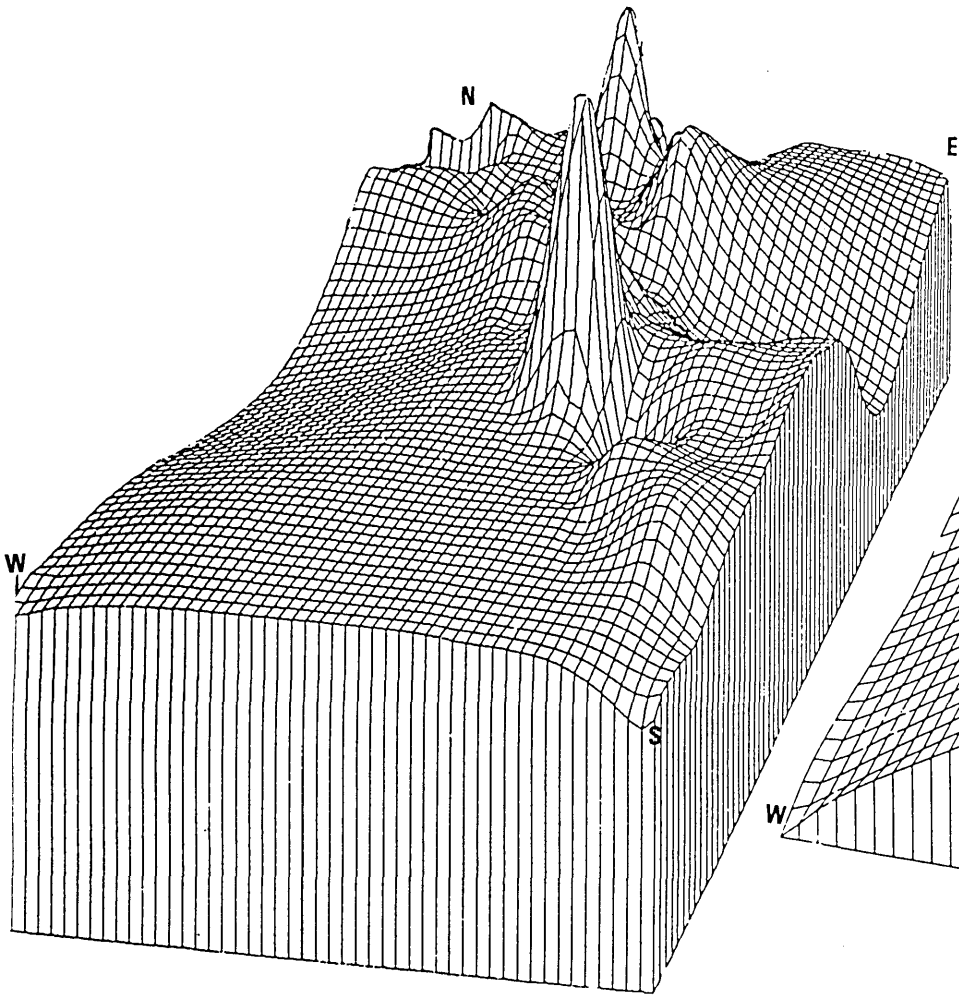


Fig.9.38 Solid surface distribution of U in the phosphate group.

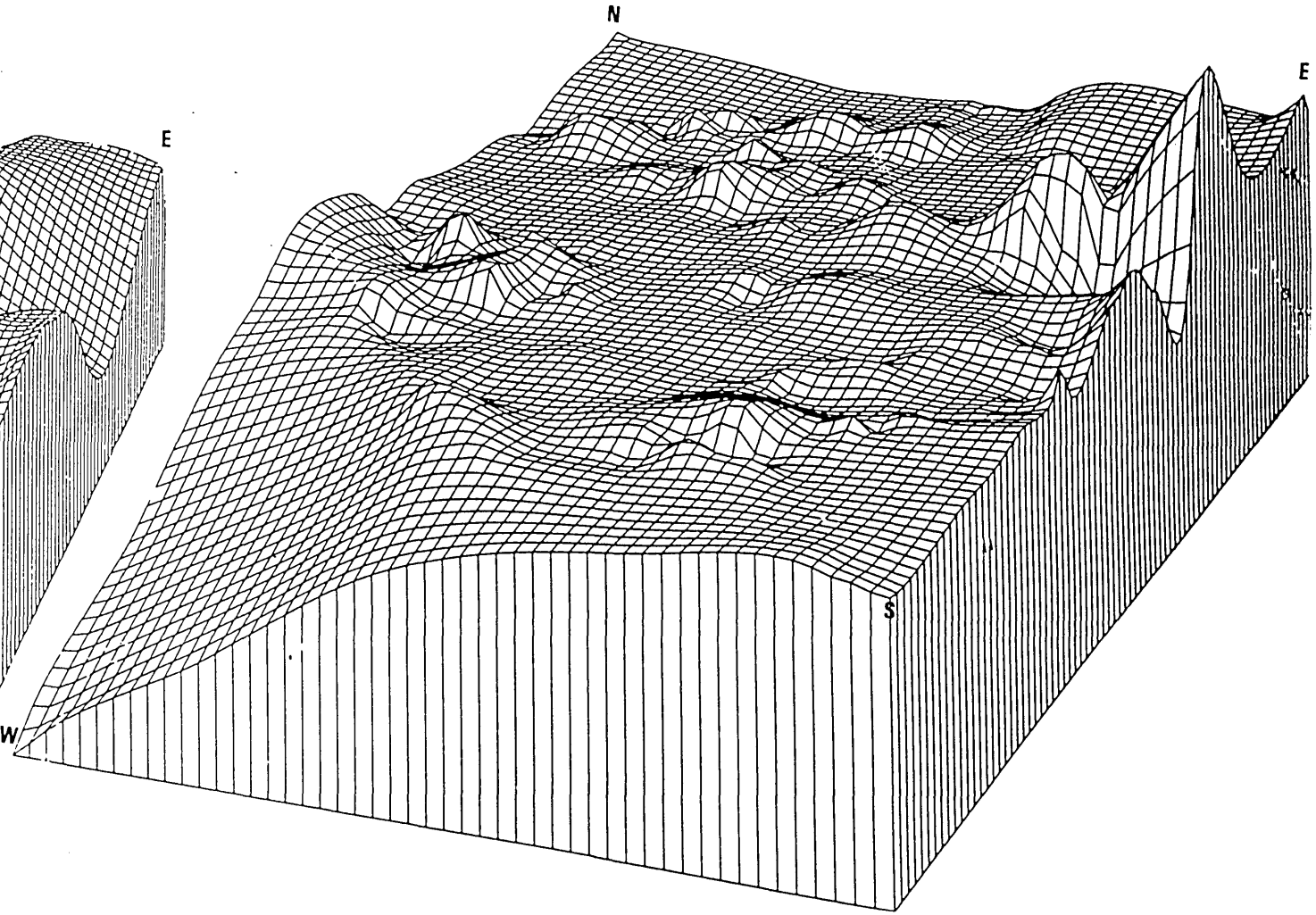
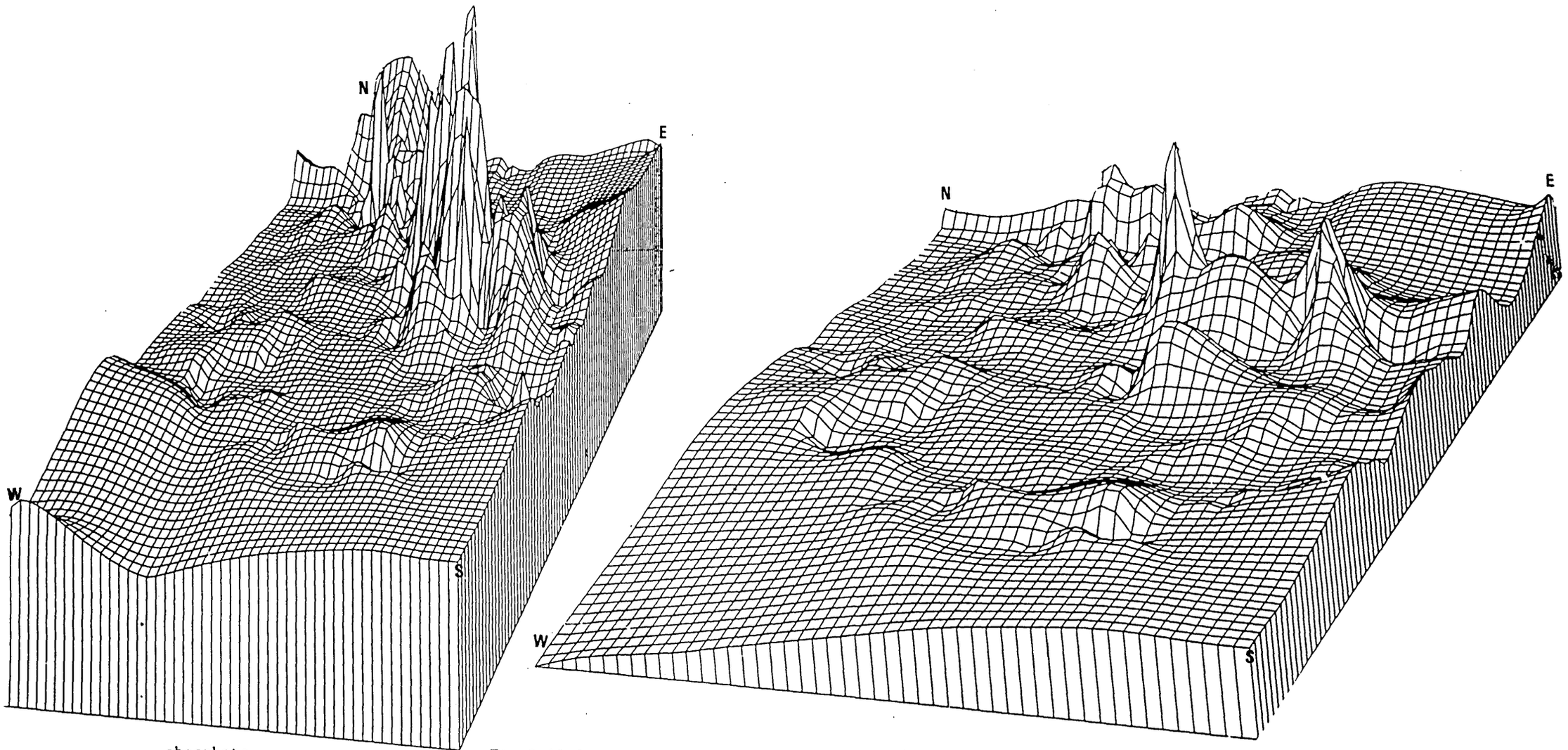


Fig.9.42 Solid surface distribution of U in the nonphosphate group.



phosphate

Fig.9.43 Solid surface distribution of CPS in the phosphate and nonphosphate groups.

nonphosphate

(see above), therefore, such influential factors should always be kept in mind when discussing these distribution patterns.

9.7.4 Distribution of U and associated elements in the nonphosphate group.

For comparison, the solid surface distributions of U, CPS, Th As and Se in the nonphosphate group were constructed (Figs. 9.42 to 9.46 respectively). The pattern for U distribution (Fig. 9.42) clearly outline two moderately positive U anomalous trends over nonphosphate rocks; the first is closley related to the clayey glauconitic limestones and marls of the Lower Palaeogene rocks on the eastern side which seems to be more enriched in U than the adjacent Upper Palaeogene, Neogene and Quaternary rocks. Therefore this trend shows a decrease of the peak intensities from east to west which corresponds nicely with the dominance of these various lithologies. It is of interest to compare this pattern with that in Fig. 9.38 for U in the phosphate rocks. The above mentioned positive trend of anomalous U levels fits nicely with the negatively anomalous trend shown in Fig. 9.38 over the same geographical location, this suggests that the clays and other non-carbonate constituents within the Palaeogene and Neogene rocks are perhaps responsible for the U enrichment in the positive trend, and not due to the phosphate presence. However, other factors such as two inferred faults running parallel to the northwestern and southeastern sides of this anomalous trend could equally be responsible for the observed enhanced levels of U in this location.

The second moderately to weakly anomalous area is located in

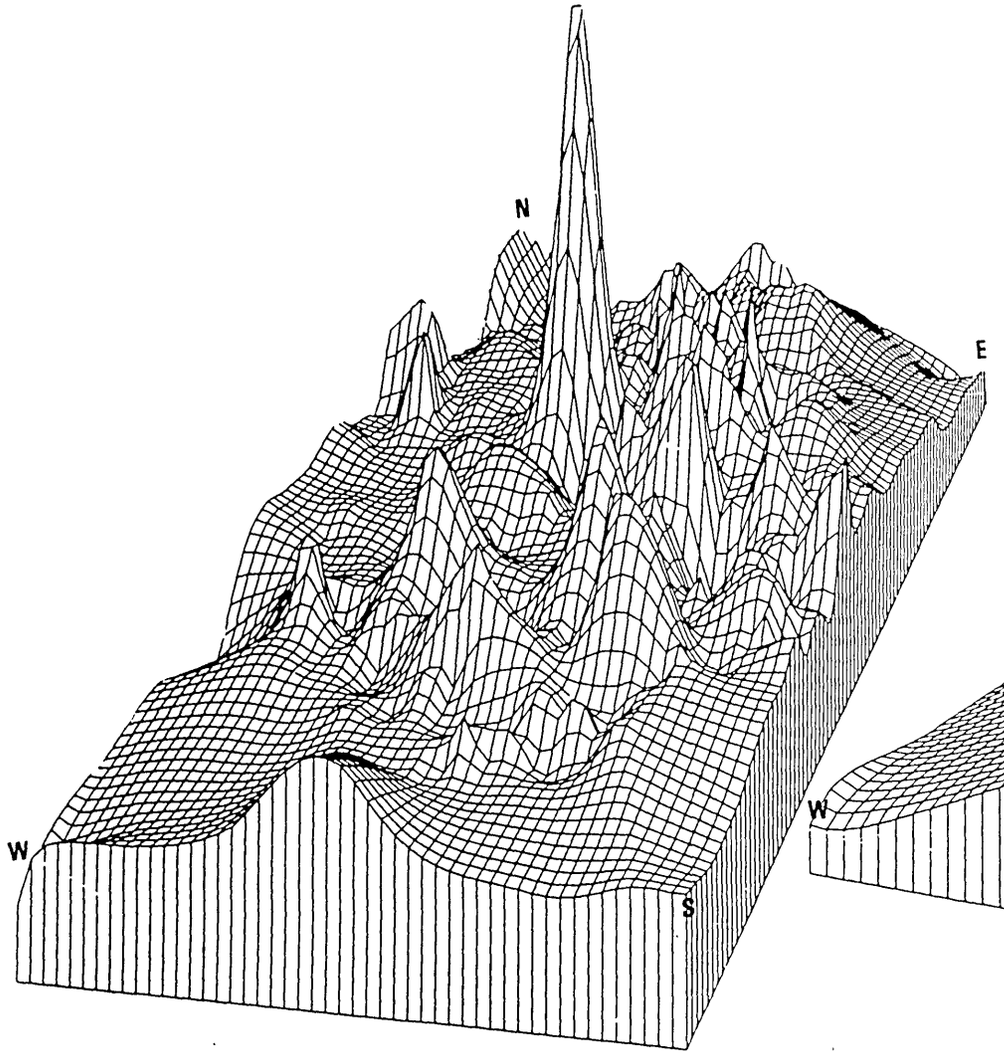


Fig.9.39 Solid surface distribution of Th in the phosphate group.

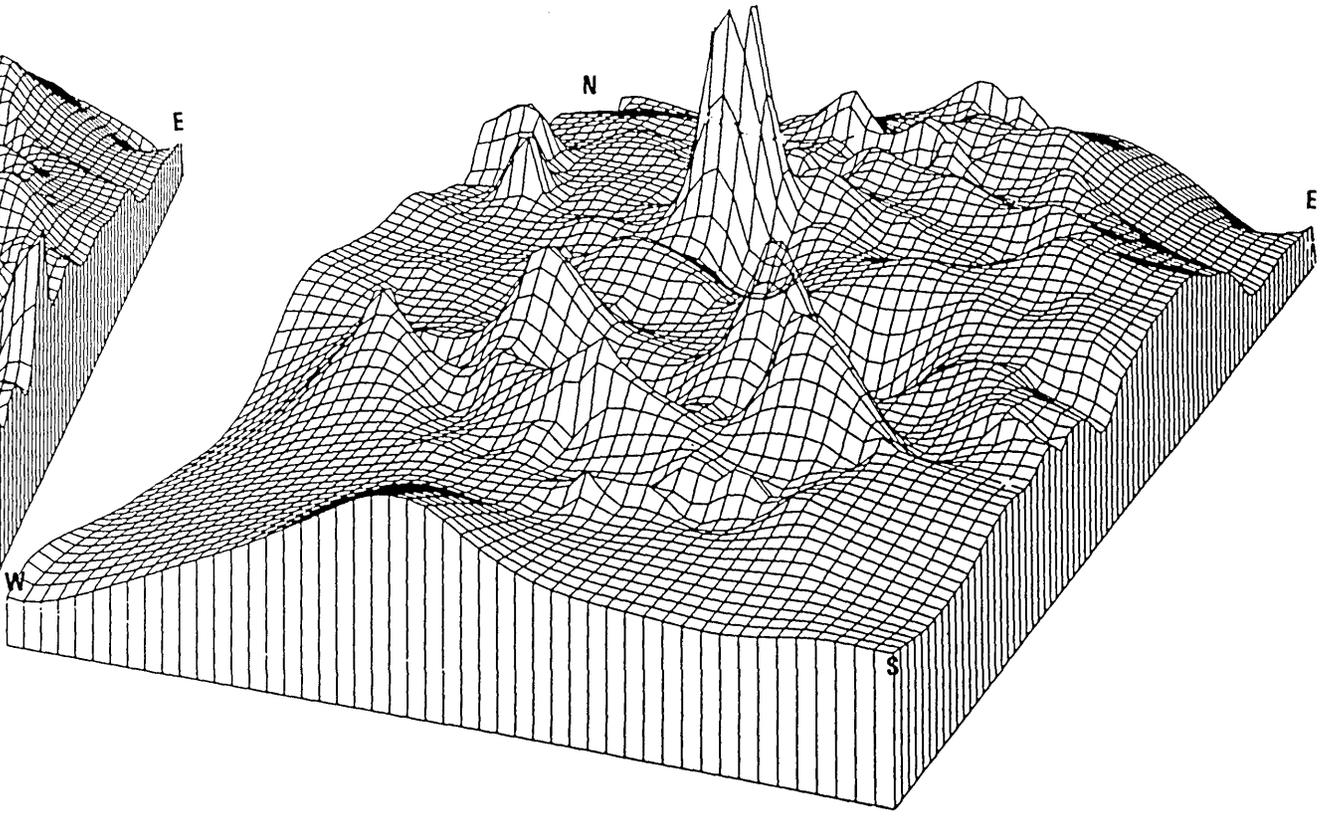


Fig.9.44 Solid surface distribution of Th in the nonphosphate group.

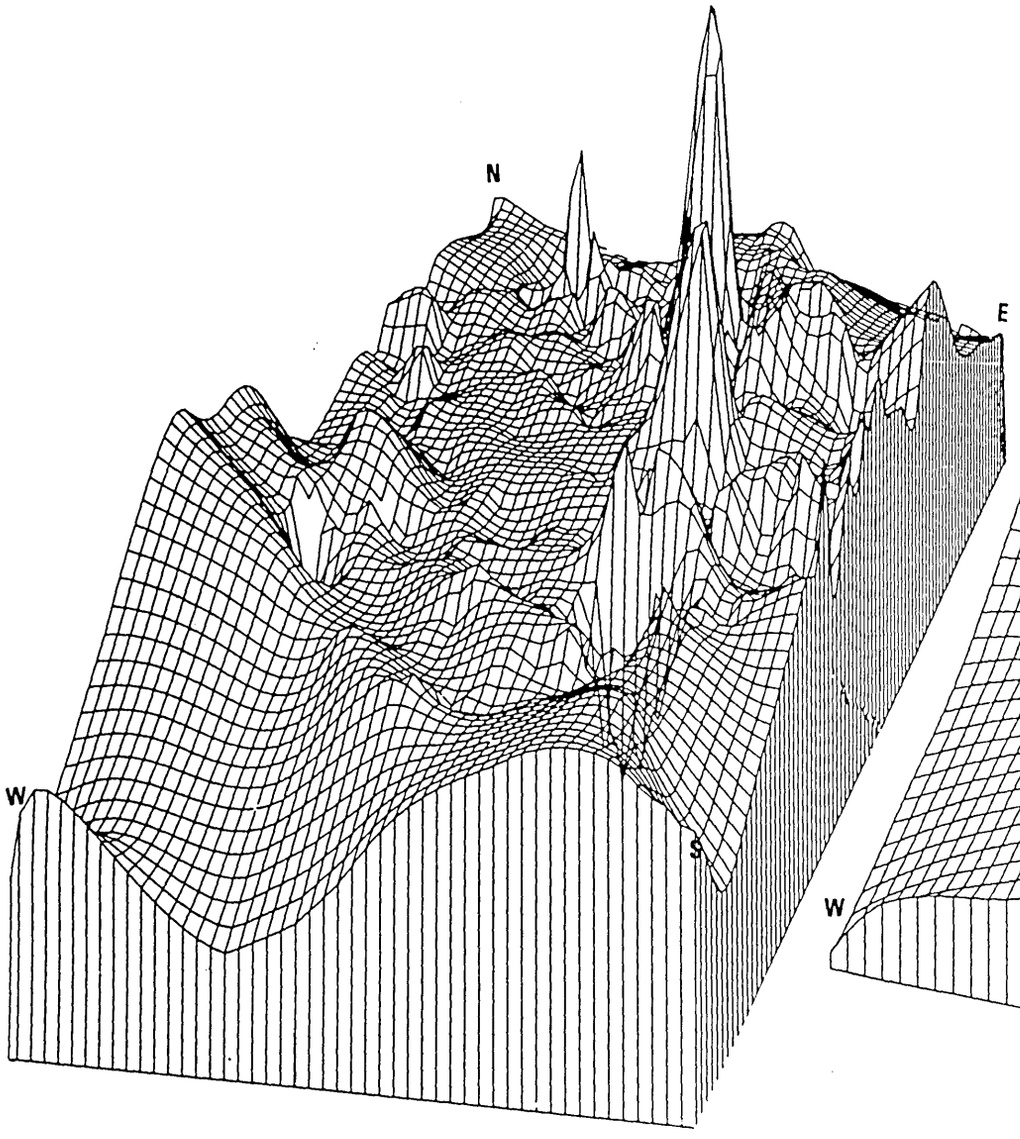


Fig.9.40 Solid surface distribution of As in the phosphate group.

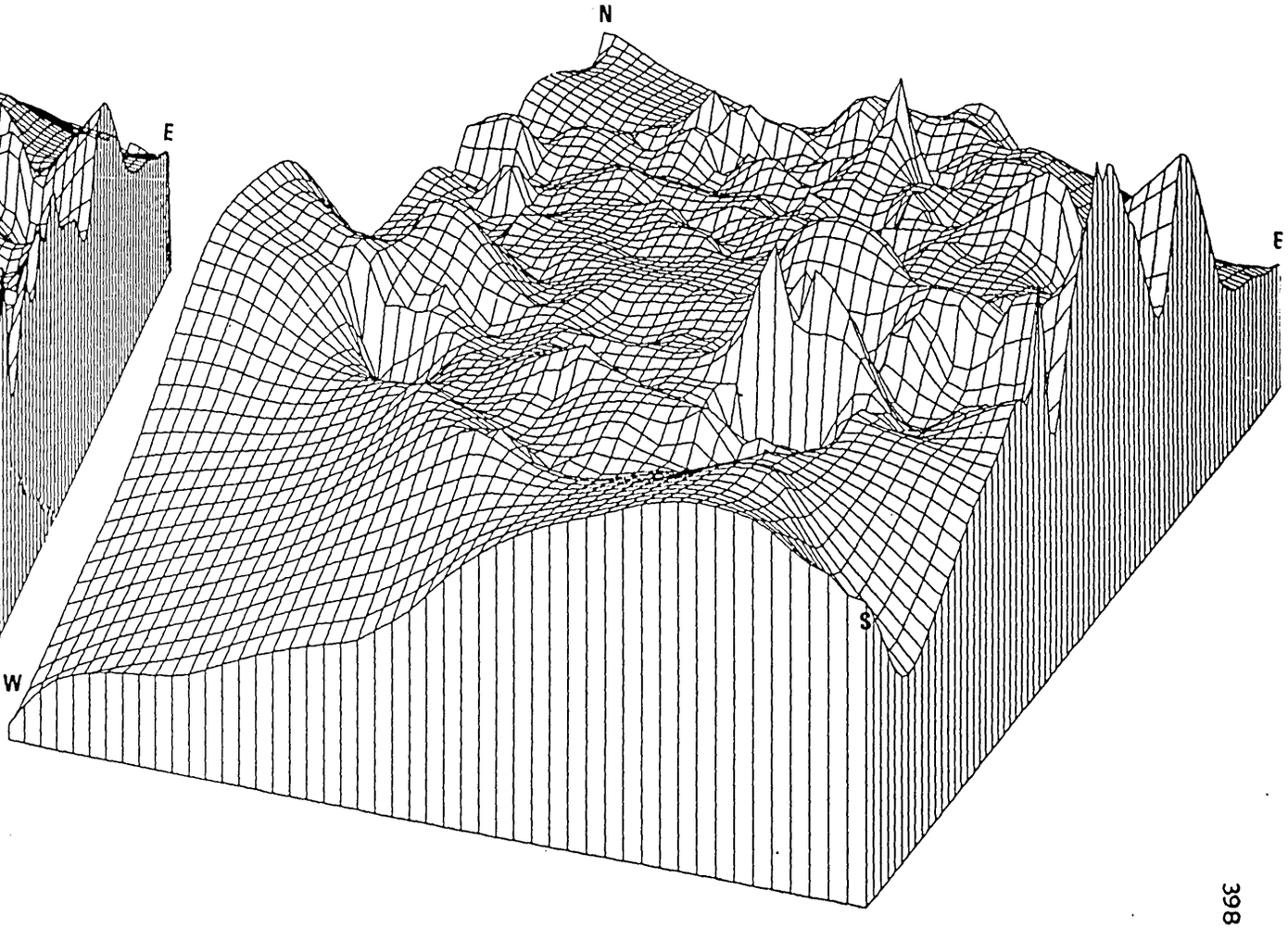


Fig.9.45 Solid surface distribution of As in the nonphosphate group.

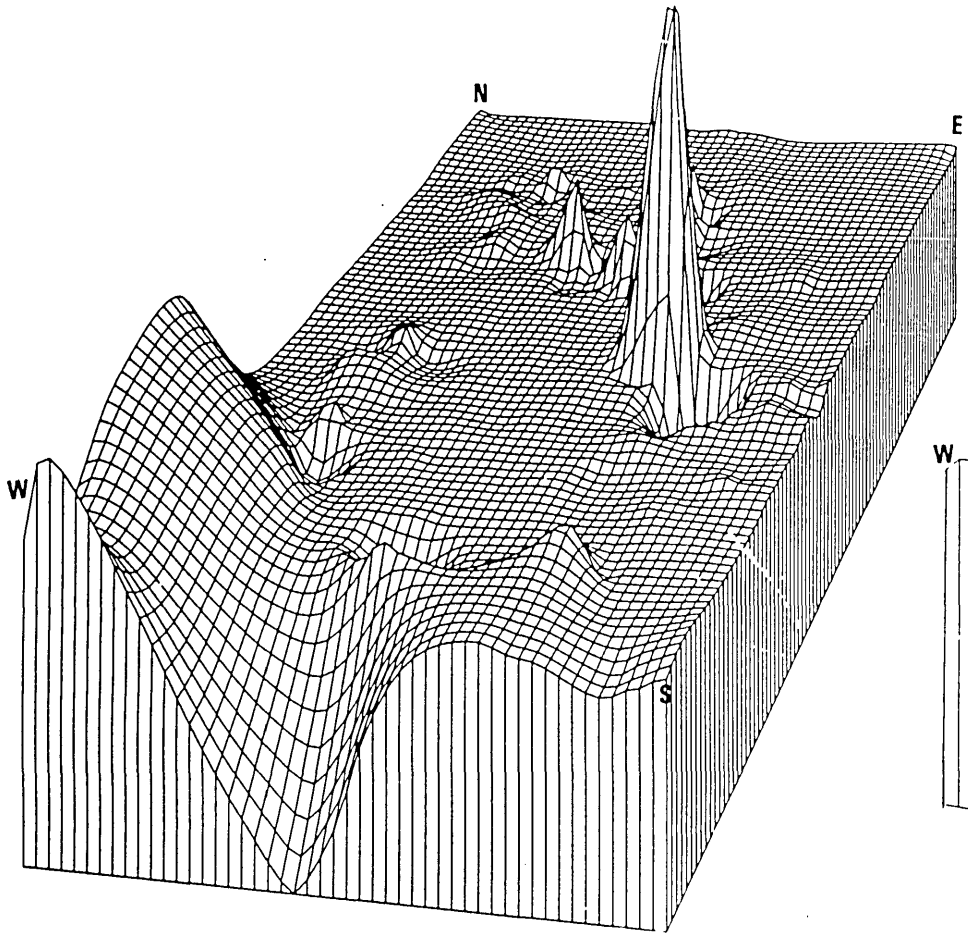


Fig.9.41 Solid surface distribution of Se in the phosphate group.

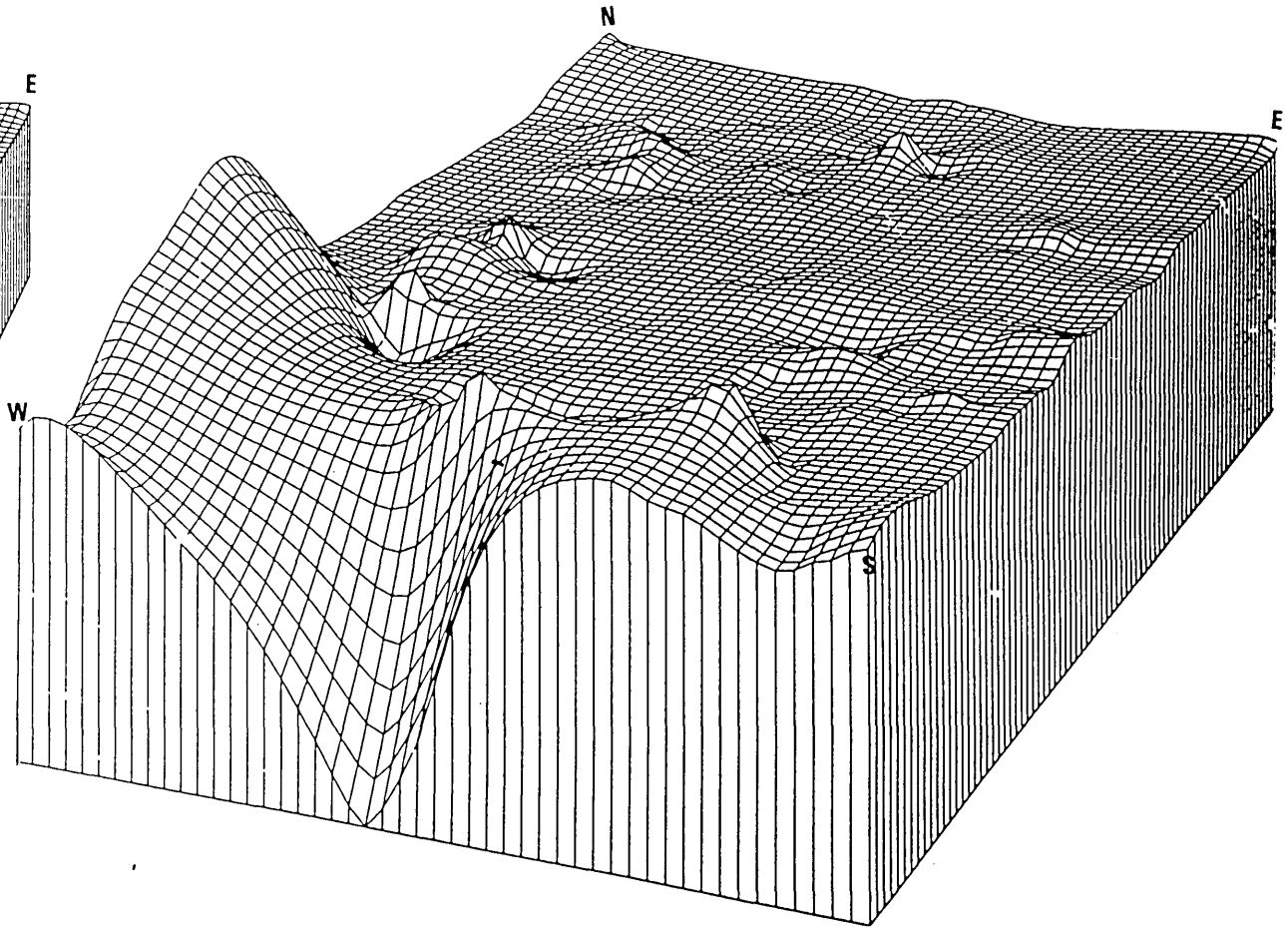


Fig.9.46 Solid surface distribution of Se in the nonphosphate group.

the west of the region near J. Abou Rabah, where U enrichment occurs particularly at the eastern and western flanks as well as at the northern plunge of this ridge. The rocks are mainly of Santonian, Campanian, Maestrichtian and Lower Eocene age, composed of strongly fractured limestones, marls and flints. It can be inferred, however, that this anomalous area extends under the Neogene and Quaternary cover towards a third weakly enriched area situated in the northern and western suburbs of the T.4. This area is represented by a cluster of small peaks. Uranium enrichment in this locality was first detected along with Se in the Palaeogene aquifer (Fig. 9.47) by the hydrogeochemical survey (see section 7.5.7 and 7.6) close to the unconformity between the Miocene (Neogene) sediments and the Palaeogene rocks. The northernmost peak of the cluster in this area is related to a tiny outcrop of marly limestone of Maestrichtian and/or Danian age, whereas the highest value however, belongs to a complex fault contact between brownish to greenish gypsiferous clays and clay limestones of Miocene (Neogene) sediments and grey marly limestone of older Palaeogene rocks. In addition to these areas, a few scattered and relatively weak to moderate high U values can be found along the eastern margin further south of the first anomaly and between J. Bassiri and J. Rmah.

The pattern of radioactivity (Fig. 9.43) also brings out the first and third U enriched areas, and shows signs of the third one. It also emphasizes the upnormal and unexplained high anomaly in the vicinity of the town of Palmyra.

The pattern of Th (Fig. 9.44) is almost totally different

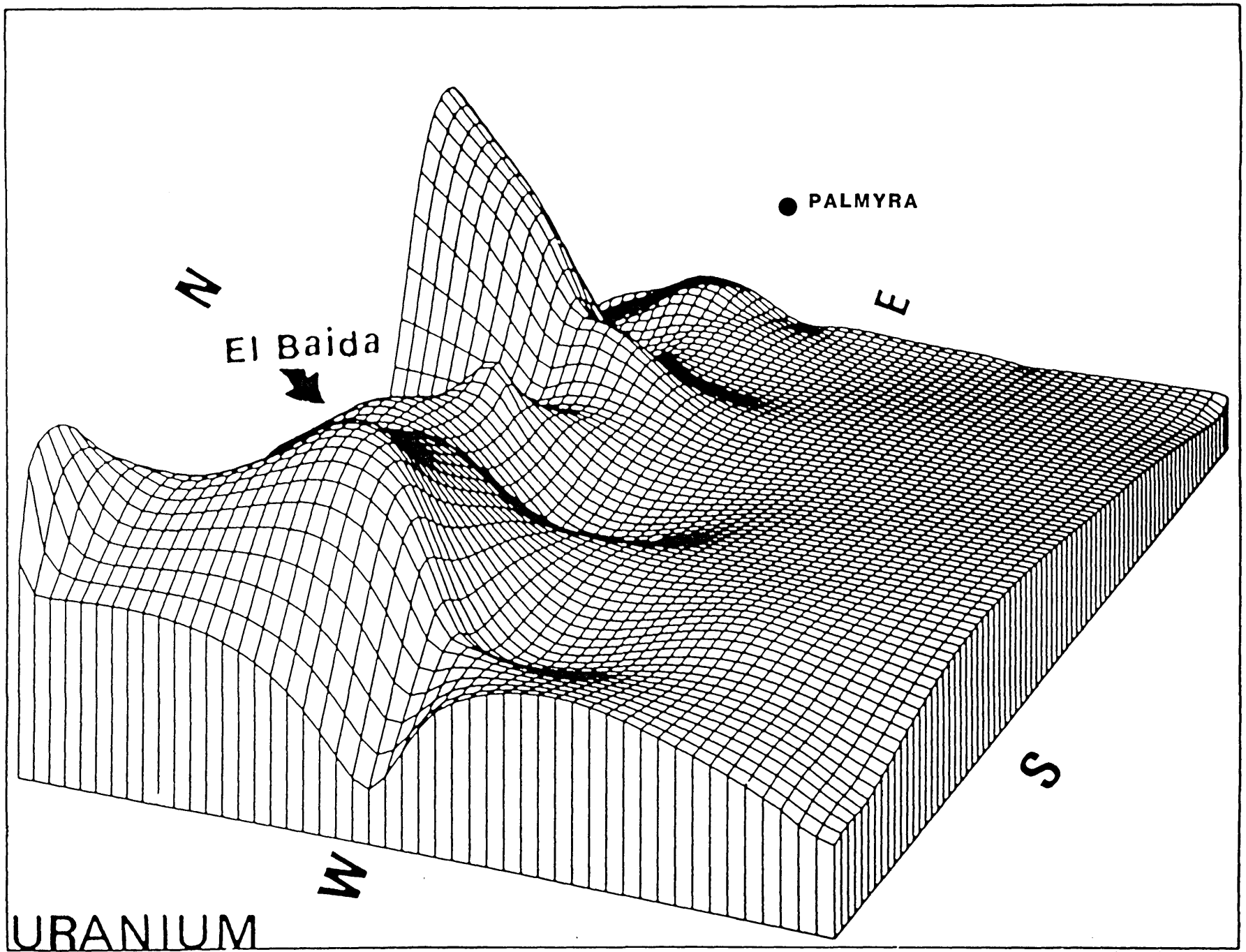


Fig.9.47 Solid surface distribution of U in the hydrogeochemistry.

from that of U and radioactivity, it clearly illustrates the main structural trends of NE-SW; NW-SE and E-W; while the pattern of As (Fig. 9.45) reflects all three anomalous areas, and particularly enhances the second one (near J. Abou Rabah) and that close to J. El Bassiri. The Se pattern (Fig. 9.46) supports only the second area, the inferred connection with the third, especially west to the T.4, and to a lesser degree some of the scattered peaks near J. Rmah and the eastern margin.

9.7.5 Uranium and Phosphorus in the phosphorite deposits.

Most of the elements of interest to this research (U, Th, As, Se, V, Mo and Sr) in addition to P are markedly enriched in the phosphorite deposits of the Palmyrides compared to the phosphate and other groups of rocks (see Table 9.4). However, as mentioned earlier the primary objective of sampling and studying of this group of rocks is to compare the results of U and P with those results for the same phosphorite deposits obtained by Hunting (1975). It should be noted that U measurements were made using similar analytical techniques in these two studies. The results in Table 9.5 indicate a very good agreement between the obtained means of U concentration for each of the phosphorite deposits, the table clearly confirms the conspicuous variation in the U contents between the variuos phosphorite formations that was observed during the course of the present work as well as reported in earlier phosphorite studies (Liaschenko and Tatarnikove, 1968; Atfeh, 1967 and Otaky in Mouty et al., 1983). However, contrary to these earlier reports, this study, along with that of Hunting (1975), shows that a linear relationship between U and P in the

phosphorites cannot be supported by the geochemical data (Fig. 9.48 and see Fig. 5.21).

Values of P_2O_5 in the present study are, however, slightly lower than those of hunting, especially for the "Eastern" deposits (but still within one standard error, see Table 9.5), and this difference is thought to be due to the use of more representative bulk samples by Hunting, whereas only 250mg of the surface rock samples were analysed in this study.

9.7.6 Uranium in fault-controlled zones.

Based on the foregonig observation that faults in the region exhibit a strong control over the distribution of almost all the elements involved, an attempt is made here to separate from the data all of those rock samples that were collected from strongly distorted areas, along or close to main faulted zones. The aim is to investigate the effect of faulting on geochemical dispersion patterns.

Surprisingly, the statistical parameters in Table 9.4 show generally smaller standard deviations for most of the elements from fault zones relative to other groups. The greater variance shown by Ni, V, Zn and Cd is due to their extremely high levels in sample 710, 712 and 119. With these samples excluded, the remaining group of samples appears to be more geochemically homogeneous than others. Moreover, comparing of its geochemical data with that of the phosphorite deposits reveals other characteristics which can be summarized as:

Table 9.5 Comparison of U and P_2O_5 contents of this study with that of Hunting (1975).

Phosphorite deposit	This study			Hunting (1975)		
	No. of samples	U ppm	P_2O_5	No. of samples	U ppm	P_2O_5
Kneifiss	11	107.6 ±15.6	30.2 ±2.1	12	112.3 ±13.2	32.2 ±2.1
(Eastern) Ash-Shariqueih	11	49.3 ±9.2	24.9 ±4.2	22	44.2 ±23	28.6 ±3.5
Al-Abter	09	133.7 ± 23	27.3 ±2.7	-	-	-
Om-Jorm-Baktal	10	488 ± 94	32.6 ±3	-	-	-
Non-commercial phosphorite	16	287.4 ± 77	11.7 ±4.6	-	-	-

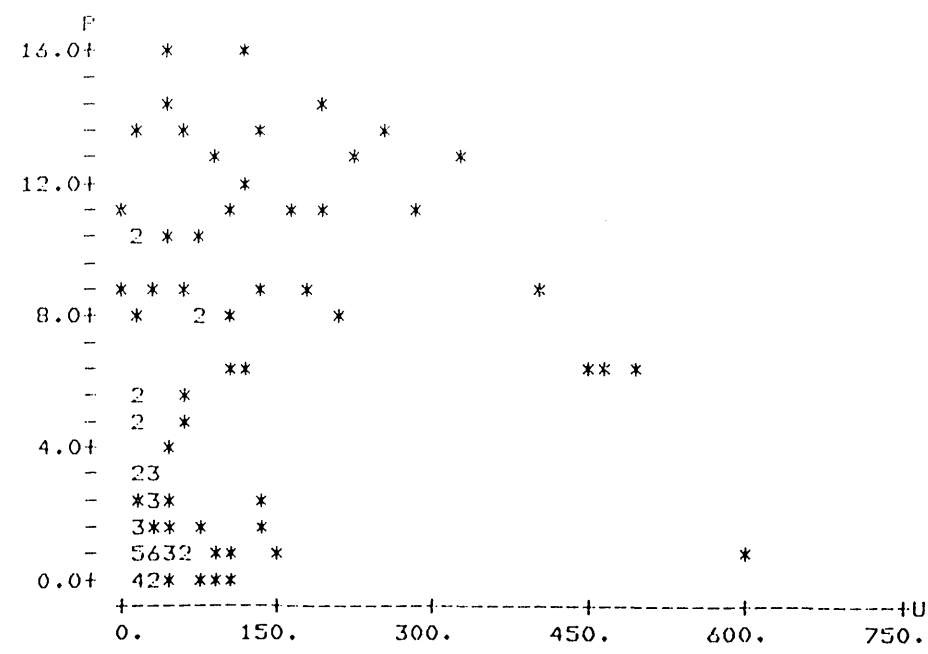


Fig.9.48 Scatterplot showing the relationship of U and P_2O_5 in the phosphate group.

a) higher means U, CPS, Se, V, Mo, Zn, Ni and Cd, typically up to three folds those shown by the phosphorite group; two folds for As and Cu and significantly higher Cr, Th, La and to lesser degree Al.
b) lower P, Ca, Ba and to lesser degree Na; other elements are unchanged.

Another important factor is the occurrences of multielement mineralized phases (Mo, Pt, Zn, Cu and Fe with S, Ba, and U) in some fault-controlled samples occupying macro and microfractures (Plates 21 and 22)

Although, the number of samples prohibited further investigations and comments at present, more detailed work in these areas should be considered.

9.7.7 Geochemistry of various lithostratigraphical units.

9.7.7.1 General characteristics

The 405 samples are divided into six different lithostratigraphical units on the basis of their age (1 to 6 starting from Quaternary), similarities in sedimentary environment and their general petrography and mineralogy. The means and standard deviations of the measured elements in each of these units are listed in Table 9.6. The Upper Cretaceous Unit 5 (103 samples) consists largely of phosphate rocks and will not be discussed further. However, it should be noted that this unit shows the highest mean of U content of 69 ppm.

Table 9.6 Summary statistics of various lithostratigraphic units.

ELEMENTS	LITHOSTRATIGRAPHIC UNIT 1 QUATERNARY N=73		UNIT 2 NEOGENE N=54		UNIT 3 U & M PALEOGENE N=87		UNIT 4 L PALEOGENE N=83		UNIT 5 U CRETACEOUS N=103		UNIT 6 L CRET. TO JURASSIC N=5	
	$\bar{X}$	S.D	$\bar{X}$	S.D	$\bar{X}$	S.D	$\bar{X}$	S.D	$\bar{X}$	S.D	$\bar{X}$	S.D
U ppm	3.00	1.10	3.90	2.00	7.50	6.40	18.00	12.00	69.00	109.00	0.82	0.24
C.P.S	103.00	28.80	86.90	37.70	119.00	90.20	176.00	72.00	376.00	371.00	59.40	16.20
Th ppm	3.00	4.20	2.90	2.70	2.50	2.40	2.90	2.10	5.30	4.80	1.34	0.58
As "	3.90	1.90	3.80	3.70	4.90	5.50	6.20	5.00	9.30	11.20	1.57	1.98
Se "	0.70	0.70	0.60	1.00	0.70	1.40	1.80	4.40	3.40	8.90	0.02	0.03
Li "	13.90	7.00	10.00	9.50	9.50	7.00	9.70	9.90	9.10	6.90	19.18	22.70
Sr "	732.00	731.00	796.00	969.00	687.00	536.00	1144.50	775.00	1025.00	938.00	686.20	811.00
Ba "	469.00	381.00	480.00	465.00	422.00	487.00	290.80	314.00	362.00	401.00	21.70	12.40
La "	15.30	5.30	10.90	7.90	12.40	8.70	12.20	9.70	19.60	17.90	4.50	1.62
Ti "	1281.00	754.00	834.00	841.00	1020.00	1611.00	737.50	777.00	829.00	865.00	504.68	440.00
V "	70.50	65.90	48.20	30.70	61.60	36.50	68.50	45.20	155.60	177.00	13.78	8.08
Cr "	52.90	28.70	42.00	38.80	53.20	48.50	55.80	35.60	83.00	78.00	5.82	4.60
Mo "	5.50	6.70	5.80	9.90	5.60	10.10	6.40	4.50	13.90	22.00	4.78	3.38
Mn "	218.00	131.00	105.50	94.40	142.00	198.00	112.00	131.00	145.00	197.00	35.16	33.70
Co "	9.30	4.50	8.50	11.60	7.80	8.90	5.70	4.50	7.60	8.10	3.82	2.78
Ni "	50.40	28.90	43.00	38.20	49.00	45.60	48.60	30.00	146.00	893.00	9.32	5.88
Cu "	19.80	8.70	19.60	25.10	22.50	18.30	22.70	13.90	34.80	50.00	5.24	1.63
Zn "	76.1	88.1	101.60	268.00	101.00	149.00	79.90	71.70	299.00	818.00	10.96	7.95
Cd "	2.90	4.90	5.70	25.60	5.90	14.70	4.70	13.70	26.00	64.00	0.31	0.42
Pb "	27.60	15.20	27.70	32.70	22.90	16.70	21.60	13.90	28.00	25.00	15.42	11.40
P %	0.69	1.74	0.20	0.17	0.53	0.75	0.82	1.10	3.20	4.50	0.02	0.01
Na %	0.34	0.63	0.30	0.43	0.22	0.38	0.38	0.39	0.26	0.28	0.03	0.05
K %	0.51	0.24	0.37	0.46	0.34	0.36	0.30	0.28	0.31	0.28	0.30	0.27
Mg %	1.70	1.10	1.15	1.56	1.30	2.00	1.21	1.31	1.10	1.00	3.46	4.84
Ca %	20.30	5.50	23.20	10.80	26.80	10.30	25.90	7.50	26.80	8.50	15.54	4.60
Al %	1.99	0.97	1.19	1.00	1.36	1.35	1.20	1.00	1.47	1.30	0.50	0.40
Fe %	1.38	0.61	0.84	0.70	0.95	1.00	0.93	0.76	0.92	0.78	0.34	0.30

N=number of samples; X=arithmetic mean; S.D=Standard deviation; C.P.S= radioactivity.

The second highest levels of U concentration are found among the Lower Palaeogene carbonate dominant unit (83 samples), with mean U contents of 18 ppm. The Upper Palaeogene Unit 3 comprises (87 samples) which are mainly fossiliferous limestones (Pecten and Nummulites) of white, yellow and grey colours, sandy algal limestones with some flint nodules and quartz sandstones, it shows lower U mean of 7.5 ppm, but still considered to be above the normal average.

It was discovered during all early radiometric investigations in the region (GEGMR, 1978; Aabaid, 1980, Jubeli, 1982 and Mouty et al. 1983) that the carbonate rocks, in general, have very low levels of gamma radiation suggesting the presence of little U content. However, worldwide, rocks such as limestone, dolomite and other sedimentary carbonates have long been considered to be among the least uraniferous of the earths crust (2.7 ppm U in continental crust and 2.3 ppm U for crust as a whole from Seigle, 1980). Higher U content was reported by Baronov et al (1956) for 128 composites of carbonate rocks from the Russian platform ranged from 1.2 to 5.4 ppm. However, Bell (1963) when reporting U in the carbonate rocks, suggested that the suspected presence of phosphatized carbonate in the samples of Baronov et al. can account for the high U values reported for these Russian samples. Because U is highly soluble in the presence of carbonate and bicarbonate ions, it follows that U should not syngenetically precipitate along with pure carbonate rocks whether they are of biogenetic or chemical origin.

On the basis of the limited fission-track studies and other

preliminary petrographic and mineralogical work of the present research, the high U content of the Palmyrides carbonate rocks can also be probably attributed to the presence of phosphatic particles and other non-carbonate impurities (clays, organic matter and muds). It is expected, therefore, that mobile uraniferous solutions in the sedimentary environment of the Upper Cretaceous and Palaeogene were subjected to complexing and intimate association with these impurities particularly those of collophane, francolite, apatite and the organic matter leading to the obtained higher than average U levels. This is suggested mainly by the finding of the fission-track work (see section 5.8.6). The strong affinity of U towards such components of the rocks is well documented by many workers elsewhere (Szalay, 1964; Schmitt Collerus, 1979; and McArthur, 1980). The remaining three lithostratigraphical units show in general lower U levels, the arithmetic mean of 3.9 ppm U is found in the Neogene Unit 2 that consists of 54 samples of lacustrine, alluvial and other clastic sediments. Except for the existence of some individual anomalous values up to 13.5 ppm in the greenish fine grained lacustrine conglomerate rocks of calcareous cement, located along the unconformity with the older Palaeogene rocks, and very few Pliocene (Upper Neogene) gypsiferous brown and greenish clays from the faulted zones, the levels of U concentration of the Neogene unit can be considered as typical background value (1-3 ppm U).

The geochemistry of the Quaternary Unit 1 (73 samples) does not bear a clear relationship to the primary dispersion of the measured elements, increased levels of Fe, Al, Ti, Li,K, Na and Mg reflect the formation of weathering products. These are, however,

typical background concentrations of U in the Quaternary sediments averaging 3 ppm.

The lowest mean of 0.8 ppm U content is shown by Unit 6 which comprises 5 samples of gypsum, dolomitic limestone and dolomite rocks that are older in age than Upper Cretaceous (Lower Cretaceous-Triassic). The low levels of U in these rocks indicate that the sedimentary environment during the early stages of the Mesozoic times was not favourable for U enrichment. The concentrations of other elements are also relativley low and closley correspond to the low background values in other lithostratigraphical units of the region.

9.7.7.2 Boxplots.

The variation of U, CPS, P, Th, As, Se, V, Mo, Sr, Ca and K contents between the rock units was studied using Boxplot technique (Wainer, 1981; see chapter 7). The plots Figs. 9.49 to 9.51 show that the highest U median and the widest range is found (as expected) in the Upper Cretaceous Unit 5, whereas the lowest U median and narrowest range is found in the older Unit 6 (Lower Cretaceous-Triassic). Similar behaviour is shown by CPS, P, Th, As and to lesser degree V. Although the median of Se is also slightly higher in Unit 5, but, the differences between the Units 1 to 4 (Quaternanry to Lower Palaeogene) are not significant, in fact, no difference is shown between the Neogene and Upper Palaeogene units, very low Se content is found in the older rocks (Unit 6). In contrast, K shows its highest median in both the Quaternary unit 1 and the older rocks (Unit 6), whereas the lowest one for the Upper

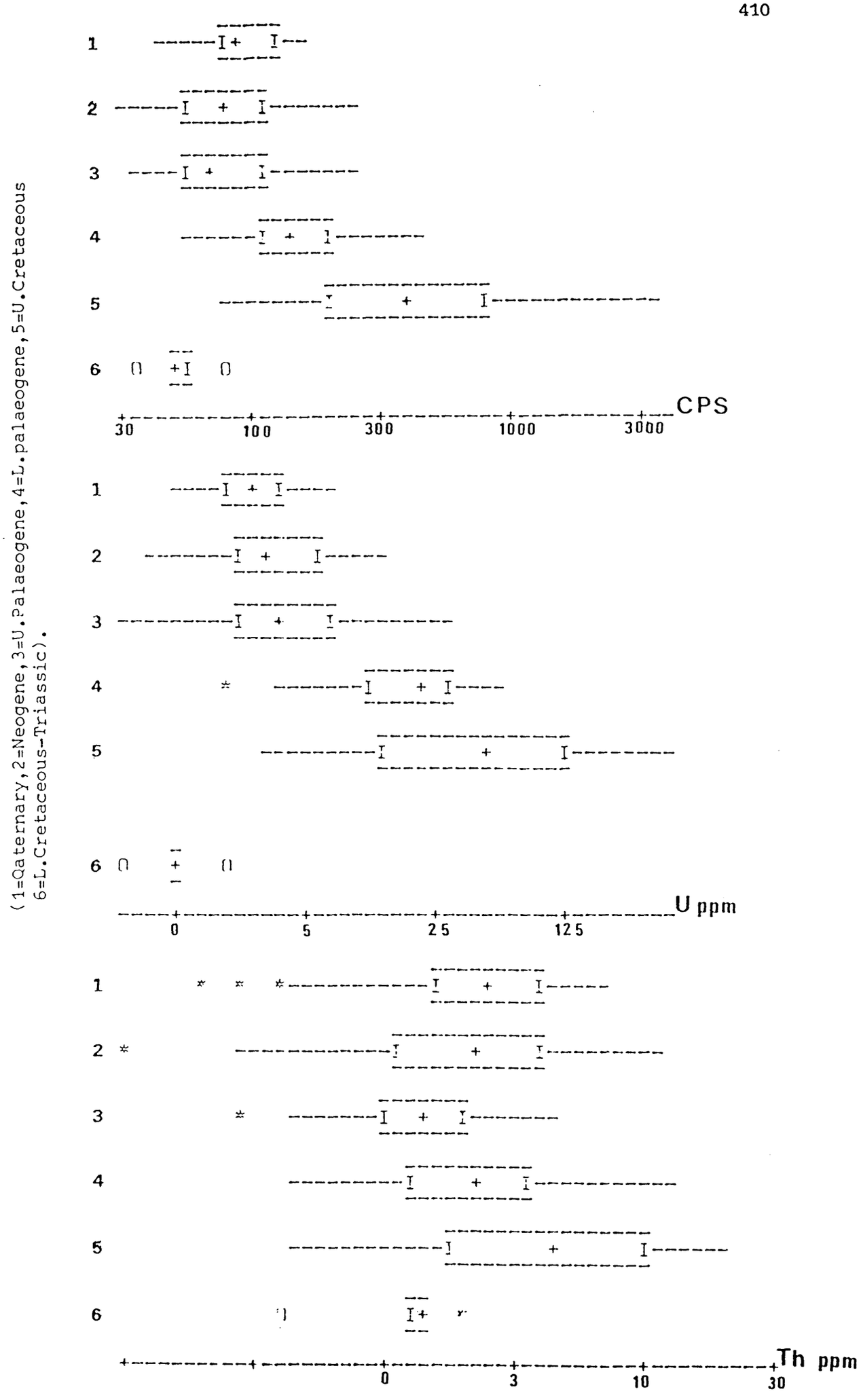


Fig.9.49 Boxplot of U, CPS and Th by rock type.

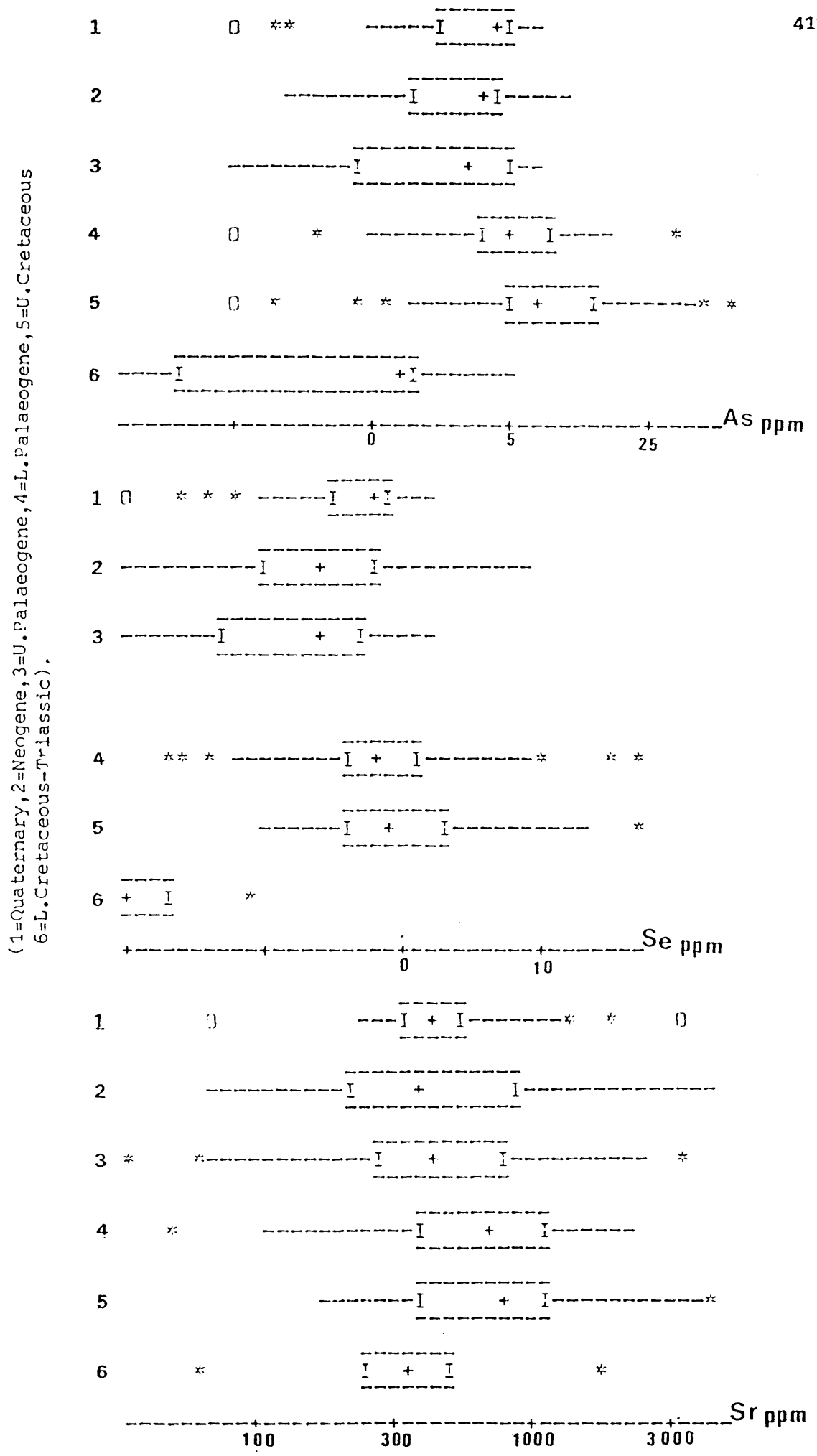


Fig.9.50 Boxplot of As, Se and Sr by rock type.

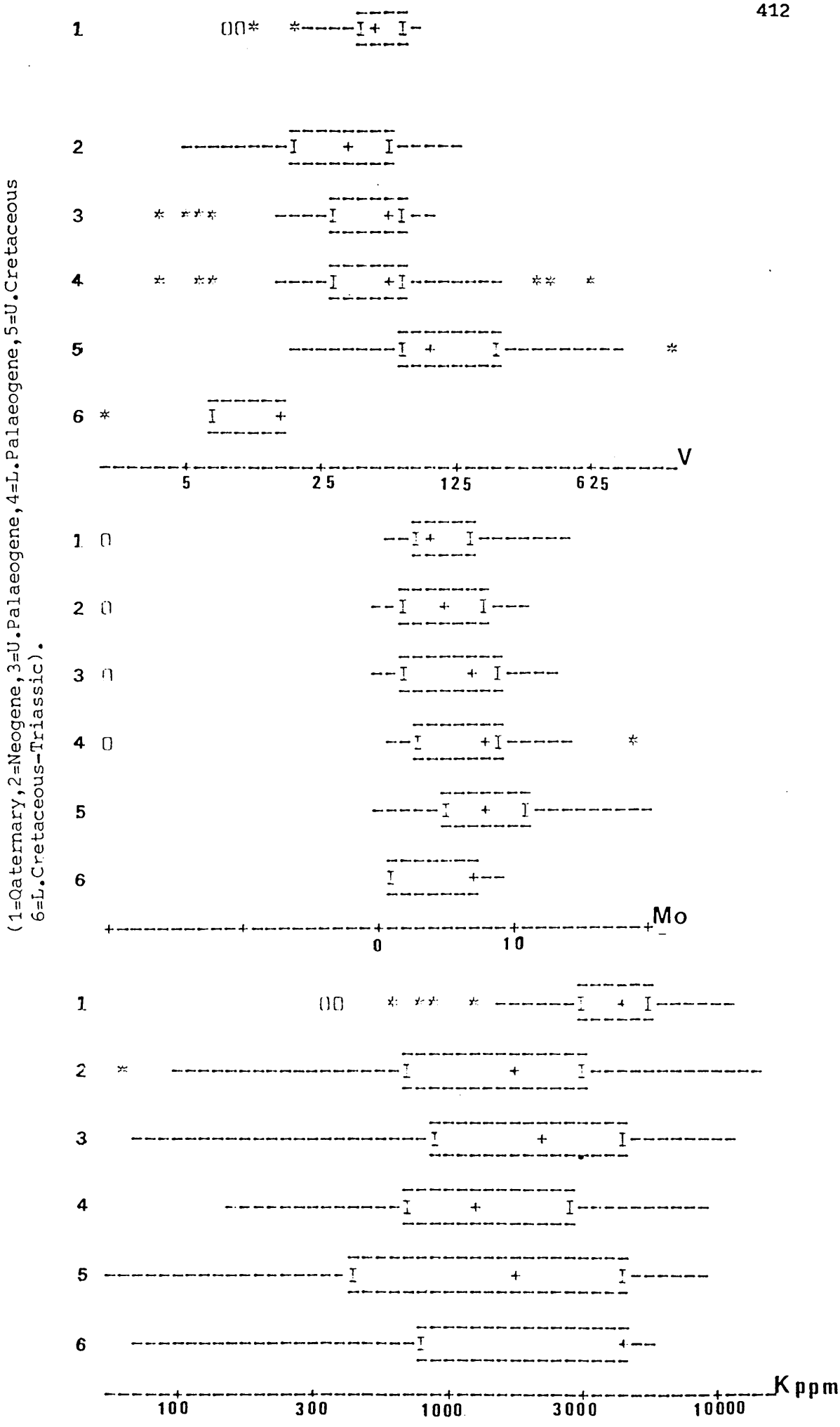


Fig.9.51 Boxplot of V, Mo and K by rock type.

Cretaceous (Unit 5) reflecting the depletion of the phosphate rocks with respect to K content, this latter unit, however appears to have the widest range of K concentrations. No significant difference in the median values of the Mo content between variuos units is detectable from the plot, owing to the small variation shown by Mo concentrations.

9.7.7.3 Lithogeochemistry of typical regional traverses.

The distribution patterns of U and its associated elements Th, As, Se, K, Sr, V, Mo, P, Ca, Li and radioactivity in both traverses 600 and 100, adequately illustrate the principal geochemical features of these elements over the outcrops of various lithostratigraphical units of the region (Figs. 9.52 to 9.59). The main features in the two traverses appears to be, in general, similar. The patterns of CPS, U and P (Figs. 9.52 and 9.53) display distinct similarities in both traverses, but with much extensive anomalous peaks in traverse 600 especially for CPS, P and to lesser degree U. The traverse geochemistry confirms the findings of the areal distribution patterns and proved to be in good agreement with the corresponding elemental contents within each of the lithostratigraphical units. Uranium correlates strongly with the phosphates of Upper Cretaceous (Unit 5) and Lower Eocene rocks (Unit 4) particularly over the two limbs of the Southern Palmyrides mountains and to a lesser degree over the clayey limestones of Lower Paleogene in both eastern and western sides of the traverses. Minor anomalous peaks of U higher than the general background level (that can be estimated from the figures as 15 and 8 ppm U for traverses 600 and 100 respectively) can be seen over the

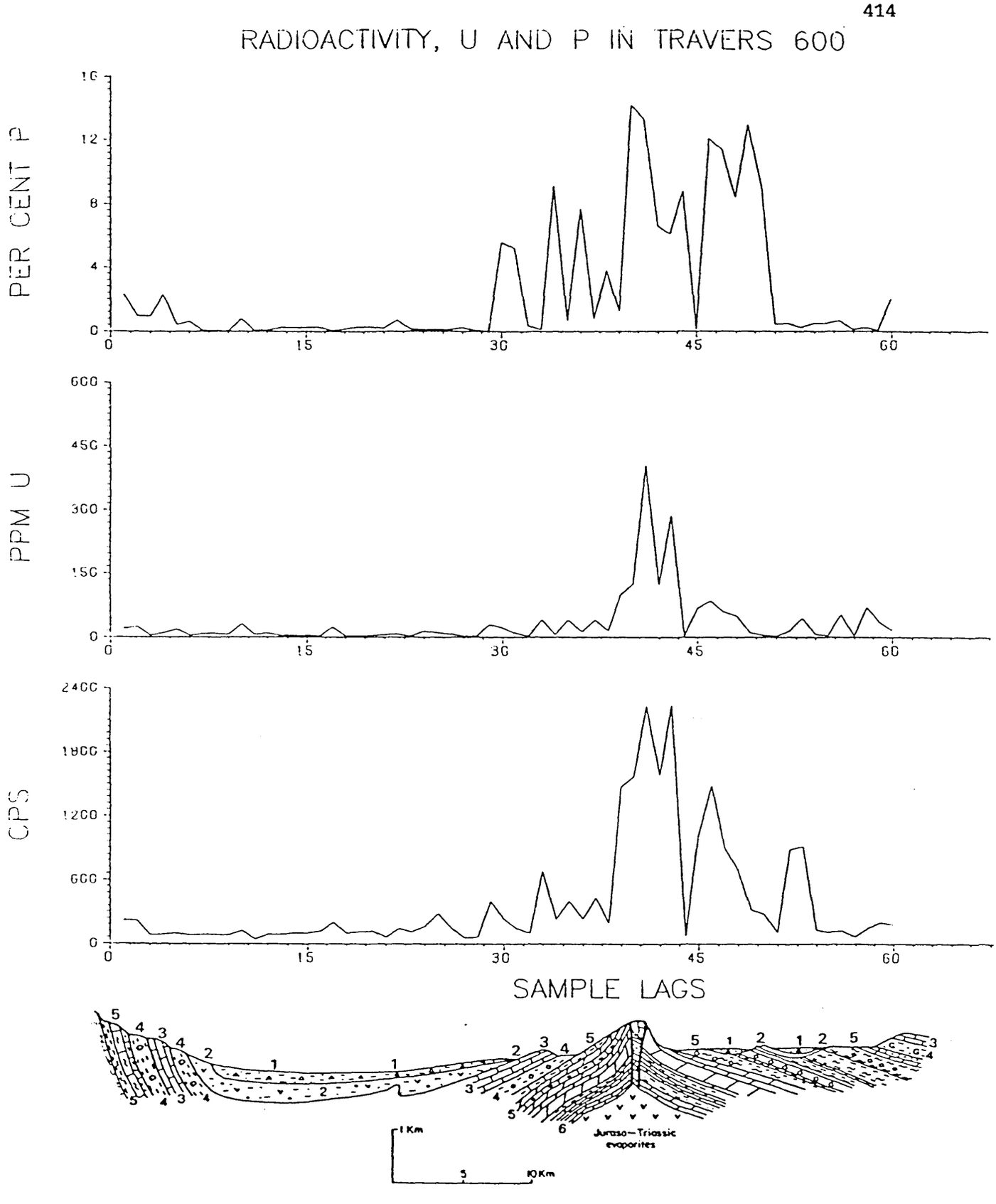


Fig.9.52 Distribution of CPS, U and P along traverse 600.

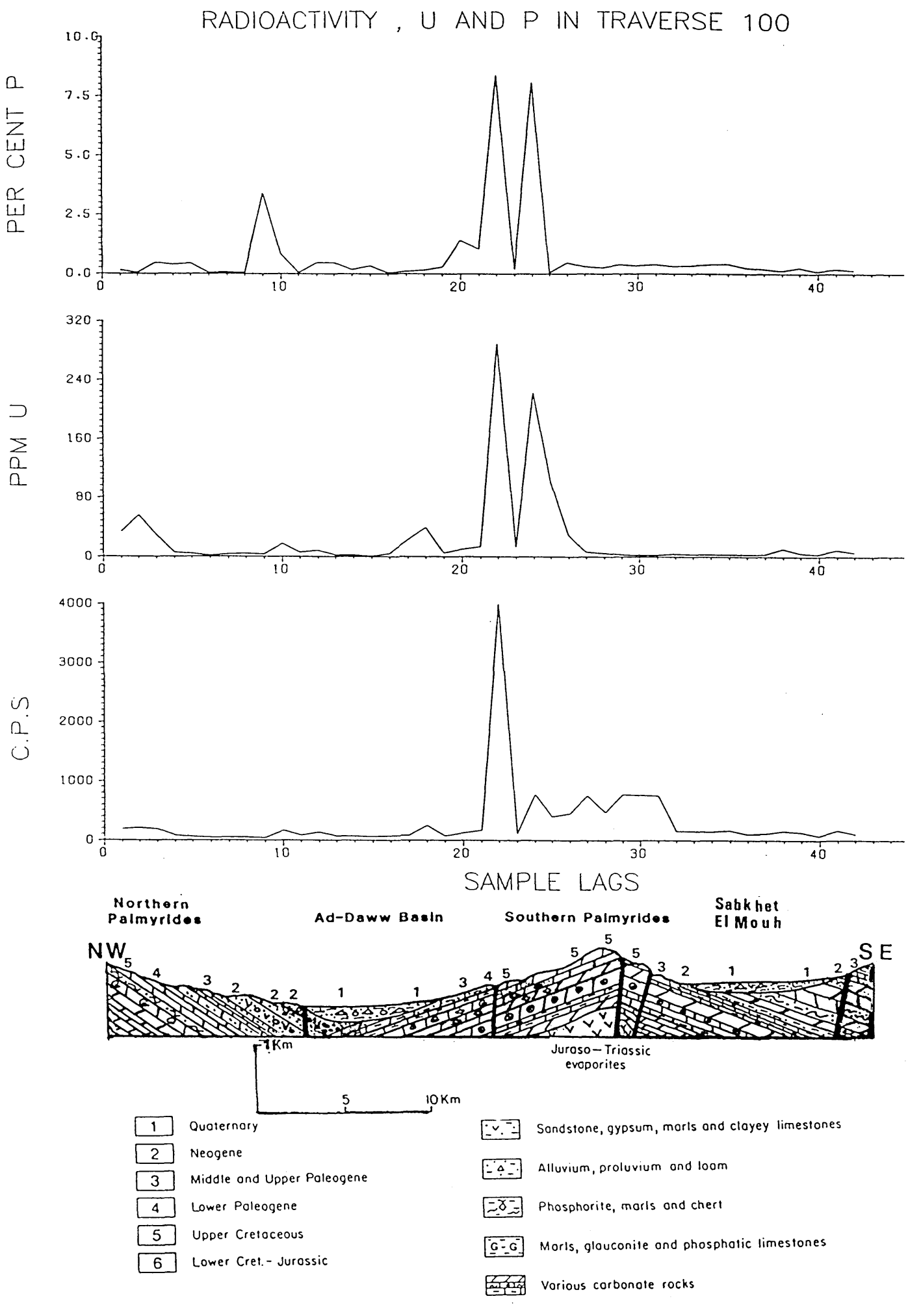


Fig.9.53 Distribution of CPS, U and P along traverse 100.

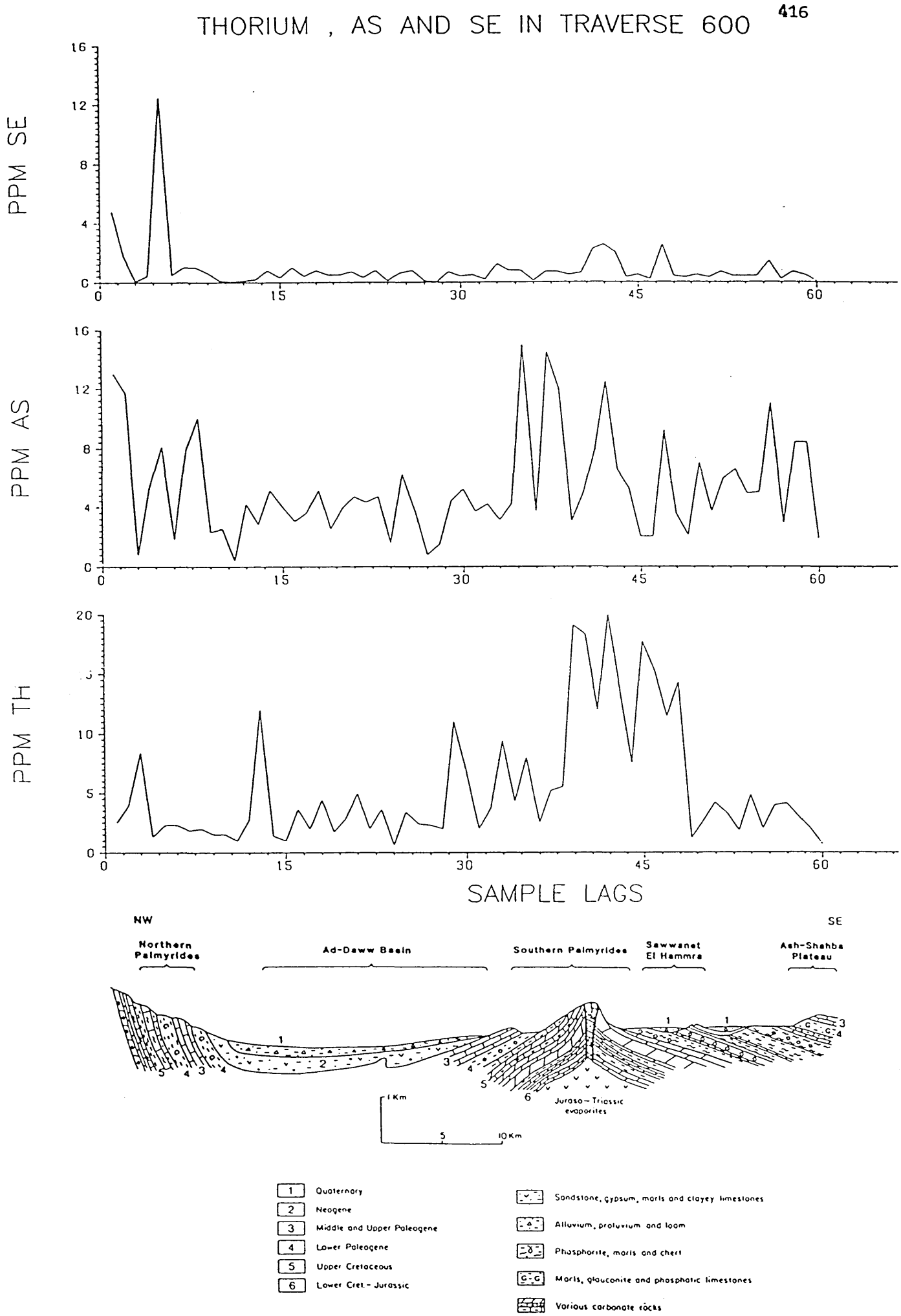


Fig.9.54 Distribution of Th, As and Se along traverse 600.

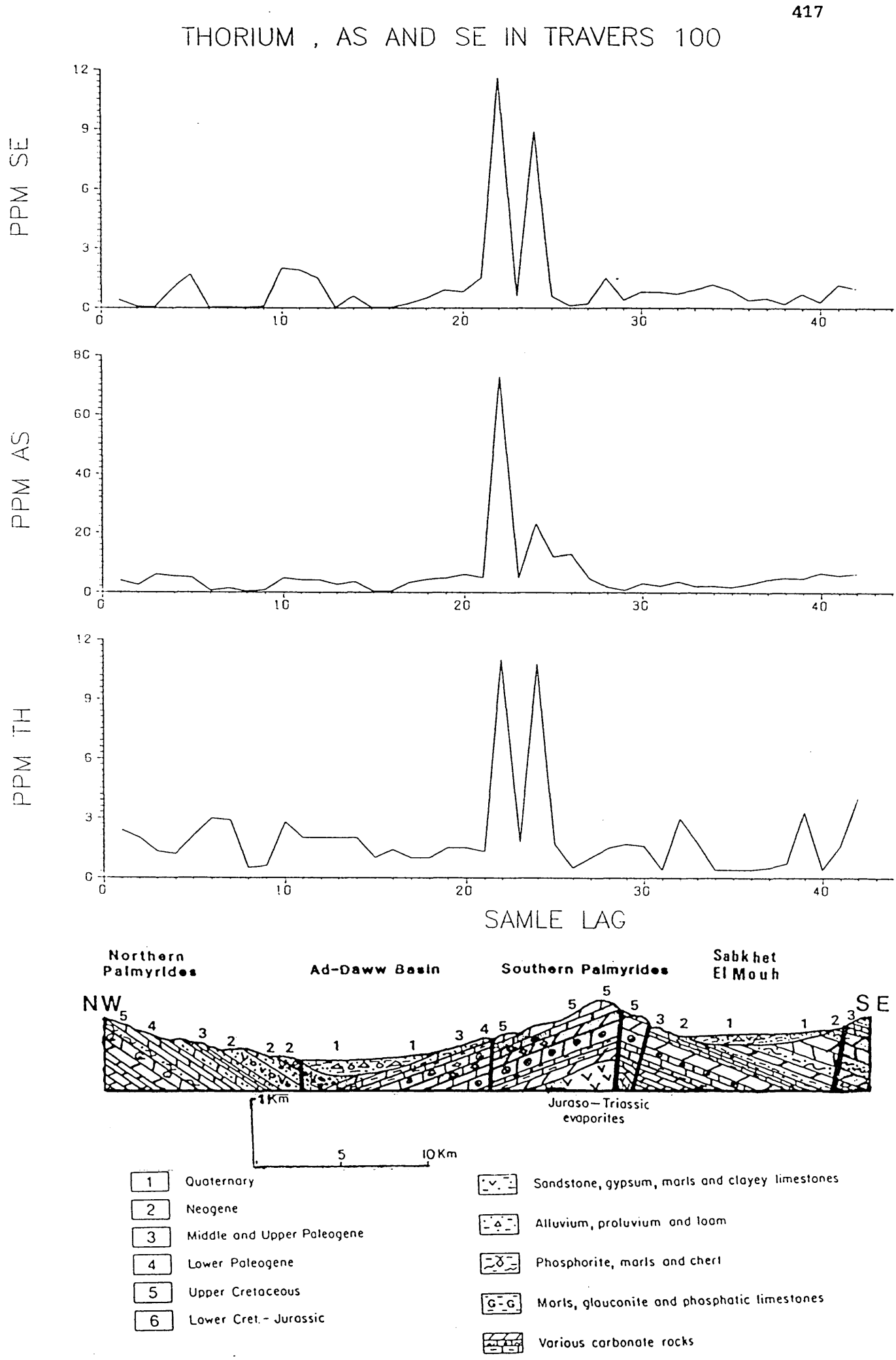


Fig.9.55 Distribution of Th, As and Se along traverse 100.

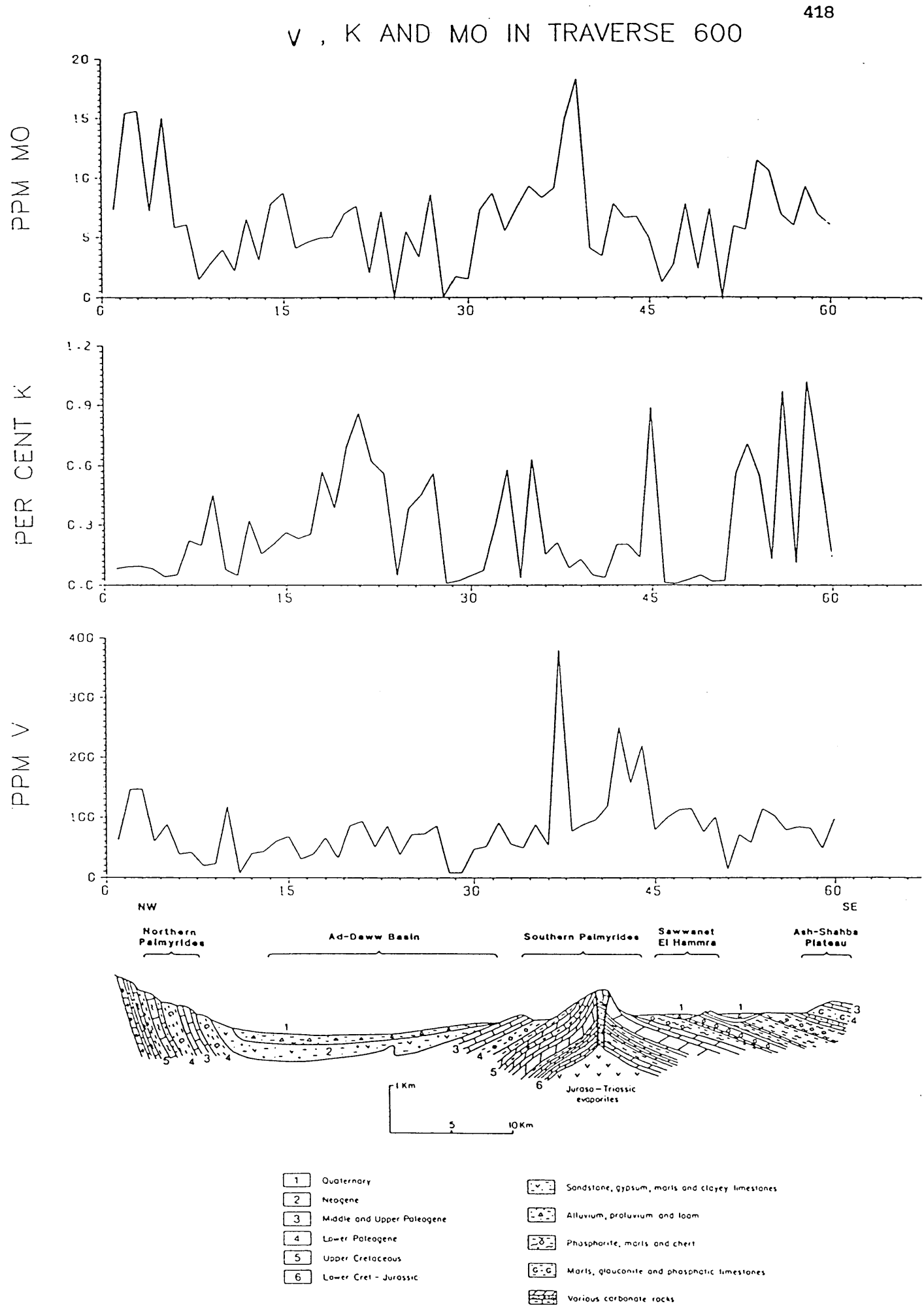


Fig.9.56 Distribution of V, Mo and K along traverse 600.

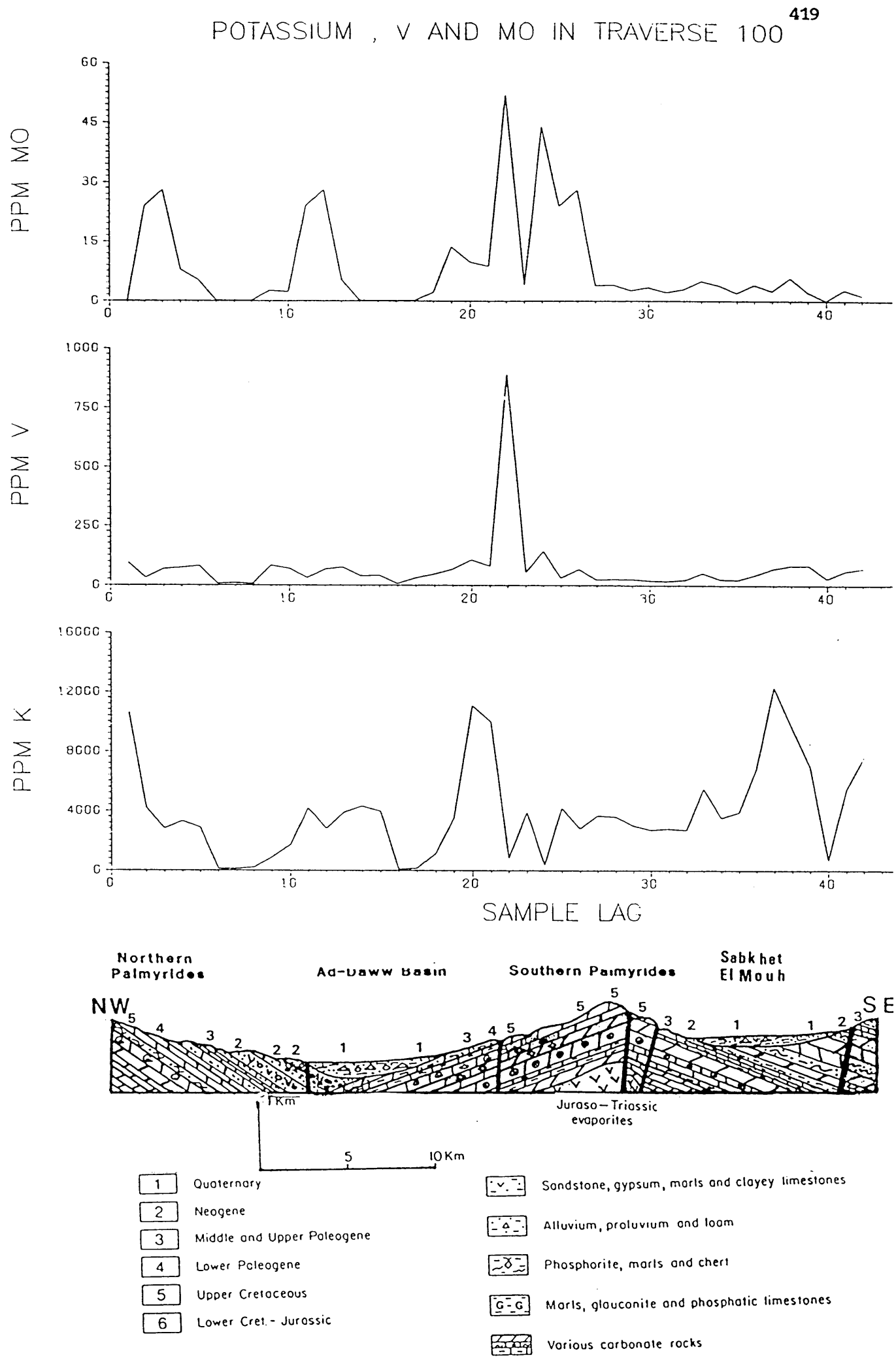


Fig.9.57 Distribution of V, Mo and K along traverse 100.

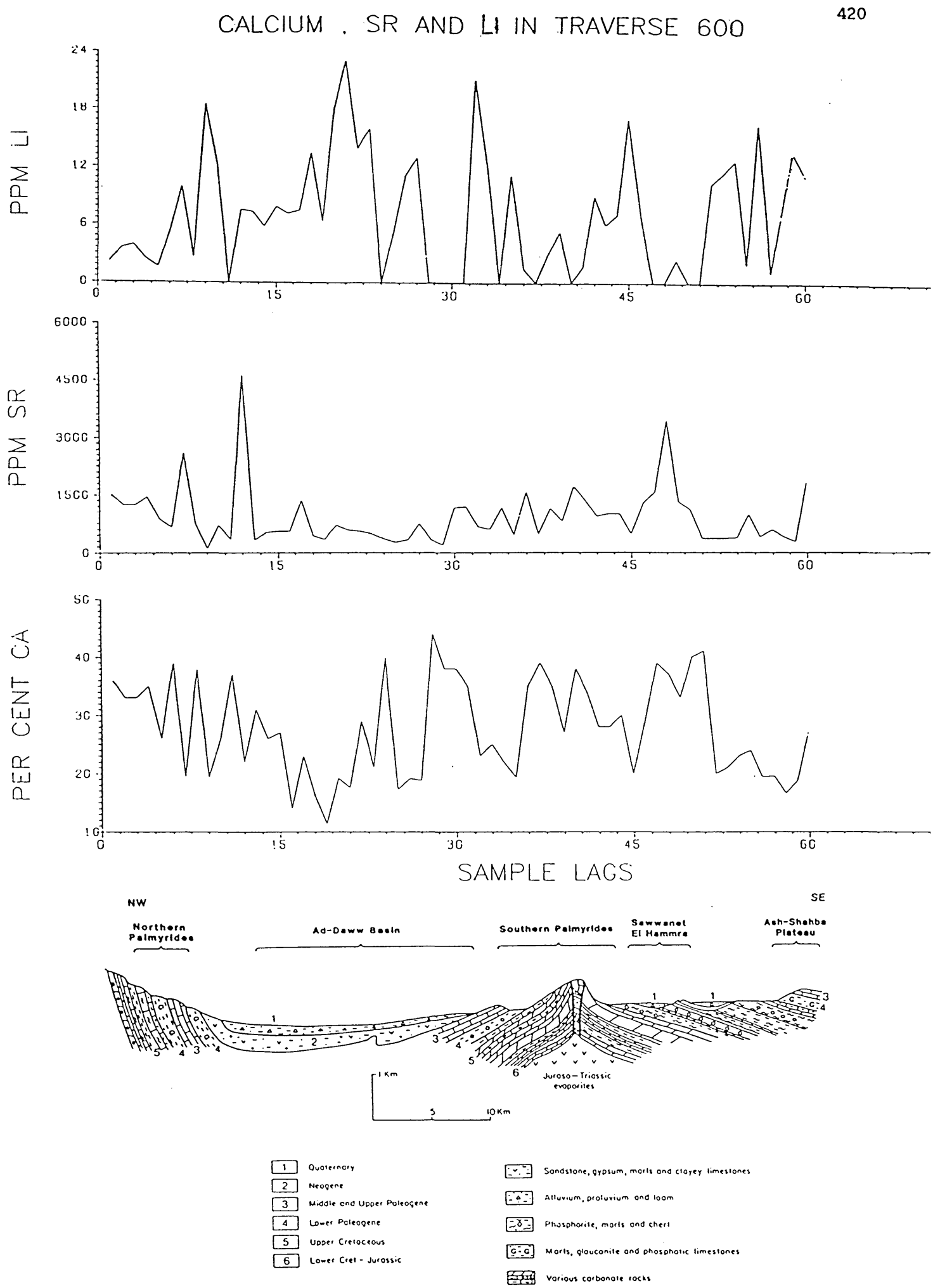


Fig.9.58 Distribution of Ca, Sr and Li along traverse 600

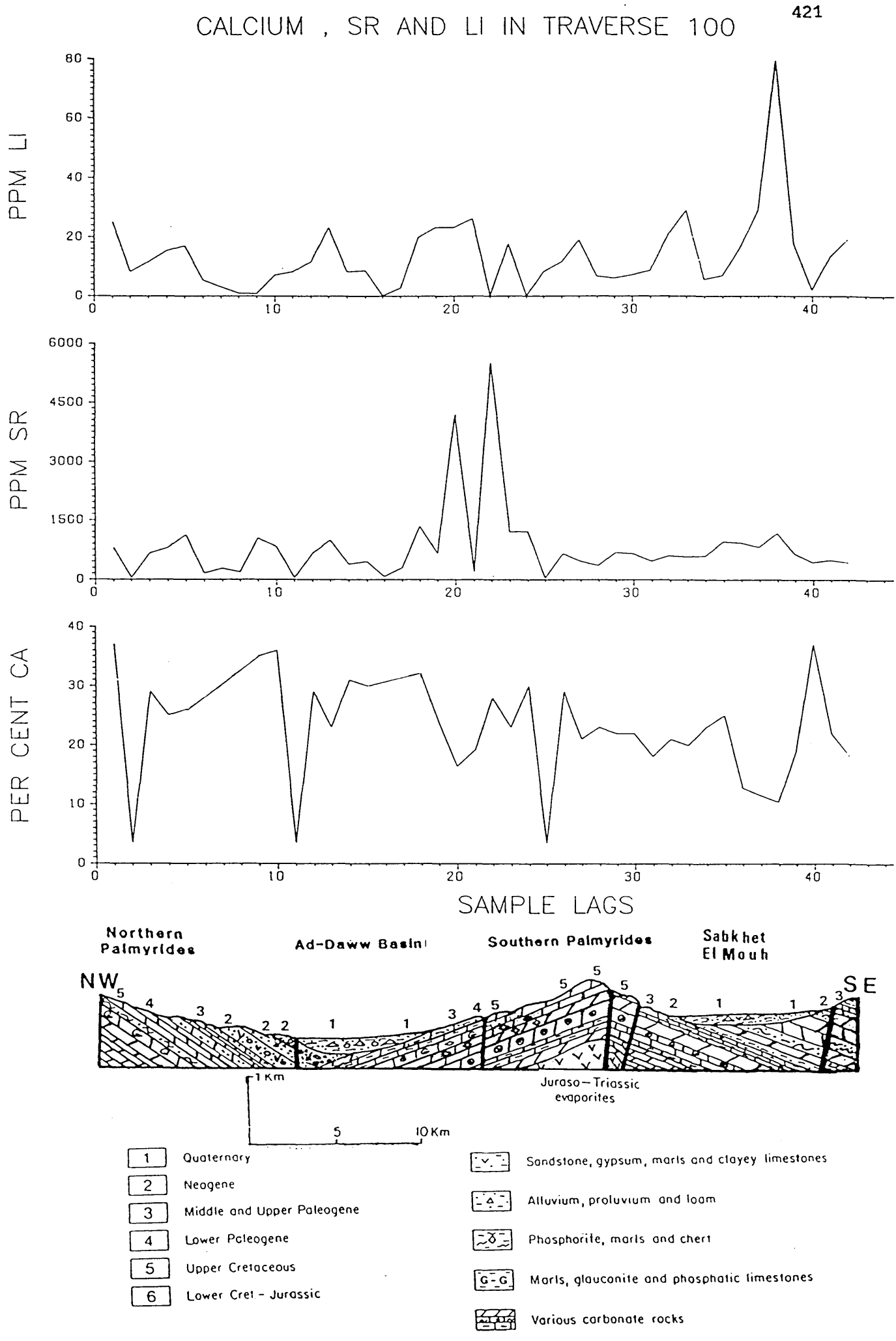


Fig.9.59 Distribution of Ca, Sr and Li along traverse 100.

unconformity contact between the Palaeogene rocks and the Neogene sediments, this contact occurs clearly only in the western sides of the traverses. Comparison of the anomalous peaks of U and P, close to this contact suggests that, contrary to P, uranium shows enrichment towards the Neogene sediments, whereas P is enriched towards the Palaeogene rocks.The enhanced U level in these Neogene sediments can nicely be confirmed by the hydrogeochemical data in the western side od Ad-Daww basin. Similar characteristics are shown by Th, K, Mo and to a lesser degree V and As. Selenium, however, varies considerably between traverse 600 (Fig. 9.54) and 100 (Fig. 9.55), in the former, it shows lower values over J. An-Naquaqueh of the Southern Palmyrides that is underlain by rocks of Units 5 and 4, while it shows high levels over corresponding sites of traverse 100, the reason for this contrasting feature is related to the presence of major faults in the latter traverse, that thought to be responsible for the observed enrichment here. Its pattern in both the eastern and western parts of the two traverses appears to be similar. Other intersecting features are shown by the contrast expressed by the patterns of Ca and Sr in both traverses (Figs. 9.58 and 9.59), marked enhancement of Sr over the Neogene and Palaeogene Units 2, 3, and 4 is contrary to the depletion can be seen, moreover, Sr shows similar behaviour to Se in many aspects. The patterns of Li (Figs. 9.58 and 9.59) show two main worth noting lithogeochemical characteristics:

a) A general enhancement over the Quaternary formations (Unit 1)

b) A marked depletion over the phosphate rocks in Units 5 and 4, therefore its pattern, is in contrast with that of P in Figs. 9.52 and 9.53, but similar to that of K in Fig. 9.57.

Finally, the enrichment of V over the lithologies in the eastern half of the region, relative to the western one is well expressed by its pattern in traverse 600 (Fig. 9.56).

9.8 Interelement correlation analysis

Correlation analysis for the whole of the lithogeochemical data set of the Palmyrides region were obtained by Box-Cox power transformation of the data and by the robust technique. There are few differences in the resulting coefficients, such that the robust technique gave higher coefficients, at a better confidence level for the correlation between U and P. The coefficients of the robust correlation are presented in Table 9.7. Strong linear positive correlations exist, at the 99% confidence level, between U, CPS, As, Se, V, Zn, Mo, P, Ni, Cd, Th and Cr. The strongest negative correlation among the various variables is that between V, Zn, Ni and Cu on one side and Fe, Al, Ti and K on the other, indicating that the former group of trace elements are not scavenged or adsorbed to Fe-oxihydroxides or clay fractions that are represented by the latter group of major elements. No significant negative correlation is found between U and any of the measured variables.

Thorium, P and radioactivity show somewhat weak, but still significant correlation at the 99% confidence level. The scatter plots of Th, K and U versus the radiomentric measurements clearly confirm that U is the major contributor to the radioactivity of the Palmyrides rocks (Fig. 9.60); the plot of P versus the radioactivty and the U content (Fig. 9.61), demonstrates a good linearity at the background levels which is thought to be a function of the typical

Table 9.7 Robust correlation matrix of the lithogeochemical data.

	U	CFS	TH	AS	SE	LI	NA	K
CFS	.782							
TH	.308	.396						
AS	.626	.633	.148					
SE	.607	.400	.143	.542				
LI	-.076	-.120	-.040	-.061	-.021			
NA	-.021	.006	.063	-.031	-.044	.080		
K	-.137	-.116	-.040	-.063	-.052	.754	.057	
MG	-.073	-.028	-.043	-.066	.008	.348	.099	.329
CA	.097	.121	.013	.082	-.065	-.584	.005	-.611
SR	.130	.089	.172	.050	.041	-.166	.070	-.281
BA	-.003	.081	.042	.097	.013	.013	.063	.009
AL	-.065	-.062	-.016	.021	.038	.712	.080	.831
LA	.143	.216	.144	.159	.085	.137	.074	.291
TI	-.092	-.081	-.036	-.079	-.060	.607	.148	.699
V	.552	.157	.126	.294	.604	.012	-.013	-.054
CR	.288	.226	.161	.239	.266	-.061	.185	-.038
MO	.501	.394	.098	.499	.474	-.018	.021	-.028
MN	-.119	-.087	-.014	-.108	-.089	.593	.061	.688
FE	-.122	-.100	-.041	-.035	-.042	.717	.119	.827
CO	-.071	-.076	-.026	-.084	-.048	.514	.058	.436
NI	.457	.036	.110	.194	.596	.051	-.008	-.031
CU	.398	.093	.050	.250	.514	.011	.091	-.017
ZN	.540	.160	.104	.344	.602	-.031	-.005	-.088
CD	.333	.238	-.022	.345	.181	-.156	-.006	-.136
PB	.122	.049	.112	.043	-.021	.314	.000	.167
P	.497	.572	.404	.264	.126	-.233	.036	-.256

Table 9.8 Summary of the correlations of U with other variables in the six lithostratigraphic units.

Elements.	Lithostratigraphic Units.					
	1	2	3	4	5	6
	U	U	U	U	U	U
CFS	.230	.310	.530	.504	.661	.696
TH	-.065	-.093	.084	.098	.125	.130
AS	.256	.140	.208	.118	.622	.908
SE	.192	.001	.184	-.078	.646	.869
LI	.129	.117	.062	-.111	.077	.010
NA	.055	.200	.149	-.212	-.138	.033
K	.104	-.010	-.194	-.028	-.098	.805
MG	.030	.124	.175	-.067	-.000	.184
CA	.140	.070	.071	.184	-.111	.407
SR	.167	.233	.298	-.083	-.062	.744
BA	.110	.127	.055	-.096	.111	.930
AL	.042	-.017	-.153	-.015	-.066	.766
LA	.228	-.020	.004	-.086	-.145	.827
TI	-.119	-.011	-.112	.011	.031	.556
V	-.051	.171	.140	.097	.501	.735
CR	.229	.289	.013	.023	.084	.544
MO	.031	.026	.194	-.052	.411	.419
MN	-.055	-.008	-.156	.021	-.147	.968
FE	.081	-.003	-.159	-.076	-.139	.731
CO	-.057	.017	-.105	-.002	-.054	.280
NI	.150	.141	.028	-.002	.487	.338
CU	.184	.151	-.003	.028	.377	.312
ZN	-.061	.008	.147	.119	.516	.387
CD	-.077	-.031	.137	.208	.225	-.073
PB	.072	.151	-.030	-.149	.138	.096
P	.273	.160	.257	.007	.047	.901

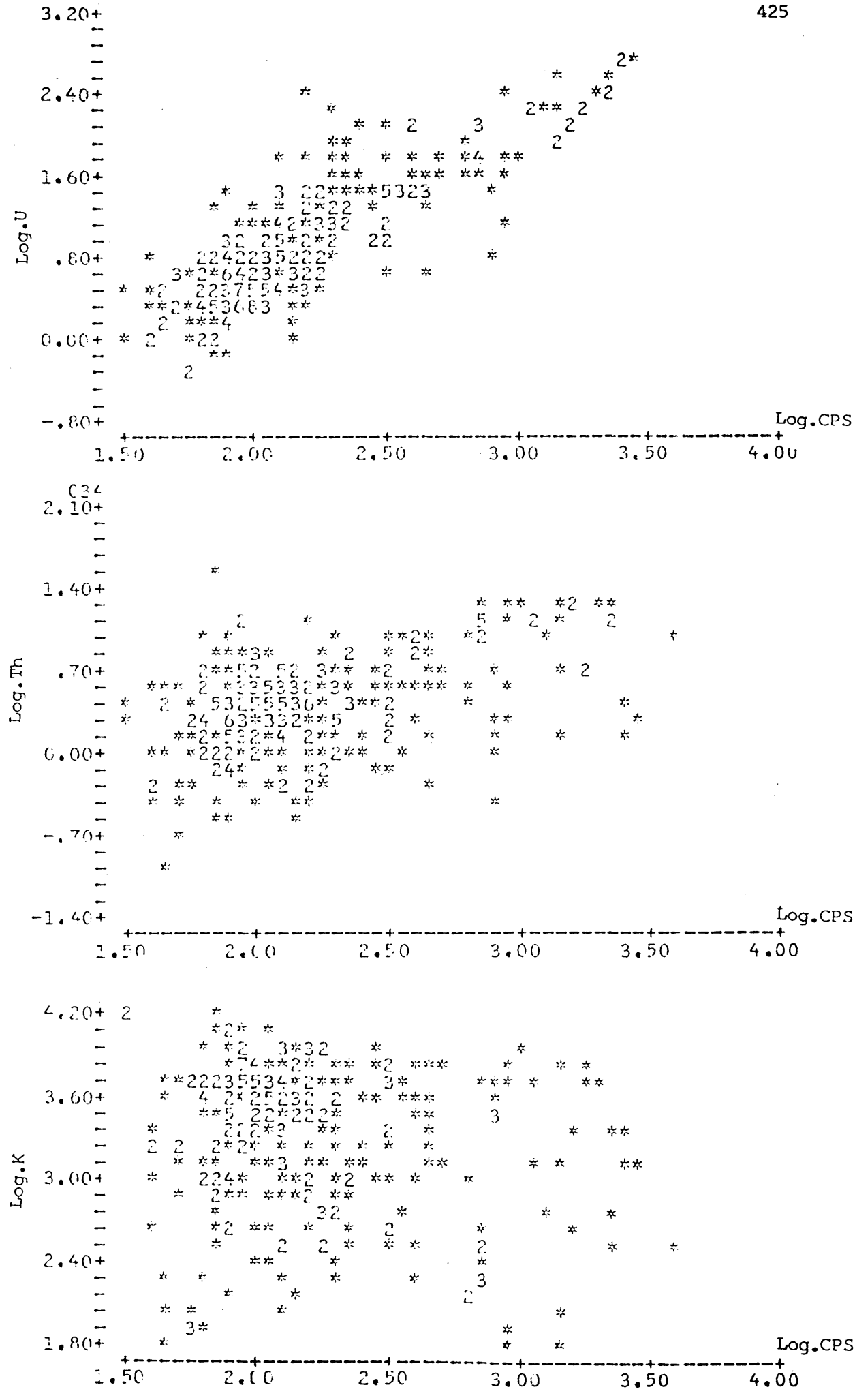


Fig.9.60 Scatterplots of U, Th and K contents of the rocks Vs CPS.

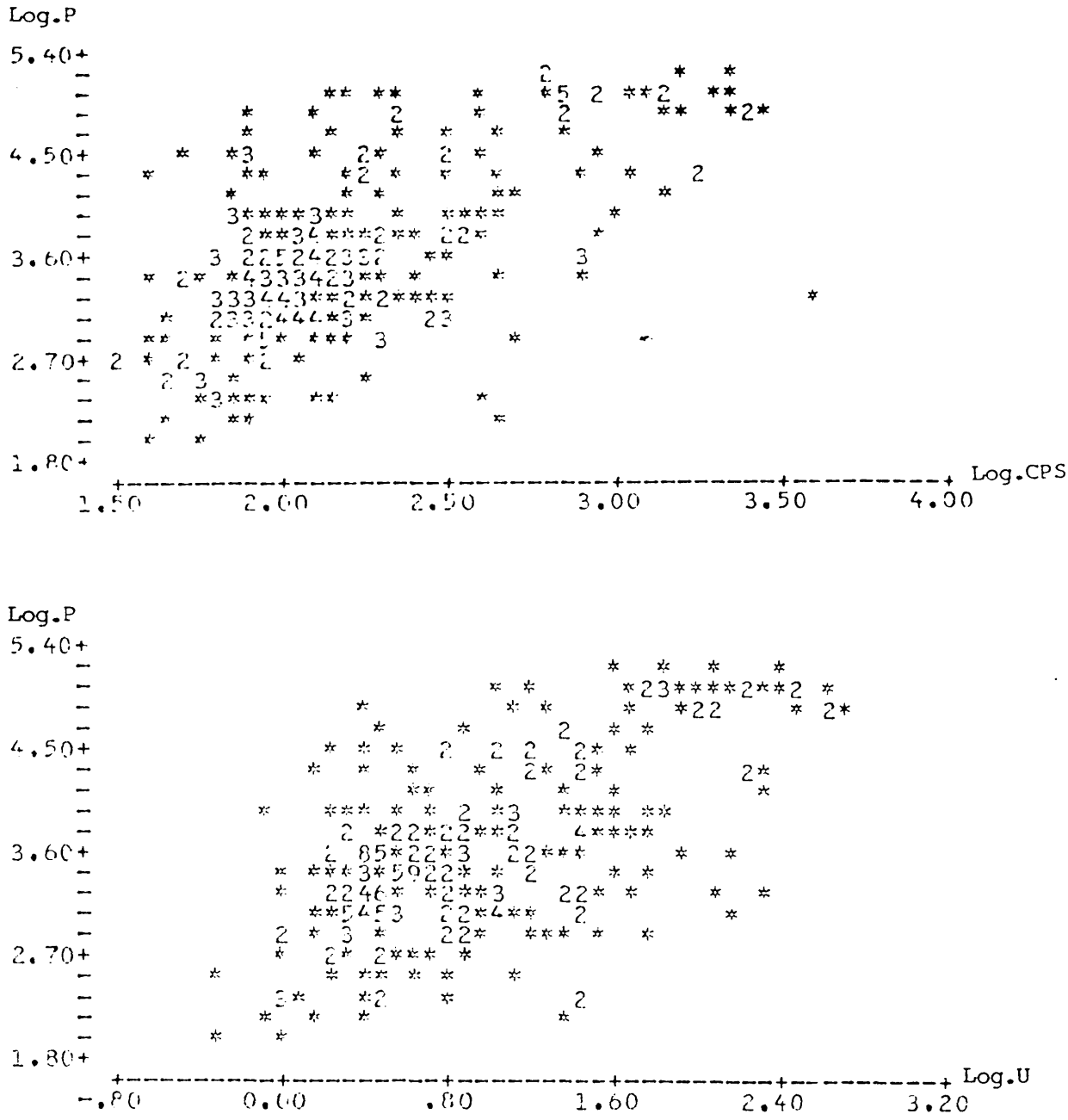


Fig.9.61 Scatterplot of P content in the rocks Vs CPS and U

U content in the phosphate rocks. However, in agreement with the orientation survey, and the earlier findings of Hunting (1975) (see Fig. 2.15), the relationship of P and CPS in the reconnaissance lithogeochemical samples, is indeed indirect above a threshold of 9.1% P (equivalent to 20.8 P_2O_5), and the linearity seems to depend only on the high levels of U in the rocks.

The weak positive correlation coefficient (0.49) for U and P and even the lower coefficient (0.18) obtained by the Box-Cox matrix perhaps indicates that, the substitution of U within the apatite and other phosphate minerals may not be the dominant phase in which U is present in the phosphates, this interpretation however, could find some support by the fission-track results.

Similar correlation matrices are computed for rocks of the two major lithogeochemical groups (the phosphate and nonphosphate samples). A summary of the correlation coefficients between U, CPS and P with selected variables is presented in Fig. 9.62. It indicates that the significant positive correlations within the two groups are; U, CPS, As, Se, Mo, V and Cd on one side and P, Th and Ca on the other in the phosphate group; and U and CPS; CPS and Th; and to a lesser degree U and Th in the nonphosphate rocks.

Phosphorus in the phosphate group significant negative correlations with Fe and K, and no correlation with the remaining major elements, this may confirm the lack of any sizeable detrital components in these rocks, whereas in the nonphosphate rocks P shows good correlation with La, Sr, Cd, V, Mo and Ca, suggesting mutual substitutions of these elements within the phosphate

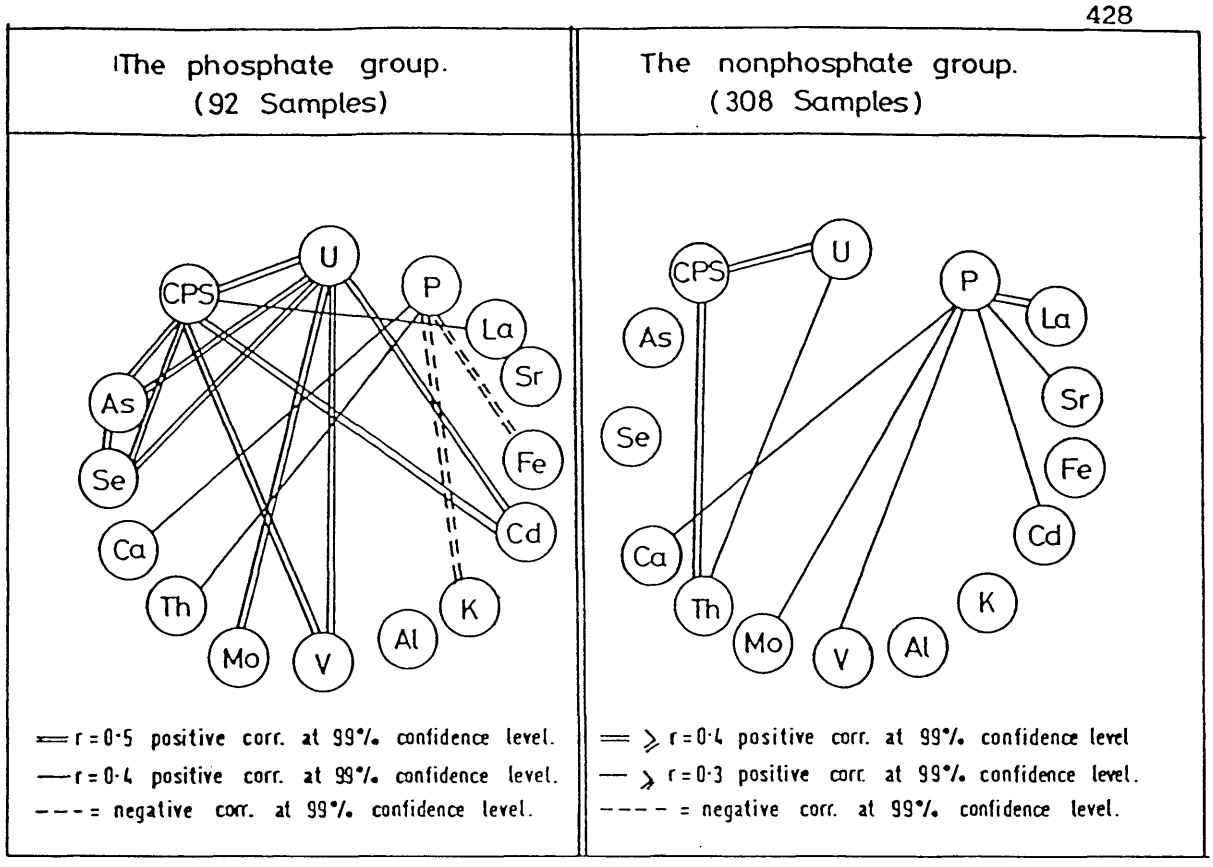
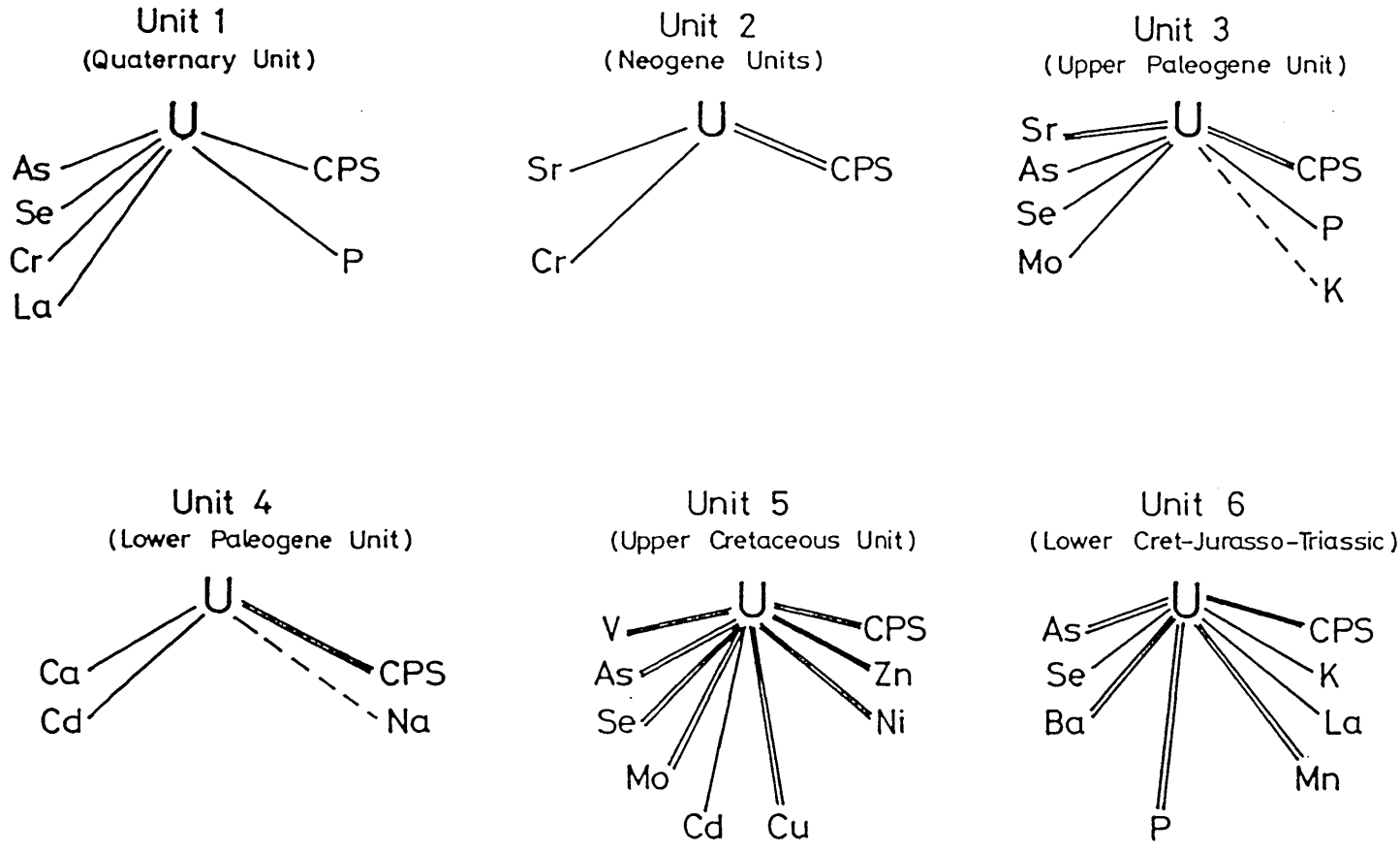


Fig. 9.62: Summary of the correlations between U, CPS and P with selected elements in the two main lithogeochemical groups.



positive correlation at 95°/. confidence level.

positive correlation at 90°/. confidence level.

significant negative correlation.

Fig. 9.63 Levels of U correlations in the Lithostratigraphical Units.

minerals.

Correlation coefficient matrices were also calculated for the geochemical data of the six lithostratigraphical units. For brevity the significant correlations of U with selected variables at the 95% and 90% confidence levels are presented in Fig. 9.63 and Table 9.8.

Results of the correlation analysis emphasizes the close association of U with As, Se, mo, V and to lesser degree P and Sr, the significance of this association is due to:

a) it persists in both the primary and secondary environments, and was shown by almost all sampling media used in this research;

b) it characterizes well known sedimentary U deposits world-wide.

9.9 Cluster analysis.

Twenty elements together with U, Th and the radioactivity measurements are considered in terms of R-mode cluster analysis in order to clarify the results of the correlation. The power-transformed data are standardized to generate the best cophenetic correlation coefficient, which is a measure of degree of fit. It was found that the highest cophenetic coefficient is obtained using either Wards or the Centriod clustering methods (r= 0.67). The dendogram (Fig. 9.64) summarizes the element groupings. Four distinct clusters are apparent:

1) Al, Fe, K, Ti, Mg, Mn and Li;

2) Ca, P, Sr, Th and Na;

3) CPS, U, As, Se, Ba and La;

4) Cr, Cd, Mo, V and Zn.

The second, third and to a lesser degree the fourth clusters are also mutually correlated at a significant level.

The first cluster, however, implies an association of elements of the clay fraction and Fe and Mn oxihydroxides. The second suite is mainly related to the prominent phosphorite lithology in which Sr and Na reside almost exclusively in apatite (McArthur, 1980), Sr as a major substituent of Ca and Na to balance the charge resulted from CO_3^{2-} and PO_4^{3-} substitution; Th seems to be trapped in the lattice during phosphorite formation. The third cluster is an obvious correlation which is found in all the present geochemical investigations regardless of the sampling medium used, and it appears to reflect a leachate solution derived from a source which seems most likely to be the phosphorite lithology, during reworking processes. The fourth cluster exemplifies the element association that has been shown to be significantly enriched along the fault zones, but is not apparently dependent on any one phase; it shows, however, a low level of association with both cluster 2 and 3.

Uranium and CPS show again close association and similarity, it is of interest, however, to know to which group U belongs in the case of excluding the radioactivity measurements. A repeat R-mode cluster analysis was, therefore, undertaken with the exclusion of CPS and the element association (Zn, Cd, Cr, Mo, Li, Ti, Mn and La) that has shown to be least associated with U in the first cluster. In the dendogram (Fig. 9.65), U shows an association with Th, As and Se, suggesting also a possibility of U partial enrichment with

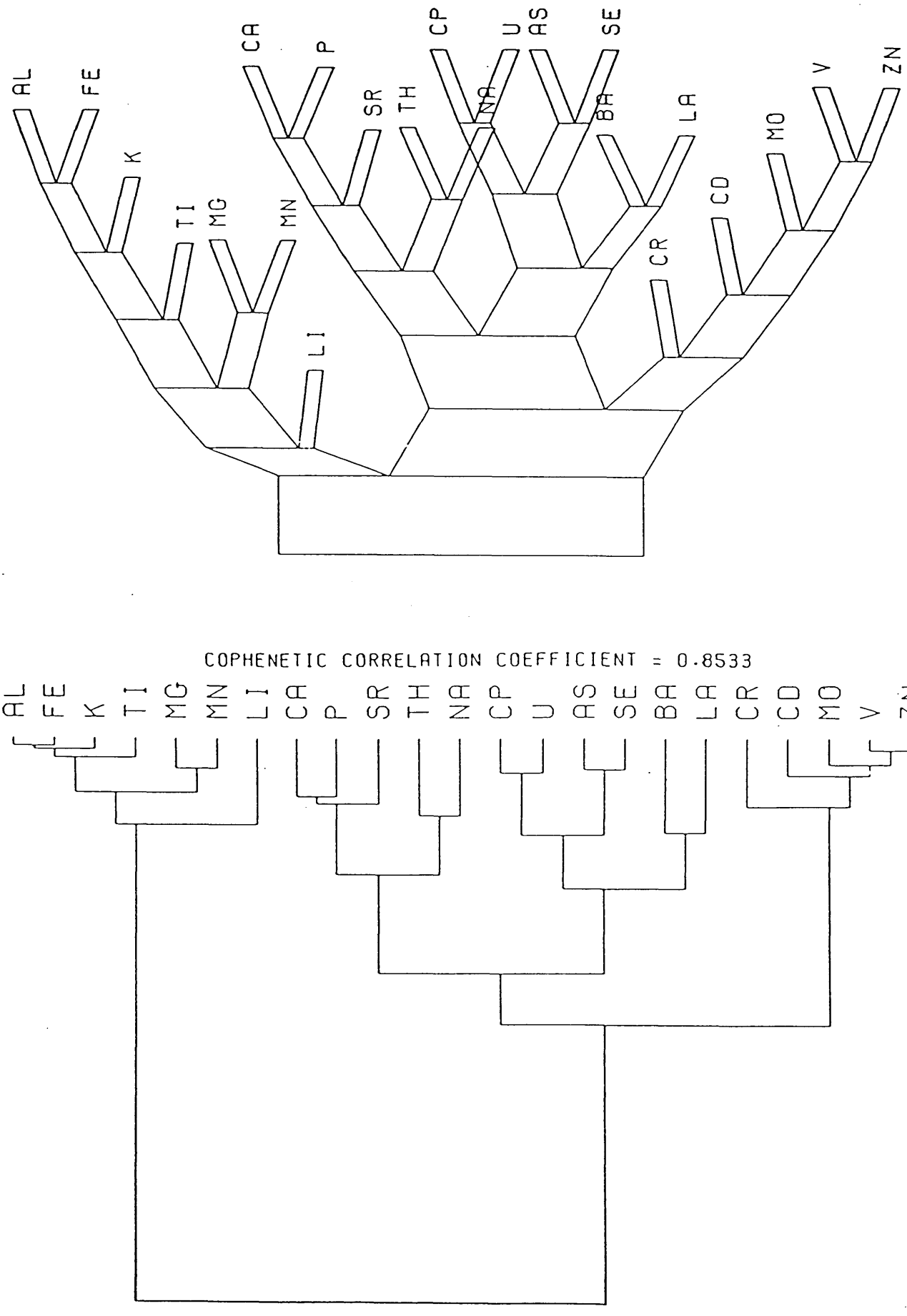
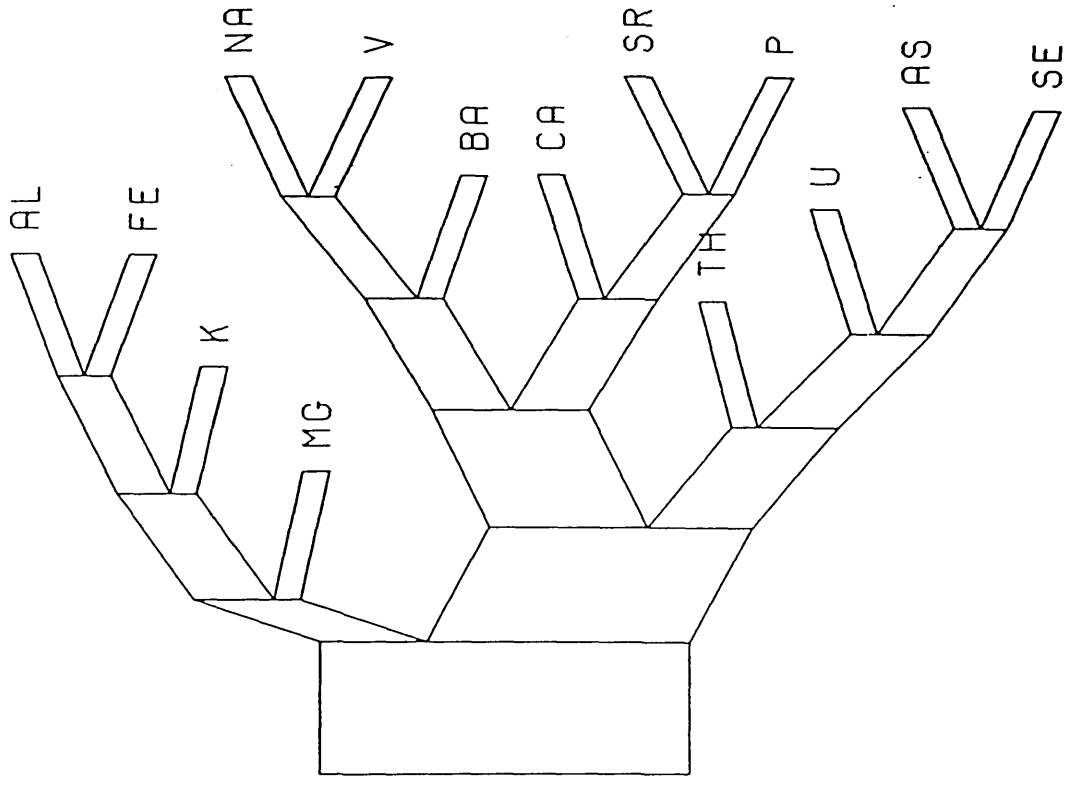


Fig.9.64 Dendrogram of R-mode cluster analysis of 20 variables of the litogeochemistry.



CLUSTER OF ALL SAMPLES

COPHENETIC CORRELATION COEFFICIENT = 0.6522

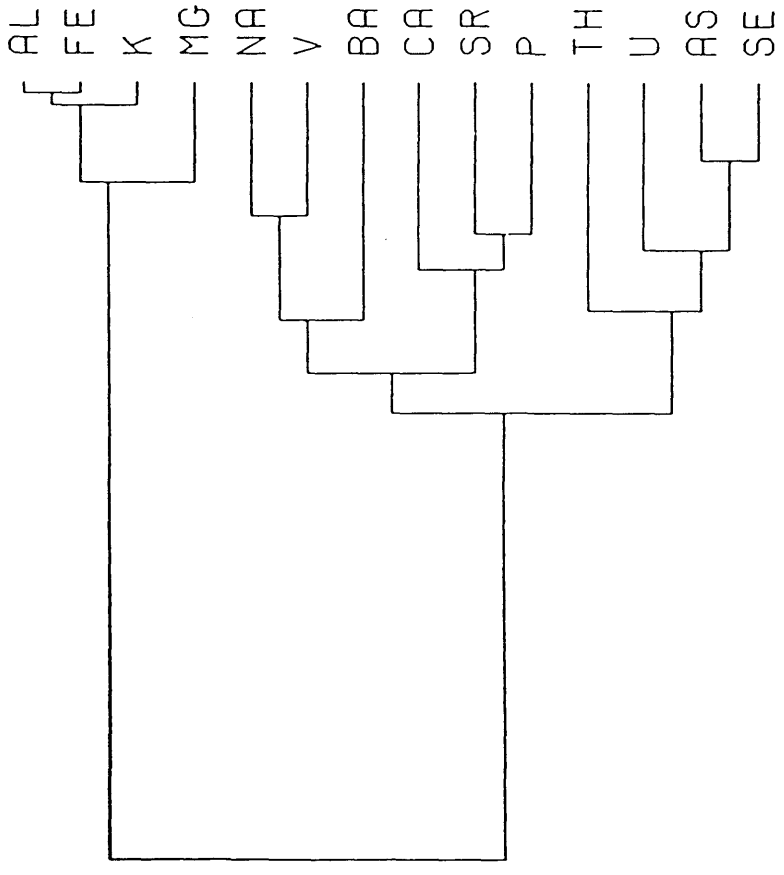
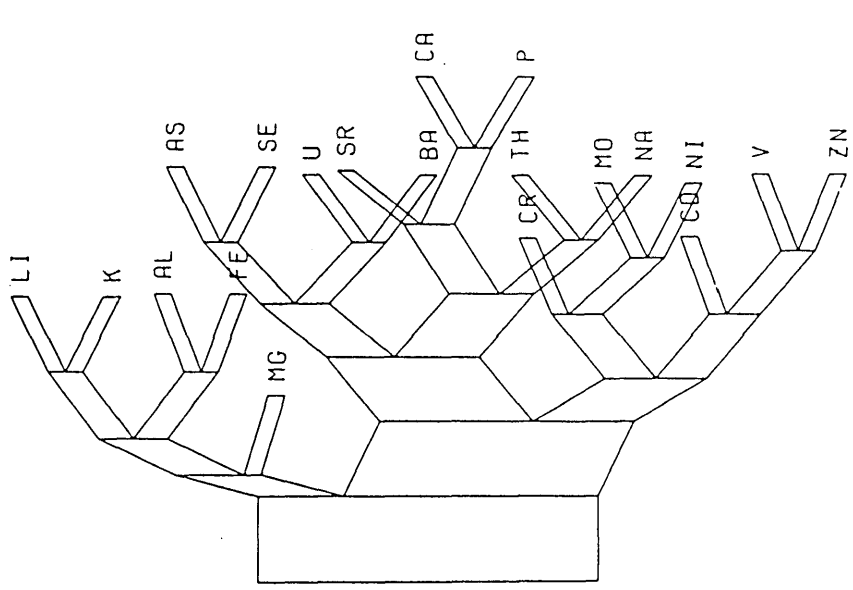
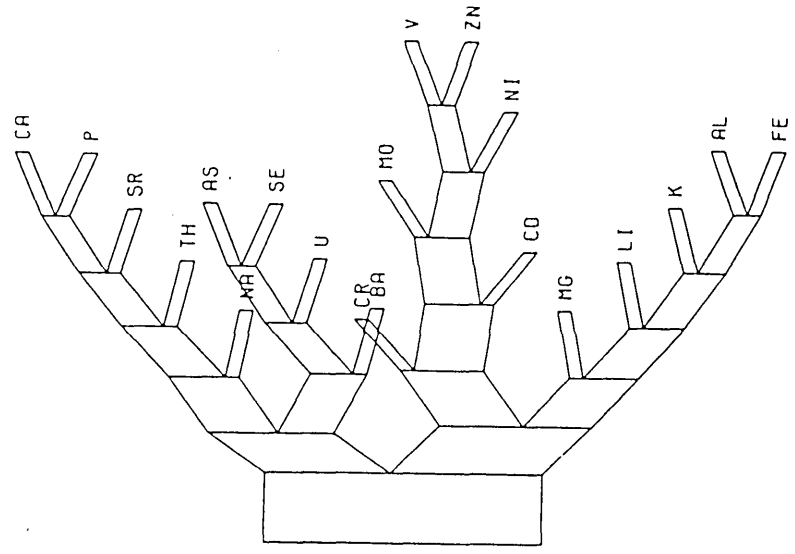


Fig.9.65 Dendrogram of R-mode cluster analysis of 14 variables of the lithogeochemistry.

these elements in a form of leachate. The observed close association of Th and U in a primary dispersion does not appear to have been detected during the orientation survey, possibly because it has not been preserved in the secondary environment. To this marked difference is added that shown by Ba and V which together with Na form a distinct cluster which reveals a significant association with that of the phosphorite group.

The dendograms of R-mode clustering of the two phosphate and nonphosphate groups (Figs. 9.66 and 9.67) have not revealed any interesting differences from an exploration standpoint. There is however, relevant detail in the clusters shown by the dendogram of the lithogeochemical data of the phosphate rocks (Fig. 9.66). Among the strong clusters, P and Ca are closely associated (as should be expected) and U, Ba Se, As on one side and Th and Na on the other seem to have varying degrees of association with P. However, for the nonphosphate group (Fig. 9.67), the strongest cluster is shown by V, Zn, Ni, Mo, Cd and Cr which exhibits at the same time a low level of association with a second cluster comprising of Fe, Al, K, Li and Mg. On the other hand Ca, P, Sn, Th and Na form a third cluste which is associated at a significant level with a fourth cluster which consists of As, Se, U and Ba. These four clusters summarize the relationships of the elements without being strongly affected by abundant P minerals or content. Hence the correlation shown by the first cluster (V, Zn, Ni, Mo, Cd and Cr) and the second one (Fe, Al, K, Li and Mg) could somewhat indicate a possible intimate relationship of these two associations that could result from weathering or reworking processes in which the former cluster of elements can be adsorbed or scavenged by the latter





WARDS METHOD

CLUSTER ANALYSIS

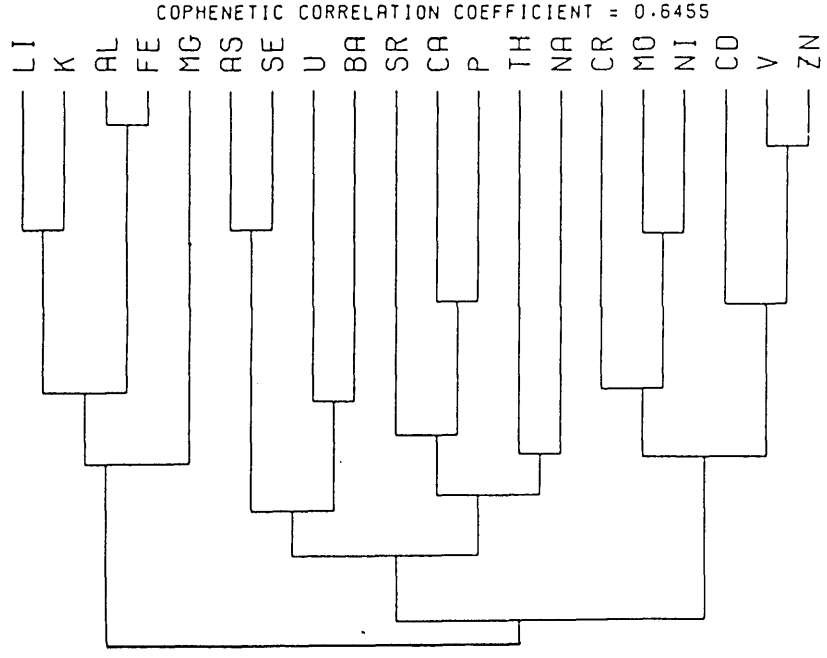


Fig.9.66 Dendrogram of R-mode cluster analysis of 20 variables in the phosphate group.

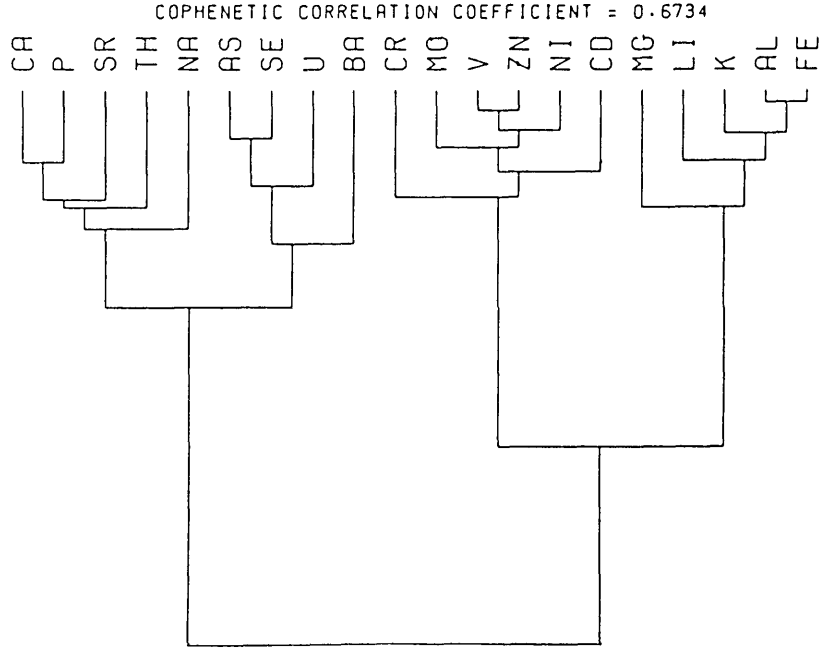


Fig.9.67 Dendrogram of R-mode cluster analysis of 20 variables in the nonphosphate group.

cluster (Fe, Al, K) in the form of clays and/or Fe-Mn oxi-hydroxide fractions.

9.10 Factor Analysis.

9.10.1 General

The principal aims of factor analysis were outlined in Chapter VIII. Factor analysis can be used to overcome interpretative problems caused by the compositional variations in the samples. The use of the factor scores rather than element data reduces erratic trends caused by mineralogical and chemical variations and perhaps can improve the interpretation by adjusting for rock-type in an appropriate way. Selenius (1983) has shown the value of reducing skewness in geochemical data prior to factor analysis, while Bolivar et al. (1983) successfully applied this technique to establish the geological relationships in the case of a complex data set.

Factor analysis is employed in the present work in order to assist recognition of underlying controls on the dispersion patterns of U and its associated elements, as well as outlying areas of exploration interest.

9.10.2 The six factor model.

A principal components of the Box-Cox transformed data were computed for the matrix of 405 samples and 24 variables. Although, using the robust technique would be slightly preferable, it was not

done because the procedure requires excessive computation time and limits manoeuvring with samples and variables. Taking into consideration the varimax criterion, a six factor model was selected for data analysis with respect to underlying controls that could be related to geological features and/or environmental processes. Elements which have a factor loading in the range of 0.25 to 1.0, regardless of the sign, have been considered as representative members of each particular association that results from the chosen factor model.

The variables, rotated factors, and their loadings are presented in Table 9.9. The model produced explains 73.6% of the total data variance, it is worth noting that a 12 factors model is needed to explain 81% of the variance, hence, the six factor model is considered to be satisfactorily acceptable.

Factor 1 is characterized by the strong loadings of Zn, Ni, Cu, V, Cr, Mo and Cd with lower loadings of U, P, Fe and Al. It explains 19.9% of the total variance, and seems to reflect a primary process acting during deposition of the rocks in a marine environment, especially under intense tectonism or submarine volcanism. Although the elements association of this factor suggest magmatic activity of basic composition, there is no field evidence to relate such association to terrestrial basic rocks, and at present, there is an absence of outcrops of these rocks in the immediate vicinity of the sampling area. However, it is worth noting that, there was active volcanisms in the region during the Cretaceous as a result of (previously mentioned) movements of the Afro-Arabian plate against Anatolia and otherEurasian microplates

Table 9.9 Loadings of the six factor model for the Palmyrides lithogeochemistry.

NEW ROTATED FACT LOADINGS

****

	FACT 1	FACT 2	FACT 3	FACT 4	FACT 5	FACT 6
CPS	-.2550	.1452	-.7277	-.0008	.0573	.1580
U	-.2606	-.0049	-.7670	.0119	.1592	-.0512
TH	-.0306	-.0900	-.2226	-.0020	.0857	.8773
AS	-.1376	-.2256	-.7074	-.0602	.0819	.1714
SE	-.1511	.0267	-.5690	.1022	-.3466	.0097
LI	-.2709	-.6826	-.0168	-.0745	-.1391	.1615
NA	-.3556	-.3610	-.2603	.0636	.3389	-.1958
K	-.2071	-.9088	.0647	-.1180	-.0514	.0735
MG	-.1457	-.7927	-.0192	.0417	.1002	-.0289
CA	-.0904	.4280	-.2646	.5051	.2952	-.2204
SR	-.4660	.1388	-.1046	.4318	.3147	.1933
BA	-.1118	-.2835	.0048	-.1370	.6848	.0402
AL	-.3685	-.8807	-.0040	-.0811	.0256	.0691
V	-.7952	-.2556	-.3340	-.0780	.1122	.0388
CR	-.7102	-.3004	-.2604	.0581	.3066	.0114
MO	-.6661	-.1582	-.1625	-.2151	-.1486	.1058
MN	.1310	-.7730	-.1126	-.1347	.1534	-.1398
FE	-.3199	-.9023	-.0031	-.0764	.0499	.0774
CO	-.0023	-.5528	-.0670	-.4806	.2781	-.0852
NI	-.8075	-.4052	-.0990	.0029	.1104	-.0469
CU	-.8069	-.2716	-.0845	.0517	.1038	-.0959
ZN	-.8384	-.0984	-.2444	-.0330	.1473	.0596
CD	-.5930	.1168	-.2425	-.4930	.1091	.0356
PB	-.1638	-.1139	.0138	-.7352	.1923	.0058
P	-.2948	.1693	-.0557	-.0502	.4599	.0833

VARIANCE ACCOUNTED FOR BY COMPNTS.

COMPNT	VARIANCE PERCENT	CUM VAR
1	19.9384	19.9384
2	21.5621	41.5005
3	10.0272	51.5277
4	6.7218	57.5211
5	7.7107	65.2318
6	8.3815	73.6133

(Dewey, 1973; Singor et al.; 1982). The volcanic rocks of that age are represented in the region by strongly weathered basalt, dolorite and anamesite which are richer in their contents of those elements strongly loaded in this factor, than any of the known sedimentary rocks. It is feasible, therefore, that similar volcanic activities or deep taphrogenic vents can account perhaps for the introduction of the elements V, Zn, Ni, Cr, Cu, Cd and Mo into the environment of sedimentation. The low loadings of Fe, Al and Na in this factor suggest that an insignificant detrital supply was incorporated into these rocks during deposition; thus it rules out any consideration of weathering products that could be derived from above mentioned older volcanic rocks. In general, factor 1 appears to reflect a sedimentary environment in which tectonisms and submarine volcanisms are active in generating the association of elements that are significantly heavily loaded in this factor.

The areal distribution of the factor scores (Fig. 9.68) shows quite clearly three trends of high values. The first and second trends are running in a northeasterly direction between J. Rmah (south) and J. Abou El Fawaress (northwest of Palmyra). It can be inferred from this figure that the two trends run nearly parallel to the Southern Palmyrides mountains along its eastern and western sides coincident with the fault system in the Southern Palmyrides zone. The third trend seems to coincide with the regional lineament found along the western side of the Ad-Daww basin which represents another possible subsurface fault. Therefore the elemental association of factor 1 reveals trace element enrichment along structurally controlled sedimentary environments. The geographic distribution of the scores outlines areas for further exploration

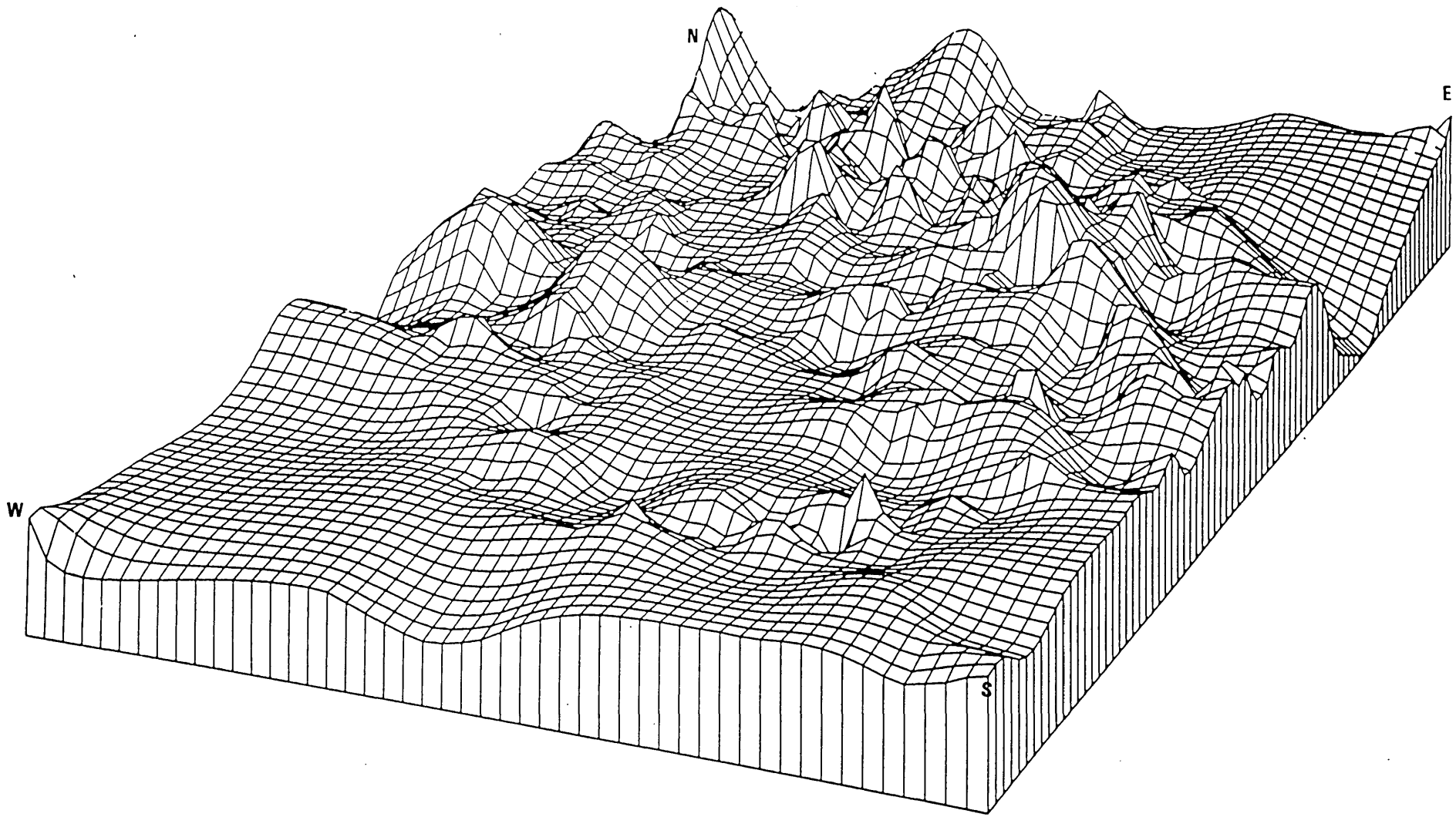


Fig.9.68 Solid surface distribution of the scores of factor 1 in the whole data set.

if the elements involved are of interest.

Factor 2 explains 21.5% of the variability of the geochemical data in terms of a strong association of K, Fe Al, Mg, Mn, Li and Co with highly significant loadings of 0.90, 0.90, 0.8, 0.79, 0.77, 0.69 and 0.65 respectively). The underlying process expressed by this association is related to the presence of the clay fraction in the sediments and to a lesser degree that of Fe oxihydroxides and glauconite. The strong loading of Mg with a much lower loading of Ca in this factor, could perhaps indicate that these clays are Mg-rich (palygorskite?) and minimizes the possibility that Mg can be attributed to dolomite or evaporite components. Therefore, if marine sedimentary phosphorite is concerned, this factor is an important one for phosphogesis (El-Bassam and Al-Allak, 1985). The areal distribution of the factor scores (Fig. 9.69) should outline formations with a prominent clayey influence, either as the main cementing material or reflecting marly and clayey carbonate lithologies. The main high scores of factor 2 are confined to the western part of the region and other scattered localities, especially in the southern part of the region in the vicinity of J. Rmah. No particular highs are found in the phosphorite domain, suggesting that clays are not present as a major fraction in the Palmyrian phosphorites.

Factor 3 is characterized by strong negative loadings of U (0.76), radioactivity (0.72), As (0.70), Se (0.56) and V (0.33) with somewhat lower Ca and Cr loadings. It explains 10% of the variability of the data and reflects enrichment processes leading towards higher contents of elements of this association. Such

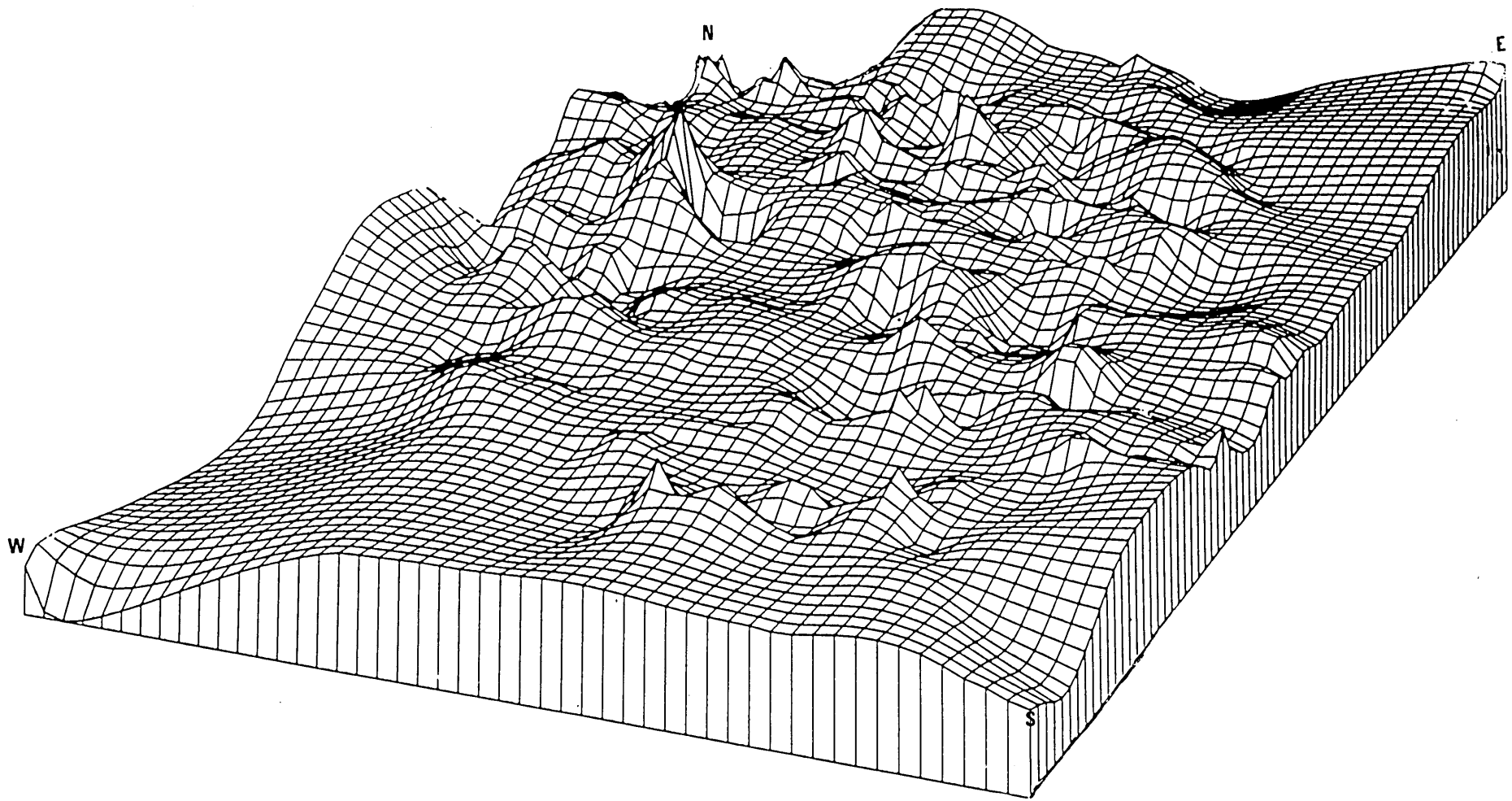


Fig.9.69 Solid surface distribution of the scores of factor 2 of the whole data set.

enrichment could result from either primary processes by adsorption or precipitation of these elements from sea and pore waters during the formation of the rocks, and/or from other solution brought into the depositional basin via fractures or upwelling. Alternatively it could occur as a result of secondary processes such as in situ reworking of the rocks and interaction with groundwater. Factor 3, however, ought to be considered as U, As, Se and to a lesser degree V concentration factor, which could outline by its high scores areas of interest for exploration.

The areal distribution of the scores is presented in Fig. 9.70. It reveals a cluster of highs to the east, north and west of the Ad-Daww basin. This distribution pattern resembles to a certain degree that shown by the scores of factor 1 and the areal distribution of the phosphorites in the region. It is therefore assumed that factor 3 represents a combination of two underlying controls acting together. The first seems to be structurally related to areas along the northeasterly trending faults along the two flanks of the Southern Palmyrides mountains, and also along the regional lineament in the western part of the region. The second is a lithological influence related spatially and possibly genetically to the phosphorite domain. This in turn, according to the author's personal viewpoint, may have resulted from major plate tectonic activity responsible for creating the favourable environment for the formation of phosphorites and their enrichment in U and associated elements. It is worth noting, however, that the pattern shown by the scores of factor 3 confirms the presence of a structural control on the distribution patterns of a few trace elements as discussed earlier. The role of faulting in producing

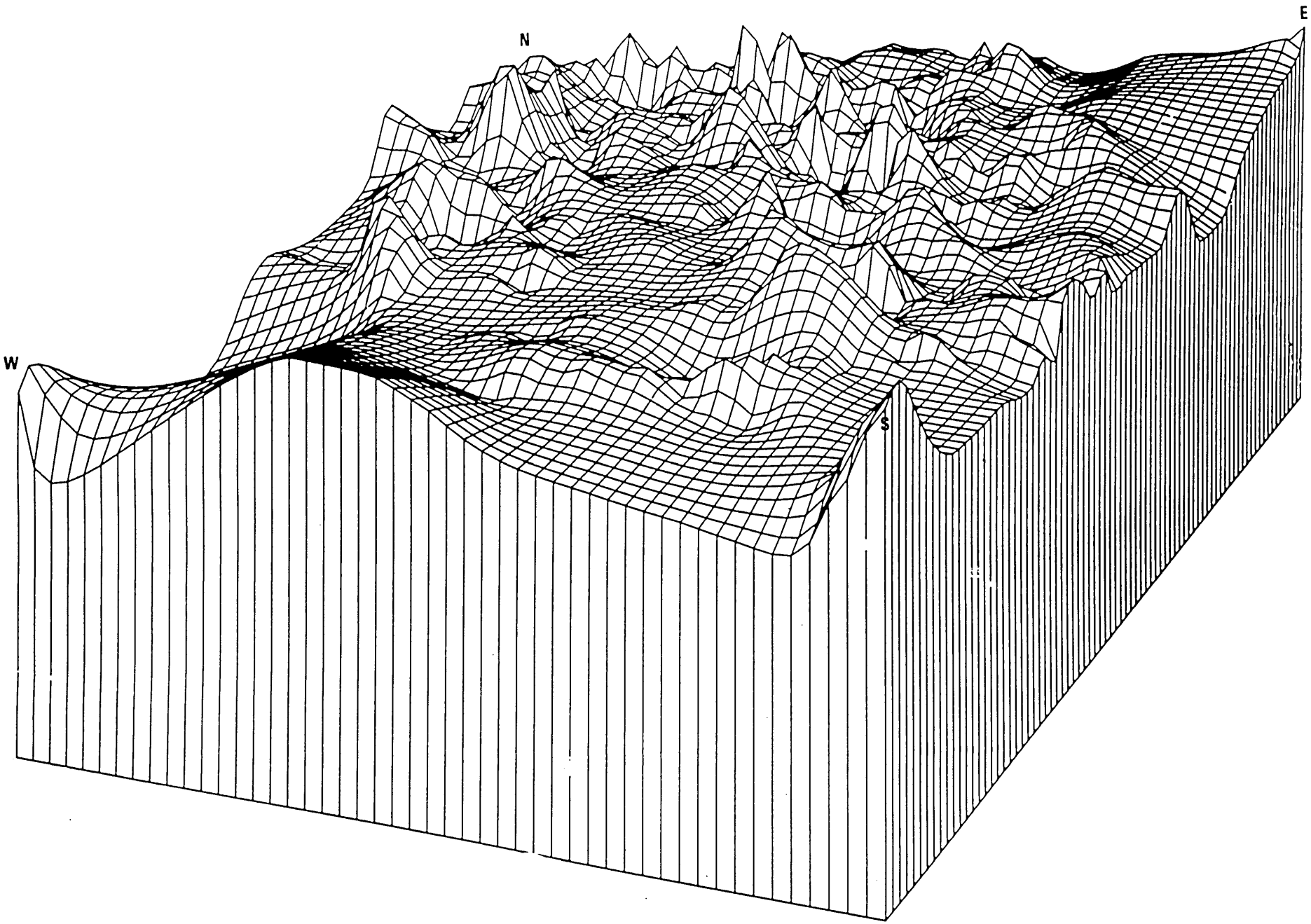


Fig.9.70 Solid surface distribution of the scores of factor 3 in the whole data set.

trace elements enrichment is well known world-wide, and the decisive role of plate tectonics for U enrichment in some Palmyrides rocks can be supported, at least in some aspects, by the plate tectonic related model reported by Simpson et al. (1979) and Watson and Plant (1979) for explaining U enrichment within the Caledonides of Scotland.

The fourth factor accounts for the lowest percentage of the total variance (6.7%), and represents an association of negatively but significantly loaded elements such as Pb (0.73), Cd (0.49) and Co (0.48) along with positively loaded Ca (0.50) and Sr (0.43). Geochemically, this group of elements represents lagoonal carbonate facies which seem to be deposited in a very shallow high salinity environment. The main underlying controls detected by factor 4, therefore, are of a geological and environmental nature.

The geographical distribution pattern of the factor scores (Fig. 9.71) clearly defines the paleogeography of the lagoonal carbonate environment in the region. These facies are outlined by the high scores. They are found mainly in three locations: (1) the southeastern corner of the region (J. Aida and Ash-Shahba Plateaux); (2) the vicinity of Sabkhet El Mouh (the Palaeogene rocks of the hills surrounding the Sabkha especially in its western side); (3) the vicinity of the T4 oilpumping station, and extending southwestwards Sharifeh hills and its surroundings. It is suggested that the carbonate rocks found in these aras possibly represent reef, back reef and lagoonal facies.

Factor 5 is characterized by significant positive loadings of

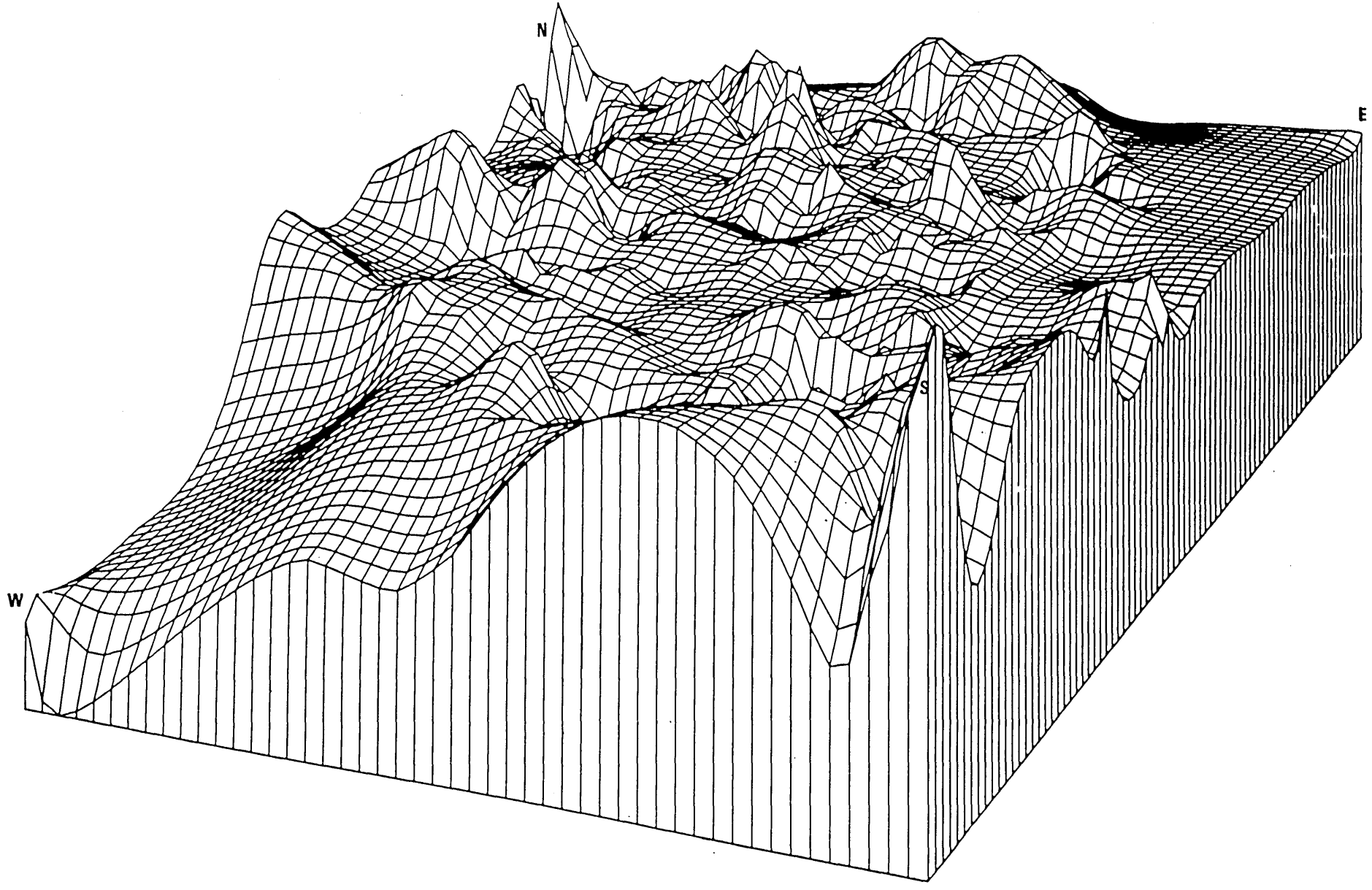


Fig.9.71 Solid surface distribution of the scores of factor 4 in the whole data set.

P (0.46), Ba (0.68), Na (0.33), Sr (0.31), Cr (0.3), Ca (0.30) and Co (0.28) and negative loadings of Se (0.34). This association explains 7.7% of the data variance. It appears to be closely related to apatite components and expresses the affinity of the elements involved to phosphorite precipitation. Factor 5, therefore, ought to be thought of as a phosphorite factor and should be widespread but with particular prominence within the vicinity of the commercial phosphorite deposits.

The areal distribution of the factor scores, shown in Fig. 9.72, reveals a general high level of background values above which only a rather subdued northeasterly trend of relatively high scores coincide with known phosphorite deposits. In addition, a few scattered high values are found, particularly in the northwestern corner, seemingly influenced by the presence of very small outcrops of Upper Cretaceous rocks. It must be kept in mind that the presence of barite could account for the two most obvious highs near Palmyra and T.4, this however, seems to reflect additional environmental control on this factor.

Factor 6 explains 8.3% of the total variance and is heavily loaded on Th (0.89). Weak loadings on Ca (0.22) and Sr (0.20) could lead to the assumption that Th perhaps is linked to some form of carbonate fraction as a result of secondary processes. However, little confidence can be attributed to such an intepretation, and it is preferable to view factor 6 as simply Th distribution, largely independent of lithology and element association.

Although the distribution pattern of the factor scores (Fig.

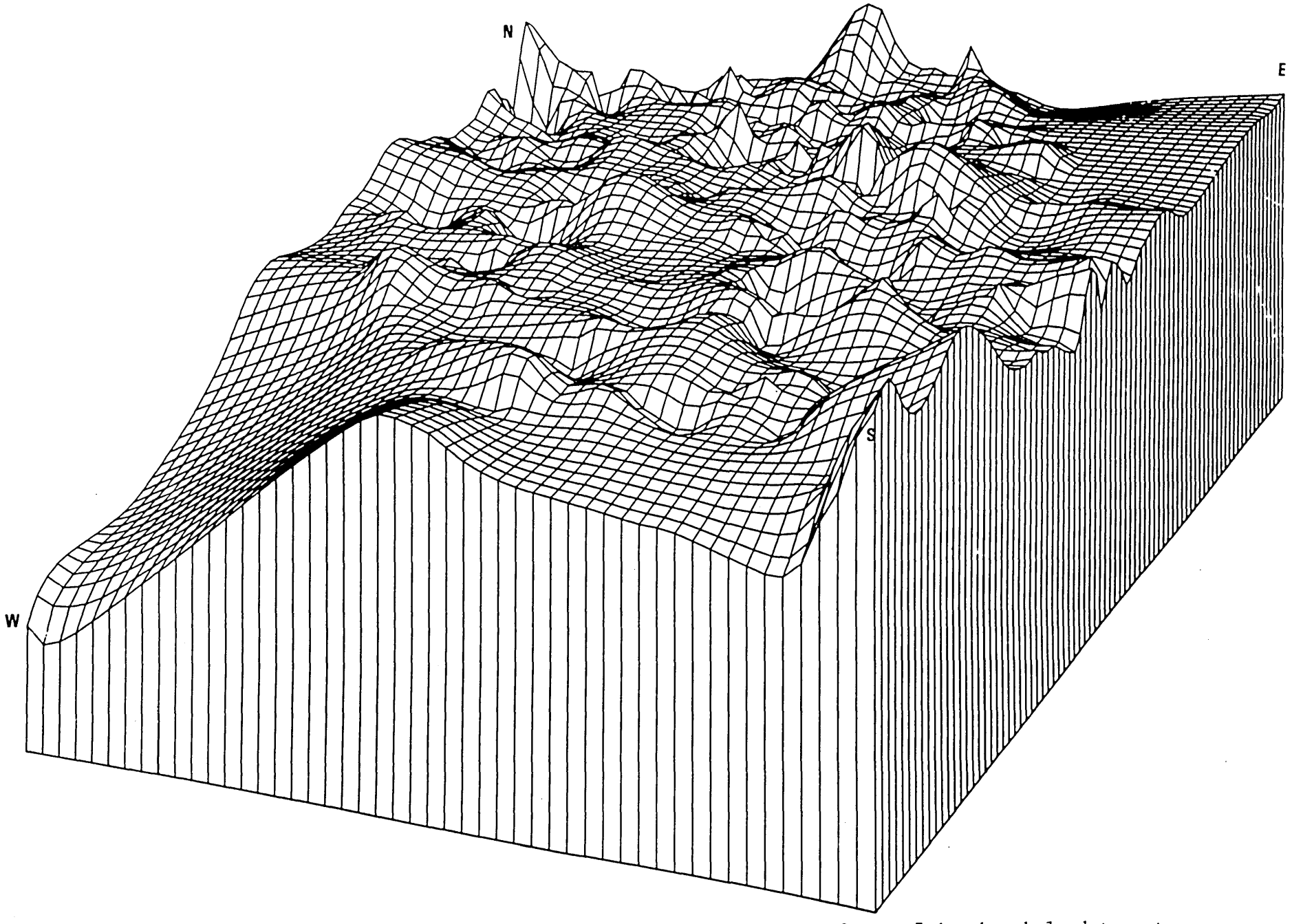


Fig.9.72 Solid surface distribution of the scores of factor 5 in the whole data set.

9.73) failed to provide any further interpretational evidence it is possible to trace a few slightly higher scores from the southeastern part of the Sawwanet El Hammra hills towards the northwestern vicinity of Palmyra. The significance of this trend is not at all clear. In addition a comparison of this pattern with the geochemical dispersion pattern for Th in Fig. 9.22 reveals a coincidence of the anomalies in the immediate vicinity of Sabkhet El Mouh and along the western side of the region. This confirms that factor 6 is essentially a primary dispersion factor of Th with weaker influence of a supergene factor, which otherwise cannot be interpreted in terms of the underlying geological and environmental controls. It is of importance to point out at this stage that the remaining 27% of the data variance can be accounted for by much larger number of additional factors and related processes and it is beyond the scope of this research work to further investigate these.

9.10.3 Factors controlling U in the phosphate rocks.

Factor analysis is of particular value in the investigation of the behaviour of U in the 92 phosphate and phosphatic limestone rocks. Therefore, the Box-cox transformed geochemical data of the phosphate group of rocks were used to generate a principal component matrix for U, Th, P and the ten other variables listed in Table 9.10 along with the factor loadings.

The resulting 5 factor model shown in Table 9.10 was considered cable in explaining the distribution of U and associated elements within the data; It accounts for 76.1% of the variability.

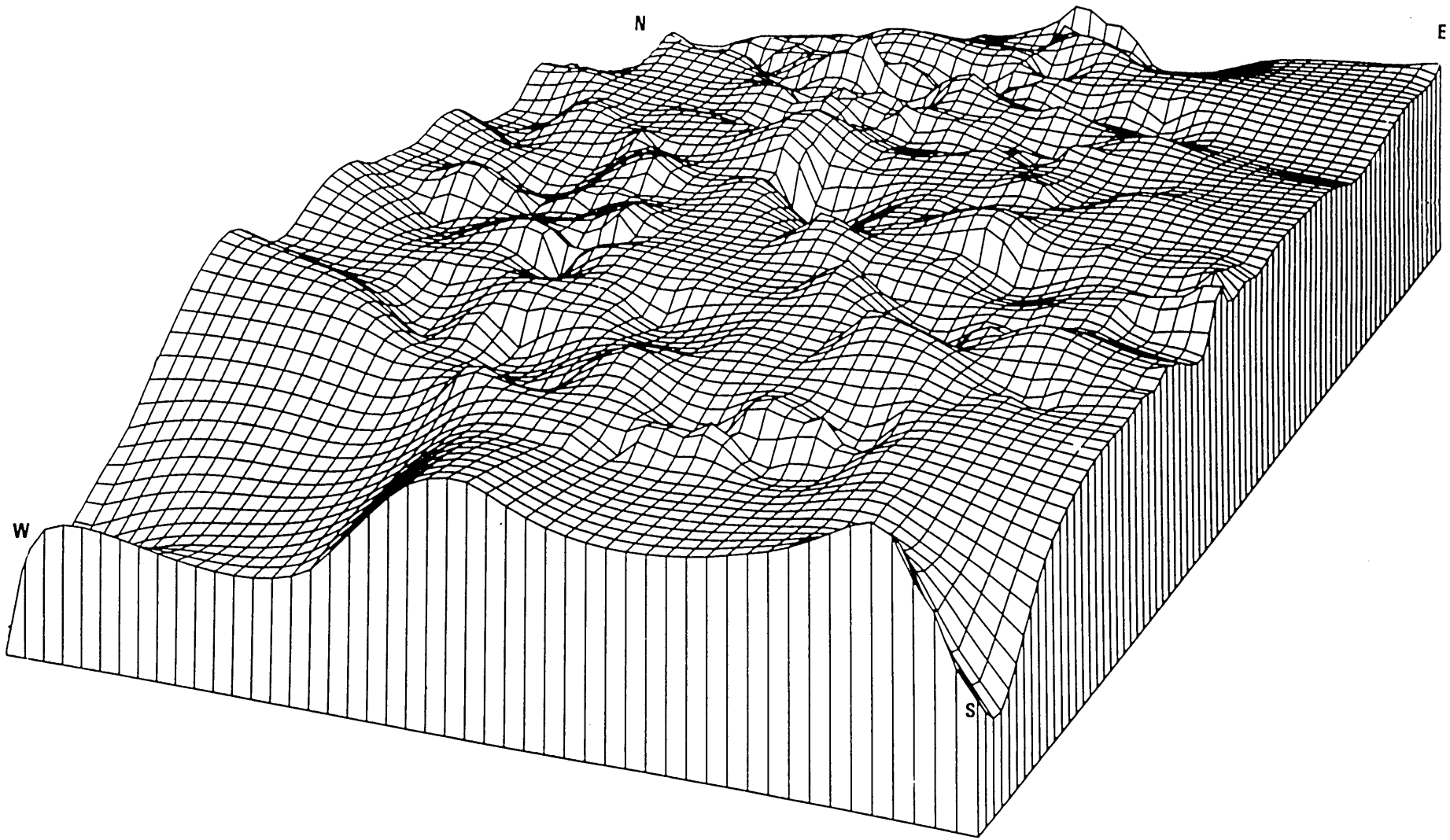


Fig.9.73 Solid surface distribution of the scores of factor 6 in the whole data set.

Table 9.10 Loadings of the five factor model for the phosphate and phosphorite rocks.

1 NUMBER OF ROTATION AND VARIANCE AT EACH STEP

0	.2207570
1	.4901239
2	.5052451
3	.5055830
4	.5055894
5	.5055894
6	.5055894
7	.5055894
8	.5055894

NEW ROTATED FACT LOADINGS

****

	FACT 1	FACT 2	FACT 3	FACT 4	FACT 5
U	.3894	-.4273	.4046	.1536	-.4802
TH	.1898	.0567	.0477	.5756	.0682
AS	-.0071	-.9181	-.0159	-.0260	-.0077
SE	.0076	-.8562	.2260	.0567	-.0390
MG	-.8980	.0000	-.1484	-.0422	-.1156
CA	.5977	-.3449	-.4215	.1487	.1054
SR	.0066	.0136	-.0951	.7810	-.1011
BA	-.0459	-.0026	-.1742	.0614	-.9317
AL	-.7480	-.0342	.3919	-.3864	.1501
V	.0155	-.0841	.9174	-.1131	.0762
MO	-.3185	-.1778	.7699	.1144	.1125
FE	-.7725	-.0693	.2488	-.4024	.1840
P	.2262	-.1991	.0220	.7793	-.0975

VARIANCE ACCOUNTED FOR BY COMPNTS.

COMPNT	VARIANCE PERCENT	CUM VAR
1	20.4828	20.4828
2	15.1166	35.5994
3	16.2051	51.8045
4	14.9296	66.7341
5	9.4145	76.1486

On the basis of the accepted range of loading (>=.3 to 1.0), it can be seen that factors 1,4 and possibly 3 are underlain by lithological controls and factors 2 and 5 are considered to be uranium enrichment and mineralization factors. Uranium has its greatest negative loadings in factors 2 and 5 and significant positive loadings in factors 1 and 3. This indicates that the geochemical behaviour of U in the phosphate rocks is a complex one which is controlled by more than one factor.

In factor 1, which explains 20.5% of the total variance, a stong association of Mg (0.89), Fe (0.77), Al (0.74), Ca (0.59), U (0.39) and Mo (0.32) suggests that the underlying control is related to some sort of Mg-rich clays (palygorskite?) either as a major constituent of the rock (phosphatized clayey limestones, particularly those of the Upper Cretaceous or Lower Palaeogene series or as cement in other phosphatic carbonate rocks. Uranium, showing a significant loading in this factor seems to be adsorbed onto these clay fractions, and therefore might be easily mobilised into solution under alkaline oxidizing environmental conditions.

The distribution pattern of the factor scores (Fig. 9.74) shows the following characteristics;

(i) high background of the element association over most of the region;

(ii) a marked depletion in the midwestern area;

(iii) a trend of high scores at the westen side of the southern Palmyrides range up to the northern Palmyrides mountains.

This trend of high scores coincides with outcrops of the Upper Cretaceous to Lower Eocene which includes a sequence of Phosphatized carbonate, marly limestones with intercalations of phosphatic horizons and clayey limestones. These formations seem likely to contain Mg-rich clays and glauconites thought to characterize the association.

Factor 2 accounts for 15.1% of the variance in the data; it is represented by a strong negative loading of As (0.92), Se (0.86), U (0.43) and to a lesser degree Ca (0.34). Such association clearly indicates an elemental enrichment process, where a carbonate/bicarbonate alkaline solution seems to be percolating the rocks and leaching, redistributing and precipitating these elements. This process could lead to depletion in some parts of the region and enrichment in others, exact localities depending on many textural, structural, petrographical, topographical and other rock and environmental characteristics, including the groundwater regime.

Therefore this factor ought to be considered as an As, Se and U enrichment factor caused by carbonate/bicarbonate solutions.

The areal distribution of the scores (Fig. 9.75) outlines by its highs the enriched parts of the region and by its lows the depleted ones. Most of the enriched rocks are situated in the eastern half of the region extending from Palmyra in the northeast into the eastern foot of J. Rmah, including Wadi Ghadir El Hamel in the southeast. A shorter east-west ridge can be traced in the vicinity of Khneifiss-Ash-Sharquieh (Eastern) phosphorite mines,

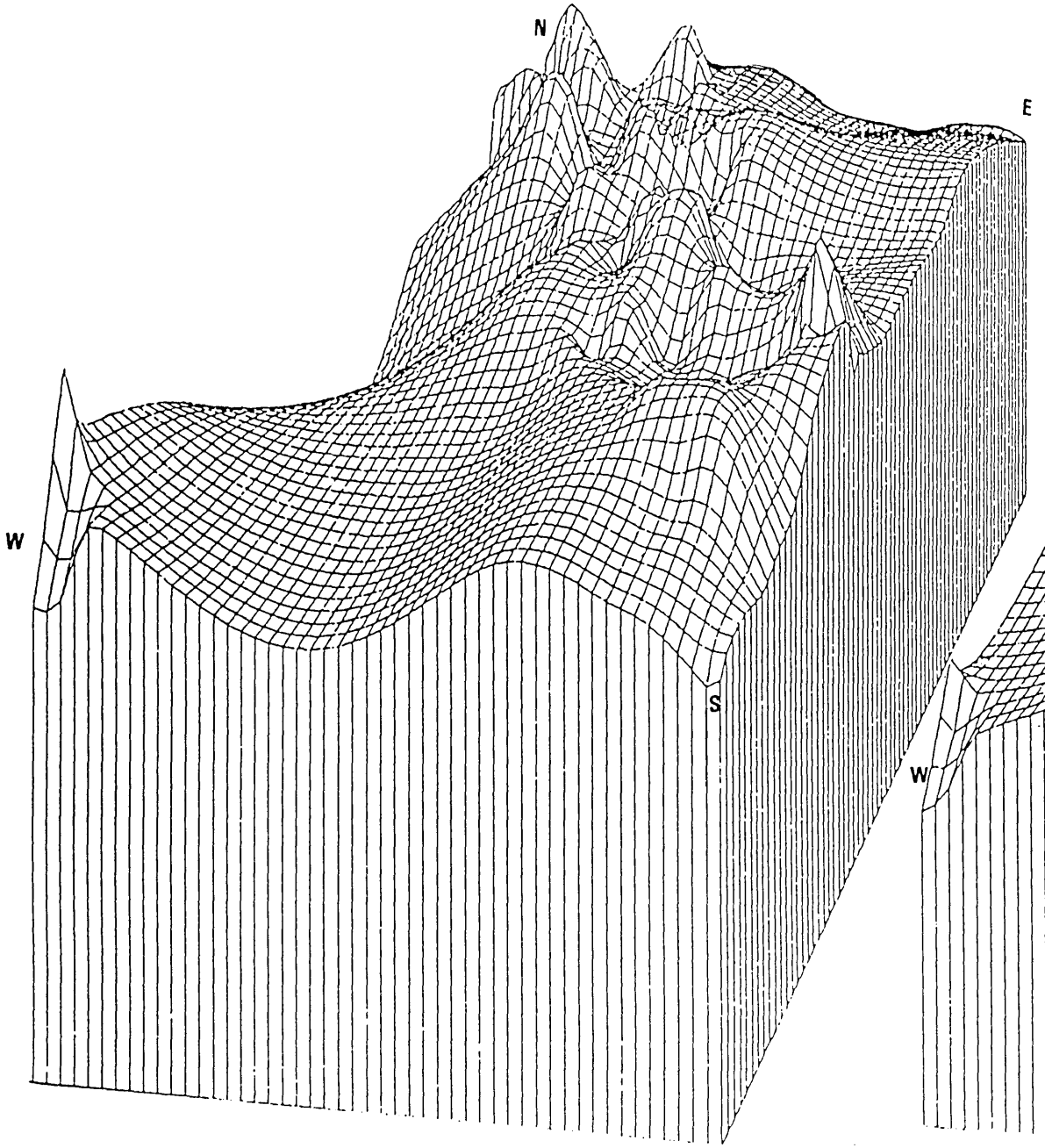


Fig.9.74 Solid surface distribution of the scores of factor 1 in the phosphate rocks.

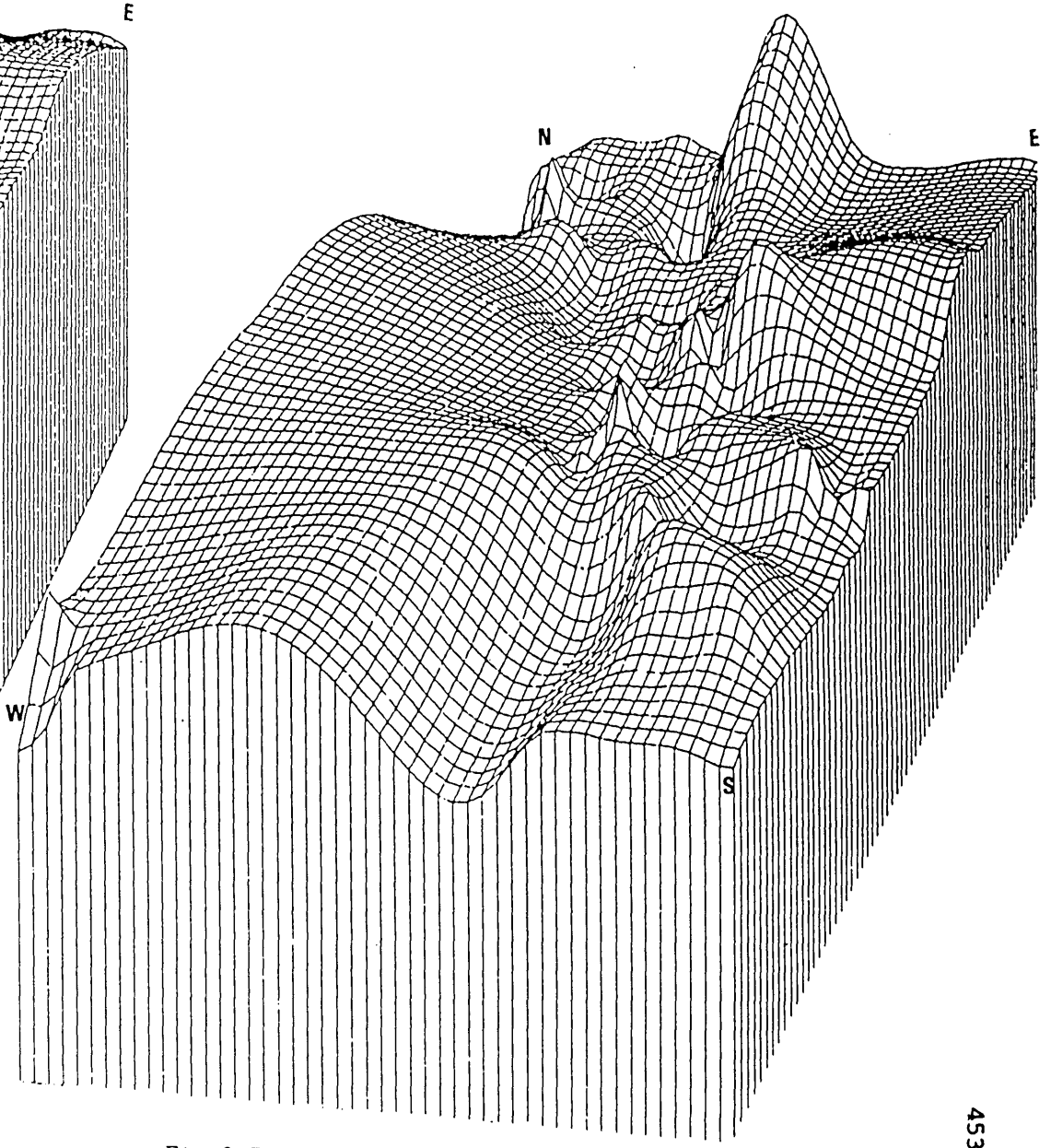


Fig.9.75 Solid surface distribution of the scores of factor 2 in the phosphate rocks

the magnitude of the anomalous peaks perhaps reflects the relative U enrichment in Khneifiss phosphorites compared to Ash-Sharquieh (Eastern) phosphorites. Uranium enriched solutions could have moved along some of the earlier discussed E-W trending faults which exist in the Khneifiss area, re-exposing its phosphorites to interaction with these solutions or causing reworking and in situ enrichment of its constituents. The lack of evidence of similar structural siting in Ash-Sharquieh could perhaps explain the poorer U content of its phosphorites (see Table 9.5), hence, the relatively low factor scores than in Khneifiss deposits.

Factor 3 explains 16.2% of the data variance, and shows strong positive loadings for V (0.92), Mo (0.77), U (0.40), slightly less Al (0.39), and a negative loading for Ca (0.42). This association suggests interpretation as an underlying U mineralizing factor in which V plays a significant role.

This factor can, therefore, account for the many occurrences of carnotite and other urano-vanadate secondary minerals. The possible enrichment of these elements in an organic phase in these rocks must also be considered. Such a relationship is widely accepted geochemically and well documented. Although, no quantitative organic carbon analyses were carried out, many signs of the presence of such a phase in the phosphorite and phosphatic carbonate samples were found through microscopic and other optical studies of thin sections. Therefore, factor 3 represents either V, U and Mo mineralization factor or enrichment due to adsorption onto organic matter.

Surprisingly the distribution pattern of the scores (Fig. 9.76) suggests an alternative explanation for the source of enrichment of these elements in this factor, which could also explain the loadings of Al and Ca and the finding of Pt mineral grains in a thin section of sample 119 of this group of rocks (see Plate 22 and Fig. 9.77), the pattern of the high scores coincides exactly with the locations of samples taken from fault zones. Those samples are particularly enriched in V, Mo and U (along with other trace elements which were not included in computing the principal component matrix). In the light of the factor finding and that of the SEM and microprobe results, it is perhaps more accurate to relate the pattern of high value in this factor to mineralizing fluids comming into contact with these rocks through fault conduits. Two possible sources for these enriched solutions can be suggested;

i) adviction of low temperature fluids from underlaying sedimentary sequence, the evidence of which is given by the mineralized low temperature quartz veins found in similar fault sitting (see the X-R diffractogram Fig. 9.17).

ii) migrated fluids from where they have been discharged or expelled along extentional faults. The X-R diffractogram of sample 119 (Fig. 9.78 and Plate 22) gave evidence of $BZn(PO_3)_2$, Ba, Ti phosphate mineral of high temperature environment. Further inspection of the distribution pattern indicates that the majority of high scores form an inverted triangle in the northern half of the region. This shape is caused by the intersection of trends in three different directions (SE to NW; SW to NE; and E to W). It is worth noting that these fault zones require more detailed investigations.

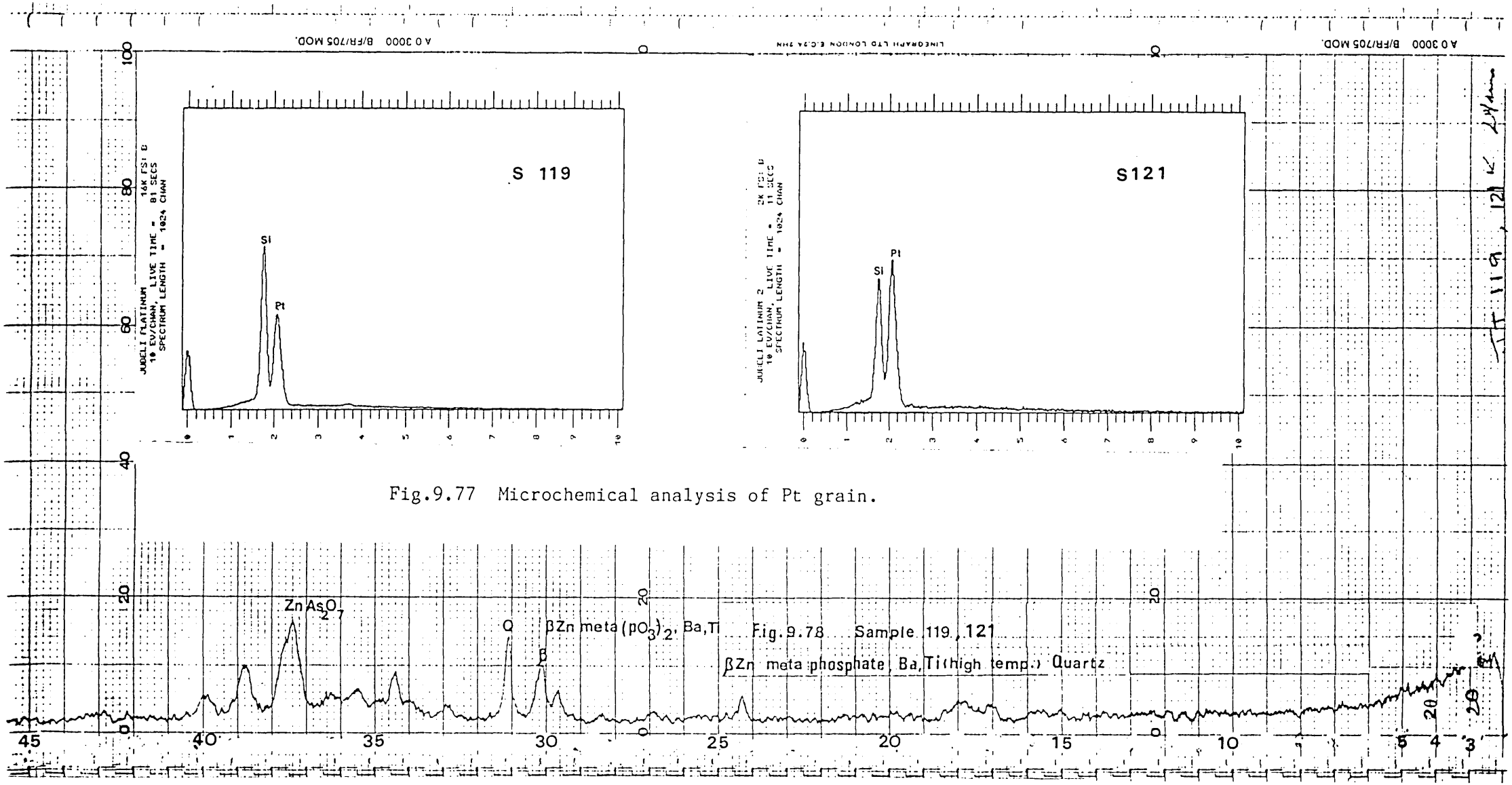


Fig.9.77 Microchemical analysis of Pt grain.

Fig.9.78 X-ray diffraction of sample 119 showing high temperature minerals.

In factor 4 which accounts for 14.9% of the variance, the strong positive loadings of P (0.78), Sr (0.78) and Th are clearly accounted for by the abundant phosphorite rocks in which Sr and possibly Th substitutes for Ca within the apatite minerals. Many of the phosphorites and phosphatic limestones are rich in glauconite, which can explain the negative loadings of Fe (0.40) and Al (0.38) in this factor. Therefore the underlying control on this association of elements is a lithological one; factor 4 can be called the phosphorite factor.

The distribution pattern of the scores (Fig. 9.79) indicates two locations dominated by low negative scores in sharp contrast with the generally even surface of high positive scores. The rocks in these two negative locations are mainly Lower and Upper Palaeogene rocks which include much phosphatized glauconitic clayey carbonate and relatively little phosphorites and highly phosphatized rocks. The link between negative scores and lithology finds particular significance in terms of pH of the sedimentary basin and the environment of deposition. It is well known that sedimentation of phosphorites and of carbonates occurs within very narrow, but different ranges of slightly alkaline conditions and a relatively small shift in pH will favour overwhelming precipitation of one at the expense of the other. generally carbonate sedimentation dominates above pH 7.8 while phosphorites precipitate at about pH 7.5 (Krumbein and Garrels, 1952).

Factor 4, therefore, can be considered as a pH indicator and suggests that the pH conditions were slightly higher in the domains of the negative scores where there has been the precipitation of

phosphatized carbonates instead of phosphorites. More evidence is needed to elaborate on this interpretation.

Factor 5 is characterized by strong negative loadings for Ba (0.93) and U (0.48), and explains a fairly low percentage of the total variance (9.4%). Barium is a large cation which can replace K in some clays and other detrital fragments and/or be adsorbed onto the surfaces of these fractions and the bone debris of phosphorites. Thus rocks with high positive scores are perhaps located in relative proximity to palaeo shorelines or have since been subjected to stronger than average post-depositional weathering. In both cases the part of U represented in this factor suggests a mixture of primary and secondary dispersion processes, with perhaps the latter being the more dominant. In addition of providing somewhat Palaeographical indications, factor 5 expresses secondary environmental apects and weathering features.

The areal distribution of the scores is presented in Fig. 9.80. A sharp contrast between the high and lows seems to indicate old palaeogeographical boundaries within the Palmyrides sedimentary environment. The areas of high scores reflect shallower depositional waters, inferred from Fig. 9.70 to be predominant in the eastern, southeastern and the northwestern corner of the region. A much deeper water environment prevailed in the western and southwesten parts. The marked east-west mount shown by the scores coincides with the Ash-Sharquieh phosphorite mines; lower values, however, are found in the domain of Khneifiss deposit.

It is suggested in the light of the factor association and

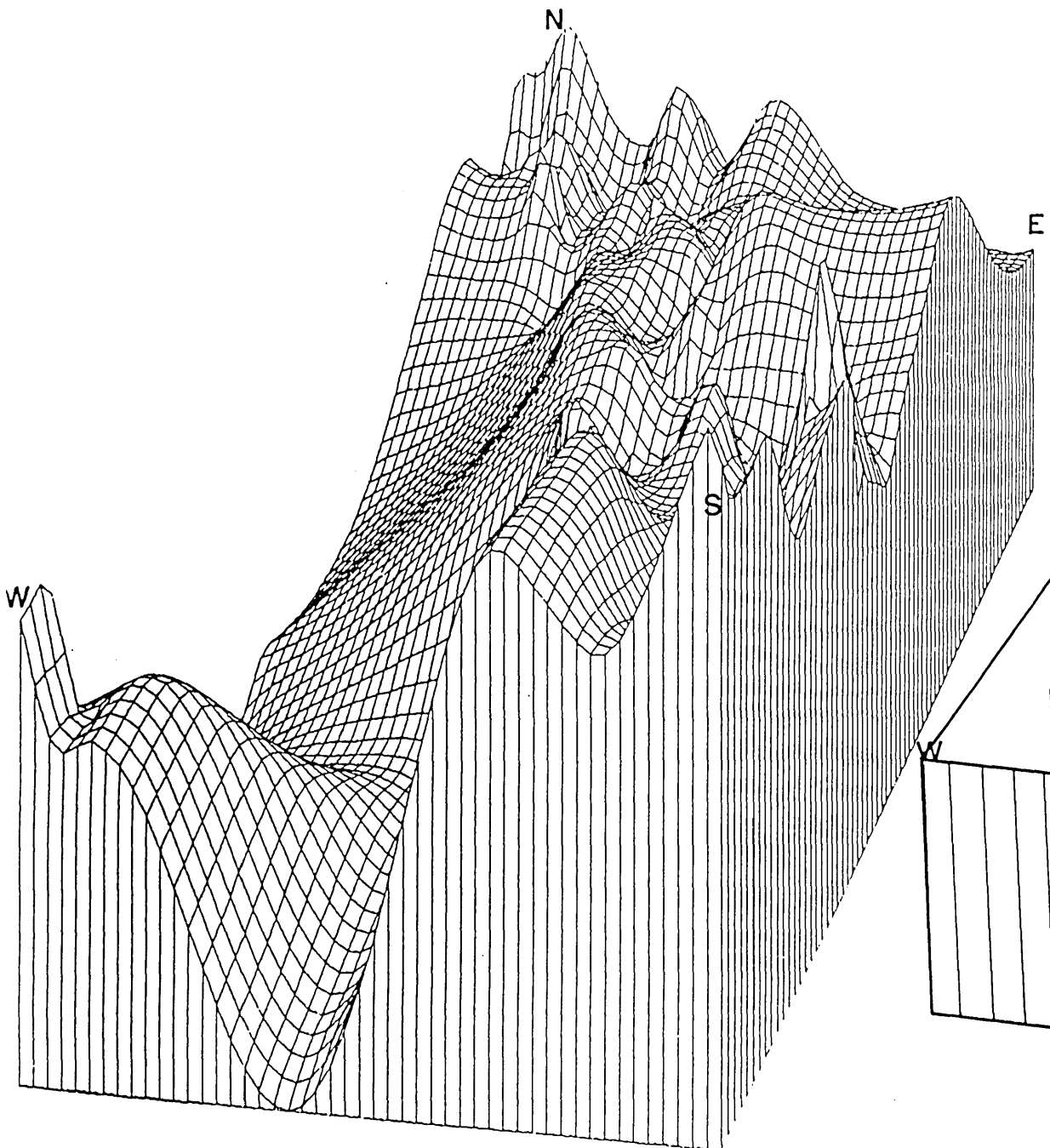


Fig.9.80 Solid surface distribution of the scores of factor 5 in the phosphate rocks.

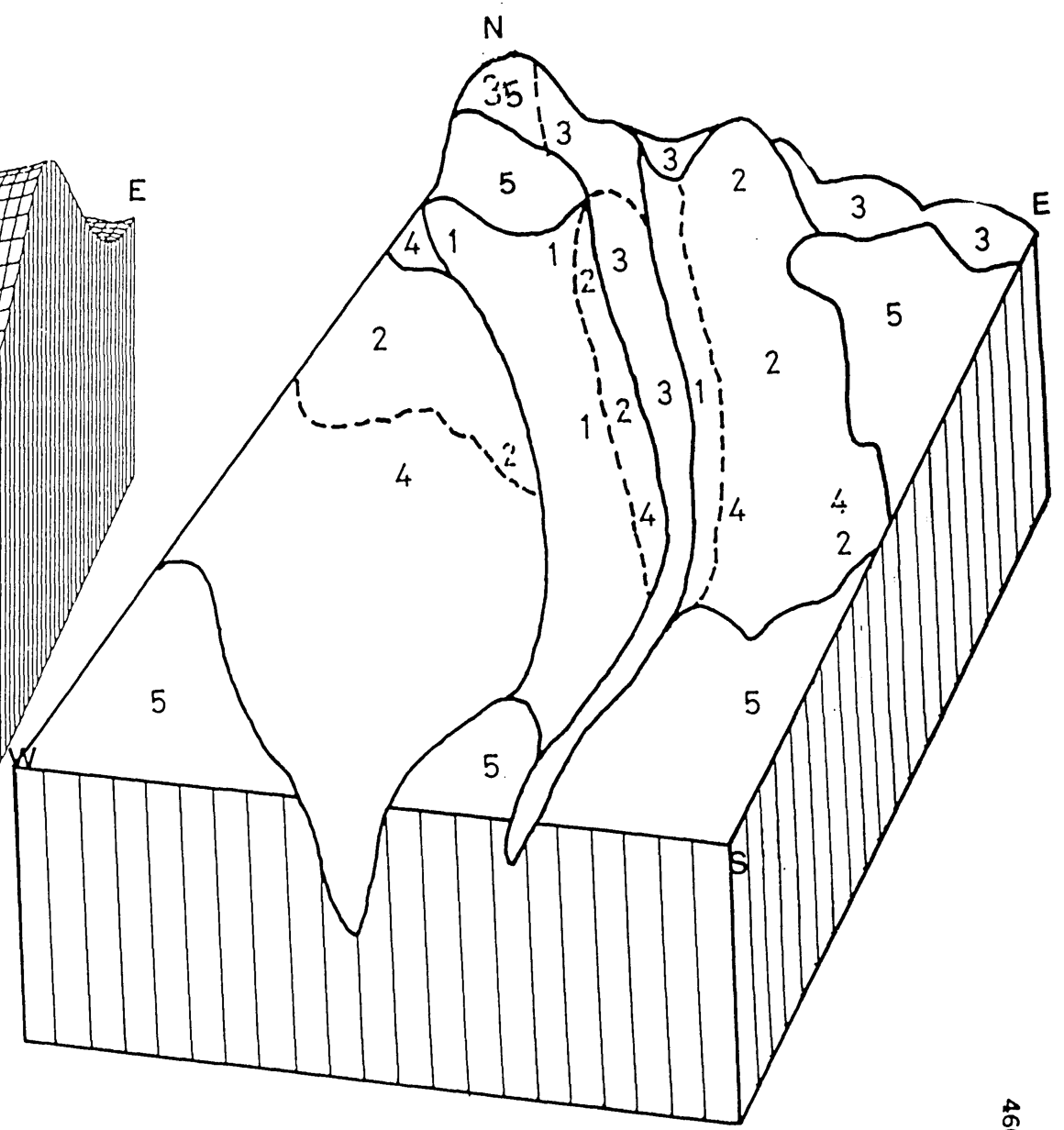


Fig.9.81 Zonation shown by the regional distribution of the scores of the five factors.

the distribution pattern of the scores that, relative to the Khneifiss phosphorite, the Eastern ones show:

i) a larger proportion of detrital supply which seems to be coming from both the east and northwest;

ii) shallower and perhaps warmer waters;

iii) probably more active postdepositional weathering.

These characteristics could partially explain the lower P_2O_5 and U contents in the Eastern phosphorite deposits compared to those at Khneifiss by depletion with the detrital supply. Furthermore they could be responsible for the conspicuous variations in the lithogeochemistry of the various phosphorite deposits.

More detailed inspection of the score distribution patterns for the factors suggests a subtle regional zonation (although the anomalous peaks of these factors show some overlap especially in the central and northern part of the region). The pattern, schematically illustrated in Fig. 9.81, reveals that the central part is mainly dominated by factors 1, 2 and to a lesser degree 3, whereas factor 5 dominates the southern, western and to a lesser degree northern corners, in addition to a large part of the southeastern margin where it is shared by factor 3 in the eastern corner and factor 2 in the mid-southeasten side. Factor 3 dominates the northeastern side, especially the two northern and easten corners. Factor 4 shows large coverage nearly over the whole region and overlaps particularly in the central part and the southeastern side of the region. Its distribution is characterized by generally high background which manifests itself in the mid-western side of

the region relative to other factors.

Underlying controls of the observed zonation are largely related to the following:

i) particular enrichment of U and the elemental associations which are represented by factors 1, 2 and 3 over the central and northeastern parts which are occupied by the Southern Palmyride mountains and the adjacent Palaeogene hills owing to two possible sources;
   a) primary dispersion from the highly mineralizing fluids which are incorporated into the rocks via fault conduits, as well as due to elevated levels of these elements, in a phosphate sour rocks (factors 3, 2 and 4)
   b) secondary enrichment possibly caused by the interaction of faults and fracture-circulated groundwaters with the dominant rocks (clayey carbonates, marls, glauconitic phosphatized limestones and phosphates) leading to secondary U mineralization (factor 1 and 3), and perhaps adsorption onto the Mg-rich clay constituents of these rocks (factor 1).

ii) the pattern shown by factor 5 reflects an increase of the detrital components along the peripheral margins of the region acting with a strong framework of structural, lithological and environmental factors close to the eastern, northeasten and northern margins. This latter effect is represented by the overlap of the highest peaks of the scores of factors 2, 3, 5 and to a lesser degree 1.

The triple points resulted from the intersection of the

SSE-NNW trends of these factors especially those of factors 2 and 3 west of Palmyra and near to the northern corner are worth particular exploration interest owing to being both U enrichment factors.

9.11 Regression analysis.

9.11.1 Regression models

Multivariate ridge regression was applied to determine relative importance of different combinations of exploratory variables (predictors) to the behaviour of U in the total lithogeochemical data of the Palmyrides. Since nearly all the variables are subjected to severe skewness due to outlier problems, Box-Cox power transformed data were used in order to ensure that the regression model is not seriously distorted by outliers.

In the first regression attempt U in rocks was regressed against 21 exploratory variables, excluding radiometric measurements (CPS). The ridge regression coefficients (Table 9.11) and the ridge trace (Fig. 9.82) illustrate that, at a ridge constant of K=0.06, As, Se, V and Ca are the most stable positive predictors of U, while Ba and Fe are the stable negative predictors. The R^2 and F-ratio of the ridge regression indicate that it is an acceptable and significant regression solution. In the conventional least squares regression solution (K=0), V and Fe are, respectively, the best positive and negative predictors.

After eliminating 14 outliers from the sample population, a

Table 9.11 Standardized estimators of U in the 22 variable model of ridge regression and the regression coefficient.

STANDARDIZED ESTIMATORS

	RIDGE CONSTANT 0.00	.02	.04	.06★	.08	.10	.15
TH	.1238	.1221	.1203	.1185	.1167	.1150	.1112
AS	.2131	.2128	.2120	.2107	.2091	.2073	.2023
SE	.1714	.1716	.1710	.1702	.1691	.1680	.1650
LI	.1536	.1351	.1212	.1101	.1009	.0931	.0778
NA	-.0195	-.0147	-.0114	-.0088	-.0068	-.0052	-.0021
K	-.0335	-.0569	-.0655	-.0686	-.0693	-.0689	-.0662
MG	.0145	.0173	.0182	.0181	.0176	.0169	.0147
CA	.2100	.1966	.1856	.1763	.1684	.1616	.1476
SR	.0708	.0724	.0737	.0745	.0749	.0751	.0748
BA	-.0897	-.0943	-.0968	-.0980	-.0984	-.0981	-.0961
AL	-.1695	-.1355	-.1153	-.1017	-.0917	-.0841	-.0707
V	.4355	.3732	.3292	.2965	.2711	.2507	.2142
CR	-.0104	-.0161	-.0165	-.0150	-.0128	-.0104	-.0045
MO	.0653	.0581	.0531	.0495	.0470	.0451	.0422
MN	.1993	.1520	.1227	.1023	.0872	.0754	.0546
FE	-.2206	-.1751	-.1454	-.1261	-.1124	-.1021	-.0847
CO	.0071	.0074	.0078	.0079	.0077	.0073	.0058
ZN	-.1428	.1083	-.0833	-.0643	-.0496	-.0378	-.0166
CD	-.0395	-.0203	-.0075	.0017	.0084	.0136	.0224
PB	.0249	.0268	.0270	.0268	.0264	.0258	.0245
P	.0687	.0701	.0704	.0704	.0702	.0699	.0690
MAXIMUM VIF	18.79	12.62	9.53	7.67	6.43	5.54	4.13

STANDARDIZED ESTIMATORS DATA MATRIX % OBSERVATIONS 25 VARIABLES

	RIDGE CONSTANT 0.00	.02	.04	.06	.08★	.10	.15
TH	.0423	.0509	.0577	.0633	.0678	.0716	.0787
AS	.3432	.3373	.3327	.3286	.3246	.3207	.3111
SE	.1313	.1432	.1509	.1562	.1598	.1624	.1660
LI	.0334	.0280	.0251	.0234	.0220	.0210	.0188
NA	.0009	.0025	.0029	.0029	.0026	.0022	.0010
K	.1337	.0937	.0695	.0532	.0416	.0329	.0187
MG	-.0165	-.0099	-.0056	-.0026	-.0004	.0012	.0039
CA	.0336	.0351	.0357	.0359	.0359	.0357	.0351
SR	-.0362	-.0323	-.0294	-.0270	-.0250	-.0232	-.0195
BA	.0149	.0078	.0027	-.0012	-.0042	-.0065	-.0103
AL	-.2450	-.1903	-.1565	-.1336	-.1170	-.1046	-.0836
LA	-.3014	-.2722	-.2482	-.2280	-.2108	-.1959	-.1661
TI	.1843	.1600	.1428	.1295	.1186	.1095	.0917
V	.3130	.2744	.2460	.2240	.2063	.1917	.1643
CR	-.1052	-.1095	-.1088	-.1062	-.1028	-.0991	-.0898
MO	.3443	.3107	.2847	.2640	.2470	.2329	.2058
MN	.2039	.1621	.1360	.1180	.1046	.0942	.0758
FE	-.0955	-.0638	-.0479	-.0388	-.0331	-.0293	-.0239
CO	-.0546	-.0441	-.0364	-.0304	-.0258	-.0220	-.0153
NI	.0151	-.0024	-.0113	-.0159	-.0183	-.0193	-.0190
ZN	-.2849	-.2209	-.1789	-.1489	-.1265	-.1089	-.0782
CD	.0056	.0010	.0003	.0012	.0028	.0046	.0092
PB	-.0037	.0056	.0119	.0165	.0201	.0229	.0280
P	.5332	.5048	.4801	.4585	.4394	.4224	.3869
MAXIMUM VIF	15.57	11.08	8.63	7.09	6.02	5.24	3.96

Table 9.12 Standardized estimators of U in the optimum regression and the regression coefficients.

DATA MATRIX % 401 OBSERVATIONS 16 VARIABLES

STANDARDIZED ESTIMATORS

	RIDGE CONSTANT 0.00	.02	.04	.06	.08★	.10	.15
CPS	.6011	.5834	.5671	.5520	.5380	.5249	.4954
TH	.0182	.0205	.0228	.0249	.0269	.0288	.0328
AS	.1650	.1644	.1635	.1625	.1616	.1606	.1584
SE	.0269	.0335	.0397	.0452	.0503	.0548	.0641
LI	.1337	.1233	.1140	.1058	.0985	.0920	.0784
NA	.0087	.0098	.0105	.0111	.0116	.0120	.0131
K	-.1157	-.1036	-.0946	-.0877	-.0821	-.0776	-.0692
MG	.0045	.0038	.0029	.0021	.0013	.0006	-.0008
CA	.1184	.1156	.1128	.1102	.1078	.1055	.1005
SR	.0390	.0406	.0418	.0428	.0437	.0444	.0460
BA	-.0648	-.0669	-.0683	-.0693	-.0700	-.0705	-.0709
AL	-.1118	-.0881	-.0755	-.0674	-.0616	-.0572	-.0494
V	.1947	.1859	.1794	.1741	.1696	.1657	.1578
CR	.0178	-.0059	-.0174	-.0238	-.0277	-.0302	-.0332
P	-.0671	-.0547	-.0445	-.0357	-.0280	-.0212	-.0073
MAXIMUM VIF	14.88	10.35	7.99	6.53	5.54	4.82	3.65

Table 9.13 Statistics of the regression and

ANALYSIS OF VARIANCE % RIDGE

SOURCE OF VARIATION	SUM OF SQUARES	DEGREES OF FREEDOM	MEAN SQUARES	F-RATIO
REGRESSION	184.75	15	12.32	60.7663
RESIDUAL	78.03	385	.20	
TOTAL VARIATION	262.78	400		

MULT. R-SQUARED = .7030 STD. ERROR OF EST. = .4502
VARIANCE OF ERROR TERM = .2027

★ = Selected ridge constant.

RIDGE TRACE

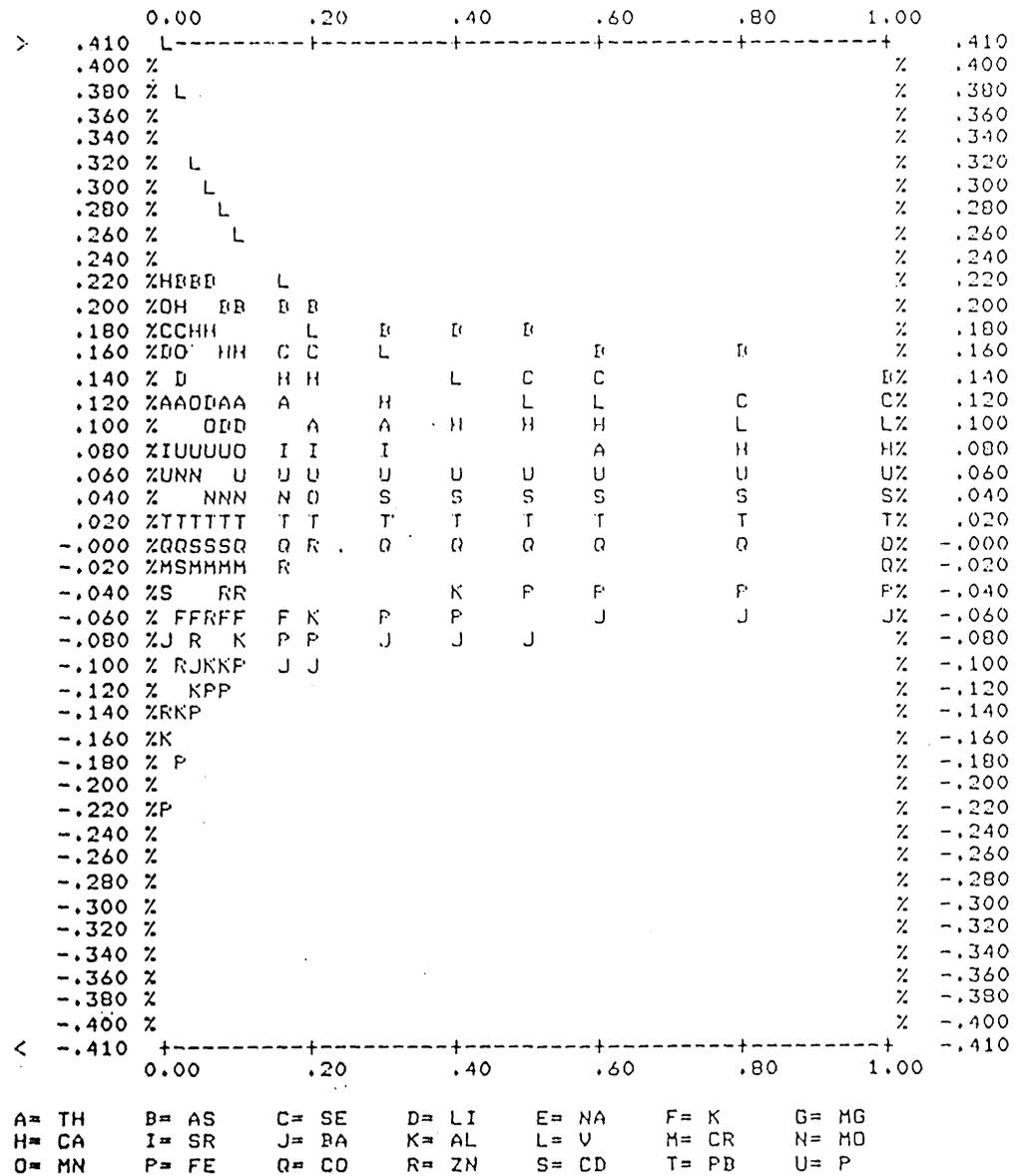


Fig.9.82 Ridge trace of U regression against 20 variables of the lithogeochemical data.

RIDGE TRACE

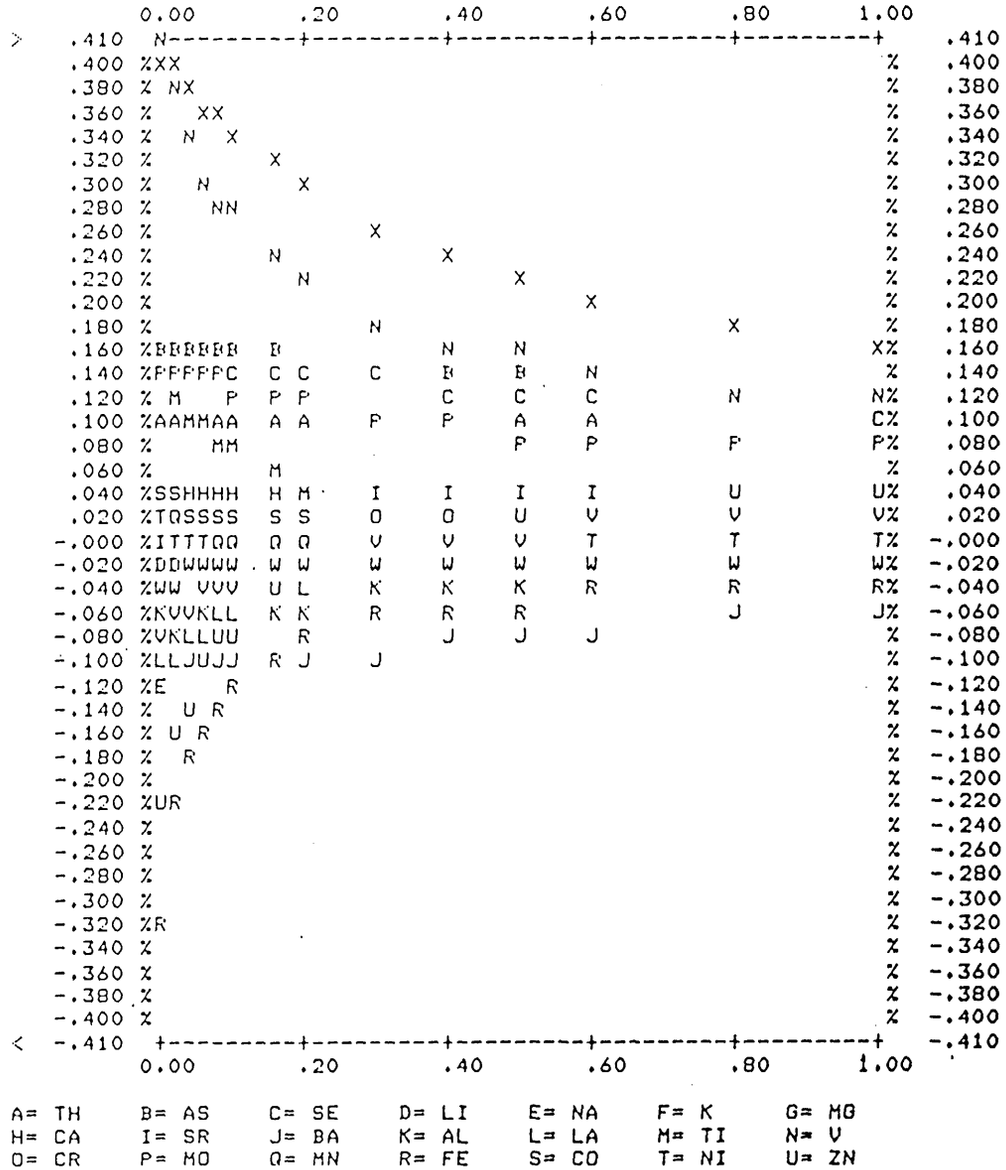


Fig.9.83 Ridge trace of U regression of the lithogeochemical data.

second regression for U against other variables excluding radioactivity produced the ridge trace shown in Fig. 9.83. It can be seen that, at the chosen ridge constant of K=0.08, the best positive predictors for U in the rocks are P, As, Mo, V and Se. The most stable negative predictors are La, Zn, Al and Cr.

The marked change in the suite of negative predictors and the addition of P and Mo to the positive ones probably reflects the complexity of U behaviour in various lithologies or lithological units as well as the effect of eliminating anomalous samples. From the two regression models it can be inferred that the behaviour of U is;

a) antipathetic with Fe and Al which represents the clay fraction as both being negative predictors;
b) a function of the mineralizing fluids or leachate solutions (represented by V, Mo, As and Se as the positive predictors;
c) influenced by the phosphate lithologies, represented by P and Ca as positive predictors; and
d) possibly affected to a minor degree by a detrital fraction or weathering product, represented by Ba, Cr and Fe as negative predictors.

A third regression was carried out to assess the predictivity of the ground radiometric measurements, using 16 variables. The selection of these variables was optimized based on their geochemical properties, which could represent both geological and environmental features. The results shown in Table 9.12 and Fig. 9.84 indicate that the radioactivity of the rocks is the best positive predictor of U content, followed by V, As and Se. Barium

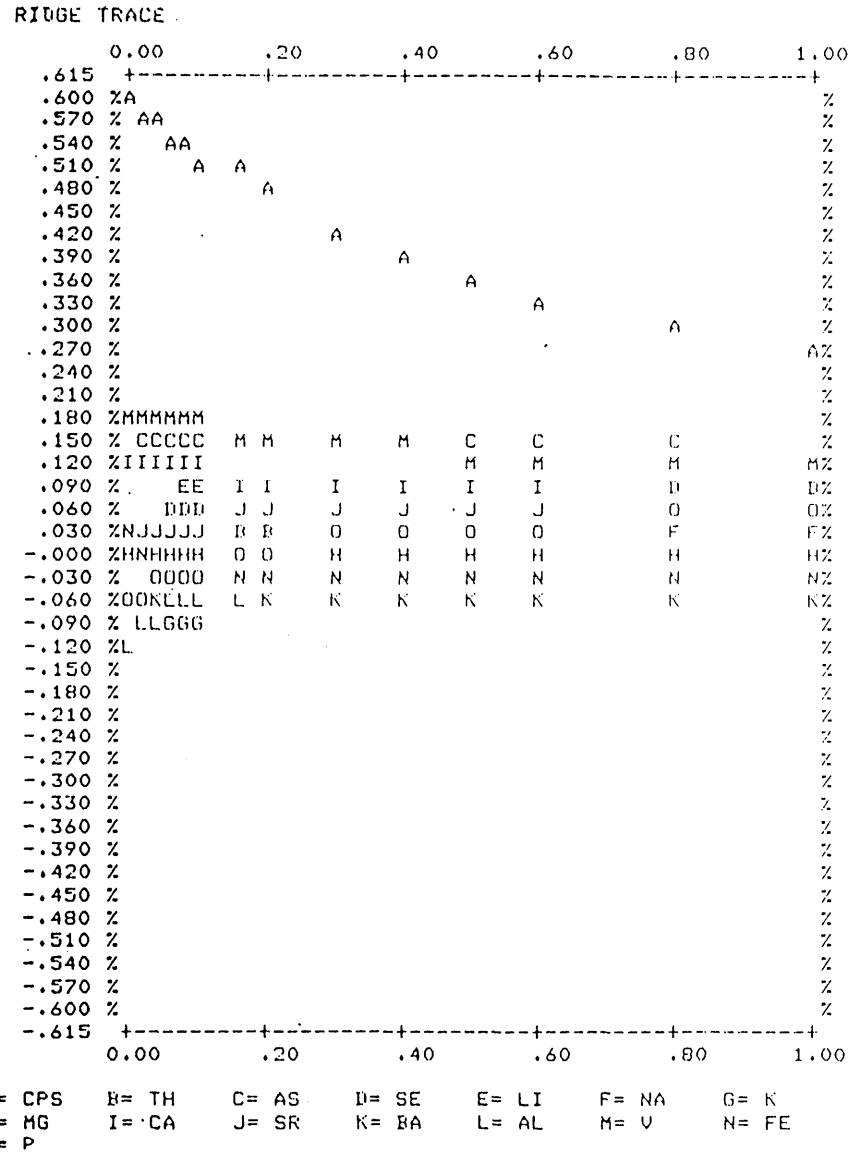


Fig.9.84 Ridge trace of the optimum U regression model with 16 variables of the lithogeochemical data.

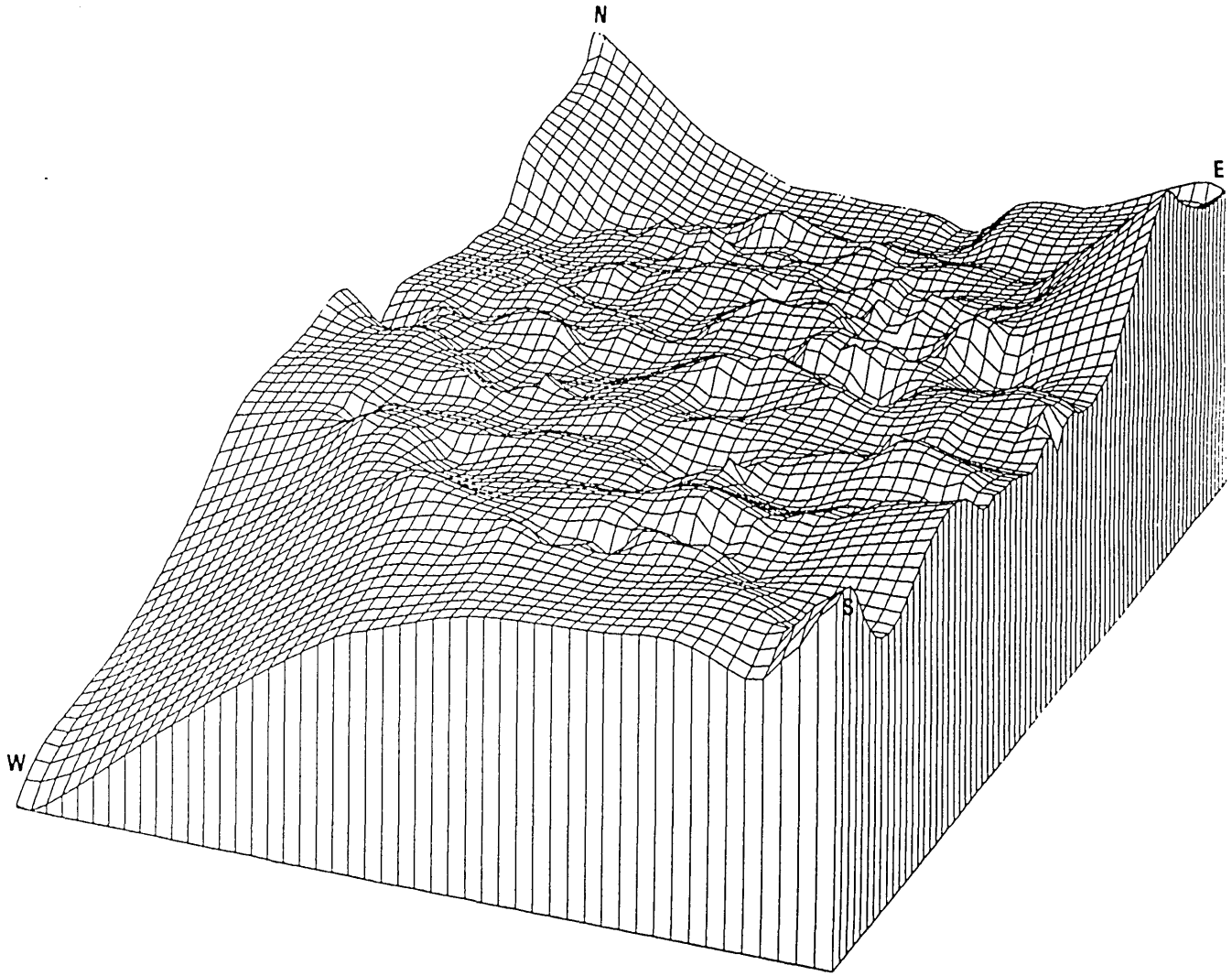


Fig.9.85 Solid surface distribution of U residuals after ridge regression of the lithogeochemical data.

along with Al and Fe are the best negative predictors. The predictivity of P although still positive, seems to be less pronounced than previously indicated; radiometric measurements seem to relegate its importance or significance. From Table 9.13 it was found that this regression solution has the highest R^2, and hence the best goodness-of-fit, therefore only the resulted U residuals are considered for further mapping and discussion.

9.11.2 Interpretation of the residuals

The U residuals obtained from the third ridge regression analysis are plotted as a spatial solid surface distribution (Fig. 9.85). The anomalies are reduced in magnitude because the residuals were log transformed and therefore the anomaly contrast for the residuals is not as sharp as shown by the factor scores or the simple element geochemical patterns. Three different features can still be seen in the distribution of the residuals:

1) A relatively marked depletion (negative residuals) is confined to the extreme southwestern corner of the region, which is underlain by Middle and Upper Palaeogene chalky limestone and other carbonate rocks. It seems that this area is the least interesting for further exploration work.
2) The central area and a large part of the western margin are void of any significant positive residual anomalies except for the vicinity of J. Abou Rabah and the extreme northwestern corner. The former is an area strongly affected by faults and numerous fractures, and is located within the trend of the regional lineament mentioned earlier, and the rocks are mainly Upper Cretaceous in age. The latter seems to be either affected by detrital supply generated from the known Er-Kheime phosphorite

deposit located further northwestwards, or influenced by the groundwater regime, which proved to be enriched in U, Se and associated elements. Moving eastward from the centre scattered very weak positive residuals can be found, the significance of which is unclear.

3) A trend of anomalous positive residuals runs along the southeastern boundary of the Palmyrides region, with peaks pointing towards the East. The trend seems to be particularly coherent in its northeastern corner, where Neogene and Lower Palaeogene are the major formations. However, elsewhere along the trend the dominant lithologies are generally those of the Lower and Upper Palaeogene.

It should be pointed out at this stage that definite controls for the anomalous residuals are not reliably provided by the regression analysis, therefore, considering only the regression results, it is not clear whether the distribution pattern of the residuals represents lithological or structural controls or expresses a combination of various other underlying natural processes. In the light of the results of both factor analysis and regression analysis, however, the three U residual features seem to have lithological, environmental and stuctural controls.

The distribution patterns of the U residuals is in good agreement with the distribution patterns shown by the scores of U factors. Both results outline areas of potential importance for further work.

9.11.3 Regression of U in the phosphate rocks.

In an attempt to evaluate the U predictivity by some elements usually found in U enriched phosphate rocks, a regression analysis was carried out for U against 13 other variables in a combined group of samples formed by the 92 phosphate rocks plus the 57 samples collected from the phosphorite deposits. The variables were selected on the basis of including the main constituents of typical phosphorite rocks.

a) phosphorite minerals represented by P and Ca;

b) substituents such as Th, Sr, Mg, Ba, Se, As, Cr, Mo and U; and

c) adsorbants represented by Al and Fe.

The ridge regression coefficients along with that of the least square regression at K=0 are given in Table 9.14, and the corresponding ridge trace is presented in Fig. 9.86.

Vanadium, Ba, As, Se and Sr proved to be the best positive predictors for U in the Palmyrides phosphate rocks, and the best negative predictors are Mg, Cr and Fe. The analysis of variance shows that the R^2 and F-ratio suggest tha the regression equation obtained provides a significant regression solution. Accordingly, this indicates that the behaviour of U content in these phosphorite samples can be predicted by the levels of V, Ba, As, Se and Sr in decreasing order of their predictivity. Phosphorus proved insignificant as a possible predictor of U content in the phosphate rocks. Comparable results have been already found in many cases during this work, and in particular the lack of significant high linear correlation between U and P, especially in the primary

Table 9.14 Standardized estimators of U in the phosphate and phosphorite rocks and the regression coefficients.

STANDARDIZED ESTIMATORS

	RIDGE CONSTANT						
	0.00	.02	.04	.06	.08*	.10	.15
TH	.1509	.1484	.1458	.1431	.1404	.1378	.1316
AS	.2953	.2806	.2688	.2589	.2504	.2430	.2279
SE	.1557	.1671	.1756	.1821	.1870	.1908	.1964
MG	-.2695	-.2607	-.2531	-.2461	-.2396	-.2336	-.2201
CA	.0088	.0037	.0006	-.0013	-.0026	-.0034	-.0040
SR	.2318	.2174	.2049	.1940	.1844	.1759	.1584
BA	.3017	.2959	.2897	.2834	.2771	.2710	.2566
AL	.3192	.2509	.2067	.1749	.1508	.1316	.0971
V	.4632	.4424	.4220	.4033	.3863	.3709	.3385
CR	-.2099	-.1903	-.1744	-.1612	-.1502	-.1406	-.1217
MO	-.1693	-.1493	-.1319	-.1168	-.1038	-.0925	-.0698
FE	-.1937	-.1546	-.1330	-.1197	-.1108	-.1047	-.0954
P	.1427	.1278	.1166	.1080	.1013	.0959	.0865
MAXIMUM VIF	10.03	7.65	6.21	5.25	4.56	4.03	3.15

STANDARDIZED ESTIMATORS

	RIDGE CONSTANT						
	.20	.30	.40	.50	.60	.80	1.00
TH	.1259	.1159	.1075	.1005	.0944	.0845	.0767
AS	.2162	.1987	.1857	.1754	.1667	.1525	.1412
SE	.1987	.1980	.1940	.1887	.1828	.1712	.1603
MG	-.2083	-.1889	-.1735	-.1609	-.1504	-.1337	-.1210
CA	-.0036	-.0015	.0010	.0034	.0056	.0092	.0119
SR	.1448	.1248	.1107	.1002	.0921	.0800	.0715
BA	.2435	.2207	.2019	.1862	.1727	.1511	.1345
AL	.0737	.0441	.0260	.0139	.0055	-.0054	-.0118
V	.3125	.2730	.2440	.2215	.2034	.1756	.1552
CR	-.1075	-.0871	-.0728	-.0621	-.0537	-.0413	-.0327
MO	-.0528	-.0297	-.0149	-.0050	.0020	.0106	.0153
FE	-.0903	-.0846	-.0811	-.0783	-.0759	-.0716	-.0678
P	.0806	.0739	.0705	.0684	.0669	.0647	.0628

* = Selected ridge costant.

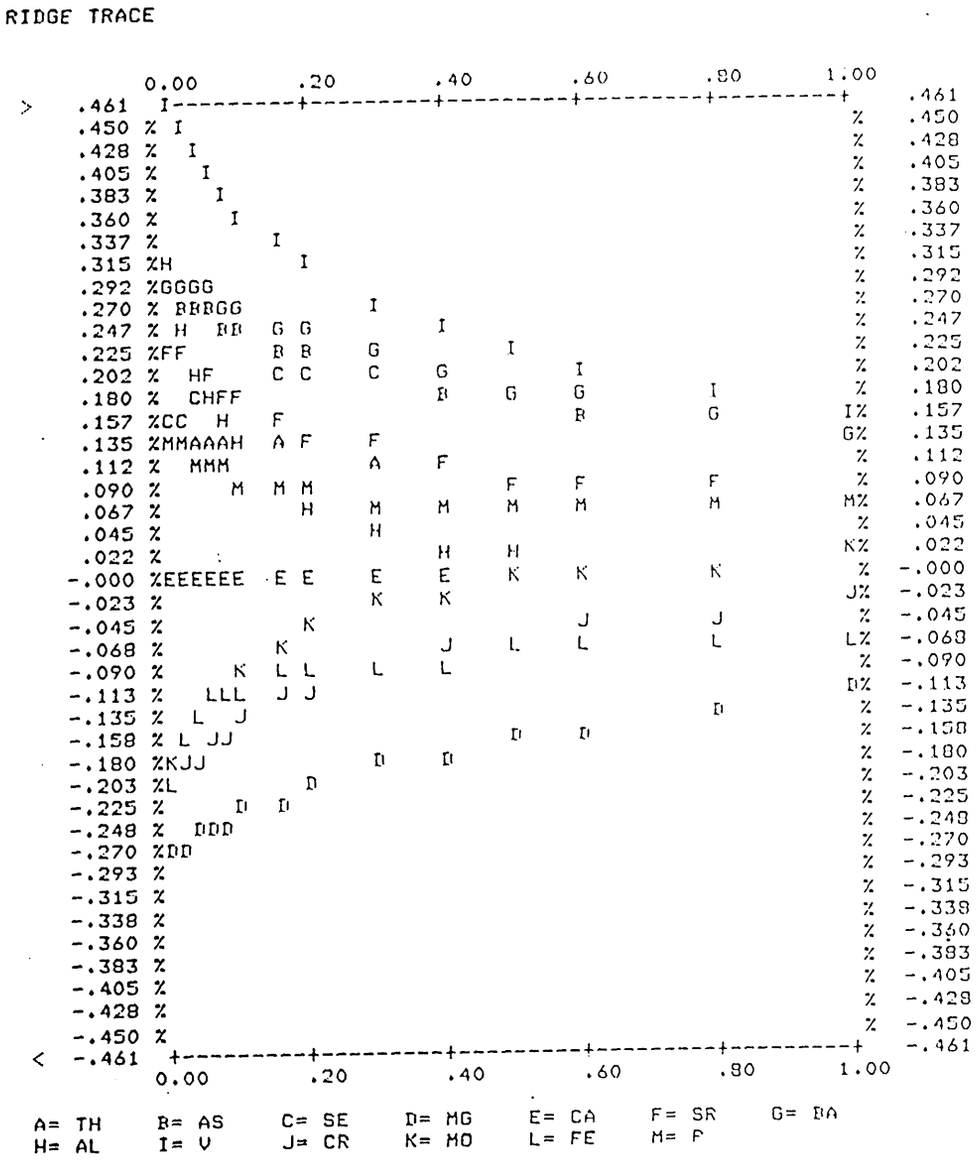


Fig.9.86 Ridge trace of regression for U vs 13 variables of the phosphate rocks.

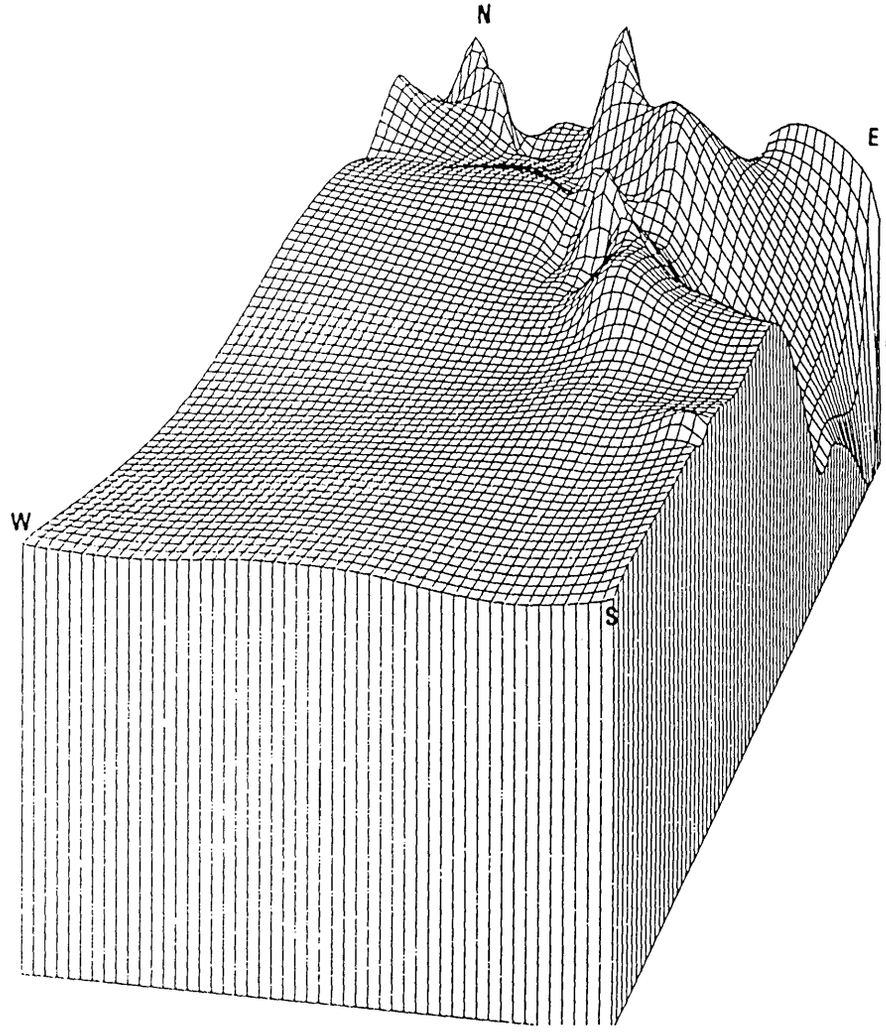


Fig.9.87 Solid surface distribution of U residuals in the phosphate rocks.

haloes.

The distribution of U residuals (Fig. 9.87) delineate within the phosphorite domain a trend of anomalous residuals striking SE to NW. The highest values are found;

i) in the vicinity of khneifiss phosphorite deposits;

ii) west to northwest of Palmyra; and

iii) in the northwestern corner of the region.

The first two locations coincide with strongly faulted sites characterized by pronounced enrichment in V, Ni, Zn, U, As, Se and Sr. It should be stressed that even within the phosphorite group, these highly enriched samples are confined or spatially related to fault zones. Other moderately positive anomalies are closely related to the above mentioned trend extending southeastwards beyond the boundary of the surveyed region towards the Syrian Desert in the east and the western part of the Northern Palmyrides mountains in the north. Adjacent to the Ash-Sharquieh (Eastern) phosphorite mines, a short East-West trend of very low negative residuals can be found, which seems to act as a sharp boundary for the phosphorite formations. This may indicate that rocks along this trend contains lesser phosphorite constituents than the adjacent phosphate domain (Khneifiss). This is in good agreement with the finding of factor analysis, the scores of factor 4 (Fig. 9.79) provide strong support to this interpretation.

Finally, it is worth noting that, ridge regression has not included all possible predictor variables of U in the primary environment, for example, despite the great influence of the

organic matter on U behaviour, it was impossible to predict such a role using ridge regression due to the lack of quantitative measurements of organic carbon content in the rocks involved.

Generally, in comparison with the results of other multivariate analysis,correlation, cluster and especially factor analysis, the regression results seem to outline similar features; this indicates good agreement between these techniques in aiding the interpretation of the Palmyrides lithogeochemical data.

9.12 Conclusions

The following conclusions can be derived from the foregoing lithogeochemical data interpretation;

1) Reconnaissance scale multielements geochemistry is capable of revealing geochemical characteristics pertinent to U exploration in the Palmyrides region.
2) The lithogeochemical investigations shows a strongly contrasing pattern of U dispersion, varying from very low (0.5 ppm) to very high (>600 ppm) levels; U and most other measured trace elements are enriched in the phosphate and clayey glauconitic carbonate rocks relative to other lithologies of the region.
3) The degree of trace metal enrichment in the rocks seems to be controlled by not only lithological, but also structural and environmental controls.
4) The mean concentrations of the measured elements in the lithostratigraphical units indicates a general decrease in their contents on passing from Upper Cretaceous to recent. This emphasizes;

a) the role of faulting, rifling and other Neo-Tethys tectonism in enhancing the concentration levels of these elements in the Palmyrides rocks because their enrichment seems to coincide with these major tectonic events that began in Upper Cretaceous; and

b) it indicates an inverse relationship between the enrichment processes and the age of the rocks.

5) It can be inferred from the present lithogeochemical study that the elevated U contents in the carbonate rocks can be attributed to non-carbonate constituents (impurities) such as clays, phosphate particles and possibly organic matter, reflecting the depositional environment characteristics.

6) A close association of U, V, Mo, As, Se, Sr, K, Cd, Ba and to a lesser degree P is evident in the primary dispersion patterns throughout the region. However, elements such as Ni, Zn and Cr are also associated with U especially in strongly fault-distorted areas.

7) The formation of the Palmyrides phosphorites, including its U enrichment is a result of combined Mesozoic to Cenozoic plate tectonics (first subduction and then collision), and more ancient taphrogenic events still actively acting along deep-seated faults.

8) Radioactivity within the region is mainly a function of U concentration,and is not as equally related to K or Th contents; It also shows no direct linear relationship with P_2O_5.

9) The sites classified as anomalous by factor analysis and regression analysis suggest a close spatial association with the above-mentioned taphrogenic vents. These sites are found along three structural directions known in the region, namely, SW-NE,

E-W and SE-NW. When SW-NE faults intersect NW-SE faults, the anomalous lithogeochemical response related to U is best developed.

10) The lithogeochemical dispersion patterns of U and its associated elements, especially Se and V are considerably affected by the interaction between the groundwater regime and the rocks, particularly in the central north and northwestern parts of the region and along both the eastern and western sides of Ad-Daww basin.

11) The factors loadings and scores facilitate the complex lithogeochemical data of the Palmyrides, and provide useful indications of potentially interesting areas for further investigations.

Chapter X

10. Summary, conclusions and recommendations for further work.

10.1 Summary

The dispersion patterns of U and associated elements in rocks, wadi and playa sediments, overburden and groundwaters of the Palmyrides region have been studied using multielement geochemistry coupled with ground scintillation gamma ray measurements. This approach to the research was successful in achieving all the aims and objectives. Furthermore, this research work demonstrated the relationship between geochemical variations and lithostratigraphy geology), structural and environmental features of the region, as well as revealing for the first time evidence of weak hydrothermal mineralization in very restricted areas.

Statistical treatment of the data greatly assisted the research. Investigation of the frequency distribution of 27 elements used in the reconnaissance data showed that the majority of these elements were not normally distributed; in many cases log-transformation proved unsuccessful in normalizing the data. Therefore,generalized power transformations(Box-Cox) were used and were found helpful in recognizing the relationships between various elements and variables involved in the study. Uni-variate data, presented as symbolic areal distribution maps, satisfactorily outlined general trends of anomalous values in relation to broad geographical and geological sub-regions. Solid surface spatial distributions of factor scores and the residuals of regression

analysis proved to be helpful in establishing causal controls on the geochemistry that could be related to geology, mineralization, structures and environmental conditions. Correlation and cluster analysis of normalized data emphasized many of the associations shown by factor and regression analysis.

10.2 General conclusions

10.2.1 Approach

Reconnaissance multielement geochemistry using various sampling media was effective in outlining the overall element dispersion patterns and delineating areas and zones of particular exploration interest for follow-up work. Areas with highly anomalous U concentrations and mineralization factors such as U, V, Ni, Zn, Cu, Mo and Cd, as well as areas with high U residuals, are considered to be of great importance. These areas occur in J.Bassiri, J.Abou El Fawaress, J.Tabaque, the hills situated between J.Abtar and J.Om Jorm , and zones along the eastern and western margins of the region, especially towards the Syrian Desert.

10.2.2 Radioactivity measurements

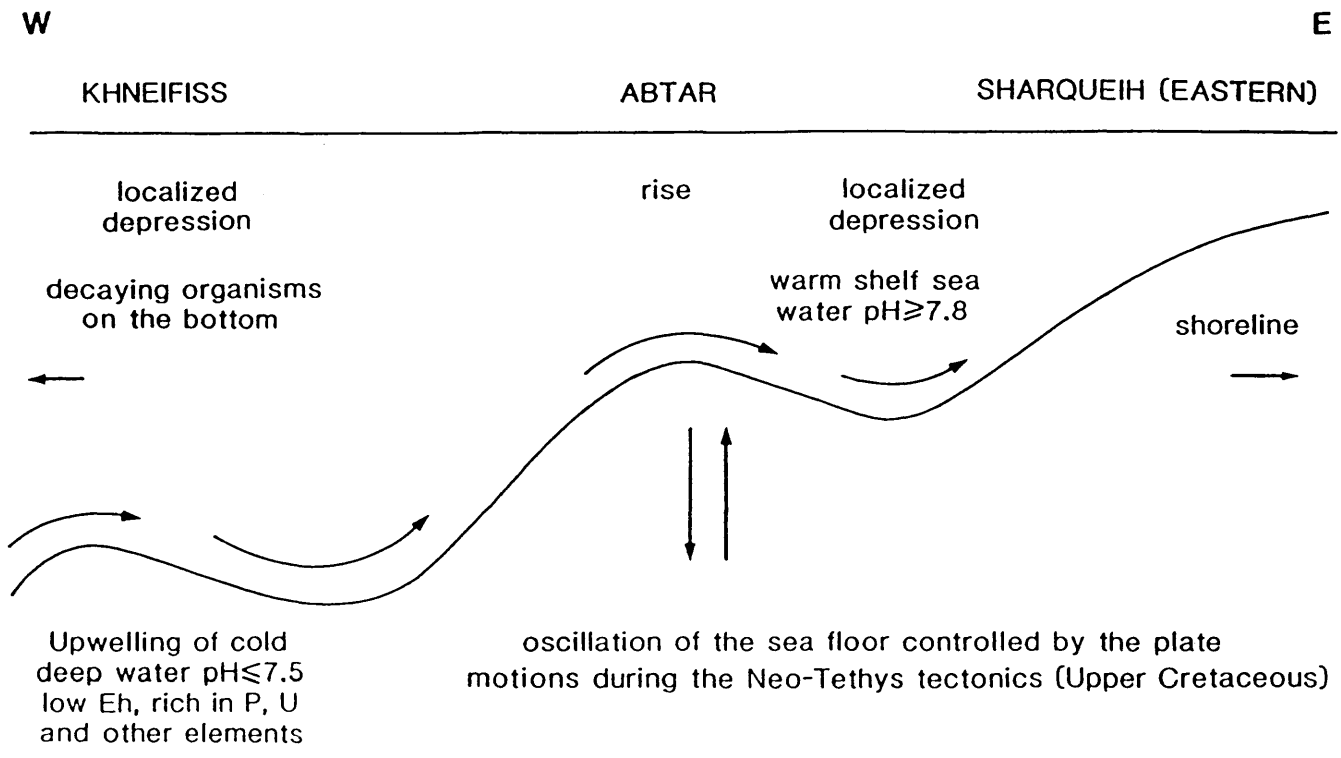
Gamma-ray radioactivity within the region was found to be mainly a function of U content rather than a response to Th and K concentrations. Although scintillometry is a convenient qualitative exploration tool for U, it was found that it cannot provide reliable quantitative determinations of U content, and, in some cases, it yielded equivalent U values unsupported by NAA geochemical

data. This might be caused by a disequilibrium problem which is a major drawback of the radiometric techniques; lithogeochemical methods can be used to overcome such shortcomings. Furthermore, in the Palmyrides region, gamma-ray measurements indicate mainly uraniferous phosphates, and are neither particularly efficient at discriminating these from mineralization, nor delineating mineral occurrences.

10.2.3 Geology

From integrated geological, structural and geochemical data presented in this thesis, it can be concluded that the formation of phosphorite and U incorporation in the Palmyrides region was linked to plate tectonic activities.

A)- The phosphogenesis in the Palmyrides was contemporaneous with intensive Neo-Tethys tectonisms during Upper Cretaceous times, which can be genetically related to the lateral movement of the Arabia plate towards the zone of collision with the Anatolia plate. Two phases of tectonic activities contributed to the enrichment in P, U and associated elements. The first is a rifting stage which permits taphrogenic fluids (deep rooted in the lower crust or upper mantle) to be incorporated into the sedimentary environment via conduits such as faults and fractures. The second is a general subsidence of the whole region during the Upper Cretaceous which was characterized by oscillations of the sea floor (Fig. 10.1). These plate tectonic activities were a response to ridge-push forces acting at the southern border of the Palmyrides aulacogene. This effect was intensified due to the location of this depression between the



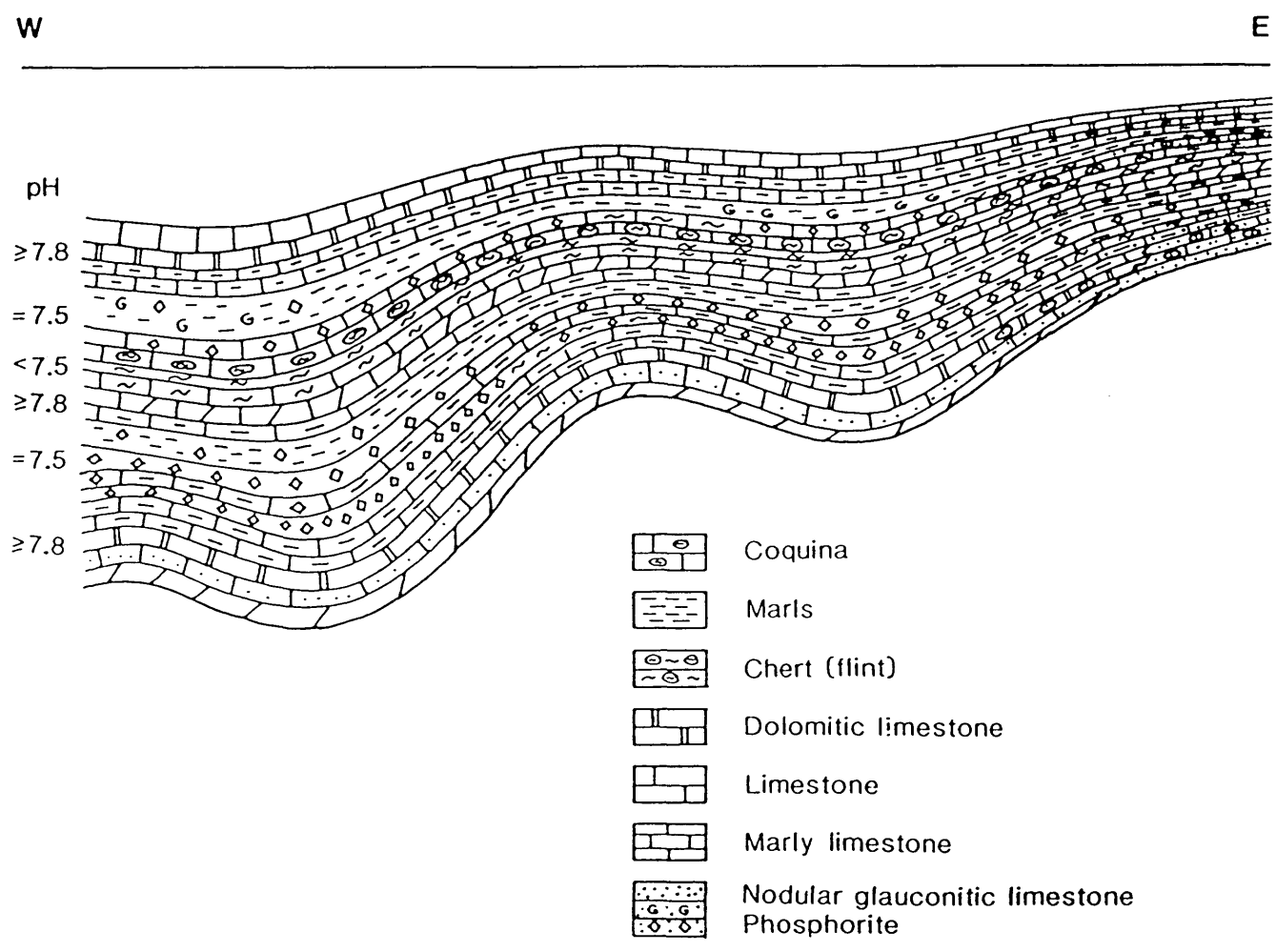


Fig. 10.1. A suggested framework for a model of phoshogenesis in the Palmyrides region during the Upper Cretaceous plate tectonics of the Middle East.

two basement highs (Rutbah and Halab) and was aided by the lubrication effect of the Triasso-Jurassic evaporites. The ridge-push force was originally generated at the Gulf of Suez triple junction.

B)- Upwelling of deep sea water, rich in dissolved P, U and other elements, cold, and at low pH and Eh relative to the oxygenated and warm shallow shelf sea water, was generated owing to the changes in the sea floor configuration. Such an upwelling theory was first discussed by Kazakov (1937), and was said to account for Turkish phosphorite by Sheldon (1964). More recently it was considered valid by many workers to explain models of phosphogenesis world wide (Cook and McElhinny, 1979; Riggs, 1985, 1984; El Bassam et al., 1985, 1983; Lucas et al., 1984).

C)- Within the Palmyrides, localized depressions were developed during Campanian-Maestrichtian times to different degrees. Khneifiss depression perhaps shows signs of more subsidence and proximity to deep open-sea conditions than Ash-Sharqueih and Al-Abtar deposits. This was reflected by less detritus, shell fragments and higher P and U contents.

D)- Major changes in climatic and physico-chemical conditions of the sedimentary environment (pH, Eh, temperature, organic matter) have resulted from an interaction of the upwelling body of sea water with the shallow shelf water in depressions. The conditions prior to the begining of the tectonic activities and plate movements seem to have favoured dominantly carbonate sedimentation. However, such interaction and mixing of the two bodies of sea waters have resulted in a slight fall in the pH from perhaps above 7.8 (which favours carbonate precipitation)

to approximately 7.5 (which favours the precipitation of phosphorite) (Krumbein and Garrels, 1952; Reeves and Saadi, 1971). This appears to have been accompanied by a slight fall in Eh and temperature leading to accumulations of phosphorite formations.

E)- This was accompanied by the syngenetic incorporation of a significant part of the U content into the phosphorite and their phosphate minerals and particles. The results of fission track and SEM studies indicated that further, post-depositional, U enrichment occurred as well. Geochemical data also showed conspicuous variations in U content even within one phosphorite bed, apart from larger variations between Khneifiss and Sharquieh phosphorite deposits. It is inferred, however, that these post-depositional U enrichments occurred due to an increase in anaerobic conditions which may have developed over a stagnation period within the localized depressions immediately after the upwelling event. In these circumstances, recently formed phosphorite, still in contact with mineralizing pore waters, subarial reworking of the already formed phosphorites (McClellan, 1980; Lucas et al., 1979; McArthur, 1984),and decaying organisms on the bottom of the depression would lead to increasing adsorption of U into the bituminous matter,and to an increased amount of P beyond the normal nutritional need of the biota mass.

F)- The peculiar alternation of thin beds of phosphorite, carbonate, chert, phosphatized limestone and layers totally made of bone fragments suggests alteration of high and low sea water levels. Therefore, cycles of upwelling appear to have taken place intermittently over the phosphogenesis epoch. Hence,

the changes in sedimentation conditions that favour the phosphorite formation were also intermittent and closely followed the upwelling periods which themselves are controlled by the tectonic activities.

G)- Chert beds, poor in CO_3^{2-}, P and U, mark the Campanian as well as other phosphorite formations all over the region. They indicate a drop in pH and reflect shallow water conditions in the alternation cycle. They also seem to precipitate under more oxidizing conditions within a high energy environment, indicating relative proximity to the shoreline.

H)- Two mechanisms of phosphatization can be inferred from such model of phosphogenesis.

1) Direct bioclastic, biogenic and chemical precipitation of phosphorite from the sea water in the localized depressions of the sea floor of the region.

2) Replacement of calcite by apatite and other phosphate minerals. This seems to follow resetting of the climatic and environmental conditions after the depletion of P and associated elements from each upwelling body of water in the first process. Continuation of this type of replacement in the shallow shelf deposition environment may explain the widespread phosphatized limestone lithologies found in the Palmyrides and mirrored through microscopic examination of the thin sections, which showed carbonate grains being partially replaced by phosphate matter.

I)- The sources of P, U and other elements appear to be as follows.

1) The available soluble P, U and other elements in the sea water together with an increase caused by the upwelling flux.

2) A significant supply of these elements, especially P, U, V, Zn, Ni and Cd, is derived by erosion and weathering of the extensive volcanic rocks which erupted during the first rifting stage within the Lower Cretaceous sequence and which are particularly evident in J.Rmah and J.Naqnaqueh in the Palmyride mountains. The rapid cycles of uplift and subsidence which preceeded the phosphogenesis epoch enhanced the weathering and released important amounts of these elements into the sea.

3) The most important source is possibly related to some types of mineralizing fluid which made their way through ancient taphrogenic conduits into the Palmyrides basin. Evidence of such fluid was found in J.Bassiri, Om-Jorm and J.Abou El Fawaress in the form of small mineralized veins within the Upper Cretaceous rocks, including phosphorites, and other rocks in similar geological and structural settings.

10.2.4 Uranium minerals

A) From the overall results of the mineralogical studies of the mineralized specimens it was concluded that almost all secondary U minerals are tiny, euhedral, tabular scales and laths, flattened, elongated and in some cases curved, with micaceous cleavage, and probably simulating orthorhombic symmetry. These minerals are carnotite, tyuyamunite, meta-tyuyamunite and an unnamed uranyl-vanadate lead hydroxide closely similar to ferghanite, all of which are of the carnotite group. In rare cases a uranyl sulphate (schoeckingerite) was found. Particularly conspicuous from the scanning electron microscope

images is an intimate association of U minerals with celestite [$SrSO_4$]. However, despite the abundant phosphate rocks in the region, no autunite (uranyl phosphate) minerals were found owing perhaps to the presence of dissolved V or vanadate.

B) From combined drainage, groundwater and rock geochemistry it can be concluded that the secondary U minerals have been formed during modification and mobilization of the primary U present in the phosphorite and other mineralized rocks by circulating groundwater. Due to the continued leaching of U into oxidizing solutions and the availability of complexing agents, secondary enrichments in calcrete and gypcrete formations occur. The lateral-flow of the groundwater has transported and dispersed U via fractures, whereas evaporites, sorption onto clays and precipitation were responsible for the widespread formation of secondary U minerals in the Palmyrides.

10.2.5 Fission track registrations

A) This technique proved very useful and efficient in mapping the distribution of U content in the samples; and in agreement with the conclusions drawn by Bowie et al. (1972); Simpson et al. (1976) it was found that the fission tracks provide valuable and sensitive means of distinguishing between levels of uranium in the rocks studied.

B) The track density demonstrates that U enrichment closely follows the phosphate constituents (ovules, pellets, coprolites, fish teeth and the isotropic and anisotropic bone fragments), and the phosphate minerals (apatite, francolite, hydroxyfluorapatite, collophane), as well as the organic matter of these samples. No U

enrichment was found in the glauconite grains or the calcite crystals. Micro-fissures within the phosphate rocks were particularly enriched in U, which can be accounted for by post-depositional enrichment processes.

C) Total U content of the phosphorite is largely controlled by the accessory phases (organic matter, collophane muds, pellets) and the diagenetic processes, and not by apatite alone, as had been suggested by earlier studies elsewhere in the world.

10.2.6 Drainage geochemistry

A) Reconnaissance and semi-detailed wadi sediment sampling at intervals of approximately 10 to 15m have been shown to be suitable means of locating anomalous U dispersion trains or source areas. Samples have to be collected in the main drainage channels and above each confluence in drainage networks directly confined to the mountain slopes. This is because anomalies and dispersion trains cannot be readily recognized in the wadis on lowland areas owing to enormous dilution.

B) Dispersion trains for most of the elements are rather short and transport is largely mechanical. Anomalies do not persist more than tens of meters from known mineral occurrences and rarely more than 150m. However, a hydromorphic influence on U and associated elements, when present, do not significantly modify the bedrock-sediment relationship. This was also reflected in the grain size distribution which is dominated by the silt and coarser fraction with only a minor clay size fraction (<3%) being developed.

C) Uranium in the wadi sediments is found in two geochemical

associations:

U, Se, P, As, Ba, V and Sr; and

U, V, Zn, Ni, Mo, Cr, Cu, Cd and As.

Judging from the lack of any correlations between U and Al, Fe, Mn and alkalis, both U associations are not greatly influenced by secondary environmental processes; hence, they are related to primary haloes. The first association is found where U mineralization originated by leaching of the prominent phosphate rocks. The second association is formed by subsurface magmatic or low temperature hydrothermal activities.

Therefore, the underlying controls of the geochemical variation in the drainage sediments of the region are:

1) bedrock in general and phosphate rocks in particular; and
2) mineralizing solutions enriched in U, V, Ni, Zn, Mo, Cr, Cu, Cd and As of deep rooted origin incorporated into the wadi sediments via fault and fracture conduits.

D)- The drainage survey shows that U is dispersed beyond the phosphate domain.

E)- Examination of U distribution with respect to grain size of the wadi sediments showed that different size fractions could exhibit different dispersion patterns. The 500-250 μm size fraction was found suitable for routine analysis.

10.2.7 Hydrogeochemistry

A) Notwithstanding that the hydrogeochemical sampling scheme was

not optimal, multielement hydrogeochemistry of the region proved advantageous in providing good understanding of the behaviour of U and associated elements in the Palmyrides groundwaters. It is, therefore, considered a very useful tool for U exploration in this semi-arid region, provided boreholes or wells are available.

B) Among the four aquifers present in the region, the Neogene aquifer appeared to be of particular importance with respect to U enrichment, followed by the Palaeogene aquifer.

C) Two partially separated zones of anomalous dissolved U concentrations are found within the Neogene aquifer separated by a topographic rise of the less permeable and older Palaeogene base. East of this rise, towards the El-Maqssam area, U enrichment is accompanied by high levels of V, Mo, Se, As and, to a lesser degree, Sr; whereas the zone to the west of El Baida is strongly enriched in dissolved Se, U and Sr (see Fig. 7.21). Both geological and lithogeochemical evidence suggest that the enrichment in both sides of the rise occurs along the unconformity contact between the Neogene and Palaeogene rocks and possibly coincides with the regional lineament in the western side of the Ad-Daww basin. The spatial relationship and the geochemical association in these two anomalous zones indicate the possible development of a redox front, which is close to the oxidizing side in the west (Se, Sr and U) and more reducing further east (U, V, Mo, As, Se and Sr) of the above mentioned rise. This seems to resemble the worldwide, well reported zonation found in the sandstone roll-front type of U deposits (Adler, 1970; Rose and Wright, 1980; Chester, 1984). The persistence of U anomalies in the two depressions could

perhaps, be related to the development of localized reducing bottom conditions owing to sulphate reduction.

However, the groundwater circulation within the Neogene and Quaternary aquifers does not favour multiple cycles of reduction-oxidation and repeated mobilization-precipitation processes which lead to significant accumulation of U.

D) Although widespread occurrences of secondary U minerals in the region may indicate the availability of dissolved U, V and K within the groundwater regime this also indicates the unfortunate ease with which U is being dispersed under the prevailing environmental conditions. The factors controlling the groundwater circulation, therefore, are important in determining the eventual fate of U and its associated elements as was also concluded earlier by Dall Aglio et al. (1974).

E) Uranium and the multielement associations that characterize its hydrogeochemical anomalies appear to be mobilized initially by carbonate complexes under oxygenated, slightly alkaline groundwaters, but this relationship with carbonate suffered from later alteration due to other factors such as the dissolution of chlorides and sulphates. This greatly increased the content of total dissolved solids(TDS),such high TDS now characterizes the majority of the Palmyrides groundwater samples. The unstable and generally weak relationships between U and TDS shown by correlation, cluster and regression analysis may indicate that the dissolution of sulphates and chlorides occurred withouta corresponding increase in U content.

10.2.8 Playa geochemistry

A) Influences of the secondary environment on Sabkhet El Mouh geochemistry are apparent. The playa survey provides evidence for the continuous geochemical modification of the playa sediments under surficial conditions. Some of these processes have produced weakly U-enriched hydromorphic dispersion patterns reflected in the silt and clay fractions (>70%) which dominate the grain size distribution. Processes such as erosion, leaching, migration, deposition and diagenesis are relatively active.

B) Coprecipitation on clays and Fe-hydroxides of most trace elements, including U and As, is proposed to explain the close association of Fe, Al, Ti, Mo, As, U, V, Ni, Zn, Cu, Cr, K, Li indicated by correlation, cluster and principal component factor analysis. Such a relationship in the Palmyrides geochemistry was found only in the Playa sediments. It may have resulted from interaction between both ground and surface waters with the infilling sediments.

C) Uranium in the playa sediments appears to be present in more than one mode. Its strongest association was found with As, Sr and V. This association was also emphasized by factor and regression analysis, suggesting an origin of a leachate solution derived from one source. The areal distribution of the corresponding factor scores indicated that the high score values coincide with a fault-controlled drainage channel trending SW-NE across the sabkha. This seems to be the only interesting zone for follow up work, since it is not seriously affected by scavenging, coprecipitation or other surficial influences.

D) R-mode factor analysis confirmed the presence of the following underlying controls on U and associated elements.

1 - Clay and Fe-hydroxide fractions control the secondary surficial distribution.

2-A Strong evaporatic component, represented by the association of Na, Li, Mg, K, Si and, to a lesser degree, Ca, reflecting environmental control.

3 - Possible structural control which may cause further interaction between the hydrologic regime, the sediments and the main bedrock lithologies, leading to leaching and redistribution of the elements, especially U, V, Mo, Sr and As.

4 - Diagenetic control is operating at present.

10.2.9 Lithogeochemistry

A) The Palmyrides lithogeochemical survey provided a fundemental knowledge about the primary dispersion patterns of the elements determined in the rocks of the region. Great variation of U content was found in the phosphate group reflecting the important influence of the presence of phosphate upon the trace element geochemistry in general and U in particular. However, it was also found that the U variation was not linearly related to P_2O_5 content, suggesting that U in the phosphate rocks does not occupy only substitutional sites in apatite (as was originally believed), but seems to be incorporated in more than one phase and may be of syngenetic and/or epigenetic origin. The strongest contrast between background and anomalous populations was achieved using rock samples.

B) The basic statistical parameters of U and its associated elements Se, As, V, Mo, Cd, Zn, Sr and to lesser degrees Ni, Cr, Cu and La, show that the degree of their enrichment seems to be primarily controlled by structural factors.

C) A marked lithogeochemical vertical zoning can be concluded from the current data. All the above mentioned elements and P show very low levels in the rocks older than Upper Cretaceous (Unit 6). However, in the time span of Upper Cretaceous to Recent (Holocene) the concentration levels of these elements begin to increase during Coniacian and Santonian. The U enrichment culminates in the Campanian-Maestrichtian coinciding with major rifting events, with maxima in the phosphorite and phosphate rocks of Unit 5, and especially in active fault zones. Concentrations decrease in the overlying Lower and Upper Palaeogene rocks (Units 4 and 3), reach an even lower level in the Neogene rocks (Unit 2), and reach the lowest background values in the Quaternary formations (Unit 1); the regression of such a younging feature is illustrated in Fig. 10.2.

D) Laterally, U and its associated elements are enriched along the two eastern and western margins of the study area, the two sides of Ad-Daww basin and parallel to the flanks of the mountain ranges. Particular enrichment of these elements occurs when SW-NE faults intersect NW-SE and E-W faults, where an anomalous lithogeochemical response in U, V, Mo, As, Se, Ni, Cd, Zn and Cu is best developed, as illustrated in Fig. 10.3. This suggests that the present reconnaissance survey successfully outlined

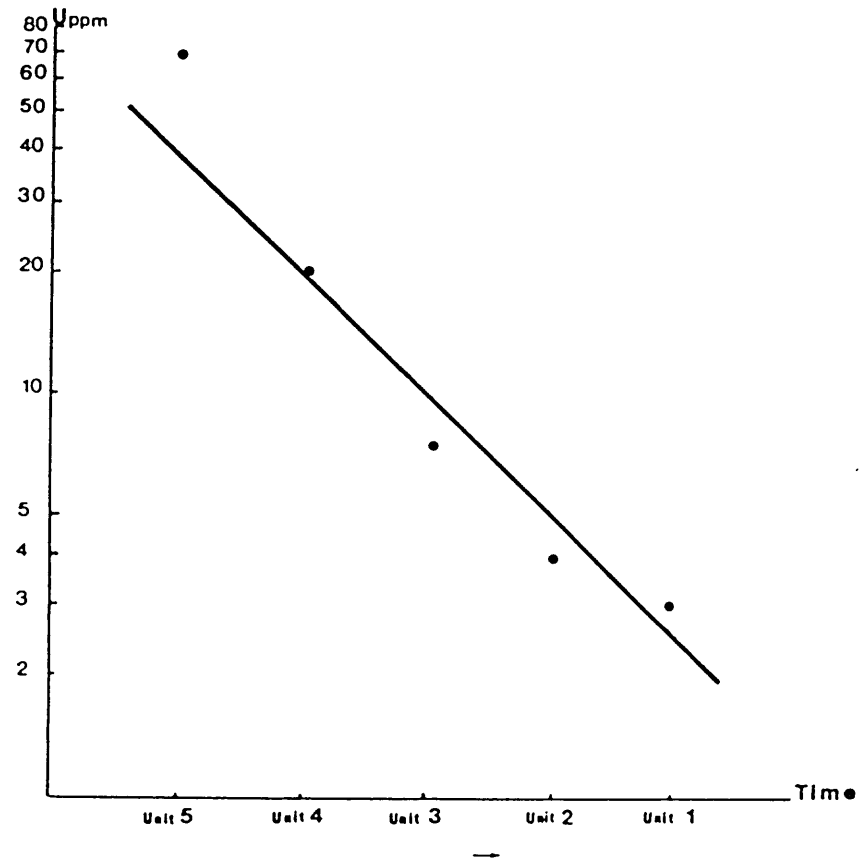


Fig.10.2 Variation of U contents with geological history since Upper Cretaceous to Recent.

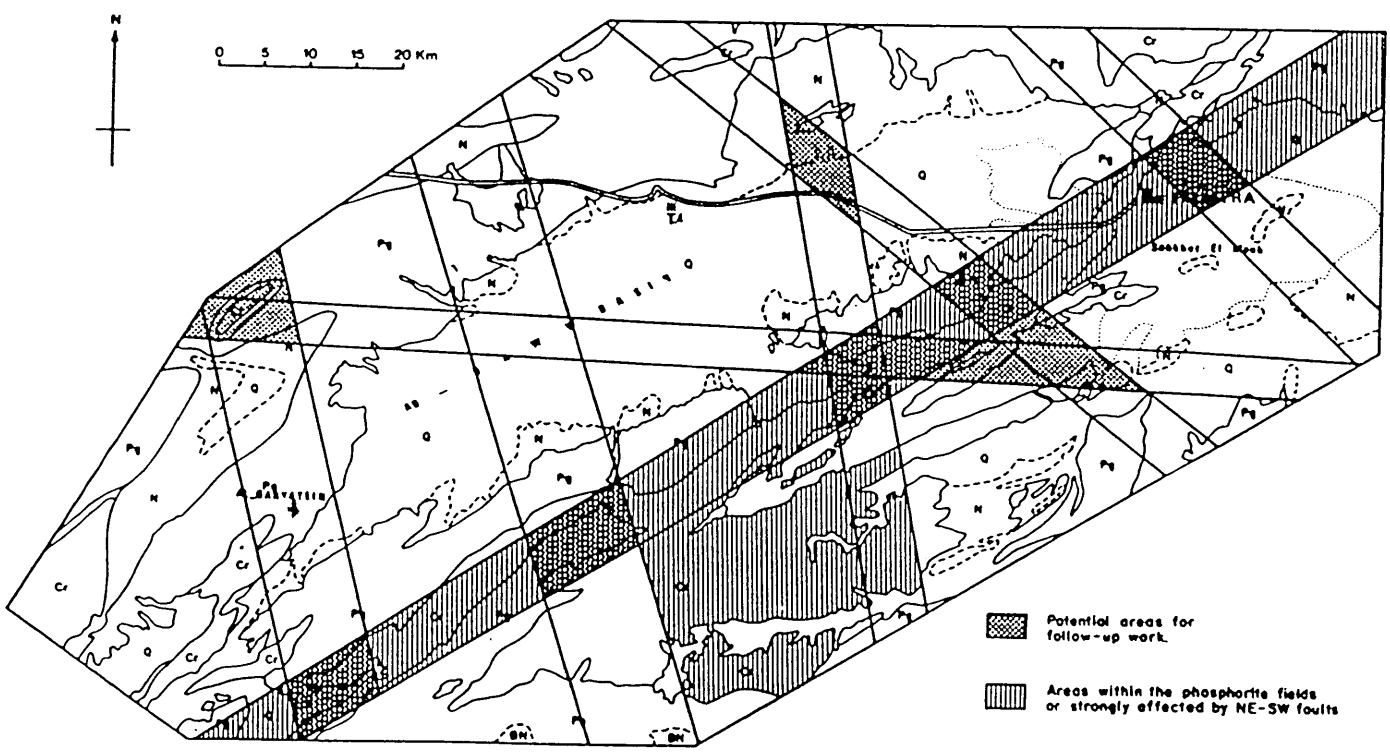


Fig.10.3 Structurally controlled U enriched areas in the Palmyrides region (areas for follow-up work).

potentially interesting areas for follow-up U exploration in the region.

E) Distinct lithogeochemical associations were revealed by the multivariate techniques used, particularly cluster, regression and factor analysis:

1 - U, CPS, Se, V, As, Mo, Ni, Zn, Cu, Cr and Cd.

2 - P, Th, U, Ba, Sr, La, Ca, Na, Cr and Co.

3 - Fe, Al, K, Ti, Mg, Mn and Li.

4 - Ni, Zn, V, Mo, Cr, Cu, Cd and U.

5 - Ca, Sr, Pb, Cd, Zn and Co.

6 - Th, Ca, Sr.

These associations can be explained in terms of causal factors as follows:

I) Structural control, which is represented by the group of elements, Ni, Zn, V, Mo, Cr, Cu, Cd and U (and sometimes P), that are derived from metalliferous fluids debouched onto the sea floor (during major tectonic activities) through fault conduits and since incorporated within diagenetically formed rocks. Both phosphate enriched rocks, as well as small, structurally controlled, mineralized veins, are characterized by such an association. Comparison of the contour maps for U and P (Figs. 10.4 and 10.5) clearly support this conclusion.

II) Lithological control, represented by three distinct associations:

P, Th, U, Ba, Sr, La, Ca, Na, Cr and Co (of phosphate

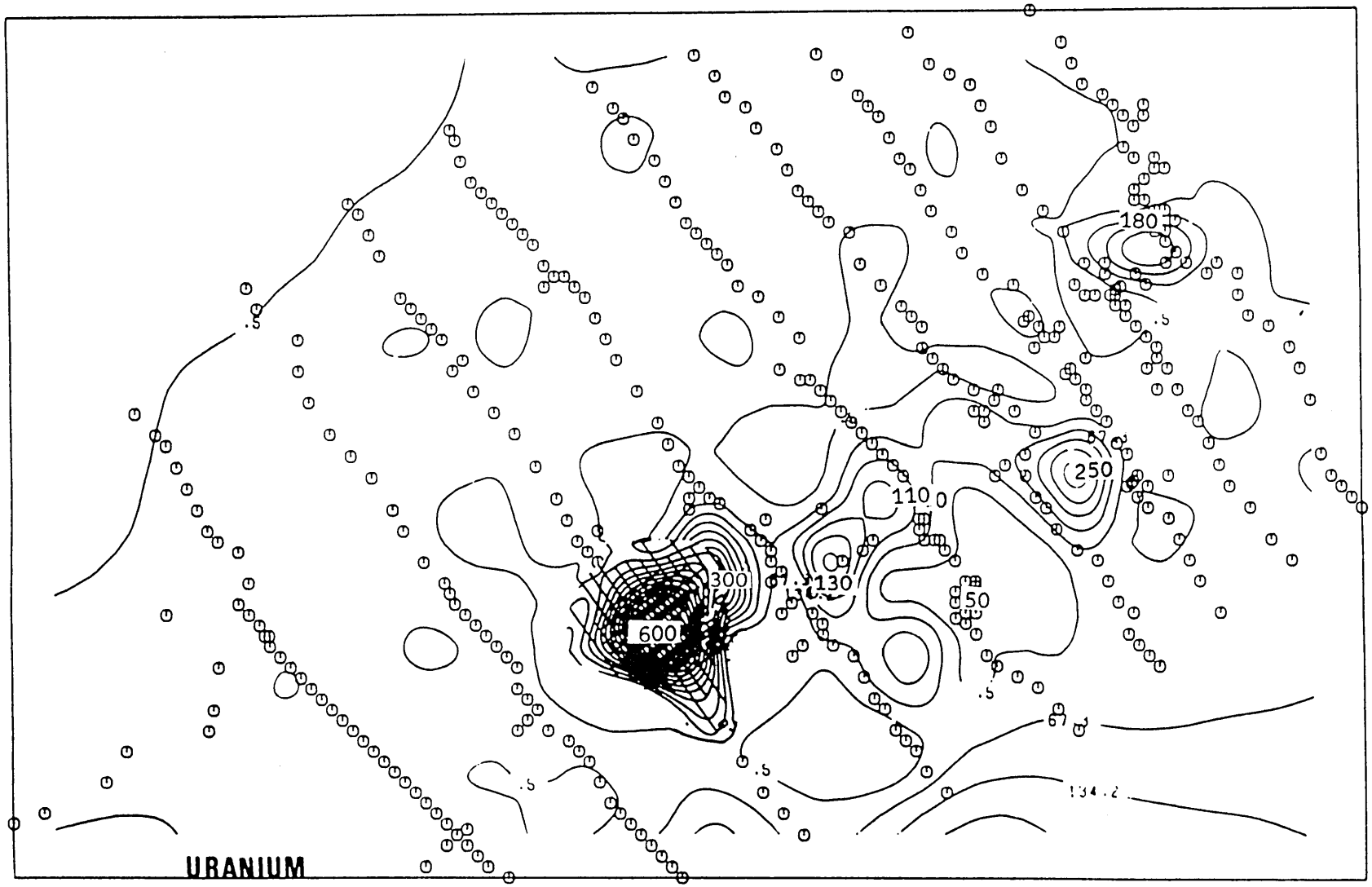


Fig.10.4 Contour map of U in the Palmyrides region.

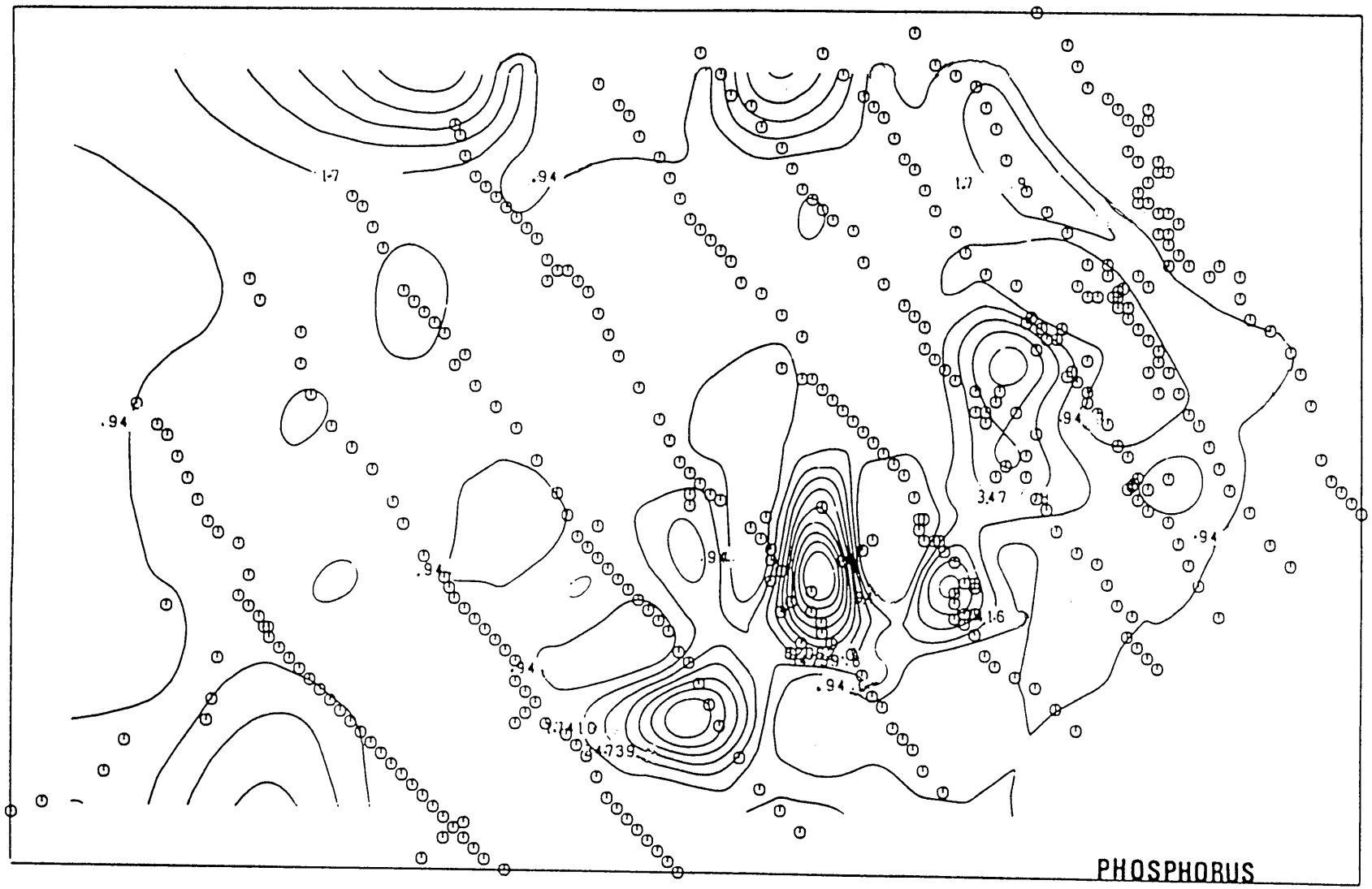


Fig.10.5 Contour map of P in the Palmyrides region.

origin);

Ca, Sr, Pb, Cd, Zn and Co (of carbonate origin); and

Th, Ca and Sr (of carbonate origin).

III) Environmental control, indicated by enhanced levels of K, Li, Sr and other alkalis, owing to climatic control on solutions derived from the interaction between the ground water regime and the rocks. This considerably affects the dispersion pattern of Sr, Se, K, Li, V and to a lesser degree U. The evapotransport of the desired solutions may explain the formation of secondary U minerals along with the formation of calcrete and gypcrete duricrusts. It shows also that U and associated elements have been variously leached out of the phosphorite source rock in many weathered profiles.

IV) The association Fe, Al, K, Ti, Mg, Mn and Li identifies clay or Fe-Mn hydroxide fractions. This could result from secondary processes and/or may reflect the primary clay component in the marls, marly limestones and clayey limestones or both. However, the great role that groundwaters may have played along the unconformity contact between the Neogene lacustrine deposits and the older Palaeogene rocks as well as the above mentioned influence on the contents of Se, Sr, U, V, Mo and As clearly indicates the presence of secondary surficial or subsurficial weathering processes.

E) It is concluded also that the above mentioned U enrichment in

the carbonate rocks of the Palaeogene can be attributed to the non-carbonate impurities.

F) From an exploration viewpoint, the obvious similarities between drainage, groundwater and rock geochemical data regarding the close association of U, V, As, Se, Mo, Cd and to a lesser degree Sr and K is of particular interest. Two conclusions can be drawn : the first is that although the lithogeochemical anomalies are more useful in defining areas for detailed investigation, favourable indications derived from anomalous patterns shown by all three sampling media are superior to any single one medium; the second one is that this persistent association of elements clearly reveals a leaching process from a source which could be either the phosphorite rocks and/or metalliferous aureoles in rocks situated closely above or below the localities involved. Both implications are significant for further exploration work.

10.3 Further work and recommendations

The conclusions outlined above lead to recommendations for

A) Follow-up U exploration work in the Palmyrides region. Further geochemical surveys should be undertaken in more detail over the areas delineated with high U contents, high residuals and high scores of those factors indicating U enrichment and/or mineralization. This should be preceeded as well as accompagnied by detailed structural studies and geological analysis in order to establish the exact field relationship between the localized strongly faulted and brecciated zones and the main areal and

regional structures, and to point out, if possible, some lithostratigraphic guides(see Fig.10.3).

B) An exploration drilling operation along the northwestern flank of the southern Palmyride mountains should be planned and executed over selected sites in a zone 500m wide connecting anomalous localities in J. Bassiri, Bardeh, Om-Jorm, Qal-Tabaque and Abou El Fawaress, and concentrated at those sites with taphrogenic features proved by recent earthquake studies to be still active. Mineralogical, petrogeochemical and geochemical studies should be carried out on the borehole cores. Analysis must include U and the elements found by the present research to be in close relationship with U, such as V, Mo, Se, As, Cd, Zn, Ni, Cr, Sr, K, P (and the precious metals Au, Ag and Pt, which were found at least in one small mineralized vein). The use of geostatistics can aid in the design of drilling programmes and interpretation of borehole data, and its application is strongly recommended.

C) As discussed earlier, exploration for U is essentially the search for suitable geologic, structural and environmental settings in which the prevailing conditions may produce anomalous concentrations of U by deposition from U enriched solutions. Therefore, in the light of the findings of the present hydrogeochemical and lithogeochemical surveys, it is strongly recommended to trace and map in detail the unconformity contact between the Neogene lacustrine and clastic sediments and the older Palaeogene rocks, in order to investigate the potential for sandstone or basal type U deposits. Sampling of this contact and analysis for U and its associated elements

should also be carried out as soon as possible, given the great assistance that multielement geochemistry can provide. Q-mode cluster analysis can be used to classify the samples and establish a test set for further discriminant analysis.

D) In the region, little is known of the fundamental relationship between U and the mechanism of complexing, transport and adsorption by the organic matter. The present work has suggested, although not fully shown, that urano-vanadate complexes similar to those of carbonate and phosphate may be responsible for U complexing and transport in solutions. Therefore investigations along these lines are recommended, especially when bearing in mind that nearly all secondary U minerals are of the urano-vanadate type.

E) Further hydrogeochemical investigations should be carried out covering areas within central and eastern Syria and the Syrian Desert, if boreholes and wells are readily available. Analysis of groundwater radium, ^{226}Ra and ^{222}Rn, is also recommended. The Ra^{2+} results can then be used as an exploration guide to a nearby and perhaps concealed ^{230}Th or its parent ^{234}U. Similarly, the high mobility of ^{222}Rn, which is a gaseous daughter product of ^{226}Ra, can be used in exploration to locate deeply buried U deposits.

F) Application of the "saturation index" of Lueck (1978) and the concept of solution-mineral equilibria (Langmuir, 1978, 1980; Miller et al., 1984; Watny et al., 1985) in order to compute the solubility index of dissolved U is strongly recommended. Therefore, variables such as Eh, pH, temperature, water depth and

flow, dissolved U, V, TDS and other cations and anions(such as CO_3^{2-}, SO_4^{2-}, PO_4^{3-}, NO_3^-) should be measured during sampling and analysis and the list of the thermodynamic properties and data should be prepared for such a computation. It should be stressed that no tetravalent U minerals were found in the region, because it seems that U was transported in solution in the form of U^{6+} which could be derived from all of the three U isotopes. However, the ^{234}U isotope is likely to comprise part of the signal of U^{6+} because it is normally more mobile in natural waters (Levinson and Coetzee, 1978). Coward and Osmond (1977) reported such an isotopic signal which was discernable for a number of kilometres in the direction of groundwater flow.

G) The U equilibrium and disequilibrium problems should be fully investigated in the region through future follow-up work in order to answer the following two questions:

   i) whether or not U is leached out of the source and the daughters remain.

   ii) whether the formation of the so called "young U" has or has not reached equilibrium with its daughter products.

H) Gas and vapour geochemistry using, particularly, the soil ^{222}Rn, ^{220}Rn and He have been extensively used in U exploration world-wide (Dyck, 1983; Hambleton-Jones, 1984; and Lovell et al., 1980). It should be noted however, that in the case of calcrete-type U deposits, these daughter products of U proved unsatisfactory (Severne, 1978), but it is suggested that these measurements, coupled with the soil Hg, could provide useful information if they were applied in detailed investigations over the fault zones and other strongly fractured outcrops.

To summarize, it is hoped that this study has provided the first necessary step and insight into some of the factors controlling the Palmyrides geochemistry. In particular, it is hoped that the completely unexpected presence, although at present insignificant, of small mineralized veins of possibly hydrothemal origin will stimulate further investigations into such systems.

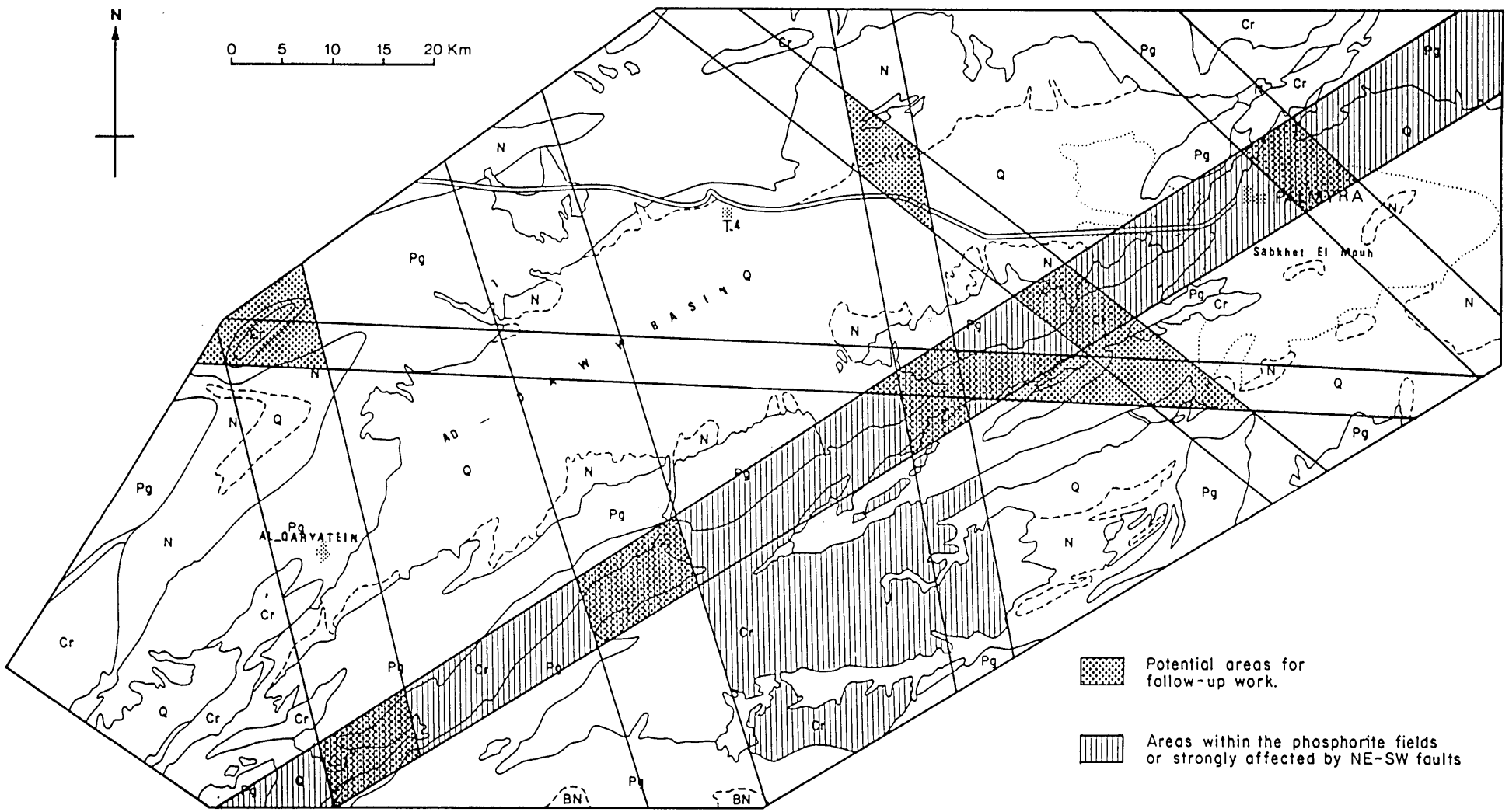


Fig.10.3 Structurally controlled U enriched areas in the Palmyrides region (areas for follow-up work).

REFERENCES

1. AABAID, K. 1980. Radiometric measurments in the Palmyrides Region. Rep. GEGMR, Damascus, SAR.
2. ABDUL-MONEIM, A.A. 1959. Report on airborne radiometric survey in Syria between 19 September to 21 October, 1959. D.G.S.M.R., S.A.R.
3. ADAMS, J.A.S. AND GASPARINI, P. 1971. "Gamma-Ray Spectrometry of Rocks", Elsevier, Amsterdam.
4. ADAMS, S.S. AND SAUCIER, A.E. 1980. Geology and recognition criteria for uraniferous humate deposits, Grants uranium region. New Mexico. Open File Rep. U.S.DOE GJBX-2(81), 226p.
4. ADLER, H.H. 1977. Geochemical factors contributing to uranium concentration in alkalic igneous rocks. (IAEA, Tc-25/4), 34-45, Vienna, 1977.
5. ADLER, H.H. 1974. Concepts of uranium-ore formation in reducing environments in sandstone and other sediments. In: IAEA, Uranium Ore Deposits, 141-168,
6. ADLER, H.H. 1973. Exploration for Uranium in Sandstones. In: IAES, Uranium Exploration Methods, 155-169, Vienna.
   Vienna, STI/Pub/374, 1974.
7. ADLER, H.H. 1970. Interpretation of colour relations in sandstone as a guide to uranium exploration and ore genesis, Uranium Exploration Geology, IAEA, Vienna, 1970, 331-344.
8. AGHA, W.R. AND DROUBI, A. 1983. Study of the water resources of Ad-Daww Basin, Vol. II, pp249, ACSAD DM/T37, Damascus, SAR.
9. AGHA, W.R. 1976. Use of Geophysical Methods for the Study of the Groundwater Resources of the Dawwa Basin, ACSAD/HS/P6.
10. AHRENS, L.H. (ed). 1968. Origin and Distribution of the Elements. Pergamon Press Ltd., Oxford, 1178p.
11. AL-BASSAM, K.S. AND AL ALLAK, M.M. 1985. Factors controlling the deposition of some Tethyan phosphorite of Iraq. Chemical Geology, 51, 199-212.
12. AL-BASSAM, K.S. AND HAGOBIAN, D. 1983. Lower Eocene phosphorites of the Western Desert, Irag. Sediment. Geol., 33: 295-316.
13. AL-MALEH, A.K. 1976. Etude tratigraphique, petrographique, sedimentologique et geochemique due Cretace du N W Syrien (Kurd Dagh et environs d'Afrine). Les aspects petroliers de la region. These Univ. Pierre et Marie - Curie Paris VI)
14. ALTSCHULER, Z.S. 1980. The geochemistry of trace elements in marine phosphorites : I Characteristics, abundances and enrichment. Soc. Eco. Paleontologists Mineralogists Spec. pub. 29, p19-30.
15. ALTSCHULER, Z.S. 1980(b). The bearing of geochemistry on the recovery of uranium and rare earths in phosphorites: Internat. Cong. Phosphorus Compounds, 2nd, Boston, April, Proc. p605-625.
16. ALTSCHULER, Z.S., CLARKE, R.S. Jr. AND YOUNG, E.J. 1958. Geochemistry of uranium in apatite and phosphorite. Geol. Survey Prof. Paper 314-D Washington, U.S. Govt. Print, off. p.45-90.

17. ANDERSON, R.F. 1985. Redox behaviour of uranium in an anoxic marine basin. In: Concentration mechanism of uranium in geological environments. Proceeding of Int. Meet. Nancy.
18. ANDREOLI, M.A.G., ROBB, L.J., MEYER, M., AINSLIE, L.C. AND HART, R.J. 1985. Granitoids of the Pre-Witwatersrand Basement: Clues to the source of uranium placer mineralization. In: Recotnition of Uranium Provinces. Proceeding of an IAEA Technical Committee Meeting, London, 18-20 September.
19. ANDREWS ET AL. 1985. A radiochemical, hydrochemical and dissolved gas study of groundwaters in the Molasse Basin of Upper Austria. Earth and Planetary Science Letter, 73, 317-332.
20. ANDREWS, J.N. AND KAY, R.L.F. 1983. The uranium content and U^{234}/U^{238} activity ratios of dissolved uranium in groundwater from some triassic sandstone in England. Isotope Geosciences, 1, No. 2, 101-117.
21. ANON, 1976. How Track-Each Measure Radon Gas as a Clue to U^{308} bodies. World Mining, March.
22. APPLEYARD, S.J. 1984. Uranium in groundwater near Uarov, Western Australia: distribution and relevance to mineralization. (Abst). In: Geochemical Exploration in arid and deeply weathered terrains. Davy and Mazzuchelli (eds). J. Geochem. Explor., 22: 355.
23. APPLIN, K.R. AND LANGMUIR, D. 1978. Groundwater Geoch geochemistry as a Prospecting Tool for Uranium Deposits in Pennsylvania. GJO-1659-4.
24. ARAMBOURGE, C., DUBERLRET, L., SIGNEUX, J. AND SOVNAY, J. 1959. Contributions a la stratigraphie et al paleontologie du Cretace et de Nummultique de la marge N W de la peninsula Arabique. Notes et mem. Moyen-Orient, Paris, 1959, 7.
25. ARMSTRONG, F.C. 1976. Uranium in Plutonic Rocks. Amer. Assoc. of Pet. Geol. Bull. 60, 1389.
26. ARMSTRONG, F.C. 1974. Uranium resources of the future uranium ore deposits, IAEA, Athens, Vienna, STI/PUB/379, 625-635.
27. ARENDT, J.W., BUTZ, T.R., CAGLE, G.W., KANE, U.E. AND NICHOLS, C.E. 1979. Hydrogeochemical and Stream Sediment Reconnaissance Procedures of the Uranium Resource Evaluation Project. Oak Ridge Gaseous Diffusion Plant, Tennessee, December 31, 1979. UC-51, Nuclear Raw Material.
28. ARENDT, J.W 1978. Hydrogeochemical and stream sediment reconnaissance basic data for Seguin NIMS quadrangle, Texas. U S Dept. Energy Report K/UR-108.
29. ATFEH, S. 1970. Uranium in Syria, Report GEGMR, 790. Syria.
30. ATFEH, S. 1964. Phosphorite and Uranium in Syria : Data collected from explanatory notes of 1:200,000 scale geological map of Syria. Report DGSMR., 546, S.A.R.
31. ATFEH, S. 1967. The Phosphorite Deposits of Syria. Unpub. Ph.D. Thesis, University of London, King's College, July 1967.
32. ATFEH, S. AND FARADJEV, V.A. 1965. Radioactivity of Phosphorites in Syria. "Report G.E.G.M.R., 571, S.A.R.".

33. ATFEL, S. 1967. Mineralogy and Chemical Composition of the Upper Cretaceous Phosphate Deposits of Syria. (Paper Int. Colloquium Rock Phosphate, Toulouse, France, May.
34. AZZAROLI, A. 1968. On the Evolution of the Gulf of Aden. Proc. 23rd Int. Geol. Congr., 1: 125-134.
35. BADALOV, S.T., BELOPOLSKAYA, T.L. PRIKHIDKO, P.L. AND TURESELKOVA. 1969. Geochemistry of Selenium in Sulphate-Sulphide Mineral Paragenesis. Geochem. Intern. V. 6 (4), p799-802.
36. BAILEY, R.V. AND CHILDERS, M.O. 1977. Applied Mineral Exploration with Reference to Uranium, Westview Press, Boulder, Colorado. 542p.
37. BARAKSO, J.J. 1979. Geochemical Dispersion of Uranium in Overburden-covered Regions. CIM, April, 1979.
38. BARBIER, J., BAURBRON, J.C., BOSCH, B., BRIOT, P. AND JACOBS, C. 1980. Donnees preliminaires sur les isotopes dusoufre dans les calcretes uraniferes: un cas dans la province de Mudugh (Somalia). Comptes Rendu Academie Sciences, Paris, Vol. 290, Serie D, ppl047-1050.
39. BARNE S, I. AND HERN, J.D. 1973. Chemistry of Subsurface Waters. Ann. Rev. Earth Plan. Sci. 1, 157-181.
40. BARONOV, D.I., RONOV, A.B. AND KUNASHOVA, K.G. 1956. On the Geochemistry of Dispersed Thorium and Uranium in Clays and Carbonate Rocks of the Russian Platform: Geochemistry (Moscow) No. 3, p3-8.
41. BARRETTO, P.M.C. 1985. Identification of Uranium Provinces in Brazil. In: Recognition of Uraniun Provinces. Proceedings of an IAEA Technical Committee Meeting, London, 18-20 September.
42. BARRINGER, A.R. 1985. Rapid Reconnaissance Techniques for Oil and Mineral Exploration in Desert Terrains. In: Prospecting in Desert Terrain. Instn. Min. Metall. London, p273-283.
43. BARTHEL, F. AND HAHN, L. 1985. Sedimentary Uranium Occurrences in Eastern Europe with Special Reference to Sandstone Formations. IAEA, Tec. Doc. 328, Vienna, 51-68.
44. BARTON, P.B., JJr. 1956. Fixation of Uranium in the Oxidized Base Metal Ores of the Goodsprings District,
45. BASHAM, I.R., BALL, T.K., BEDDOE-STEPHENS, B. AND MICHIE, U. Mcl. 1982. Uranium bearing accessory minerals and granite fertility: I Methods of identification and evaluation. II Studies of granites from the British Isles. OECD/NEA/IAEA, Paris, 385.
Clark Co., Nevada. Econ. Geol., V, 51, pl78-191.
46. BASHAM, I.R. 1980. Charged-particle track analysis in the assessment of sandstone-type uranium ore from Pakistan. Nucl. Tracks. Vol. 4, pp33-40.
47. BASHAM, I.R. 1981. Some applications of autoradiographs in textural analysis of uranium bearing samples - A discussion. Econ. Geol. Vol. 76, pp974-982.
48. BATES, R.L. AND JACKSON, J.A. 1980. Glossary of Geology. 2nd edition. American Geological Institute (Falls Church, Virginia).
49. BATURIN, G.N., KOCHENOV, A.V. AND SHIMKUS, K.M. 1967. Uranium and rare metals in sediments of black and Mediterranean Seas. Geochem. Int. 4, p.29.

50. BATURIN, G.N., KOCHENOV, A.V. AND SENIN, YU. M. 1971. Uranium concentration in recent oceanic sediments in zones of rising currents. Geochem. Int. 8.
51. BELL, L. 1982. Uranium Exploration Technology Developments Under the U.S. NURE Program. In: Proc. OECD/NEA/IAEA, Paris, 859-873.
52. BELL, K.G. 1963. Uranium in Carbonate Rocks. U.S. Geol. Surv. Prof. Paper. 474-A; 29.
53. BEN-AVRAHAM, Z. 1978. The structure and tectonic setting of the Levant continental margin, Eastern Mediterranean. In: O.H. Oren (ed), Structure and Tectonics of the Eastern Mediterranean. Tectonophysics 46: 313-331.
54. BENES, P. AND STEINNES, E. 1975. Migration forms of trace elements in natural fresh waters and the effect of the water storage. Water Research V.g., p741-749.
55. BENNETT, G.D. 1978. Introduction to groundwater hydraulics. A programmed text for self instructors. (U.S. Geol. Survey. Techniques of Water Resources Investigations. Boob 3, Chapter B2). 172pp.
56. BENSON, L.V. AND LEACH, D.L. 1979. "Uranium Transport in Walker River Basin, California and Nevada. J. Geochem. Explor., 11: 227-247.
57. BERTHOLLET, P. 1958. Methodes d'analyses utilisee par la section de Geochemie; France. C.E.A. Note 250.
58. BEUS, A.A. AND GRIGORIAN, S.V. 1977. Geochemical exploration methods for mineral deposits. (Wilmette, III: Applied Publishing) 287pp.
59. BINNS, R.A. McANDREW, N., SUN, S.S. 1980. Origin of Uranium Mineralization at Jabiluka. In: Uranium in the Pine Creek Geosyncl. Inter. Atomic Energy Agency, Vienna, 543-562.
60. BLAKE, W.P. 1902. The caliche of Southern Arizona : an example of deposition by the Vadose Circulatio. Trans. Am. Inst. of Mining and Metallurgical Engineers, 31: 220-226.
61. BLANK, H.R. AND TYNES, E.W. 1965. Formation of Caliche Insitu. Geol. Soc. Am. Bull., 76: 1387-1392.
62. BLISKOVISKIY, V.Z., EFIMOVA, L.V. AND ROMANOVA, L.V. 1967. The strontium content of phosphorites: Geochem. Int. 4, p1186.
63. BLISKOVSKIY, V.Z., ROMANOVA, L.V. AND SMIRNOVA, A.I. 1968. Trace elements in the interstatial waters of marine sediments. Geochem. et Cosmochim. Acta, 32, p397.
64. BOBERG, W.W. AND RUNNELLS, D.D. 1971. Reconnaissance study of uranium in the South Platte River, Colorado. Econ. Geol., 66: 435-450.
65. BOLIVER, S.L., CAMPBELL, K. AND WECKSUNG, G.W. 1983. R-mode factor analysis applied to uranium exploration in the Montrose quadrangle, Colorado. In: G.R. Parslow (ed), Geochemical Exploration 1982. J. Geochem. Explor., 19: 723-743.
66. BOURCART, J. 1940. Recherches Stratigraphiques sur le Pliocene et le Quaternaire du Levant. Bull. Soc. Geol. Fr., 10, p207.
67. BOWIE, S.H.U. 1979. The mode of occurrence and distribution of uranium deposits. Philos. Trans. R. Soc. London Ser. A., 291: 289-300.

68. BOWIE, S.H.U. 1977. Where to prospect for uranium. In: Recognition and Evaluation of Uraniferous Areas. Proceedings of IAEA, Vienna, p151-164.
69. BOWIE, S.H.U. 1976. Whither Uranium? Trans. IMM, London, Vol. 85, p163.
70. BOWIE, S.H.U. 1970. Some geological concepts for consideration in the search for uranium provinces and major uranium deposits. IAEA, Vienna, p285.
71. BOWIE, S.H.U. AND CAMERON, J. 1976. Existing and New Techniques in Uranium Exploration. In: Symposium and Exploration for Uranium Ore Deposits, Vienna, IAEA.
72. BOWIE, S.H.U., SIMPSON, P.R., RICE, C.M. 1973. Application of Fission-track and Neutron Activation Methods to Geochemical Exploration for Uranium. J. Geochem. Expl. (1972). London, IMM, 1973.
73. BOWIE, S.H.U., BALL, T.K. AND OSTLE, D. 1971. Geochemical methods in the detection of hidden uranium deposits. In: CIM Special Vol. No. 11, Proc. 3rd Int. Explor. Symp., Toronto, 1970, 103-111.
74. BOWMAN, W.W. 1977. Neutron activation analysis for uranium and associated elements. In: Symposium on Hydrochemical and Stream Sediment. Reconnaissance for Uranium in the United States. U.S. Department of Energy Grand Junction, Colorado, Document GJBX-77, (77p), 79-91.
75. BOX, G.E.P. AND COX, D.R. 1964. An analysis of transformations. J. Royal Slat. Soc., Sev. B, 26, p211-243.
76. BOYLE, D.R. 1985. Geological environments for basal-type uranium deposits in sedimentary host rocks. In: Geological Environments of Sandstone-type Uranium Deposits. IAEA, Tec. Doc. 328, Vienna, 363-382.
77. BOYLE, D.R. 1984. The genesis of surficial uranium deposits. In: Surficial Uranium Deposits. IAEA, Tec. Doc. 322, Vienna, 45-52.
78. BOYLE, D.R. 1982. The formation of basal-type uranium deposits in South-Central British Colombia, Canada. Econ. Geol. 77.
79. BOYLE, D.R. AND BALLANTYNE, S.B. 1980. Geochemical Studies of Uranium Dispersion in South-Central British Colombia, CIM Bull. (73/820) 89-108.
80. BOYLE, D.R. 1978. The dispersion of uranium around miocene "basal type" uranium occurrences in the Lassie lake Area, South Central British Colombia, Geological Survey of Canada, paper 79-1A.
81. BOYLE, R.W. 1982. Geochemical prospecting for thorium and uranium deposits. Elsevier Scientific Publication Company.
82. BRADSHAW, P.M.D., CLEWS, D.R. AND WALKER, J.L. 1980. Exploration Geochemistry (2nd edition) Part 8, pp50-54.
82. BRAITSCH, O. 1971. "Solid deposits, their origin and composition. Springer-Verlag, Berlin, 297pp.
83. BRAMLETT, L.B., REYHER, S.L. AND SOUTHARD, G.G. 1983. Uranium Geology and Geochemistry, Copper Mountain, Wyoming: AIMI Trans. 272, 1891-1901.
84. BREGER, I.A. 1974. The role or organic matter in the accumulation of uranium. IAEA 74, pp99-124.

85. BRINCK, J.W. 1974. The geochemical distribution of uranium as a primary criterion for the formation of ore deposits. Proceedings of a symposium on formation of uranium ore deposits. IAEA, STI/PUB/374, Vienna, p21-32.
86. BRIOT, P. 1984. Surficial uranium deposits in Somalia. In: Surficial Uranium Deposits, IAEA, Tec. Doc. 322, 217-220.
87. BRISTOW, Q. AND KILLEEN, P.G. 1982. Natural-gamma spectral logging using scintillation detectors. OECD/NEA/IAEA, Paris, 77.
88. BROOKINS, D.G., DELLA VALLE, R.S. AND BALAGNA, J.P. 1979. Trace element exploration geochemistry of uranium occurrences in the San Juan Basin, South-western U.S. (Abstr.) Geol. Soc. Am. Abstr. with programs.
89. BROOKS, R.R., BAKER, A.J.M., RAMAKRISHNA, R.S. AND RYAN, D.E. 1985. Botanical and geochemical exploration studies at the Suruwila Copper-Magnetite prospect in Sri Lanka.
90. BROOKS, R.A., AND CAMPBELL, J.A. 1976. Preliminary investigation of the elemental variation and diagenesis of a tabular uranium deposit. La Sal Mine, San Juan County, Utah. U.S. Geol. Surv. Open File Rep. 76-287, 30pp.
91. BROOKS, R.R. 1972. Geobotany and Biogeochemistry in Mineral Exploration. Harper and Row.
92. BROWN, E., SKONGSTAD, M.W. AND FISHMAN, M.J. 1970. Techniques of Water Resources Investigations of the United States Geological Survey. U.S. Government Printing Office, Washington, D.C. 160p.
93. BRYNARD, H.J. AND ABDREOLI, M.A.G. 1985. An overview of the regional, geochemical and structural setting of the uraniferous granites in the Damara Orogen, South-west Africa/Namibia. In: Recognition of Uranium Provinces. Proceeding of an IAEA Tec. Committee Meeting, London, 18-20 September.
94. BRYNARD, H.J. 1983. Fission-track studies of uranium distribution in geological samples. Spec. Publ. Geol. Soc. S. Afr., 7: 413-417.
95. BUBULIS, D. 1979. New techniques in uranium exploration. Can. Min. J. April, pp35-42.
96. BUGROV, V. 1974. Geochemical sampling techniques in the Eastern Desert ofEgypt. J. Geochem. Explor., 3, 67-75.
97. BURDON, D.J. 1961. Groundwater Development and Conservation in Syria. Final Report, FAO Puch, Rome.
98. BURNS, R.G. AND FYFE. 1966. Distribution of elements in geological processes. Chemical Geology 1(1): 49-56.
99. BUSHINSKIY, G.I. 1964. On shallow water origin of phosphorite sediments: in the Turayf region, northern Saudi Arabia. U.S. Geol. Surv. Prof. paper, 600C, p4.
100. BUTT, C.R.M. 1985. Major uranium provinces : Yilgarn Block and Gascoyne Province, Western Australia. In: Recognition of Uranium Provinces. Proceedings of an IAEA Tec. Committee Meeting, London 18-20 Sept.

101. BUTT, C.R.M., MANN, A.W. AND HORWITZ, R.C. 1984. Regional setting, distribution and genesis of surficial uranium deposits in calcretes and associated sediments in Western Australia. In: Surficial Uranium Deposits, IAEA, Tec. Doc. 322, Vienna, 121-128.
102. BUTT, C.R.M. AND WILDING, I.G.P. 1976. Geochemical exploration special publication.
103. BUTZ, T.R. (1977). Uranium geochemical survey of the Crystal City-Beville quadrangles, Texas. U.S. Dept. Energy, Open File Report GJBX-(77) 77, p99-132.
104. BUTZ, T.R. 1977. Groundwater sampling in uranium reconnaissance. DoE Open File Rep. GJBX (77), 93-98.
105. CAMERON, E.. (Ed). 1983. Uranium exploration in Athabasca basin, 310pp. Saskatchewan Energy and Mines Geological Survey of Canada, Ottawa, Canada.
106. CAMERON, E.M., BECK, L.S. AND DARNLEY, A.G. 1983. Introduction: In E.M. Cameron (Ed) Uranium Exploration in Athabasca Basin.
107. CAMERON, E.M. 1980. Geochemical exploration for uranium in northern lakes. In: R.H. Carpenter (ed). J. Geochem. Explor. V. 13, p221-250.
108. CAMERON, E. 1976. Uranium in Calcrete Environment Western Australia, 47th ANZAAS Congress, Hobart.
109. CAMERON, E. 1976. Geochemical reconnaissance for uranium in Canada: Notes on methodology and interpretation of data. Geol. Surv. Canada paper 76-1C, p229-236.
110. CAMERON, E.M. AND HORNBROOK, E.H.W. 1976. Current approaches to geochemical reconnaissance for uranium in the Canadian Shield, IAEA-SM-208/31, p241-264.
111. CAMERON, E.M., BECK, L.S. AND DARNLEY, A.G. 1982. A review of exploration research and development projects in the NEA/IAEA Athabasca Basin test area. Saskatchewan. Proc. OCED/NEA/IAEA, Paris, 909-931.
112. CAMERON, E. AND FLETCHER, C.I. 1976. "Yeelirrie". In: Smith et al (eds). Surficial Mineral Deposits and Exploration Geochemistry. Yilgarn Block, Western Australia. 25th Int. Geol. Cong. Excursion Guide 41C, 41-45.
113. CAMERON, E., MAZZUCHELLI, R.H. AND ROBBINS, T.W. 1980. Yeelirrie Calcrete Uranium Deposits, Murchison Region, Western Australia. In: Butt, C.R.M. and Smith, R.E. (eds). Conceptual Models in Exploration Geochemistry, Journal of Geochemical Exploration, Vol. 12, pp350-353.
114. CANNON, H.L. 1964. Geochemistry of Rocks and Related Soil and Vegetation in the Yellow Cat. Area, Grant County, Utah. U.S. Geol. Surv. Bull., 1976: 1-127.
115. CARELLA, R. AND SCARPA, N. 1962. Geological results of exploration in Sudan by AGIP Mineraria. 4th Arab Petrol. Congr., 5-12 Nov. 1962, 23H. Beirut, Lebanon.
116. CARLISLE, D. 1984. Surficial uranium occurrences in relation to climate and physical setting. In: Surficial Uranium Deposits. IAEA, Tec. Doc., 322, 25-35.

117. CARLISLE, D. 1983. Concentration of Uranium and Vanadium in Calcretes and Gypcretes. In: Wilson, R.C.L. (ed). Residual Deposits : Surface Related Weathering Processes and Materials. Geol. Soc., London, 258.
118. CARLISLE, D., MERIFIELD, P.M., ORME, A.R.R., KOHL, M.S. AND KOLKER, O. 1978. The distribution of clacretes and gypcretes in South Western United States and their uranium favourability based on a study of deposits in Western Australia and South-West Africa (Namibia). U.S. Dept of Energy, Open File Rpt. GJBX-29 (18), 274.
119. CATHCART, J. 1978. Uranium in phosphate rock, U.S.G.S. prof. paper, 988-B, A1-A6.
120. CATHELINEAU, M., CHAROY, B., CUNEY, M., DUBESSY, J., LEROY, J., NGUYENTRUNG, C., POTY, B., ROMBOZ, C. AND WEISBROD, A. 1985. Contrasting behaviour of U and Sn-W at the hydrothermal stage in the West-Hyrcynian Chain : an interpretation in the light of mineralogy, fluid inclusion chemistry, solubility and speciation data. In: Concentration mechanism of U in geological environments. Int. Meeting, Nancy.
121. CHAMBERLAIN, J.A. 1964. Hydrogeochemistry of Uranium in the Bancroft-Halibration Region, Ontario. Geol. Surv. Can. Bull., 118.
122. CHARLET, J.M., DUPUIS, C.H., QUINIF, Y., BOUKO, P.H. AND LAIR, P.H. 1982. Natural thermoluminescence of quartz and feldspars, application of a new method in U exploration. OECD/NEA/IAEA, Paris, 545.
123. CHATTERJEE, A.K. AND STRONG, D.F. 1984. Discriminant and factor analysis of geochemical data from granitoid rocks hosting the Millet Brook, uranium mineralizations, South Mountain Batholith, Nova Scotia, Uranium, 1. 289-305.
124. CHENEVART, C. 1950. Problems de la geologie du petrole. A propos de l'usage des cartes a isopaques : quelques faits observes dans le Cretace de la Palmgrene, Syrie. mein. Soc. Vaudaise Sci. Nat. No. 61, V. 9, No. 4, 34p.
125. CHILD, D. 1973. The essentials of factor analysis in geology : Holt, Rinehart and Winston, London, 107pp.
126. CHRISTOPHER, D.A. AND KALNINS, T. 1977. Exploration for basal type uranium deposits in British Colombia. Western Miner., 50, pp75-79.
127. CHU, L.H., CHAND, F.C. AND AHMED, J. 1984. Favourable geological environments for uranium mineralization, peninsular Malaysia. J. Geochem. Explor. V. 20, No. 2, p205-219.
128. CLARKE, R.S. AND YOUNG, E.J. 1958. Geochemistry of Uranium in apatite and phosphorite. U.S. Geological Survey. Prof. paper 314-D. 90p.
129. CLOSS, L.G. AND NICHOL, I. 1975. The role of factor and regression analysis in the interpretation of geochemical reconnaissance data. Can. J. Earth Sci., 12 : 1316-1330.
Econ. Geol. Vol. 74, 315-330.
130. COKER, W.B. 1980. A geological orientation for uranium of the Montreal river area, District of Algoma, Ontario. Geol. Surv. Can. Paper 79-18, 27.

131. COKER, W.B. AND NICHOL, I. 1975. Metal dispersion in lake sediments related to mineralization and its use in reconnaissance in northern Ontario. In: I.L. Elliot and W.K. Fletcher (eds)., Geochemical Exploration, 1974, Elsevier, Amsterdam, pp549-553.
132. COLE, M.M. 1985. Simple remote sensing in prospecting for gold, uranium and base metals in desert areas in Australia and Africa : Some case studies. In: Prospecting in Areas of Desert Terrains.
133. COMTE, D., BLACHERE, H. AND VARLET, M. 1985. Geological environment of uranium deposits in the Perrman of Lodeve Basin, France. In: IAEA, Tec. Doc. - 328, 69-82, Vienna.
134. CONDIE, K.C. 1978. Geochemistry of Proterozoic Granitic Plutons from New Mexico, U.S.A. Chemical Geology, 21, p.131-149.
135. CONDIE, K.C. 1976. "Plate Tectonics and Crustal Evolution", Pergamon, 288pp.
136. COOK, P. AND MCELHINNY. 1979. A re-evaluation of the spatial and temporal distribution of sedimentary phosphate deposits in the light of plate tectonics.
137. COOK, P.J. 1972. Petrology and geochemistry of the phosphate deposits of northwest Queensland, Australia. Econ. Geol. V. 67, 1193-1213.
138. CORDFUNKE, E.H.P. 1969. The Chemistry of Uranium, Elsevier publ. Co., Amsterdam, 250p.
139. CORNELIUS, K.D. 1976. Preliminary rock type and genetic classification of uranium deposits. Econ. Geol. V. 71, 941-943.
140. COWART, J.B. AND OSMOND, J.K. 1977. Uranium isotopes in groundwater: their use in prospecting for sandstone type uranium deposits. J. Geochem. Explor. 8: 365-379.
141. CULBERT, R.R., BOYLE, D.R. AND LEVINSON, A.A. 1984. Surficial Uranium Deposits in Canada. In: Surficial Uranium Deposits, IAEA, Tec. Doc. 322, 179-192.
142. CULBERT, R.R., LEIGHTON, D.G. 1978. Uranium in Alkaline Waters - Kanagan Area, B.C., CIM Canadian Inst. of Mining and Metallurgy Bulletin, 71, No. 793.
143. CUNEY, M. 1985. Physicochemical parameters controlling accessory minerals paragenesis in granitic rocks. In: Concentration Mechanisms of Uranium in Geological Environments, Int. Meeting, Nancy, 2-5 Oct. 1985.
144. CUNEY, M. 1982. Comportement de l'uranium et du thorium au course du metamorphisme progressif. In: Uranium Exploration Methods, OECD-NEA/IAEA, Paris. 217-218.
145. CUNEY, M. 1978. Geological environment, mineralogy and fluid inclusions of Bois Nois - Limouzat Uranium Vein, Forez, France Econ. Geol., 73, 1567-1610.
146. DAHLKAMP, F.J. 1979. Uranium exploration techniques - their applicability and limitations. Inst. of Uranium, London, 1979.
147. DAHLKAMP, F.J. 1978. Classification of uranium deposits. Min. Deposita, 13, 83-104.
148. DAHLKAMP, F.J. 1977. Geochronological - Metallogenetic correlation of uranium mineralization. IAEA, Tec. Doc., 25/8, Vienna.

149. DALL'AGLIO, M., GRAGNANI, R. AND LOCARDI, E. 1974. Geochemical factors controlling the formation of the secondary minerals of uranium. In: Formation of Uranium Ore Deposits, IAEA, Athens (1974) 33-40.
150. DALL'AGLIO, M. 1971. A study of the Circulation of Uranium in the Supergene Environment in the Italian Alpine Range : Geochim. et Cosmochim. Acta, V. 35, p.47-59.
151. DANIELSSON, A., RONNHOLM, B. AND KJELLSTROM, L.E 1973. Fluorometric method for the determination of uranium in natural waters. Talanta, 20 : 185-192.
152. DARNLEY, A.G. 1985. Geophysical and geochemical maps pertinent to Athabasca and Elliot Lake uranium deposits. In: Recognition of Uranium Provinces. Proceedings of an IAEA Tec. Committee meeting, London, 18-20, Sept.
153. DARNLEY, A.G. 1975. Geophysics in Uranium Exploration. Geol. Surv. Can. Paper, 75-26, p21-31.
154. DARNLEY, A.G., CHARBONNEAU,B.W. AND RICHARDSON, K.A. 1977. Distribution of uranium rocks as a guide to the recognition of uraniferous regions. In: Recognition and Evaluation of Uraniferous Areas, IAEA, Vienna, STI/PUB/450 p55-86.
155. DARNLEY, A.G., CAMERON, E.M. AND RICHARDSON, K.A. 1975. The Federal-Provincial Uranium Reconnaissance Programme. In: Uranium Exploration 75; Geol. Surv. Canada paper 75-26, p49-68.
156. DAVIDSON, C.F. AND BOWIE, S.H.U. 1956. Methods of prospecting for uranium and thorium. In: Proc. Int. Conf. Peaceful Uses Atom. Energy, Geneva, 1955 (New York : U.N., 1956 Vol. 6, 659-662.
157. DAVIDSON, C.F. AND ATKIN, D. 1953. On the Occurrence of Uranium in Phosphate Rock. In: Internat. Geol. Congr. 19th 1952, Sect. 11 : 14-31.
158. DAVIDSON, C.F. AND BOWIE, S.H.U. 1951. On thucholite and related hydrocarbon-uranium complexes. Bull. Geol. Surv. Gt. Britain, 3, 1-19.
159. DAVIS, J.C. 1973. Statistics and data analysis in Geology. John Wiley and Sons, 549pp.
160. DEANE, K. AND SMITH, J.R. 1984. Uranium mineralogy. In: Uranium Geochemistry, Mineralogy, Geology, Exploration and Resources. De Vivo et al (eds), Instn. Min. Metall. London, 1984, 43-88.
161. DEER, W.A., HOWIE, R.A. AND ZUSSMAN, J. 1964. Rock forming minerals (phosphates) : Longmans, London, Vol. V, p323-338.
162. DELANEY, M.L. AND BOYLE, E.A. 1983. Uranium and Thorium Concentration in Foraminiferal Calcite. Earth and Planetary Science Letters, Vo. 62, No. 2.
163. DELANY, A.C. AND FLEISCHER, R.L. 1978. Increase in uranium concentration in stream draining rocky flats, Colorado. J. Geochem. Explor., 9: 53-62.
164. DEMET'YEV, V.S. AND SYROMYATNIKOV, N.G. 1968. Condition of formation of a sorption barrier to the migration of uranium in an oxidizing environment. Geochem. Int. 1(3) : 394-400.
165. DENSON, N.M., ZELLER, H.D. AND STEPHENS, J.D. 1956. Water sampling as a guide in the search for uranium and its use in evaluating widespread volcanic units as potential source beds for uranium : U.S. Geol. Survey, prof. paper 300p, 673-680.

166. DEUTSCHER, R.L., MANN, A.W. AND GIBLIN, A.M. 1980. Groundwater geochemistry in the vicinity of the Jabiluka deposit. In: Uranium in the Pine Creek Geosynetine, Ferguson and Goleby (eds). IAEA, Vienna, 477-486.
167. DE VOTO, 1984. Uranium exploration. In: Uranium Geochemistry Mineralogy, Geology, Exploration and Resources. De Vivo et al (eds). Instn. Min. Metall. London, 101-108.
168. DEWEY, J.F. 1977. Episodicity, Sequence and Style at Convergent Plate Boundaries. In: Strangway, D.W. (ed). The Continental Crust and its Mineral Deposits. Geol. Assoc. Can. Spec. paper. 20 : 553-573.
169. DEWEY, J.F. AND BURKE, K.C. 1973. Tibetan, Variscan and Precambrian Basement Reactivation : Products of Continental Collison. J. Geology 81 : 683-692.
170. DICKSON, B.L. 1984. Uranium series disequilibrium in the carnotite deposits of Western Australia. In: Surficial Uranium Deposits. IAEA, Tec. Doc. 322.
171. DICKINSON, W.R. 1980. Plate tectonics and key petrologic associations. In: Strangway, D.W. (ed) The Continental Crust and its Mineral Deposits. Geol. Assoc. Can. Spec. Paper 20 : 341-360.
172. DIXON, C.J. AND PEREIRA, J. 1974. Plate tectonics and mineralization in the Tethyan Region, Mineral Deposita, Vol. 9, p185-198.
173. DODD, P.H. 1976. Uranium exploration technology. In: Geology Mining and Extractive Processing of Uranium. Instn. Min. Metall. London, 1976. 158-171.
174. DODSON, R.G. 1972. Some environments of formation of uranium deposits. In: Bowie et al (eds). Uranium Prospecting Handbook, London, IMM, p33-44.
175. DODSON, R.G., NEEDHAM, R.S., WILKES, P.G., PAGE, R.W., SMART, P.G. AND WATCHMAN, A.L. 1974. Uranium mineralization in Rum Jungle Alligator Rivers Province, Northern Territory Australia. In: Formation of Uranium Ore Deposits : Vienna IAEA, p551-568.
176. DOI, K., SHUICHIRO, H. AND SAKAMAKI, Y. 1975. Uranium mineralization by groundwater in sedimentary rocks, Japan : Econ. Geol., V. 70, p628-646.
177. DOOLEY, J.R. Jr., TATSUMOTO, M. AND ROSHOLT, J.N. 1964. Radioactive disequilibrium studies of roll features, Shirley Basin, Wyoming : Econ. Geology, V. 59, No. 4 p586-595.
178. DONGARRA, G. 1984. Geochemical behaviour of uranium in the supergene environment. In: Uranium Geochemistry, Geology Mineralogy, Exploration and Resources. De Vivo et al (eds) Instn. Min. Metall., London, 18-22.
179. DUBERTRET, L. 1965. Carte geologique de la Syrie et du Liban au 1 : 1000,000^{e} Beyrouth, 1965.
180. DUBERTRET, L. 1933. La tectonique de la Syrie Septentrionale a la fin du Cretace et au debut du Tertiaire. Notes et mem. Syrie et Liban, 1933, 1.
181. DUBERTRET, L., KELLER, A. AND VAUTRIM, H. 1932. Contribution a' l'etude de la region desertique Syrienne. C.r. Acad. Sci., Paris, 194, p1000-1002.

182. DUBERTRET, L., KELLER, A. AND VAUTRIM, H. 1932. Contribution a la geologie de la Djezireh. Cr. Acad. Sci., Paris, 194.
183. DUBERTRET, L. 1933. Sur la structure de lacote oriental de la Metiterranee. Cr. 4 Acad. Sci., Paris, 1933. 197, p458.
184. DUBRETRET, L. 1930. Note preliminaire sur la structure geologique des Etat du Levant sous Mandat francais. C.R. Somm. Soc. Geol. Fr., 1930, 30, No. 6, p43-45.
185. DUBERTRET, L. 1932. Les formes structurales de la Syrie et de la Palestine; leur origine. C.R. Acad. Sci., Paris, 1932, 194, p1964-1966.
186. DUBERTRET, L. 1932. Les formes structurales de la Syrie et de la Palestine; leur origine, C.R. Acad. Sci., Paris, 1932, 195, p66-68.
187. DROVENIK, F. 1957. Possibilite de prospection pour l'uranium en Syrie. Report D.G.S.M.R., 127, S.A.R.
188. DUNN, C.E. 1983. Uranium geochemistry of the NEA/IAEA Athabasca test area. In: Cameron (ed)., Uranium Exploration in Athabasca Basin. Saskatchewan Energy and Mines Geol. Survey
189. DUNN, C.E. 1982. The massive Wallastone Uranium Biogeochemical Anomaly in the Boreal Forest of Northern Saskatchewan, Canada. OECD/NEA/IAEA, Paris, 477- .
190. DURAY, J.R. 1982. Direct-uranium Logging : Neutron-based techniques. In: Uranium Exploration Methods, OECD/NEA/IAEA Paris, 793-806.
191. DYCK, W. 1983. Geochemical studies of lakes near the Midwest and McClean uranium deposits. In: Cameron (ed)., Uranium Exploration in Athabasca Basin, Saskatchewan, Energy and Mine Geol. Survey, 1983.
192. DYCK, W. 1980. Uranium, radon, helium and other trace elements and gases in well waters of parts of the St Lawrence Lowlands, (Ottawa region), Canada, Journ. Geoch. Explor. V.13, No. 1, p27-39.
193. DYCK, W. 1980a. Regional well water geochemical reconnaissance data, Cypress Hills, Saskatchewan, Geol. Surv. Canada, Open File 678.
194. DYCK, W., WHITAKER, S.H. AND CAMPBELL, R.A. 1976. Well water uranium reconnaissance, southwestern Saskatchewan, In: Report of Activities, Part C, Geol. Surv. Can., paper 76-1C, p249-253.
195. DYCK, W. 1975. Geochemistry applied to uranium exploration : "Uranium Exploration" 75, Geol. Surv. Can. paper 75-26, p33-47.
196. DYCK, W. 1974. Geochemical studies in the Surficial Environment of Beaverlodge area, Saskatchewan : Canada Geol. Surv. Can. paper 74-32, 30p.
197. DYCK, W. 1968. Radon-222 emanations from a uranium deposit, Econ. Geol. V. 63, p288-289.
198. EARLE, S.A.M. AND DREVER, G.L. 1983. Hydrogeochemical exploration for uranium within the Athabasca basin Northern Saskatchewan. In: G.R. Parslow (ed), Geochemical Exploration 1982, J. Geochem. Explor., 19 : 57-73.
199. EDMUNDS, W.M. 1977. Groundwater geochemistry control and process. Water Research Centre, Medmenham, England. 115-147.

200. EJEL, F. 1968. Etude geologique et micropaleontologique du Cretace Superieur et du Paleogene dans la Region de Damas. Theses de Doclorate, Faculte de Paris CNRS No. 2225 (unpublished).
201. EK, J. 1982. Uranium in soil, forest litter and living plant material above three urnium mineralizations in northern Sweden. OECD/NEA/IAEA, Paris, 465- .
202. ERDMAN, J.A. AND HARRACH, G.H. 1981. Uranium in big sagebrush from western U.S. and evidence of possible mineralization in the Owyhee Mountains of Idaho. J. Geochem. Explor., 14, 81-94.
203. EVARHART, D.L. 1985. Tectonic settings of the world's sandstone-type uranium deposits. IAEA Tec. Doc. 328, Vienna 21-46.
204. EWERS, G.R., NEEDHAM, R.S., STUART-SMITH, P.G. AND CRICK, I.H. 1985. Geochemistry of Low-grade Early Proterozoic Sedimentary Sequence in the Line Creek Geosyncline, Northern Territory. Aust. Jour. Earth. Sci.
205. EWERS, G.R., FERGUSON, J. AND DONNELLY, T.H. 1983. The Nabarlek uranium deposit - petrology, geochemistry and some constraints on genesis. Econ. Geol. 78, 823-837.
206. FARADZHEV, V.A. AND LONIKA, R.P. 1966. The geological map of Syria, 1:200,000. Explanatory notes, sheet I-37 XIV (Al Qaryatein) (Technoexport, USSR, 1966).
207. FARRELL, B.L. 1984. The use of "Loan" concentrate in geochemical exploration in deeply weathered arid terrains. J. Geochem. Explor., 22 : 101-118.
208. FAUTH, H. 1973. Hydrogeochemical reconnaissance prospecting Uranium Exploration Methods. IAEA, Vienne, p209-218. Univ. California Press, 605p.
209. FELMLEE, J.K. AND CADIGAM, R.A. 1979. Radium and uranium concentrations and associated hydrogeochemistry in groundwater in southwestern Pueblo County, Colorado U.S. Geol. Surv., Open File, Rep. 79-974 : 54pp.
210. FERGUSON, J. 1985. The Uranium Cycle. In: Recognition of Uranium Provinces. Proceeding of an IAEA Tec. meeting, London 18-20 September.
211. FERGUSON, J. AND WINER, P. 1980. Statistical treatment of whole-rock chemical data. Proceedings of the International Uranium Symposium on the Pine Creek Geosyncline.
212. FINCH, W.I. 1985. Sandstone-type uranium deposits - Summary and Conclusions. In: Geological environment of sandstone type uranium deposits. IAEA, Tec. Doc. 328, Vienna 401-408.
213. FINCH, W.I. 1985b. Map and index list of sandstone type uranium deposit in North America, IAEA Tec. Doc. 328, Vienna.
214. FINCH, W.I. 1985c. Map and index list of sandstone type uranium deposits in South America. IAEA Tec. Doc. 328, Vienna.
215. FINCH, W.I. 1967. Geology of epigenetic uranium deposits in sandstone in the United States. U.S. Geol. Surv. prof. paper. 538, 121pp.
216. FIX, P.F. 1956. Hydrogeochmical exploration for uranium. U.S. Geol. Surv. Prof. paper 300, p667-671.

217. FLASCHER, M. AND ALTSCHULER, Z.S. 1969. The relationship of the rare earth composition of minerals to geological environment. Geochem. et Cosmochim. Acta, 33, p725.
218. FLEISCHER, R.L., PRICE, P.B. AND WALKER, R.M. 1975. Nuclear tracks in solids : principles and applications.
219. FORD, I.A. 1951. Radioactivity of rock, an improvement in the photographic technique. Nature, Vol. 167, p273-275.
220. FRASER, W.J. 1980. Geology and exploration of the Rum Jungle uranium field. In: Uranium in the Pine Creek Geosyncline, Ferguson and Coleby (eds) IAEA Vienna, 287-298.
221. FRASS, O. 1977. Juraschichten am Hermon. Neues Jahrb Mineral, 1877, p17-30.
222. FRIEDMAN, G.M. 1964. Early diagenesis and lithification in carbonate sediments : J. Sediment Petrol., 34 : 777-813.
223. FRIEDMAN, G.M., GEBELEIN, C.D. AND SANDERS, J.E. 1971. Miorite envelopes of carbonate grains are not exclusively ofphotosyntehtic algal origin. Sedimentology, 16 : 89-96.
224. FRONDEL, C. 1958. Systematic mineralogy of uranium and thorium. Bull. U.S. Geol. Surv. 1064, 400p.
225. FYFE, W.S. 1979. The geochemical cycle of uranium. Phil. Trans. R. Soc. London. A291, 433-445.
226. GABELMAN, J.W. 1977. Origin and taphrogenic uranium concentration. In: Recognition and Evaluation of Uraniferous Areas. Proceedings of an IAEA Tech. Committee meeting, Vienna, 1975.
227. GABELMAN, J.W. 1977. Remote sensing in uranium exploration. In: Recognition and Evaluation of Uraniferous Areas. Proceedings of an IAEA Tech. Committee meeting, Vienna, 1975.
228. GABELMAN, J.W. 1977. Migration of Uranium and Thorium - Exploration Significance. AAPG Pub. No. 3, Tulsa, Oklahoma, U.S.A.
229. GABELMAN, J.W. 1975. Sedimentary and Uranium Prospecting : Sediment. Geol. V. 6, No.3, p145-186.
230. GALAKTIONOV, A.B., FARADZHEV, V.A., KAZMIN, V.G. AND MIKHAILOV, I.A. 1967. The geology of Syria Part II. Explanatory Notes. Mineral deposits and underground water resources (Technoexport, USSR).
231. GALLAGHER, M.L. 1972. Exploration for uranium in the Northern Highlands of Scotland : a case history. In: Uranium Prospecting Handbook, Bowie et al. (eds). Inst. Min. Metall., London 313-319.
232. GALLOWAY, W.E. 1985. The depositional and hydrogeologic environment of Tertiary uranium deposits, South Texas Uranium Province. In: Geological Environment of Sandstone type Uranium Deposits, IAEA Tec. Doc. 328, Vienna 199-214.
233. GALLOWAY, W.E. 1978. Uranium mineralization in a costal-plain fluvial aquifer system: Catahoula Formation, Texas. Econ. Geol. Vol. 73, pp1655-1676.
234. GAMBLE, D.S. 1984. The Lake Raeside Uranium Deposit : In: Surficial Uranium Deposits. IAEA, Tec. Doc. 322, Vienna, 141-148.
235. GANDHI, S.S. 1978. Geological setting and genetic aspects of uranium occurrences in the Kaipokok Bay-Big River Area, Labrador. Econ. Geol., 73 : 1492-1522.

236. GARFUNKEL, Z. 1981. Internal structure of the Dead Sea leaky transform (rift) in relation to plate kinnetics. J. Tectonophysics, 80, 81-108.
237. GARFUNKEL, Z., SAK, I. AND FREUND, R. 1981. Active faulting in the Dead Sea rift. Tectonophysics 80, 1-26.
238. GARRETT, R.G., KANE, V.E. AND ZIEGLER, R.K. 1980. The management and analysis of regional geochemical data, Journ. Geochem. Explor. V.13, p115-152.
239. GARRETT, R.G. AND GOSS, T.I. 1979. The evaluation of sampling and analytical variation in regional geochemical surveys. In: J.R. Watterson and P.T. Throbald (eds), Geochemical Exploration 1978, Assoc. Explor. Geochem. Spec. Vol. 7, Toronto, p371-383.
240. GARRETT, R.G. AND LYNCH, J.J. 1976. A comparison of neutron activation delayed neutron counting versus fluorometric analysis in large-scale geochemical exploration for uranium; in Exploration for Uranium Ore Deposits, IAEA, Vienna, STI/PUB/434, p321-334.
241. GARRETT, R.G. 1974. Field data acquisition methods of applied geochem. surveys at the Geological Survey of Canada. Geol. Surv. Can. paper, 74-62:36pp.
242. GARRETT, R.G. 1971. Molybdenum, tungsten and uranium in acid plutonic rocks as a guide to regional exploration, S.E. Yukon, Can. Min. J. V.92, No. 4, p37-40.
243. GASPARINI, P. 1984. History of Radioactivity. In: Uranium, Geochemistry, Mineralogy, Geology, Exploration and Resources. De Vivo et al (eds), London Instn. Min. Metall., 1-11.
244. GASBARRINI, C. AND WILLIAMSON, R.G. 1981. Mineralogy of Uranium Ores. In: Process Mineralogy ed. by Donald M. Hansen & Won C. Park.
245. GASPARINI, C. 1980. The role of the ore microscope and electron microprobe in the mining industry. CIM Bull. 73, p73-85.
246. GEORGE, D.C. 1982. Total count gamma-ray logging : Correcting factors and logging model grade assignments. OECD/NEA/IAEA, Paris, 729.
247. GEORGE, D.C. AND SCOTT, J.H. 1982. Review of magnetic susceptibility logging and its application to uranium exploration. OECD/NEA/IAEA, Paris, 837.
248. GIBLIN, A.M. 1985. Applications of groundwater geochemistry to genesis theories and exploration methods for early Tertiary sediment hosted uranium deposits in Australia. Proceeding of Inter. Meeting Nancy, 2-5 October.
249. GIBLIN, A.M. AND DICKSON, B.L. 1984. Hydrogeochemical interpretation of apparent anomalies in base metals and radium in groundwater near Lake Maurice in the Great Victoria Desert (Abstr.). J. Geochem. Explor. 22: 361.
250. GIBLIN, A.M. AND SNELLING, A.A. 1983. Application of hydrogeochemistry to uranium exploration in the Pine Creek Geosyncline, Northern Territory, Australia. In: G.R. Parslow (ed), Geochemical Exploration 1982, J. Geochem. Explor., 19 : 33-55.

251. GIBLIN, A.M. 1980. The role of clay adsorption in genesis of uranium ores. In: Uranium in the Pine Creek Geosyncline, Ferguson and Goleby (eds). IAEA, Vienna, 521-529.
252. GILE, L.H., PETERSON, F.F. AND GROSSMAN, R.B. 1966. Morphological and genetic sequences of carbonate accumulation in desert soils. Soil Sci., 101:347-360.
253. GINGRICH, J.E. 1983. Radon as a geochemical exploration tool. J. Geochem. Explor. 21 : p19.
254. GINGRICH, J.E. 1981. Simplicity advantage of track etch in exploration; Northern Miner., V. 67, No. 6, pD3-D6.
255. GINGRICH, J.E. 1974. Results from a new uranium exploration mthod; Soc. Min. Eng. A.I.M.E., No. 79-S, 16, 9p.
256. GOLDHABER, M.B. 1979. Origin of marcasite and its implications regarding the genesis of roll-front uranium deposits: U.S. Geol. Surv. Open File Rept. 79-1696, 38p.
257. GOLDHABER, M.B., REYNOLDS, R.L. AND RYE, R.O. 1978. Origin of a south Texas roll-type uranium deposit : II Sulphide petrology and sulphur isotopic studies: ECON. GEOL. V.73, p1690-1705.
258. GOLDHABER, M.B. AND REYNOLDS, R.L. 1977. Geochemical and mineralogical studies of a south Texas roll-front uranium deposit. U.S. Geol. Surv. Open File Rept. 77-821, 34p.
259. GORDON, G.E., RANDLE, K., GOLES, G.E., CORLISS, J.B., BEESON, M.H. AND OXLEY, S.S. 1968. Instrumental activation analysis of standard rocks with high resolution gamma-ray detectors. Geochim. et Cosmochim. Acta 32, 369-396.
260. GOTT, G.B., WOLCOTT, D.E. AND BOWLES, C.G. 1974. Stratigraphy of the Iyan Kara Group and Localization of Uranium Depsoits, Southern Blackhills, South Dakota and Wyoming : U.S. Geol. Survey, Prof. paper 763, 57p.
261. GOVETT, G.J.S. 1983. Rock geochemistry in mineral exploration. In: Handbook of Exploration Geochemistry, G.J.S. Govett (ed), Vol. 3, Elsevier Scientific Publication, Amsterdam, 461p.
262. GOVETT, G.J.S. AND PWA, A. 1981. Regional reconnaissance exploration rock geochemistry for massive sulphides, New Brunswick, Canada. J. Geochem. Explor. V.15, p139.
263. GOUDIE, A. 1973. Duricrusts in tropical and subtropical landscapes : Oxford University Press, 174p.
264. GRAF, D.L. 1960. Geochemistry of Carbonate Sediments and Sedimentary Carbonate Rocks, Illinois State Geological Survey Division. Part II Sedimentary carbonate rocks, Circular, 298, 413p. Part III Minor element distribution, Circular 301, 71p.
265. GRANGER, H.C. AND FINCH, W.I. 1985. The Colorado Plateau Uranium Province, U.S.A. In: Recognition of Uranium Provinces. Proceeding of an IAEA Tec. Committee meeting, London, 18-20 September.
266. GRANGER, H.C. 1978. Some speculations on the genetic geochemistry and hydrology of roll-type uranium deposits: Wyoming Geol. Assoc. Ann. Conf., 30th, Guidebook, p349-361.

267. GRANGER, H.C. 1974. Zoning in the altered tongue associated with roll-type uranium deposits, In: Formation of Uranium Ore Deposits : Vienna, Intern. Atomic Energy Agency, p185-200.
268. GRANGER, H.C. AND WARREN, C.G. 1969. Unstable sulphur compounds and the origin of roll-type uranium deposits Econ. Geol., V.64, p160-171.
269. GRANGER, H.C. 1968. Localization and control of uranium deposits in the Southern San Juan mineral belt, New Mexico - An hypothesis : U.S. Geol. Surv. Prof. paper 600-B, p60-70.
270. GRANGER, H.C. 1966. Ferroselite in a roll-type uranium deposit, Powder River Basin, Wyoming : U.S. Geol. Survey Prof. paper 550-C, pC133-C137.
271. GRANGER, H.C., SANTOS, E.S., DEAN, B.G., AND MOORE, F.B. 1961. Sandstone-type uranium deposits at Ambrosia Lake, New Mexico - an interim report. Econ. Geology V.56, No. 7, p1179-1210.
272. GRANTER, H.C. AND RAUP, R.B. 1969. Geology of uranium deposits in the Dripping Spring Quartzite, Gila County, Arizona : U.S. Geol. Surv. Prof. paper 595, 108p.
273. GRASTY, R.L. 1982. Utilising experimentally derived multi-channel gamma-ray spectra for the analysis of airborne data. OECD/NEA/IAEA, Paris, 653.
274. GRASTY, R.L. 1979. Gamma-Ray Spectrometric Methods in Uranium Exploration - Theory and operational procedures, In: Geophysics and Geochemistry in the Search for Metallic Ores; Peter J. Hood (d), Geological Survey of Canada, Economic Geology Report 31, p147-161.
275. GREGORY, A.F. 1983. Interpretive geological mapping as an aid to exploration in the NEA/IAEA Athabaska test area In: Uranium Exploration in Athabaska Basin, Cameron, E.M. (ed). Saskatchewan Energy and Mines Geol. Surv.
276. GRIFFITHS, J.C. 1971. Problems of sampling in geoscience. Trans. Inst. Min. Metall., Ser. B, 80: 346-356.
277. GRIGORIAN, S.V. ET AL. 1974. On geochemical criteria for rejecting zones of dispersed ore mineralization. In: Criteria for the Interpretation of Geochemical Anomalies, p54-63. Moscow.
278. GRIGORIAN, S.V. 1965. Increasing the depth of prospecting for concealed uranium ore bodies by means of t primary aureol; Sov. Atom. Energy, V.18, I, p57.
279. GRIMALDI, F.S. 1956. The analytical chemistry of uranium and thorium. In: U.S. Geol. Surv. Prof. paper 300, p605-617.
280. GRIMALDI, F.S., MAY, I., FLETCHER, M.H. AND TITCOMB, J. (Compilers). Collected papers on methods of analyses for uranium and thorium, U.S. Geol. Surv. Bull. 1006, 184p.
281. GRIMBERT, A. 1972. Use of geochemical techniques in uranium prospecting. In: Uranium Prospecting Handbook, Bowie et al (eds), Instn. Min. Metall., London, 110-119.
282. GRUTT, E.W. Jr. 1972. Prospecting criteria for sandstone-type uranium deposits. In: Uranium Prospecting Handbook, Bowie et al. (eds). Instn. Min. Metall. London, 47-76.

283. GULBRANDSEN, R.A. 1966. Chemical composition of phosphorites of the phosphoria formation. Geochem. et Cosmochemica Acta, 769-777.
284. GUSTAFSON, L.B. AND CURTIS, L.W. 1983. Post-Kombolgie Metasomatism at Jabiluka Northern Territory, Australia and its significance in the formation of high-grade uranium mineralization in Lower Proterozoic rocks. Econ. Geol. Vol.78, pp26-56.
285. HABASHI, F. 1962. Correlation between the uranium content of marine phosphate and other rock constituents. Econ. Geology, Vol.57, p1081-1084.
286. HALE, M. AND JUBELI, Y. 1985. Multielement drainage reconnaissance of the Ad-Daww Region, Central Syria. In: Prospecting in Areas of Desert Terrain. Instn. Min. Metall., London, p173-182.
287. HALE, M. 1981. Pathfinder applications of arsenic, antimony and bismuth in geochemical exploration. In: A.W. Rose and H. Gundlach (eds), Geochemical Exploration 1980. J. Geochem. Explor., V.15, p307-323.
288. HALL, G.E.M. 1979. A study of the stability of uranium in waters collected from various geological environments in Canada. In: Current Research, Part A, Geol. Surv. Canada, paper - 79-1A, p361-365.
289. HAMBLETON-JONES, B.B., HEARD, R.G. AND TOENS, P.D. 1984. Exploration for surficial uranium deposits. In: Surficial Uranium Deposits, IAEA, Tec. Doc. 322, Vienna, 61-64.
290. HAMBLETON-JONES, B.B. AND CAITHNESS, A. 1984. The application of Landsat imagery for delineating potential surficial uranium deposits in Namibia. In: Surficial Uranium Deposits. IAEA, Tec. Doc. 322, Vienna, 71-79.
291. HAMBLETON-JONES, B.B. 1978. Theory and practice of geochemical prospecting for uranium. Minerals Sci. Engng. Vol.10, No.3.
292. HARSHMAN, E.N. 1972. Geology and Uranium Deposits, Shirley Basin, Wyoming. U.S. Geol. Surv. Prof. paper 745,p82.
293. HARSHMAN, E.N. 1966. Genetic implications of some elements associated with uranium deposits, Shirley Basin, Wyoming, U.S. Geol. Surv. Prof. paper550-C, pC167-173.
294. HARSHMAN, E.N. 1962. Alterations as a guide to uranium ore, Shirley Basin, Wyoming. In: Short papers in Geology, Hydrology and Topography, U.S. Geol. Surv. Prof. paper 450-D, pD8-D10.
295. HARSHMAN, E.N. 1961. Paleotopographic control of a uranium mineral belt, Shirley Basin, Wyoming. In Short papers in Geology, Hydrology and Topography. U.S. Geol. Surv. Prof. paper 424C, pC4-C6.
296. HASKIN, L.A., ET AL. 1966. "Physics and Chemistry of the Earth" L.A. Eyring (ed), Pergamon Press, New York, Vol.7, p167.
297. HATHAWAY, L.R. 1977. Interpretation of uranium content of groundwater in west-central Kansas: Short papers of the U.S. Geol. Surv. Uranium Thorium Symposium - Campbell, J.A. (ed). U.S. Geol. Surv. Circ. 753, p65-66.
298. HAWKES, H.E. AND WEBB, J.S. 1962. Geochemistry in mineral exploration, Harper and Row, New York, 415p.

299. HAWKINS, D.B., HOK, C.I., FORBES, R.B. AND DINKEL, D. 1980. Geology and Geochemistry of Arsenic in water, soil and rock, Fairbanks, Alaska Area. G.S.A. Programmes with Abs. 12 (7) p443.
300. HENDERSON, P. AND WILLIAMS, C.T. 1981. Application of Intrinsic GE Detectors to the Instrumental Neutron Activation Analysis for Rare Earth Elements in Rocks and Minerals. J. Radionanlytical Chemistry V.67, No.2, p445-52.
301. HENSON, F.R.S. 1951. Observations on the geology and petroleum occurrences of the Middle East. Proc. Third World Petrol. Congr. Sect. I, p118-140.
302. HENSON, F.R.S. 1937. Larger foraminerifera from Aintab, Turkish, Syria. Eclogae. Geol. helv. Bale, 30.
303. HEIN, J.R., KOSKI, R.A. AND MORGENSON, L.A. 1982. Uranium and Thorium Enrichment in Rocks from the base of DSDP Hole 465A, Hess Rise, Central Pacific. Chem. Geol., 36:237-251.
304. HENRY, B.H., GARY, C.D. AND JAMES, O.E. 1978. Instrumental Analysis. Allyn and Bacon Inc.
305. HOAG, R.B. AND WEBBER, G.R. 1976. Significance for mineral exploration of sulphate concentrations in groundwaters. Bull. Can. Inst. Min. Metall. 69,86-91.
306. HOERL, A.E. AND KENNARD, R.W. 1980. Ridge regression: Advances, algorithms and applications. Technometrics.
307. HOEVE, J. AND SIBBALD, T.I.I. 1978. Uranium metallogenesis and its significance to exploration in the Athabasca Basin. In: G.E. Parslow (ed), Uranium Explorations Techniques Sask. Geol. Soc., Spec. Publ., 4:161-188.
308. HOFFMAN, S.J. 1983. Geochemical exploration for unconformity-type uranium deposits in permaforest terrain, Hornby Bay Basin, Northwest Territories, Canada. In: G.R. Parslow (ed), Geochemical Exploration 1982. J. Geochem. Explor., 19:11-32.
309. HORNBROOK, E.H.W. AND GARRETT, R.G. 1976. Regional Geochemical Lake Sediment Survey, East-Central Saskatchewan, Canada Geological Survey, Ottawa, paper 75-41.
310. HOSTLER, P.B. AND GARRELS, R.M. 1962. Transportation and precipitations of uranium and vanadium at low temperature, with special references to sandstone-type uranium deposits. Econ. Geol., V.57, p137-167.
311. HOWARD, J.H. III. 1977. Geochemistry of selenium: formation of ferroselite and selenium and selenium behaviour in the vicinity of oxidizing sulphide and uranium deposits. Geochim. et Cosmochim Acta 41: 1665-1678.
312. HOWARTH, R.J. 1984. Statistical applications in geochemical prospecting: a survey of recent developments. J. Geochem. Explor., 21:41-61.
313. HOWARTH, R.J. AND MARTIN, L. 1979. Computer-based techniques inthe compilation, mapping, and interpretation of exploration geochemical data. In: P.J. Hood (ed). Geophysic and Geochemistry in the Search of Metallic ores. Geol. Surv. Can., Econ. Geol. Rep., 31: 545-574.
314. HOWARTH, R.J. AND EARLE, S.A.M. 1979. Application of a generalized power transformation to geochemical data. Mathematical Geology, V.11, No.1, p45-63.

315. HOWARTH, R.J. 1973. The pattern recognition problem in applied geochemistry. In: Geochemical Exploration 1972, M.J. Jones (ed). Inst. Min. Metall. London, p259.
316. HOWARTH, R.J. 1971a. An empirical discriminant method applied to sedimentary-rock classification from major element geochemistry. Math. Geol., 3:51-60.
317. HOWARTH, R.J. 1971b. An empirical discriminant classification of regional stream-sediment geochemistry in Devon and East Cornwall. Inst. Min. Metall. Trans., Sect. B, 80: 142-149.
318. HOWARTH, R.J. AND LOWENSTEIN, P.L. 1971. Sampling variability of stream sediments in broad scale regional geochemical reconnaissance. Tran. Inst. Min. Metall. Ser. B, 80:363-372.
319. HOWER, J. 1961. Some factors concerning the nature and origin of Glauconite. Am. Min. 46, p313.
320. HUNTER, J. AND MICHIE, U. MCL. 1985. Uranium provinces and the exploration industry. In: Recognition of Uranium Provinces. Proceedings of an IAEA Technical Committee Meeting, London, 18-20 Septembr.
321. HUNTING GEOLOGY AND GEOPHYSICS LIMITED. 1975. Mineral Exploration and Development in Syria. "Report on Consultancy".
322. HUSSEIN, H.A.M., ABDEL-GAWAD, A.M., ABDEL-HALIM, A. AND ABDEL GHAFOUR, M. 1961. On the geology and mineralogy of uranium occurrence in the Palmyrian Chain, Syria, 4th Arab Science Congress, Cairo.
323. HUTCHINSON, R.W., AND BLACKWELL, J.D. 1984. Time, Crustal Evolution and Generation of Uranium Deposits. In: Uranium Geochemistry, Mineralogy, Geology, Exploration and Resources. De Vivo et al (eds). Instn. Min. Metall. London, 89-100.
324. INGLESRUD, I., CHOCHOLAK, J. AND STEPHAN, E.F. 1948. Chemical processes to recover U from phosphate rock. U.S. Atomic Energy Comm., B.M.I., JDS-126, 29pp.
325. INTERNATIONAL ATOMIC ENERGY AGENCY. 1985. Geological Environments of Sandstone-type Uranium Deposits. IAEA, Tec. Doc. 328, Vienna.
326. INTERNATIONAL ATOMIC ENERGY AGENCY. 198 . Proterozoic Unconformity and Stratabound Uranium Deposits. IAEA Tec. Doc. 315, Vienna.
327. INTERNATIONAL ATOMIC ENERGY AGENCY. 1984. Surficial Uranium Deposits, IAEA, Tec. Doc. 322, Vienna.
328. INTERNATIONAL ATOMIC ENERGY AGENCY. 1980. Uranium in the Pine Creek Geosyncline, IAEA, Proc. of Inter. Symp. Sydney, 1979, Vienna 1980.
329. INTERNATIONAL ATOMIC ENERGY AGENCY. 1972. Uranium Exploration Geology (proceedings panel, Vienna, 1970), IAEA Vienna.
330. INTERNATIONAL ATOMIC ENERGY AGENCY. 1974. Formation of Uranium Ore Deposits (Proceedings Symp., Athens, 1974), IAEA, Vienna.
331. INTERNATIONAL ATOMIC ENERGYAGENCY. 1976. Exploration for Uranium Ore Deposits (Proc. Symp. Vienna, 1976). IAEA, Vienna, 1976.
332. INTERNATIONAL ATOMIC ENERGY AGENCY. 1977. Recognition and Evaluation of Uraniferous Areas, IAEA, Tec. Committee Meeting, Vienna.

333. IYER ET AL. 1973. Application of Fission Track Registration Technique in the Estimation of Fissile Material ^{235}U content in Natural and Depleted Uranium Samples and Total Uranium in Solutions: Nucl. Instrum. Methods V.109, p453-459.
334. IYER ET AL. 1974. Fission Track Registration in Solid-State Track Detectors Immersed in Fissile-material Solutions. Nucl. Instrum. Methods V. 115, p23-27.
335. JACQUET, R. 1933. Une faune du Miocene moyen dans la vallee du Nahr el Kebir (Nord de Lattaquie, Syrie). Cr. Soc. Geol. Fr., (5e) t.3, p67.
336. JAMES, G.W. 1977. Parts per million determinations of uranium and thorium in geologic samples by X-ray spectrometry and chem., 49: 967-969.
337. JAMES, G.W. AND HATHAWAY, L.R. 1976. Recent advances in analytical methods for determining uranium in natural waters and geological samples. In: Exploration for Uranium Ore Deposits, IAEA, Vienna.
338. JAMES, N.P. 1972. Holocene and Pleistocene Calcareous Crusts (Caliche) Profiles. Criteria for Ruaerial Explosure. J. Sediment Petrol., 42:817-836.
339. JENKS, G.F. 1973. The Evolution and Prediction of Visual Clustering in Maps Symblized with Proportional Circles. Display and Analysis of Spatial Data, p311-327. John Wiley, New York.
340. JONES, T.A. 1972. Regression. Math. Geol. 4: 203-218.
341. JORESKOG, K.G., KLOVAN, J.E. AND REYMENT, R.A. 1976. Geological Factor Analysis. Methods in Geomathematics 1, Elsevier, New York, N.Y. 178pp.
342. JUBELI, Y. AND PARRY, S. 1986. A New Appliction of Neutron Activation Analysis with ^{239}U to Determine Uranium in Groundwaters. J. Radioanal. Chem. (in press).
343. JUBELI, Y. 1982. Radiometric and Geological Investigations in Part of Central Syria. Report 1, AEC, S.A.R.
344. JUBELI, Y., GHALEB, B. AND SANAWBARA, M. 1982. Interpretation of Gamma Logs of 21 Boreholes from the Yarmouk Basin, Syria. Report 2 AEC, S.A.R.
345. JUBELI, Y. 1981. Effectiveness of Selective and Sequential Extraction Techniques in Separating Natural Geochemical Anomalies of Pb and Zn from those associated with Contamination. Unpublished M.Sc Thesis, ITC, Delft, The Netherlands.
346. KAHLE, C.F. 1977. Origin of subaerial holocene calcareous crusts: role of algae, fungi and sparmicritization. Sedimentology, 24: 413-435.
347. KAJITANI, K. 1970. A Geochemical study on the genesis of ningyoite the special calcium uraneous mineral, Econ. Geol. 65, 470p.
348. KANE, V.E., LARSON, N.M. AND NALL, V.C. 1977. A computer program to generate Pearson, Spearman and Kendall Correlations, Union Carl Oak Ridge, Tennessee, K/UR-8. U.S. Dept. of Energy, Grand Junction, Colorado [GJBX-18 (78].
349. KAPLAN, H., UZ, S. AND CETINTURK, I. 1974. Formation of uranium ore deposits. IAEA, pp437-452.
350. KARPOFF, R. 1957. Sur l'existence due Maestrichtien au nord du Djeddeh (Arabie Seondite). C.R. Acad. Sci. Paris, 245: 1322-1324.

351. KATMEH, E. 1968. Report on the possibility of gravels and pebbles found along Homs-Khneifiss-Sawaneh route, 2 volumes, Report GEGMR, 712 and 713, Syria.
352. KATMEH, E. 1969. Preliminary report on outcrop of limestones, semi-marble and coloured rocks in Palymra. Report GEGMR, 755, Syria.
353. KAZAKOV, A.V. 1937. The phosphorite facies and the genesis of phosphorites in geological investigations of agricultural ores. Sci. Inst. Fert. Insecto-Fungic. Trans. (USSR), 142: 95-113.
354. KENNETH, R. APPLIN, AND LANGMUIR, DONALD. 1978. Groundwater Geochemistry as a Prospecting Tool for Uranium Deposits in Pennsylvania. The Pennsylvania State University, Dept of Geosciences, Sepember.
355. KHOURI, J. AND HADJ, M. 1983. Study of the water resources in Ad-Daww Basin (SAR), Part I, ACSAD/DM/T-36, 205p.
356. KHOURI, J. AND DROUBI, A. 1981. Groundwater movement in the fractured carbonate rocks, ACSAD/DM110, 60p.
357. KHOURI, J. AND AGHA, W.R. 1979. Hydrogeological and hydrogeophysical study of soft water intrusion in the Central area of the Dawwa Basin in the Syrian arid zones. ACSAD/HS/P5, Damascus, 27p.
358. KHOURI, J. 1973. Hydrochemical investigations in some arid and semi-arid zones in the Syrian Arab Republic and its aid to groundwater explorations. Porc. Seminar on Groundwater, UNESCO-Foundation of Scientific Research Bagdad.
359. KHOURI, J. 1972. Groundwater in the arid zones of the Syrian Arab Republic: 12th Conf. of Arab Engineers, Cairo.
360. KHOURI, J. 1971. Investigation of groundwater flow system in arid zones. The Arab Engineer, No. 34, Damascus.
361. KHOURI, J. 1970. Hydrogeology in Intermountain Basin. The Arab Engineer, No. 30, Damascus.
362. KHOURI, J. 1966. Problems of groundwater exploitation in desertic areas. The Arab Engineer No. 19, Damascus.
363. KILLEEN, P.G. 1979. Gamma-ray spectrometric methods in uranium geochemistry in the search for metallic ores. P.J. Hood (ed). Geol. Surv. Canada, Econ. Geol. Report 31, pp163-229.
364. KILLEEN, P.G. 1982. Primary Calibration of a Gamma-Ray Spectrometer for the Measurement of Potassium, Uranium and Thorium. Proceeding.
365. KILLEEN, P.G. AND BRISLOW, Q. 1976. Uranium exploration by borehole gamma-ray spectrometry using off-the-shelf instrumentation. In: Exploration for U ore deposits, IAEA, Vienna.
366. KIM, K.H. AND BURNETT, W.C. 1983. Gamma-ray spectrometric determination of uranium-series nuclides in marine phosphorite Analy. Chem. 55, 1796.
367. KIMBERLEY, M.M. (ed). 1978. Uranium deposits, their mineralogy and origin. Mineral. Assoc. Canada. Short Course Handbook, Vol.3.
368. KITANO, Y. AND OOMORI, T. 1971. The coprecipitation of uranium with calcium carbonate. J. Oceanogr. Soc. Jpn. 27.
369. KLEINER, B. AND HARTIGAN, J.A. 1981. Representing points in many dimensions by trees and clusters. J.A.S.A. V.76, p260-269.

370. KLEMINE, H.H. 1958. Regional geology of circum-mediterranean region: Am. Assoc. Petroleum Geologists, V.42, p477-512.
371. KING, J.W. AND AUSTIN, S.R. 1966. Some characteristics of roll-type uranium deposits at Gas Hills, Wyoming: Mining Eng., v.18, p73-80.
372. KOCH, G.S. AND LINK, R.F. 1971. Statistical analysis of geological data, Vol. 2. John Wiley and Sons, New York, N.Y., 438pp.
373. KOCH, R.C. 1960. Activation Analysis Handbook, Academic Press, New York.
374. KOSTOV, I. 1977. Crystallochemical differentiation and localization of uranium ore deposits in the earth's crust (IAEA, Tc - 25/2), Vienna.
375. KOTTLOWSKI, F.E. 1971. Origin of Evaporite. F.E. Kottlowski (Ed.) Reprint from: AAPG Bull. Vol.21, No. 9. 1973.
376. KOVAL, P.V. 1984. The role of regional lithogeochemistry in mineral exploration. In: Geochemical exploration Bjorklund (ed). J. Geochem. Explor. 21: 201-208.
377. KRAL, J. AND BURCHART, J. 1983. Dispersion of uranium in accessory apatite in crystalline rocks and its possible petrogenetic meaning. Earth and Planetary Sci. Lett., 63, p34-40.
378. KRASHENINNKOV, V.A. 1965. Stratigraphie Zonales des depots Daniens. Acad. Sci. URSS. Inst. Geol. Fasc. 133, 5-26 (translation from Russian).
379. KRISCHE, E.U. AND QUIEL, F. 1984. The application of supervised classification to Landsat data in the exploration for surficial uranium deposits - An example from Western Australia. In: Surficial Uranium Deposits. IAEA, Tec. Doc. 322, Vienna, 65-69.
380. KRUGER, P. 1971. Principles of Activation Analysis. Wiley Interscience.
390. KRUMBEIN, W.C. AND GRAYBILL, F.A. 1965. An introduction to statistical models in geology. McGraw-Hill, New York, N.Y., 475pp.
391. KRUMBEIN, W.C. 1960. The "geological population" as a framework for analysing numerical data in geology. Liverpool Manchester Geol. J., 2(3): 341-368.
392. KRUMBIEN, W.C. AND SLACK, H.A. 1956. Statistical Analysis of Low-level Radioactivity of Pennsylvannian Black Fissile Shale in Illinois. Geol. Soc. Am. Bull., 67 (6): 739-762.
393. KRUMBEIN, W.C. AND GARRELS, R.M. 1952. Origin and Classification of Chemical Sediments. J. Geol., 60: 1-33.
394. KUNZENDORF, H., PLUGER, W.L. AND FRIEDRICH, G.H. 1983. Uranium in Pacific deep-sea sediments and manganese nodules. In: Geochemical Exploration 1982. G.R. Parslow (d). J. Geochem. Explor. 19: 147-162.
395. KUNZENDORF, H. AND LOVBORG, L. 1981. Elemental interferences in the analysis of uranium by delayed-neutron counting. In: A.W. Rose and H. Gundlach (eds). Geochemical Exploration 1980. J. Geochem. Explor. 15: 585-595.
396. KUTINA, J. 1981. Concentration of uranium in areas where the Appalachian folded belt is intersected by major east-west trending fracture zones. Global Tect. Metall. 3, 255-275.

397. LANDAIS, P. AND DEPPE, J.M. 1985. A chemical study of the carbonaceous material from the Carswell structure. In: "The Carswell Structure Uranium Deposits, (Saskatchewan) G.A.C. Special Paper 29. R. Laine, D. Alonso and M. Svab (eds.), ppl65-174.
398. LANG, A.H., GRIFFITH, J.W. AND SLEACY, H.R. 1962. Canadian deposits of uranium and thorium. Geo. Surv. Can., Econ. Geol. Sur. No. 16. (second edition).
399. LANGFORD, F.F. 1974. A supergene origin for vein-type uranium ores in the light of the Western Australia Calcrete-carnotite deposits. Econ. Geol., 69, 516-526.
400. LANGMUIR, D. AND CHATHAM, J.R. 1980. Groundwater prospecting for sandstone-type uranium deposits: a preliminary comparison of merits of mineral-solution equilibria, and single element tracer methods. J. Geochim. Explor., 13: 201-219.
401. LANGMUIR, D. 1979. Uranium Resource/Technology Seminar II Colorado S.M.
402. LANGMUIR, D. 1978. Uranium solution-mineral equilibria at low temperatures with application to sedimentary ore deposits. Geochim et Cosmochim Acta 42: 547-569.
403. LARGE, D. 1981. The geochemistry of the sedimentary rocks in the vicinity of the Tom Pb-Zn-Ba deposit, Yukon Territory, Canada. J. Geochem. Explor. V.15, p203- .
404. LEACH, D.L. 1977. Geochemical reconnaissance for uranium in the arid regions of the western United Sates. Symposium on Hydrogeochemical and stream-sediment reconnaissance for uranium in the United States. GJBX-77.
405. LEACH, D.L., PUCHLIK, K.P. AND GLANZMAN, R.K. 1980. Geochemical exploration for uranium in playas. In: R.H. Carpenter (ed), Geochemical Exploration for Uranium. Journal of Geochemical Explor., 13: 251-283.
406. LENIKAN AND THOMSON. 1965. Activation analysis; principles and applications. Academic Press, New York.
407. LE PICHON, X. AND FRANCHETEAU, J. 1978. A plate-tectonic analysis of the Red Sea-Gulf of Aden Area. In: O.H. Oven (ed), Structure and Tectonics of the Eastern Mediterranean. Tectonophysics, 46: 369-406.
408. LEVINSON, A.H. AND COETZEE, G.L. 1980. Implications of Disequilibrium in Exploration for Uranium Ores in the Surficial Environment Using Radiometric Techniques. A Review.
409. LEVINSON, A.A. 1974. Introduction to exploration geochemistry (Calgari, Alberta: Aplied Publishing Ltd.) 612p.
410. LIASCHENKO, K.P. AND TATARNIKOV, A.A. 1968. Estimation of uranium deposits in the territory of the Syrian Arab Republic. Report Dept. Geol. Surv and Mineral Research (Syria).
411. LITTLE, H.W. 1970. Distribution of types of U deposits and favourable environments for U exploration; Proc. Series IAEA, Vienna, p35.
412. LOBATO, L.M., FORMAN, J.M.A., FUZIKAWA, K., FYFE, W.S. AND KERRICH, R. 1983. Uranium in overthrust Archean basement. Bahia, Brazil. Canadian Mineralogist, Vol. 21: 647-654.

413. LOCARDI, E. 1985. Uranium provinces and mantle anomalies. In: Recognition of Uranium Provinces. Proceedings of an IAEA Technical Committee meeting, London, 18-20 September.
414. LOCARDI, E. 1977. Recent volcanic and uranium mineralizations, IAEA - Tec. Doc. 25/5.
415. LOPATKINA, A.P. 1964. Characteristics of migration of uranium in the natural waters of humid regions and their use in the determination of the geochemical background for uranium. Geochem. Int., 4, 788-795.
416. LOVBORG, L. 1972. Assessment of uranium by gamma-ray spectrometry. In: Bowie, S.H.U., Davis, M. and Ostle, D. (eds). Uranium Prospecting Handbook, London, Inst. Min. Metall. ppl57-173.
417. LOVBORG, L., KUNZENDORF, H. AND HANSEN, J. 1968. Use of field gamma spectrometry in the exploration of uranium and thorium deposits in South Greenland. Nuclear Techniques and Mineral Resources, IAEA, Vienna, ppl97-211.
418. LOVELL, J.S., HALE, M. AND WEBB, J.S. 1980. Vapour geochemistry in mineral ekxploration. Mining Magazine, 229-239.
419. LOVELL, J.S., HALE, M. AND WEBB, J.S. 1980. Vapour Geochemistry in Mineral Exploration. Mining Magazine, September.
420. LOVERING, T.G. AND MCCARTHY, J.H. 1978. Conceptual Models in Exploration Geochemistry. The basin and range province of the Western United States and Northern Mexico; J. Geochem. Explor. V.9, No.2/3, pl13-276.
421. LOWENSTEIN, T.K. AND HARDIE, L.A. 1985. Criteria for the recognition of salt-pan evaporites. Sedimentology, 32, 627-644.
422. LUCAS, J. AND PREVOT, L. 1984. Synthese de l'apatite Par Voie baclerienne a partir de matiere organique phosphate et de divers carbonates de calcium dans eaux douce et marine naturelles. Chem. Geol., Vol. 42, No. 1/4, ppl01-118.
423. LUCAS, J. FLICOTEAUX, R., NATHAN, Y., PREVOT, L. AND SHAHAR, Y. 1980. Differential aspects of phosphorite weathering. SEPM, Sp. Pub. 29, 117-137.
424. LUDWIG, K.R., GOLDHABER, M.B., REYNOLDS, R.L. AND SIMMONS, K.R. 1982. U-Pb isotope isochron age and preliminary sulphur isotope systematics of the Felder uranium deposit, south Texas. Econ. Geol., V.77, p557-563.
425. LYON, W.S.Jr. 1964. Guide to Activation Analysis. Published by: Van Nostrand Company.
426. MACKENZIE, A.B., BOWDEN, P. AND KINNARD, J.A. 1984. Combined neutron activation and particle track analysis of element distributions in a rock slice of mineralized granite. J. Radioanal. Chem., 82/2, 341-352.
427. MANCEY, S.J. AND HOWARTH, R.J. 1980. Power-transform-removal of skewness from large data sets. IMM, London.
428. MANN, A. W. AND HORWITZ, R.C. 1979. Groundwater calcrete deposits in Australia: some observations from Western Australia. Journal of the Geological Society of Australia, Vol.26, p293-303.
429. MANN, A.W. AND DEUTSCHER, R.L. 1978. Genesis principles for the precipitation of carnotite in calcrete drainages in Western Australia, Econ. Geol. 73, 1724-1737.

430. MASON, B. 1966. Principles of Geochemistry, 3rd Edition. John Wiley & Sons, New York, 329p.
431. MANSKAYA, S.M. AND DROZDOVA, T.V. 1968. Geochemistry of organic substances. Pergamon Press, Oxford.
432. MARTIN, H., LEFIN, J.P., DEJONGHE, L. AND HENRY, J. 1983. Stream-sediments geochemical prospecting for chromium in the paleozoic of the Belgian Ardennes. In: G.R. Parslow (ed), Geochemical Exploration, 1982. J. Geochem. Explor., 19: 25-26 (Abs.).
433. McARTHUR, J.M. 1984. Francolite geochemistry-compositional controls during formation, diagenesis, metamorphism and weathering. Geochim et Cosmochim Acta, Vol.48.
434. McARTHUR, J.M. 1978. Element partitioning in ferruginous and pyritic phosphorite from the Continental margin off Morocco. Mineralogical Magazine, June 1978, Vol.42, pp221-228.
435. McKELVEY, V.E. AND CARSWELL, L.D. 1956. Uranium in the phosphoria formation. Prof. paper U.S. Geol. Surv. 300, 483-7.
436. McKENZIE, D.P. 1972. Active tectonics of the Mediterranean region. Geophys. J.R. Astron Soc., 30: 109-185.
437. McKENZIE, D.P., DAVIES, D. AND MOLNAV, P. 1970. Plate tectonics of the Red Sea and East Africa. Nature, 226: 243-248.
438. McLENNAN, S.M. AND TYLOR, S.R. 1980. Rare earth elements in sedimentary rocks, granites and uranium deposits of the Pine Creek Geosyncline. In: Uranium in the Pine Creek Geosyncline, Ferguson and Coleby (eds). IAEA, Vienna, 175-190.
439. McMILLAN, R.H. 1978. Genetic aspects and classification of important Canadian uranium deposits. In Short Course in uranium deposits: their mineralogy and origin. M.M. Kimberley (ed.). Toronto: The University Press for Mineralogical Association of Canada, 187-204.
440. McSWIGGEN, P.L., MOREY, G.B. AND WEIBLEN, P.W. Uranium (1986) in early Proterozoic phosphate-rich melasedimentary rocks of East-Central Minnesota. Econ. Geol. Vol. 81, pp173-183.
441. MAHADEVAN, T.M. 1985. Characterization and genesis of the Singhbham uranium province, India. In: Recognition of Uranium Provinces. Proceedings of an IAEA Technical Committee Meeting, London, 18-20 September.
442. MCLENNAN, S.M. AND TAYLOR, S.R. 1980. Thorium and U in sedimentary rocks: crustal evolution and sedimentary recycling. Nature, Vol.285: 621-624.
443. MACMURDO, K.W. AND BOWMAN, W.W. 1977. Assay of fissile materials by a cyclic method of neutron activation and delayed neutron counting. Nucl. Instrum. Methods, 141: 299-306.
444. MELIN, R.E. 1969. Uranium deposits in Shirley Basin, Wyoming: Wyoming Univ. Contr. Geology, V.8, No.2, p143-149.
445. MELIN, R.E. 1964. Description and origin of uranium deposits in Shirley Basin, Wyoming: Ecn. Geol. V.59, p835-849.
446. MELVYN CASCOYNE. 1981. A simple method of uranium extraction from carbonate groundwater and its application to $^{234}U/^{238}U$ disequilibrium. J. Geochem. Explor., V.14: 199-207.

447. MICHEL, D. 1983. Les oxy-hydroxydes de fer: Leur role dans la distribution de l'uranium dans le milieu supergene, These Nancy.
448. MIDDLETON, W.G. 1984. An assessment of the use of hydrogeochemistry in exploration for calcrete uranium in Australia. In: Surficial Uranium Deposits, IAEA, Vienna.
449. MIESCH, A.T. 1977. Logtransformation in geochemistry. Matt. Geol., 9(2): 191-194.
450. MIESCH, A.T. 1976. Geochemical survey of Missouri - methods of sampling, laboratory analysis and statistical reduction of the data. U.S. Geol. Surv., Prof. paper, 954-A, 39pp.
451. MIESCH, A.T. 1975. Variograms and variance components in geochemistry and ore evaluation. In: E.H.T. Whitten (ed), Quantitative Studies in the Earth Sciences. Geol. Soc. Am. Mem., 142: 333-340.
452. MIFFLIN, M.D. 1968. Delineations of groundwater flow systems in Nevada, Desert Research Institute, Technical Report Series H-W, Pub. No.4, Reno, U.S.A.
453. MILANOVKSY, E.E. 1981. Aulacogens of ancient platforms: problems of their origin and tectonic development. In: J.H. Illies (ed), Mechanism of Graben Formation. Tectonophysics, 73: 213-248.
454. MILLARD, H.T. Jr. 1976. Determination of uranium and thorium in USGS standards by the delayed neutron technique. U.S. Geol. Surv. Prof. paper 840, p61-65.
455. MILLER ET AL. 1984. Application of Mineral-Solution Equilibria to Geochemical Exploration for Sandstone-hosted Uranium Deposits in Two Basins in West Central Utah. Econ. Geol. V.79, p266-283.
456. MILLER, J.M. AND LOOSEMORE, W.R. 1972. Instrumental technique for uranium prospecting handbook, London. Inst. of Mining and Metallurgy, p135-146.
457. MILTON, C. 1971. Authigenic minerals of the Green River Formation. Contrib. Geol. (Trona Issue) Univ. Wyoming, 10, 57-63.

458. MOKADDEM, M. AND FUCHS, Y. 1984. Depots Superficiels D'Uranium en Algerie. In: Surficial Uranium Deposits, IAEA, Tec. Doc. 322, Vienna, p107-112.
459. MOON, C.J. 1983. Factors Controlling the Surficial Dispersion of Arsenic, Antimony, Bismuth and Selenium from Mineral Deposits in the British Isles. Unpub. PhD Thesis, Univ. of London.
460. MOON, C.J. 1977. A geological appraisal of the uranium mineralization in the Karoo System (IAEA-Tec.Doc.25/17) Vienna.
461. MOOR, P.J. 1971. Contributions to discussion of paper entitled "Methods of Analysis of Subsurface Waters". "Trans. Inst. Min. Metall. 80: B53-B54.
462. MOTT, L.V. AND DREVER, J.I. 1983. Origin of Uraniferous Phosphatic Beds in Wilkins Peak Member of Green River Formation, Wyoming. Am. Assoc. Petr. Geologists Bull. V.67, No.1: 70-82.
463. MOTTS, W.S. 1958. Caliche genesis and rainfall in the Pecos Valley area of south eastern New Mexico. Geol. Soc. Am., 69: 1737 (Abs.).

464. MOUAQADEH, F. 1964. Summary of deposits of sulphur in Suheira Cave, Palinyra. REport. GEGMR., Syria.
465. MOUAQADEH, F. 1967. A report on prospecting works for sands at Rimayleh-Al-Qaryatein, Report, GEMR., 660, Syria.
466. MOUAQADEH, F. 1968. Opoka occurrence at Al-Housaya and Ghadir El Hamal. Report. GEGMR, 724, Syria.
467. MOUTY, M. 1984. Le Jurassique dans la chaine Palmyrides (Syrie Centrale). 27th Int. Geol. Congr. Moscow-USSR.
468. MOUTY, M. 1978. Donnes nouvelles sur le Jurassique dans la Palmyrides. Syr. Geol. Mag. No.2, p20-22.
469. MOUTY, M. 1973. On the Jurassic rocks in Palmyrid chaine, Arab Scientific Conferences - Cairo.
470. MOUTY, M., EL MALEH, A.K., OTAKI, M., ABOU LABAN, H. AND JUBELI, Y. 1983. Geological studies of selected traverses in the Palmyrides region, Report, GEGMR., Damascus.
471. MURATA ET AL. 1951. Hydration and base exchange properties of carnotites, tynyamanite and related compounds. Am. Mineralogist, V.35, p323-324.
472. NARGOLWALL, S.S. AND PRZYBYLOWICZ, E.P. 1973. Activation analysis with neutron generators. Wiley Interscience Publications.
473. NASH, J.T., GRANGER, M.C. AND ADAMS, S.S. 1981. Geology and concepts of genesis of important types of uranium deposits. In: Skinner, B.J. (ed). Economic Geology Seventy-fifth Anniversary Volume, p63-116.
474. NEAL, J.T. (Ed.). 1975. Playa and dried lakes. Benchmark Paper in Geology Vol. 20, Halsted Press, 399pp.
475. NEAL, J.T. 1975. Playas and dried lakes. Benchmark Papers in Geology 120, U.S. Air Force Weapons Laboratory, 411pp.
476. NEEDHAM, R.S., EWERS, G.R. AND FERGUSON, J. 1985. Pine Creek Geosyncline. In: Recognition of U provinces. Proceedings of an IAEA Technical Committee Meeting, London, 18-20 September.
477. NESBITT, H.W. 1979. Mobility and Fractionation of Rare Earth Elements during Weathering of a Granodiorite, Nature 279: 206-210.
478. NETTERBERG, F. 1971. Calcrete in road construction, Nat. Inst. for Road Research, S. Afr., CSIR Bull. 10 Report, 286, 73.
479. NETTERBERG, F. 1969. The interpretation of some basic calcrete types, S. Afr. Archaeol. Bull., 24, 117-122.
480. NICHOLLS, G.D. 1967. Trace elements in sediments: an assessment of their possible utility as depth indicators. Marine Geol. 5, p539.
481. NICHOLS, C.E. 1984. Uranium exploration technique in De Vivo et al (eds). Uranium Geochemistry, Mineralogy Geology, Exploration and Resources, IMM.
482. NININGER, R.D. 1977. Recognition of uranium districts. In: Recognition and Evaluation of Uraniferous Areas. Proceedings of an IAEA Technical Committee Meeting, Vienna, 1975, 1-11.
483. NOETING, F. 1887. Die Jura am Hermon. Eine geognostische Monographie. Stuttgart.
484. NUR, A. AND BEN AVRAHAM, Z. 1978. The Eastern Mediterranean and the Levant: Tectonics of Continental Collision. Tectonophysics, 46, p297-311.

485. OBIAL, R.C. AND JAMES, C.H. 1973. Use of cluster analysis ingeochemical prospecting with particular reference to southern Derbyshire, England. In: M.J. Jones (ed), Int. Geochem. Explor. Symp. 1972, IMM, London, p237-257
486. OLADE, M.A. AND GOODFELLOW, W.D. 1978. Lithogeochemistry and hydrogeochemistry of uranium and associated elements in the Tombstone Batholite, Yokon, Canada. J. Geochem. Explor., V.
487. OLMSTED, F.H., LOETZ, O.J. AND IRLAN, B. 1973. Geohydrology of the Yuma Ared, Arizona and California. U.S. Geol. Surv. Prof. paper 486-H, 227p.
488. OSTLE, D. 1982. Recognition of uranium provinces. In: Uranium exploration methods, OECD-NEA in collaboration withthe IAEA, Paris, 953-954.
489. OSTLE, D., BALL, T.K. 1973. Some aspects of geochemical surveys for uranium. "Uranium Exploration Methods" (Proc. Panel, Vienna, 1972), IAEA, Vienna, 171.
490. OSTLE, D., COLEMAN, R.F. AND BALL, T.K. 1972. Neutron activation analysis as an aid to geochemical prospecting for uranium. In: Uranium Prospecting Handbook. (S.H.U. Bowie et al (eds)). Inst. of Min. and Metallurgy, London.
491. OSTLE, D. 1954. Geochemical prospecting for uranium. Mining Mag., London, 91, 201-208.
492. OTTON, J.K. 1984. Surficial uranium deposits in the United States of America. In: Surficial Uranium Deposits. IAEA, Tec. Doc. 322, 237-242.
493. OTTON, J.K. AND ZIELINSKI, R.A. 1985. Movement and concentration of uranium in young, organic-rich sediments, Stevens County, Washington. In: Concentration Mechanisms of Uranium in Geological Environments. Inst. Meeting, Nancy.
494. PACER, J.C. 1982. Radon measurement techniques for uranium exploration. OECD/NEA/IAEA, Paris, 495.
495. PAGE, L.R. 1960. The source of U in ore deposits. In: Rep. 21st Int. Geol. Congr., Copenhagen: Berlingske Bogtrykkori, 1960, pt 15, 149-64.
496. PAGEL, M. 1984. Petrology, Mineralogy and Geochemistry of Surficial Uranium Deposits. In: Surficial Uranium Deposits, IAEA, Tec. Doc. 322, 37-44.
497. PAHLAVANPOUR, B., PULLEN, J.H. AND THOMPSON, M. 1980a. Determination of trace concentrations of selenium in soils and sediments by the introduction of hydrogen selenide into inductively coupled plasma source for emission spectrometry. Analyst, 105: 274-278.
498. PAHLAVANPOUR, B., THOMPSON, M. AND THORNE, L. 1980b. Simultaneous determination of trace amounts of arsenic, antimony and bismuth in soils and sediments by volatile hydride generation and inductively coupled plasma spectrometry. Analyst, 105: 756-761.
499. PARAK, T. 1973. Rare earths in the apatite iron ores of Lappland, together with some data about Sr, U, and Th content of these ores. Econ. Geol. 68, p210.
500. PARANOV, V.I. 1956. "Radiometry". Publishing house of the Academy of Sciences, USSR, Moscow.
501. PARRY, S.J. AND JUBELI, Y. 1986. Rapid determination of submicrogram quantities of uranium in geological material by epithermal neutron activation analysis. (In preparation).

502. PARRY, S.J. 1982. Epithermal Neutron Activation Analysis of short-lived Nuclides in Geological Materials. Journal of Radioanalytical Chemistry, Vol.72, No.1-2, p195-207.
503. PARSLOW, G.R. 1985. Basement as a source material for HHP granites: Data from Saskatchewan Shield, Canada. In: HHP Granites, Hydrothermal Circulation and Ore Genesis, a Conference organised by the Instn. Min. Metall., St Austell, Cornwall, 251-262.
504. PARSLOW, G.R. AND GASKARTH, J.W. 1984. Geochemistry of the East Amisk Area. Saskatchewan Energy and Mines, Open File Report, 84-23, pp156.
505. PARSLOW, G.R. 1982. Chemical ages as indicators of regional uranium potential. In: Uranium exploration methods, OECD-NEA, IAEA, Paris, 209-216.
506. PARSLOW, G.R. AND DWAIRI, I. 1977. Precision and accuracy of the fluorometric determination of uranium in lake sediments. In: C.E. Dunn (ed), Uranium in Saskatchewan Sask. Geol. Surv. Spec. Publ., 3: 169-192.
507. PEACOCK, J.D. AND WILLIAMSON, R. 1961. Radon determination as a prospecting technique. Tran. Inst. Min. and Metall., 71, 75-85.
508. PERTLIK, F. ET AL. 1969. Uranium in Handbook of Geochemistry, II-5 Wedepohl K.H. (ed) (Berlin: Springer Verlag), 50p.
509. PERVES, M. 1948. La prehistoire de la Syrie et du Liban. Syrie, 1946-1948, 25 No.1-2.
510. PETERS, W.C. 1978. "Exploration and Mining Geology". John Wiley, New York, 696pp.
511. PETER, G., WHITKOP, E.I. AND DUPONT DE, N. AND COMPANY. 1982. Determination of uranium in aqueous samples by laser-induced fluorescence spectrometry. Anal. Chem., 54, p2475-2477.
512. PIRC, S. AND ROSE, A.W. 1981. Uranium anomalies in paleo-aquifers near sandstone-type uranium deposits in the Devonian Catskill-Formation of Pennsylvania. In: A.W. Rose and H. Gundlach (eds), Geochemical Exploration. J. Geochem. Explor., 15: 219-231.
513. PIRIE, I.E. AND NICHOL, I. 1981. Geochemical dispersion in wallrocks associated with the Norbec deposit, Noranda, Quebec. In: A.W. Rose and H. Gundlach (eds), Geochemical Exploration 1980. J. Geochem. Explor., 15: 159-180.
514. PLANT, J. 1971. Orientation studies on stream-sediment sampling for a regional geochemical survey in Northern Scotland. Trans. Inst. Min. metall. Ser.B. 80:324-345.
515. PLANT, J.A., O'BRIEN, C., TARNEY, J. AND HURDLEY, J. 1985. Geochemical criterial for the recognition of high heat production granite. In: HHP Granites, Hydrothermal Circulation and Ore Genesis, a Conference organised by Instn. Min. Metall., St Austell, Cornwall, p263-285.
516. PLANT, J.A., SIMPSON, P.R., GREEN, P.M., WATSON, J.V. AND FOWLER, M.B. 1983. Metalliferous and mineralized Caledonian granites in relation to regional metamorphism and fracture systems in northern Scotland. Trans. Instn. Min. Metall. (Sect.B) 92, B33-42.

517. PLANT, J.A., BROWN, G.C., SIMPSON, P.R. AND SMITH, R.T. 1980. Signatures of metalliferous granites in the Scottish Caledonides. Trans. Instn. Min. Metall. (Sect. B) 89, B198-210.
518. PLANT, J., GOODE, G.C. AND HERRINGTON, J. 1976. An instrumental neutron activation method for multielement geochemical mapping. J. Geochem. Explor. 6, 299-319.
519. POCHET, R. 1982. Dosumetrie de L'Helium et du radon dans L'eau et dans les sols satures non consolides. OECD/ NEA/IAEA, Paris, 505.
520. PONIKAROV ET AL. 1966. The Geological Map of Syria scale 1:1000,000. (Technoexport, USSR).
521. POTY, B.B., LEROY, J. AND CUNY, M. 1974. Les inclusions granitique du limosin et due Forez (Massif Central, France). Op. Cit (5) pp569-583.
522. PRETORIUS, D.A. 1981. Gold and uranium in quartz-pebble conglomerates. Econ. Geol. 75th Anniversary, Vol. p117-138.
523. PRICE, W.A. 1933. Reynos a problem of south Texas and origin of caliche. Am. Assoc. petrol. Geologists Bull., 17: 488-522.
524. PRICE, V. AND FERGUSON, R.B. 1980. Stream sediment geochemical survey for uranium. In: R.H. Carpenter (ed), Geochemical Exploration for Uranium. J. Geochem. Explor., 13: 285-304.
525. QUENNELL, A.M. 1958. The structure and geomorphic evolution of the Dead Sea rift. Quarterly journal of the Geological Society of London, 114, 1-24.
526. RACKLEY, R.I. 1976. Origins of western states uranium mineralization. In: Handbook of Stratabound and Stratiform Ore Deposits, Wolf, K.H. (ed). Elsevier Publ. Company, Amsterdam, V.7, p89-156.
527. RANKIN, A.H. AND ALDERTON, D.H.M. 1985. Fluids in granites from southwest England. In: HHP Granites, hydrothermal circulation and ore genesis, a conference organised by the Instn. Min. Metall., St Austell, Cornwall.
528. RANKIN, A.H., ALDERTON, D.H.M., THOMPSON, M. AND GOULTER, J.E. 1982. Determination of uranium: carbon ratios in fluid inclusion decrepitates by ICP. Mineralogical Mag. Vol.46, p179-186.
529. READ, J.F. 1974. Calcrete deposits and quarternay sediments, Edel Province, Shark Bay, Western Australia. Am. Assoc. Petrol. Geologists Memoir, 22: 250-282.
530. REEVES, C.C. Jr. 1978. Economic significance of Playa Lake deposits. Spec. Publs. Int. Ass. Sedimentologists.
531. REEVES, C.C. Jr. 1970. Origin, classification and geologic history of caliche on the southern high plains, Texas and eastern New Mexico. J. Geol., 78: 352-362.
532. REEVES, M.J. AND SAADI, T.A. 1971. Factors controlling the deposition of some phosphate bearing strata from Jordan. Econ. Geol. Vol.66, 451-465.
533. REIMER, G.M. 1985. Induced polarization and electromagnetic field surveys of sedimentary uranium deposits. In: Geological Environment of Sandstone type Uranium Deposits. IAEA, Tec. Doc. 328, Vienna, 335-346.

534. REIMER, G.M. 1975. Uranium determination in natural water by the fission track technique. J. Geochem. Explor., 4, 425-31.
535. REISS, Z.I. 1955. Micropaleontology and the Cretaceous-Tertiary Boundary in Israel. II. Remarks on the age of some late cretaceous and early Tertiary stratigraphic units.
536. RENFRO, A.R. 1974. Genesis of evaporite-associated stratiform metalliferous deposits - A. Sabkha Process. Econ. Geol. Vol.69, 33-45.
537. REYNOLDS, R.L. 1983. Iron disulphide minerals and the genesis of roll-type uranium deposits. Econ. Geol. Vol.78(1).
538. REYNOLDS, R.L., GOLDHABER, M.B. AND CARPENTER, D.J. 1982. Biogenic and non-biogenic ore-forming processes in the south Texas uranium district: Evidence from the Panna Maria deposit. Econ. Geol. V.77, p541-556.
539. REYNOLDS, R.L. AND GOLDHABER, M.B. 1978. Origin of a south Texas roll-type deposit: I. Alteration of iron-titanium oxide minerals. Econ. Geol. V.73, p1677-1689.
540. REYNOLDS, R.L., GOLDHABER, M.B. AND GRAUCH, R.I. 1977. Uranium associated with iron-titanium oxide minerals and their alteration products in a south Texas roll-type deposit. In: Campbell, J.A. (ed). Short papers of the U.S. Geol. Surv. Uranium-thorium Symposium. U.S. Geol. Survey Circ. 753, p37-39.
541. RICH, R.A., HOLLAND, H.D. AND PATERSON, U. 1977. Hydrothermal uranium deposits. Elsevier, 264p.
542. RIGGS, S.R. 1985. Cyclic sediments, changing climate, and neogene phosphogenesis. Int. Geol. Corre. Prog. Project 156, Tallahassee, Florida.
543. RIGGS, S.R. 1984. Paleoceanographic model of neogene phosphorite deposition, U.S. Atlantic Continental margin. Science, Vol. 223, p123-231.
544. ROBB, L. AND MEYER, M. 1985. Uranium distribution and concentration mechanisms in the hinterland of the Witwatersrand basin. In: Concentration Mechanisms of Uranium in Geological Environments. Int. Meeting, Nancy.
545. ROBBINS, J.C. AND CASTLEDINE, C. 1979. Laser fluorescence as a basic analytical technique for uranium in the mining industry; Bull. Can. Inst. Min. Metall. V.72, No. 803, p98.
546. ROBBINS, J.C. 1978. Field technique for the measurement of uranium in natural waters. Bull. Can. Inst. Min. Metall., 71, 61-67.
547. ROBERTS, D.E. 1985. The Olympic Dam Copper-Uranium-Gold Deposit. In: Recognition of Uranium Provinces. Proceeding of an IAEA Technical Committee meeting, London, 18-20 September.
548. ROBINSON, B.W. AND NICKEL, E.H. 1979. A useful technique for mineralogy: the backscattered electron low vacuum mode of scanning electron microprobe operation. Am. Mineralogist, 64, 1322-1328.
549. ROGERS, J.J.W., RAGLAND, P.C., NISHMORI, R.K., GREENBERG, J.K. AND HANK, S.A. 1978. Varieties of granitic uranium deposits and favourable exploration areas in the Eastern United States. Econ. Geol. 73, p1539-1555.

550. ROGERS, J.J.W. AND ADAMS, J.A.S. 1969. Thorium and Uranium. In: Handbook of Geochemistry, Wedepohl, K.E. (ed). (Berlin; Springer, 1978), II-V, Pt. 90, 39p and Pt 92, 50p.
551. RONOV ET AL. 1967. Geochemistry of the rare earths in the sedimentary cycle. Geochem. Int. 4, p.1.
552. ROSE, A.W., WESOLOWSKI, D. AND SMITH, A.T. 1983. Groundwater geochemistry of uranium and other elements, Monticello area, New York. In: G.R. Parslow (ed). Geochemical Exploration, 1982. J. Geochem. Explor., 19: 163-186.
553. ROSE, A.W. AND WRIGHT, R.J. 1980. Geochemical exploration models for sedimentary uranium deposits. J. Geochem. Explor. (13).
554. ROSE, A.W., HAWKES, H.E. AND WEBB, J.S. 1979. Geochemistry in mineral exploration, 2nd edition. Academic Press, London, 657pp.
555. ROSE, A.W. 1977. Geochemical exploration for U. DOE Open File, GJBX-77, p303-352.
556. ROSE, A.W., KEITH, M.L. AND SHUR, N.H. 1976. Geochemical drainage surveys for uranium: sampling and analytical methods based on trail surveys in Pennsylvania. DoE, Open File, GJBX-28, 33p.
557. ROSSMAN, G.I., SYCHEV, I.V. TARKHANOVIA, G.A. ET AL. 1972. Use of Radiogenic Pb^{206} Halos in Prospecting for Uranium in Acid Volcanic Rocks. Int. Geol. Rev. 14, 332-337.
558. RUNNELL, D.R. AND LINDBERG, R.D. 1981. Hydrogeochemical Exploration for Uranium Ore Deposits: Use of the Computer Model WATEQFC. J. Geochem. Explor., 15: 37-50.
559. RUGLESS, C.S. AND GOVETT, G.J.S. 1984. Exploration rock geochemistry for Pinnacles-type mineralization at Broken Hill, N.S.W., Australia. J. Geochem. Explor. 22: 133-160.
560. RUZICKA, V. 1985. Geology and genesis of uranium deposits in the early Proterozoic Blind-River-Elliot Lake Basin, Ontario, Canada. In: Recognition of Uranium Provinces. Proceedings of an IAEA Technical Committee Meeting, London, 18-20 September.
561. RUZICKA, V. 1971. Geological comparison between East European and Canadian uranium deposits. Geol. Surv. Can. Paper, 70-48: 1-196.
562. SAFADI, C. 1954. Hydrogeologie du bassin d'Ed-Daou (Ad-Daww). A pub. de (AIH) No. 37, Assemblee Generale de Rome, tome II. p308-314.
563. SAMAMA, J.C. 1984. Uranium in lateritic terrains. In: Surficial Uranium Deposits. IAEA Tec. Doc. 322, Vienna, 53-60.
564. SANFORD, R.F. 1982. Preliminary model of regional mesozoic groundwater flow and uranium deposition in the Colorado Plateau. Geology, 10, 348-352.
565. SANFORD, R.F. 1985. Origin of Sandstone-hosted Uranium Deposits, Frome Embayment, South Australia. IAEA, Tec. Doc. 328, 297-313.
566. SAWKINS, F.J. 1984. Metal deposits in relation to plate tectonics. Springer-Verlag Berlin Heidelberg, 325pp.
567. SCHMIDT-COLERUS, J.J. 1979. Investigation of the relationship between organic matter and uranium deposits. Open File Rep. U.S. DoE, GJBX-130(79), 281p.

568. SCHOCK, H.H. 1977. Comparison of a coaxial Ge(Li) and a planar Ge detector in instrumental neutron activation analysis of Geologic materials. J. Radioanal. Chem. 36, 557-563.
569. SCLATOR ET AL. 1980. The heat flow through oceanic and continental crust and theheat loss of the earth. Rev. Geophys. Space Phys. 18: 269-311.
570. SELINUS, O. 1983. Factor and discriminant analysis to lithogeochemical prospecting in an area of Central Sweden. In: G.R. Parslow (ed), Geochemical Exploration 1982. J. Geochem. Explor., 19: 619-642.
571. SENGOR, A.M.C. AND YILMAZ, Y. 1981. Tethyan evolution of Turkey: a plate tectonic approach. Tectonophysics, 75: 181-241.
572. SHAFIQ, S. 1952. Sulphur occurrence northeast of Palmyra. Report, GEGMR, Syria.
573. SHARP, R.R. Jr. 1977. The LASL approach to uranium geochemical reconnaissance. DoE, Open File, GJBX 77 (77), 353-366.
574. SHAW, D.M. 1974. R-Mode factor analysis on enslatite chondrite analysis. Geochim et Cosmochim Acta, 38: 1607-1613.
575. SHAW, D.M. 1961. Element Distribution Laws in Geochemistry Geochim et Cosmochim. Acta, 23, 116-134.
576. SHATSKY, N.S. AND BODGANOV, A.A. 1961. An international tectonic map of Europe, scale 1:2,5000,000, Izv. Akad. Nauk. USSR, Serv. Geol., (4) (in Russian).
577. SHEARMAN, D.J. 1978. Evaporite of Coastal Sabkhas. Marine Evaporite, Dean et al (eds), SEPM Short Course, No. 4, Oklahoma City.
578. SHEARMAN, D.J. 1966. Origin of marine evaporites by diagenesis: Instn. Min. Metall. Trans., V,B75, p207-215.
579. SHELDON, R.P. 1981. Ancients marine phosphorites. Ann. Rev. Earth Planet Sci. 9, 251-284.
580. SHELDON, R.P. 1964. Exploration of phosphorite in Turkey a case history. Econ. Geol. V.59, p1159-1175.
581. SIBBALD, T.I.I. 1985. Geology and genesis of the Athabasca Basin uranium deposits. In: Recognition of Uranium Provinces. Proceedings of an IAEA Technical Committee Meeting, London, 18-20 September.
582. SIEGEL, F.R. (Ed.). 1979. Review of research on modern problems in geochemistry. Int. Asso. Geochem. and Cosmochem., UNESCO.
583. SILVER, L.T. 1982. A note on the magnitude of possible uranium losses from granites of the conterminous United States. OECD/NEA/IAEA, Paris, 457- .
584. SIMOV, S.D. 1985. Formation of U deposits. In: Recognition of Uranium Provinces. Proceedings of an IAEA Technical Committee meeting, London, 18-20 Sept.
585. SIMPSON, C.J., HUNTINGTON, J.F., LISHMAN, J. AND GREEN, A.A. 1980. A study of the Pine Creek Geosyncline using integrated Landsat and Aeromagnetic data. In: Uranium in the Pine Creek Geosyncline, Ferson and Goleby (eds). IAEA, Vienna, 141-155.
586. SIMPSON, P.R. AND HURDLEY, J. 1985. Granites as indicators of uranium provinces. In: Recognition of Uranium Provinces. Proceedings of an IAEA Technical Committee meeting, London, 18-20 Sept.

587. SIMPSON, P.R. AND HURDLEY, J. 1985. The relationship between metalliferous mineralisation and High Heat Production Granites in Bushveld Complex, South Africa. In: HHP Granites, Hydrothermal Circulation and Ore Genesis, a Conference organised by the Instn. Min. Metall., St Austell, Cornwall.
588. SIMPSON, P.R., TWIST, D. AND HURDLEY, J. 1985. The uranium potential of the Bushveld complex, South Africa: A Study of the acid igneous rocks. In: Concentration Mechanisms of Uranium in Geological Environments. Proceedings of Int. Meeting, Nancy, 2-5 October.
589. SIMPSON, P.R. AND PLANT, J.A. 1984. Role of high heat production granites in uranium province formation. In: Uranium Geochemistry, Mineralogy, Geology, Exploration and Resources. De Vivo et al (eds), London, Instn. Min. Metall., 167-78.
590. SIMPSON, P.R., PLANT, J.A., WATSON, J.V., GREEN., P.M. AND FOWLER, M.B. 1982. The role of metalliferous and mineralized uranium granites in the formation of uranium provinces. In: Uranium Exploration Methods. Symposium organised by the OECD-NEA in collaboration with the IAEA, Paris, 157-170.
590. SIMPSON, P.R. AND BOWLES, J.F.W. 1981. Detrital uraninite and pyrite: are they evidence for a reducing atmosphere? U.S. Geol. Surv. prof. paper 1161, S12p.
591. SIMPSON, P.R., BROWN, G.C., PLANT, J.A. AND OSTLE, D. 1979. Uranium mineralization and granite magmatism in the British Isles. Phil. Trans. R. Soc., London, A291, 385-412.
592. SIMPSON, P.R. AND BOWLES, J.F.W. 1977. Uranium minerlization of the Witwatersrand and Dominion Reef Systems. Phil. Trans. R. Soc. London, A286, 527-548.
593. SIMPSON, P.R., PLANT, J. AND COPE, M.J. 1976. Uranium abundance and distribution in some granites from northern Scotland and southwest England as indicators of uranium provinces. In: Geology, Mining and Extractive Processing of Uranium. Instn. Min. Metall. London, 126-139.
594. SIMPSON, P.R. 1968b. Substitution in apatite: II, low temperature fluoride-hydroxyl apatite. Am. Miner. 53, p.1953.
595. SIMPSON, P.R. 1967. Effect of pH and solution concentration on the composition of carbonate-apatite. Am. Miner. 52, p896.
596. SMEE, B.W. AND BAILES, R.J. 1986. The use of lithogeochemical patterns in wall rock as a guide to exploration drilling at the Jason lead-zinc-silver-barium deposit, Yukon Territory. In: C.E. Nichols (ed) Exploration for Ore Deposits of the North American Cordillera. J. Geochem. Explor., 25: 217-230.
597. SMIT, C.J.B. 1982. Radiometric determination of uranium using a collemated face scanner. OECD/NEA/IAEA, Paris, 681.
598. SMITH, D.K. Jr. 1984. Uranium mineralogy. In: B. De Vivo F. Ippolito, G. Capaldi and P.R. Simpson (eds), Uranium, Geochemistry, Mineralogy, Geology, Exploration and Resources (London, IMM), 43-88.

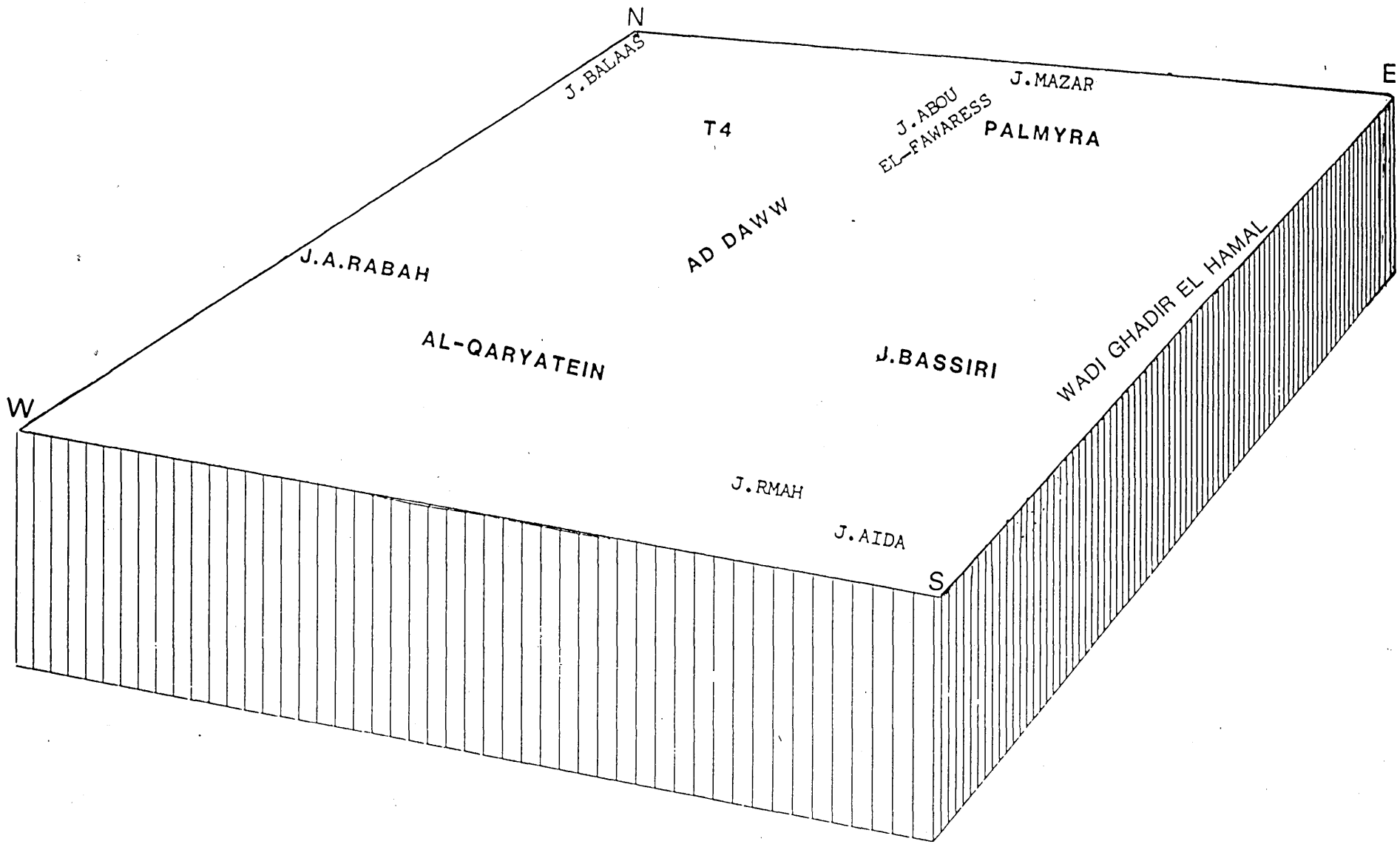
599. SMITH, A.Y. AND LYNCH, J.J. 1969. Field and Laboratory Methods used in Geochemical Prospecting by the Geological Survey of Canada, No. 11, Uranium in Soil, Stream Sediment and Water. Geol. Survey Can. Paper, 69-40.
600. SNEDECOR, G.W. AND COCHRAN, W.C. 1967. Statistical methods, 6th ed., Iowa State University Press, Ames.
601. SNELLING, A.A. 1984. A soil geochemistry orientation survey for uranium at Koongarra, Northern Territory. In: Geochemical exploration in arid and deeply weathered terrains, Davy and Mazzucchelli (eds). J. Geochem. Explor. 22: 83-99.
602. SNELLING, A.A. 1980. Uraninite and its alteration products Koongarra uranium deposit. In: Uranium in the Pine Creek Geosyncline, Ferguson and Goleby (eds). IAEA, Vienna, 487-498.
603. SONNENFELD, P. 1984. Brines and Evaporites. Academic Press Inc. 613pp.
604. SOPUCK, V.J., DE CARLA, A., WRAY, E.M. AND COOPER, B. 1983. The Application of Lithogeochemistry in the Search for Unconformity-type Uranium Deposits, Northern Saskatchewan, Canada. In: G.R. Parslow (ed), Geochemical Exploration 1982. J. Geochem. Explor., 19: p77-99.
605. SORENSEN, H. 1977. Features of the distribution of uranium concentration in alkalic igneous rocks. IAEA, Tec. Doc., 25/10, Vienna, 47-54.
606. SORENSEN, H. 1970. "Low-grade uranium deposits in agpaitic nepheline syenites, South Greenland". In: Uranium Exploration Geology (IAEA, Vienna, 151-168).
607. SOULIDI-KONDRATIEV, E.D. AND PONIKAROV, V.P. 1966. The geological map of Syria, scale 1:200,000. Explanatory notes, sheet I-37-XV (Tudmor/Palmyra) (Technoexport, USSR).
608. SPEER, J.A., SOLBELG, T.N. AND BECKER, S.W. 1981. Petrography of the uranium-bearing minerals of the liberty Hill pluton, South Carolina: Phase assemblages and migration of uranium in granitoid rocks. Econ. Geol. Vol. 76, pp2162-2175.
609. SPIRAKIS, C. 1977. The role of semi-permeable membranes in the formation of certain vanadium-uranium deposits. Econ. Geol., 72, 1442-1448.
610. STARINSKY, A., KUTZ, A. AND KOLODNY, Y. 1982. Incorporation of uranium into diagenetic phosphorite. Geochim. et Cosmochim Acta, V.46, p1365-1374.
611. STEENFELT, A. AND KUNZENDORF, H. 1978. Geochemical methods in uranium exploration in Northern East Greenland. In: Geochemical Exploration. J.R. Watterson and P.K. Theobald (eds). 429-442.
612. STEVENS, D.N., ROUSE, G.E., DE VOTO, R.H. 1971. Radon-222 in soil-gas: three uranium case histories in the western United States. CIM special vol. No.11, 258-264.
613. STUART, D.C. AND RYAN, D.E. 1981. Epithermal neutron activation analysis with SLOWPOKE nuclear reactor. National Research Council of Canada.
614. STUCKLESS, J.S. 1985. Applications of U-Th-Pb isotope systematics to investigations of uranium source rocks. In: Concentration mechanisms of uranium in geological environments. Int. Meeting, Nancy.

615. STUCKLESS, J.S. AND NKOMO, I.T. 1978. Uranium-Lead Isotope Systematics in Uraniferous Alkali-rich Granites from the Granite Mountains, Wyoming: Implications for uranium source rocks. Econ. Geol., V.73, p427-441.
616. SUMMERHAYES, C.P. 1973. Phosphate in sediments off S.W. Africa. Nature, 243, p509.
617. SUMMERHAYES, C.P. 1970. Phosphate Deposits on the Northwest African Continental Shelf and Slope. Unpublished PhD Thesis, Imperial College, Univ. London, 282pp.
618. SUN, S.S. 1982. Chemical composition and origin of the earth's primitive mantle. Geochim. Cosmochim Acta, 46, 179-92.
619. SZALAY, A. 1958. The significance of humus in the geochemical enrichment of uranium. In: Porc. 2nd Int. UN Conf. Peaceful Uses Atomic Energy, Geneva, 1731.
620. TECHNOEXPORT, V.O. 1966. Explanatory notes of each 1:200,000 geology map sheets.
621. TECHNOEXPORT, V.O. 1967. Explanatory notes of Geological Map of Syria at 1:500,000 scale Vol. 1. Stratigraphy Igneous Rocks, Tectonics. Vol. 2. Mineral Deposits and Undergraound-water Resources.
622. THEIS, N.J. 1979. Uranium-bearing and associated minerals in their geochemical and sedimentological context, Elliot Lake, Ontario. Canada Geol. Surv. Bull. 304, 50p.
623. THOMPSON, M.E. 1954. Further studies of the distribution of uranium in rich phosphate beds of the phosphoria formation. U.S. Geol. Surv. Bull. 1009-D.
624. THOMPSON, M. 1983. Control procedures in geochemical analysis. In: Statistics Data Analysis in Geochemical Prospecting. (ed) R.J. Howarth. Handbook of Exploration Geochemistry, Vol.2, Elsevier Publication, Amsterdam.
625. THOMPSON, M., RAMSEY, M. AND PAHLAVANPOUR, B. 1982. Water analysis by Inductively Coupled Plasma Atomic Emission Spectrometryafter a rapid pre-concentration. Analyst, Vol.107: 1330-1334.
626. THOMPSON, M. AND HOWARTH, R.J. 1978. A new approach to estimation of analytical precision. J. Geochem. Explor., 9: 23-30.
627. THOMPSON, M. AND HOWARTH, R.J. 1976. "Duplicate analysis in geochemical practice". Analyst, London 101: 690.
628. THOMPSON, M. AND HOWARTH, R.J. 1973. The rapid estimation and control of precision by duplicate determinations. Analyst, 98: 153-160.
629. TOENS, P.D., HAMBLETON-JONES, B.B. 1984. Definition and classification of surficial uranium deposits. In: Surficial Uranium Deposits. IAEA, Tec. Doc. 322,9-14.
630. TOENS, P.D. 1981. Uranium provinces and their time-bound characteristics. Trans. Geol. Soc. S. Afr., 84, 293-312.
631. TOOMS, J.S., SUMMERHAYES, C.P. AND CRONAN, D.S. 1969. Geochemistry of marine phosphate and manganese deposits. Oceanogr. Ann. New York Acad. Sci., 85, p145.

632. TOURTELOT, H.A. 1964. Minor element composition and organic carbon content of marine and non-marine shale of Late Cretaceous age in the western interior of the United States. Geochim. Cosmochim. Acta., V.28, 1573-1609.
633. TUREKIAN, K.K. 1977. Geochemical distribution of elements. In: Encyclopedia of Science and Technology, 4th edn. 627-630. McGraw Hill, New York.
634. TUREKIAN, K.K. AND CHAN, L.H. 1971. The marine geochemistry of the uranium isotopes. ^{230}Th and ^{231}Pa In: Activation analysis in geochemistry and cosmochemistry. A.O. Brunfelt and E. Steinnes (eds). (Universitets forlaget, Oslo: 311-320).
635. TURNER, B.R. 1985. uranium Mineralization in Karoo Basin, South Africa. Econ. Geol. V.80, pp256-269.
636. TURNER, A.B. 1982. Direct uranium logging by high resolution gamma-ray spectrometry. OECD/NEA/IAEA, Paris, 793- .
637. URANIUM SUPPLY AND DEMAND. (The U Institute, Mining Journal Books Ltd., London), 1976, 1977, 1978, 1982.
638. VICKERS, R.C. 1957. Alteration of sandstone as a guide to uranium deposits and their origin, Northern Black Hills, South Dakota. Econ. Geol. Vol.52, p599-611.
639. VINE, J.D. 1972. Geology of uranium in Coaly and Carboniferous rocks: U.S. Geol. Surv. Prof. paper 356-D, p113-170.
640. VINOGRADOVE, A.P. Geochemistry of rare and dispersed elements in soil, 254pp. Publishing House of the AN, USSR, Moscow.
641. WALD, M. AND WIEG, G. 1973. Determination of manogram U content in solutions by the fission track method. Radiochim Acta, V.19, p37.
642. WANTY, R.B., CHATHAM, J.R. AND LANGMUIR, D. 1985. The solubilities of some major and minor element minerals in groundwaters associated with a sandstone-hosted uranium deposit.
643. WARD, F.N. AND PRICE, V. 1980. Analytical Methodology for Uranium Exploration and Retrospective and Prospective. In: R.H. Carpenter (ed), Geochemical Explorations for Uranium. J. Geochem. Explor., 13, 97-113.
644. WARD, F.N. AND BONDER, W.F. 1979. Analytical methodology in search for metallic ores. In: P.J. Hood (ed), Geophysics and Geochemistry in the Search for Metallic Ores. Geol. Surv. Can., Econ. Geol. Rep., 31: 365-383.
645. WARREN, C.G. 1975. Selenium associated with uranium deposits; U.S. Geol. Surv. Open File Report, 75-595, p52-53.
646. WATSON, A. 1983. Evaporite sedimentation in non-marine environments. In: Geochemical Sediment, and Geomorphology by A.S. Goudie and Kenneth Pye. Academic Press, 439pp.
647. WATSON, J.V. AND PLANT, J. 1979. Regional geochemistry of uranium as a guide to deposit formation; Phil. Trans. R. Soc. London, A, V.291, p321-338.
648. WATSON, J., FOWLER, M.B., PLANT, J., SIMPSON, P.R. AND GREEN, P.M. 1982. Uranium provinces in relation to metamorphic grade and regional geochemistry. In: Uranium exploration methods, OECD/NEA/IAEA, Paris, 235-248.

649. WATERBURY, G.R. 1977. Fluorimetric analyses for uranium in natural waters in HSSR Sumposium, pp395, GJBX-77(77).
650. WALTERS, R.A. 1983. Geochemical exploration for uranium and other metals in tropical and subtropical environments using heavy mineral concentrates. In: G.R. Parslow (ed), Geochemical Exploration, 1982. J. Geochem. Explor., 19: 103-124.
651. WATTERSON, J.R. AND THEOBALD, P.K. 1978. Geochemical exploration. Proceeding of the 7th Int. Geochem. Explor. Symp. Golden, Colorado.
652. WEBB, J.S. AND THOMPSON, M. 1977. Analytical requirements in exploration geochemistry. Pure Appl. Chem., 49: 1507-1518.
653. WEBB, J.S. 1970. Some geochemical applications of regional geochemical reconnaissance. Geol. Assoc. Proc. 81 (3), 385-594.
654. WEBB, J.S. AND MILLAMAN, A.P. 1950. Heavy metals in natural waters as a guide to ore. Inst. Min. Metall. Trans. 60, 475-504.
655. WEEKS, A.D. AND EARGLE, D.H. 1960. Uranium at Palangana Salt Dom, Duval County, Texas. U.S. Geol. Surv. Prof. paper 400B, pB48-B52.
656. WENRICH, K.J. 1985. Hydrogeochemical and stream sediment sampling for uranium in the sandstone environment. In: Geological Environments of Sandstone-type Uranium Deposits, IAEA, Tec. Doc. 328, Vienna, p317-334
657. WENRICH-VERBECK, K.J. 1977. Uranium and co-existing element behaviour in surface waters and associated sediments with varied sampling techniques used for uranium exploration. J. Geochem. Explor. 8, 337-355.
658. WENNERVIRTA, H. 1967. Geochemical methods of uranium prospecting in Finland. In: "Geochemical Prospecting in Fennoscandia". (A. Kvalheim, ed.), 155-170. Interscience, New York.
659. WETZEL, R. AND MORLON, D.M. 1959. Contribution a la geologie de la Transjordanie. Notes et mem. Moyen-Orient, 7.
660. WILSON, M.R. 1984. Uranium enrichment in European peat bogs. In: Surficial Uranium Deposits, IAEA, Tec. Doc. 322, Vienna, 197-203.
661. WODZIAKI, A. 1959. Geochemical prospecting for uranium in the Lower Buller Gorge, New Zealand. N.Z. J. Geol. Geophys. 2, 602-612.
662. WYANT, D.G., SHARP, W.N. AND SHERIDAN, D.M. 1956. Reconnaissance study of uranium deposits in the Red Desert, Sweetwater County, Wyoming. U.S. Geol. Surv. Bull. 1030-I, p237-308.
663. YEMA, P.J.M. AND HOCHMAN, M.B.M. 1985. A thermoluminescence study of the role of a Middle Proterozoic unconformity in controlling uranium mineralization, as shown at the Eyre Peninsula, South Australia. In: Concentration Mechanisms of Uranium in Geological Environments. Int. Meeting, Nancy.
664. YOUNG, R.G. 1984. Uranium deposits of the world, excluding Europe. In: Uranium Geochemistry, Mineralogy, Geology, Exploration and Resources. De Vivo et al (eds). Instn. Min. Metall. London, 117-139.

665. YOUNG, R.G. 1964. Distribution of uranium deposits in the White Canyon - Monument Valley District, Utah-Arizona. Econ. Geol. V.59, p850-873.
666. ZIEGLER, V. AND DARDEL, J. 1984. Uranium deposits in Europe. In: Uranium geochemistry, mineralogy, geology, exploration and resources. De Vivo et al (eds). Instn. Min. Metall. London, 140-161.
667. ZIEGLER, V. 1974. Essai de classification metallo-tectonique des gisments d'uranium. IAEA-SM-183/16, STI/374, Vienna.
668. ZIELINSKI, R.A. 1983. Tuffaceous sediments as source rocks for uranium. A case study of the White River Formation, Wyoming: J. Geochem. Explor. (18) (3) 285-306.
669. ZIELINSKI, R.A. 1982a. The mobility of uranium and other elements during alteration of phyolite ash to montmorillorite: a case study in the troublesome formation, Colorado. Chem. Geol. 35 (314), p185-204.
670. ZIELINSKI, R.A. 1982b. Uraniferous opal, Virgin Valley, Nevada: conditions of formation and implications for uranium exploration. J. Geochem. Explor. 16(3), p197-216.
671. ZIELINSKI, R.A. AND ROSHOLT, J.N. 1978. Uranium in waters and aquifer rocks at the Nevada test site, Nye County, Nevada, J. Res. U.S. Geol. Surv., 6 (4): 489-498.



An overlay block diagram for approx location of key sites mentioned in the elements distribution and mapping the factor scores and residuals of the Palmyrides lithogeochemistry.